Neuromethods 56

Springer Protocols

Michael Aschner
Cristina Suñol
Anna Bal-Price *Editors*

Cell Culture Techniques

Humana Press

NEUROMETHODS

Series Editor
Wolfgang Walz
University of Saskatchewan
Saskatoon, SK, Canada

For further volumes, go to
http://www.springer.com/series/7657

Cell Culture Techniques

Edited by

Michael Aschner

Departments of Pediatrics and Pharmacology, and the Kennedy Center for Research on Human Development, Vanderbilt University Medical Center, Nashville, TN, USA

Cristina Suñol

Institut d'Investigacions Biomèdiques de Barcelona, CSIC-IDIBAPS, and CIBERESP, Barcelona, Spain

Anna Bal-Price

In-Vitro Methods Unit, Institute for Health and Consumer Protection, European Commission Joint Research Centre, Ispra, VA, Italy

Humana Press

Editors
Michael Aschner
Department of Pediatrics
Vanderbilt University Medical Center
Garland Avenue 2215-B
Nashville, TN 37232, USA
michael.aschner@vanderbilt.edu

Anna Bal-Price
Inst. for Health & Consumer Protection,
ECVAM In-Vitro Methods Unit
Via Enrico Fermi 1
Ispra 21026, Varese, Italy
Anna.Price@jrc.it

Cristina Suñol
Institut d'Investigacions Biomèdiques,
Neurochemistry & Neuropharmacology
CSIC C/ Rosselló 161
Barcelona 08036, Spain
csendqi@iibb.csic.es

ISSN 0893-2336 e-ISSN 1940-6045
ISBN 978-1-61779-076-8 e-ISBN 978-1-61779-077-5
DOI 10.1007/978-1-61779-077-5
Springer New York Dordrecht Heidelberg London

Library of Congress Control Number: 2011922382

Humana Press is part of Springer Science+Business Media (www.springer.com)

Preface to the Series

Under the guidance of its founders Alan Boulton and Glen Baker, the Neuromethods series by Humana Press has been very successful since the first volume appeared in 1985. In about 17 years, 37 volumes have been published. In 2006, Springer Science + Business Media made a renewed commitment to this series. The new program will focus on methods that are either unique to the nervous system and excitable cells or which need special consideration to be applied to the neurosciences. The program will strike a balance between recent and exciting developments like those concerning new animal models of disease, imaging, *in vivo* methods, and more established techniques. These include immunocytochemistry and electrophysiological technologies. New trainees in neurosciences still need a sound footing in these older methods to apply a critical approach to their results. The careful application of methods is probably the most important step in the process of scientific inquiry. In the past, new methodologies led the way in developing new disciplines in the biological and medical sciences. For example, Physiology emerged out of Anatomy in the nineteenth century by harnessing new methods based on the newly discovered phenomenon of electricity. Nowadays, the relationships between disciplines and methods are more complex. Methods are now widely shared between disciplines and research areas. New developments in electronic publishing also make it possible for scientists to download chapters or protocols selectively within a very short time of encountering them. This new approach has been taken into account in the design of individual volumes and chapters in this series.

Wolfgang Walz

Preface

Societal, ethical, and cost-related issues, not to mention the need for sound scientific methods, have led to new and/or refined methods for the evaluation of health risks associated with neurotoxic compounds. To be effective, they must be relevant and predictive of exposure, relatively inexpensive, and preferably amenable to high throughput analysis and a reduction in animal use. Ultimately, they also have to be of value to public health regulators, providing them with sound guidelines upon which to base exposure limits to adverse neurotoxic compounds. In other cases, they need to provide clues on neurotoxic mechanisms, identifying potential targets for the development of new treatment modalities.

While this book contains traditional chapters, such as those on various cell cultures which describe methods that have evolved over years, we made a valiant attempt to include also innovative approaches to neurotoxicologic testing, recognizing that the Decade of the Brain (1990–2000) has brought about a revolution in neurobiology and neurotoxicology. Accordingly, we describe how stem cells, computational biology, and other novel powerful methods can now be applied to address the challenges of neurotoxic testing.

We hope that the chapters will enlighten both the novice and the experienced neurotoxicologist and provide them with a renewed sense of the state of the art of *Neuromethods* that can facilitate the study of adverse changes in the developing and mature brain alike, addressing molecular mechanisms of neurotoxicity as well as genetic susceptibility. While for the foreseeable future, animal testing is unlikely to be completely replaced, marshaling and improving upon methods that reduce the need for animal testing will undoubtedly continue. We hope that the series of chapters compiled herein will amass a renewed wave of interest transforming neurotoxicology testing into mechanistically driven, cost-effective, and high throughput series of tests that are met by contemporary challenges.

Nashville, TN ***Michael Aschner***
Barcelona, Spain ***Cristina Suñol***
Ispra, Italy ***Anna Bal-Price***

Contents

Contributors

Asad A. Aboud • *Department of Neurology, Vanderbilt Kennedy Center for Research on Human Development, Vanderbilt University Medical Center, Nashville, TN, USA*

Michael D. Aleo • *Pfizer Worldwide Research and Development, Drug Safety Research and Development, Groton 06340, CT, USA*

Michael Aschner • *Departments of Pediatrics and Pharmacology, and the Kennedy Center for Research on Human Development, Vanderbilt University Medical Center, Nashville, TN, USA*

Anna Bal-Price • *In-Vitro Methods Unit, Institute for Health and Consumer Protection, European Commission Joint Research Centre, Ispra, VA, Italy*

João Batista Teixeira da Rocha • *Departamento de Química, Centro de Ciências Naturais e Exatas, Universidade Federal de Santa Maria, Santa Maria, RS, Brazil*

Jordi Berenguer • *Department of Cell Death and Proliferation, IIBB, CSIC-IDIBAPS, Barcelona, Spain*

Aaron B. Bowman • *Department of Neurology, Vanderbilt Kennedy Center for Research on Human Development, Vanderbilt University Medical Center, Nashville, TN, USA*

Joseph Bressler • *Center For Alternatives In Animal Testing, Department of Environmental Health Sciences, Bloomberg School of Public Health and Hugo Moser Institute at the Kennedy Krieger, Baltimore, MD, USA*

Guy C. Brown • *Department Biochemistry, University of Cambridge, Cambridge, UK*

Guy A. Caldwell • *Department of Biological Sciences, The University of Alabama, Tuscaloosa, AL, USA; Departments of Neurology and Neurobiology, Center for Neurodegeneration and Experimental Therapeutics, University of Alabama at Birmingham, Birmingham, AL, USA*

Kim A. Caldwell • *Department of Biological Sciences, The University of Alabama, Tuscaloosa, AL, USA; Departments of Neurology and Neurobiology, Center for Neurodegeneration and Experimental Therapeutics, University of Alabama at Birmingham, Birmingham, AL, USA*

Sandra Ceccatelli • *Department of Neuroscience, Karolinska Institutet, Stockholm, Sweden*

Roméo Cecchelli • *Université Lille Nord de France, Lille, France; Laboratoire de la Barrière Hémato-Encéphalique, EA 2465, IMPRT-IFR 114, Faculté des Sciences Jean Perrin, Université d'Artois, Lens, France*

Simona G. Codreanu • *Department of Biochemistry, Vanderbilt University, Nashville, TN, USA*

Sandra Coecke • *In-Vitro Methods Unit, Institute for Health and Consumer Protection, European Commission Joint Research Centre, Ispra, VA, Italy*

Lucio G. Costa • *Department of Environmental and Occupational Health Sciences, University of Washington, Seattle, WA, USA; Department of Human Anatomy, Pharmacology, and Forensic Science, University of Parma Medical School, Parma, Italy*
Rosa Cristòfol • *Institut d'Investigacions Biomèdiques de Barcelona, CSIC-IDIBAPS, Barcelona, Spain*
Maxime Culot • *Université Lille Nord de France, Lille, France; Laboratoire de la Barrière Hémato-Encéphalique, EA 2465, IMPRT-IFR 114, Faculté des Sciences Jean Perrin, Université d'Artois, Lens, France*
Lucie Dehouck • *Université Lille Nord de France, Lille, France; Laboratoire de la Barrière Hémato-Encéphalique, EA 2465, IMPRT-IFR 114, Faculté des Sciences Jean Perrin, Université d'Artois, Lens, France*
Marie-Pierre Dehouck • *Université Lille Nord de France, Lille, France; Laboratoire de la Barrière Hémato-Encéphalique, EA 2465, IMPRT-IFR 114, Faculté des Sciences Jean Perrin, Université d'Artois, Lens, France*
Yannick Delplace • *Cellial Technologies, Faculté des Sciences Jean Perrin, Lens, France*
Kevin C. Ess • *Department of Neurology, Vanderbilt Kennedy Center for Research on Human Development, Vanderbilt University Medical Center, Nashville, TN, USA*
Marcelo Farina • *Departamento de Bioquímica, Centro de Ciências Biológicas, Universidade Federal de Santa Catarina, Florianópolis, Santa Catarina, Brazil*
John Flaskos • *Laboratory of Biochemistry and Toxicology, Faculty of Veterinary Medicine, Aristotle University of Thessaloniki, Thessaloniki, Greece*
Anna Forsby • *Department of Neurochemistry, The Arrhenius Laboratory for Natural Sciences, Stockholm University, Stockholm, Sweden*
Michael Fricker • *Department Biochemistry, University of Cambridge, Cambridge, UK*
Daniel A. García • *Cátedra de Química Biológica, Departamento de Química. Facultad de Ciencias Exactas, Físicas y Naturales, Universidad Nacional de Córdoba, Córdoba, Argentina*
Jean-François Ghersi-Egea • *INSERM UMRS842, Université Lyon-1, Lyon, France*
Gennaro Giordano • *Department of Environmental and Occupational Health Sciences, University of Washington, Seattle, WA, USA*
Marina Guizzetti • *Department of Environmental and Occupational Health Sciences, University of Washington, Seattle, WA, USA*
Dorothée Hallier-Vanuxeem • *Cellial Technologies, Faculté des Sciences Jean Perrin, Lens, France*
Alan J. Hargreaves • *School of Science and Technology, Nottingham Trent University, Nottingham, UK*
Paul Honegger • *Department of Physiology, University of Lausanne, Lausanne, Switzerland*
Wan Norhamidah Wan Ibrahim • *Department of Neuroscience, Karolinska Institutet, Stockholm, Sweden*
Walter Kaufmann • *Hugo Moser Institute, Department of Environmental Health Sciences, Bloomberg School of Public Health, Baltimore, MD, USA*
Agnieszka Kinsner-Ovaskainen • *In-Vitro Methods Unit, Institute for Health and Consumer Protection, European Commission Joint Research Centre, Ispra, VA, Italy*

Anne-Marie Lenfant • *Université Lille Nord de France, Lille, France; Laboratoire de la Barrière Hémato-Encéphalique, EA 2465, IMPRT-IFR 114, Faculté des Sciences Jean Perrin, Université d'Artois, Lens, France*
Daniel C. Liebler • *Departments of Pharmacology, Biochemistry, and Biomedical Informatics, Vanderbilt University, Nashville, TN, USA*
Karsten K. Madsen • *Department of Pharmacology and Pharmacotherapy, Faculty of Pharmaceutical Sciences, University of Copenhagen, Copenhagen, Denmark*
Cathleen Marshall • *Hugo Moser Institute, Department of Environmental Health Sciences, Bloomberg School of Public Health, Baltimore, MD, USA*
BethAnn McLaughlin • *Departments of Neurology and Pharmacology, Vanderbilt Kennedy Center for Research on Human Development, Vanderbilt University, Nashville, TN, USA*
Dejan Milatovic • *Department of Pediatrics, Vanderbilt University Medical Center, Nashville, TN, USA*
Michaela Moors • *Department of Neuroscience, Karolinska Institutet, Stockholm, Sweden*
Toshio Narahashi • *Department of Molecular Pharmacology and Biological Chemistry, Feinberg School of Medicine, Northwestern University, 303 E. Chicago Avenue, Chicago, IL, USA*
M. Diana Neely • *Department of Neurology, Vanderbilt Kennedy Center for Research on Human Development, Vanderbilt University Medical Center, Nashville, TN, USA*
Jonas J. Neher • *Department Biochemistry, University of Cambridge, Cambridge, UK*
Cliona O'Driscoll • *Hugo Moser Institute, Department of Environmental Health Sciences, Bloomberg School of Public Health, Baltimore, MD, USA*
Sebastián Pons • *Department of Cell Death and Proliferation, IIBB, CSIC-IDIBAPS, Barcelona, Spain*
Magda Sachana • *Laboratory of Biochemistry and Toxicology, Faculty of Veterinary Medicine, Aristotle University of Thessaloniki, Thessaloniki, Greece*
Coral Sanfeliu • *Institut d'Investigacions Biomèdiques de Barcelona, CSIC-IDIBAPS, Barcelona, Spain*
Arne Schousboe • *Department of Pharmacology and Pharmacotherapy, University of Copenhagen, Faculty of Pharmaceutical Sciences, Copenhagen, Denmark*
Juan Segura-Aguilar • *Molecular and Clinical Pharmacology, ICBM, Faculty of Medicine, University of Chile, Santiago, Chile*
Emmanuel Sevin • *Université Lille Nord de France, Lille, France; Laboratoire de la Barrière Hémato-Encéphalique, EA 2465, IMPRT-IFR 114, Faculté des Sciences Jean Perrin, Université d'Artois, Lens, France*
Marta Sidoryk-Węgrzynowicz • *Department of Pediatrics, Vanderbilt University Medical Center, Nashville, TN, USA*
Carme Solà • *Institut d'Investigacions Biomèdiques de Barcelona, CSIC-IDIBAPS, Barcelona, Spain*
Ursula Sonnewald • *Department of Neuroscience, NTNU, Faculty of Medicine, MTFS, Trondheim, Norway*
Jeannette N. Stankowski • *Neuroscience Graduate Program and Vanderbilt Kennedy Center for Research on Human Development, Vanderbilt University, Nashville, TN, USA*

Nathalie Strazielle • *Brain-i, Lyon, France*
Cristina Suñol • *Institut d'Investigacions Biomèdiques de Barcelona, CSIC-IDIBAPS, and CIBERESP, Barcelona, Spain*
Christoffer Tamm • *Department of Neuroscience, Karolinska Institutet, Stockholm, Sweden*
Andrew M. Tidball • *Department of Neurology, Vanderbilt Kennedy Center for Research on Human Development, Vanderbilt University Medical Center, Nashville, TN, USA*
Roshan Tofighi • *Department of Neuroscience, Karolinska Institutet, Stockholm, Sweden*
Aviva M. Tolkovsky • *Department Biochemistry and Cambridge Centre for Brain Repair, University of Cambridge, Cambridge, UK*
Michelle L. Tucci • *Department of Biological Sciences, The University of Alabama, Tuscaloosa, AL, USA*
Elodie Vandenhaute • *Université Lille Nord de France, Lille, France; Laboratoire de la Barrière Hémato-Encéphalique, EA 2465, IMPRT-IFR 114, Faculté des Sciences Jean Perrin, Université d'Artois, Lens, France*
Helle S. Waagepetersen • *Department of Pharmacology and Pharmacotherapy, Faculty of Pharmaceutical Sciences, University of Copenhagen, Copenhagen, Denmark*
Dieter G. Weiss • *Cell Biology and Biosystems Technology, Institute of Biological Sciences, University of Rostock, Rostock, Germany*
H. Steve White • *Anticonvulsant Drug Development Program, Department of Pharmacology and Toxicology, University of Utah, Salt Lake City, UT, USA*
Marie-Gabrielle Zurich • *Department of Physiology, University of Lausanne, Lausanne, Switzerland*

Chapter 1

Guidance on Good Cell Culture Practice (GCCP)

Anna Bal-Price and Sandra Coecke

Abstract

The use of various in vitro systems is expanding dramatically not only in basic research, but also to meet regulatory requirements for chemicals and products of various kinds. Further significant developments are certain to result from the use of in vitro systems for high-throughput screening in pharmacology and toxicology. Because the maintenance of high standards is fundamental to all good scientific practice and is essential for maximising the reproducibility, reliability, credibility, acceptance and proper application of any results produced, guidelines have been developed to define minimum standards in cell and tissue culture to be called as Good Cell Culture Practice (GCCP). The scope of this chapter has been broadly defined to include systems based on cells and tissues obtained from humans and animals, issues related to the characterisation and maintenance of essential characteristics, as well as quality assurance; recording and reporting; safety, education and training; and ethics.

This GCCP guidance lists a set of six principles intended to support best practice in all aspects of the use of cells and tissues in vitro, and to complement, but not to replace, any existing guidance, guidelines or regulations.

Key words: Maintenance, Characterisation, Standardisation, Documentation, Storage, Hazards, Facilities, Primary culture, Cell lines

1. Introduction

The aim of Guidance on Good Cell Culture Practice (GCCP) is to promote the maintenance of high standards and to reduce uncertainty in the development and application of animal and human cell and tissue culture procedures and products by encouraging the greater international harmonisation, rationalisation and standardisation of in vitro laboratory practices; quality control systems; safety procedures; recording and reporting; and compliance with laws, regulations and ethical principles. Here, the basic concepts of GCCP principles will be discussed in order to demonstrate their

Michael Aschner et al. (eds.), *Cell Culture Techniques*, Neuromethods, vol. 56,
DOI 10.1007/978-1-61779-077-5_1, © Springer Science+Business Media, LLC 2011

role in the development, optimisation and validation of in vitro test methods to ensure more robust (relatively insensitive to minor changes in the protocol) and easy transferable test methods. The GCCP document (a full version see (1)) provides the basis for an internationally agreed-upon and consistent scientific high quality approach for the development of new alternative cell- and tissue-based test methods (2) with potential regulatory applicability and is referenced in the OECD Advisory Document on The Application of the Principles of GLP to In Vitro Studies (3,4).

This guidance is not only required to meet regulatory requirements for toxicity testing of chemicals and products of various kinds but also to serve the rapidly expanding use of in vitro systems in basic research as well. Furthermore, significant developments are certain to result in the use of in vitro systems for high-throughput screening in pharmacology and toxicology and systems biology approaches (5); the enlarging fields of genomics, proteomics and metabonomics; the field of stem cell development and standardisation; and the use of biomarkers of disease, susceptibility, exposure and effect.

2. The Principles of GCCP

The GCCP sets the minimum standards for any in vitro work involving cell and tissue cultures. However, its detailed implementation depends on the nature of the work involved. Based on review by a broad range of experts and organisations, the aim of GCCP is to foster consensus among all concerned with the use of cell and tissue culture systems, in order to:

- Establish and maintain best cell and tissue culture practice.
- Promote effective quality control systems.
- Facilitate education and training.
- Assist journal editors and editorial boards.
- Assist research funding bodies.
- Facilitate the interpretation and application of conclusions based on in vitro work.

The GCCP guidance is based upon the following six operational principles.

2.1. First GCCP Principle

Establishment and maintenance of a sufficient understanding of the in vitro system and of the relevant factors which could affect it.

The essential elements for assuring reliable and accurate work when using in vitro cell- and tissue-based systems are as follows:

- Authenticity, including identity of the system, e.g. provenance and confirmation of genotypic and/or phenotypic characteristics.
- Purity, e.g. freedom from biological contamination.
- Stability and functional integrity of the system in relation to its intended use.

The standardisation of in vitro systems begins with the original animal or human donor and the cells or tissues derived, and also embraces their subsequent manipulation, maintenance, and preservation. Standardisation is a difficult task, because cells and tissues are prone to change in culture and inevitably are subjected to physical and/or chemical insults during their isolation, culture, use and storage. However, by establishing a framework of procedures for factors that can be controlled, variation and other adverse effects on reproducibility and reliability can be minimised. The availability of well-characterised and quality-controlled stocks of cells and tissues, and of media and other critical reagents, further reduces variability.

Various classifications have been published, which define different types of in vitro cell and tissue systems (6). Three different broad categories will be considered in this guidance (see Fig. 1), namely:

- Isolated organs or tissues
- Primary and early passage cultures
- Cell lines (including finite, continuous and stem cell lines)

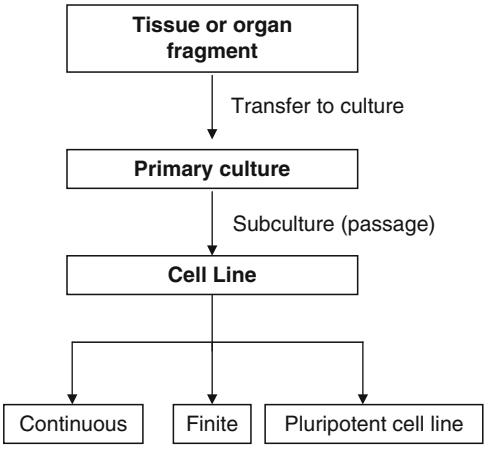

Fig. 1. Relationships between the main types of in vitro systems.

2.1.1. Cells and Tissues

2.1.1.1. Isolated Organs or Tissues

Isolated organs and tissues, taken for direct use from animal or human donors, are used for a wide variety of in vitro applications. These systems are difficult to standardise, because they often have complex environmental and nutritional needs, and because of variation between donors.

Tissues or organ fragments can be used in a variety of systems and devices. Such in vitro systems, including isolated skin and eye models, are very popular for toxicological applications, due to their similarity with the in vivo situation. It is important to be able to study an adequate number of replicates in such experiments, and one approach is to use slice technology. Ultra-thin slices of tissues, such as liver, lung, kidney or brain, can be used to provide a preparation retaining some of the structural and functional features of the original organ. Inevitably, however, such features tend to be rapidly lost.

Methods involving the isolation and reaggregation of cells from organs, such as skin, brain and liver, can lead to the reconstruction of three-dimensional structures, again with some of the structural and functional properties of the original organ or tissue.

Cells from blood and other body fluids are readily prepared as homogenous preparations, which are very useful for in vitro studies. Umbilical cord blood and bone marrow are rich sources of stem cells and have become the basis for expanding the range of other systems.

2.1.1.2. Primary Cultures and Early Passage Cultures

The initial in vitro culture of harvested cells and tissues taken directly from animals and humans is called *primary culture*. In many cases, such cultures also exhibit key characteristics similar to those seen in vivo, so they are widely used for basic research and for a number of in vitro applications.

Although cells in some primary cultures can proliferate and can be subcultured (as *early passage cultures*), they generally have a limited life span and are known to change their differentiated characteristics with time in culture. They commonly require complex nutrient media, supplemented with animal serum and other non-defined or ill-defined components, although serum-free medium formulations are becoming increasingly available. Primary cultures often represent heterogeneous cell populations, and are difficult to standardise and to reproduce, because of uncontrollable variations between preparations.

Primary cultures have traditionally been maintained either in suspension or, more commonly, as monolayers on glass or plastic surfaces. However, methods employing extracellular matrix components, and innovative techniques such the as co-culture of different cell types and three-dimensional culture, now offer much greater potential for maintaining differentiated structure and function.

2.1.1.3. Cell Lines

Cell lines comprise cells that are able to multiply for extended periods in vitro and can therefore be maintained by serial subculture. They can be subdivided into finite cell lines, continuous cell lines and stem cell lines.

Finite Cell Lines Finite cell lines are cultures of cells that possess the ability to be subcultured numerous times, but which eventually cease replication an d enter a state of senescence in which cell division has stopped, but the cells remain viable and may also retain some functional activity.

Finite cell lines have a useful life span in vitro and can be maintained as well-characterised and quality-controlled deposits in cell banks. However, changes occur as they approach senescence, so they should not be used above defined population doubling limits, which are established by experimental investigation.

Numerous finite cell lines have been established. Many of them are human diploid fibroblast cell lines, which are genetically stable and remain diploid for many passages, but which generally reach senescence after 60–70 population doublings.

Continuous Cell Lines Certain cell lines show an apparent ability to be subcultured indefinitely and are known as continuous cell lines. They do not show the senescence experienced with finite cell lines. Continuous cell lines are typically derived from tumours or normal embryonic tissues.

While many continuous cell lines have proven to be stable over long-term passage in vitro, they may undergo substantial and irreversible changes. It is therefore important to avoid subjecting cell lines to variable culture and passage conditions, and to establish cryopreserved stocks of early passage cells.

Some continuous cell lines can be a heterogeneous mixture of phenotypes (e.g. human promyelocytic HL-60 leukaemia cells, RD, SH5Y-SY). Other cell lines may undergo changes to the differentiation state due to culture conditions (e.g. when adherent cultures are allowed to reach confluency, such as CaCo-2, MDCK). In such cases, the potential for the selection of certain cell types as a result of in vitro maintenance, handling and preservation is a significant risk for in vitro cell-based methods.

Continuous cell lines may arise spontaneously or can be produced by using a variety of other methodologies, such as:

- Exposure of normal cells and tissues to irradiation and/or treatment with chemical mutagens or carcinogens.
- Isolation from cultures infected with viruses (e.g. Epstein–Barr virus).
- Genetic modification of cells by transfection with cloned genes (e.g. SV40 large T-antigen, adenovirus E1, telomerase).

Stem Cell Lines Stem cell lines retain the characteristics of stem cells and can produce a diverse series of differentiated cell types. They require great care in their maintenance, handling and preservation in order to ensure that their stem cell characteristics and capacity for differentiation are retained.

Embryonic stem cell lines are usually established and maintained on embryonic mouse fibroblasts or other feeder cell layers, which are critical to their successful culture. Although serum-free and feeder-free culture methods are currently being developed, the effects of these new developments on the stability and quality of the cultures have yet to be ascertained.

Standardisation for Specific Uses Standardisation of cell lines used for specialised studies and for production purposes will require attention to specific characteristics, as well as to the fundamental issues which apply to all cell cultures. They should be checked, and rechecked at appropriate times, for the expression of critical functions and markers (e.g. the pathways for biotransformation of xenobiotics, specific cytoskeletal markers, and characteristic morphology and ultrastructure). The number of passages for which they remain usable should be established.

2.1.2. In Vitro Culture Conditions

Cell and tissue culture environments differ in many respects from those found in vivo. Key elements of in vitro culture conditions include culture media, supplements and other additives, culture ware and incubation conditions.

2.1.2.1. Basal Medium

In vitro work is generally performed in complex nutritive media. Depending on the circumstances, the basal culture medium can be serum supplemented (as in traditional cell culture methods) or serum free, but supplemented with additives necessary for obtaining satisfactory cell proliferation and production, or for maintaining a desired differentiation status.

Many slightly different formulations exist under the same general medium names, and even subtle changes in the medium formulation can substantially alter the characteristics of certain cells and tissues. Therefore, the medium to be used should be precisely specified, and it is important to check that new supplies of medium meet the required specifications.

2.1.2.2. Serum

Serum is essential for the maintenance and/or proliferation of many cell types. It is a complex mixture of a large number of constituents, including low and high molecular weight biomolecules with a variety of physiologically balanced growth promoting and growth inhibiting activities. However, due to its complexity and batch-to-batch variation, serum introduces unknown variables into a culture system and can interfere with its performance.

Animal serum can be derived from adult, newborn or foetal sources. Bovine sera are the most commonly used, and during the last few decades, foetal bovine serum (FBS) has become the standard supplement for cell culture media. It is a cocktail of most of the factors required for cell proliferation and maintenance, and thus is an almost universal growth supplement.

Since the composition of serum is highly variable, it is important that, when an existing batch of serum is substantially depleted, a new set of serum batches should be evaluated in parallel with the current in-use batch. A range of growth promotion tests can be used for this purpose, one of the most convenient and most widely used of which is the plating efficiency test.

It may be also useful for individual users to define serum specifications that meet their particular needs, including the maximum acceptable levels of serum components, such as immunoglobulins (which may have inhibitory effects), endotoxins (indicative of bacterial contamination) and haemoglobin (indicative of haemolysis during clotting).

Animal sera are a potential source of microbiological contaminants, notably mycoplasma, bovine viruses and possibly the agent causing bovine spongiform encephalopathy (BSE). Suppliers use a variety of techniques, including filtration, irradiation and heat inactivation, to reduce microbial contamination. Nevertheless, it is wise, and for some applications, obligatory, to specify sourcing of serum from countries where there is a low risk of infection, and, in the case of bovine sera, from animals of less than 30 months old.

The use of human serum is restricted to specialised applications, as carries with it additional risks, such as the potential presence of human pathogenic viruses. Its use must be subject to the strictest quality controls, including documentation on origin and viral safety.

2.1.2.3. Alternatives to Serum

Because of the disadvantages inherent in the use of animal and human sera, there have been many attempts to find alternatives. These have included the use of poorly defined supplements (e.g. pituitary extracts, chick embryo extracts, bovine milk fractions, bovine colostrums) and various plant extracts (e.g. vegetal serum). In some cases, it is possible to use fully chemically defined media with appropriate hormones and growth factors. A compilation of commercially available serum-free media was published recently and can be found at http://www.focusonalternatives.org.uk.

2.1.2.4. Nutritional Status

The exhaustion or inactivation of essential nutrients in cell culture media, and rising levels of metabolites will inhibit cell growth and cell function, will ultimately cause cell death. Planning an appropriate programme for medium replenishment is therefore essential. This should also be considered when using conditioned medium from one culture in an attempt to promote the growth of another.

2.1.2.5. Antibiotics

It is important to remember that antibiotics are agents that arrest or disrupt fundamental aspects of cell biology, and, whilst being most effective against prokaryotic cells (i.e. bacteria), they are also capable of causing toxic responses in animal cells. Not surprisingly, antifungal agents, being directed at higher order, eukaryotic micro-organisms, are likely to be more toxic to animal cell cultures. Given these obvious contraindications, the use of antibiotics in cell and tissue culture should be focused in two areas: (1) protection of tissues, organs and primary cultures from contamination and (2) the positive selection of recombinant cell clones based on the expression of antibiotic resistance genes. In addition, it is important to obtain antibiotics from companies that are willing to provide certification for the concentration and purity of the antibiotics they supply.

Where possible, the use of antibiotics should be avoided. It should not become routine in the cell and tissue culture laboratory and can never be relied on as a substitute for effective aseptic techniques.

2.1.2.6. Cell Culture Surface/Matrix

The surfaces to be used for cell cultures may need to be pre-washed or pre-treated, e.g. to achieve the comprehensive wetting of a complex matrix. Where coating materials are used, washing before cell seeding may be necessary. There may be batch-to-batch variation in coatings of biological origin, so pre-use testing is essential.

2.1.3. Handling and Maintenance

Care should be taken not to expose the cells or tissues to inappropriate conditions (e.g. excessive time out of the incubator or cryostorage system). Key items of equipment, including incubators, laminar air flow and microbiological safety cabinets, and cryostorage systems, must be used by trained personnel only.

Aseptic techniques, where appropriate, should be rigorously applied. The routine isolation, handling and maintenance protocols for cells and tissues should be established as standard operating procedures (SOPs).

2.1.3.1. Temperature

The optimal culture temperature depends on the type of cells involved. Insect cells have an optimal growth temperature between 25 and 28°C and their growth characteristics may be altered at higher temperatures. The culture of mammalian cells at temperatures above 38°C may induce apoptosis, whilst growth at 34°C may slow replication but may also enhance the expression of certain cell proteins. Recombinant cell lines expressing the temperature-sensitive form of SV40 large T antigen will replicate at around 33°C, but not at 37°C.

2.1.3.2. Atmosphere

Oxygen and carbon dioxide are known to be vital for cell growth and variations in the levels of these gases can have significant effects on cell cultures. High levels of both gases will be toxic and

very low levels will inhibit cell growth and may result in cell death. Oxygen levels may need to be optimised for particular purposes, e.g. to promote growth in large-scale cultures in bioreactors. For most cell cultures, the appropriate atmosphere would be 5% v/v carbon dioxide in air.

2.1.3.3. pH

The optimal pH for cell culture is usually pH 7.4, and variation outside a relatively narrow pH range may have significant effects on cell phenotype, growth and viability.

2.1.3.4. Cell Detachment and Subculture

Detachment solutions, such as trypsin/EDTA, can have significant effects on cell cultures. Residual detachment solutions can lead to adverse effects, and therefore should be removed after cell dissociation.

Most cell lines are subcultured before they reach confluency. In some cases, cell differentiation occurs progressively after confluency is reached. The repeated passage of some cell lines after they have reached full confluency may result in the loss of desired characteristics. For example, the subculture regime can affect the productivity of recombinant cell lines and the differentiation capacity of Caco-2 cells.

2.1.4. Cryopreservation

Cells and tissues can be cryopreserved for limited or prolonged periods. The cryopreservation process includes freezing, storage and recovery. The following points must be considered:

- Cell or tissue type.
- Status of cells (differentiation, adherence).
- Growth phase (usually, cells should be harvested during exponential growth).
- Cryoprotectant (type and concentration, e.g. 10% v/v DMSO).
- Additives to improve cell survival (e.g. serum).
- Cooling rate (freezing at controlled rate in the presence of the selected cryoprotectant).
- Storage conditions (temperature, liquid nitrogen vapour or liquid phase).
- Recovery method (e.g. rate of thawing, gradual dilution to minimise osmotic shock and replacement of cryoprotectant).

Storage in the liquid phase of nitrogen provides the lowest, most stable and most convenient storage temperature, but vapour phase storage is generally considered to be safer. Electrical storage systems provide a very practical and maintenance-free, low temperature storage solution. However, in a multi-user environment, such systems are prone to the effects of temperature fluctuations in stored material, and in the absence of liquid nitrogen or carbon dioxide back-up systems, they are at high risk in the event of loss of power supply.

The failure of liquid nitrogen refilling procedures can result in the loss of valuable cells and tissues, so it is vital that there are effective training and monitoring procedures for the filling and maintenance of liquid nitrogen containers. In addition, it is advisable to store aliquots of important stocks at more than one storage site.

2.1.5. Microbial, Viral and Cellular Cross-Contamination

Contamination with bacteria, yeast and other fungi can result in the complete loss of cultures. Undetected contamination with slow growing micro-organisms, or with micro-organisms resistant to antibiotics, can have a significant impact on the quality and/or validity of data obtained from in vitro systems. The most common example of such an infection is mycoplasma.

There are various potential sources of viral contamination, including the operator, cell culture reagents of animal origin and the cells or tissues of origin. All cell and tissue culture facilities should therefore have appropriate measures for detecting and minimising the risk of the microbial and viral infections.

Viruses can cause lytic infections, thus destroying the host cells, but may also become established as persistent, sub-lethal infections, which are maintained with passage of the host cell line. Many cells lines both carry and express viral gene sequences. In a small number of cases, infectious human pathogens are released into the culture medium (e.g. Epstein–Barr virus from the NAMALWA cell line and human T-lymphotrophic virus II from MT4 cells). Animal viruses are expressed by some cell lines (e.g. bovine viral diarrhoea virus in bovine cell lines). Mammalian genomes contain many retrovirus-like sequences, which, whilst not overtly infectious, may be released in large quantities as retrovirus-like particles in murine myeloma cells, hybridomas and other cell lines (e.g. CHO cells and BHK cells). The expression of such virus-like sequences is also observed at the mRNA level in many human cancer cell lines and other primate cell lines.

Cross-contamination of cell lines with other cell lines is a real, but often neglected, problem. Whenever possible, cells should be obtained from certified sources and appropriate procedures should be applied to minimise the risk of cross-contamination during their storage and use in the laboratory.

2.2. Second GCCP Principle

Assurance of the quality of all materials and methods, and of their use and application, in order to maintain the integrity, validity and reproducibility of any work conducted.

The aim of quality assurance is to confirm the consistency, traceability and reproducibility of in vitro cell and tissue work. Each laboratory should have designated persons to oversee the quality assurance of:

- The cells and tissues.
- All other materials.

- The methods, protocols and SOPs.
- The equipment and its maintenance.
- The recording procedures.
- The expression of results.

2.2.1. Cells and Tissues

A laboratory should have specific protocols and SOPs for the receipt of new or incoming cells and tissues, and for the handling, maintenance and storage and of all cells and tissues, with regular monitoring for compliance. The following are among the factors to be considered:

- Authenticity.
- Morphological appearance.
- Viability.
- Growth rate.
- Passage number and/or population doublings.
- Functionality.
- Differentiation state.
- Performance controls specific to the application.
- Contamination and cross-contamination.

2.2.2. Other Materials and In Vitro Culture Conditions

The quality control of media, supplements and additives is both time consuming and expensive. Since most of these materials are obtained commercially, the supplier should be expected to operate according to standards appropriate to their supply and use, and to provide the relevant quality control documentation.

The user laboratory has the responsibility:

- To confirm that all the materials to be used are suitable for their intended purposes.
- To ensure that all materials are appropriately handled, stored and used.
- To monitor batches of materials with regard to changes or variations which may affect their use (for certain critical reagents, e.g. serum, pre-use testing may be necessary).

In the case of critical reagents, the manufacturer cannot be expected to know the user's specific requirements. The user should therefore define a specification to include general details of the reagent, such as quality controls for identity, purity and activity and stability. Where relevant, the specification should include compliance with international standards (such as ISO standards or pharmacopoeial protocols).

All other working materials that come in direct or indirect contact with cell and tissue cultures should be regularly monitored and appropriate procedures should be in place for ensuring

the quality of culture vessels and surface coatings, the cleanliness and sterility of any re-used equipment (e.g. glassware) and lack of toxicity (e.g. plastic and rubber components).

Appropriate procedures are necessary for the purchase, installation, commissioning, correct use, performance monitoring (e.g. calibration) and maintenance of the following:

- Low temperature storage refrigerators.
- Incubators.
- Laminar air flow and safety cabinets, and other sterile work areas.
- Automatic pipettes and pipettors.
- Sterilisation ovens and autoclaves.
- Analytical and production equipment.

2.3. Third GCCP Principle

Documentation of the information necessary to track the materials and methods used, and to permit the repetition of the work and report the information required to enable the target audience to understand and evaluate the work.

In cell and tissue culture, as in any practical science, clear documentation of the systems used and procedures followed is mandatory, in order to permit the traceability, interpretation and repetition of the work. Therefore, accurate records of cell type, origin, authentication and characterisation, and of the materials used and the culture techniques performed, are essential.

The documentation should be retrievable and should include:

- The objective of the work.
- The rationale for the choice of procedures and materials used.
- The materials and equipment used.
- The origin and characterisation of the cells and/or tissues.
- The laboratory records, including results, raw data and quality control records.
- Cell and tissue preservation and storage procedures.
- The protocols and SOPs used, and any deviations from them.

In some circumstances, e.g. where compliance with GLP or GMP is required, there should be formal procedures for retrieval and review, and for resolving any questions or disputes that may arise.

2.3.1. Origins of Cells and Tissues

A minimal set of information is essential when working with cells (primary or cell lines) or tissues of animal or human origin such as (if applicable) source, species/strain, sex, age, number of donors, health status, any special pre-treatment, organ/tissue of

origin, cell type(s) isolated, isolation technique, date of isolation, operator, supplier, material transfer agreement, medical history of donor, pathogen testing, shipping conditions, state of material on arrival, cell line identification and authentication and mycoplasma testing.

2.3.2. Handling, Maintenance and Storage

It is essential that records should be kept on the following:

- Culture media (including all supplements and additives) and other solutions and reagents (including details of supplier, batch, storage requirements, expiry date), and methods of preparation (these may be specified in SOPs for research and development work, but the traceability of each procedure to ensure the use of appropriate reagents may be required, in line with other specific quality standards).
- Culture substrate (type and supplier of coating material [e.g. collagen, fibronectin, laminin, poly-D-lysine], basal membrane [e.g. Matrigel®]) and recording of the coating procedures, where applicable.
- Procedures for preparation or use of cells or tissues.

The records on handling, maintenance and storage related to cultureware and equipment should include:

- Type and origin of culture ware (types and suppliers of flasks, Petri dishes, t-flasks, roller bottles, etc.).
- Laminar air flow and safety cabinet testing, calibration, maintenance and repair.
- Monitoring of humidity (if appropriate), temperature and CO2 levels in incubators.
- Monitoring of refrigerator and freezer temperatures.
- Monitoring of liquid nitrogen level and/or temperature in storage containers.
- Sterility controls (e.g. autoclaving, sterility tests).
- Regular maintenance and calibration of all other critical apparatus (according to manufacturers' manuals).

With regard to the in vitro system, critical information must be recorded to permit tracing of the history of the biological material, its characteristics and the treatments, manipulations, measurements and procedures applied to it, including statistical procedures used to analyse the results obtained.

Cell and tissue preservation and storage details should include (but not be limited to) the following:

- Type of cell or tissue and passage/identity number.
- Cryoprotectant used and its concentration.
- Number of cells and volume per cryovial.

- Position in container.
- Viability and plating efficiency after thawing.
- Date and operator.

Any changes in storage location should be formally recorded and, when appropriate, relevant notification should be given (e.g. to the owner, safety officer or quality control personnel).

The disposal procedures for culture laboratory waste (used solutions, toxic treatments, biological materials, etc.) must be documented and compliance with them should be ensured.

Examples of requirements for documentation concerning the handling, maintenance and storage of cells (primary or cell lines) and tissues animal or hum (if applicable): ethics, morphology, histopathology, quarantine, purity of isolation, phenotype, state of differentiation, type of culture, culture medium, feeding cycles, growth and survival characteristics, initial passage number, confluency at subculture, induction of differentiation, identification and authentication, ageing, mycoplasma testing.

2.3.3. Reporting

Effective communication is an essential part of cell and tissue culture work, so careful attention should be given to the reporting procedures used.

The format of a report will depend on the target audience, e.g. in-house personnel, a client or sponsor, a regulatory body, the scientific community or the general public. The person(s) responsible for the report should be identified. Where appropriate, the report should be formally authorised for its intended purpose.

A high-quality scientific report should cover the objective of the work, the protocols and SOPs used, planning and experimental design, the execution of the study, data collection and analysis and a discussion of the outcome.

It should also be made clear that the whole study was established and performed in accordance with any relevant standards, regulations, statutes, guidelines or guidance documents, and safety and quality assurance procedures.

When submitting the report of the cell and tissue culture work, a minimum set of information should be included, which covers the origins of the cells, the characterisation, maintenance and handling of the cells and the procedures used. A statement of compliance with the GCCP principles should also be included.

Details to be included in papers for publication in journals are as follows: type of culture, cell/tissue type, species, origin, catalogue/product number, basic culture medium, serum, antibiotics, other additives, complete medium, frequency of medium change, type of culture plates/flasks, surface coating, subculture frequency, subculture split ratio, detachment solution, usable passage range, passage number at use, maintenance conditions, storage conditions.

2.4. Fourth GCCP Principle

Establishment and maintenance of adequate measures to protect individuals and the environment from any potential hazards.

National and local laws, based on moral and ethical principles, govern safety in the workplace in most countries. Many countries also issue guidelines on occupational health and laboratory safety, and individual laboratories may also have rules which reflect local circumstances. Thus, the guidance on safety in the cell culture laboratory given here in no respect replaces these laws and regulations, but rather draws attention to certain aspects of them and highlights issues specific to the in vitro culture of animal and human cells and tissues.

Identifying and evaluating risks, and taking appropriate action to avoid or minimise them, are the foundations on which safety is built (11). In the work environment, and particularly in the laboratory, where hazards may be complex and their evaluation requires specialist knowledge, risk assessment should be performed in a structured way. Furthermore, the results of such risk assessments should be recorded not only to confirm that they have been carried out and appropriate action taken, but also to act as a reference document for individuals performing the tasks assessed. These assessments should be reviewed at regular intervals to take into account any changes in local practice, national or international regulations, or increases in scientific knowledge.

It is important to pay particular attention to risks, which may be specific to, or more significant in, certain groups of workers. For example, where there is the possibility that women of reproductive age may carry an undiagnosed pregnancy and would be at greater risk from the effects of certain chemicals, such as teratogens or biological agents, and persons with a diminished immune response (e.g. due to medication or to a medical condition) should seek expert medical advice before they are allowed to work in a laboratory where cell and tissue culture is performed.

The safety conditions highlighted below relate not only to the safety of individual cell and tissue culture workers, but also to that of their colleagues, the general public and the environment.

All personnel must be made aware of the potential hazards associated with their work and must be trained in the designated safety procedures, as well as in the appropriate use of the safety equipment required (including personal protective equipment) and the appropriate handling of spills.

Risk assessment should be carried out under the following headings, but should not be limited to them, depending on the circumstances:

- Facilities (e.g. laboratories, offices, storage and sanitation): For example, are they appropriate and adequate for the intended use, well maintained and properly heated/ventilated?

- Security: Depending on the work, are special security precautions required (e.g. for restricted access to site/laboratories and for removal of hazardous material from the site)?
- Health and safety of staff: Is the health and safety monitoring of staff regularly carried out and documented?
- Laboratory equipment: Is the equipment used certified as sufficiently safe for its specific and intended purpose?
- Infectious/biohazardous materials: Are hazard classification, receipt, processing, containment, storage and disposal conducted correctly, with use of the appropriate protective ware, clothing and other precautions?
- Chemicals and radioactive substances: Are the receipt, handling, storage and disposal of hazardous materials (e.g. toxic compounds, flammable liquids) conducted according to the correct procedures?
- Hazard prevention: Are appropriate hazard prevention plans established, are staff regularly trained in these procedures (e.g. fire evacuations) and are they applied correctly.
- Waste disposal: Is a waste management procedure established that ensures prompt and safe removal from the clean cell culture areas followed by disposal according to approved procedures?

Typical precautions to be used to ensure operator safety when handling cells and tissues

- Hands should be washed or disinfected before and after handling cells.
- An appropriate gown or laboratory coat should be worn, to be put on when entering the laboratory and removed when leaving it.
- Personal accessories (e.g. rings, watches), which might compromise cell and tissue culture activities, should be removed or covered up to prevent contamination.
- If appropriate, gloves should be worn, and replaced immediately if torn or punctured.
- When handling cell and tissue cultures, workers must avoid transferring contamination on the hands from the culture work to unprotected body parts (e.g. eyes or mouth), clothing or items in the open laboratory environment.
- As far as reasonably practicable, all cell and tissue work should be performed in a Class II cabinet or other appropriate (micro) biological safety cabinet. NB: Certain cabinets, such as horizontal flow cabinets, protect the cells and tissues, but not the user or the general environment.

- Mouth pipetting must be strictly prohibited.
- All procedures should be undertaken by using methods that minimise the production of aerosols that might spread contamination by micro-organisms or cells.
- All disinfectants used should be effective and appropriate for the work.
- All work surfaces should be cleaned with an appropriate disinfectant (e.g. 70% ethanol), before and after use.
- The use of sharps should be avoided as far as is possible. Any used sharps should be disposed of safely according to approved procedures.
- All cultures should be clearly and unambiguously labelled.

2.4.1. Hazards Related to Cell and Tissue Culture Work

Hazards can be categorised into three main groups: physical hazards, chemical hazards and biological hazards. A risk assessment plan should consider all these hazards in relation to the proposed work. Risk assessment is not only limited to the laboratory and laboratory personnel, but also to people in the entire facility, people in the external environment and to the environment itself. This is not only a vital aspect of basic research and testing, but is particularly important when cultured cells and tissues are used for diagnostic purposes or for producing therapeutic products, or when the cells and tissues themselves are used for therapeutic purposes.

2.4.1.1. Physical Hazards

The cell and tissue culture laboratory does not pose any specific physical hazards. However, laboratories and workspaces should always be kept clean and tidy, and free of material stored on the floor or anywhere where it can cause risk to other people. Any equipment or apparatus used should meet national safety guidelines. Equipment such as autoclaves and laminar flow or microbiological safety cabinets should have a programme of maintenance for safe use, usually carried out at a minimum frequency of once a year. The correct operation of equipment should also be regularly checked. Procedures should be in place for ensuring the safest possible use of equipment connected with ultraviolet light, liquid nitrogen and pressurised gases.

2.4.1.2. Chemical Hazards

The cell and tissue culture laboratory is not a particularly dangerous place to work with regard to chemical hazards. However, some chemicals have ill-defined or unknown biological effects, so general safety standards should always be maintained to protect workers against these uncertain hazards. Material Safety Data Sheets for all chemicals used in the laboratory should be requested from the suppliers. For any substances which are potentially hazardous to health (e.g. mutagens, cryoprotectants and labelling dyes),

these data should form the basis of a risk assessment for the use of this chemical, as the level of risk will vary, depending on, for example, the quantities being used and the techniques being employed. This is covered by national legislation in some countries. Correct waste disposal procedures should always be followed.

Materials being tested in in vitro toxicity tests represent a particular problem, particularly if the study requires that they be coded and supplied via an independent, external source. Although the concentrations used in the final test solutions may be very low, the storage of the bulk material and its handling can represent a significant potential risk. It should always be possible to break the code in the event of an accident. Particular care should be taken with certain kinds of materials, such as when women of reproductive age may be exposed to teratogenic test materials during an in vitro reproductive toxicity study.

2.4.1.3. Biological Hazards

Many different issues related to potential biological hazards must be considered and, in certain cases, monitored in the cell and tissue culture laboratory.

Risk assessments should address issues that could arise from the species of origin, the health status of donor, the available data from microbiological screening tests and the culture and storage history. Although not usually dangerous to the user, cells and tissues have the potential to permit the replication of viruses potentially pathogenic to humans and should therefore be routinely treated as if they are a potential health risk.

All cells and tissues new to the laboratory should be handled under a strict quarantine procedure, including suitable precautions to prevent the spread of potential contamination with additional controls, as necessary (e.g. use of separate dedicated media and equipment, and work by dedicated staff). It is not advisable to use horizontal laminar flow cabinets when handling cells, as such cabinets are designed to protect only the work area and the air flow is directed toward the user.

Where the nature of the work means that there is a significant risk of biological hazard, special precautions must be taken in accordance with national requirements, most of which, where infectious organisms are concerned, are based on the WHO classification for human pathogens.

If the cells or tissues originate from a certified source, such as a recognised cell bank, which provides certification of freedom from certain contaminants, this documentation may suffice for risk assessment, provided that the cells have not been exposed to potential sources of contamination since leaving the bank. However, it is recommended that, as a minimum and where advisable, mycoplasma testing should be carried out on all samples received.

Due to the risk that the operators' immune systems may not protect them against, for example, the tumourigenic growth of their own cells which may have been altered via the in vitro procedures (e.g. by transformation, immortalisation, infection or genetic modification), most national guidelines make it unacceptable for operators to culture cells or tissues derived from themselves or from other workers in the same laboratory, nor to genetically manipulate such cells or tissues, or treat them with potentially pathogenic organisms.

Many countries have national safety committees, which establish guidelines for work with genetically modified organisms (GMOs) and help and require scientists to classify and perform their work at the appropriate biosafety level. Recombinant cells (i.e. those produced by genetic engineering or genetic modification [terms used to cover most techniques used to artificially alter the genetic make-up of an organism by mixing the nucleic acids of different genes and/or species together]) will generally fall within the requirements of such guidelines. The classification and control of this kind of work differs between countries, and countries may decide to classify work at a higher or lower level when new information on a particular vector/host system becomes available.

Risk assessment is clearly a dynamic process and has to take into account new developments and the progress of science. It is the responsibility of the scientists involved to keep up to date with developments in this expanding field of activity and at all times to respect national and international guidelines and requirements.

2.4.2. Risk to the Environment

Risks to the environment are generally due to poor waste disposal, leading to contamination of water, air or soil, or the escape from containment of hazardous materials. The environment can also be contaminated by release of biological material due to accidents, including transport accidents, and systems should be put in place either to prevent or minimise the potential for such damage.

2.4.2.1. Waste Disposal

Methods of waste disposal appropriate to the work in hand must be identified during the risk assessment process. These methods must protect not only the individual tissue culture workers themselves, but also their colleagues, the wider population and the environment. Work with known pathogens and GMOs must be performed according to the relevant regulations (see above), including methods of waste disposal. Where methods are not specified in these regulations, there is a requirement to assess and justify all proposed methods of waste disposal as part of the risk assessment. Similarly, the appropriate method of disposal of hazardous chemicals must be identified before work with them is undertaken.

In line with the precautionary principle, the following minimum precautions should be taken when disposing of waste from the cell culture laboratory:

- All liquid waste, with the exception of sterile media or solutions, should be either chemically inactivated (e.g. by using sodium hypochlorite or another disinfectant) or autoclaved before disposal.
- All solid waste should either be autoclaved before leaving the laboratory or should be placed in rigid, leak-proof containers before being transported elsewhere for autoclaving or incineration.

2.4.2.2. Transport

The transportation of any biological materials, chemicals (including liquid nitrogen) or other materials (e.g. dry ice) of potential risk to humans, animals, plants and/or the environment must comply with national or international regulations (http://www.iata.org/whatwedo/dangerous_goods). They should be packed so as to prevent spills in the case of breakage, be correctly labelled (with appropriate hazard symbols) and have the appropriate accompanying documentation (e.g. materials safety data sheet, import form, export form and CITES permit, if applicable). Where appropriate, the International Air Transport Association (IATA) guidelines should be followed, as they are stringent and are recognised internationally. Before arranging transport, the various legal requirements for export and import into the recipient country should be considered, including ethical issues (e.g. the use of human cells or tissues of embryonic origin), disease transmission, endangered species regulations and bioterrorism regulations.

Biological material is usually classified for shipping purposes as:

- Diagnostic specimens
- Infectious specimens
- Biological products
- GMOs

2.5. Principle 5: Compliance with Relevant Laws and Regulations, and with Ethical Principles

From an ethical and legal point of view, it is desirable that high standards for cell and tissue culture should be established and maintained worldwide, so that accountability, safety and ethical acceptability can be universally guaranteed, insofar as that it is reasonably practicable. The ethical and associated legal issues raised are extremely complex and beyond the scope of these GCCP guidelines. However, all concerned should maintain a sufficient level of awareness of the ethical issues related to cell and tissue culture work, and of public opinion and the relevant legislation at the national and international levels.

At present, there are no ethical guidelines relating specifically to general cell culture practices, but various guidelines, regulations and laws are in place for dealing with cells and tissues of specific origin and/or use.

Before any studies are initiated, matters of ethical significance must be carefully considered. These can be subdivided, from a GCCP point of view, into general ethical considerations and more-specific considerations.

From a general perspective, good practice leads to data of high value, in turn leading to less waste of effort and greater confidence in the outcome of the study, to the benefit of all concerned, including the general public.

The more-specific considerations include the ethical implications of using material of animal and human origin, and GMOs.

2.5.1. Laws and Regulations

At present, there are no international laws specifically governing cell and tissue culture practices. However, any work involving animal or human pathogens has to be performed in compliance with national and international requirements. Some countries have, or are preparing, legislation or regulations to control specific areas, such as the use of material of human origin. New controls are also being drafted in response to the challenges and opportunities presented by transplantation, regenerative medicine, stem cell research and GMOs. Ownership of cell lines and patents must also be dealt with appropriately and special conditions may apply where cell cultures are involved (7). In addition, there are international agreements relating to the provision of organisms and cell cultures that may be used for bioterrorism.

2.5.2. The Use of Animal Material

In general, any work involving animal material should be in compliance with local and national legislation on animal experimentation and the Three Rs (reduction, refinement and replacement) principles of Russell and Burch (8). In addition, other ethical issues may arise in certain circumstances. Examples include the use of cells derived from endangered species (http://www.cites.org/), the production of monoclonal antibodies by the ascites method (see *References: Monoclonal antibodies and ethics*) and the pre-treatment of animals with chemical inducers to provide cells for culture with specific biochemical properties (e.g. hepatocytes with elevated CYP450 enzyme levels).

In order to minimise pain and distress, donor animals should be handled according to the appropriate and approved procedures. As foetuses of many mammalian species can already feel pain long before birth (8), they should also be treated with the utmost care, again according to appropriate procedures.

Serum, and especially FBS, is a commonly used component of animal cell culture media. It is harvested from bovine foetuses taken from pregnant cows during slaughter. Here again, the current practice of foetal blood harvesting poses ethical problems (blood is usually taken via cardiac puncture, without any form of anaesthetic (9,10)). Efforts are being made to reduce the use of animal serum and, where possible, to replace it with synthetic

alternatives. A wide range of other cell culture materials derived from animals (e.g. tissue extracts, extracellular matrix materials) also raise ethical concerns.

Legal issues can also arise if animal-derived cells and tissues are found to be infected with viruses which could infect wildlife or species of agricultural importance. For this reason, the discovery of certain viruses in cells and tissues may need to be notified to the relevant authorities and appropriate action taken.

2.5.3. The Use of Human Material

The use of human biological material is critical for medical research. It is particularly important that researchers are aware of the need to handle such material in a responsible manner and in accordance with local and national requirements.

Those involved with the procurement, supply and use of human biological material should maintain proper records to ensure appropriate traceability and control of the applications of the material in ways which are consistent with the nature of the consent given by, or on behalf of, the donor. All use of human tissue should be approved by the appropriate ethics committee and copies of such approvals should be kept for reference. Where samples are provided to third parties, the custodian is responsible for the safe keeping of the code which enables samples to be linked to individual donors, where appropriate and when necessary.

Human material is usually procured either from specialised cell and tissue banks or from hospitals (11). Currently, most of the banks are run on a not-for-profit basis. Nevertheless, some of them have been set up by private industries, particularly for the production of engineered tissues. This raises serious ethical concerns (including the transfer of human material for profit), and has not yet been dealt with adequately at the national level in most countries or internationally.

Confidentiality with respect to the provision and use of human tissue is governed both by law and by professional guidelines. A legal requirement in most countries is that, when dealing with human material, informed consent must be sought either from the donor or from the donor's family.

Human tissue banks should be recognised as the most legally and ethically acceptable approach to the procurement and distribution of donated non-transplantable human tissue for research, as they are best equipped to deal with, and advise on, the complex issues involved, including ethics, consent, safety and logistics as well as scientific questions.

The removal of blood samples from human volunteers should only be performed by qualified personnel and particular precautions should be followed to minimise any risks. Such volunteers should also be considered to be donors and some form of documented informed consent will be required.

The use of human stem cells involves serious ethical questions, because of their origins and their potential uses. This is a relatively new research area, and, while some countries already have strict controls, other countries are currently considering what laws and regulations should be introduced in the public interest.

The procurement of stem cells from early embryos and foetuses is a particularly sensitive issue, because of the circumstances in which such embryos and foetuses become available. Stem cells can also be obtained from adult tissues and from umbilical cord blood, where the ethical considerations to be taken into account are similar to those involved in obtaining other human tissues, but it is the use of the stem cells which requires effective regulation.

Before any human material is used for the establishment of a new cell line, ethical approval should be obtained from the relevant authority.

2.5.4. Genetically Modified Cells

The creation, storage, transport, use and disposal of genetically engineered cells are currently subject to the requirements that apply to GMOs. This is a rapidly expanding field and its long-term consequences are as yet unknown. It involves manipulating genes and cells in ways that do not occur in nature, and for this reason, it raises sensitive ethical issues. The above activities are regulated in many countries, where, before any work is initiated, relevant approval must be sought.

2.6. Principle 6: Provision of Relevant and Adequate Education and Training for all Personnel to Promote High Quality of In Vitro Work and Safety

The range of applications for cell culture is expanding rapidly and involves an ever-broadening range of technical manipulations (e.g. chemically induced and genetic modifications) for use in basic and applied science, manufacturing, diagnosis, and efficacy and safety testing procedures as well as for providing therapeutic materials.

The competence of staff to perform their duties in a laboratory is central to ensuring that work is performed according to the standards of the organisation in relation to its scientific, legal and safety requirements and obligations. This requires education and training as well as the regular monitoring of performance.

A good basic education should be given in the nature and purposes of cell and tissue culture which is an essential basis for any future training programme. The basic principles of in vitro work, aseptic technique, cell and tissue handling, microscopy, basic culture procedures (cell viability testing, cell counting, subculturing etc), quality assurance, use and maintenance of all equipment, laboratory safety, waste disposal and ethics should be included. It is also important that those working with material of animal or human origin should have a sufficient understanding of any additional laws or regulations that will apply.

Much of the training required may best be given on a one-to-one basis in the laboratory. However, there are a number of

principles that can be covered in organised courses that may involve participants from more than one laboratory.

Training should be seen as an ongoing process for improving and developing practical skills and maintaining competence. Given its critical importance to the success of any laboratory work, there should be a formally documented training and development programme for all members of staff, including training records and regular reviews of training needs.

When new staff join a laboratory staff, their skills and experience should be assessed, and the need for further training procedures in relation to their new jobs should be identified. These needs may include a variety of general and specific procedures, covering SOPs, general laboratory maintenance, and safety and emergency procedures.

Training can be provided in-house by experienced members of staff and/or visiting experts via accredited on-line programmes and/or through attendance at external courses. For certain applications including product manufacture and testing, and processing of cells and tissues for clinical use, training must be formally recorded and reviewed.

Acknowledgements

The authors would like to thank GCCP Task Force: Balls M, Bowe G, Davis J, Gstraunthaler G, Hartung T, Hay R, Merten OW, Schechtman L, Stacey G. and Stokes W. for their contribution.

References

1. Coecke S, Balls M, Bowe G, Davis J, Gstraunthaler G, Hartung T, Hay R, Merten OW, Price A, Schechtman L, Stacey G, Stokes W (2005) Guidance on good cell culture practice. Altern Lab Anim 33:261–287
2. Hartung T, Gstraunthaler G, Balls M (2000) Bologna statement on good cell culture practice (GCCP). ALTEX 17:38–39
3. OECD (2004) Organisation for Economic Co-operation and Development series on Principles of Good Laboratory Practice and Compliance Monitoring. Number 14. Advisory Document of the Working Group on Good Laboratory Practice: The Application of the Principles of GLP to in vitro Studies, OECD Environmental Health and Safety Publications, Environment Directorate: ENV/JM/MONO(2004)26. Paris, France: OECD
4. OECD (2004) Draft Advisory Document of the OECD Working Group on GLP on the Application of GLP Principles to In Vitro Studies. 18pp. Paris, France: OECD
5. Gupta K, Rispin A, Stitzel K, Coecke S, Harbell J (2005) Ensuring quality of in vitro alternative test methods: issues and answers. Regul Toxicol Pharmacol 43:219–224
6. Schaeffer WI (1990) Terminology associated with cell, tissue and organ culture, molecular biology and molecular genetics. In Vitro Cell Dev Biol 26:97–101
7. Russell WMS, Burch RL (1959) The principles of humane experimental technique. London, Methuen, p 238pp
8. van der Valk J, Mellor D, Brands R, Fischer R, Gruber F, Gstraunthaler G, Hellebrekers L, Hyllner J, Jonker FH, Prieto P, Thalen M,

Baumans V (2004) The humane collection of fetal bovine serum and possibilities for serum-free cell and tissue culture. Toxicol In Vitro 18:1–12

9. Jochems CEA, van der Valk JBF, Stafleu FR, Baumans V (2002) The use of fetal bovine serum: ethical or scientific problem? Altern Lab Anim 30:219–227
10. Anderson R, O'Hare M, Balls M, Brady M, Brahams D, Burt A, Chesné C, Combes RD, Dennison A, Garthoff B, Hawskworth G, Kalter E, Lechat A, Mayer D, Rogiers V, Sladowski D, Southee J, Trafford J, van der Valk J, van Zeller A-M (1998) The availability of human tissue for biomedical research. The report and recommendations of ECVAM workshop 32. Altern Lab Anim 26:763–777
11. Jones BPC (1998) Laboratory practice. In: Stacey G, Doyle A, Hambleton P (eds) Safety cell and tissue culture. Kluwer Academic, Dordrecht, The Netherlands, pp 64–86

Chapter 2

Induced Pluripotent Stem Cells (iPSCs): An Emerging Model System for the Study of Human Neurotoxicology

M. Diana Neely, Andrew M. Tidball, Asad A. Aboud, Kevin C. Ess, and Aaron B. Bowman

Abstract

This chapter describes the materials and methods necessary to generate human induced pluripotent stem cells (iPSCs) from primary human fibroblasts and direct their differentiation into neural progenitor cells. Application of such methods is an emerging model for the study of neurotoxicity focused on human neurons and glia derived from specific patients. The techniques described here include primary human fibroblast culture, lentiviral/retroviral-mediated iPSC inductions, iPSC clonal expansion and maintenance, validation of pluripotency markers, and neuronal differentiation of iPSCs. Methods and applications using iPSCs are rapidly changing: here we describe the current methods used in our laboratories. The iPSC induction method featured in this chapter is based on a two-step viral transduction approach described by Dr. Shinya Yamanaka and colleagues (Cell 131:861–872, 2007) modified following the protocol of Dr. Sheng Ding and collaborators (Nat Methods 6:805–808, 2009). The neuralization method featured in this chapter is based on the method described by Lorenz Studer and colleagues (Nat Biotechnol 27:275–280, 2009). Maintenance and cryostorage methods were developed in our lab by optimizing a combination of approaches described in the literature. This chapter is not meant to be comprehensive, but instead focuses on the core competencies needed to begin working with human iPSCs and neuralization of these cells for toxicological studies.

Key words: Induced pluripotent stem cells, Human models of neurotoxicity, Neuronal differentiation, Patient-derived fibroblasts

1. Introduction

A major breakthrough was announced in 2007 by two independent labs, headed by Drs. Shinya Yamanaka and James Thomson, reporting the generation of human induced pluripotent stem cells (iPSCs) from adult human dermal cells with a developmental potential seemingly equivalent to human embryonic stem cells (hES cells) (1, 2). iPSCs can generate cells from all three embryonic germ layers, and thus are very similar to hES cells (1–3). Because of these traits,

Michael Aschner et al. (eds.), *Cell Culture Techniques*, Neuromethods, vol. 56,
DOI 10.1007/978-1-61779-077-5_2, © Springer Science+Business Media, LLC 2011

iPSCs open a new and exciting branch of human stem cell based toxicological and disease research. The study of neurotoxicology represents an almost ideal application of this technology given the complexities of Human diseases with diverse genetic and environmental risk factors. Furthermore, the ability to differentiate neurons and glia from patient iPSCs offers a chance to examine in detail changes in both the development and maintenance of neural function resulting from complex genetic inheritance patterns. Finally, the relative ease to expand, maintain, culture, and differentiate iPSCs will enable utilization of this resource by a broader range of laboratories around the world, expanding both the scope and depth of research into human disease.

Environmental stressors are thought to interact with an individual's genetic makeup to influence or cause neurological disease. These toxicological actions may occur at any point during development as well as later during adulthood. The multigenic inheritance pattern of environmental susceptibility makes it difficult to evaluate the risk that environmental agents pose for specific diseases or persons. The advent of iPSC technology will enable researchers to generate in vitro cultures of patient-specific neurons to assess patient-specific susceptibility to neurotoxicants. This technology opens the opportunity to characterize the cellular, physiological, pharmacological, and molecular properties of living human neurons with identical genetic determinants as individuals with neurological disease (Fig. 1). Furthermore, if a comprehensive clinical history of the patients is known, iPSC-based studies can compare patient populations showing sensitivity to particular environmental agents, divergent clinical outcomes, and differing co-morbidities. Thus, iPSC technology has the potential to revolutionize scientific approaches to human health.

The application of human pluripotent stem cell technology to toxicological risk assessment posits that cells differentiated from patient-derived stem cells will model the toxicant sensitivity of the patient's own cells. A number of technical and theoretical hurdles need to be overcome before the utility of this approach can be realized. For example, efficiency and consistency of stem cell derivation; contribution of epigenetic changes; and protocols for differentiation, exposure paradigms, and assessment of toxicity need to be optimized. Perhaps though the most fundamental issue that must be addressed soon is whether the methods for generating patient-derived pluripotent stem cells are capable of yielding a consistent model of sensitivity to environmental toxicants. Several groups, including our own, are currently performing research and development to validate iPSCs as a model of human toxicological risk.

This chapter describes current methods to generate and validate iPSCs using the basic method developed by Yamanaka and colleagues of lentiviral transduction of fibroblasts to allow expression of the mouse retroviral receptor, *Slc7a1,* followed by mouse

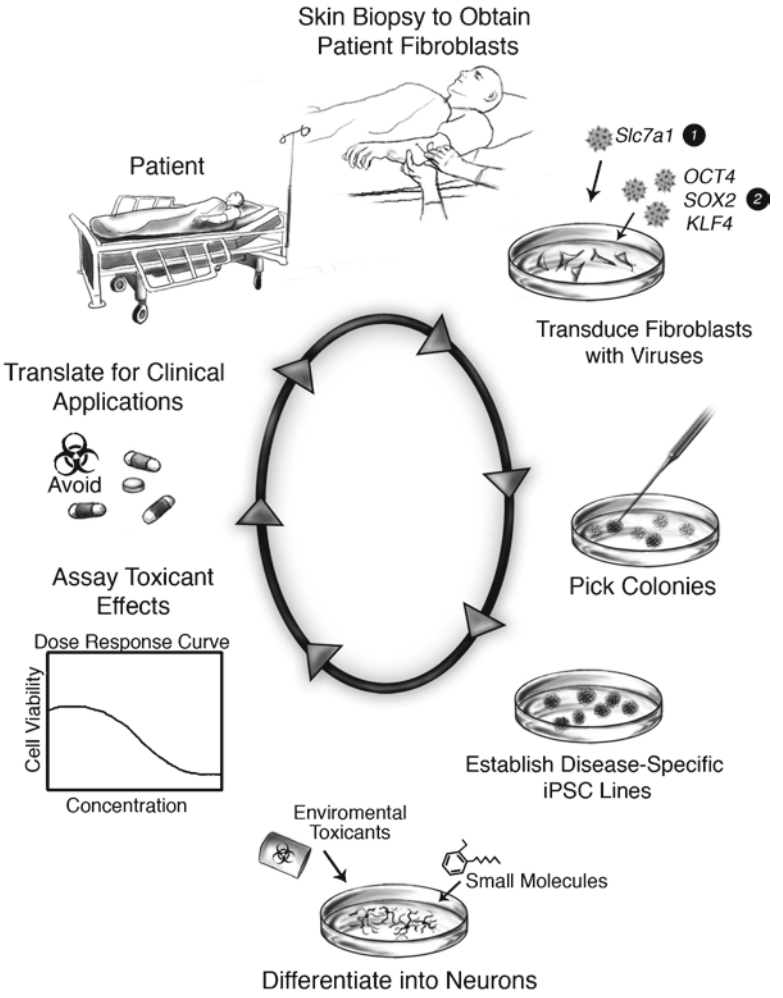

Fig. 1. Scientific approach: from bedside to bench and back again. A schematic overview is given of the steps involved in deriving patient-specific neurons and how observations from experimentation with these neurons can potentially benefit patients. Fibroblasts harvested from a skin biopsy are transduced to become patient-specific human induced pluripotent stem cells (iPSCs). The human iPSCs are then differentiated into neurons that can be assessed for their response to the neurotoxicants of interest. The knowledge obtained from these experiments may directly benefit the patients or allow the testing of novel hypotheses related to disease pathogenesis.

ecotropic retroviral transduction with the three genes shown to be sufficient for induction of pluripotency, *SOX2, KLF4, and OCT3/4* (1, 4). We provide detailed methods from our laboratory's adaptation of a variety of available methods. The topics covered include culturing of primary human fibroblasts from skin biopsies, preparation of virus for transductions, induction of pluripotency in human fibroblasts, isolation of human iPSC colonies, basic maintenance and expansion of human iPSC lines, and a discussion of first step validation protocols to confirm the human

iPSC phenotype. Finally, we discuss methods we have adapted from the work of Lorenz Studer and colleagues to induce neural progenitors from human iPSCs (5). Throughout this chapter, we refer the reader to key publications that offer alternative methods or expanded approaches in working with human iPSCs.

2. Materials

The selection of basic materials for iPSC culture and differentiation is critical for success. Indeed, for many of the reagents it is highly recommended that these specific vendors and catalog numbers be utilized. A list of antibodies, including dilutions and vendor information, are provided in Table 1. A complete list of the stock reagents needed, including catalog number and vendor name, is provided in Table 2. Cell culture conditions for all procedures in this chapter utilize a standard tissue culture incubator, with a 5% $CO_{2,}$ humidified environment at 37°C. Due to the use of viruses and primary human cells, human iPSC cultures and human fibroblast reprogramming should be carried out in a biosafety level 2 (BSL2) approved facility. Below we provide the recipes for all of the media and solutions described in the methods Sect. 3.

Volume	Component	Final concentration
Complete DMEM media		
440 mL	DMEM (Mediatech, Inc. #10-013-LV)	
50 mL	Fetal Bovine Serum (FBS) (Sigma # F2442)	10%
5 mL	Pen/Strep (100×, Mediatech # 30-002-CI)	1×
5 mL	Non-essential amino acids (100×, Sigma # M7145)	1×
hES media		
385 mL	DMEM/F12 (Invitrogen #11330-032)	
100 mL	Knockout Serum Replacement (Invitrogen #10828)	20%
2.5 mL	Glutamax (100×, Invitrogen #35050-061)	2 mM
5 mL	Pen/Strep (100×, Mediatech # 30-002-CI)	1×
5 mL	Non-essential amino acids (100×, Sigma # M7145)	1×
0.2 mL	rhFGF, basic (20 μg/mL in D-PBS, Promega # G5071)	8 ng/mL
3.5 μL	β-Mercaptoethanol (Sigma # M3148)	100 μM
Neuralization media		
410 mL	Knockout DMEM (Invitrogen #12660)	
75 mL	Knockout Serum Replacement (Invitrogen #10828)	15%
5 mL	Glutamax (100×, Invitrogen #35050-061)	2 mM
5 mL	Pen/Strep (100×, Mediatech #30-002-CI)	1×
5 mL	Non-essential amino acids (100×, Invitrogen # M7145)	1×
1.93 μL	β-Mercaptoethanol (Sigma # M3148)	55 μM

Fibroblast freezing solution		
12 mL	DMEM (Mediatech, Inc. #10-013-LV)	60%
6 mL	FBS (Sigma # F2442)	30%
2 mL	DMSO (Sigma # D8418)	10%
Feeder-free iPSC freezing solution		
9 mL	mTeSR1 (StemCell Technologies. Item#05850)	90%
10 µL	Rho Associated Kinase (ROCK) inhibitor Y-27632 (1,000× in H_2O, Tocris Bioscience #1254)	10 µM
1 mL	DMSO (Sigma # D8418)	10%
CTK solution		
5 mL	2.5% (w/v) trypsin (Invitrogen #15090-046)	0.25%
5 mL	1 mg/mL collagenase IV (Invitrogen #17104-019) (in D-PBS)	0.1 mg/mL
0.5 mL	0.1 M $CaCl_2$ in cell culture grade H_2O (Sigma # C7902)	1 mM
10 mL	Knockout Serum Replacement (Invitrogen #10828)	20%
30 mL	Cell culture grade H_2O (Invitrogen #15230-147)	

Table 1
Primary and secondary antibodies

	Dilution	Source and item number
Primary antibodies		
TRA-1-60	1:100	Millipore. Item# MAB4360
CD57/HNK-1	1:100	Sigma. Item# C6680
NESTIN	1:200	Millipore. Item# AB5922
OCT4	1:200	Cell Signaling Technology. Item# 2750
PAX6	1:200	Covance. Item# PRB-278P
SSEA3 (MC-631)	1:100	Millipore. Item# MAB4303
SSEA4 (MC-813-70)	1:200	Dev. Studies Hyb Bank. Item# MC-813-70
SSEA4-Alexa Fluor 488	1:100	BD Pharmingen. Item# 560308
TRA-1-60-Alexa Fluor 555	1:25–50	BD Pharmingen. Item# 560121
TRA-1-81-Dylight 488	100	Stemgent. Item# 09-0069
Secondary antibodies		
DyLight 649 Affinity Purified Donkey Anti-Mouse IgG (H + L)	1:400	Jackson Immunoresearch Laboratories. Item# 715-495-150
DyLight 649 Affinity Purified Donkey Anti-Rabbit IgG (H + L)	1:400	Jackson Immunoresearch Laboratories. Item# 711-495-152
DyLight 549 Affinity Purified Donkey Anti-Mouse IgG (H + L)	1:800	Jackson Immunoresearch Laboratories. Item# 715-505-150
DyLight 549 Affinity Purified Donkey Anti-Rabbit IgG (H + L)	1:800	Jackson Immunoresearch Laboratories. Item# 711-505-152
DyLight 649 Affinity Purified Goat Anti-Rat IgM, µ chain specific	1:400	Jackson Immunoresearch Laboratories. Item# 112-495-020

Table 2
Materials and reagents

Reagent	Source and item number
293-FT cell line	Invitrogen. Item# R700-07
Accutase	Innovative Cell Technologies. Item# AT-104
BD Matrigel™ hESC-qualified Matrix	BD Biosciences. Item# 354277
Blasticidin S	Invitrogen. Item# R210-01
Dispase	StemCell Technologies. Item# 07923
D-PBS	Mediatech. Item# 21-031-CV
Normal donkey serum	Jackson Immunoresearch Laboratories. Item# 017-000-121
Fugene 6 transfection reagent	Roche Applied Science. Item# 11814443001
Geneticin (G418)	Mediatech. Item# MT61234RG
Hoechst (bisBenzimide H 33258)	Sigma. Item# B1155
Leukocyte Alkaline Phosphatase Kit	Sigma. Item# 85L1-1KT
LIF (leukemia inhibitory factor)	Millipore. Item# LIF1010
Lipofectamine 2000 transfection	Invitrogen. Item# 11668-019
Mitomycin-C	Sigma. Item# M4287
mTeSR1 medium	StemCell Technologies. Item# 05850
Noggin	R&D Systems. Item# 719-NG
OPTI-MEM I reduced-serum medium	Invitrogen Corporation. Item# 11058-021
16% Paraformaldehyde solution	Electron Microscopy Sciences Item# 15710
PBS (10× solution)	Mediatech Item# 46-013-CM
PD0325901	Cayman Item# 13034
PLAT-E cells	Cell Biolabs, Inc. Item# RV-101
pLenti6/UbC/mSlc7a1	Addgene. Plasmid 17224
pMXs-hc-MYC	Addgene. Plasmid 17220
pMXs-hKLF4	Addgene. Plasmid 17219
pMXs-hOCT3/4	Addgene. Plasmid 17217
pMXs-hSOX2	Addgene. Plasmid 17218
Polybrene	Millipore. Item# TR-1003-G
Puromycin	Sigma. Item# P8833
ROCK inhibitor, Y-27632	Tocris Bioscience. Item# 1254
SB431542	Stemgent. Item# 04-0010

(continued)

Table 2 (continued)

Reagent	Source and item number
SNL cells	MMRRC at University of California, Davis. Item# 015892-UCD
Thiazovivin	Stemgent # 04-0017
Triton X-100	Sigma. Item# T8787
Trypsin-EDTA (0.05%) 1×	Invitrogen Corporation. Item# 25300-054
ViraPower™ Bsd Lentiviral Support Kit	Invitrogen Corporation. Item# K4970-00

3. Methods

3.1. Procurement, Propagation, and Preservation of Human Fibroblasts

Human iPSCs are derived from human somatic cells by the transgenic expression of a small number of factors (see Sect. 3.3). Human adult dermal fibroblasts are widely used for the production of patient-specific iPSCs, but derivation of iPSCs from human keratinocytes has also been reported (6). Human fibroblast cultures can be established from skin biopsies or can be obtained from commercial sources. Organizations offering primary human fibroblasts include:

American Type Culture Collection, ATCC, http://www.atcc.org
Cell Applications, http://www.cellapplications.com

Coriell Institute for Medical Research, http://ccr.coriell.org/

European Collection of Cell Cultures, ECACC, http://www.ecacc.org.uk

Japanese Collection of Research Bioresources, http://cellbank.nibio.go.jp

Lonza, http://www.lonza.com/group/en.html

Riken Biosource Center, http://www.brc.riken.jp

3.1.1. Obtaining Fibroblasts from a Human Skin Biopsy

To obtain patient-specific tissue, we perform 3 mm punch skin biopsies using an Acu Punch (Acuderm, Inc). The removed tissue is cultured under standard culture conditions and after 3–7 days, fibroblasts migrating out from the skin punch can be observed (Fig. 2). Two weeks later these fibroblasts can be passaged for derivation of iPSCs and cryostocks generated for future use.

3.1.1.1. Procedure

1. Skin biopsies should be obtained only with Institutional Review Board approval.
2. Obtain skin biopsies (about 3 mm punch biopsy) from patients using standard sterile methods.

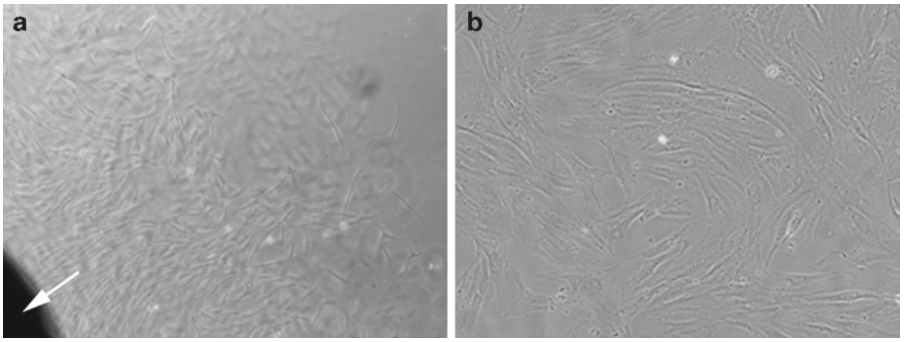

Fig. 2. Procurement of human fibroblasts. (**a**) The tissue of a skin biopsy is transferred into a cell culture dish and maintained in complete DMEM media. Over the next 2 weeks, fibroblasts migrate out of the tissue and proliferate in the dish. This is an image taken 11 days after the biopsy was performed. Fibroblasts have migrated away from the skin tissue (*arrow*). After about 2 weeks, the fibroblasts are harvested and are ready for propagation. (**b**) The fibroblasts shown were harvested from the same biopsy tissue seen in (**a**). These fibroblasts have been passaged three times and are shown here at about 80% confluency. At this point the human fibroblasts are ready for another passage or can be used for iPSC generation.

3. The tissue is transferred to a 35 mm dish containing 1 mL complete DMEM media.
4. Skin sample is transferred to a tissue culture hood and halved with a scalpel or sterile scissors (sterilized tools should to be used for tissue from each patient to prevent any cross-contamination).
5. Put each half of the biopsy tissue into a well of a 6-well plate containing 0.5 mL of complete DMEM media. It is important that the tissue makes contact with the dish surface at this stage; if necessary a sterile glass cover slip (22 × 22 mm) can be put on top of the skin tissue for additional weight to ensure contact between the tissue and the culture dish surface.
6. When the tissue is in contact with the culture dish surface, slowly add 1.5 mL of complete DMEM media.
7. Move dish carefully into a standard tissue culture incubator (5% CO_2, humidified environment at 37°C).
8. Aspirate media and add additional 2 mL complete DMEM media 48 h later.
9. Feed cultures every 3–4 days with complete DMEM media.
10. Fibroblasts will migrate out of the biopsied tissue and are ready for propagation 1–2 weeks later.

3.1.2. Propagation of Human Fibroblasts

Human fibroblasts are best split when they reach about 80% confluency (Fig. 2b). The first passage is performed on fibroblasts growing in 6-well plates from which they are transferred into 10 cm dishes for further propagation. Volumes of media and enzyme needed for the first (when the cells are in 6-well plates) and later

propagations (when the fibroblasts are grown in 10 cm dishes) are both indicated, with the latter appearing in parentheses.

3.1.2.1. Procedure

1. Before the first passage move the cover slip (if present) into an empty well of the dish with the side that had faced the tissue up and remove the biopsied tissue punch from the well.
2. Wash fibroblasts and the cover slip two times with 2.5 mL (10 mL) of D-PBS to remove all media and serum.
3. Incubate cells and cover slip (present only for the first propagation) each with 1 mL (1 mL) of 0.05% trypsin-EDTA for about 5 min (check under the microscope for progress starting at 3 min).
4. Stop digestion by adding 2 mL (10 mL) of complete DMEM media.
5. Harvest fibroblasts and transfer cells from 1-well (dish) each into a 15 mL (50 mL) conical tube.
6. Add another 2.5 mL (10 mL) of complete DMEM media into each well and repeat the washing step.
7. Add solution containing trypsinized cells to conical tube from previous step.
8. Spin cells at $200 \times g$ for 5 min at room temperature.
9. Aspirate supernatant and resuspend cell pellet.
10. First passage only – resuspend cell pellet from each well of the 6-well plate in 10 mL complete DMEM media and plate cells into 10 cm dish.
11. Later passages only – resuspend cell pellets obtained from each 10 cm dish in 30–40 mL of complete DMEM media and plate cells into three to four new 10 cm dishes.
12. Label each culture with date, fibroblast identity, and passage number (see Note 1).
13. Feed cells with complete DMEM media every other day.

3.1.3. Freezing and Thawing of Human Fibroblasts

Derivation of human iPSCs is most likely to be successful if attempted with early passage fibroblasts (ideally less than passage 5). Thus, early passage human fibroblasts should be frozen for future iPSC inductions should your first attempts not meet with your expectations.

3.1.3.1. Procedure

Freezing of Human Fibroblasts

1. Proceed with steps 2–9 as described previously (Sect. 3.1.2).
2. Resuspend cell pellets in 3–4 mL of fibroblast freezing solution (usually we freeze at a concentration of about 2×10^5 cells/mL).
3. Pipette 1 mL of cell suspension into 1.5 mL Nalgene cryogenic vials (#5000-1020).

4. Put cryo-vials into a Nalgene cell culture cryofreezing container for overnight freezing at –80°C.
5. Transfer the cells into the liquid nitrogen storage facility the next day.

Thawing of Human Fibroblasts

1. Rapidly transfer the cryo-vial containing the fibroblasts from the liquid nitrogen storage into a 37°C water bath.
2. Thaw the cells by gentle agitation until most, but not all, of the contents is thawed.
3. Remove the vial from the water bath and let the reminder of the cells thaw.
4. Rinse the vial with 75% ethanol before transferring it into the tissue culture hood.
5. Transfer the thawed cell suspension into a 15 mL conical tube.
6. Slowly add 9 mL prewarmed complete DMEM media to the cells.
7. Spin the cells at $200 \times g$ for 5 min at room temperature.
8. Resuspend the cell pellet (about 2×10^5 cells) in 10 mL of complete DMEM media.
9. Plate cells into a 10 cm dish.
10. Follow the growth and passage of the cells when they are about 80% confluent.

3.2. iPSC Induction: Lentivirus and Retrovirus Production

Reprogramming adult human fibroblasts into iPSCs is mediated by viral expression of transcription factors that are involved in maintaining the pluripotent state. The original report by Shinya Yamanaka's laboratory identified four transcription factors needed to reprogram cells: *OCT3/4*, *SOX2*, *KLF4*, and *c-MYC* (1, 7, 8). We prefer to omit *c-MYC* from the transcription factor cocktail due to concerns of its potential to increase the number of partial iPSC colonies and its oncogenic character, as described by a subsequent paper from Yamanaka and colleagues (4).

Retroviruses containing the human cDNAs for *OCT3/4*, *SOX2*, and *KLF4* are used to drive expression of these genes in fibroblasts. For safety and efficiency reasons, ecotropic retroviruses are used. This approach requires the expression of the mouse membrane receptor protein gene, *Slc7a1*, for retroviral transduction of human fibroblasts. The *Slc7a1* gene is introduced into the fibroblasts by lentiviral transduction prior to retroviral transduction of the 3 factors. Lentiviruses are produced in the viral packaging cell line 293FT, while retroviruses are made in PLAT-E cells. Production of lentivirus requires co-transfection of pLenti6/UbC/mSlc7a1 with plasmids expressing the virus

packaging genes. Production of retrovirus in PLAT-E cells does not require co-transfection with additional viral packaging genes, as the cells stably expresses these factors already. Generation of retrovirus is done by transfection of single constructs encoding the genes for induction of pluripotency (pMXs-*h*, pMXs-*hKLF4*, pMXs-*hOCT3/4*, or pMXs-*hSOX2*). Viruses are obtained by collecting the supernatants from the transfected packaging cells. Retrovirus containing supernatant is pooled for transduction of the fibroblasts. Although some groups have reported freezing virus-containing supernatants at –80°C for later transduction, we prefer to use fresh virus-containing supernatants due to concerns of loss of viral titer resulting from the freeze–thaw cycle. The days marked in the timelines of this section correspond to those found in the timelines for fibroblast passaging and transduction (Sect. 3.3). All plasmids containing the cDNAs needed for virus production are available from Addgene and are listed in Table 2.

3.2.1. Passaging Packaging Cell Lines 293FT or PLAT-E

1. Aspirate the complete DMEM media from a 10-cm tissue culture dish when the cells have reached 80–90% confluency.
2. Wash once with 10 mL of D-PBS and aspirate.
3. Add 1 mL of 0.05% trypsin-EDTA and incubate at 37°C for 2 min.
4. Add 9 mL of complete DMEM media and gently pipette up and down to detach cells creating a single-cell suspension.
5. Place cells in a 15 mL conical tube and centrifuge at 200×*g* for 5 min.
6. Aspirate media and resuspend the cell pellet in 2 mL complete DMEM media. For PLAT-E cells, add 1 μg/mL puromycin and 10 μg/mL blasticidin S to the media while expanding to maintain the expression of the viral packaging vector which contains resistance genes for these antibiotics. For 293FT cells, add 0.5 mg/mL G418 (geneticin) to the media.
7. Either propagate cells at a ratio of 1:4 to 1:6 for continued propagation or count the cells and dilute them to the appropriate concentration for transfection (4×10^6 per 10 cm dish for 293FT cells or 3.6×10^6 per 10 cm dish for PLAT-E cells) into complete DMEM media.

3.2.2. Transfecting 293FT Cells

1. One day prior to transfection (day 1), plate 4×10^6 293FT cells onto a 10-cm dish and incubate overnight in complete DMEM media *without* G418 in a standard tissue culture incubator.
2. The next day (day 2) pipette 1.5 mL of OPTI-MEM I media into a microcentrifuge tube, add 9 μg of ViraPower lentivirus packaging mix, and 3 μg of pLenti6/UbC plasmid DNA.

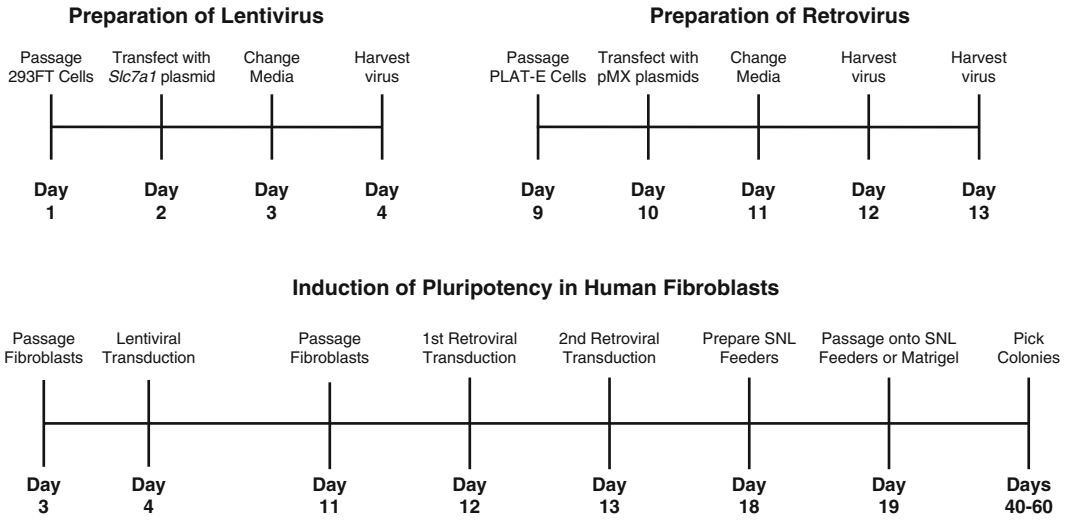

Fig. 3. Timeline for human iPSC induction. The induction of human fibroblast to become human iPSCs requires the preparation of several different agents (viruses and cells) at defined time intervals. The three timelines provided are set to the same schedule to allow the reader to organize the many steps required for the reprogramming of human fibroblasts.

3. In a separate tube, mix 1.5 mL of OPTI-MEM I with 36 μL of Lipofectamine 2000 by finger tapping and incubate for 5 min at room temperature.
4. Combine the DNA- and Lipofectamine containing solutions, mix by finger tapping, and incubate for 20 min at room temperature.
5. Change the complete DMEM media on 293FT cells, then add transfection mixture to the cultures dropwise, and swirl gently.
6. Incubate the 293FT cells for 24 h.
7. Change media to fresh complete DMEM (day 3).

A timeline for generation of lentivirus for transduction using this protocol is shown in Fig. 3.

3.2.3. Transfecting PLAT-E Cells

1. One day prior to transfection (day 9), seed three 10-cm dishes with 3.6×10^6 PLAT-E cells each (one for each pMX plasmid) and incubate overnight in complete DMEM media *without* puromycin or blasticidin S in a standard tissue culture incubator.
2. The following day (day 10), pipette 0.3 mL of OPTI-MEM I media into three microcentrifuge tubes, add 27 μL of Fugene 6 transfection reagent to each, mix by finger tapping, and incubate for 5 min at room temperature.
3. Add 9 μg of either *OCT3/4, KLF4,* or *SOX2* pMX plasmid to the three microcentrifuge tubes, mix by finger tapping, and incubate 15 min at room temperature.

4. Change the complete DMEM media on the PLAT-E cells, add transfection mixtures dropwise, one to each plate of PLAT-E cells, and swirl gently.
5. Incubate the PLAT-E cells for 24 h with transfection mixture (day 11).
6. Remove transfection mixture and replace with complete DMEM media.

A timeline for generation of retrovirus for transduction using this protocol is shown in Fig. 3.

3.2.4. Preparing the Virus for Transduction

1. Collect media 48 h after transfection, for PLAT-E cells also collect at 72 h (days 12, 13) into a 50 mL conical tube (the three pMX virus-containing media can be mixed together at this point).
2. Centrifuge at 3,000 × *g* for 5 min at room temperature to remove cells in the supernatant.
3. Filter supernatants using a 0.45 μm pore-size polyethersulfone syringe filter to remove remaining cells.
4. Add polybrene to a final concentration of 4 μg/mL to virus-containing media.
5. Use immediately for fibroblast transduction. The supernatant is approximately 30 mL when combined from all PLAT-E plates. The 30 mL is typically enough to transduce three 10 cm plate of fibroblasts with 10 mL of virus-containing media each.

3.3. iPSC Induction: Fibroblast Passaging and Transduction

The field of iPSC induction has changed rapidly since the initial paper by the Yamanaka group in 2006 (8) and new approaches that increase the efficiency of iPSC induction have been described (9–15). The human iPSC lines established in our laboratory so far were produced following the method developed in Shinya Yamanaka laboratory (except that we omit one of the factors, *c-MYC*) with modifications described by Sheng Ding and collaborators (1, 4, 9, 16). Here, we describe methods for iPSC induction in the presence (Sect. 3.3.1) and absence of feeder cells (3.3.2). We provide an overall timeline for the entire process of reprogramming, including preparation of virus for transduction, in Fig. 3. This timeline uses the same scheduling days across the procedure for experimental planning purposes.

3.3.1. iPSC Induction on SNL Feeder Cells

3.3.1.1. Procedure

1. Plate 5×10^5 fibroblasts 1 day prior to transduction with lentivirus (day 3) onto a 10-cm dish in complete DMEM media.
2. The following day (day 4), aspirate media and replace with prepared lentivirus-containing 293FT supernatant DMEM complete media *without* G418.

3. Incubate for 24 h and replace virus-containing media with fresh complete DMEM media (day 5).
4. Maintain cells for 7 days following transduction in complete DMEM media. Change media every 3 days. Be sure that the culture remains between 20 and 80% confluency throughout this time. If the culture reaches 80% confluency prior to day 11, passage with trypsin and replate cells at a 1:2 density (Sect. 3.1.2).
5. Passage 5×10^5 fibroblasts 1 day prior to transduction with retrovirus (day 11) onto a 10-cm dish in complete DMEM media.
6. The following day (day 12), aspirate media and replace with prepared retrovirus-containing PLAT-E supernatant complete DMEM media.
7. 24 h after first transduction replace virus-containing media with a second round of retrovirus-containing PLAT-E supernatant complete DMEM media (day 12).
8. Replace virus-containing media with complete DMEM media 24 h after second retroviral transduction (day 13).
9. Maintain cells for 7 days following initial retroviral transduction in complete DMEM media, changing the media every 3 days. Be sure that the culture remains between 20 and 80% confluency throughout this time. If the culture reaches 80% confluency prior to day 19, passage with trypsin and replate cells at a 1:2 density (Sect. 3.1.2).
10. One day prior to passaging transduced fibroblasts (day 18), prepare a 6-well plate with SNL feeder cells (Sect. 3.5.3).
11. The following day (day 19), passage and plate 1×10^5 transduced fibroblasts into each well of the SNL feeder-coated 6-well plate in complete DMEM media.
12. The following day (day 20), replace complete DMEM media with hES media.
13. Continue to replace media every other day until the culture begins to deplete the media (color of media turns yellow), then feed daily.

A timeline for iPSC induction as outlined above is shown in Fig. 3.

3.3.2. iPSC Induction Under Feeder-Free Conditions

3.3.2.1. Procedure

1. Follow steps 1–9 described in Sect. 3.3.1.
2. One hour prior to passaging transduced fibroblasts (day 19), prepare a Matrigel-coated 6-well plate.
3. Passage and plate 1×10^4 transduced fibroblasts into each well of the Matrigel-coated 6-well plate in complete DMEM media.

4. The following day (day 20), feed the cells with reprogramming media (hES media containing leukemia inhibitory factor (LIF) (10 ng/mL), PD0325901 (0.5 μM), SB431542 (2 μM), and Thiazovivin (0.5 mM).
5. Replace reprogramming media every other day until the culture begins to deplete the media (color of media turns yellow), then feed daily.

3.4. iPSC Colony Selection

After the viral transduction, the fibroblast cultures appear heterogeneous, composed of cells and cell colonies with different morphologies. The cells continuously change characteristics during the approximate 30-day period leading up to the formation of true iPSC colonies. 3-Factor induction (*OCT3/4, SOX2,* and *KLF4*) may prolong the time to the formation of human iPSCs when compared to inductions with 4 factors; however, it appears that 3-factor inductions reduce the number of partially induced iPSC colonies (4). Once presumptive colonies are identified, by light microscopy or live-immunocytochemical staining, the colonies are "picked" individually, and each is placed into a separate well of a 24-well plate and monitored by phase-contrast light microscopy. The recent development of live-cell immunocytochemistry with fluorophore-conjugated antibodies directed against stem cell surface markers has greatly increased the efficiency of selecting true iPSC colonies (17).

3.4.1. Colony Morphology Descriptions and Images

The progression of reprogramming can be monitored by morphological changes. Because cell doubling rates directly affect the rate at which somatic cells reprogram into iPSCs (18), differences in doubling rates of initial fibroblasts and their underlying epigenetic state can alter the timing of iPSC generation.

Most of the early forming colonies are likely to be non-iPSC colonies. These cells form circular patterns of distinct cells with spherical cell bodies that are often either phase bright or of a grainy darker appearance (Fig. 4a–c). These non-iPSC colonies often appear granular (phase darker) with cells piling up and have fuzzy colony margins rather than the smooth margin and flatter appearance observed with true iPSC colonies. Another class of non-iPSC colony morphology has more elongated cells that resemble small fibroblasts. These colonies vary in density and the densest colonies are easily misidentified as true iPSC colonies. True human iPSC colonies become uniformly circular as they expand (Fig. 4d), but when they are constrained by neighboring cells they can form elongated or tear-drop shaped colonies (Fig. 4e). The colony margins are defined and smooth compared to the "fuzzy" appearance of most non-iPSC colonies.

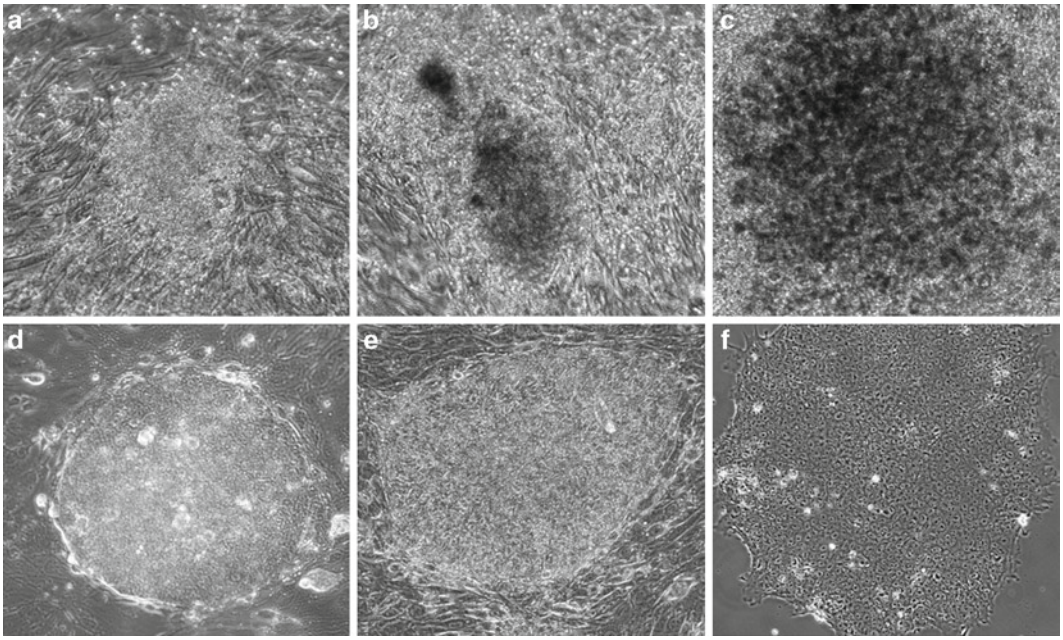

Fig. 4. Examples of various colony morphology types observed during reprogramming and propagation of iPSC colonies on feeders and Matrigel. (**a–c**) Partially reprogrammed human iPSC colonies form circular associations of cells appearing either phase bright (**a**) or phase dark (**b**, **c**). They usually do not show clearly defined colony margins and show an overall fuzzy appearance. The morphologies of these colonies are in sharp contrast to the smooth colony margins and flatter appearance of true iPSC colonies. (**d**, **e**) Human iPSCs derived from the fibroblasts of a normal subject are growing on feeder cells. These images display one human iPSC colony with surrounding SNL feeder cells. Human iPSC colonies can have a circular or oval/tear-drop shape. (**f**) The same human iPSC line can be grown under feeder-free conditions. One human iPSC colony growing on a Matrigel substrate is shown. The high nuclear to cytoplasmic ratio and prominent nucleoli typical for iPSCs is more easily appreciated in colonies growing on Matrigel than on feeder cells. All panels were imaged on a Zeiss microscope using a 10× phase contrast objective.

Human iPSCs have large round nuclei with prominent nucleoli and display a large nuclear to cytoplasmic ratio with the cytoplasm appearing phase darker than the nucleus. The overall cell shape is typically trapezoidal, but cell size and shape varies with colony size. These features are demonstrated in the higher magnification images of an iPSC colony grown on Matrigel (without feeders) shown in Fig. 7a. As a colony becomes larger, the cells are more tightly packed causing the cells to appear smaller. Cells in small colonies or at the margins of colonies growing in feeder-free conditions appear larger than the cells in the colony center. Borders between iPS cells often appear phase bright under a light microscope.

3.4.2. Live Imaging of Human iPSC Markers

For live imaging, cells are incubated with fluorophore-conjugated antibodies against iPSC markers (Fig. 5). Live staining can therefore only be performed with antibodies directed against cell surface-associated antigens. We typically use fluorophore-conjugated antibodies against SSEA4, TRA-1-60, and TRA-1-81 (for source

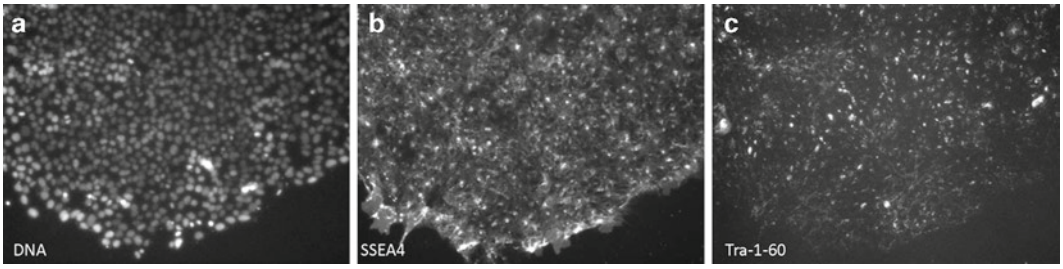

Fig. 5. Live staining of presumptive human iPSC colonies. This human iPSC colony was triple stained with Hoechst (DNA) to visualize all cell nuclei and the two iPSC surface markers SSEA4 and TRA-1-60.

and dilution of antibodies see Table 1). Live staining permits the early identification of emerging reprogrammed cells and therefore is a useful technique for picking human iPSC colonies, but is also helpful for monitoring the status of established iPSC lines and their differentiation. The following protocol was adapted from a published method (17).

3.4.2.1. Procedure

1. Dilute TRA-1-60-Alexa Fluor 555 and SSEA4-Alexa Fluor 488 (see Table 1) in warm mTeSR1 media.
2. Gently aspirate media from cultures to be stained.
3. Add antibody-containing media to cells (0.25 mL/well or 0.75 mL/well for 24- or 6-well plates, respectively).
4. Incubate for 1.5 h at 37°C.
5. Add Hoechst dye to wells (0.5 μg/mL final concentration).
6. Incubate for 30 min at 37°C.
7. Wash three times with DMEM/F12 media.
8. Image in hES media or mTeSR1 media.
9. Colonies can be directly picked under epifluorescence with the following protocol. Alternatively, the plate can be marked with a pen and the colony can be picked under phase-contrast light microscopy in a laminar flow hood to maintain sterility (see Note 2).

3.4.3. Picking Colonies onto SNL Cell Coated Culture Dishes

3.4.3.1. Procedure

1. Make a SNL cell 24-well feeder plate 1 day prior to picking colonies (Sect. 3.5.3).
2. Just prior to picking, wash the SNL plate twice with PBS and add 0.5 mL hES media with ROCK inhibitor, Y-27632 at a final concentration of 10 μM.
3. Identify colonies by morphology or live cell imaging (Sect. 3.4.2).
4. Pick colonies using a pulled-glass scraper (Fig. 6a). Since each colony represents one separate hiPSC cell line, it is important that colonies are kept separate by ensuring that they are

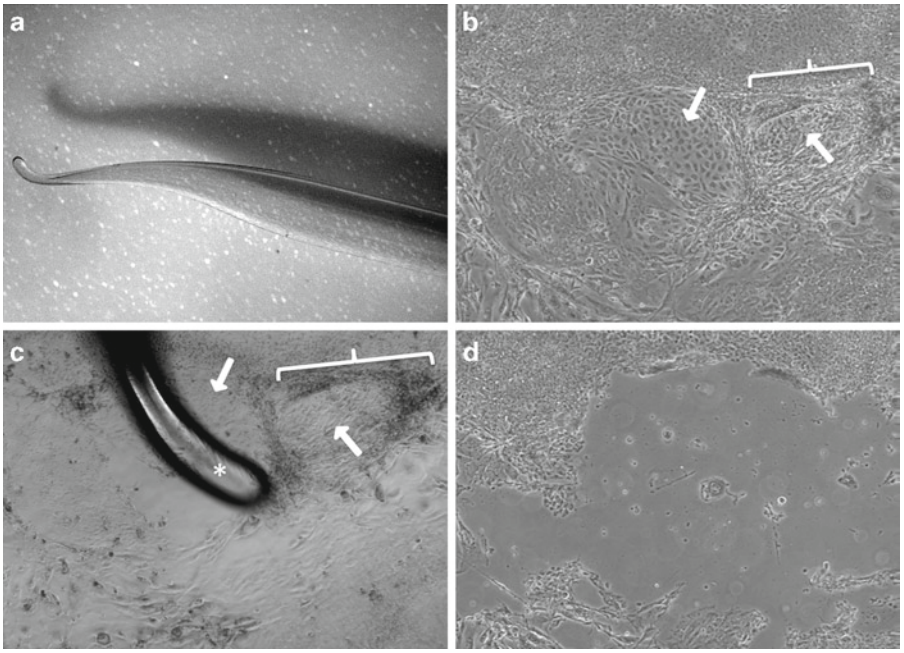

Fig. 6. Removal of differentiated cells from iPSC colonies. During propagation some spontaneous differentiation of a subset of human iPSCs is to be expected. To maintain the purity of the culture, these cells must be removed before passaging. (**a**) We prepare a scraping tool from Pasteur pipettes for that purpose. (**b**) We routinely observe two types of differentiation, cells that appear more spread out and are somewhat phase darker than human iPSCs (*arrows*). These cells are usually observed in the center or the edge of a colony. The other types of changes resemble more a piling up of human iPSCs often in the center or the edge of the colony (*area under bracket*). (**c**) These cells are scraped from the dish surface using the glass scraper (*star*) and then aspirated. The areas of differentiation from (**b**) are highlighted again (*with arrows* and *under the bracket*). (**d**) Area of differentiation has been removed with the scraping tool. The remaining human iPSCs are then passaged. (**b–d**) Imaged on a Zeiss microscope using a 10× phase contrast objective.

individually picked and transferred to the new culture dish. With a glass scraper gently separate the colonies one at a time from the SNL feeder cells.

5. Transfer the colony or colony fragments by pipetting them slowly into a 1 mL glass serological pipette and then place each colony (or the fragments of one colony) into a separate well of a SNL-coated 24-well plate.
6. Once colonies have grown substantially, the hiPSCs are passaged using the CTK method (see Sect. 3.5.3) and plated into 1 well of a 12-well SNL cell-coated culture dish.
7. For the next passage, plate the cells into 1 well of a SNL cell-coated 6-well dish.
8. Then continue to expand the hiPSC lines for verification, cryopreservation, and experiments as needed (a minority of original colonies picked will actually expand into iPSC lines).

3.4.4. Picking Colonies onto Matrigel-Coated Culture Dishes

1. Coat a 24-well tissue culture plate with Matrigel following the vendors' protocol.
2. Add fresh reprogramming media (hES media containing LIF (10 ng/mL), PD0325901 (0.5 μM), SB431542 (2 μM) and thiazovivn (0.5 μM)) to the cultures from which colonies will be picked.
3. Remove Matrigel solution and add 0.5 mL of reprogramming medium containing 10 μM ROCK inhibitor to each well.
4. Since each colony represents one separate hiPSC cell line it is important that colonies are kept separate by ensuring that they are individually picked and transferred to the new culture dish. With a pulled-glass scraper (Fig. 6a) gently remove the fibroblasts surrounding the hiPSC colony and carefully separate the colony from the Matrigel-coated dish surface. If the colony is large, break it into several pieces; small colonies should be kept intact if at all possible.
5. Transfer the colony fragments by pipetting them slowly into a 1 mL glass serological pipette and placing each colony (or the fragments of one colony) into a separate well of the Matrigel-coated 24-well plate.
6. One day after picking, feed the cells with reprogramming media (without ROCK-inhibitor).
7. Next day feed the cells with media containing 75% reprogramming media + 25% mTesr1 media (note that the concentration of LIF, PD0325901, Thiazovivin, and SB431542 will be reduced with increasing increments of mTeSR1 medium).
8. Next day change to 50%/50% reprogramming/mTeSR1 media.
9. Next day change to 25%/75% reprogramming/mTeSR1 media.
10. Next day change to 100% mTeSR1.
11. Once colonies have grown substantially, scrape away any non-iPSC-like cells with a glass scraper, and passage the hiPSCs using dispase (see Sect. 3.5.1) and plate them into 1 well of a 12-well Matrigel-coated culture dish.
12. When passaging the cells again plate them into 1 well of a Matrigel-coated 6-well dish.
13. Then continue to passage and expand the hiPSC lines for verification, cryopreservation, and experiments as needed (a minority of original colonies picked will actually expand into iPSC lines).

3.5. Maintenance and Expansion of iPSC Colonies

Once primary iPSC colonies have been picked, they have to be expanded for long-term storage and validation (for validation of human iPSCs, see Sect. 3.6). Human iPSCs require a combination of different factors for their survival and proliferation.

Traditionally, these factors are provided by co-cultured feeder cells or media conditioned by mouse embryonic fibroblasts (MEF) (2, 3). We use mitomycin-C inactivated SNL cells (1, 7), which are a derivative of the STO mouse fibroblast cell line which secretes murine LIF and is transformed with neomycin resistance (19). Irradiated MEF have also been used as feeder cells and may be substituted for the SNL cells described here (2, 3). Examples of typical human iPSC colonies growing on SNL feeder cells are portrayed in Fig. 4d, e. As observed previously (16), we noticed that the time point and plating density of SNL cells can greatly affect iPSCs growth. Thus, care should be taken that SNL cells are plated at the appropriate density 1–2 days before the passage of the iPSCs.

More recently, human stem cells have also been successfully cultured in the absence of feeder cells (20–22). Growing iPSCs in the absence of feeder cells has several advantages which include the possibility to use defined media, unobstructed visualization of human iPSC colonies, elimination of the need to maintain and prepare an additional cell type (feeder cells), avoidance of potentially confounding feeder cells during iPSC differentiation, and better recovery of frozen iPSCs. We describe methods for culturing human iPSCs on SNL feeder cells as well as under feeder-free conditions on dishes coated with Matrigel, a commercially available mixture of extracellular matrix proteins. However, for the reasons mentioned above, we now almost exclusively culture human iPSCs on Matrigel. A human iPSC colony growing on Matrigel is shown in Fig. 4f.

Freezing and reconstituting iPSCs can be a challenge and various methods for freezing and thawing stem cells have been described (16, 20, 23). In our hands, a rapid freeze/rapid thaw procedure proved best for human iPSCs that are to be plated onto SNL feeder cells. However, for plating human iPSCs onto Matrigel a slow freeze/rapid thaw approach was more successful.

All our protocols have been adapted to human iPSC cells grown in standard 6-well tissue culture plates; and thus, all volumes indicated need to be adjusted if other culture dish sizes are used.

3.5.1. Passaging Human iPSCs on Matrigel

To culture human iPSCs under feeder-free conditions, the cells are seeded and maintained in culture dishes coated with Matrigel. Matrigel is a soluble basement membrane extract mainly composed of laminin, collagen IV, entactin, and heparan sulfate proteoglycan (24, 25). Human iPSCs growing on Matrigel are maintained in a defined serum-free media (mTeSR1) that is changed daily. Once seeded onto Matrigel, the colonies expand and need to be passaged about every 4–5 days or when about 80% of the culture surface is covered with colonies.

As human iPSCs are maintained in culture, a subset of the cells spontaneously differentiate. The two most frequent types of differentiation we observe are shown in Fig. 6b. These differentiated cells need to be removed before each passage. We remove these cells scraping them off the dish surface with glass scrapers that we prepare by pulling glass Pasteur pipettes in a flame (Fig. 6a). To maintain sterility of the iPSC cultures, we move an inverted light microscope into the tissue culture hood. If the media is changed daily and the cells are passaged at appropriate intervals (4–5 days), the percentage of cells that differentiate should not exceed 5–10%. Extending the time between passaging or omitting daily media changes results in increased differentiation of the cells. In addition, we found that the degree of differentiation varies among different human iPSC lines, even among lines derived from the same fibroblasts.

3.5.1.1. Procedure

Although widely performed, we found that a preincubation with ROCK inhibitor before enzymatic treatment of human iPSCs is not necessary.

Preparation for Passaging

1. At least 1 h before cell passaging, the culture dishes to be used are coated with Matrigel using the protocols provided by the manufacturer.
2. The differentiated cells characterized by the morphologies described above are removed with a glass scraper prepared from Pasteur pipettes (Fig. 6) with the aid of an inverted light microscope that is moved into the tissue culture hood.

Enzyme Treatment

1. Aspirate media including the scraped differentiated iPSCs from the cultures.
2. Wash cultures once with DMEM/F12 media.
3. Add 1 mL/well of dispase and incubate for 8–13 min depending on the lot of enzyme. Start observing the cultures after about 8 min; the edges of colonies first will become phase bright and then start to curl up (Fig. 7b). When the edges along the full perimeter of the colonies just begin curling up (Fig. 7c), stop the digestion by aspirating the dispase solution (Note 4). Do not allow the dispase to act past the degree of curling shown in Fig. 7d because that will result in loss of cells.
4. Gently wash the cells three times with 2.5 mL DMEM/F12 media.

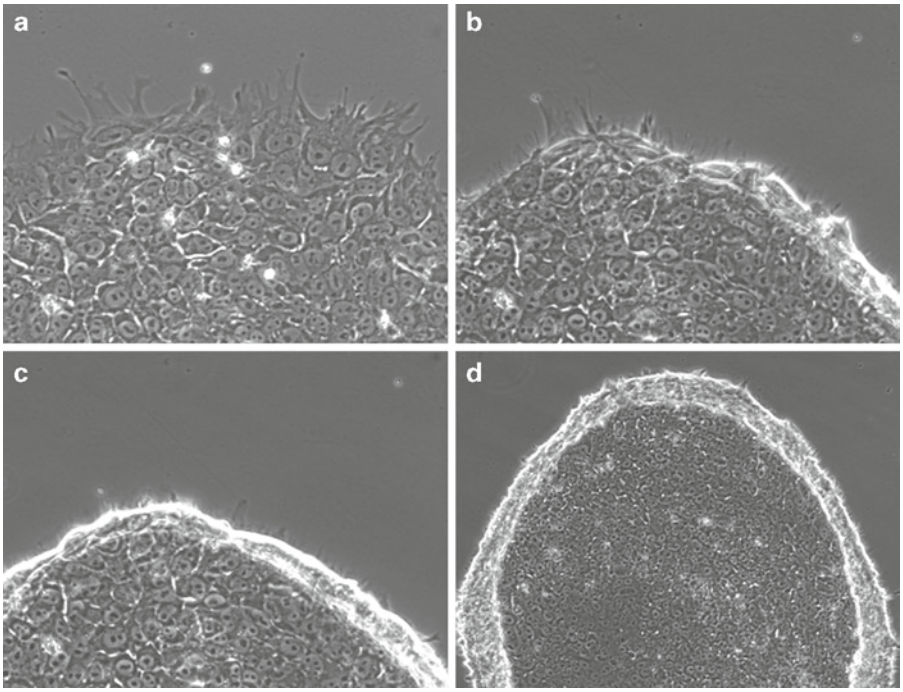

Fig. 7. Treatment of human iPSC colonies with dispase. (**a**) Human iPSC colonies growing on Matrigel have a very flat appearance with the edges of the colonies tightly adhering to the Matrigel covered dish surface. Of note, the high nuclear to cytoplasmic ratio and the prominent nucleoli typical for iPSCs are easily appreciated in these close-up images. (**b**) Exposure to dispase for ~11 min results in the curling of the edges of the colonies. (**c**) Two minutes later (~13 min) is the time when dispase treatment should be stopped and colonies harvested. Images (**a–c**) were obtained using a 20× objective. (**d**) An image of the same iPSC colony obtained with a 10× objective provides a view of a larger area of the dispase treated colony. Do not allow the dispase treatment to continue past this stage; otherwise you risk losing the colonies.

Harvesting and Replating the Cells

1. Add 2 mL/well of mTeSR1 media containing 10 μm ROCK inhibitor Y-27632, a compound that promotes the survival of dissociated human stem cells (26).
2. Scrape colonies with a cell scraper (see Note 5).
3. Transfer the cell suspension into a 50 mL conical tube.
4. Add an additional 2 mL of mTeSR1 media containing 10 μm ROCK inhibitor into each well to remove remaining cells.
5. Transfer cell suspension into same 50 mL conical tube.
6. Add an additional 6 mL of mTeSR1 media containing 10 μm ROCK inhibitor to the 50 mL conical tube. This procedure dilutes iPSCs by a factor of 5; depending on the desired dilution of the iPSCs, volume of media added can be modified. We found splitting ratios between 1:3 and 1:5 to be optimal.
7. Further break up colonies by gently pipetting the cell suspension up and down three to five times with a 5 mL glass serological pipette (see Note 6).

8. Transfer cells onto Matrigel-coated dishes (2 mL/well) using a glass serological pipette. If a transfer of human iPSCs from Matrigel to feeder cells is desired, the human iPSCs can at this stage be plated onto prepared feeder cells instead of Matrigel (see also Sect. 3.5.3).
9. Put plates in incubator and move them back and forth and left to right a few times (this will result in an even distribution of human iPSC clumps over the whole surface).
10. Feed and observe daily for growth of colonies.

3.5.2. Freezing and Thawing of Human iPSCs for Propagation on Matrigel

3.5.2.1. Procedure

Human iPSCs should be frozen at the time when they are ready for passaging or the day before. We have obtained optimal recovery of frozen cells by freezing cells harvested from 1 well of a 6-well plate in 1 mL of freezing solution and replating these cells back into 1 well of a 6-well plate.

Freezing Human iPSCs

To prepare human iPSCs for freezing, follow steps 2–5 described previously (Sect. 3.5.1) with the following modifications:

(a) ROCK inhibitor does not need to be included in the mTeSR1 media for the collection of the cells from the dishes.
(b) Cells from each well are collected in a separate 15 mL conical tube (cells collected from each well will be frozen in a separate cryo-vial).

then continue as outlined:

1. Spin cell suspensions at 120 × *g* for 5 min at room temperature.
2. Aspirate media.
3. Add 1 mL feeder-free iPSC freezing solution to the cell pellet and transfer the resuspended cells into a cryo-vial using a 1 mL glass serological pipette (pipetting while resuspending the cell pellet should be kept to an absolute minimum).
4. Put cryo-vials into Nalgene freezing container for overnight freezing at −80°C.
5. Transfer the cells into liquid nitrogen storage facility the next day.

Thawing and Plating of Human iPSCs

1. Coat culture dish with Matrigel at least 1 h before thawing the cells.
2. Rapidly transfer the cryo-vial containing the human iPSCs from the liquid nitrogen storage into a 37°C water bath.
3. Thaw the cells by gently agitating until most but not all of the content is thawed.

4. Remove the vial from the water bath and let the remainder of the cells thaw.
5. Rinse the vial with 75% ethanol before transferring it into the tissue culture hood.
6. Transfer the thawed cell suspension into a 15 mL conical tube using a 1 mL glass serological pipette.
7. Slowly add 9 mL prewarmed mTeSR1 media to the cells.
8. Spin cells at 120 × *g* for 5 min at room temperature.
9. Aspirate media and resuspend the cell pellet in 2.5 mL of mTeSR1 media containing 10 μm ROCK inhibitor.
10. Plate the cells into 1 well of a 6-well culture dish coated with Matrigel.

3.5.3. Passaging Human iPSCs onto SNL Feeder Cells

Commonly iPSCs have been grown on feeder cells to maintain pluripotency. We use SNL feeder cells that are propagated and mitomycin-C treated according to published protocols (16). We passage human iPSC cells growing on SNL cells about once every 5 days. Shorter and longer intervals between passaging result in lower yields and increased human iPSC differentiation, respectively. Immediately before passaging, differentiated human iPSCs identified by the morphologies described previously (Fig. 6) are removed by scraping. To passage human iPSCs on SNL cells, we use a protocol similar to the procedure described by Yamanaka and colleagues (16).

3.5.3.1. Procedure

Preparation for Passaging

1. The day before passaging, SNL cells are seeded into gelatin-coated dishes at a density of 2.5×10^4 cells/cm^2 in complete DMEM media.
2. Shortly before passaging, the differentiated human iPSCs are removed with a glass scraper as described previously (Sect. 3.5.1).
3. On the day the iPSCs are passaged, the SNL cells are washed two times with D-PBS and then transferred into hES media until plating of the human iPSCs.

Enzyme Treatment

1. Aspirate media from the cultures.
2. Wash cells with 2.5 mL D-PBS once.
3. Aspirate D-PBS completely.
4. Incubate cells in 400 μL/well of CTK solution for 3–5 min in incubator (start observing detachment of SNL cells at 3 min, too long of an enzyme exposure will result in the loss of human iPSC colonies).

5. When 90% of SNL cells are detached, add 2.5 mL of D-PBS to the wells.
6. Aspirate CTK/D-PBS solution and repeat washing step once.
7. Remove D-PBS completely.

Harvesting and Replating the Cells

1. Add 2 mL of hES media to each well.
2. Scrape human iPSC colonies using a cell scraper.
3. Transfer cells into 50 mL conical tube.
4. Rinse each well with 2 mL of hES media and add to the 50 mL conical tube.
5. Repeat step 4.
6. Break the colonies into smaller clumps by pipetting up and down (three to five times) with 5 mL glass serological pipette.
7. Replate cells onto mitomycin-C treated SNL cells (see Note 7).
8. Put plates in the incubator and move a couple of times back and forth and left and right to distribute cells evenly on the dish surface.
9. Feed and observe daily.

3.5.4. Freezing and Thawing of Human iPSCs for Propagation on SNL Feeder Cells

For freezing and thawing human iPSCs to be plated onto SNL feeder cells, we follow the procedures described by Ohnuki et al. (16).

3.6. Validation of Human iPSCs

Once human iPSC lines are established, their pluripotency status has to be validated. This is achieved by evaluating a set of criteria that has been established by multiple groups. Typically, the first tests to be performed are analysis of cell and colony morphology and the presence of alkaline phosphatase activity. These tests are relatively cheap, easy, and quickly performed and thus serve as an early screen for potential human iPSC clones. Karyotyping of the human iPSCs is typically performed after human iPSCs have been propagated to demonstrate that these cells maintain a stable karyotype that is equivalent to the fibroblast line they have been derived from. Expression of pluripotency markers is assessed by immunocytochemistry and RT-PCR. Bisulfite genomic sequencing is used to assess the methylation status in the promoter regions of pluripotency-associated genes. Finally, pluripotency must be demonstrated by the potential of the human iPSCs to differentiate in vitro and/or in vivo into cell types derived from the three embryonic germ layers: ectoderm, mesoderm, and endoderm.

3.6.1. Assessment of Colony and Cell Morphology

Colony and cellular morphological characteristics are assessed by phase/contrast microscopy. Typical human iPSC colonies are formed from tightly packed cells, are of round or oval shape with well-defined edges. The cells within these colonies show a high nuclear to cytoplasmic ratio and prominent nucleoli (Figs. 4d–f and 7a).

3.6.2. Assessment of Alkaline Phosphatase Activity

Alkaline phosphatase activity has been proposed to be the most reliable pluripotency marker for human stem cells (27). In order to assess the pluripotency of potential human iPSCs, the colonies need to be propagated in duplicate, one culture is used for alkaline phosphatase activity (fixation is needed for this step and thus this procedure terminates the culture), the sister culture is used for propagation if alkaline phosphatase staining confirms the potential iPSC character of the line. We test for alkaline phosphatase enzymatic activity of the human iPSCs using an alkaline phosphatase staining kit available from Sigma exactly following the manufacturer's recommendations.

3.6.3. Immunocyto chemical Assessment of Pluripotency Markers

Pluripotency markers identified in hES cells are also markers of human iPSCs and include SSEA3, SSEA4, TRA-1-60, and TRA-1-81 surface antigens and transcription factors such as OCT4, NANOG, and SOX2. An example of immunofluorescence staining of a human iPSC line made in our lab for the markers OCT4, SSEA3, SSEA4, and TRA-1-60 is shown in Fig. 8. Staining for surface markers has the advantage that live staining can be performed (see Sect. 3.4.2). For the staining of intracellular

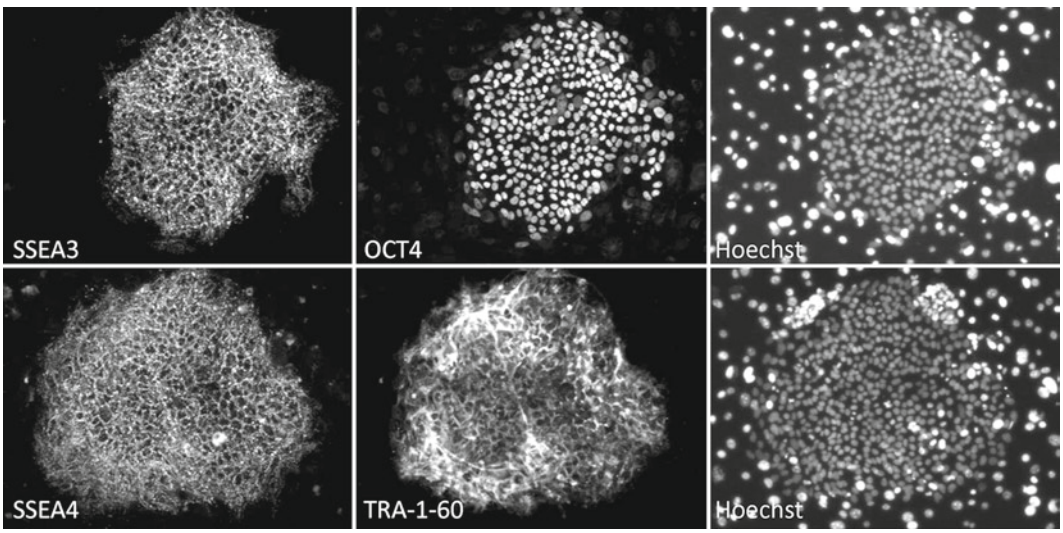

Fig. 8. Validation of human iPSC lines by immunocytochemistry. These human iPSCs cells (BG8 line) derived from a skin biopsy of a normal subject were assessed for the expression of human iPSC marker proteins. Here we show one colony that was stained for the surface marker SSEA3 and the transcription factor OCT4. Another colony of the same cell line demonstrates co-expression of the surface markers SSEA4 and TRA-1-60. The cultures were counter stained with the Hoechst dye to visualize all cell nuclei. Intensely stained feeder cell (SNL) nuclei are seen outside the perimeter of the human iPSC colonies.

proteins, the cells have to be fixed, a procedure that terminates the cultures. In order to better evaluate the results obtained from a new human iPSC line under investigation, it is critical to include an already established human iPSC or hES cell line in the staining procedure as a positive control. Counterstaining with a Hoechst (DNA) dye that labels the nuclei of all cells allows the investigator to determine the percentage of cells that expresses a particular marker of interest (Fig. 8). Since these methods are not able to accurately measure relative expression levels, assessment of gene expression by quantitative RT-PCR (see Sect. 3.6.4) is often used as a companion validation approach.

3.6.3.1. Procedure

1. Aspirate media.
2. Rinse cells once with D-PBS.
3. Fix cells with 4% paraformaldehyde in PBS for 30 min at room temperature.
4. Wash cells 3× 5 min with PBS.
5. Permeabilize cells with 0.2% Triton X-100 in PBS for 20 min at room temperature.
6. Incubate cells in PBS^{++} (PBS + 5% donkey serum + 0.05% TX-100) for 2 h at room temperature or overnight at 4°C.
7. Incubate cells with primary antibodies (see Table 1) diluted in PBS^{++} overnight at 4°C.
8. Wash cells 5× 10 min with PBS^{+} (PBS + 0.05% Triton X-100).
9. Incubate cells with secondary antibodies (see Table 1) diluted in PBS^{++} for 3 h at room temperature or overnight at 4°C.
10. Wash cells 5× 10 min with PBS^{+} at room temperature.
11. Wash 1× 5 min in PBS at room temperature.
12. Stain with Hoechst dye at 2 μg/mL for 5 min in PBS.
13. Wash 3× 5 min in PBS.
14. Image with a light microscope equipped for epifluorescence.

3.6.4. Additional Assays Used for the Validation of Human iPSCs

In addition to the above described assays, other criteria are used to characterize and validate human iPSC lines, including evaluation of expression levels of iPSC markers, assessment of gene activation, chromosomal stability, and potential of the cells to differentiate (see Sect. 3.6.5). Activation of the endogenous alleles of the pluripotency inducing factors (i.e., *c-MYC*, *SOX2*, *KLF4*, *OCT4*) as well as other key markers of pluripotency (e.g., *NANOG*) coupled with downregulation of the viral expressed factors are critical steps in generating iPSCs (1–3, 17, 28). Quantitative RT-PCR is a valuable tool to assess expression of stem cell markers. With this assay, relative expression levels can be assessed over time or between different iPSC lines for activation of endogenous genes, as well as monitoring expression of the viral transgenes. As these assays are

relatively straight forward, detailed methods are not provided here. The assay begins with the extraction of RNA from the iPSCs, which is then used as a template by a reverse-transcriptase reaction to generate cDNA. The cDNA of interest, determined by the primers chosen, is quantified by PCR amplification and product levels monitored as a function of real time to provide a measure of the initial concentration of RNA (29, 30). There are numerous commercially available kits for RNA purification, primer design, cDNA generation, and RT-PCR that have been successfully used. Table 3 provides a list of primers that we have successfully used in

Table 3
Validated human iPSC primers for SYBR green real-time RT-PCR

Primer	Tm	Sequence
GDF3 Forward	60.0	AAATGTTTGTGTTGCGGTCA
GDF3 Reverse	60.0	TCTGGCACAGGTGTCTTCAG
ACTB Forward	60.4	TGAAGTGTGACGTGGACATC
ACTB Reverse	58.4	GGAGGAGCAATGATCTTGAT
NANOG Forward	58.4	TGAACCTCAGCTACAAACAG
NANOG Reverse	58.4	TGGTGGTAGGAAGAGTAAAG
hTERT Forward	58.4	TGTGCACCAACATCTACAAG
hTERT Reverse	60.4	GCGTTCTTGGCTTTCAGGAT
OCT4 endogenous Forward	60.4	CCTCACTTCACTGCACTGTA
OCT4 endogenous Reverse	58.4	CAGGTTTTCTTTCCCTAGCT
OCT4 total Forward	60.4	AGCGAACCAGTATCGAGAAC
OCT4 total Reverse	60.4	TTACAGAACCACACTCGGAC
SOX2 endogenous Forward	60.2	CCCAGCAGACTTCACATGT
SOX2 endogenous Reverse	60.4	CCTCCCATTTCCCTCGTTTT
SOX2 total Forward	60.4	AGCTACAGCATGATGCAGGA
SOX2 total Reverse	60.4	GGTCATGGAGTTGTACTGCA
KLF4 endogenous Forward	60.4	GATGAACTGACCAGGCACTA
KLF4 endogenous Reverse	60.4	GTGGGTCATATCCACTGTCT
KLF4 total Forward	62.4	TCTCAAGGCACACCTGCGAA
KLF4 total Reverse	60.4	TAGTGCCTGGTCAGTTCATC
DNMT3B Forward	60.4	ATAAGTCGAAGGTGCGTCGT
DNMT3B Reverse	58.4	GGCAACATCTGAAGCCATTT

Primer sequences match those published by Chan et al. (17).

our lab for validation of human iPSCs with SYBR green real-time RT-PCR. Sequences of additional primers used for the assessment of human iPSC lines can be obtained from published protocols (7, 16, 17, 31). The reader is encouraged to consult these publications for information on the details of these assays.

Gene activation is determined in part by the epigenetic status of promoter DNA methylation. Methylated CpG islands are usually clustered around regulatory regions of genes and are associated with gene inactivation. Thus, the determination of the methylation status of promoters flanking pluripotency markers is another useful tool to evaluate human iPSCs, where the promoter regions of *OCT4*, *NANOG*, and other pluripotency markers should be hypomethylated relative to the DNA methylation status of the parent fibroblast cells. The methylation status of genomic DNA can be determined by bisulfite sequencing. In this procedure, bisulfite treatment of genomic DNA is performed using commercially available kits (for example, the EpiTect Bisulfite Kit by Qiagen) according to the manufacturer's recommendations. The modified DNA is then amplified by PCR using primers within the promoters of interest. The amplified sequences are cloned and randomly selected clones sequenced. For procedures and PCR primer information, the reader is referred to published methods (6, 8).

Cell propagation can result in chromosomal instability. Thus, karyotyping is performed to ensure that propagated human iPSCs maintain a stable karyotype that is equivalent to the one of the fibroblasts they were derived from. Different methods for karyotyping have been developed and the reader is referred to protocols used in the context of iPSCs (20, 22, 32).

3.6.5. Assessment of the Potential of Human iPSCs to Differentiate

If the presumptive iPSCs are indeed pluripotent stem cells, they should be capable of differentiation into cells derived from any of the three embryonic germ layers. The in vivo pluripotency of human iPSCs can be assessed by their potential to form teratomas in immunocompromised mice. Human iPSCs are injected into the mice and the resulting teratomas histologically assessed according to published protocols (6, 8, 22). True pluripotent human iPSCs should form teratomas comprised of tissues derived from all three embryonic germ layers. This technique, however, takes at least 8 weeks to perform and requires specialized care and evaluation of immunocompromised mice. Alternatives include in vitro differentiation to see if putative iPSC lines can form cells derived from all three embryonic germ layers. The protocols to induce differentiation in vitro into different cell types vary greatly depending on the desired cell type, and the reader is referred to the literature most appropriate to the cell type to be derived. The potential of human iPSCs to differentiate into any cell type of interest makes them a powerful tool for developing human models of toxicity. Here, we will describe a two-step method to derive neurons from human iPSCs. In the first step, human iPSCs are induced to

form neuronal progenitors, which are then further differentiated into neurons in the second step.

3.6.5.1. Derivation of Neuronal Progenitor Cells

Recently, methods have been published to perform neuronal inductions on a feeder-free system (5). Derivation of neurons from human iPSCs in the absence of feeder cells has several advantages, including higher yield of neurons, faster differentiation, and easier assessment of derived neurons. We perform all our neuronal differentiations with human iPSCs growing on Matrigel. SMAD signaling has been shown to play an important role during neural induction in several different systems (33–36). A recent study provides evidence that the combined use of Noggin, a bone morphogenic protein (BMP) inhibitor and SB431542, an inhibitor of the Lefty/Activin/TGFβ pathways greatly increases the efficiency of neural induction (5).

To induce neuronal progenitor cells, human iPSC colonies are dissociated with Accutase, and the resulting single-cell suspension is plated onto Matrigel-coated 24-well plates. The density at which the human iPSCs are plated at this time affects their tendency to differentiate towards PAX6 positive CNS or PAX6 negative neural crest-like progenitors, with higher plating densities favoring differentiation towards PAX6 positive cells (5). Three to five days after plating, neuralization is initiated by incubating the cells in neuralization medium containing two different compounds that inhibit SMAD signaling (5). The potential neuroprogenitor cells are evaluated by their expression of neuronal progenitor cell markers (PAX6, NESTIN) and the absence of human iPSC markers (OCT4, TRA-160, TRA-1-81, SSEA4) using the immunocytochemical staining and quantitative RT-PCR described in Sects. 3.6.3 and 3.6.4, respectively (Fig. 9).

Procedure

Preparation

1. Prepare Matrigel-coated 24-well plates according to manufacturer's instructions.
2. Remove all differentiated colonies or parts of colonies from the culture.
3. Immediately before use thaw Accutase solution.

Neuralization of human iPSCs

1. Aspirate media.
2. Wash cells with D-PBS once (2.5 mL/well).
3. Aspirated D-PBS completely.
4. Incubate with 1 mL/10 cm^2 of culture surface (i.e., 1 mL/well of a 6-well plate) of Accutase solution in the incubator for no more than 8 min.

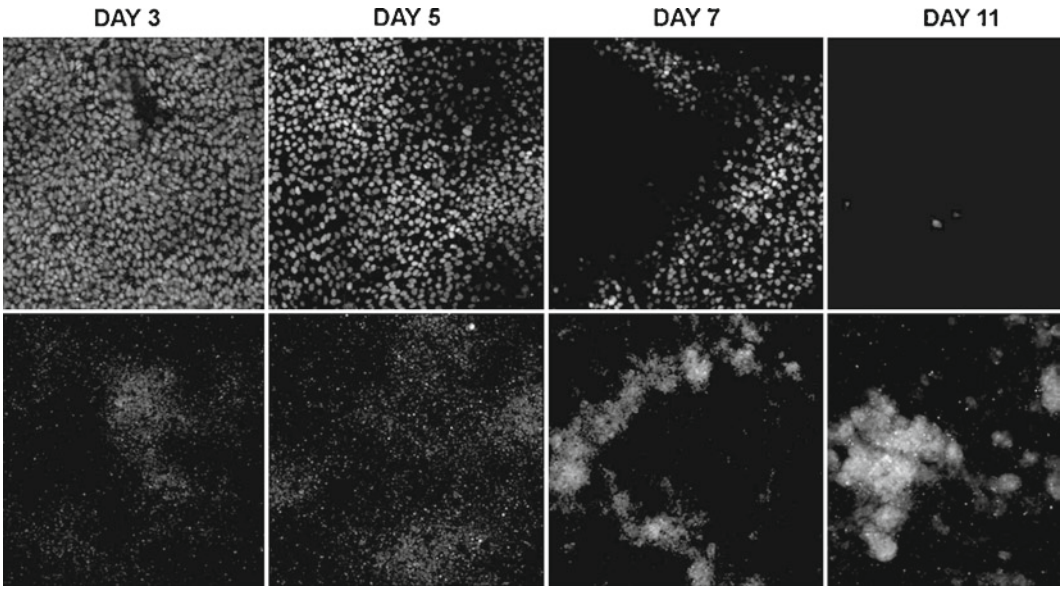

Fig. 9. Neural induction. Human iPSC line BG8 was exposed to noggin, a bone morphogenic protein (BMP) inhibitor and SB431542, a compound that inhibits the Lefty/Activin/TGFβ pathways to induce the formation of neural progenitor cells. The expression of the iPSC marker OCT4 (*top*) and the neural progenitor marker PAX6 (*bottom*) as well as other markers of neuralization (data not shown) was examined by immunofluorescence staining. Over a 3–11 day period of neural induction, the level of OCT4 expression decreases while the signal of PAX6 increases.

5. Add 3 mL of mTeSR1 media containing 10 μm ROCK inhibitor for every 1 mL of Accutase solution.
6. Pipette cells up and down several times to wash cells off the dish surface and to break up the remaining cell clumps into a single-cell suspension using 5 mL glass serological pipettes.
7. Transfer cell suspension into 15 mL conical tube.
8. Centrifuge cells 200 × *g* for 5 min at room temperature.
9. Aspirate medium and resuspend cells in 4 mL of mTeSR1 media containing 10 μm ROCK inhibitor.
10. Centrifuge cells 200 × *g* for 5 min at room temperature.
11. Resuspend cells in 1 mL of mTeSR1 media containing 10 μm ROCK inhibitor.
12. Count cells and dilute them to appropriate concentration: for the derivation of anterior CNS progenitor cells we plate at 18,000 cells/cm^2 as reported by others (5).
13. Plate cells onto Matrigel-coated dishes (we usually use 96-well plates for neuronal differentiations).
14. Feed and observe cells daily.
15. Within 3–5 days (depending on the human iPSC line) the cells are confluent and neuralization is initiated.

16. Cells are exposed to 10 μm SB431542 and 500 ng/mL Noggin in neuralization media for 5 days with a daily change of media.
17. Neuronal differentiation is initiated between day 5 and 11 and the protocols vary depending on the neuron type desired.

Once neuronal precursors have been derived and validated, they can be differentiated into different types of neurons. Depending on the neuronal type to be derived, the neuronal progenitor cells are exposed to varying series of combinations of factors for varying time periods. The description of all the different neuronal patterning protocols is beyond the scope of this chapter and the reader is referred to the diverse published methods. In principle, methods that have been developed for differentiation of hES cells are often transferrable to human iPSCs. For example, Studer and colleagues have reported the directed differentiation of both midbrain dopamine and spinal motor neurons from hES cells and human iPSCs using the same method (5). Indeed, these methods were originally developed with hES cells (37, 38). A selection of recently published papers and reviews with methods for generating a variety of neural cell types (e.g., neural progenitors, neural crest cells, peripheral sensory neurons, dopaminergic neurons, spinal motor neurons, serotonergic neurons, striatal DARPP32 positive neurons, inhibitory GABAergic, and excitatory glutamatergic neurons) is provided as a reference (37–47).

4. Notes

1. It is important to keep track of the number of passages performed with the fibroblasts. iPSCs appear to be more easily derived from early passage fibroblasts, thus cryopreservation of early passage fibroblasts is crucial.
2. The intensity of immunofluorescence in live cell imaging is much less than seen in typical immunocytochemistry. For this reason, positive and negative controls are vital for proper interpretation of live-cell fluorescence images. For optimal results, antibody concentrations should be titrated on positive control cells such as established human iPSC lines or hES lines.
3. Matrigel and SNL feeders along with the corresponding media (mTeSR1 and hES respectively) are both adequate methods for maintaining iPSC cells. However, Matrigel is preferable when growing to high density, live-cell imaging, or freezing.
4. It is important to closely watch the progress of the dispase digestion. As soon as the edges of the iPSC colonies start to

curl up, the enzyme solution has to be aspirated and the cells washed. Extending the dispase treatment by even just 1–2 min can result in the colonies lifting of the dish surface and therefore in the loss of the cells.

5. We observed no difference in colony number or size between iPSCs obtained from scraping colonies with a 5 mL glass serological pipette or a cell scraper; we typically use cell scrapers because they are easier to use.
6. We observed that pipetting human iPSC colonies with glass serological pipettes (rather than plastic pipettes) leads to larger cell aggregates and better survival of the cells during passaging and the freeze/thawing procedure.
7. If at this stage a transfer of the human iPSCs onto Matrigel is required, the cells can be plated onto dishes precoated with Matrigel as described in Sect. 3.5.1. We observed that since the CTK treatment so efficiently eliminates the SNL feeder cells preadsorption of SNL cells on gelatin before the transfer of the human iPSCs to Matrigel is not necessary.

Acknowledgments

We would like to thank Angela Ellen Tidball for the artwork and illustration of Fig. 1 of this chapter. Also, we are grateful to Dr. Lorenz Studer and Stuart Chambers for personal communications on implementing their published neuralization protocols. AMT was supported by the Vanderbilt Brain Institute. KCE was supported by a Doris Duke Clinical Scientist Development Award, NIH/NINDS K08NS050484, and the Tuberous Sclerosis Alliance. This work was further supported by a Hobbs Discovery Award from the Vanderbilt Kennedy Center (KCE, ABB), an equipment grant from the Vanderbilt Institute for Clinical and Translational Research 1UL 1RR024975 NCRR/NIH (KCE, ABB), core support from NIH NICHD grant P30HD15052 (ABB), and research support from the NIH/NIEHS grant RO1ES016931 (ABB).

References

1. Takahashi K, Tanabe K, Ohnuki M, Narita M, Ichisaka T, Tomoda K, Yamanaka S (2007) Induction of pluripotent stem cells from adult human fibroblasts by defined factors. Cell 131:861–872
2. Yu J, Vodyanik MA, Smuga-Otto K, Antosiewicz-Bourget J, Frane JL, Tian S, Nie J, Jonsdottir GA, Ruotti V, Stewart R, Slukvin II, Thomson JA (2007) Induced pluripotent stem cell lines derived from human somatic cells. Science 318:1917–1920
3. Park IH, Zhao R, West JA, Yabuuchi A, Huo H, Ince TA, Lerou PH, Lensch MW, Daley GQ (2008) Reprogramming of human somatic cells to pluripotency with defined factors. Nature 451:141–146

4. Nakagawa M, Koyanagi M, Tanabe K, Takahashi K, Ichisaka T, Aoi T, Okita K, Mochiduki Y, Takizawa N, Yamanaka S (2008) Generation of induced pluripotent stem cells without Myc from mouse and human fibroblasts. Nat Biotechnol 26:101–106
5. Chambers SM, Fasano CA, Papapetrou EP, Tomishima M, Sadelain M, Studer L (2009) Highly efficient neural conversion of human ES and iPS cells by dual inhibition of SMAD signaling. Nat Biotechnol 27:275–280
6. Aasen T, Raya A, Barrero MJ, Garreta E, Consiglio A, Gonzalez F, Vassena R, Bilic J, Pekarik V, Tiscornia G, Edel M, Boue S, Belmonte JCI (2008) Efficient and rapid generation of induced pluripotent stem cells from human keratinocytes. Nat Biotechnol 26:1276–1284
7. Takahashi K, Okita K, Nakagawa M, Yamanaka S (2007) Induction of pluripotent stem cells from fibroblast cultures. Nat Protoc 2:3081–3089
8. Takahashi K, Yamanaka S (2006) Induction of pluripotent stem cells from mouse embryonic and adult fibroblast cultures by defined factors. Cell 126:663–676
9. Lin T, Ambasudhan R, Yuan X, Li W, Hilcove S, Abujarour R, Lin X, Hahm HS, Hao E, Hayek A, Ding S (2009) A chemical platform for improved induction of human iPSCs. Nat Methods 6:805–808
10. Hockemeyer D, Soldner F, Cook EG, Gao Q, Mitalipova M, Jaenisch R (2008) A drug-inducible system for direct reprogramming of human somatic cells to pluripotency. Cell Stem Cell 3:346–353
11. Hong H, Takahashi K, Ichisaka T, Aoi T, Kanagawa O, Nakagawa M, Okita K, Yamanaka S (2009) Suppression of induced pluripotent stem cell generation by the p53-p21 pathway. Nature 460:1132–1135
12. Kaji K, Norrby K, Paca A, Mileikovsky M, Mohseni P, Woltjen K (2009) Virus-free induction of pluripotency and subsequent excision of reprogramming factors. Nature 458:771–775
13. Okita K, Nakagawa M, Hyenjong H, Ichisaka T, Yamanaka S (2008) Generation of mouse induced pluripotent stem cells without viral vectors. Science 322:949–953
14. Woltjen K, Michael IP, Mohseni P, Desai R, Mileikovsky M, Hämäläinen R, Cowling R, Wang W, Liu P, Gertsenstein M, Kaji K, Sung H-K, Nagy A (2009) piggyBac transposition reprograms fibroblasts to induced pluripotent stem cells. Nature 458:766–770
15. Yoshida Y, Takahashi K, Okita K, Ichisaka T, Yamanaka S (2009) Hypoxia enhances the generation of induced pluripotent stem cells. Cell Stem Cell 5:237–241
16. Ohnuki M, Takahashi K, Yamanaka S (2009) Generation and characterization of human induced pluripotent stem cells. Curr Protoc Stem Cell Biol Chapter 4:Unit 4A.2
17. Chan EM, Ratanasirintrawoot S, Park IH, Manos PD, Loh YH, Huo H, Miller JD, Hartung O, Rho J, Ince TA, Daley GQ, Schlaeger TM (2009) Live cell imaging distinguishes bona fide human iPS cells from partially reprogrammed cells. Nat Biotechnol 27:1033–1037
18. Hanna J, Saha K, Pando B, van Zon J, Lengner CJ, Creyghton MP, van Oudenaarden A, Jaenisch R (2009) Direct cell reprogramming is a stochastic process amenable to acceleration. Nature 462:595–601
19. Friedrich G, Soriano P (1993) Insertional mutagenesis by retroviruses and promoter traps in embryonic stem cells. Methods Enzymol 225:681–701
20. Sjögren-Jansson E, Zetterström M, Moya K, Lindqvist J, Strehl R, Eriksson PS (2005) Large-scale propagation of four undifferentiated human embryonic stem cell lines in a feeder-free culture system. Dev Dyn 233:1304–1314
21. Xu C, Inokuma MS, Denham J, Golds K, Kundu P, Gold JD, Carpenter MK (2001) Feeder-free growth of undifferentiated human embryonic stem cells. Nat Biotechnol 19:971–974
22. Amit M, Carpenter MK, Inokuma MS, Chiu CP, Harris CP, Waknitz MA, Itskovitz-Eldor J, Thomson JA (2000) Clonally derived human embryonic stem cell lines maintain pluripotency and proliferative potential for prolonged periods of culture. Dev Biol 227:271–278
23. Mollamohammadi S, Taei A, Pakzad M, Totonchi M, Seifinejad A, Masoudi N, Baharvand H (2009) A simple and efficient cryopreservation method for feeder-free dissociated human induced pluripotent stem cells and human embryonic stem cells. Hum Reprod 24:2468–2476
24. Kleinman HK, McGarvey ML, Liotta LA, Robey PG, Tryggvason K, Martin GR (1982) Isolation and characterization of type IV procollagen, laminin, and heparan sulfate proteoglycan from the EHS sarcoma. Biochemistry 21:6188–6193
25. Bissell DM, Arenson DM, Maher JJ, Roll FJ (1987) Support of cultured hepatocytes by a laminin-rich gel. Evidence for a functionally significant subendothelial matrix in normal rat liver. J Clin Invest 79:801–812

26. Watanabe K, Ueno M, Kamiya D, Nishiyama A, Matsumura M, Wataya T, Takahashi JB, Nishikawa S, Nishikawa S-i, Muguruma K, Sasai Y (2007) A ROCK inhibitor permits survival of dissociated human embryonic stem cells. Nat Biotechnol 25:681–686
27. O'Connor MD, Kardel MD, Iosfina I, Youssef D, Lu M, Li MM, Vercauteren S, Nagy A, Eaves CJ (2008) Alkaline phosphatase-positive colony formation is a sensitive specific, and quantitative indicator of undifferentiated human embryonic stem cells. Stem Cells 26: 1109–1116
28. Silva J, Nichols J, Theunissen TW, Guo G, van Oosten AL, Barrandon O, Wray J, Yamanaka S, Chambers I, Smith A (2009) Nanog is the gateway to the pluripotent ground state. Cell 138:722–737
29. Lutfalla G, Uze G (2006) Performing quantitative reverse-transcribed polymerase chain reaction experiments. Methods Enzymol 410:386–400
30. Wong ML, Medrano JF (2005) Real-time PCR for mRNA quantitation. Biotechniques 39:75–85
31. Ungrin M, O'Connor M, Eaves C, Zandstra PW (2007) Phenotypic analysis of human embryonic stem cells. Curr Protoc Stem Cell Biol Chapter 1:Unit 1B.3
32. Totonchi M, Taei A, Seifinejad A, Tabebordbar M, Rassouli H, Farrokhi A, Gourabi H, Aghdami N, Hosseini-Salekdeh G, Baharvand H (2010) Feeder- and serum-free establishment and expansion of human induced pluripotent stem cells. Int J Dev Biol 54(5): 877–886.
33. Elkabetz Y, Panagiotakos G, Al Shamy G, Socci ND, Tabar V, Studer L (2008) Human ES cell-derived neural rosettes reveal a functionally distinct early neural stem cell stage. Genes Dev 22:152–165
34. Lee H, Shamy GA, Elkabetz Y, Schofield CM, Harrsion NL, Panagiotakos G, Socci ND, Tabar V, Studer L (2007) Directed differentiation and transplantation of human embryonic stem cell-derived motoneurons. Stem Cells 25:1931–1939
35. Smith JR, Vallier L, Lupo G, Alexander M, Harris WA, Pedersen RA (2008) Inhibition of Activin/Nodal signaling promotes specification of human embryonic stem cells into neuroectoderm. Dev Biol 313:107–117
36. Valenzuela DM, Economides AN, Rojas E, Lamb TM, Nuñez L, Jones P, Lp NY, Espinosa R, Brannan CI, Gilbert DJ (1995) Identification of mammalian noggin and its expression in the adult nervous system. J Neurosci 15:6077–6084
37. Li X-J, Du Z-W, Zarnowska ED, Pankratz M, Hansen LO, Pearce RA, Zhang S-C (2005) Specification of motoneurons from human embryonic stem cells. Nat Biotechnol 23:215–221
38. Perrier AL, Tabar V, Barberi T, Rubio ME, Bruses J, Topf N, Harrison NL, Studer L (2004) Derivation of midbrain dopamine neurons from human embryonic stem cells. Proc Natl Acad Sci U S A 101:12543–12548
39. Hu B-Y, Zhang S-C (2009) Differentiation of spinal motor neurons from pluripotent human stem cells. Nat Protoc 4:1295–1304
40. Aubry L, Bugi A, Lefort N, Rousseau F, Peschanski M, Perrier AL (2008) Striatal progenitors derived from human ES cells mature into DARPP32 neurons in vitro and in quinolinic acid-lesioned rats. Proc Natl Acad Sci U S A 105:16707–16712
41. Zhang X-Q, Zhang S-C (2010) Differentiation of neural precursors and dopaminergic neurons from human embryonic stem cells. Methods Mol Biol 584:355–366
42. Carpenter M, Inokuma M, Denham J, Mujtaba T, Chiu C, Rao M (2001) Enrichment of neurons and neural precursors from human embryonic stem cells. Exp Neurol 172:383–397
43. Gaspard N, Bouschet T, Hourez R, Dimidschstein J, Naeije G, Van Den Ameele J, Espuny-Camacho I, Herpoel A, Passante L, Schiffmann SN, Gaillard A, Vanderhaeghen P (2008) An intrinsic mechanism of corticogenesis from embryonic stem cells. Nature 455:351–357
44. Goldstein RS, Pomp O, Brokhman I, Ziegler L (2010) Generation of neural crest cells and peripheral sensory neurons from human embryonic stem cells. Methods Mol Biol 584: 283–300
45. Ozolek JA, Jane EP, Esplen JE, Petrosko P, Wehn AK, Erb TM, Mucko SE, Cote LC, Sammak PJ (2010) In vitro neural differentiation of human embryonic stem cells using a low-density mouse embryonic fibroblast feeder protocol. Methods Mol Biol 584:71–95
46. Fasano CA, Chambers SM, Lee G, Tomishima MJ, Studer L (2010) Efficient derivation of functional floor plate tissue from human embryonic stem cells. Cell Stem Cell 6:336–347
47. Cooper O, Hargus G, Deleidi M, Blak A, Osborn T, Marlow E, Lee K, Levy A, Perez-Torres E, Yow A, Isacson O (2010) Differentiation of human ES and Parkinson's disease iPS cells into ventral midbrain dopaminergic neurons requires a high activity form of SHH, FGF8a and specific regionalization by retinoic acid. Mol Cell Neurosci 45:258–266

Chapter 3

Neural Stem Cells

Roshan Tofighi, Christoffer Tamm, Michaela Moors, Wan Norhamidah Wan Ibrahim, and Sandra Ceccatelli

Abstract

Cells can be defined as "stem cells" when able to self-renew and differentiate into tissue-characteristic cells. Neural stem cells (NSCs) derived from the nervous system are able to generate neuronal and glial cells and are present not only in the developing nervous system, but also in specific regions of the adult brain. While embryonic NSCs play an essential role in the development and maturation of the nervous system, adult NSCs may have a role in the normal functions of the brain, including learning, memory, and emotional responses. Growing evidence points to developmental exposure to chemicals as a possible cause of nervous system disorders. The developing nervous system is particularly vulnerable to toxic agents, which may cause long-lasting effects that may be manifested later in life. The majority of the chemicals in commerce have not been tested for developmental neurotoxicity and the limited information currently available points to the need for more experimental research specially designed to address this issue. We have implemented the use of NSCs as experimental models for developmental neurotoxicity studies. Here, we provide a short overview of some data obtained with NSCs and a detailed description of the cell culture protocols.

Key words: Neural stem cells, Neurotoxicity, Proliferation, Differentiation, Migration

1. Introduction

Over recent years, there has been an increasing interest for the use of stem cells in various biomedical applications, including pharmacological and toxicological research. We have established neural stem cell (NSC) cultures as in vitro models for neurodevelopmental toxicity studies with the aim to implement new experimental systems to test chemicals and predict potential neurotoxicity. The following chapter provides a short overview of practical applications of NSCs in neurotoxicology, based on the experience of our group. The continuous ongoing work to optimize the NSC-derived in vitro models is expected to provide novel and powerful

Michael Aschner et al. (eds.), *Cell Culture Techniques*, Neuromethods, vol. 56,
DOI 10.1007/978-1-61779-077-5_3,

assays to directly address one of the most relevant public health issues namely developmental neurotoxicity.

1.1. Neural Stem Cells

Cells can be defined as "stem cells" when they fulfill two main criteria:

1. Self-renewal – The cells have to be able to divide and proliferate in a way that gives rise to at least one new stem cell, and this can be achieved by either symmetric or asymmetric cell division. Symmetric cell division results in two daughter cells exhibiting similar properties as the dividing cell, whereas asymmetric cell division generates two different daughter cells. Most often one cell remains a de facto stem cell, while the other becomes a progenitor cell with more lineage restrictions. During neurodevelopment it is thought that at early stage there is mainly symmetric cell division (1), while later on, it shifts to asymmetric cell division with generation of cells differentiating into postmitotic neural cells and new stem cells.
2. Multilineage differentiation – Many cells can proliferate and bring about descendants of the same cell type (e.g., fibroblasts and myoblasts). Stem cells are able to differentiate into two or more cells characteristic of the tissue from which they have been isolated. For example, a NSC can differentiate into cells present within the central nervous system (CNS), such as neurons, astrocytes, and oligodendrocytes (2, 3).

This minimal definition has lead to a classification of cells, which possess these properties based on the tissue organ from where the cells have been isolated. Hence, NSCs are derived from the CNS, whilst embryonic stem cells are derived from the blastocysts. Tissue-specific stem cells, other than NSCs, have been identified in the hematopoietic system, pancreatic islets, liver, intestine, and skin. Stem cells have been described in a wide range of tissues, and these cells have been shown to be able to divide, self-renew, and differentiate into tissue-characteristic cells (4). In their respective organs, the stem cells reside in designated stem cell niches, which provide a controlled environment for proliferation and differentiation. The NSC niches include characteristic cytoarchitectures of the specific anatomical areas of the CNS, and several other cellular and molecular prerequisites, such as proximity to the cerebrospinal fluid and blood vessels, cell-to-cell interactions and signaling, and unique basal lamina and extracellular matrix (5). It is generally agreed that NSCs exist in a variety of developmental time stages. So far multipotent fetal NSCs have been found and isolated from numerous different brain regions of the embryonic CNS, such as the olfactory bulb, subventricular zone (SVZ), hippocampus, cerebellum, cerebral cortex, and spinal

cord (6–12). Although some suggest that not all CNS stem cells can be identified by the expression of a single protein (13, 14), the class VI intermediate filament protein nestin (an acronym for neuroepithelial stem cell protein) (15) has been shown to be transiently expressed in most neural stem or progenitor cells. Upon differentiation nestin is downregulated and replaced by other intermediate filament proteins such as glial fibrillary acidic protein (GFAP) in astrocytes or neurofilaments in neuronal cells (14–16).

During early brain development, NSCs take on positional identity within the neural tube via adjacent tissue-secreted morphogen signaling. Positional characteristics along the anteroposterior axis are specified by fibroblast growth factors (FGF), Wnt, and retinoid family ligands, whereas the dorsoventral axis is specified by the antagonistic actions of bone morphogenetic proteins (BMPs), transforming growth factor β (TGFβ) ligands, and Sonic Hedgehog (SHH) (17). FGF2 promotes proliferation of cortical NSCs in vivo (18), but is as well, together with epidermal growth factor (EGF), the only ligand known to promote NSC proliferation in vitro (19). Part of NSC proliferation signaling involves the suppression of programmed cell death. For example, the absence of retinoic acid, erythropoietin, or Notch receptor signaling markedly increases apoptosis during early gestation CNS and decrease proliferation (20–22). Notch signaling is also known to inhibit neuronal differentiation and maintain NSCs in a proliferative state (23). Activation of Notch leads to upregulation of Hes1 and Hes5, transcription factors with a conserved basic helix-loop-helix (bHLH) domain in their DNA binding region. Although Notch and Notch ligands are not expressed during early CNS development, NSCs obtained from later developmental stages seem to depend on Notch signaling to stay alive, proliferative, and undifferentiated (24). Hes1 and Hes5 upregulation induce NSCs proliferation and repression of the neurogenic bHLH genes (25, 26). The neurogenic bHLH transcription factors, such as Math1/2, Ngn1/2, Mash1, and NeuroD, are required for promoting neurogenesis and inhibition of gliogenesis (27, 28). These neurogenic bHLH genes also seem to be essential for sustaining the stemness in nearby NSC via Notch signaling (29). Overall, NSCs change their competency during development and sequentially give rise to different cell types. Thus, the maintenance of NSCs until the late developmental stages is essential to warrant the correct magnitude and diversity of cells. Cultures of NSCs in vitro can be induced to differentiate simply by removing mitogens, which leads to spontaneous differentiation to various proportions of neurons, astrocytes, and oligodendrocytes (2). By adding various growth factors, such as platelet-derived growth factor (PDGF), ciliary neurotrophic factor (CNTF), BMPs, or the thyroid hormone T3, the commitment of the differentiating

cells can be altered and directed depending on during which developmental stage the NSCs were derived (2, 30–32).

1.2. Adult Neural Stem Cells

In contrast to formerly held beliefs that the adult brain is a static system without scope for cell replacement and regeneration, there is now good evidence for the differentiation of neural cells from stem cells in the adult brain with the ability to integrate into the complex circuitry of the CNS (see (33)). Scientists started to suspect active mitosis in the adult brain tissue in the years spanning from beginning of the twentieth century to the 1960s (34, 35). Due to methodological limitations, this could not been shown until the middle of the 1960s when Altman started to label dividing cells with (^{3}H)-thymidine incorporated into the newly formed DNA (36, 37). Kaplan combined this labeling with electron microscopy (38) and showed that neurogenesis occurred in the 3-month-old adult brain of rodents. Neurogenesis has been characterized in at least two areas in the adult brain: the hippocampus (37–39) and the olfactory bulb (40, 41). The source of these newly formed neuronal cells has also been a subject to investigation and the two brain regions, which primarily have been ascribed the formation of the neurons, are the subgranular zone (SGZ) of the dentate gyrus in the hippocampus (42) and the SVZ of the lateral ventricle (LV) (3). The SVZ is the larger germinal zone and is situated adjacent to the ependyma of the LV wall. Cells from this area have been found to migrate to the olfactory bulb where they differentiate into mature granule cells and periglomerular cells, the two foremost interneurons in this part of the brain (43). Since it has been estimated that approximately 30,000 new interneurons are formed everyday in the mouse adult brain all through life, this level of neurogenesis led to the belief that there exists asymmetrically dividing self-renewing stem cells within the SVZ (40).

When cultured, cells from the SVZ grow adherently in cell culture dishes in serum-free medium supplemented with EGF and/or fibroblast growth factor-2 (FGF2). These act as mitogens for the cells both in vitro (11, 44) and in vivo (45, 46). After a while, the cells detach from the substrate and produce characteristic free floating aggregates of closely grouped cells, referred to as neurospheres. In their proliferative state, cells in the neurosphere express the stem cell-specific intermediate filament protein nestin. Immunohistochemical staining of brain sections also show nestin-expressing cells in the SVZ as well as the ependymal layer of the LV (47, 48). Adult NSCs (aNSCs) can also differentiate into neurons, astrocytes, and oligodendrocytes upon removal of EGF and FGF (11, 49). Nestin-expression, self-renewal, and multilineage differentiation properties confirm that these cells are tissue-specific stem cells, although clonal analyses of neurosphere cells have shown that only ~16% of the cells can be considered to

be de facto stem cells (50). The main part of the remaining cells is stem cell-derived progenitors with a more limited proliferation and differentiation potential (51). However, it is still unclear which cells in the SVZ are the resident aNSCs. Several cell types have been proposed, including astrocytes (52), multiciliated ependymal cells (53), and subependymal cells (48).

1.3. Neural Stem Cell Biomedical Applications

The wide interest in NSCs is mainly based on the perceived therapeutic potential these cells could offer in repair after brain injury or in the treatment for neurodegenerative diseases. Brain injuries, e.g. subsequent to stroke, have been shown to stimulate proliferation in both the SGZ and the SVZ with subsequent migration to the damaged area (54–56). Alterations in the aNSC-containing brain areas have also been seen in chronic degenerative neurological disorders, such as Huntington's disease and Alzheimer's disease. In these diseases, proliferation and neurogenesis are increased (57, 58). On the other hand, in Parkinson's disease, proliferation in these areas has been shown to be impaired (59). The harvesting of stem cells, which can be amplified in culture and later used for repair and regeneration in cell replacement therapies, has been the driving force that has made stem cells currently one of the hottest topics in science.

An additional application of stem cell-based systems is in the area of drug development and toxicity testing. Exposure to chemical agents, either man-made or naturally occurring, can cause alterations in the normal activity and/or structure of various target organs, including the nervous system.

1.4. Neurotoxicity

The complexity and the special features of the nervous system make it particularly vulnerable to insults of various origins. The very high metabolic rate makes the CNS dependent on continuous aerobic glycolysis and subsequently, very sensitive to any aberrations in the supply of glucose and oxygen (see (60)). The high oxygen consumption, together with a moderate level of antioxidant activity and a high quantity of polyunsaturated fatty acids, renders the nervous system a prime target for oxidative stress (see (61)).

The adult brain is protected by the blood–brain barrier, an anatomical barrier formed by specialized endothelial cells with tight junctions. Consequently, many endogenous and exogenous toxic agents are prevented to enter the adult brain, although some toxicants can cross the barrier by passing through the membranes of the endothelial cell by diffusion or by active transport. In the developing nervous system, the blood–brain barrier is not fully developed until at roughly 6 months of age in humans (62), which predisposes fetuses and young infants to brain injuries by toxicants that do not affect the adult nervous system.

Brain development occurs in different phases and each developmental stage is reached according to a tightly regulated program.

The different parts of the nervous system are built by cell proliferation, migration, and differentiation, and proper functioning requires a precise number of cells in the right place with the correct characteristics (63). Insults interfering with these mechanisms can consequently result in adverse changes in the nervous system. For instance, disruption of proliferation can inhibit the formation of subpopulations of neurons that were forming at the specific time point of the insult. Migration is even more sensitive, because it can be disrupted either directly or by effects on neighboring cells or important supporting structures, e.g. radial glia. Moreover, disruptions in programmed cell death, which is regulated by growth factors, cytokines, and neurotransmitters (64–66), can kill neurons that should not have been removed, or promote the survival of redundant cells, which are produced during neurogenesis to ensure the correct formation of a given structure and, under normal conditions, afterwards are eliminated. In addition to neuronal cells, glial cells can also be affected by developmental injuries. The brain growth spurt, which is the period when the brain grows most rapidly, is predominantly characterized by the proliferation of astrocytes and oligodendrocytes, glial cells that are responsible for a variety of functions, such as neuronal support and maintenance, and myelin production. This stage of development has been shown to be sensitive to toxic insults, suggesting that glial cells are also a target for neurotoxicants (see (67)). Interestingly, the consequences of a developmental damage may not necessarily be apparent until a critical age when a neurodevelopmental defect may be unmasked or precipitated by a subsequent insult (see (68)).

During this modern era, the number of new chemicals appearing annually has increased enormously. Exposure to toxic substances before or after birth has been identified as one key risk factor for neurodevelopmental disorders. Consequently, the need for developmental neurotoxicity studies of environmental/industrial chemicals has been deemed to be of utmost importance. Due to the vast number of chemicals, the amount of animals needed for safety evaluation has substantially increased. Progress in mechanistic research and the increasing awareness of the need to reduce, replace, and refine animal testing has led to the development of alternative methods. Increasingly, in vitro methods have been applied in many research fields, including toxicology. The use of different cell culture models for predicting in vivo effects of neurotoxic chemicals has been developed in the attempt to provide rapid screening systems with a battery of highly sensitive assays. Although alternative testing will not be able to give the extent of information that can be retrieved from animal testing, in vitro systems allow a valuable prescreening function prior to in vivo testing. On this background, our group has established and implemented the use of rodent and human NSC as model systems for in vitro neurodevelopmental toxicity studies.

1.5. Neural Stem Cells in Neurotoxicity Studies

As mentioned above, embryonic development is a continuous process of a precisely orchestrated sequence of events, including cell proliferation, migration, differentiation, and maturation, driven by gene expression changes that are programmed both in time and space. Toxic interference with these programs will most likely give rise to malformations and/or malfunctions. NSCs appear already during the neural plate formation and are generally agreed to exist throughout the various developmental stages. It has been suggested that NSCs in fact constitute the major cell type of the early ectoderm. Hence, for studies with focus on cellular mechanisms of toxicant effects during brain development, NSCs appear an ideal in vitro model. With increased knowledge of mechanisms and the identification of measurable endpoints, it should be possible to identify patterns, i.e. unique signatures, for different classes of neurotoxicants.

These endpoints should include cell viability/death followed by mechanistic investigations at biochemical and molecular levels. NSCs also provide the unique possibility to identify and investigate alterations in the differentiation and migration potential, thereby recognizing selective targets and windows of susceptibility to a certain neurodevelopmental insult. Using these experimental approaches and the NSC line C17.2, primary culture of rat embryonic NSCs, rat and murine aNSCs, and human neurospheres as experimental models, we have investigated the effects of several neurotoxic agents and identified NSCs as highly vulnerable targets. First of all, we tested whether these cells would have the capability to undergo apoptosis via the intrinsic and extrinsic apoptotic pathways. Interestingly, we observed that while classical apoptosis inducers, such as staurosporine, could activate the mitochondrial caspase-dependent pathway, the FasL/CD95 could not induce cell death in spite of the presence of the Fas receptor and procaspase 8 (69, 70). We also studied the toxic effects of the neurotoxic metals methylmercury (MeHg) and manganese (Mn) in rat primary embryonic cortical NSCs and in the murine NSC line C17.2. Our results showed that NSCs are more sensitive to both MeHg and Mn than differentiated neuronal or glial cells. Both toxicants induce apoptosis via Bax-activation, cytochrome *c* release, and activation of downstream caspases. In addition, a parallel calpain-dependent cell death pathway could be detected upon MeHg exposure. Remarkably, exposure to MeHg at concentrations lower than those detected and observed in cord blood from Swedish pregnant women inhibits spontaneous neuronal differentiation of NSCs via activation of the Notch signaling pathway (71–73).

In an attempt to address the complex issue of sex-related differences in the response to neurotoxicants, we have used aNSCs prepared from rodents of both sexes, which are easily identified as compared to rodent embryos at day 14 (74, 75). We exposed

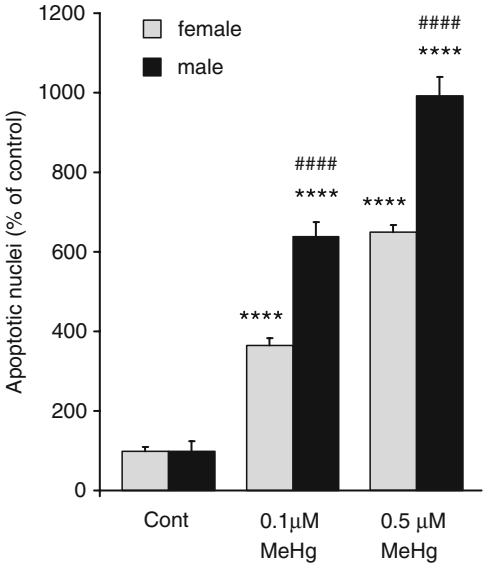

Fig. 1. Male or female aNSCs were prepared from six pooled 8-week-old mice and cells were exposed to 0.1 or 0.5 μM MeHg for 16 h. Fixed cells were stained with Hoechst 33342 and the nuclei were scored at the fluorescence microscope. The percentage of apoptotic nuclei, characterized by smaller size and brighter chromatin, was calculated. Male aNSCs showed higher sensitivity to MeHg than female aNSCs. Values are means ±SEM of 4 determinations. Statistical analysis was carried out with the one-way analysis of variance ANOVA followed by Fisher's protected least significant difference (PLSD) test (**** significantly different than control cells, $p \leq 0.0001$ and #### significantly different than female cells, $p \leq 0.0001$).

aNSCs to 0.1 and 0.5 μM MeHg for 16 h and observed that aNSCs prepared from males were significantly more sensitive to the toxic effects of MeHg than cells obtained from females, as shown by the higher number of apoptotic nuclei (Fig. 1). It is interesting to note that experimental (76–78) and epidemiological studies of children (79, 80) have shown a higher susceptibility of males to developmental exposure to MeHg. A detailed review of the published data on neurotoxicity studies done in NSCs is out of the scope of this chapter; however, we have shortly summarized some of the available data in Table 1.

1.6. NSC Cultures and General Culture Conditions

Generally, when growing cells in vitro, the volume of cell media should be kept constant, because differences in surface area allow different gaseous exchange through the medium over to the cells (81). Also the density of cultured cells is of great importance, because cells plated at high density exhibit increased Bcl-2 and Bcl-xL levels, suggesting that cell-to-cell contact may promote cell survival. In addition, when a cell culture becomes confluent and/or nutrient depleted, the activation of G1 CDK/cyclins is inhibited resulting in growth arrest (reviewed by (82)). When working with NSCs, the ascertainment of the right cell density is

Table 1
Neurotoxicity studies with NSCs

Cell model	Agent	Observed effects	References
Rodent neural progenitor cell line from cerebellum	Staurosporine (STS), DMNQ, FasL/CD95	Induction of caspase-dependent cell death by STS and DMNQ activation of ERK by FasL	Tamm et al. (70)
Rodent neural progenitor cell line from cerebellum and rodent eNSCs from dorsal cortex	Methylmercury	↑ Apoptotic cell death ↓ differentiation of neuronal cells	Tamm et al. (71)
Rodent eNSCs from dorsal cortex	Methylmercury	Activation of Notch signaling pathways	Tamm et al. (72)
Rodent neural progenitor cell line from cerebellum and rodent eNSCs from dorsal cortex	Manganese	Mitochondrial-mediated apoptosis	Tamm et al. (73)
Rodent eNSCs from dorsal cortex	STS	Activation of Na+-channel during apoptosis	Akanda et al. (87)
Rodent eNSCs from striatum, ventral mesencephalon and cortex	Lead	↓ Proliferation ↓ differentiation of neurons and oligodendrocytes↑ differentiation of astrocytes	Huang and Schneider (88)
Rodent eNSCs from telencephalon	Ethanol	↓ Differentiation of neurons	Tateno et al. (89)
Rodent aNSCs from SVZ	STS, FasL/CD95	Induction of caspase-dependent cell death by STS but not by FasL	Sleeper et al. (69)
Rodent aNSCs from SVZ, derived from glucocorticoid (GC) treated rats during pregnancy	Hydrogen peroxide	↑ Sensitivity to oxidative stress in offspring of dams exposed to GC	Ceccatelli et al. (90)
Rodent aNSCs from SVZ, derived from ARE-hPAP transgenic mice	Methylmercury	Chromatin condensation and induction of hPAP	Onishchenko et al. (77)
Human neural progenitor cells	PCBs	↑ Differentiation of oligodendrocytes	Fritsche et al. (91)

(continued)

Table 1
(continued)

Cell model	Agent	Observed effects	References
Human neural progenitor cells (gestation week 16–19)	Mercury, ethanol	↓ Migration	Moors et al. (92)
Human neural progenitor cells (gestation week 16–19)	Methylmercury chloride, mercury chloride	↓ differentiation of neurons↓ migration	Moors et al. (93)
Human neural progenitor cells	PBDE	↓ Differentiation of neurons and oligodendrocytes ↓ migration	Schreiber et al. (94)
Human NSC line derived from umbilical cord blood	Methylmercury chloride	↓ Proliferation and ↑ apoptosis in stem cell Loss of astrocytic cells in differentiated cells	Buzanska et al. (95)
Human NSCs from cortex (gestation week 16, male)	Rotenone	Caspase-independent apoptosis ↑ in undifferentiated cells. Caspase-dependent apoptosis ↑ in differentiated cells	Li et al. (96)

Table 2
Different cultures of NSCs described in this chapter

Species	Name	Origin	Developmental period
Rodent	C17.2	Neonatal cerebellum (immortalized cell line)	Four days old mice (97)
Rodent	Cortical neural stem cell (cNSCs)	Dorsal cortex (primary culture)	E15 rat embryos
Rodent	aNSCs	Subventricular zone (primary culture)	Eight weeks old mice
Human	Neural progenitor cells (neurospheres)	Human fetal brain tissue (primary culture)	Gestation week 8–20

even more critical because seeding of the cells at different densities affects the outcome of the differentiated cell types, as shown by Tsai and McKay (83).

Both NSC primary cultures and immortalized cell lines can be used for experimental studies. Primary NSC cultures can be grown either as dissociated adherent cells grown in protein-coated culture dishes or in suspension as aggregates defined as neurospheres, which are formed in culture and maintain cell–cell contacts in a 3D structure in a sort of in vivo-like organization. The dissociation procedure results in loss of histological tissue organization, but allows single cell analysis. A major advantage of using cell lines is the homogeneity of the cell population that facilitates the design and execution of experimental investigations. However, they may have different characteristics, for instance in terms of gene expression, as compared to primary NSCs. It is then an advisable strategy to use multiple NSC in vitro models for developmental neurotoxicity testing and mechanistic studies. Here, we provide detailed protocols for culturing the NSC models that we have successfully implemented and applied in our laboratory; the multipotent neural precursor cell line C17.2, primary cultures of rodent embryonic and aNSC and human neurospheres (see Table 2).

2. NSC Culture Protocols

2.1. Cell Line C17.2 Cells

2.1.1. Preparation of Medium

Final volume is 600 mL.

1. Take 500 mL DMEM (+4.5 g/L-glucose, +L-glutamine, +Pyruvate).
2. Add 60 mL fetal calf serum (10%).

3. Add 30 mL horse serum (5%).
4. Add 7 mL fungizone conc (kept at –20°C).
5. Add 4 mL Gentamycin conc (kept at room temperature (RT)).
6. Add 200 mM L-glutamine (kept at –20°C).

2.1.2. Preparation of Differentiation Medium

The differentiation medium is prepared as described above except that fetal calf serum and horse serum should not be added.

2.1.3. Preparation of Plates

Cells can be grown on uncoated dishes. When grown on glass coverslips, coat with 50 µg/mL poly-L-lysine at 37°C for 2 h.

2.2. Primary Cell Culture of Embryonic Cortical Stem Cells (cNSCs)

2.2.1. Preparation of Medium (500 mL)

1. Take 495 mL of DMEM/F12 (keep 5 mL for transferrin, see below).
2. Add transferrin (50 mg dissolved in 5 mL of DMEM/F12).
3. Add insulin (12.5 mg dissolved in 2.5 mL of 10 mM NaOH).
4. Add 1 M putrescine, 500 µM sodium selenite, and 100 µM progesterone.
5. Filter sterile the medium.
6. Add 5 mL penicillin/streptomycin and keep at 4°C.

2.2.2. Hanks Buffer

1. 50 mL 10× HBSS.
2. Add 81.5 mM $NaHCO_3$.
3. Add 1 M HEPES.
4. Adjust the pH to 7.2 and store in RT.

2.2.3. Preparation of Plates

1. Add poly-L-ornithine (15 µg/mL) solution to each plate and incubate the plates at 37°C for at least 2–3 h.
2. Remove poly-L-ornithine solution and wash 3 times with PBS.
3. Remove PBS and add fibronectin (1 µg/mL).
4. Incubate at 37°C for at least 1 h.
5. Wash twice with PBS and remove the PBS.
6. Add new PBS and incubate the plates in the cell culture incubator until seeding cells.

2.3. Primary Cell Culture Adult Neural Stem Cells (aNSCs)

2.3.1. Solutions/Buffers

1. Solution 1 (S1) of total volume of 500 mL: add 50 mL 1× HBSS, 9.0 mL D-glucose, and 7.5 mL HEPES. Adjust to 7.5.
2. Solution 2 (S2) of total volume of 500 mL: 25 mL 1× HBSS and 154 g sucrose. Adjust to 7.5.
3. Solution 3 (S3) of total volume of 500 mL: 20 g BSA, 10 mL of 1 M HEPES solution, and 490 mL 1× EBSS. Adjust the pH to 7.5.

2.3.2. Dissociation Media

1. Take 10 mL of S1.
2. Add 13.3 mg trypsin, 7 mg hyaluronidase, 2 mg kynerenic acid, and 200 µL DNase.

2.3.3. Neurosphere Media

1. Take 47 mL of DMEM/F12.
2. Add 1 mL B27 supplement, 0.5 mL penicillin/streptomycin, and 0.4 mL HEPES.

2.3.4. Preparation of Plates

Coat the plates with poly-D-lysine (0.1 mg/mL) for 2 h at 37°C.

2.4. Human Neural Progenitor (HNP) Cells

1. Take 322 mL DMEM+Glutamax.
2. Add 161 mL F12+Glutamax.

2.4.1. Proliferation Media (500 mL)

3. Add EGF (20 ng/mL) and FGF (20 ng/mL).
4. Add 10 mL 50× B27 and 5 mL penicillin/streptomycin and keep at 4°C.

2.4.2. Differentiation Media (500 mL)

1. Take 200 mL DMEM + Glutamax.
2. Add 100 mL F12+Glutamax and 3 mL 100× N2 and keep at 4°C.

2.4.3. Preparation of Plates

1. Incubate the plates with poly-D-lysine (0.1 mg/mL) for 2 h at 37°C.
2. Wash twice with sterile water.
3. Incubate the plates with laminin (5 µg/mL) for 2 h at 37°C.
4. Wash twice with sterile water.
5. Add sterile PBS and store the plates at 4°C.

3. Dissection

3.1. cNSCs

1. Sacrifice E14.5–15.5 timed pregnant mother and take out the embryos and put them in HANKS at RT.
2. Dissect the embryos from the amnion and separate the head.
3. Using a pair of tweezers immobilize the head by placing one fork through the eye socket and caudally towards the neck. Peel back using the tweezers to expose the dorsal surface of the brain (see Note 1).
4. Free the brain from the skull, cut away the cerebellum, and separate the hemispheres of the cerebrum.
5. Cut away the olfactory bulb if present and immobilize the hemisphere by the most rostral point.
6. Cut away the developing thalamus/striatum (see Note 2).

7. Cut away the dorsal part of the developing cortex and transfer into HANKS in a 15 mL falcon.
8. Allow the dissected cortices to settle to the bottom.
9. Aspirate the HANKS from the cortices leaving 2 mL.
10. Dissociate the cortices by pipetting up and down for 15 times gently using a 1 mL pipette tip.
11. Add 10 mL of prewarmed DMEM/F12 medium (including the supplements) and mix gently two times with a 5 mL pipette.
12. Count the cells with trypan blue and seed 15,000 cells/cm^2.

3.2. aNSCs

1. Kill the mice via cervical dislocation and take out the brain from the skull.
2. Put the brain into ice cold PBS (see Note 3).
3. Under the dissection microscope cut 2/3 of the cerebrum. Take the frontal part. Divide the two hemispheres into two parts.
4. Make visible the LV wall.
5. Make a thin hole underneath the LV using small scissor.
6. Cut out the LV and put into ice cold PBS.
7. Dissolve the enzymes in 5 mL of solution 1 (15 mL falcon tube).
8. Place the enzyme mix in 37°C during fine dissections.
9. Sterile filter the enzyme mix and add DNase to the mixture.
10. Place ventricle walls in the enzyme mix and pipette very gently for 15 times using a blue pipette tip.
11. Incubate the ventricle walls in the enzyme mix for 20–30 min at 37°C and pipette carefully when half of the incubation time has gone.
12. Pipette the mix until most of the tissue dissolve.
13. Add 5 mL S3 to the tissue–enzyme mix.
14. Filter through a 70 μm cell strainer and centrifuge at 1,500 rpm for 10 min.
15. Remove supernatant and resuspend cells in 10 mL ice-cold S2.
16. Centrifuge at 2,000 rpm for 10 min.
17. Remove supernatant and resuspend cells in 2 mL ice-cold S3.
18. Fill a new 15 mL tube with 12 mL of ice-cold S3.
19. Gently apply the 2 mL cell suspension to the top of the new tube.
20. Centrifuge at 1,500 rpm for 7 min.
21. Remove supernatant and resuspend in prewarmed neurosphere media.
22. Seed all the cells in a 100 mm cell culture dish (CORNING) in 15 mL neurosphere medium.

23. Add 10 ng/mL EGF.
24. Add 10 ng/mL EGF on day 3 without changing medium (see Note 4).

4. Methods

4.1. Passaging C17.2 Cells

- Remove medium from the cell culture dish.
- Wash with PBS.
- Add 2 mL 1× TED/10 cm dish (trypsin + EDTA) for 30 s.
- Remove 1.5 mL TED after 30 s and wait for 1.5 min.
- Add new medium and dissociate cells by pipetting.
- Count the cells with trypan blue.
- Seed the cells into a new dish at 4,000 cells/cm^2.

4.2. Passaging cNSCs

1. Remove the medium from dish.
2. Add 5 mL HANKS/100 mm dish and incubate for 5 min in culture incubator.
3. Remove 4 mL HANKS from the dish and leave 0.5 mL.
4. Scrape cells gently with cell scraper.
5. Collect all cells in one dish and transfer them into a 50 mL falcon tube.
6. Dilute cells with 9 mL DMEM/F12 medium (including the supplements).
7. Count the cells using trypan blue.
8. Seed the cells at 2,500 cells/cm^2 in DMEM/F12 medium (including the supplements).
9. Wait until cells have settled, then add 10 ng/mL FGF.
10. Every 24 h add 10 ng/mL FGF.
11. Every 48 h change the medium and add 10 ng/mL FGF (see Note 5).

4.3. Passaging aNSC

4.3.1. Passaging aNSC Neurospheres

1. Collect all neurospheres in a 15 mL falcon tube (see Note 6) and centrifuge at 1,500 rpm for 10 min.
2. Resuspend the pellet in 1 mL TED and mix for 15 times with a yellow pipette tip and incubate for 10 min at 37°C in the water bath.
3. Mix gently using a yellow pipette tip and continue incubation for 5–10 min at 37°C.
4. Mix gently for 10× using a yellow pipette tip.
5. Add 9 mL fresh medium and centrifuge at 1,500 rpm for 10 min.

6. Discard supernatant and resuspend the pellet in 5 or 10 mL fresh medium depending on the pellet's size.
7. Count the cells with trypan blue.
8. Seed cells at 80,000 cells/cm^2 in 15 mL medium and add (10 ng/mL) EGF and (10 ng/mL) FGF.
9. Place the cells inside the incubator and add (10 ng/mL) EGF and (10 ng/mL) FGF every third day (see Notes 4 and 7).

4.3.2. Passaging aNSC as Single Cells for Experiment

1. Coat plates with poly-D-lysine (0.1 mg/mL) for 2 h.
2. Repeat steps (1–7) from 4.3.1.
3. Add 1% filter sterilized FCS to the medium. Do not add EGF or FGF!
4. Seed 160,000 cells/cm^2 in FCS-containing medium.
5. Let the cells grow overnight.
6. Gently discard the medium containing FCS and add 1 mL fresh medium containing (10 ng/mL) EGF and (10 ng/mL) FGF.

4.4. Passaging hNPC

The HNP can be passaged by mechanical or enzymatic disruption of the sphere structure, but their medium should be changed as follows.

1. Put 10 mL proliferating medium in a new plate.
2. Discard 10 mL of the old medium.
3. Use the rest of the old medium for transferring the spheres to the new plate (see Note 8).
4. Separate the spheres very well with a yellow pipette tip (see Note 9).

4.4.1. Mechanical Passaging of HNP

For mechanical passaging, use a McIlwain tissue chopper.

1. Transfer spheres in a dish that fits in the holder of the McIlwain tissue chopper.
2. Remove the medium.
3. Cut the spheres in smaller sections of a size about 0.2–0.25 mm.
4. Add 1 mL medium and transfer the spheres in a new dish with fresh proliferation medium.
5. Separate the spheres very well with a yellow pipette tip (see Note 7).

4.4.2. Enzymatic Passaging of HNP

For enzymatic digestion, incubate spheres in trypsin solution.

1. Transfer spheres in a falcon tube.
2. Centrifuge for 5 min at 1,500 rpm.

3. Discard supernatant and add 0.5 mL TrypLE™ Express.
4. Incubate for 6 min at 37°C in the water bath by shaking.
5. Add 6 mL proliferation medium.
6. Centrifuge for 5 min at 1,500 rpm.
7. Add an appropriate amount of medium and resuspend the cell pellet mechanically to achieve a single cell suspension.
8. Count the cells with trypan blue and seed 50,000 cells/cm^2.

5. Differentiation

5.1. Differentiation of C17.2 Cells

Upon removal of serum, C17.2 cells can differentiate into neurons, astrocytes, and oligodendrocytes (84). For differentiation assays, C17.2 cells are grown in serum-containing DMEM medium. Following cell attachment, the medium is replaced with serum-free medium and the cultures are incubated for 1 day before performing experiments. Cell differentiation process can be evaluated by immunocytochemistry analysis of the neuronal marker β-III tubulin and the astrocyte marker GFAP. C17.2 cells grown in serum-containing conditions can also be differentiated by incubating the cultures in media supplemented with, for example, brain-derived neurotrophic factor (BDNF; 4 ng/mL), neurotrophin-3 (NT-3; 10 ng/mL), ciliary neurotrophic factor (CNTF; 10 ng/mL), and glial-derived neurotrophic factor (GDNF; 5 ng/mL) (85).

5.2. Differentiation of cNSCs

cNSCs have the capacity of differentiating into major cell types found in the telencephalon, including pyramidal- and interneurons, astrocytes and oligodendrocytes, as well as smooth muscle cells (2). Upon mitogen withdrawal, cNSCs spontaneously differentiate into mainly neurons and astrocytes, but can also be differentiated specifically into astrocytes by treatment with interleukin-related compounds such as ciliary neurotrophic factor (CNTF) or oligodendrocytes by thyroid hormone (T3) treatment. Spontaneous differentiation of cNSCs is induced as follows:

1. When cells have reached the right confluency (about 5–7 days after previous passaging), passage the cells as discussed in Sect. 4.2 (1–10).
2. Seed the cells at the density 500 cells/cm^2 and add 10 ng/mL FGF every day.
3. After 48 h, remove the old media and add media. Do not add FGF.
4. Change the media every 2 days, but do not add FGF.
5. Check the morphology. After about 1 week in culture, the cNSCs will appear more differentiated.

5.3. Differentiation of aNSCs

Upon removal of EGF and FGF, cells can differentiate into neurons, astrocytes, and oligodendrocytes (3, 11, 49). Differentiation of aNSCs have been described by two methods, either as dissociated cells or as neurospheres. The latter is typically used to demonstrate that individual spheres are multipotent (86). For spontaneously differentiation of dissociated aNSCs, follow the protocol in Sect. 4.3.2 and wait until the cells have differentiated sufficiently (about 1 week in culture).

5.4. Differentiation of hNPC

Differentiation of hNPC cells can be initiated in spheres or single cell suspensions (see Sect. 4.3) under growth factor withdrawal. Therefore, hNPC should be plated on poly-D-lysine/laminin coated surfaces and grown in differentiation medium for up to 4 weeks. After 2–4 days, a decrease in NSC can be determined.

6. Notes

1. Autoclave the dissection tools 1 day before the dissection.
2. The tissue looks white under the dissecting microscope and is located caudally and ventrally in the hemisphere.
3. The brains can be kept on ice maximum for 2 h.
4. Flush up everyday the spheres to prevent attachment to the bottom of the dish.
5. Look for the morphological changes and at 80% confluency, passage the cells.
6. Flush all the bottom of the plate with fresh medium to take all the spheres that might have been left.
7. After 3 days, aNSCs start to form neurospheres again.
8. Some spheres will be attached to the bottom of the old plate. These spheres should be discarded because they have started to differentiate and hence are stuck to the bottom of the plate.
9. The spheres should be separated far away from each other before they are placed inside the incubator, otherwise they will stick together and make a new big sphere.

7. Conclusions

Extensive evidence indicates that many diseases must be understood in a life-long perspective, as processes that start in utero and manifest later in life. Adverse prenatal events, such as exposure to toxic environmental agents, have been associated to

neurodevelopmental disorders as well as neurodegenerative diseases. The use of NSCs as in vitro models allows the design of experimental studies aimed at identifying the mechanisms behind possible developmental damage and/or functional alterations induced by early insults. Moreover, NSCs offer the possibility to perform large-scale in vitro developmental neurotoxicity studies, including screening of chemicals and pharmaceutical drugs. Considering that NSCs are also present in the adult nervous system, where they may have a role in learning, memory, and response to injuries, neurotoxicity studies on NSCs may provide novel information relevant to various types of nervous system disorders.

References

1. Caviness VS Jr, Takahashi T, Nowakowski RS (1995) Numbers, time and neocortical neuronogenesis: a general developmental and evolutionary model. Trends Neurosci 18:379–383
2. Johe KK, Hazel TG, Muller T, Dugich-Djordjevic MM, McKay RD (1996) Single factors direct the differentiation of stem cells from the fetal and adult central nervous system. Genes Dev 10:3129–3140
3. Reynolds BA, Weiss S (1992) Generation of neurons and astrocytes from isolated cells of the adult mammalian central nervous system. Science 255:1707–1710
4. Cai J, Rao MS (2002) Stem cell and precursor cell therapy. Neuromolecular Med 2:233–249
5. Doetsch F (2003) A niche for adult neural stem cells. Curr Opin Genet Dev 13:543–550
6. Palmer TD, Takahashi J, Gage FH (1997) The adult rat hippocampus contains primordial neural stem cells. Mol Cell Neurosci 8:389–404
7. Davis AA, Temple S (1994) A self-renewing multipotential stem cell in embryonic rat cerebral cortex. Nature 372:263–266
8. Lee A, Kessler JD, Read TA, Kaiser C, Corbeil D, Huttner WB, Johnson JE, Wechsler-Reya RJ (2005) Isolation of neural stem cells from the postnatal cerebellum. Nat Neurosci 8:723–729
9. Marmur R, Mabie PC, Gokhan S, Song Q, Kessler JA, Mehler MF (1998) Isolation and developmental characterization of cerebral cortical multipotent progenitors. Dev Biol 204:577–591
10. Pagano SF, Impagnatiello F, Girelli M, Cova L, Grioni E, Onofri M, Cavallaro M, Etteri S, Vitello F, Giombini S, Solero CL, Parati EA (2000) Isolation and characterization of neural stem cells from the adult human olfactory bulb. Stem Cells 18:295–300
11. Reynolds BA, Tetzlaff W, Weiss S (1992) A multipotent EGF-responsive striatal embryonic progenitor cell produces neurons and astrocytes. J Neurosci 12:4565–4574
12. Uchida N, Buck DW, He D, Reitsma MJ, Masek M, Phan TV, Tsukamoto AS, Gage FH, Weissman IL (2000) Direct isolation of human central nervous system stem cells. Proc Natl Acad Sci USA 97:14720–14725
13. Kukekov VG, Laywell ED, Thomas LB, Steindler DA (1997) A nestin-negative precursor cell from the adult mouse brain gives rise to neurons and glia. Glia 21:399–407
14. Dahlstrand J, Lardelli M, Lendahl U (1995) Nestin mRNA expression correlates with the central nervous system progenitor cell state in many, but not all, regions of developing central nervous system. Brain Res Dev Brain Res 84:109–129
15. Lendahl U, Zimmerman LB, McKay RD (1990) CNS stem cells express a new class of intermediate filament protein. Cell 60:585–595
16. Messam CA, Hou J, Major EO (2000) Coexpression of nestin in neural and glial cells in the developing human CNS defined by a human-specific anti-nestin antibody. Exp Neurol 161:585–596
17. Altmann CR, Brivanlou AH (2001) Neural patterning in the vertebrate embryo. Int Rev Cytol 203:447–482
18. Vaccarino FM, Schwartz ML, Raballo R, Rhee J, Lyn-Cook R (1999) Fibroblast growth factor signaling regulates growth and morphogenesis at multiple steps during brain development. Curr Top Dev Biol 46:179–200
19. Ford-Perriss M, Abud H, Murphy M (2001) Fibroblast growth factors in the

developing central nervous system. Clin Exp Pharmacol Physiol 28:493–503

20. Lutolf S, Radtke F, Aguet M, Suter U, Taylor V (2002) Notch1 is required for neuronal and glial differentiation in the cerebellum. Development 129:373–385
21. Shingo T, Sorokan ST, Shimazaki T, Weiss S (2001) Erythropoietin regulates the in vitro and in vivo production of neuronal progenitors by mammalian forebrain neural stem cells. J Neurosci 21:9733–9743
22. Schneider RA, Hu D, Rubenstein JL, Maden M, Helms JA (2001) Local retinoid signaling coordinates forebrain and facial morphogenesis by maintaining FGF8 and SHH. Development 128:2755–2767
23. Gaiano N, Fishell G (2002) The role of notch in promoting glial and neural stem cell fates. Annu Rev Neurosci 25:471–490
24. Hitoshi S, Seaberg RM, Koscik C, Alexson T, Kusunoki S, Kanazawa I, Tsuji S, van der Kooy D (2004) Primitive neural stem cells from the mammalian epiblast differentiate to definitive neural stem cells under the control of Notch signaling. Genes Dev 18:1806–1811
25. Ohtsuka T, Sakamoto M, Guillemot F, Kageyama R (2001) Roles of the basic helix-loop-helix genes Hes1 and Hes5 in expansion of neural stem cells of the developing brain. J Biol Chem 276:30467–30474
26. Nakamura Y, Sakakibara S, Miyata T, Ogawa M, Shimazaki T, Weiss S, Kageyama R, Okano H (2000) The bHLH gene hes1 as a repressor of the neuronal commitment of CNS stem cells. J Neurosci 20:283–293
27. Nieto M, Schuurmans C, Britz O, Guillemot F (2001) Neural bHLH genes control the neuronal versus glial fate decision in cortical progenitors. Neuron 29:401–413
28. Farah MH, Olson JM, Sucic HB, Hume RI, Tapscott SJ, Turner DL (2000) Generation of neurons by transient expression of neural bHLH proteins in mammalian cells. Development 127:693–702
29. Kageyama R, Ohtsuka T, Hatakeyama J, Ohsawa R (2005) Roles of bHLH genes in neural stem cell differentiation. Exp Cell Res 306:343–348
30. Panchision DM, McKay RD (2002) The control of neural stem cells by morphogenic signals. Curr Opin Genet Dev 12:478–487
31. Gross RE, Mehler MF, Mabie PC, Zang Z, Santschi L, Kessler JA (1996) Bone morphogenetic proteins promote astroglial lineage commitment by mammalian subventricular zone progenitor cells. Neuron 17:595–606
32. Li W, Cogswell CA, LoTurco JJ (1998) Neuronal differentiation of precursors in the neocortical ventricular zone is triggered by BMP. J Neurosci 18:8853–8862
33. Gross CG (2000) Neurogenesis in the adult brain: death of a dogma. Nat Rev Neurosci 1:67–73
34. Bryans WA (1959) Mitotic activity in the brain of the adult white rat. Anat Rec 133:65–71
35. Hamilliton A (1901) The division of differentiated cell in the central nervous system of the white rat. J Comp Neurol 11:297–320
36. Altman J (1962) Are new neurons formed in the brains of adult mammals? Science 135:1127–1128
37. Altman J, Das GD (1965) Autoradiographic and histological evidence of postnatal hippocampal neurogenesis in rats. J Comp Neurol 124:319–335
38. Kaplan MS, Hinds JW (1977) Neurogenesis in the adult rat: electron microscopic analysis of light radioautographs. Science 197:1092–1094
39. Taupin P, Ray J, Fischer WH, Suhr ST, Hakansson K, Grubb A, Gage FH (2000) FGF-2-responsive neural stem cell proliferation requires CCg, a novel autocrine/paracrine cofactor. Neuron 28:385–397
40. Lois C, Alvarez-Buylla A (1994) Long-distance neuronal migration in the adult mammalian brain. Science 264:1145–1148
41. Hinds JW (1968) Autoradiographic study of histogenesis in the mouse olfactory bulb. II. Cell proliferation and migration. J Comp Neurol 134:305–322
42. Gage FH, Kempermann G, Palmer TD, Peterson DA, Ray J (1998) Multipotent progenitor cells in the adult dentate gyrus. J Neurobiol 36:249–266
43. Alvarez-Buylla A, Garcia-Verdugo JM (2002) Neurogenesis in adult subventricular zone. J Neurosci 22:629–634
44. Gritti A, Vescovi AL, Galli R (2002) Adult neural stem cells: plasticity and developmental potential. J Physiol Paris 96:81–90
45. Li B, DiCicco-Bloom E (2004) Basic fibroblast growth factor exhibits dual and rapid regulation of cyclin D1 and p27 to stimulate proliferation of rat cerebral cortical precursors. Dev Neurosci 26:197–207
46. Craig CG, Tropepe V, Morshead CM, Reynolds BA, Weiss S, van der Kooy D (1996) In vivo growth factor expansion of endogenous subependymal neural precursor cell populations in the adult mouse brain. J Neurosci 16:2649–2658

47. Doetsch F, Garcia-Verdugo JM, Alvarez-Buylla A (1997) Cellular composition and three-dimensional organization of the subventricular germinal zone in the adult mammalian brain. J Neurosci 17:5046–5061
48. Morshead CM, Reynolds BA, Craig CG, McBurney MW, Staines WA, Morassutti D, Weiss S, van der Kooy D (1994) Neural stem cells in the adult mammalian forebrain: a relatively quiescent subpopulation of subependymal cells. Neuron 13:1071–1082
49. Gage FH, Ray J, Fisher LJ (1995) Isolation, characterization, and use of stem cells from the CNS. Annu Rev Neurosci 18:159–192
50. Gritti A, Parati EA, Cova L, Frolichsthal P, Galli R, Wanke E, Faravelli L, Morassutti DJ, Roisen F, Nickel DD, Vescovi AL (1996) Multipotential stem cells from the adult mouse brain proliferate and self-renew in response to basic fibroblast growth factor. J Neurosci 16:1091–1100
51. Mayer-Proschel M, Kalyani AJ, Mujtaba T, Rao MS (1997) Isolation of lineage-restricted neuronal precursors from multipotent neuroepithelial stem cells. Neuron 19:773–785
52. Doetsch F, Caille I, Lim DA, Garcia-Verdugo JM, Alvarez-Buylla A (1999) Subventricular zone astrocytes are neural stem cells in the adult mammalian brain. Cell 97:703–716
53. Johansson CB, Momma S, Clarke DL, Risling M, Lendahl U, Frisen J (1999) Identification of a neural stem cell in the adult mammalian central nervous system. Cell 96:25–34
54. Arvidsson A, Collin T, Kirik D, Kokaia Z, Lindvall O (2002) Neuronal replacement from endogenous precursors in the adult brain after stroke. Nat Med 8:963–970
55. Kokaia Z, Lindvall O (2003) Neurogenesis after ischaemic brain insults. Curr Opin Neurobiol 13:127–132
56. Parent JM (2003) Injury-induced neurogenesis in the adult mammalian brain. Neuroscientist 9:261–272
57. Jin K, Peel AL, Mao XO, Xie L, Cottrell BA, Henshall DC, Greenberg DA (2004) Increased hippocampal neurogenesis in Alzheimer's disease. Proc Natl Acad Sci U S A 101:343–347
58. Curtis MA, Penney EB, Pearson AG, van Roon-Mom WM, Butterworth NJ, Dragunow M, Connor B, Faull RL (2003) Increased cell proliferation and neurogenesis in the adult human Huntington's disease brain. Proc Natl Acad Sci U S A 100:9023–9027
59. Hoglinger GU, Rizk P, Muriel MP, Duyckaerts C, Oertel WH, Caille I, Hirsch EC (2004) Dopamine depletion impairs precursor cell proliferation in Parkinson disease. Nat Neurosci 7:726–735
60. Heiss WD (1981) Cerebral blood flow: physiology, pathophysiology and pharmacological effects. Adv Otorhinolaryngol 27:26–39
61. Evans PH (1993) Free radicals in brain metabolism and pathology. Br Med Bull 49:577–587
62. Risau W, Wolburg H (1990) Development of the blood-brain barrier. Trends Neurosci 13:174–178
63. Rodier PM (1994) Vulnerable periods and processes during central nervous system development. Environ Health Perspect 102(Suppl 2):121–124
64. Johnson EM Jr, Deckwerth TL (1993) Molecular mechanisms of developmental neuronal death. Annu Rev Neurosci 16:31–46
65. Henderson CE (1996) Programmed cell death in the developing nervous system. Neuron 17:579–585
66. Ikonomidou C, Bittigau P, Koch C, Genz K, Hoerster F, Felderhoff-Mueser U, Tenkova T, Dikranian K, Olney JW (2001) Neurotransmitters and apoptosis in the developing brain. Biochem Pharmacol 62:401–405
67. Aschner M, Allen JW (2000) Astrocytes in methylmercury, ammonia, methionine sulfoximine and alcohol-induced neurotoxicity. Neurotoxicology 21:573–579
68. Reuhl KR (1991) Delayed expression of neurotoxicity: the problem of silent damage. Neurotoxicology 12:341–346
69. Sleeper E, Tamm C, Frisen J, Zhivotovsky B, Orrenius S, Ceccatelli S (2002) Cell death in adult neural stem cells. Cell Death Differ 9:1377–1378
70. Tamm C, Robertson JD, Sleeper E, Enoksson M, Emgard M, Orrenius S, Ceccatelli S (2004) Differential regulation of the mitochondrial and death receptor pathways in neural stem cells. Eur J Neurosci 19:2613–2621
71. Tamm C, Duckworth J, Hermanson O, Ceccatelli S (2006) High susceptibility of neural stem cells to methylmercury toxicity: effects on cell survival and neuronal differentiation. J Neurochem 97:69–78
72. Tamm C, Duckworth JK, Hermanson O, Ceccatelli S (2008) Methylmercury inhibits differentiation of rat neural stem cells via Notch signalling. Neuroreport 19:339–343
73. Tamm C, Sabri F, Ceccatelli S (2008) Mitochondrial-mediated apoptosis in neural stem cells exposed to manganese. Toxicol Sci 101:310–320
74. Du L, Bayir H, Lai Y, Zhang X, Kochanek PM, Watkins SC, Graham SH, Clark RS

(2004) Innate gender-based proclivity in response to cytotoxicity and programmed cell death pathway. J Biol Chem 279:38563–38570

75. Reisert I, Engele J, Pilgrim C (1989) Early sexual differentiation of diencephalic dopaminergic neurons of the rat in vitro. Cell Tissue Res 255:411–417
76. Gimenez-Llort L, Ahlbom E, Dare E, Vahter M, Ogren S, Ceccatelli S (2001) Prenatal exposure to methylmercury changes dopamine-modulated motor activity during early ontogeny: age and gender-dependent effects. Environ Toxicol Pharmacol 9:61–70
77. Onishchenko N, Tamm C, Vahter M, Hokfelt T, Johnson JA, Johnson DA, Ceccatelli S (2007) Developmental exposure to methylmercury alters learning and induces depression-like behavior in male mice. Toxicol Sci 97:428–437
78. Rossi AD, Ahlbom E, Ogren SO, Nicotera P, Ceccatelli S (1997) Prenatal exposure to methylmercury alters locomotor activity of male but not female rat. Exp Brain Res 117:428–436
79. Grandjean P, Weihe P, White RF, Debes F (1998) Cognitive performance of children prenatally exposed to "safe" levels of methylmercury. Environ Res 77:165–172
80. McKeown-Eyssen GE, Ruedy J, Neims A (1983) Methyl mercury exposure in northern Quebec. II. Neurologic findings in children. Am J Epidemiol 118:470–479
81. Pfaller W, Balls M, Clothier R, Coecke S, Dierickx P, Ekwall B, Hanley BA, Hartung T, Prieto P, Ryan MP, Schmuck G, Sladowski D, Vericat JA, Wendel A, Wolf A, Zimmer J (2001) Novel advanced in vitro methods for long-term toxicity testing: the report and recommendations of ECVAM workshop 45. European Centre for the validation of alternative methods. Altern Lab Anim 29:393–426
82. Knudsen KE, Diehl JA, Haiman CA, Knudsen ES (2006) Cyclin D1: polymorphism, aberrant splicing and cancer risk. Oncogene 25:1620–1628
83. Tsai RY, McKay RD (2000) Cell contact regulates fate choice by cortical stem cells. J Neurosci 20:3725–3735
84. Doering LC, Snyder EY (2000) Cholinergic expression by a neural stem cell line grafted to the adult medial septum/diagonal band complex. J Neurosci Res 61:597–604
85. Parker MA, Anderson JK, Corliss DA, Abraria VE, Sidman RL, Park KI, Teng YD, Cotanche DA, Snyder EY (2005) Expression profile of an operationally-defined neural stem cell clone. Exp Neurol 194:320–332
86. Deleyrolle LP, Reynolds BA (2009) Isolation, expansion, and differentiation of adult mammalian neural stem and progenitor cells using the neurosphere assay. Methods Mol Biol 549:91–101
87. Akanda N, Tofighi R, Brask J, Tamm C, Elinder F, Ceccatelli S (2008) Voltage-dependent anion channels (VDAC) in the plasma membrane play a critical role in apoptosis in differentiated hippocampal neurons but not in neural stem cells. Cell Cycle 7:3225–3234
88. Huang F, Schneider JS (2004) Effects of lead exposure on proliferation and differentiation of neural stem cells derived from different regions of embryonic rat brain. Neurotoxicology 25:1001–1012
89. Tateno M, Ukai W, Ozawa H, Yamamoto M, Toki S, Ikeda H, Saito T (2004) Ethanol inhibition of neural stem cell differentiation is reduced by neurotrophic factors. Alcohol Clin Exp Res 28:134S–138S
90. Ceccatelli S, Tamm C, Zhang Q, Chen M (2007) Mechanisms and modulation of neural cell damage induced by oxidative stress. Physiol Behav 92:87–92
91. Fritsche E, Cline JE, Nguyen NH, Scanlan TS, Abel J (2005) Polychlorinated biphenyls disturb differentiation of normal human neural progenitor cells: clue for involvement of thyroid hormone receptors. Environ Health Perspect 113:871–876
92. Moors M, Cline JE, Abel J, Fritsche E (2007) ERK-dependent and -independent pathways trigger human neural progenitor cell migration. Toxicol Appl Pharmacol 221:57–67
93. Moors M, Rockel TD, Abel J, Cline JE, Gassmann K, Schreiber T, Schuwald J, Weinmann N, Fritsche E (2009) Human neurospheres as three-dimensional cellular systems for developmental neurotoxicity testing. Environ Health Perspect 117:1131–1138
94. Schreiber T, Gassmann K, Götz C, Hübenthal U, Moors M, Krause G, Merk HF, Nguyen N-H, Scanlan TS, Abel J, Rose CR, Fritsche E (2010) Polybrominated diphenyl ethers induce developmental neurotoxicity in a human in vitro model: evidence for endocrine disruption. Environ Health Perspect 118:572–578
95. Buzanska L, Sypecka J, Nerini-Molteni S, Compagnoni A, Hogberg HT, del Torchio R, Domanska-Janik K, Zimmer J, Coecke S (2009) A human stem cell-based model for

identifying adverse effects of organic and inorganic chemicals on the developing nervous system. Stem Cells 27:2591–2601

96. Li J, Spletter ML, Johnson DA, Wright LS, Svendsen CN, Johnson JA (2005) Rotenone-induced caspase 9/3-independent and -dependent cell death in undifferentiated and differentiated human neural stem cells. J Neurochem 92:462–476
97. Ryder EF, Snyder EY, Cepko CL (1990) Establishment and characterization of multipotent neural cell lines using retrovirus vector-mediated oncogene transfer. J Neurobiol 21:356–375

Chapter 4

Primary Cultures for Neurotoxicity Testing

Carme Solà, Rosa Cristòfol, Cristina Suñol, and Coral Sanfeliu

Abstract

Cell cultures are widely used in biomedical research. Primary cultures are directly obtained from fresh tissue and reproduce during days or weeks the major characteristics of the original tissue cells. Primary cell culture systems have shown their usefulness for studying the specific activities and the underlying mechanisms of a variety of test compounds. Brain primary cultures have become a powerful tool to analyze the toxic effects and mechanisms of potentially harmful agents in the different brain cell types.

Key words: Primary cultures, Neurons, Astrocytes, Microglia, Oligodendrocytes

1. Introduction

1.1. Brain Cultures

Many studies of neurotoxicity in vitro rely on the use of cultured cells that model neurons or glial cells. Primary cultures from brain tissue yield standardized preparations of living cells that maintain their specific physiological characteristics for a number of days and which may be used for testing a multiplicity of neural end points. For instance, a mouse embryo litter will give about 6–8 multiwell plates or the corresponding Petri dishes of neuron cultures, enough to test between 4 and 20 agents, depending on the procedure.

The embryological time of differentiation or "birthday" of each neuron type (1) will determine the optimal moment for its culture. Some neuron types and, in general, glial cells require postnatal tissue for culture.

Although cultures may be prepared with brain tissue from any experimental animal, neuron and glia cultures from rats and mice are the most common and the best characterized. The yield

Michael Aschner et al. (eds.), *Cell Culture Techniques*, Neuromethods, vol. 56,
DOI 10.1007/978-1-61779-077-5_4, © Springer Science+Business Media, LLC 2011

of the two species is very similar, and mice are increasingly popular due to the many transgenic lines that can also be used for neurotoxicity studies.

Human embryo tissue discarded from abortions is also a useful source of brain cultures. Although its availability is low, human cultures may be useful to confirm selected results. Indeed, there are reported discrepancies between test results in rodent and human brain cultures (2, 3).

1.2. General Procedure

Selected brain tissue at the precise state of maturation is dissected from the animal postmortem. Tissue is mechanically triturated and chemically disaggregated, before being washed and seeded on appropriated culture surfaces. Throughout the procedure, cells are maintained in physiological solutions under sterile conditions and are finally seeded with a culture medium that mimics the blood bicarbonate buffering system. Cultures are maintained in a CO_2 humidified incubator at 37°C until use. Sterility must be maintained throughout the procedure.

Many variations in procedures or in the composition of the culture medium have been described. In the following protocols, mouse neuron culture procedures are based on those originally described by the group of Schousboe (4, 5). Mixed glial cultures are prepared according to the method of Giulian and Baker (6), with some modifications, and microglia cultures according to Saura et al. (7). Mouse oligodendrocyte culture and the various CNS human cultures are adapted from the work of Kim's group (8–10).

Animal culture procedures meet the ethical guidelines for animal research, but they should also be approved by the local animal ethics committee. For human cultures, approval from the local ethics committee for human research must also be obtained. Human tissue is collected by a physician or nurse, who must be previously provided with the relevant informed-donation form and sterile flasks containing preserving solution in which to store the tissue.

2. Materials

The basic material needed to be able to obtain and maintain primary cell cultures in a research laboratory consists of the following specific equipment and disposables.

2.1. Culture Equipment

1. Sterilized stainless steel surgical instruments to dissect the tissue of interest.
2. Stereoscopic microscope to help in the dissection process.
3. Room temperature centrifuge with swinging bucket rotor.

4. Laminar flow cabinets (or biological safety cabinets in the case of biological risk material such as human tissue), with vacuum connection.
5. Thermostatic water bath with linear shaking.
6. Neubauer hemocytometer.
7. Cell culture CO_2 incubators.
8. Inverted microscope.
9. Fridge and freezer.
10. Autoclave.

2.2. Disposable Laboratory Material

1. Sterilized tips for automatic micropipettes.
2. Disposable sterilized capped centrifuge tubes and serological pipettes, Pasteur pipettes and filters.
3. Sterilized glass bottles of different volumes.
4. Sterilized plastic material to be used as culture support, such as T-flasks, Petri dishes, and multiwell culture plates. Depending on the type of cell culture it may be necessary to coat the culture support with a product that increases cell adhesion to the cell culture support, such as poly-L- or poly-D-lysine and laminin.

2.3. Solutions and Culture Media

Different types of buffers and solutions, as well as a wide variety of cell culture media, are commercially available and the choice will depend on the type of culture. Some of them are mentioned below for the different cell cultures presented.

3. Methods

3.1. Primary Mouse Neuron Cultures

3.1.1. Cerebellar Granule Cells

To prepare cerebellar granule cell cultures, cerebella are harvested from a mice litter (8–10 pups) on a postnatal day (P) 7.

3.1.1.1. Stock Solutions

1. Krebs buffer: 120.9 mM NaCl, 4.83 mM KCl, 1.22 mM KH_2PO_4, 25.5 mM $NaHCO_3$, 12 mM glucose, 3 g/L bovine seroalbumin, and 0.015 g/L phenol red. Filter through a 2 μm filter to sterilize and store at 4°C.
2. Phosphate buffer saline solution (PBS): 135 mM NaCl, 7.5 mM $Na_2HPO_4.2H_2O$, and 1.5 mM KH_2PO_4.
3. Insulin solution: dissolve 1 mg insulin (25 i.u.) in 100 μL 0.01 N HCl and add insulin buffer solution (32.4 mM Na_2HPO_4, 7.6 mM NaH_2PO_4, 10 g/L albumin) to a total of

10 mL. Then make a 1:100 dilution with insulin buffer solution. Filter and store in aliquots at –20°C.

4. 150 mM $MgSO_4$ solution: dissolve 1.48 g $MgSO_4$ in 40 mL distilled water. Filter and store at 4°C.
5. 10 mg/mL trypsin solution: dissolve 100 mg trypsin in 10 mL PBS. Filter and store in aliquots at –20°C.
6. 10 mg/mL deoxyribonuclease I (DNase) (Sigma, D5025) solution in double distilled water. Filter and store in aliquots at –20°C.
7. 10 mg/L poly-L-lysine or 25 mg/L poly-D-lysine solution: prepare in distilled water. Autoclave and store at 4°C. Coat culture supports with the solutions. Maintain overnight in a CO_2 incubator, then aspirate the poly-L- or poly-D-lysine and rinse with sterile distilled water. Keep dry until use.
8. 2 mM cytosine β-D-arabinofuranoside (Ara-C) solution: 4.86 mg Ara-C (Sigma, C1768) in 10 mL distilled water. Filter and store in aliquots at –20°C.
9. Fetal bovine serum (FBS) (Invitrogen, 10270), heat-inactivated by incubation at 56°C for 30 min. Store in 50 mL aliquots at –20°C.

3.1.1.2. Culture Medium

Dulbecco's Modified Eagle medium (DMEM) (Biochrom AG, F0455) pH 7.0 supplemented with 26.2 mM $NaHCO_3$, 25 mM KCl, 25 mM glucose, 0.2 mM L-glutamine, 100 mU/L insulin, and 7 μM *p*-aminobenzoic acid. Filter under sterile conditions and add 10% FBS and 100 μg/mL gentamicin (Invitrogen, 15750).

3.1.1.3. Disaggregation Solutions

Prepare the following Krebs solutions in sterile glass bottles immediately before culture preparation:

1. Solution 1: 80 mL Krebs buffer and 0.62 mL $MgSO_4$ solution.
2. Solution 2: 20 mL Solution 1, 0.1 mL DNase, and 0.5 mL trypsin.
3. Solution 3: 20 mL Solution 1, 0.1 mL DNase, and 0.2 mL $MgSO_4$. Separate 5 mL to dissolve 10.4 mg soybean trypsin inhibitor, filter to sterilize and add back to the Solution 3.
4. Solution 4: 16.8 mL Solution 1 and 3.2 mL Solution 3.

Equilibrate these solutions by bubbling 5% CO_2/95% O_2 with a sterile cotton-plugged Pasteur pipette connected to the gas source until a red-orange color is yielded by the pH indicator (phenol red). Warm the solutions at 37°C.

3.1.1.4. Procedure

1. Clean head and neck with 70% ethanol and kill the animals by decapitation in a flow cabinet. Transfer heads to a Petri dish on ice.

2. Peel away the scalp and the skull and take out the brain using a spatula or scissors. Place it in a fresh dish on ice.
3. Separate cerebellum from brain with a pair of forceps and place them in a 100 mm Petri dish containing cold PBS. Then strip off the meninges. Dissect preferably under a stereoscopic microscope.
4. Transfer the dissected material to a 35 mm Petri dish containing sterile cold PBS and keep on ice while proceeding with all the brains.
5. Put the cerebella dissected from the whole litter onto a sterile Teflon plate (5 × 5 cm). Chop the tissue thoroughly into small pieces using a sterile razor blade.
6. Transfer the minced tissue using a sterile Pasteur pipette filled with Solution 1 into a 50 mL tube. Rinse the plate with more Solution 1. Add Solution 1 to a total volume of 10 mL. Disperse the tissue gently up and down twice with a Pasteur pipette.
7. Centrifuge briefly at 200×*g* and carefully remove the supernatant.
8. Add 2 mL of Solution 2, pipette gently to avoid the formation of bubbles, and transfer the suspension to the bottle containing the remainder of Solution 2.
9. Incubate for 15 min in a 37°C shaking water bath at 100 rpm.
10. Add 20 mL of Solution 4 to inhibit trypsin activity and transfer the cell suspension to a 50 mL tube.
11. Centrifuge for 5 min at 200×*g* and carefully remove the supernatant.
12. Add 7 mL of Solution 3. Disperse the softened tissue using a 10 mL syringe with a cannula attached.
13. Move the suspension slowly up and down ten times until it is translucent. Allow to stand for 3–5 min so that all the pieces of nondispersed tissue settle to the bottom of the tube.
14. In the meantime, prepare a 50 mL tube with 10 mL of culture medium at 37°C. Transfer the suspension using a Pasteur pipette, taking care not to transfer any lumpy tissue.
15. Centrifuge for 5 min at 200×*g* and carefully remove the supernatant.
16. Add 2 mL of culture medium and pipette gently to disaggregate the pellet. Add up to 10 mL or more depending on the size of the pellet.
17. Take a small aliquot of the cell suspension in order to determine the cell density using a hemocytometer.
18. Obtain the desired cell density to be plated by diluting the cell suspension in culture medium.

19. Seed cells at 4×10^5 cells/cm^2 in appropriate culture plates and place them into a humidified 37°C, 5% CO_2 incubator.
20. One or 2 days after seeding, add 10 μM Ara-C in order to avoid proliferation of non-neuronal cells. Cultures are mature after 6–8 days in vitro (DIV).

3.1.2. Cerebral Cortical Neurons

To prepare cerebral cortical neuron cultures the cerebral cortices are harvested from embryonic day (E) 15 mouse brains (E16 and E17 can also be used).

3.1.2.1. Stock Solutions

All the stock solutions described for cerebellar granule cell cultures (Sect. 3.1.1).

3.1.2.2. Culture Medium

Cortical neurons are not cultured in a depolarized medium. Therefore, do not add KCl to the DMEM medium. Otherwise, the culture medium is the same as that described for cerebellar granule cells (Sect. 3.1.1).

3.1.2.3. Disaggregation Solutions

Cortical neurons are more sensitive to the deleterious effects of trypsin, so only add 0.4 mL of trypsin solution in Krebs Solution 2. Otherwise, use the disaggregating solutions described in Sect. 3.1.1.

3.1.2.4. Procedure

1. Kill pregnant mouse by cervical dislocation.
2. In a flow cabinet, clean the abdomen with 70% ethanol and perform a length-wise incision in the midline with scissors.
3. Open the abdomen and remove the uterus using forceps, transferring it to a Petri dish. Take out the embryos and transfer them to a Petri dish containing cold PBS.
4. Cut off the heads and open the scalp and the skull by using fine forceps or ophthalmological scissors. Remove out the brain and place in a fresh dish with PBS.
5. Dissect both cerebral cortices by using forceps and place them in a Petri dish with fresh PBS. Then strip off the meninges. Dissect preferably under a stereoscopic microscope.
6. Transfer the dissected material to a 35 mm Petri dish containing sterile cold PBS and keep on ice while proceeding with all the brains.
7. Transfer the cortices obtained from the whole litter to a sterile Teflon plate and follow the same culture method described above for preparing cerebellar granule cell cultures (steps 5–18, Sect. 3.1.1). Take care to avoid excessive chopping of the tissue.

8. Seed cells at 3×10^5 cells/cm^2 in appropriate culture plates previously coated with poly-L- or poly-D-lysine, and place them in a humidified 37°C, 5% CO_2 incubator.
9. One or 2 days after seeding add 2 µM Ara-C in order to avoid proliferation of non-neuronal cells. Cultures are mature after 6–8 DIV.

3.1.3. Hippocampal Neurons

To prepare hippocampal neuron cultures, hippocampi are harvested from E18 mouse brains (E17 and E19 can also be used).

3.1.3.1. Stock Solutions

All the stock solutions described for cerebellar granule cell cultures (Sect. 3.1.1).

3.1.3.2. Culture Medium

Culture medium described for preparing cerebral cortical neuron cultures (Sect. 3.1.2).

3.1.3.3. Disaggregation Solutions

All the disaggregation solutions described for preparing cerebral cortical neuron cultures (Sect. 3.1.2).

3.1.3.4. Procedure

Steps 1–3 as for cerebral cortical neuron cultures (Sect. 3.1.2).

4. Cut off the heads and peel away the scalp and the skull using finer forceps.
5. Take out the brain using a spatula or scissors and place it in a dish with cold PBS under a stereoscopic microscope.
6. Remove the cerebellum, separate the two hemispheres, and remove the meninges. Take one cerebral hemisphere and remove the midbrain using forceps in order to expose the hippocampus. This forms a half-circle ring connected at the convex side to the cortex and at the concave side to the meninges.
7. Dissect the hippocampus away from the cortex using ophthalmological scissors and clean off the meninges.
8. Transfer the dissected material to a 35 mm Petri dish containing cold PBS and keep on ice while proceeding with all the brains.
9. Transfer the hippocampi from the whole litter to a sterile Teflon plate and follow the same culture method described previously for preparing cerebellar granule cell cultures (steps 5–18, Sect. 3.1.1).
10. Seed cells at 2×10^5 cells/cm^2 in appropriate culture plates previously coated with poly-L- or poly-D-lysine, and place them into a humidified 37°C, 5% CO_2 incubator.
11. Two days after seeding add 6–8 µM Ara-C in order to avoid proliferation of non-neuronal cells, but remove it by changing the medium after 3 days of culture. Cultures are mature after 6–8 DIV.

3.2. Primary Mouse Glial Cultures

3.2.1. Mixed Glial Cultures

Mixed glial cultures are prepared from the cerebral cortices of P2–P4 C57BL/6 mice.

3.2.1.1. Stock Solutions

1. Serum: heat-inactivated FBS.
2. Antibiotics: 10,000 i.u. penicillin and 10,000 µg/mL streptomycin (Invitrogen, 15140).
3. Antimycotic: 250 µg/mL amphotericin B (Fungizone®, Invitrogen, 15290).
4. Trypsin solution: 0.25% trypsin-1 mM EDTA in Hanks' balanced salt solution (HBSS, Invitrogen, 25200).
5. DNase solution: 40 mg DNase in 10 mL PBS.

   All these products can be stored in aliquots at –20°C.

3.2.1.2. Culture Medium

DMEM:F12 (Invitrogen, 31330038, with glutamine and HEPES), to which 10% serum, 1/1,000 antibiotics, and 1/500 amphotericin B is added.

3.2.1.3. Procedure

1. Use 6–8 animals. Clean head and neck with 70% ethanol and kill the animals by decapitation in a flow cabinet. Transfer heads to a Petri dish.
2. Dissect the brain and place it in a fresh 60 mm Petri dish with cold PBS. Remove the cerebellum and midbrain and dissect the meninges under a stereoscopic microscope.
3. Transfer the dissected material to a 35 mm Petri dish contai-ning cold PBS and keep on ice while proceeding with all the brains.
4. Cut the cortical tissue into small pieces with a scalpel, transfer to a capped 50 mL plastic centrifuge tube, and add PBS to a final volume of approximately 20 mL.
5. Centrifuge at 200×*g* for 2 min.
6. Remove the supernatant through aspiration with a Pasteur pipette connected to vacuum and resuspend the pellet in 12 mL of trypsin solution. Incubate at 37°C for 25 min with shaking (100 rpm) in order to dissociate the tissue.
7. Add 12 mL of cell culture medium with serum and 0.5 mL DNase solution to the cell suspension and then pass it 20–40 times up and down through a 10 mL serological pipette. Serum components will stop trypsinization and DNase will digest nucleic acids released during the chemical and mechanical disaggregation of the tissue.
8. Centrifuge the cell suspension at 200×*g* for 7 min.

9. Carefully remove the supernatant with a Pasteur pipette connected to a vacuum.
10. Add 20 mL of cell culture medium and homogenize gently with a serological pipette.
11. Filter through a cell strainer with nylon mesh (100 µm pore size) (BD Falcon, 352360).
12. Count the cells using a Neubauer hemocytometer.
13. Adjust the cell suspension to a density of $3–3.5 \times 10^5$ cells/mL using culture medium.
14. Seed the cells in the desired T-flasks, Petri dishes, or multiwell culture plates at a density of $1.0–1.3 \times 10^5$ cells/cm^2.
15. Maintain the cell cultures in a CO_2 incubator at 37°C in humidified 5% CO_2 atmosphere.
16. Replace the medium every 5–7 days. Confluence is achieved after 10–12 DIV. Use cultures at 2–3 weeks. These cultures contain mainly astrocytes and microglial cells.

3.2.2. Astrocyte-Enriched Cultures

Astrocyte cultures are prepared from the cerebral cortices of P2–P4 C57BL/6 mice.

3.2.2.1. Stock solutions

1. All the stocks solutions listed in Sect. 3.2.1.
2. Ara-C solution: 1 mM Ara-C in distilled water. Filter to sterilize and store in aliquots at –20°C.
3. Laminin solution: 1 mg/mL laminin (Invitrogen, 23017) in distilled water. Filter and store in aliquots at –20°C. To coat the cell supports with laminin, wash the supports with sterilized PBS and incubate with 1/50 laminin solution in sterilized PBS for at least 1 h. Aspirate the laminin solution 10 min before seeding the cells.

3.2.2.2. Culture medium

The same as that for mixed glial cultures (Sect. 3.2.1).

3.2.2.3. Procedure

Steps 1–13 as for mixed glial cultures (Sect. 3.2.1).

14. Seed the cells at a density of $1.0–1.3 \times 10^5$ cells/cm^2 in laminin coated T-flasks, Petri dishes, or multiwell culture plates to facilitate the attachment of astrocytes and reduce the presence of microglial cells.
15. Maintain the cell cultures in a CO_2 incubator at 37°C in a humidified 5% CO_2 atmosphere. Replace the medium every 5–7 days.
16. Just when confluence is achieved (6–8 DIV in the presence of laminin coating) add 1/100 Ara-C solution (10 µM final concentration) to the culture medium for 4 days in order to minimize the proliferation of microglial cells.

17. Change the culture medium to fresh medium without Ara-C.
18. Use the cultures 1 day later. These cultures contain >95% of astrocytes.

3.2.3. Microglial-Enriched Cultures

Microglial cultures are obtained from the cerebral cortices of P2–P4 C57BL/6 mice. Mixed glial cultures are prepared as described above (Sect. 3.2.1), while microglial-enriched cultures are obtained by the mild trypsinization method described by Saura et al. (7) as follows.

3.2.3.1. Stock Solutions

All the solutions listed in Sect. 3.2.1.

3.2.3.2. Culture Medium

The same as that for mixed glial cultures (Sect. 3.2.1).

3.2.3.3. Procedure

Steps 1–15 as for mixed glial cultures (Sect. 3.2.1).

16. Replace the medium every 5–7 days. Once confluence is achieved (10–12 DIV), microglial cells start to proliferate. Maintain the mixed glial cultures for 18–19 DIV and then change the culture medium.
17. At 24–48 h collect the culture medium and keep it at 37°C as conditioned culture medium.
18. Rinse the cells with serum-free medium.
19. Incubate the cells with trypsin solution diluted 1:4 in serum-free culture medium for 25–35 min in the CO_2 incubator. The upper layer of the culture, constituted mainly by astrocytes, will slowly detach and a lower layer of mainly microglial cells will remain firmly attached to the support.
20. Add an equal volume of culture medium containing serum to stop the trypsinization process.
21. Remove the medium with the detached cells, and return the conditioned medium obtained in step 17 to the culture.
22. Use the cells 1 day later. These cultures contain >98% of microglial cells.

3.2.4. Primary Mouse Oligodendrocyte Cultures

Oligodendrocyte cultures are obtained from whole brains of adult mice.

3.2.4.1. Stock Solutions

1. HBSS without calcium, magnesium 1× (Invitrogen, 14170).
2. HBSS 10× (Invitrogen, 14180).
3. Percoll (Fluka, 77237).
4. 10 mg/L poly-L-lysine (see Sect. 3.1.1).
5. 2 mM Ara-C (see Sect. 3.1.1).

3.2.4.2. Culture Medium

Minimum Eagle medium (MEM) (Sigma, M4655), supplemented with 25 mM glucose, 2 mM L-glutamine and 10% FBS, 100 µg/mL gentamicin and 0.25 µg/mL amphotericin B.

3.2.4.3. Disaggregation Solutions

PBS with 0.02% EDTA, 2.5 mg/mL trypsin, and 80 μg/mL DNase. Warm at 37°C.

Procedure

1. Dissect aseptically the whole brain from 10 to 15 adult mice and place them in a Petri dish with cold PBS. Clean off the meninges and large blood vessels and transfer brains to another Petri dish with 20 mL of cold PBS.
2. Transfer one brain at a time to a Teflon plate (5 × 5 cm) and cut with a razor blade or scalpel in small blocks of approximately 3 × 3 × 3 mm.
3. Transfer minced tissue into a 100 mL glass bottle containing 20 mL of disaggregating solution. Gently disperse the tissue up and down twice with a 10 mL pipette.
4. Incubate for 30 min in a 37°C shaking water bath.
5. Add 2 mL of FBS to inhibit trypsin activity and disperse the softened tissue by gently pipetting up and down 20 times with a 10 mL pipette until the cell suspension is translucent.
6. Allow to stand for 3–5 min so that all the pieces of nondispersed tissue settle to the bottom of the bottle.
7. Take the cell suspension and filter by passing through a 100 μm nylon cell strainer settled on the top of a 50 mL tube.
8. Centrifuge the filtered cells at 500×*g* for 10 min and discard the supernatant.
9. Add 2 mL of HBSS and pipette gently to disaggregate the pellet. Add up to 20 mL HSS. Add 9 mL Percoll and 1 mL HBSS 10×. Mix to form a 30% Percoll solution and transfer to a 25 mL sterile capped glass tubes (Corex, No. 8446).
10. Centrifuge in a refrigerate centrifuge with a fixed angle rotor for 30 min at 30,000×*g* (e.g., Sorvall, rotor SA-600, at 14,400 rpm) at 4°C, without brakes.
11. After centrifugation, discard (from top to bottom) layer 1 of clear HBSS and layer 2 of myelin. Collect 10–15 mL of layer 3 of viable oligodendrocytes. Discard layers 4 and 5 of erythrocytes and debris, respectively.
12. Transfer the oligodendrocytes to a 50 mL tube containing 30 mL HBSS 1× and mix gently.
13. Centrifuge at 500×*g* for 15 min.
14. Discard the supernatant and add 2 mL of culture medium. Pipette gently to disaggregate the pellet. Add up to 10 mL.
15. Centrifuge for 10 min at 200×*g*.
16. Resuspend the pellet again in 5 mL of culture medium.
17. Take a small aliquot of the cell suspension in order to determine the cell density using a hemocytometer.

18. Obtain the desired cell density to be plated by diluting the cell suspension in culture medium.
19. Seed cells at 5×10^6 cells/flask in uncoated 25 cc T-flasks (T25), and place them in a humidified 37°C, 5% CO_2 incubator.
20. After 24 h shake gently and collect the supernatant with the oligodendrocytes. Disperse to single cells with a Pasteur pipette and medium, centrifuge at 200×*g* and seed again at 5×10^6 cells/flask in uncoated T25.
21. Repeat step 20, but this time seed at $0.5–1 \times 10^5$ cells/cm^2 on poly-L-lysine coated plates. These cultures contain >95% oligodendrocytes at 3 DIV. Thereafter, it is advisable to add 5 μM Ara-C to curtail proliferation of contaminant nonoligodendroglial cells so as to use mature oligodendrocytes after 10 DIV. Change the medium twice a week.

3.3. Primary Cultures of Human Fetal Brain

3.3.1. Human Cerebral Cortical Neurons

Primary cultures of cerebral cortical neurons are prepared from human fetal cerebral cortical tissue.

3.3.1.1. Stock Solutions

1. Preserving solution: PBS with 3 g/L bovine seroalbumin and 100 μg/mL gentamicin. Add 50 mL in 100 mL sterile plastic capped flasks and keep at 4°C until used for human fetal tissue samples.
2. Horse serum (HS) (Invitrogen, 16050), heat-inactivated by incubation at 56°C for 30 min. Store in 50 mL aliquots at –20°C.
3. Other stock solutions are the same as those described for preparing cerebellar granule cell cultures (Sect. 3.1.1).

3.3.1.2. Culture Medium

MEM (Sigma M4655), supplemented with 25 mM glucose, 2 mM L-glutamine and 5% HS, 100 μg/mL gentamicin and 0.25 μg/mL amphotericin B.

3.3.1.3. Disaggregation Solutions

Disaggregation solutions are the same as those described for preparing mouse cerebral cortical neuron cultures (Sect. 3.1.2).

3.3.1.4. Procedure

1. A piece of fetal cerebral cortical tissue is collected aseptically from a therapeutic abortion (14–18 weeks of pregnancy), immersed in the preservation solution, and kept at 4°C until used for culture, up to 24 h.
2. Tissue is washed twice with cold PBS by transferring it with forceps from one Petri dish containing PBS to another one.
3. Meninges and vessels plus any noncerebral cortical tissue that may be present are discarded.
4. Next, follow the same procedure as that for cerebellar granule neuron culture (steps 5–18, Sect. 3.1.1).

5. Seed cells at 2×10^5 cells/cm^2 in appropriate culture plates, previously coated with poly-L-lysine, and place them in a humidified 37°C, 5% CO_2 incubator.
6. Change the medium once a week. Do not add Ara-C, or only transiently as in mouse hippocampal neuron culture (step 11, Sect. 3.1.3). Cultures up to 15 DIV are highly enriched in neurons. Cultures are mature after 10–15 DIV. Use neurons up to 3 weeks old.

3.3.2. Human Cortical Astrocyte Cultures

Astrocyte cultures are obtained from human fetal cerebral cortical tissue previously processed for neuron culture.

3.3.2.1. Culture Medium

Culture medium is the same as that described for preparing human fetal cerebral cortical neuron cultures (Sect. 3.3.1).

3.3.2.2. Disaggregation Solution

PBS with 0.02% EDTA and 50 µg/mL trypsin.

3.3.2.3. Procedure

1. Use 30 DIV human fetal neuron cultures (Sect. 3.3.1) seeded in a 75 cc T-flask (T75).
2. Wash culture with PBS and incubated with 10 mL disaggregating solution for 2–5 min.
3. Cells are detached by gently pipetting with a Pasteur pipette and then transferred to a 50 mL tube containing 0.5 mL of FBS to inhibit trypsin.
4. Add 10 mL of PBS to the flask to remove all the cells and transfer to the same tube.
5. Centrifuge at 200×*g* for 5 min and carefully remove the supernatant.
6. Add 2 mL of culture medium and pipette gently to disaggregate the pellet. Add up to 30 mL and seed in two T-flasks to obtain a subculture dilution 1:2.
7. Place them in a humidified 37°C, 5% CO_2 incubator.
8. After 2 weeks, check the astrocyte cultures visually for the presence of surviving neurons. If abundant, do another subculture by following steps 2–5, and then culture astrocytes for another 2 weeks. Cultures should be nearly pure by then.
9. Trypsinize again (steps 2–5).
10. Add 2 mL of culture medium and pipette gently to disaggregate the pellet. Add up to 7 mL of medium per astrocyte T75 used.
11. Take a small aliquot of the cell suspension in order to determine the cell density using a hemocytometer.
12. Obtain the desired cell density to be plated by diluting the cell suspension in culture medium.

13. Seed astrocytes at 1×10^5 cells/cm^2 in appropriate culture plates, previously coated with poly-L-lysine, and place them back in the CO_2 incubator.
14. Change the medium once a week throughout the procedure. Use astrocytes at 3–5 days after the final seeding.

3.3.3. Human Cortical Microglia Cultures

Microglia cultures are obtained from human fetal cerebral cortical tissue previously processed for neuron culture.

3.3.3.1. Culture Medium

Culture medium is the same as that described for preparing human fetal cerebral cortical neuron cultures (Sect. 3.3.1).

3.3.3.2. Procedure

1. Use human fetal neuron cultures (Sect. 3.3.1) seeded in T75 before the first weekly change of culture medium at 7 DIV.
2. Shake flask on a shaking plate at 37°C for 2–4 h.
3. Collect medium in a 50 mL tube.
4. Centrifuge at 200×*g* for 5 min and carefully remove the supernatant.
5. Add 2 mL of culture medium and pipette gently to disaggregate the pellet.
6. Take a small aliquot of the cell suspension in order to determine the cell density using a hemocytometer. Obtain the desired cell density to be plated by diluting the cell suspension in culture medium.
7. Seed cells at $0.5–1 \times 10^5$ cells/cm^2 in appropriate culture plates, previously coated with poly-L-lysine, and place them into a humidified 37°C, 5% CO_2 incubator. Use microglia at 1–3 days after seeding.

4. Notes

1. Most laboratories can be adapted to performing cell cultures, but it is advisable to design the cell culture room by following a sterility gradient (11).
2. Mice neuron cultures are routinely used at 6–8 DIV. For differentiation studies (i.e., neurite outgrowth) or chronic studies, cultures can be treated as early as 1 DIV. Supplements added to the culture medium support neuron survival without a need for medium replacement. Human neuron cultures live longer and also mature slower than rodent cultures.
3. Other media commonly used for mice neuron cultures include formulations where the presence of serum is avoided and DMEM is supplemented with B27 supplement (Invitrogen,

L17504) or N2 supplement (Invitrogen, L17502). The medium is then periodically replaced with fresh medium. Most neurons survive with medium changes every other day, preferentially with a partial replacement, although this is not the case for mature cerebellar granule cells.

4. In this chapter, we have described a method of obtaining mouse astrocyte-enriched cultures in which microglial contamination is avoided/minimized by facilitating the adhesion of astrocytes (laminin coating) and through the use of an antimitotic agent (Ara-C) once a confluent monolayer of astrocytes is obtained (Sect. 3.2.2). The use of agents that selectively destroy macrophages, such as L-leucine methyl ester (12), as well as the use of subcultures or procedures including shaking, has also been described to increase the purity of astroglial cultures (reviewed in (13)). In fetal human astrocyte cultures, the limited passage used to get rid of neurons also decreases the presence of microglia (Sect. 3.2.2). However, the use of microglial markers is advisable in order to assess the degree of purity of astroglial cultures.
5. To prepare mouse microglia-enriched cultures, microglial cells can also be obtained by shaking from mixed glial cultures (6), as described in the human astrocyte culture protocol (Sect. 3.3.3). However, in that case only the microglial cells growing above the astroglial cell layer are detached, while the microglia growing below the astrocyte layer remain attached. The use of the method described in this chapter for mouse cultures (Sect. 3.2.3) results in a higher yield of microglial cells than does the shaking method (7).
6. Oligodendrocyte cultures can also be obtained from human tissue for selected experiments. The percentage of oligodendrocytes that can be isolated from the fetal brain is very low (10) and it is better to use tissue samples of postmortem adult-brain white matter (8). To this end, use donated tissue from adult-brain white matter obtained via autopsy (it being essential that a few hours elapse between death and culture) and follow the procedure for mice oligodendrocyte cultures (Sect. 3.2.4).
7. The use of mixed neuronal-glial cultures or co-cultures is also an interesting tool to be considered in neurotoxicology. Interactions between the different types of neural cells play an important role in the normal function of the brain, as well as in the response of the brain to negative stimuli, such as neurotoxicants. When neuronal cell cultures are grown in the absence of Ara-C, mixed neuronal-glial cell cultures are obtained. The final percentage of the different glial cell types present (mainly astroglial and microglial cells) will depend on the kind and the age of the neuronal culture and the culture medium used. Co-cultures of different types of neural cells can be obtained by seeding one type of cell over a culture of another type at a

pre-established ratio (direct contact). Thus, glial cells can be seeded over a monolayer of neuron cells or vice versa. In addition, one neural cell type can be seeded in a separate compartment (or insert) inside a culture well while another neural cell type is seeded at the bottom of the same culture well. This system allows the interchange of soluble factors in the absence of direct contact between the two cell cultures.

8. Routine observation under the inverted microscope by phase contrast is essential in order to check the correct status of the culture before using it for testing. The different brain cell types show specific morphology in culture, which can generally be appreciated in phase contrast images. Neurons extend characteristic long neurite processes. Different neurons have different morphologies, i.e., cerebellar granule cells are all small and spherical and appear bright under the phase contrast microscope, whereas cerebral cortical and hippocampal neurons are more heterogeneous, containing the larger and darker pyramidal neurons. Glial cells show morphological differences depending on the presence of other neural cell types or the density of culture. Thus, astrocytes present a flat and polygonal shape with few processes in astrocyte-enriched cultures or mixed glial cultures, but a stellate morphology with abundant and branched thin processes in neuronal-astrocyte cultures. Microglial cells present either an elongated or amoeboid morphology when they are cultured alone, but a more spherical morphology with short and thin processes when they are cultured in the presence of astrocytes. Cell-specific immunostaining is advisable in order to appreciate these differences better. The use of immunocytochemical techniques allows the cell types present in a primary culture to be identified. Commercial antibodies or histochemical stains are available as specific markers for the different kinds of neural cells, for instance: (a) anti-neuronal nuclei (anti-NeuN) or anti-microtubule associated protein 2 (anti-MAP2) antibodies as neuron markers, (b) anti-glial fibrillary acidic protein (anti-GFAP) antibody as an astrocyte marker, (c) Lycopersicon sculentum (tomato) lectin or anti-CD11b antibody as microglial markers, and (d) anti-galactocerebroside (anti-GalC) antibody as an oligodendroglial marker.

Acknowledgments

The authors acknowledge support from the following grants: PI06/1212, PI08/1396, PI10/0453 and RD06/0013/1004 from ISCIII, SAF2006-13092-C02-02 and SAF2009-13093-C02-02 from MICINN, Spain, and LSHB-CT-2004-512051 from European Commission.

References

1. Patel AJ, Lewis PD (1988) Brain cell acquisition and neurotropic drugs with special reference to functional teratogenesis. Prog Brain Res 73:389–403
2. Sanfeliu C, Cristòfol R, Torán N, Rodríguez-Farré E, Kim SU (1999) Use of human central nervous system cell cultures in neurotoxicity testing. Toxicol In Vitro 13:753–759
3. De Vera N, Martínez E, Sanfeliu C (2008) Spermine induces cell death in cultured human embryonic cerebral cortical neurons. J Neurosci Res 86:861–872
4. Hertz E, Yu ACH, Hertz L, Juurlink BHJ, Schousboe A (1989) Preparation of primary cultures of mouse cortical neurons. In: Shahar A, de Vellis J, Vernadakis A, Haber B (eds) A dissection and tissue culture manual of the nervous system. Alan R. Liss, New York, pp 203–206
5. Schousboe A, Meier E, Drejer J, Hertz L (1989) Preparation of primary cultures of mouse (rat) cerebellar granule cells. In: Shahar A, de Vellis J, Vernadakis A, Haber B (eds) A dissection and tissue culture manual of the nervous system. Alan R. Liss, New York, pp 203–206
6. Giulian D, Baker TJ (1986) Characterization of ameboid microglia isolated from developing mammalian brain. J Neurosci 6:2163–2178
7. Saura J, Tusell JM, Serratosa J (2003) High-yield isolation of murine microglia by mild trypsinization. Glia 44:183–189
8. Kim SU (1990) Neurobiology of human oligodendrocytes in culture. J Neurosci Res 27:712–728
9. Satoh J, Kim SU (1994) HSP72 induction by heat stress in human neurons and glial cells in culture. Brain Res 653:243–250
10. Satoh J, Kim SU (1994) Proliferation and differentiation of fetal human oligodendrocytes in culture. J Neurosci Res 39:260–272
11. Freshney RI (1992) Design and layout of the laboratory. In: Freshney RI (ed) Culture of animal cells, 3rd edn. Wiley-Lis, New York, pp 17–30
12. Hamby ME, Uliasz TF, Hewett SJ, Hewett JA (2006) Characterization of an improved procedure for the removal of microglia from confluent monolayers of primary astrocytes. J Neurosci Methods 150:128–137
13. Du F, Qian ZM, Zhu L, Wu XM, Qian C, Chan R, Ke Y (2010) Purity, cell viability, expression of GFAP and bystin in astrocytes cultured by different procedures. J Cell Biochem 109:30–37

Chapter 5

Preparation and Use of Serum-Free Aggregating Brain Cell Cultures for Routine Neurotoxicity Screening

Paul Honegger and Marie-Gabrielle Zurich

Abstract

The nervous system is a frequent target of industrial chemicals, pharmaceuticals, and environmental pollutants. To screen large numbers of compounds for their neurotoxic potential, in vitro systems are required which combine organ-specific traits with robustness and high reproducibility. These requirements are met by serum-free aggregating brain cell cultures derived from mechanically dissociated embryonic rat brain. The initial cell suspension, composed of neural stem cells, neural progenitor cells, immature postmitotic neurons, glioblasts, and microglial cells, is kept under continuous gyratory agitation. Spherical aggregates form spontaneously and are maintained in suspension culture for several weeks. Within the aggregates, the cells rearrange and mature, reproducing critical morphogenic events such as migration, proliferation, differentiation, synaptogenesis, and myelination. In addition to the spontaneous reconstitution of histotypic brain architecture, the cultures acquire organ-specific functionality as indicated by activity-dependent glucose consumption, spontaneous electrical activity, and brain-specific inflammatory responses. These three-dimensional primary cell cultures offer therefore a unique model for neurotoxicity testing both during development and at advanced cellular differentiation. The high number of aggregates available and the excellent reproducibility of the cultures facilitate routine test procedures. This chapter presents a detailed description of the preparation and maintenance of these cultures as well as their use for routine toxicity testing.

Key words: Aggregating brain cell cultures, Development, Maturation, Neurotoxicity, Gliotoxicity, CNS, Three-dimensional cell culture, Organ toxicity, High content analysis

1. Introduction

The introduction of new regulations for hazard evaluations and novel approaches in drug testing increased the need for in vitro systems for toxicity assessments. The central nervous system is a frequent target of industrial chemicals, pharmaceuticals, and environmental pollutants, calling for efficient in vitro systems representing the functional characteristics of this specific organ. Previous work has shown that the rotation-mediated aggregating

Michael Aschner et al. (eds.), *Cell Culture Techniques*, Neuromethods, vol. 56,
DOI 10.1007/978-1-61779-077-5_5,

brain cell cultures provide a suitable system for neurotoxicity testing, including developmental, acute, and chronic neurotoxicity. The most characteristic features of these cultures include the spontaneous formation of free-floating regular spheroids, their organotypic three-dimensional characteristics, and their extensive structural and functional maturation. The high reproducibility and robustness of these cultures are largely due to the initial mechanical dissociation of the embryonic brain tissue and to the use of a chemically defined culture medium (1). The aggregates, which form spontaneously from the initial cell suspension within the first days in vitro, are maintained under continuous gyratory agitation in a CO_2 incubator. The cell types present in the original brain tissue are also found in the aggregates, including neural stem cells, neural progenitor cells, immature neurons, glial and microglial cells. Most of the macroglia (astrocytes, oligodendrocytes) arise after culture initiation by the proliferation of precursor cells. In the newly created tissue-specific environment, the cells are able to interact by physical contacts as well as by the exchange of soluble messengers and metabolites. These intrinsic factors enable extensive cellular differentiation and the elaboration of histotypic structures such as the natural extracellular matrix, mature synapses, functional neuronal networks, and myelinated axons. This maturation process takes about 1 month. Interestingly, besides the highly differentiated neurons and glial cells present in the mature aggregates, a discrete population of undifferentiated stem/precursor cells persists, comparable with the situation in the adult brain. From the practical point of view, the cultures offer several advantages for their practical use, in particular high yield, robustness, high reproducibility, and the use in permanence of a serum-free, chemically defined culture medium.

Various aspects concerning the characterization of serum-free aggregating brain cell cultures and their use for neurotoxicological investigations have been reviewed previously (2–5). The present chapter provides a detailed description of the preparation, maintenance, and use of aggregating rat brain cell cultures for the detection of chemicals exhibiting organ-specific toxicity. Therefore, the original protocols for culture preparation, maintenance, and use were adjusted to address the routine testing of chemicals. The modifications include the use of rat whole brain (instead of only the telencephalon) as the source of the initial cell fraction; the use of only one size of culture flask for the initiation and maintenance of the cultures (no transfer of the cultures at day 2 from smaller to bigger flasks); and the use of a multiparametric (high content) assay strategy to detect nervous system-specific adverse effects, taking as endpoints gene expression, global rate of RNA synthesis, and the rate of glucose consumption.

The cultures are prepared from 16-day embryonic rat brain (comprising telencephalon, mesencephalon, and rhombencephalon).

The dissected brain tissue is dissociated mechanically into a single cell fraction by the sequential passage through nylon sieves of 200 and 100 μm pore sizes. The cells are then pelleted, washed in Puck's D1 solution by centrifugation, resuspended in cold culture medium (modified DMEM, serum-free), and aliquots transferred to the culture flasks (50-mL DeLong flasks or modified Erlenmeyer flasks). The flasks are then placed on a rotating platform (5 cm rotation diameter; 68 rpm at culture initiation, increased to a maximum of 80 rpm within the following 4 days) in a CO_2 incubator (37°C, 10% CO_2/90% humidified air). Aggregation of the dissociated cells starts immediately after incubation and continues for several hours. The amount of cells derived from one embryonic brain is sufficient for the preparation of one flask containing some 1,200–1,500 aggregates. Initially, all reaggregated cells are immature, as evidenced by low or undetectable levels of cell type-specific differentation markers. While most of the neurons are already postmitotic, the majority of the macroglia arise from glial precursor cells (astrocytes and oligodendrocytes) and continue to proliferate during the first 2 weeks in vitro. Cellular maturation progresses during about 4 weeks, giving rise to highly differentiated histotypic cultures. Throughout the culture period, the media are replenished regularly. The high culture density is beneficial for the cellular stability and maturation, but it requires frequent media replenishment and occasional subdivision (split) of the cultures to assure the adequate supply of metabolic substrates.

For the test procedure, replicate cultures are prepared, i.e., the aggregates of several flasks are pooled, randomized, and aliquoted into smaller culture vessels (e.g., 25-mL DeLong flasks). The use of replicate cultures increases both the testing capacity of the cultures and the statistical power of the data. For example, 32 replicate cultures are prepared for each test, taking the aggregates of five original flasks. With this number of replicates, five compounds at three different concentrations plus untreated controls can be assayed. The cultures are exposed for 44 h to the different chemicals. Four hours before the harvest, the cultures receive radiolabeled uridine to assess the global rate of RNA synthesis. At the time of the harvest, aliquots of the media are taken to measure the glucose concentration as indicator of the global rate of glucose consumption. Of each replicate culture, the total RNA is extracted and the total RNA content per replicate determined. Aliquots of the purified RNA are taken for liquid scintillation counting to determine uridine incorporation and for the preparation of cDNA by reverse transcription (RT) for the subsequent PCR reactions. Gene expression is measured by quantitative RT-PCR for genes representative for neurons (neurofilament protein, NF-H), astrocytes (glial fibrillary acidic protein, GFAP), oligodendrocytes (myelin basic protein, MBP), as well as for one

gene related to cellular stress (heat shock protein-32, HSP32, also called heme oxygenase-1, HO-1). Concentration–effects relationships are determined at sub-cytotoxic drug concentrations. The use of 32 replicate cultures per test is convenient for the application of robotic procedures for the determination of multiple gene expression by qRT-PCR, e.g., making use of 384-well plates and an automated workstation.

2. Materials

2.1. Animals

Timed-pregnant rats, SPF, Sprague–Dawley, 16 days in gestation, counting the day following mating as embryonic day 1 (E1). Embryos of rats mated during the day are taken in the morning of day 16 for culture preparation; embryos of rats mated overnight are taken in the afternoon of day 16 for culture preparation. For more information about the staging and dissection of rat embryos, see Dunnett and Björklund (6). For rat housing, handling, and euthanasia, the existing specific regulations and guidelines have to be followed.

2.2 .Required Special Equipment

2.2.1. Equipment for Cell Culture

Incubator: 37 ± 1°C; 90 ± 5% humidity; 10 ± 1% CO_2/air (e.g., Heraeus, which can be heat sterilized, and accommodates the gyratory shaker listed below).

Gyratory shaker, 50 mm shaking diameter, i.e., a deviation of 25 mm to each side (e.g., Kühner gyratory shaker X-SL, driven by magnetic induction, tolerates high humidity and heat sterilization, and creates only little heat in the incubator, http://www.kuhner.com/).

Osmometer (e.g., Fiske 210 Micro-Sample Osmometer, Advanced Instruments, Inc.).

Culture vessels, i.e., DeLong flasks (Bellco) or modified Erlenmeyer flasks, 25 and 50 mL. The culture flasks are custom made from Schott Duran Erlenmeyer flasks (Verrerie de Carouge; http://www.vdc.ch/), of which the necks are cylindric to accommodate a gas-permeable plastic cap.

Plastic caps for culture vessels (e.g., Bellco KAP-UTS cat no. 2007-18004; http://www.bellcoglass.com/; or Labocap 17/18, cat no. LD107-410, Verrerie de Carouge, http://www.vdc.ch/).

Pyrex glass bottles (100 mL) with air-tight closures for media.

Filtration units for sterile filtration of small volumes (Millipore cat no. SLGP033RB, 0.2 µm) and for larger volumes (Nalgene).

Dissecting tools, including per dissecting person large scissors (1), small pointed scissors (1), large forceps (1), small curved forceps (1), Vannas scissors (1), and Dumont forceps (1).

Nylon-mesh filter bags, prepared from Nitex nylon monofilament (Sefar; http://www.sefar.com/) with either 200 µm

mesh opening (cat. no. 03-200/54) or 100 μm mesh openings (cat. no. 03-100/49). The filter bags can be prepared from double sheets of nylon mesh by sealing and cutting them at once using a 40 W soldering iron. The 200-μm mesh sacs are 14 cm long and 3.5 cm large; the 100-μm mesh sacs are 5.5 cm long and 5 cm large.

Appropriate glass funnels around which the filter bags are fitted. For 200-μm mesh sacs, the funnels have a stem of 12 cm and an outside diameter of 2.5 cm (top) and 1.6 cm (bottom); for 100-μm mesh bags, the funnels have a stem of 4 cm and an outside diameter of 4.5 cm (top) and 2.5 cm (bottom). Only the dimensions of the second, shorter funnel are critical.

Glass rods for mechanical dissociation, 0.6 cm diameter, 20 cm long, with blunt, fire-polished ends.

Conical plastic tubes, sterile, 15 and 50 mL, and suitable racks.

Serological plastic pipettes, 5 and 2 mL.

(Note: For culture sampling and transfer, it is recommended to use 2-mL plastic pipettes with a relatively wide orifice to avoid damage to the aggregate).

2.2.2. Equipment for Analytical Procedures

NanoDrop spectrophotometer.

T3 Thermocycler (Biometra).

Fast Real-Time PCR system 7900 HT (Applied Biosystems).

Liquid scintillation analyzer TRI-CARB 2300TR (Packard).

Polyvials V: 20 mL plastic vials for scintillation counting (Zinsser analytic, cat. no. 3071401).

RNase-free tips (Diamond, Gilson).

Safe-Lock microtubes 1.5 mL (Eppendorf), microtubes 0.5 mL (Eppendorf), and suitable racks.

PCR strip tubes (Axygen, cat. no. PCR-0208-C) and PCR strip caps (Axygen, cat. no. PCR-02CP-C).

MicroAmp optical 96- and 384-well reaction plates (Applied Biosystem, cat. no. N801-0560).

MicroAmp optical adhesive film (Applied Biosystems, cat. no. 4311971).

ABI prism optical adhesive cover starter kit (Applied Biosystems, cat. no. 4313663).

Glucose analyzer (Beckman coulter glucose analyzer-2).

2.3. Optional Special Equipment

Dissecting block (optional) with wells for Petri dishes and perfused with cooling liquid.

Glass pipettes, 5 mL for media replenishment.

Cotton plugger for glass pipettes (convenient if recyclable glass pipettes are used for media replenishment, as cost-reducing measure).

Pyrex glass jar (10 L) for the preparation of media, PBS, and Puck's solution D1.

Water purification system (Millipore or Barnstead).
Peristaltic pump for media filtration.
Filtration units for sterile filtration of large volumes (Microgon MediaKap-10 hollow fibers).
Pyrex glass bottles with air-tight closures, 500 mL to store culture media and PBS.
Laboratory Automation Workstation Biomek 3000 (Beckman Coulter).

2.4. Chemicals and Reagents

2.4.1. Chemicals for Cell Culture

DMEM powder mix for 10 L (Gibco-BRL cat. no. 52100-039) containing high glucose (4.5 g/L) and glutamine, but no bicarbonate and no pyruvate.
Trace elements and various other salts of the highest purity available (see below).
Ultrapure water.
Ethanol absolute (Fluka, cat. no. 02860).
D-Glucose monohydrate ultrapure (Fluka, cat. no. 49158).
D-Sucrose biochem. grade (Fluka, cat. no. 84100).
Gentamicin sulfate (Sigma cat. no. G 1264).
Vitamins BME 100-fold concentrated (Sigma cat. no. B 6891)
L-Carnitine (Fluka, Buchs, Switzerland cat. no. 22018).
Choline chloride (Sigma cat. no. C 7527).
Hydrocortisone hemisuccinate (Sigma cat. no. H 2270).
Insulin (Sigma cat. no. I 5500).
Linoleic acid (Sigma cat. no. L 8134).
Lipoic acid (Sigma cat. no. T 5625).
Transferrin (human) (Sigma cat. no. T 2252).
Triiodothyronine (Sigma cat. no. T 2752).
Vitamin A alcohol (Fluka cat. no. 95144).
Vitamin B12 (Fluka, cat. no. 95190).
Vitamin E (Sigma cat. no. T 3251).
Phenol red (Fluka cat. no. 77660).

2.4.2. Products for Analytical Procedures

Uridine[5,6-^{3}H] (PerkinElmer, cat. no. NET 367).
QIAshredder (Qiagen, cat. no. 79656).
RNeasy Protect Mini Kit (Qiagen, cat. no. 74126).
Tissue solubilizer (NCS, Amersham).
Scintillation fluid Flo-Scint A (PerkinElmer, cat. no. 6013569).
TaqMan reverse transcription reagents (Applied Biosystems, cat. no. N8080234).
Primers for qRT-PCR (Microsynth).
SYBR GREEN PCR master mix (Applied Biosystems, cat. no. 4312704).
Glucose reagent kit (Beckman coulter cat. no. 671640).
Dimethyl sulfoxide (DMSO), analytical grade.
2-Mercaptoethanol (Fluka, cat. no. 63690).

3. Methods

3.1. Preparation of Solutions and Media for Cell Culture

(Protocols are given for all solution preparations, although it may be possible to purchase custom-made solutions and media. All solutions are made with ultrapure water, which is an absolute requirement when working with serum-free culture media).

3.1.1. 20× Concentrated Salts for Puck's Solution D1

Dissolve in ultrapure water 160 g/L NaCl, 8 g/L KCl, 1.5 g/L $Na_2HPO_4 \times 12\ H_2O$, 0.6 g/L KH_2PO_4, and 100 mg/L phenol red.

Sterilize by filtration and store frozen in aliquots of 100 mL.

3.1.2. 20× Concentrated Glucose/Sucrose for Puck's Solution D1

Dissolve in ultrapure water 22 g/L D-glucose monohydrate and 400 g/L D-sucrose.

Sterilize by filtration and store frozen in aliquots of 100 mL. After thawing, shake vigorously before use.

3.1.3. Gentamicin Stock Solution 500×

12.5 mg/mL of gentamicin sulfate. Sterilize by filtration and store at 4°C.

3.1.4. Puck's Solution D1

To 450 mL ultrapure sterile water add 25 mL of 20× concentrated salts for Puck's solution D1 plus 25 mL of 20× concentrated glucose/sucrose for Puck's solution D1. Check osmolarity and adjust, if necessary to 340 ± 5 mOsm. Store at 4°C. Shortly before use, adjust to pH 7.4 with sterile 0.2 N NaOH (color of solution should be "salmon" red, neither yellowish nor purplish) and add 1 mL gentamicin stock solution 500×.

3.1.5. Trace Elements, 10^4-Fold Concentrated

(Prepare the following nine aqueous solutions separately and store them at –20°C in 1 mL aliquots):

2.5 mM $Na_2SiO_3 \times 5H_2O$

0.15 mM Na_2SeO_3

0.05 mM $CdSO_4 \times 8H_2O$

0.1 mM $CuSO_4 \times 5H_2O$

0.05 mM $MnCl_2 \times 4H_2O$

0.005 mM $(NH_4)_6Mo_7O_{24} \times 4H_2O$

0.0025 mM $NiSO_4 \times 6H_2O$

0.0025 mM $SnCl_2 \times 2H_2O$

0.5 mM $ZnSO_4 \times 7H_2O$.

3.1.6. Media Supplements 10^3-Fold Concentrated

(Prepare the following five aqueous solutions separately, sterilize them by filtration, and store at –20°C in aliquots of 5–10 mL):

0.02 mM hydrocortisone hemisuccinate

0.03 mM triiodothyronine

10 mM linoleic acid

5 mg/mL insulin

1 mg/mL transferrin

3.1.7. Concentrated Mixture of Vitamins A and E

Dissolve 114 mg vitamin A in 0.2 mL absolute ethanol and mix this solution with 1.8 g of vitamin E. Store this mixture at –20°C protected from light.

3.1.8. Modified DMEM Serum-Free Culture Medium

Fill a 10-L glass jar (Pyrex) with about 8 L of ultrapure water and dissolve under gentle stirring (using a large magnetic stirring bar) DMEM powder mix for 10 L (Gibco-BRL cat. no. 52100-039), containing high glucose (4.5 g/L) and glutamine, but no bicarbonate and no pyruvate.

Add the following supplements: 1.35 g choline chloride, 20 mg L-carnitine, 2 mg lipoic acid, 13.6 mg vitamin B12.

Add 1 mL of each of the nine trace elements 10^4-fold concentrated.

Add 37 g $NaHCO_3$ and immediately adjust to pH 7.0–7.2 (color yellowish to salmon red) by bubbling CO_2 gas into the medium (note that for storage, the medium is kept slightly below the optimal pH, since it increases somewhat by warming the medium up to 37°C prior to use).

Adjust the osmolarily of the medium to 340 ± 2 mOsm by adding the required volume of ultrapure water.

Sterilize the medium by filtration using MediaKap-10 hollow fiber filters and a peristaltic pump. Store the medium in 500-mL Pyrex bottles with gas-tight closures, at 4°C in the dark. (Note: The shelf life of this medium is only about 2 months because of high glutamine, forming ammonia by its degradation).

3.1.9. Completion of the Culture Medium

Shortly before use (maximum 1 week), complete the medium by adding the following sterile supplements per 500 mL of medium:

0.5 mL of each of the five 10^3-fold concentrated media supplements, i.e., 0.02 mM hydrocortisone hemisuccinate, 0.03 mM triiodothyronine, 10 mM linoleic acid, 5 mg/mL insulin, and 1 mg/mL transferrin.

1 mL of gentamin stock solution 500×.

0.05 mL of concentrated mixture of vitamins A and E sonicated in 10 mL of medium and added to 500 mL of medium by sterile filtration (Millex-GP 0.2 μm) (note that only a small fraction of the vitamins will pass the filter).

5 mL of vitamins BME 100-fold concentrated.

(Note: The sterility of the final culture medium is checked by the incubation of a 4 mL aliquot under normal culture conditions for at least 1 day).

3.2. Washing the Glassware

Glass culture vessels and glass pipettes can be recycled by washing and sterilizing them. The detergents to be used for the washing of

culture glassware should be devoid of organic additives. Used culture glassware should never be allowed to dry before it is cleaned, but stored immersed in a special detergent solution (e.g., neodisher LM-10, 5% v/v). In the dishwasher, a special alkaline cleaning agent free from detergents (e.g., neodisher FT) is used for washing, and a neutralizer (e.g., neodisher Z) to remove alkaline residues. The glassware is then further rinsed with water, and finally with ultrapure water. After drying, the glassware is sterilized in the autoclave (except for cotton-plugged 5-mL glass pipettes used for media replenishment, which are sterilized in dry air for 2.5 h at 220°C).

3.3. Dissection, Cell Isolation, and Culture Preparation

Aggregating brain cell cultures are prepared from 16-day embryonic (E16) rat brain comprising telencephalon, mesencephalon, and rhombencephalon. The duration of the dissection should not exceed 2 h. All dissecting instruments and solutions should be sterile. From step 5 onwards, all work is done under strictly aseptic conditions. During steps 5–21, the tissue/cells remain at 0–4°C.

1. Sacrifice the pregnant rat by decapitation using a special guillotine for rats. Avoid all unnecessary stress to the animal and follow the ethical guidelines. Clean the place of decapitation for each animal to be sacrificed. (Note: When properly done, decapitation of the conscient animal proved to create less stress than using anesthetics. Periodically, the brain of a sacrificed animal is taken for the preparation of standards for the diverse assay procedures).
2. Lay the decapitated animal on its back on a adsorbent paper and rinse the abdomen with 95% alcohol.
3. Open the peritoneal cavity: Using the large forceps, grasp the skin about 1 cm above the genitalia. With the large scissors, cut through the skin and fascia, and extend the cut on both sides of the abdomen, until the entire peritoneal cavity lies open.
4. Remove the uterine horns containing the embryos, using small curved forceps and small pointed scissors, and transfer them into 50-mL plastic tube containing 25–30 mL of ice-cold Puck's solution D1.
5. Transfer the uterine horns to one of the Petri dishes placed on the cold dissecting block (or on ice, if no dissection block is available) within a horizontal laminar flow bench.
6. Using the Vannas scissors and small forceps, separate the embryos from the uterus and from their amniotic sac and placenta, and transfer them to a fresh Petri dish containing Puck's solution D1.
7. Dissect the brain of each embryo: Fix the head of the embryo in a lateral position with the aid of the Dumont forceps and make an extended lateral incision at the base of the brain

using the Vannas scissors. Lift the brain through this opening using the blunt side of the closed Vannas scissors.

8. Using a scalpel, divide the brain roughly into two halves by separating the telencephalon from the mesencephalon/diencephalon /rhombencephalon parts.
9. Transfer the dissected brain parts to a 50-mL plastic tube filled with 40 mL of Puck's solution D1.
10. Repeat steps 1–6 for each pregnant rat, and steps 7–9 for each embryo. The brain tissue collected from 50 embryos is the maximum amount to be kept in one tube. If necessary, use several tubes filled with 40 mL Puck's solution D1 to collect the dissected tissue, and replace the liquid periodically to avoid a drop of the pH.
11. At the end of dissection, rinse each batch of tissue 3× with about 40 mL of cold Puck's solution D1. Take these batches separately for the subsequent mechanical dissociation, using each time a fresh 200-μm mesh bag (see below).
12. For the dissociation procedure, place the 200-μm mesh bag (with a glass funnel fitted inside) in a 50-mL conical plastic tube containing 25 mL cold Puck's solution D1. Pour the tissue of one batch into the bag. Remove the funnel, and hold the upper ends of the closed bag against the outer side of the tube wall.
13. Using the glass rod, gently stroke downwards, from the immersed outside of the bag, to squeeze the tissue through the mesh into the surrounding solution. At the end of this first passage, remove the bag and close the tube.
14. Repeat steps 12 and 13 for every batch of dissected brain tissue.
15. Filtration of the cell suspension: Take the 100-μm mesh nylon bag attached with tape to the short glass funnel and place it on top of an empty 50-mL conical plastic tube. Using a 5-mL serological plastic pipette, transfer the cell/tissue suspension to the nylon bag and let the suspension pass through the filter by gravity flow into the 50-mL tube. Towards the end of the filtration, add Puck's solution D1 up to a final volume of 50 mL.
16. Repeat step 15 for each batch of dissociated tissue.
17. Centrifuge the filtrate(s) containing the dissociated cells (300 g, 15 min at 4°C, with slow acceleration and deceleration).
18. Of each tube, remove the supernatant, and resuspend the pellet with cold Puck's solution D1 (start with 2.5 mL) by gentle trituration (5–6 strokes up and down using a 5-mL plastic

pipette without foaming). Bring the volume to 50 mL with cold Puck's solution D1.

19. Centrifuge the cell suspension(s) (300 g, 15 min at 4°C).
20. Of each tube, remove the supernatant and resuspend the cells in cold serum-free culture medium by gentle trituration. Transfer the resulting cell suspension to a plastic culture flask for further dilution.
21. Dilute the cell suspension with cold medium to the final volume, calculated by the number of brains used per batch of cell suspension times 8 mL of medium. Thus, each flask contains an average of the cells obtained from one embryonic brain, i.e., an initial cell number of $2.5–3.5 \times 10^7$ cells per flask.

    (Note: For routine work, cell counting is not required. The method is sufficiently robust to permit considerable variations in cell number without affecting fundamental properties of the cultures. Nevertheless, it might be useful (particularly for beginners) to determine cell number and viability. To this end, an aliquot (0.1 of 50 mL of cell suspension) is taken after completion of step 18 in the isolation procedure, diluted at least 10×, and counted using either a hemocytometer or an electronic cell counter. Cell viability, determined by the exclusion of trypan blue (not described here), should be about 50%).
22. Transfer 8-mL aliquots of the final cell suspension to 50-mL culture flasks and place them onto the platform of a rotating (68 rpm) gyratory shaker in the CO_2 incubator (37°C, 10% CO_2/90% humidified air).
23. The gyratory agitation is increased stepwise to 70 rpm in the evening of the day of culture preparation (DIV 0); 74 rpm (DIV 1); 78 rpm (DIV 2); and finally 80 rpm (DIV 4 and following).

3.4. Media Replenishment

For the maintenance of aggregating brain cell cultures, regular replenishment of the culture media is required, beginning at DIV 5.

Media are replenished every third day from DIV 5 to DIV 14, and every other day in the following. Media replenishment, i.e., the replacement of 5 mL of media supernatant (of a total of 8 mL) with fresh prewarmed serum-free culture medium, is done in a sterile hood with vertical laminar air flow according to the following protocol:

1. Fill the amount of fresh medium required for replenishment into a 150-mL sterile glass bottle and warm it in a water bath at 37°C for 10 min.

2. Put 5 flasks of cultures on a slanted support and transfer them to the laminar flow bench. Using a 5-mL pipette, remove 5 mL of media supernatant and replace it by a slightly larger volume (5.2 mL, to compensate evaporation) of fresh medium. (Note: To avoid contamination, use always a fresh pipette with fresh medium. Furthermore, the rim of the caps should be shortly immersed in 100% ethanol, taking care that no ethanol enters when closing the flask).
3. Return the flasks to the incubator and continue with another group of five cultures.

(Note: The duration of media replenishment should not exceed 30 min, and the cultures should be allowed to equilibrate for at least 1.5 h before a further series of the same incubator is replenished).

3.5. Subdivision of Cultures

For acute testing, cultures are taken between DIV 18 and DIV 25. Cultures that will be used after DIV 20 are subdivided at DIV 20 because of the greatly increased metabolic activity of the now more mature cells. For subdivision, the cultures are split into two equal parts as follows:

1. Put the required number of 50-mL culture flasks into the laminar flow hood and label them.
2. Add to each flask 4 mL of cold culture medium and pre-equilibrate in the incubator under gyratory agitation for at least 1 h.
3. Transfer half of one culture (4 mL) to one of the pre-equilibrated flask: Using a 5-mL plastic pipette, quickly resuspend the aggregates by short aspiration and brisk expulsion of the supernatant medium, then quickly take a 4-mL aliquot and transfer it to the fresh flask.
4. Replenish the original flask by adding 4 mL of fresh pre-warmed medium.
5. Put the flasks back to the incubator and continue with the next series.

(Note: The duration of subdivision should not exceed 30 min. Thereafter, the cultures should be allowed to equilibrate for at least 1.5 h before a further series is put into the same incubator).

3.6. Preparation and Use of Replicate Cultures for Acute Testing

Due to their free-floating nature, aggregate cultures can be easily pooled from individual cultures and divided into aliquots for the preparation of replicate cultures. In the present approach, five replicate cultures are prepared from each original flask, each replicate receiving about 200 aggregates. For each experiment, 32 replicate cultures are prepared according to the following protocol:

1. At the day of experimentation (e.g., DIV 18), put 32 small culture flasks (25 mL) into the laminar flow hood and label them.
2. Add to each flask 3 mL of cold culture medium and pre-equilibrate in the incubator under gyratory agitation for at least 1 h.
3. Pool in a 50-mL plastic tube the aggregates of five original cultures in a total volume of 35 mL.
4. Add 1-mL aliquots of the aggregate suspension to the pre-equilibrated flasks in series of six. Using a 2-mL plastic pipette, quickly resuspend the aggregates by short aspiration and brisk expulsion of the supernatant medium, then quickly take a 1-mL aliquot and transfer it to the first flask in the row. Continue this way with the next flasks, until all six flasks have received an aliquot of aggregates. Make sure that the sequence of numbering corresponds to that of aliquoting.
5. Put the flasks back into the incubator and continue the same way with the next series.
6. Continue the same way until all aliquots are distributed.
7. Equilibrate the replicate cultures for at least 90 min before exposing them to test chemicals.
8. For the treatments, take the equilibrated replicate cultures by groups (five groups of six plus two controls) one group at the time from the incubator for the addition of the chemicals in the laminar hood.
9. To each flask, add an aliquot of stock solution (usually 2 µL) under slight agitation. For solvent control, cultures receive an equal volume of solvent.
10. Return the flasks immediately onto the shaker in the incubator.
11. Continue the same way with the other groups of replicates.
12. Keep the treated series under standard culture conditions (i.e., at 37°C in 10% CO_2/90% humidified air and under 80 rpm gyratory agitation).

3.7. Metabolic Labeling and Harvest of the Replicate Cultures

For metabolic labeling, starting 4 h before the harvest, add 5 µL of [3H]uridine stock solution (7.4 MBq/mL) to each replicate culture (final radioactivity 9.25 KBq/mL).

The harvest will be done in the same sequence as the labeling.

(Note: Due to the requirements for qRT-PCR, always use sterilized materials and solutions for the harvest, and wear disposable gloves to prevent RNase contamination).

The aggregates of individual flasks/replicates are harvested by washing twice in ice-cold PBS and final freezing according to the following protocol:

1. Taking one replicate at the time, transfer (pour) the aggregate suspension into a 15-mL plastic tube placed in ice.
2. Let the aggregates settle by gravity sedimentation.
3. Transfer 1 mL of the supernatant to labeled Eppendorf tubes for glucose determination. Keep them in ice until centrifugation (point 7).
4. Remove the remaining supernatant by suction.
5. Resuspend the aggregates with 5 mL of ice-cold PBS, let the aggregates settle and remove again the supernatant.
6. Repeat point 3 once more (second wash).
7. Remove the supernatant and store the pelleted aggregates at –80°C.

   (Note: Analyze the samples within 1 month. Longer storage requires the addition of RNA later provided with RNeasy Protect Mini Kit).

8. Centrifuge the medium supernatants prepared in step 3 (420 g 10 min) and recover 0.8 mL of each supernatant for the glucose determination. Store the samples in the freezer until analysis.

3.8. Sample Preparation and Assays by qRT-PCR and Scintillation Counting

Of each replicate culture, the total RNA is extracted using a kit from Qiagen. The total RNA content of each extract is determined. To determine the overall rate of RNA synthesis (i.e., the rate of uridine incorporation), an aliquot of the extract is taken for liquid scintillation counting. The RT is performed using the RT kit and protocols from Applied Biosystems (ABI). The RT is run with 200 ng of total RNA in a reaction volume of 50 µL. The cDNA obtained is then used for subsequent PCR reactions. The cDNA (3.2 ng) is added to the PCR mixture composed of primers (table below), 1× SYBR Green PCR master mix (ABI), and H_2O, in a final volume of 10 µL. The measurements of multiple gene expression by qRT-PCR are most conveniently done in 384-well plates using an automated workstation.

RNA extraction with RNeasy Protect Mini Kit and QIA shredder (Qiagen): containing lysis buffer, RLT buffer, RNeasy mini columns, RW1 buffer, RPE buffer, and RNase-free water. Work at room temperature until step n:

(a) Prepare two series of 32 plastic vials for scintillation counting; add 7 mL of Flo-Scint A in each vial.

(b) Thaw samples on ice.

(c) Add 600 µL of lysis buffer (add 10 µL of 2-mercaptoethanol per 1 mL buffer RLT before use) in each sample and vortex until complete lysis.

(d) Pipet the lysate directly onto a QIAshredder spin column placed in a 2 mL collection tube, and centrifuge for 2 min at maximum speed (≥13,000×*g*).

(e) Add 600 µL of 70% ethanol to the homogenized lysate, and mix well by trituration with the pipette. Do not centrifuge.

(f) Transfer the half (600 µL) onto an RNeasy mini column placed in a 2 mL collection tube. Close the tube gently, and centrifuge for 30 s at ≥8,000×*g*. Discard the flow-through and reuse the collection tube in step g.

(g) Transfer the second half (600 µL) onto the same RNeasy mini column placed in a 2 mL collection tube. Close the tube gently, and centrifuge for 30 s at ≥8,000×*g*. Discard the flow-through and reuse the collection tube in step h.

(h) Add 700 µL buffer RW1 to the RNeasy column. Close the tube gently and centrifuge for 30 s at ≥8,000×*g* to wash the column. Discard the flow-through and the collection tube.

(i) Transfer the RNeasy column into a new 2 mL collection tube. Pipet 500 µL Buffer RPE (before using this buffer for the first time, add 4 volumes of ethanol 100%, as indicated on the bottle) onto the RNeasy column. Close the tube gently and centrifuge for 30 s at ≥8,000×*g* to wash the column. Discard the flow-through and reuse the collection tube in step j.

(j) Add 500 µL Buffer RPE to the RNeasy column. Close the tube gently and centrifuge for 2 min at ≥8,000×*g* to dry the RNeasy silica-gel membrane.

(k) Transfer the RNeasy column to a new 1.5 ml collection tube. Add 200 µL RNase-free water directly onto the RNeasy silica-gel membrane. Close the tube gently and centrifuge for 1 min at ≥8,000×*g* to elute. Place the tubes in ice.

(l) Transfer 50 µL of RNA to the corresponding vial prepared under a. for [^{3}H] uridine counting.

(m) Place the vials in the liquid scintillation analyzer with a program for ^{3}H measurements.

(n) Measure the RNA concentration in 1 µL of the eluate, on the NanoDrop spectrophotometer. Store at –80°C.

Reverse transcription with TaqMan reverse transcription reagents (Applied Biosystems, cat. no. N8080234), containing: random hexamer, buffer 10×, $MgCl_2$, dNTP, RNase inhibitor, multiscribe reverse.

(a) According to the RNA concentration obtained, calculate the volume of eluate it takes to have 200 ng of RNA and the volume of RNase-free water to complete to 19.25 µL. Work

at room temperature, but keep RNA samples on ice. Pipet the calculated volume of RNase-free water for each sample into a PCR strip tube, one for each sample (Note: do not separate the PCR strip tubes, they are easier to handle attached together), then add the calculated volume of eluate to each tube.

(b) Prepare Mix A according to the following scheme. Volumes are indicated for 32 samples (including extra volume):

Random hexamer 50 µM:	84.0 µL
Buffer 10×:	168.0 µL

(c) Distribute 7.5 µL of Mix A to each tube. Close tightly the tubes with their caps.

(d) Place the tubes in PCR instrument for 10 min at 65°C.

(e) Prepare Mix B:

$MgCl_2$ 25 mM	369.60 µL
dNTP 10 mM each	336.00 µL
RNase inhibitor 20 U/µL	33.60 µL
Multiscribe reverse 50 U/µL	42.00 µL

(Note: the enzyme should return to the freezer as soon as possible).

(f) At the end of step d, remove the tubes from PCR instrument and add 23.25 µL of Mix B to each tube.

(g) Place again in PCR instrument, programmed as follows:

10 min	25°C
45 min	48°C
5 min	95°C
hold	4°C

(h) After the run, store PCR strip tubes at –80°C.

3.8.1. qPCR

(a) Prepare the SYBR green MIX according to the following Tables 1 and 2.

(b) Vortex and distribute 32.2 µL of the SYBR green MIX in 32 microtubes Eppendorf (0.5 mL), labeled with sample names.

(c) Add 2.8 µL of cDNA in each tube, vortex.

(d) Distribute 10 µL of each Mix + cDNA in three wells of a 96-well plate, to have three replicates per sample.

(e) Centrifuge briefly the plate to spin down the contents and eliminate any air bubbles from the solutions (Heraeus Multifuge 3S-R, 2 min at 1,200 rpm (200 g)).

Table 1
Sequence and final concentration of PCR primers

Gene name	Sense primer (5′-3′)	Antisense primer (5′-3′)	Final concentration (nM)
β-actin	CCCTGGCTCCTAGCACCAT	TAGAGCCACCAATCCACACAGA	150
GFAP	CCTTGACCTGCGACCTTGAG	GCGCATTTGCCTCTCCAA	150
MBP	GCACGCTTTCCAAAATCTTTAAG	AAGGAGGCTCTCAGCGTCTT	200
HSP32	AGGTGTCCAGGGAAGGCTTT	TCCAGGGCCGTATAGATATGGT	300
NF-H	CAGGACCTGCTCAACGTCAA	CTTCGCCTTCCAGGAGTTTTCT	300

(Note: Primers are in a lyophilized form. They have to be reconstituted with fresh ultrapure water, incubated 5 min at 37°C to obtain a stock concentration of 200 μM, and then stored at –80°C. Dilute this stock with fresh ultrapure water to obtain the working concentration of 10 μM, kept at –20°C).

Table 2
Preparation of SYBR green MIX

	Final concentration of primers		
	150 nM	200 nM	300 nM
SYBR green master mix (μL)	608.00	608.00	608.00
Primer forward 10 μM (μL)	18.24	24.32	36.48
Primer reverse 10 μM (μL)	18.24	24.32	36.48
H_2O (μL)	474.24	462.08	437.76

Note: The master mix should return to the cold room as soon as possible.

(f) Place the plate into the 7900HT thermocycler.

(g) Run the PCR with the following thermal cycling conditions:

10 min at 95°C	
40 PCR cycles:	15 s at 95°C
	1 min at 60°C

(h) Always perform a dissociation curve analysis to evaluate the presence or absence of any nonspecific amplification.

(Note: several steps can be automated, e.g., by using the Laboratory Automation Workstation Biomek 3000 (Beckman Coulter). In this case, actin is analyzed first in a 96-well plate, and GFAP, NF-H, MBP, and HSP32 are analyzed subsequently in a 384-well plate).

3.8.2. Calculations

Ct:	Cycle threshold indicates the fractional cycle number at which the amount of amplified target reaches a fixed threshold
ΔCt:	Difference in threshold cycles for a given gene between treated samples and the control sample C1
C1:	First control culture
C2:	Second control culture
X:	Any of the samples, including C1 and C2
F:	Fold change

a) Calculate ΔCt (7) for each individual sample:

$$\Delta Ct_x = Ct_x - Ct_{C1}$$

b) Calculate F_X for each individual sample according to the following formula:

$$F = 2^{-(\Delta_{Ct})}$$

c) Determine the standardized F_X for each individual sample relative to the mean fold change of the controls C1 and C2 (equal to 1):

$$F_x\text{standardized} = 2F_x \,/\, F_{C1} + F_{C2}$$

3.9. Glucose Determination in Medium Supernatants by the Glucose Oxidase Method

Prepare the reagents according to the manufacturer's instructions for the glucose reagent kit (Beckman coulter cat. no. 671640).

Calibrate the analyzer with calibration solution provided in the kit.

Aliquots (10 μL) of medium supernatants and of fresh medium are analyzed.

The glucose consumption of each treated replicate culture, expressed as a percentage of glucose consumption relative to the untreated control cultures, is determined from the glucose concentration measured in the culture supernatant of each treated culture (SAMPLE) and the average glucose concentration measured in the supernatants of the control cultures (CTR), as follows:

$$\%\text{ of CTR} = \frac{(\text{glucose conc. in fresh medium} - \text{glucose conc. in SAMPLE}) \cdot 100}{(\text{glucose conc. in fresh medium}) - (\text{glucose conc. in CTR})}$$

3.10. Data Analysis

Of each replicate culture, the total RNA content is determined. Drug concentrations causing drastic reductions (≥40% decrease) in the total RNA content compared to the untreated controls are taken as the drug concentrations causing general cytotoxicity.

The rate of uridine incorporation (RNA synthesis) is calculated from the data obtained by [^{3}H] liquid scintillation counting and expressed as specific incorporation (DPM/μg RNA) during the 4-h incubation. To normalize the data, percentages are calculated with respect to the untreated controls. The lowest observed effective concentration (LOEC), determined for each compound, is defined as the drug concentration causing a deviation in uridine incorporation of 25% compared to the untreated controls.

The qRT-PCR data are expressed as ΔCt for each individual gene relative to its expression in untreated controls. The LOEC, determined for each compound and each affected endpoint separately, is defined as the lowest drug concentration causing a change in gene expression compared to the controls by at least a factor of 1.7 (i.e., either a decrease to ≤0.59-fold the control value or an increase to ≥1.7-fold the control value). Specific toxic effects often result in the decreased expression of genes coding for structural proteins such as NF-H, MBP, and GFAP, while HSP32 expression usually increases. Increased GFAP expression is taken as indication for astrocytosis, an inflammatory response. Selective effects on gene expression are typical for adverse effects of chemicals below the cytotoxic level; at higher (cytotoxic) concentrations, gene expression shows a general decrease.

The relative rates of glucose consumption are deduced from the glucose measurements in the media supernatants recovered at the harvest. The LOEC, determined for each compound, is defined as the drug concentration causing 25% deviation of glucose consumption from the untreated controls. Glucose consumption is often decreased as a consequence of chemically induced adverse effects causing decreased metabolic activity. However, as shown before (8), increased glycolytic activity may occur, e.g., by the action of depolarizing drugs (increased activity-dependent glucose consumption) or by the action of drugs affecting the oxidative energy metabolism (including the Krebs cycle and oxidative phosphorylation) causing a switch to anaerobic glycolysis, also called inverse Pasteur effect.

For each experiment, criteria for the acceptance of the experimental data are applied. Previous experience showed that >90% of the tests fulfill the following conditions, taken now routinely as the criteria of acceptance: (1) the values of duplicates do not deviate from their mean value by more than 15%; (2) the control values are in the (normal) range of previously established values; and (3) effective compounds show a concentration–effect relationship. Furthermore, for gene expression, actin analysis is performed first. If acceptable according to criterion (1), the other genes are analyzed in the following. If the actin data are not acceptable, RT and q-PCR analysis are repeated.

4. Notes

4.1. Culture Preparation and Maintenance

Whereas the preparation of aggregating brain cell cultures is rather easy, their maintenance is relatively onerous because of the high culture density requiring frequent media replenishments. For the time being, there are no automated flow-through incubators available for this culture system that could reduce the costs involved in such repetitive work. Another obstacle to the rapid use of this culture system is the need for equipment that is not found in a standard cell culture laboratory. However, alternative solutions are possible, provided that the five following critical points are respected:

1. The mechanical dissociation of the embryonic brain tissue into a single cell fraction must be complete, but sufficiently gentle to provide a single cell suspension with a maximum of viable cells (at least 50% viability as judged by the exclusion of trypan blue, a basic procedure not described here). The use of Nylon mesh filter bags, glass funnels, and glass rods described here was found best in our hands. Alternate mechanical dissociation methods are described by Cole and de Vellis (9).
2. During the initial phase of cell aggregation, the geometry of the culture vessels is critical for a reproducible vortex and hence for the formation of aggregates of comparable size. Therefore, the culture vessels used for culture initiation have to be uniform. Because we found considerable variations between DeLong flasks of different batches, we now use Duran Erlenmeyer flasks modified by a glass blower. The vortex depends on the geometry of the flasks and the speed of agitation. To find the optimal vortex with a new batch of flasks, it is recommended to vary slightly the volume of medium in the culture vessels while keeping the shaking protocol unchanged. If the aggregates appear grouped at the center of the flask, the volume has to be decreased until they cover about 2/3 of the bottom surface while floating. During the early culture phase, the aggregates are very sticky. Therefore, continuous agitation is important to avoid adhesion between aggregates and care has to be taken to avoid prolonged contact while changing their media for the first time (DIV 5). The final aggregates should be even in size, with an average diameter of about 500 μm.
3. The culture vessels need to be equipped with closures that permit rapid gas exchange. While the CO_2 is important for media buffering, optimal O_2 levels are necessary because of the high metabolic activity of the cultures. The latter also requires continuous agitation of the aggregates (they should not remain immobilized for more than 15 min).

4. The developmental stage of the original tissue is critical, requiring the exact timing of pregnancy. The present protocol was established for timed-pregnant rats (Sprague–Dawley) at gestational day 16, counting the day following mating as embryonic day 1 (E1). Embryos of rats mated during the day are taken in the morning of day 16 for culture preparation; embryos of rats mated overnight are taken in the afternoon of day 16 for culture preparation.
5. Culture conditions, medium composition, and osmolarity (340 mOsm) need to be kept constant. Extreme changes in osmolarity or pH values of media should be avoided. Highest standards of purity have to be respected for culture media and glassware.

4.2. Experimental Approach and Interpretation of Data

The present experimental design was chosen for the assay of multiple endpoints (high content analysis) and in accordance with the use of an automated working station. This approach was used in a recent study aimed at the in vitro prediction of acute systemic toxicity (www.acutetox.org), where a series of reference chemicals was examined for neurotoxic adverse effects using as endpoints gene expression, global rates of RNA synthesis, and the rate of glucose consumption. The results of this study confirmed the suitability of aggregating brain cell cultures and the use of multiple endpoints for the detection of potentially neurotoxic compounds (10). In particular, it was observed that the 6 different endpoints chosen exhibited differential sensitivities to the various test compounds. Of 57 tested reference chemicals examined for their lowest observed effect concentration (LOEC), many affected more than one endpoint at LOEC, whereas for some, one endpoint was clearly more sensitive than the others (Table 3). HSP32, an indicator of oxidative stress, was found to be the most sensitive endpoint for the greatest number of compounds, followed by uridine uptake and GFAP. Nevertheless, for some specific compounds, other endpoints were clearly more sensitive, e.g., glucose consumption was most affected by pentachlorophenol, lindane, pyrene, and warfarin; NF-H mRNA expression by cyclosporin, parathion, and phenobarbital; and MBP mRNA expression by selenate and fluoride (Table 3). The finding that pentachlorophenol and lindane greatly affect the glycolytic activity is in good agreement with observations in vivo (e.g., ref. (11)). Drug-induced changes in the six endpoints used in this study appear to reflect cellular adverse effects rather than the interference with the specific molecular targets that tend to overestimate drug toxicity. For example, parathion was found to be an extremely strong inhibitor of neuronal acetylcholinesterase (AChE) in aggregating brain cell cultures ($IC_{50} = 6.8$ E-8M) (see also ref. (12)), while it affected NF-H mRNA expression as the most sensitive of the six endpoints only at a much higher

Table 3
Differential sensitivities in a set of six endpoints. Examples of compounds for which one particular endpoint was most sensitive

Endpoint	Compound	LOEC (M)
HSP32 mRNA	Arsenic trioxide	1.0 E-7
	Cadmium (II) chloride	4.0 E-7
	Mercury (II) chloride	8.0 E-7
	Cis-diamine platinum (II) dichloride	2.0 E-6
	Diquat dibromide	2.0 E-6
	Physostigmine	5.0 E-6
	Acrylaldehyde	1.0 E-5
	Rifampicine	2.0 E-5
	Chloral hydrate	4.0 E-4
Uridine uptake	Cycloheximide	3.5 E-8
	Glufosinate ammonium	5.2 E-8
	5-Fluorouracil	2.9 E-6
	Diazepam	6.5 E-6
	Carbamazepine	4.5 E-5
	Caffeine	5.2 E-4
	Methanol	6.0 E-2
GFAP mRNA	Ochratoxin A	2.5 E-9
	Digoxin	5.0 E-8
	Amiodarone hydrochloride	2.5 E-6
	Sodium valproate	2.5 E-4
	Acetylsalicylic acid	5.0 E-4
Glucose consumption	Pentachlorophenol	8.0 E-8
	Lindane	5.0 E-6
	Pyrene	5.0 E-5
	Warfarin	2.2 E-4
NF-H mRNA	Cyclosporin A	2.0 E-6
	Parathion	1.0 E-5
	Phenobarbital	2.0 E-4
	Dimethylformamide	5.0 E-2
MBP mRNA	Sodium selenate	1.0 E-5
	Sodium fluoride	2.5 E-4

concentration (LOEC = 1.0 E-5M). Similarly, physostigmine, a reversible AChE inhibitor (IC_{50} = 3.9 E-7 M in aggregate cultures) affected HSP32 mRNA expression only at 5.0 E-6M. On the other hand, glufosinate, a herbicide and irreversible inhibitor of glutamine synthetase (IC_{50} = 5.7 E-8M in aggregate cultures) affected uridine uptake as the most sensitive of the six selected endpoints at an equally low concentration (5.2 E-8M). It also affected NF-H and GFAP mRNA expression at relatively low concentrations (2.0 E-7M). These findings also indicate that

this glia-specific toxicant affected neurons at a low concentration, presumably due to the functional neuron-astrocyte interdependence occurring in this three-dimensional culture system. The fact that in vivo, glufosinate exhibits lower neurotoxicity (13) can be explained by the relatively low permeability of the blood–brain barrier for this compound.

These few examples indicate that multiple endpoints increase the likelihood to detect adverse effects at concentrations relevant to the in vivo situation. In addition, concentration-dependent effects observed on several endpoints increase the significance of the data and reduce the number of false positive findings. Clearly, the present approach could be further improved by the introduction of additional biomarkers representing common pathways of adverse effects. From the practical point of view, it would be easy to add more genomic endpoints, because of the high amount of RNA extracted from each replicate culture. Also, gene expression data are relatively unaffected by the variability of aggregate sampling, because equal amounts of RNA are taken for the measurements. In addition to genomics, the metabolomics approach appears to offer a complementary high content analysis for routine toxicity screening using aggregating brain cell cultures as in vitro model (14).

Acknowledgements

The authors are grateful to Ms Denise Tavel and Ms Brigitte Delacuisine for excellent technical assistance. This work was supported by the EU-FP6 grant (FP6-LIFESCIHEALTH-2004-512051) and by the 3R Research Foundation Switzerland.

References

1. Honegger P, Lenoir D, Favrod P (1979) Growth and differentiation of aggregating fetal brain cells in a serum-free defined medium. Nature 282:305–308
2. Honegger P, Monnet-Tschudi F (2001) Aggregating neural cell cultures. In: Fedoroff S, Richardson A (eds) Protocols for neural cell culture, 3rd edn. Humana, Totowa, NJ, pp 199–218
3. Honegger P, Schilter B (1992) Serum-free aggregate cultures of fetal rat brain and liver cells: Methodology and some practical application in neurotoxicology. In: Zbinden G (ed) In vitro techniques in neurobiology, neuropharmacology and neurotoxicology. MTC, Zollikon, pp 51–79
4. Honegger P, Schilter B (1995) The use of serum-free aggregating brain cell cultures in neurotoxicology. In: Chang LW (ed) Neurotoxicology: approaches and methods. Academic, New York, pp 507–516
5. Zurich M-G, Monnet-Tschudi F, Costa LG, Schilter B, Honegger P (2004) Aggregating brain cell cultures for neurotoxicological studies. In: Tiffani-Castiglioni E (ed) Methods in pharmacology and toxicology: in vitro neurotoxicology, principles and challenges. Humana, Totowa, NJ, pp 243–266
6. Dunnett SB, Björklund A (1992) Staging and dissection of rat embryos. In: Dunnett SB, Björklund A, Rickwood D, Hames BD (eds) Neural transplantation. A practical approach,

The practical approach series. IRL, Oxford, pp 1–19

7. Livak KJ, Schmittgen TD (2001) Analysis of relative gene expression data using real-time quantitative PCR and the 2(–delta delta C(T)) method. Methods 25:402–408
8. Honegger P, Pardo B (1999) Separate neuronal and glial Na+, K+-ATPase isoforms regulate glucose utilization in response to membrane depolarization and elevated potassium. J Cereb Blood Flow Metabol 19: 1051–1059
9. Cole R, de Vellis J (2001) Preparation of astrocytes, oligodendrocytes, and microglia cultures from primary rat cerebral cultures. In: Fedoroff S, Richardson A (eds) Protocols for neural cell culture, 3rd edn. Humana, Totowa, N.J., pp 117–127
10. Forsby A et al (2009) Neuronal in vitro models for the estimation of acute systemic toxicity. Toxicol In Vitro 23:1564–1569
11. Sanfeliu C, Solà C, Camòn L, Martinez E, Rodriguez-Farré E (1989) Regional changes in brain 2^{-14}C-deoxyglucose uptake induced by convulsant and non-convulsant doses of lindane. Neurotoxicology 10:727–742
12. Monnet-Tschudi F, Zurich M-G, Schilter B, Costa LG, Honegger P (2000) Maturation-dependent effects of chlorpyrifos and parathion and their oxygen analogs on acetylcholinesterase and neuronal and glial markers in aggregating brain cell cultures. Toxicol Appl Pharmacol 165:175–183
13. Calas A-G, Richard O, Même S, Beloeil J-C, Doan B-T, Gefflaut T, Même W, Crusio WE, Pichon J, Montécot C (2008) Chronic exposure to glufosinate-ammonium induces spatial memory impairments, hippocampal MRI modifications and glutamine synthetase activation in mice. Neurotoxicology 29:740–747
14. van Vliet E, Morath S, Eskes C, Linge J, Rappsilber J, Honegger P, Hartung T, Coecke S (2008) A novel in vitro metabolomics approach for neurotoxicity testing, proof of principle for methyl mercury chloride and caffeine. Neurotoxicology 29:1–12

Chapter 6

Cell Culture to Investigate Neurotoxicity and Neurodegeneration Utilizing *Caenorhabditis elegans*

Michelle L. Tucci, Guy A. Caldwell, and Kim A. Caldwell

Abstract

Movement disorders such as Parkinson's Disease (PD) result, in part, from the selective loss of dopaminergic (DA) neurons. Many studies associated with DA neurodegeneration and neurotoxicity have successfully applied the model organism *Caenorhabditis elegans* to address PD-related questions. However, some pharmacological studies might be limited because the thick cuticle of the intact animal could preclude complete penetration of some chemicals. It is also difficult to examine neurons within the same individual nematode, day after day, for studies of aging and neurodegeneration. More recently, methods for culturing embryonic cells from *C. elegans* have proved to be an alternative resource for addressing the caveats associated with whole nematode studies. In this regard, cultured embryonic *C. elegans* DA neurons differentiate following dissociation from early embryos. These cells adhere to culture dish surfaces that are covered with peanut lectin and subsequently differentiate into neurons. GFP-labeled DA neurons can then be followed over time and further manipulated to provide a means for examining cellular mechanisms associated with PD. For example, the DA neurons can be exposed to neurotoxins or, if the DA neurons also express a known PD gene that causes neurodegeneration, specific neurons can be scored for cumulative neurodegenerative changes on consecutive days. In contrast, control DA neurons have not been observed to undergo degenerative changes in culture. These methods have provided additional tools for exploring DA neurodegeneration in *C. elegans*, rendering primary neuronal cell culture as a complementary approach to whole nematode studies for examining neurodegeneration associated with PD.

Key words: *C. elegans*, Neurotoxicity, Cell culture, Neurons, Alpha-synuclein, Proteasome

1. Introduction

Despite major advances in understanding neurodegenerative disorders such as PD, significant gaps still exist in our knowledge of what specific factors underlie disease susceptibility, onset, and progression. Strategies to elucidate mechanisms of neurotoxicity, as well as discern specific intracellular targets for subsequent drug development, are needed to more rapidly translate basic findings to the clinic.

Michael Aschner et al. (eds.), *Cell Culture Techniques*, Neuromethods, vol. 56,
DOI 10.1007/978-1-61779-077-5_6,

The innovative application of *Caenorhabditis elegans* toward human movement disorders research is providing insights into the function of specific gene products linked to PD and dystonia (1–3). In this regard, many of the salient features of this animal are amenable for disease research. *C. elegans* is a rapidly cultured organism with a lifespan of ~17 days, whereby experimental approaches to investigate diseases of aging, such as PD, can be taken to fruition quickly and inexpensively. Furthermore, the transparent anatomy of this organism is advantageous for following GFP markers over the course of developmental time and lifespan. Moreover, mature bioinformatic and functional genomic data are readily accessible online, thus the nematode is well positioned to play an ever increasingly important role in advancing our understanding of neuronal function and dysfunction, as pertaining to disease states.

Worms are also being exploited as a system for therapeutic drug screening and/or validation to combat movement disorders (4–7), as well as for toxicity studies (8–10). However, caveats to the use of whole worms for drug screening include the thick, outer cuticle of the animal, which could potentially limit the absorption of specific compounds, or require that higher concentrations be used, which could cause toxicity to the animals. Fortunately, *C. elegans* tolerate 1–2% DMSO, thus assisting with the permeability of many common drugs and chemicals into the animal. It should be noted, though, that DMSO itself is a chemical chaperone, a problem when screening for drugs that could reduce misfolded proteins. Thus, to circumvent drug permeability problems encountered in whole animal studies, cell culture of *C. elegans* neurons is strongly preferable.

Additional features of *C. elegans* make it attractive for neuronal cell culture. For example, transgenic lines are available that express GFP exclusively within distinct neuronal subclasses such as the serotonergic, GABAergic, cholinergic, glutamatergic, and DAergic neurons. This allows researchers to follow specific neurons, day after day, in culture (see Fig. 1). When DA neurodegeneration is examined in whole worms, it is extremely difficult, if not impossible, to follow the eight (total) DA neurons in the same worm, on high magnification, for multiple days. This is because detailed neuronal analysis involves mounting an anaesthetized animal on a microscope slide for compound microscopy, before subsequent recovery. It is challenging to recover a worm once, let alone repetitively. In contrast, the ability to culture out worm neurons from select isogenic or transgenic backgrounds facilitates the capacity to quantitatively evaluate neurodegeneration with unprecedented accuracy across distinct neuronal classes.

RNA interference (RNAi) is yet another technique that can be applied in *C. elegans* cultured neurons (11). Similarly, as a complement to examining reduced gene expression through RNAi,

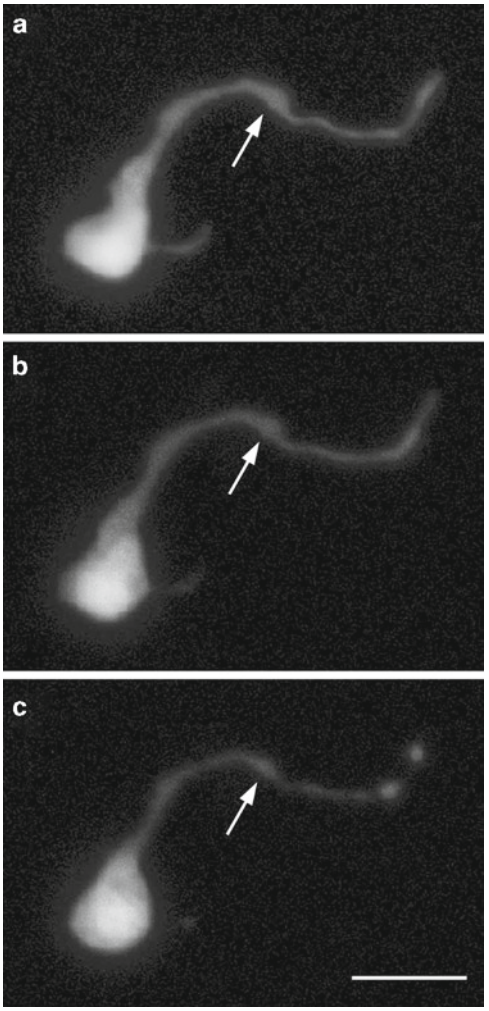

Fig. 1. An example of a *C. elegans* DA neuron cultured in vitro. Over the course of several days neurons maintain normal neuronal processes as depicted here where the same neuron was imaged following 1, 3 and 4 days of continuous culturing (parts (**a**)–(**c**), respectively). DA neurons can be highlighted using GFP driven from the DA transporter promoter (P_{dat-1}::GFP). The *arrow* depicts a neuronal process. *Scale bar* = 5 μM.

another noteworthy feature of *C. elegans* is the established availability of more than 40 years of genetic mutant strains. Of particular relevance to the field of neurodegeneration, there are mutations in six genes connected to PD (12). These include the *ubh-1* and *lrk-1* mutations associated with autosomal dominant forms of PD, linked to the human UCHL-1 and LRRK2 proteins. Autosomal recessive PD mutants include the *C. elegans pdr-1*, *pink1*, *catp-6*, as well as *djr-1.1* and *djr-1.2* genes, homologous to PRKN/parkin, PINK1, ATP13A2 and DJ-1, respectively. By genetically crossing these *C. elegans* mutants with animals expressing GFP transgenes for specific neuronal classes, neurons can be isolated

from these mutant animals, cultured, and analyzed over time, as they age. These same neurons could be further manipulated via RNAi or chemical modifiers. Likewise, specific neuronal classes of interest could be flow sorted for subsequent microarray analysis to identify coordinate changes in expression and survival (13, 14).

The methodologies and applications for *C. elegans* cell culture have been previously described for neuronal electrophysiology (15–17), as well as for muscle cell experiments (18, 19). Instead, this chapter focuses exclusively on methods required for the primary culturing of DA neurons from *C. elegans* to evaluate neurodegeneration (see Fig. 2). Here we describe how these cultures can be used to examine neurodegeneration induced by neurotoxins, as well as by the ectopic overexpression of a human PD gene,

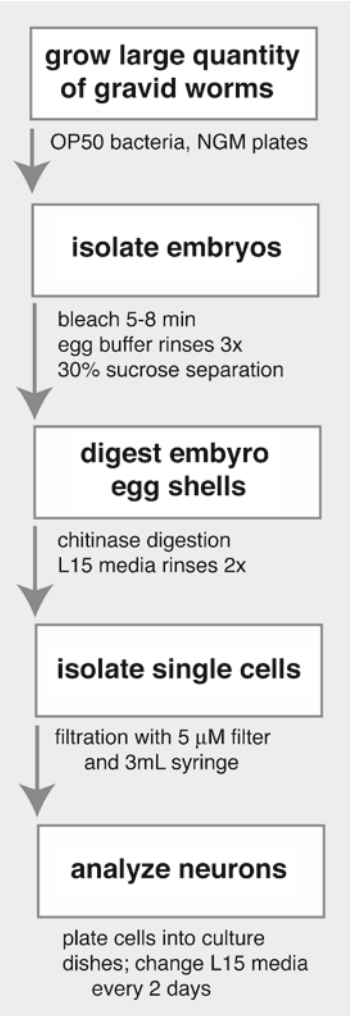

Fig. 2. The basic methodologies required for *C. elegans* cell culture utilized for neurotoxicity and neurodegeneration investigations.

alpha-synuclein, that has been transgenically integrated into the worm genome (20). Cultured DA neurons either exposed to toxins or expressing this established dominant PD gene reproducibly degenerate over time, as the neurons age, while control DA neurons do not exhibit degenerative changes. The example methodology outlined in this chapter is readily applicable to additional genetic modifiers and putative toxicological insults, either independently, or in combination, toward the goal of discerning susceptibility to environmental factors influencing neurodegeneration.

2. Materials

Suggested product sources are listed below; they are separated out based on the sequential steps of the methods described herein. Products from other suppliers that provide comparable effectiveness may also be suitable.

2.1. Materials Required for the Preparation of Culture Dishes

1. 4- or 8-well chambered coverglasses (Nunc Lab-Tek II Chambered Coverglass System (Sigma Aldrich; Z734853).
2. 0.5 mg/mL peanut lectin in sterile water (Sigma Aldrich; L0881; peanut agglutinin from *Arachis hypogaea*); gamma irradiate the bottle overnight prior to use.

2.2. Materials Required for the Growth of C. elegans

1. Worm strains used in neurodegeneration experiments: BY200 *vtIs1* (P_{dat-1}::GFP + pRF4(*rol-6*(*su1006*)) and UA44 (*baInl1*; P_{dat-1}::α-synuclein, P_{dat-1}::GFP).
2. Nematode growth medium ((NGM); see below).
3. *E. coli* OP50 strain (*Caenorhabditis* Genetics Center).
4. 60 mm non-vented Petri dishes (Tritech Research; T3308).

2.3. Materials Required for the Isolation of Embryos

1. Sterilized 10 mL glass conical tubes (Fisher Scientific; 05-507-11A).
2. Sterilized glass Pasteur pipettes (Fisher Scientific; 13-678-20B).
3. Sterilized ddH_2O.
4. Bleach/NaOH solution (prepare fresh and keep in dark; see below).
5. Egg buffer (see below); store at 4°C.
6. 30% Sucrose; store at 4°C.

2.4. Materials Required for the Preparation of Dissociated Cells

1. 1 U/mL chitinase (*Streptomyces griseus*; Sigma Aldrich; C-6137) dissolved in egg buffer (recipe below). Aliquot stocks into 500 µL individual use microcentrifuge tubes and store at −80°C for long-term use.

2. L-15 culture medium (Invitrogen; 11415-064); store at 4°C.
3. 10% Fetal Bovine Serum (Sigma Aldrich; 12107C) with 50 U/mL penicillin and 50 µg/mL streptomycin (Invitrogen 15070-063), store at –20°C.
4. 3 cc syringes (Fisher Scientific; 14-823-40).
5. 5 µM Millipore PVDF Syringe Filters (Fisher Scientific; SLSV025LS).
6. 1.7 mL sterilized microcentrifuge tubes (Fisher Scientific; 05-406-16).
7. Trypan Blue (Sigma Aldrich; T6146).
8. Hemocytometer.

2.5. Materials Required for Neuronal Analysis

1. MG-132 (EMD Biosciences; 474790).
2. DMSO.
3. *Streptomyces venezuela* (USDA-ARS ISP-5230).

2.5.1. Recipes

NGM plates (1 L media; makes 100 60-mm plates):

975 mL	ddH_2O
2.5 g	Peptone
3.0 g	NaCl
17.0 g	Bacto agar (Fisher Scientific; DF0140-07-4)

Autoclave media for 1 h and allow to cool, then add the following:

1 mL	Cholesterol (dissolve 0.125 g in 25 mL 100% ethanol)
1 mL	1 M KPO_4, pH 6.0
1 mL	1 M $MgSO_4$, 1 M $CaCl_2$
0.567 mL	Streptomycin sulfate (0.36 g/mL)
1 mL	12.1 mM nystatin (dissolved in 100% ethanol)

Pour ~10 mL agar media into each 60 mm petri dish and allow to solidify. Then seed the plates with approximately 200 µL of LB broth + OP50 bacteria and incubate overnight at 37°C (12–18 h). Store at 4°C until use.

LB broth

10.0 g	Tryptone
5.0 g	Yeast extract
10.0 g	NaCl

Add ingredients to 1 L of ddH_2O and stir until dissolved. Adjust to pH 7.0 with 5 N NaOH. Aliquot to working volumes (~75 mL). Autoclave and store at room temperature.

30% Bleach/NaOH solution (prepare fresh before each use)

1 mL	5 N NaOH
2 mL	Bleach (preferably from a fresh bottle)
7 mL	ddH_2O

Egg buffer

118 mM NaCl.
48 mM KCl.
2 mM $CaCl_2$.
2 mM $MgCl_2$.
25 mM HEPES, pH 7.3 (see Note 1), 335–340 mOsm (see Note 2).
Filter sterilize egg buffer before use and store at 4°C.

3. Methods

3.1. Preparation of Culture Dishes

1. Fill each chamber three-fourth with peanut lectin and allow to sit in a laminar flow hood for 10–20 min under UV light.
2. Remove as much solution as possible and air-dry in hood under UV light for additional 10–30 min (see Note 3).
3. Store culture dishes in a sterile container until future use (see Note 4).

3.2. Growth of C. elegans

Worms are grown on large NGM plates with OP50 bacteria (see Notes 5–7).

1. Strip dauer worms onto NGM plates with bacterial food source and grow until gravid adults (2–3 days).
2. Using glass Pasteur pipettes, wash adult worms off with distilled water into glass conical tubes (see Note 8) and centrifuge at low speed (see Note 9) at 1,000 rpm in a clinical centrifuge for 1 min.
3. Remove supernatant and repeat rinses until supernatant is clear (i.e., the bacteria have been removed).

3.3. Isolation of Embryos

1. Remove as much of the supernatant as possible without disturbing the worm pellet. Estimate the worm volume (~0.5–1 mL) and then add 3× that volume in bleach solution to the worm pellet. Gently mix and incubate at room temperature on a rocker (i.e., Nutator) for approximately 5 min.

2. Once ~80% of the worms have split open and released their embryos, add 6–7 mL egg buffer to stop the lysis reaction.
3. Centrifuge at 1,000 rpm and rinse with egg buffer 2–3 times.
4. To separate the eggs from worm carcasses, add 10 mL of 30% sucrose solution and centrifuge at 1,000 rpm for 3 min.
5. Embryos will float on the meniscus. With a sterile glass Pasteur pipette, transfer the embryos, along with approximately 3–4 mL of sucrose, to new glass conical tube.
6. Bring volume to 10 mL with ddH_2O and centrifuge at 1,000 rpm for 1 min. The embryos will pellet to the bottom or towards the middle of the conical tube.
7. Repeat step 6 2–3 more times to collect all embryos at the bottom of the centrifuge tube (by diluting out the sucrose solution).
8. Carefully transfer the pellet of embryos to a 1.7 mL microcentrifuge tube that contains 500 µL chitinase (1 U/mL).

3.4. Preparation of Dissociated Cells

1. Place tube on a rocker at room temperature for 1 h (see Note 10).
2. In order to monitor the dissociation of cells, pipette an ~10 µL aliquot of chitinase/embryo mixture onto a microscope slide. Observe the embryos under a stereoscope and when ~80% appear to be dissociated, continue on to step 3 (see Note 11).
3. Add 800 µL of L-15 media and centrifuge at 3,500 rpm for 3 min at 4°C (see Note 12).
4. Remove the supernatant and then add an additional 800 µL of L-15 media.
5. With a 1,000 µL pipetter, gently pipette up and down to dissociate cells until a large volume of dissociated cells is obtained (see Note 13).
6. Pellet dissociated cells at 4°C at 3,500 rpm for 3 min and then carefully resuspend the cells in 500 µL of L-15 media. Set aside for a minute.
7. Place a 5 µM filter on the end of a 3 cc syringe. Remove the syringe plunger and then add 1 mL of L-15 media inside the syringe. This volume will be absorbed into the filter. On top of this media, pipette 500 µL of dissociated cells (from step 6) into the syringe. Add plunger and filter these cells into a new 1.7 mL microcentrifuge tube. This step will remove any debris (larvae or undissociated cells) from the mixture.
8. Rinse the syringe filter by removing plunger and adding an additional 500 µL of L-15 media, then dispense into a second 1.7 mL microcentrifuge tube.

9. Pellet cells from both tubes at 4°C at 3,500 rpm for 3 min (see Note 14).
10. Add 100 μL of L-15 media to each tube.
11. Pool the media and cells from both tubes together and count number of cells using a hemocytometer (see Note 15).
12. Plate the appropriate volume of cells into each well of the peanut lectin-coated culture dishes. For optical imaging, ~230,000 cells/cm^2 is the suggested cell density (17) (see Notes 16 and 17).
13. Allow the cells to incubate at room temperature (22–25°C) in humid conditions (see Note 18).

3.5. Analysis of DA Neuron Degeneration

1. It will take 24–48 h for cells to differentiate into DA neurons (see Note 19).
2. Change the L-15 media every 2–3 days.
3. Do not allow the cell chambers to dry out as you aspirate the old L-15 media. Further, perform this in the laminar flow hood to maintain sterile conditions.

3.6. DA Neurodegeneration Induced by α-Synuclein Expression

These cultured cells will need to be grown for approximately 4–7 days to observe significant neurodegeneration (see Notes 20 and 21).

3.7. Pharmacological Manipulation for Induction of Neurotoxicity

3.7.1. Addition of the Proteasome Inhibitor MG-132

For neurotoxicity analysis in cultured DA neurons, MG-132 can be applied to cells (following differentiation for 24–48 h) at a final concentration of 50 μM in DMSO. A stock concentration of 10 mM in 100% DMSO should be prepared. Within hours of application, neurodegeneration can be observed (see Fig. 3). However, significant levels of neurodegeneration within the neuronal population usually occurs within 3–4 days. Lowering the concentration of the proteasome inhibitor may slow down the neurodegenerative process.

3.7.2. Addition of a Bacterial Extract from S. venezuela

Recently, the bacterial excretions of *S. venezuela*, as well as *Streptomyces coelicolor* and *Streptomyces griseus,* were administered to cultured neurons and the results compared to in vivo results with these excretions. *S. venezuela* caused significant degeneration of DA neurons both in culture (see Fig. 4) and in vivo (9). Following cell differentiation for 24–48 h, a 1:5 dilution of the stock concentration of bacterial excretions used in whole worms was applied to cell cultures. This was derived by dose–response analyses, as higher concentrations were extremely toxic to cell cultures.

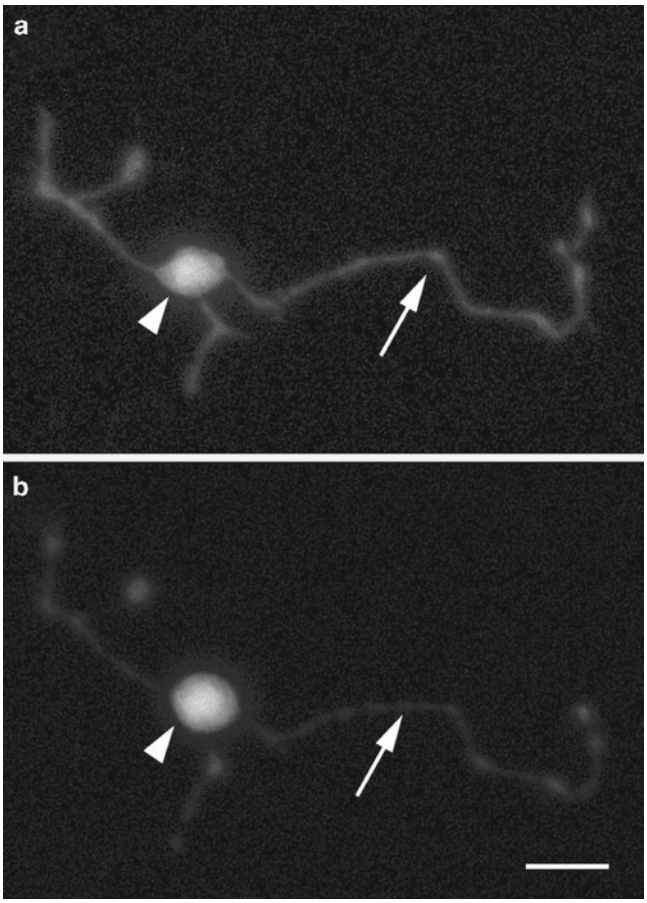

Fig. 3. Following exposure to the proteasome inhibitor MG-132, GFP-illuminated *C. elegans* DA neurons in culture degenerate. Both the cell body (*arrowhead*) and neuronal process (*arrow*) of a DA neuron display characteristic degenerative changes that are observable between the images captured on days 1 and 2 (panels (**a**) and (**b**), respectively). Notice that the cell body is rounded and the process is degenerating in (**b**). *Scale bar* = 5 μM.

4. Notes

1. Adjust pH with 1 N NaOH but do not add more than 10 mL.
2. Adjust osmolarity with sucrose; 1 L of solution usually requires ~5 g sucrose. Do not exceed 347 mOsm.
3. If the peanut lectin is not completely removed, this may cause cell clumping and poor differentiation of cells. The peanut lectin can be reused 1–2 additional times to coat future chambers. Keep track of the number times you use the peanut lectin, and throw away after three usages because UV light can break down the lectin and it will lose activity over time.

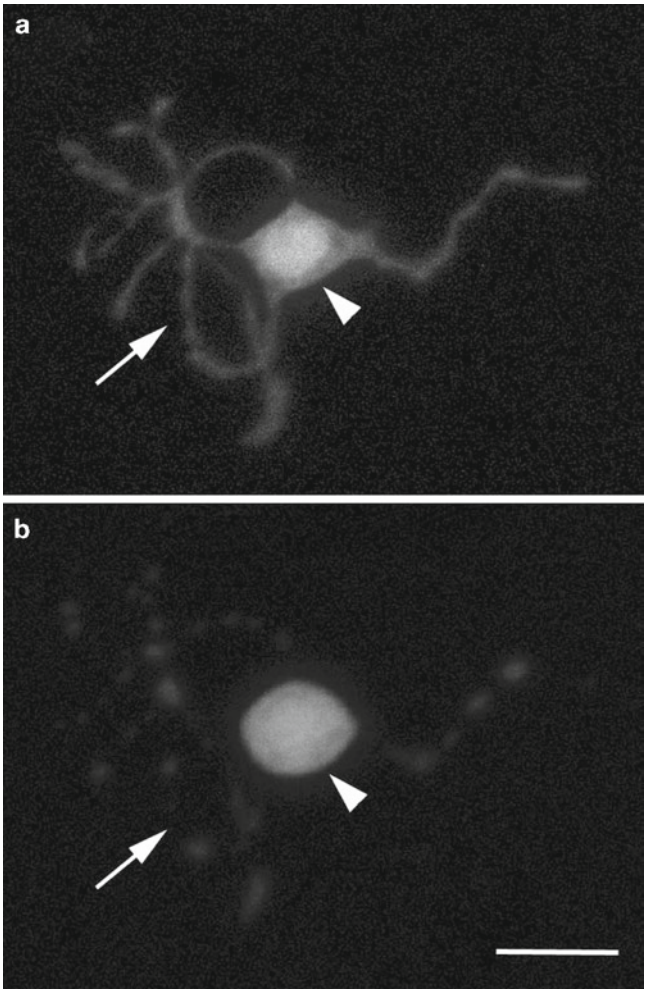

Fig. 4. A cultured *C. elegans* DA neuron degenerates in response to exposure to *S. venezuela* conditioned medium. Images depict the same GFP-labeled DA neuron on day 1 and 2, following exposure to the *S. venezuela* factor (panels (**a**) and (**b**), respectively). The *arrowhead* highlights changes in the cell body while the *arrow* provides a reference point for the degenerating neuronal process. Two degenerative changes are noticeable in (**b**), the cell body is rounded and the process is degenerating. *Scale bar* = 5 μM.

4. Coated culture dishes must be used within 2 weeks.
5. To grow LB + OP50 for seeding NGM plates, inoculate LB Broth with bacteria and streptomycin sulfate (0.36 ng/mL). Incubate in 37°C incubator for 12–18 h.
6. It has been suggested by Bianchi and Driscoll (15) that worms should be grown on an alternative media, 8P, using a different bacteria, Na22. This bacterial food source is more abundant, thus providing a larger quantity of worms. A word of warning, however, it is difficult to rinse the worms off these plates without using a large volume of water, which then may result in the potential loss of more worms.

7. For additional instructions on proper growth conditions and maintenance of *C. elegans*, refer to an additional resource (21).
8. Worms can stick to plastic. To minimize losing worms and embryos, use sterile glass conical tubes and glass Pasteur pipettes.
9. The purpose of centrifuging at low speeds is to separate bacteria from *C. elegans*.
10. The enzyme activity of the chitinase will vary between each lot, thus, egg-shell digestion will occur, on average, between 45 and 80 min.
11. Intact embryos are smooth and maintain the appearance of an eggshell while over-digested embryos will appear as loosely associated cells. Appropriately dissociated embryos will look like a cluster of grapes that still have a partially associated eggshell (see Fig. 5); these features can be detected using stereomicroscopy.
12. It is important that this step is performed using refrigeration (or in a cold room).
13. Too much, or too vigorous, pipetting can damage single cells and decrease yield.
14. Following centrifugation, a cell pellet will be visible from in the initial tube, and possibly the second tube as well.
15. Mix 10 µL cell suspension and 10 µL of Trypan Blue together in a microfuge tube. Plate 10 µL of this onto the hemocyotometer and count the total number of cells. To calculate the number of cells per mL: number of cells × 5 (hemocytometer) × 1,000 (volume) × 2 (dilution factor).
16. The volume of L-15 media added will depend upon the type of cell culture dish that is selected for the experiments. For example, single well culture dishes hold 2.4–4.5 mL of media, while 2-, 4, and 8-well culture dishes hold 1.2–2.0, 0.5–0.9, and 0.2–0.4 mL of L-15 media, respectively.
17. Cells must adhere to surface in order to differentiate. Allow 24–48 h for cells to differentiate before analysis.
18. Place the culture dishes in a Tupperware container with moist paper towels on the bottom to help minimize evaporation of the cell culture media. The lid of the container should be slightly open.
19. We determined that cells in culture expressing GFP from the DA promoter (P_{dat-1}::GFP) do not degenerate under normal conditions through 7 days in culture (see Fig. 6). This is comparable to results we have obtained from analyzing DA neurons expressing P_{dat-1}::GFP in whole animals ((see Fig. 1) and (2)).
20. When α-synuclein, a polypeptide with a propensity toward intracellular aggregation (22, 23), is overexpressed in *C. elegans* DA neurons, DA neurodegeneration occurs over

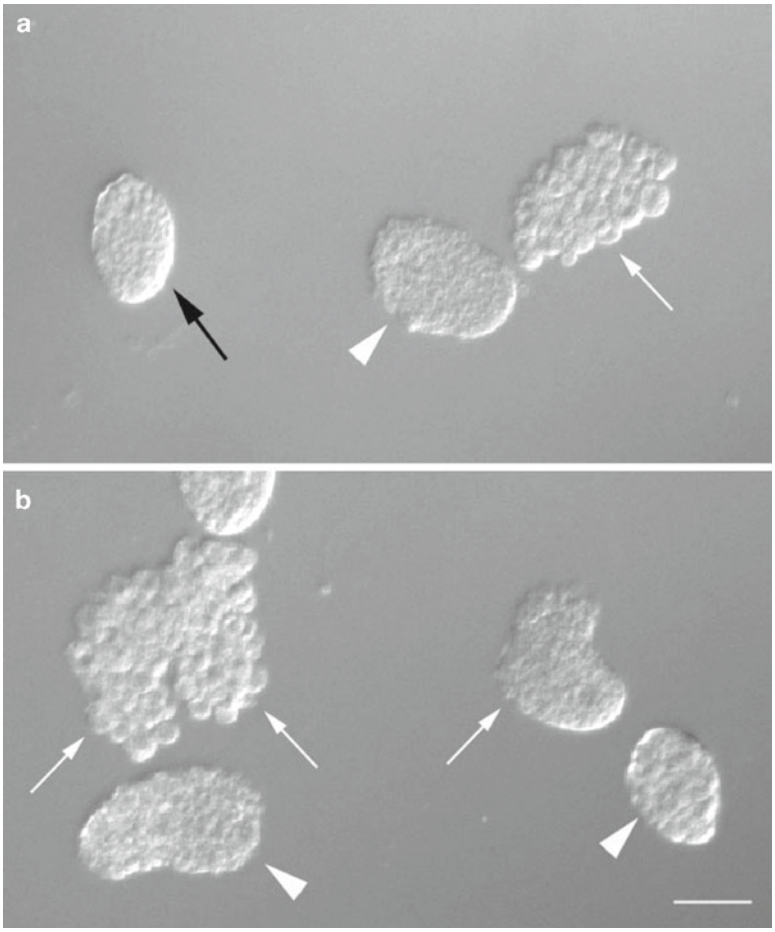

Fig. 5. *C. elegans* embryos digested with chitinase. Monitoring should be performed using microscopy. In both (**a**) and (**b**), well-digested embryos are depicted with an *arrowheads* and the dissociated cells appear as clusters of grapes that still maintain the shape of an embryo, as opposed to almost complete separation of cells as observed in examples shown with *white arrows*. In (**a**), an example of under digested embryo is also shown (*black arrow*) as well as an over-digested embryo (*white arrow*) while in (**b**), examples of over-digested embryos are provided (*white arrows*).

time in an age-dependent manner (2, 20). This phenotype is also observed in cultured neurons derived from *C. elegans* over-expressing both GFP and α-synuclein (P_{dat-1}::GFP + P_{dat-1}:: α-syn). We determined that the rate of neurodegeneration in α-synuclein-expressing cultured neurons is slower than observed in whole animals (see Fig. 1). This may be attributable to differences in excitotoxicity associated with the loss of the normal synaptic connections between neurons within intact animals vs. in cell culture. Nonetheless, by day 7, the DA neurons in culture are degenerating at a level that is comparable to that observed for DA neurons in vivo.

21. For other cell culture applications, wherein neurodegeneration and aging are not assessed, such as electrophysiology, cells in culture are often used before day 5 (17).

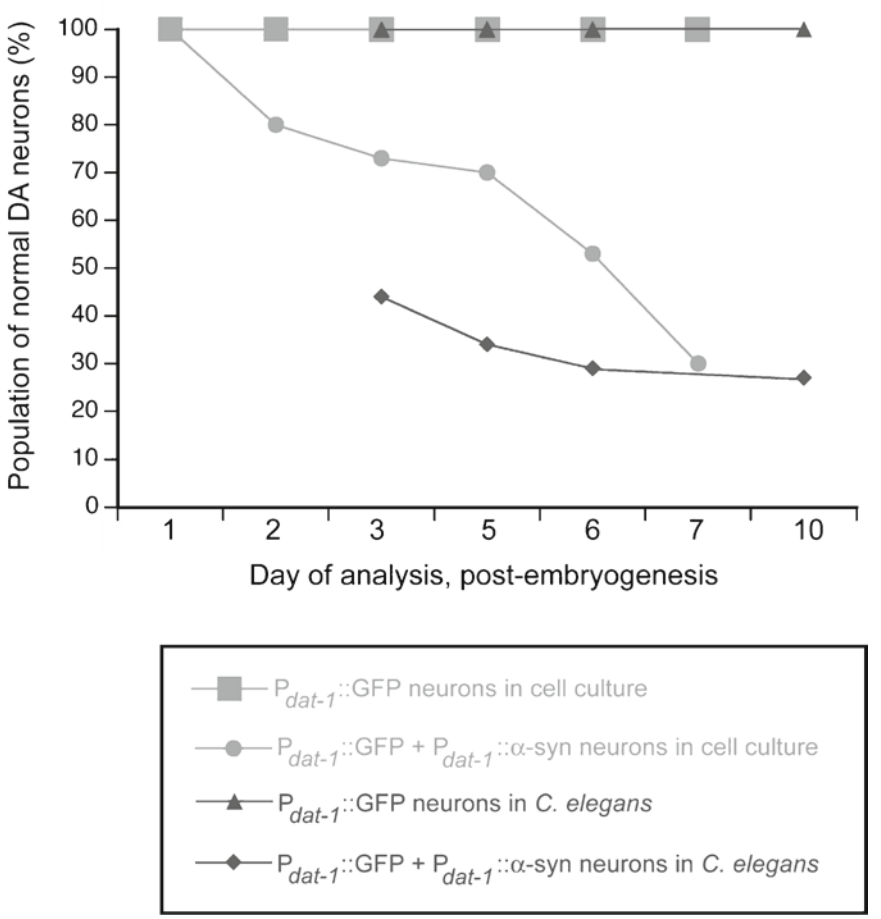

Fig. 6. Comparison of DA neuron degeneration rates between cell culture vs. intact *C. elegans.* There is no observable DA degeneration when GFP is expressed by itself from the DA promoter (P_{dat-1}::GFP) from either the cell culture experiments or within *C. elegans* (*gray boxes* or *black triangles*, respectively). However, when α-synuclein (α-syn) is co-expressed with GFP in DA neurons P_{dat-1}::GFP + P_{dat-1}:: α-syn, the nematode DA neurons (*black diamonds*) degenerate faster during the first few days of analysis than cultured neurons (*gray circles*). This may occur because the native synaptic connections within *C. elegans* are no longer maintained in cell culture.

References

1. Caldwell GA, Cao S, Sexton EG, Gelwix CC, Bevel JP, Caldwell KA (2003) Suppression of polyglutamine-induced protein aggregation in *Caenorhabditis elegans* by torsin proteins. Hum Mol Genet 12:307–319
2. Hamamichi S, Rivas RN, Knight AL, Cao S, Caldwell KA, Caldwell GA (2008) Hypothesis-based RNAi screening identifies neuroprotective genes in a Parkinson's disease model. Proc Natl Acad Sci 105:728–733
3. Gitler AD, Chesi A, Geddie ML, Strathearn KE, Hamamichi S, Hill KJ, Caldwell KA, Caldwell GA, Cooper AA, Rochet JC, Lindquist S (2009) Alpha-synuclein is part of a diverse and highly conserved interaction network that includes PARK9 and manganese toxicity. Nat Genet 41:308–315
4. Marvanova M, Nichols CD (2007) Identification of neuroprotective compounds of *Caenorhabditis elegans* dopaminergic neurons against 6-OHDA. J Mol Neurosci 31: 127–137
5. Locke CJ, Fox SA, Caldwell GA, Caldwell KA (2008) Acetaminophen attenuates dopamin-

ergic neuron degeneration in animal models of Parkinson's disease. Neurosci Lett 439: 129–133

6. Su LJ, Auluck PK, Outeiro TF, Yeger-Lotem E, Kritzer JA, Tardiff DF, Strathearn KE, Liu F, Cao S, Hamamichi S, Hill KJ, Caldwell KA, Bell GW, Fraenkel E, Cooper AA, Caldwell GA, McCaffery JM, Rochet JC, Lindquist S (2010) Compounds from an unbiased chemical screen reverse both ER-to-Golgi trafficking defects and mitochondrial dysfunction in Parkinson's disease models. Dis Model Mech 3:194–208
7. Cao S, Hewett JW, Yokoi F, Lu J, Buckley AC, Burdette AJ, Chen P, Nery FC, Li Y, Breakefield XO, Caldwell GA, Caldwell KA (2010) Chemical enhancement of torsin A function in cell and animal models of torsion dystonia. Dis Model Mech 3:386–396
8. Nass R, Hahn MK, Jessen T, McDonald PW, Carvelli L, Blakely RD (2005) A genetic screen in *caenorhabditis elegans* for dopamine neuron insensitivity to 6-hydroxydopamine identifies dopamine transporter mutants impacting transporter biosynthesis and trafficking. J Neurochem 94:774–785
9. Caldwell KA, Tucci ML, Armagost J, Hodges TW, Chen J, Memon SB, Blalock JE, DeLeon SM, Findlay RH, Ruan Q, Webber PJ, Standaert DG, Olson JB, Caldwell GA (2009) Investigating bacterial sources of toxicity as an environmental contributor to dopaminergic neurodegeneration. PLoS One 4:e7227
10. Settivari R, Levora J, Nass R (2009) The divalent metal transporter homologues SMF-1/2 mediate dopamine neuron sensitivity in *Caenorhabditis elegans* models of manganism and Parkinson Disease. J Biol Chem 284:35758–35768
11. Christensen M, Estevez A, Yin X, Fox R, Morrison R, McDonnell M, Gleason C, Miller DM 3rd, Strange K (2002) A primary culture system for functional analysis of c. *elegans* neurons and muscle cells. Neuron 33:503–514
12. Harrington AJ, Hamamichi S, Caldwell GA, Caldwell KA (2010) *C. elegans* as a model organism to investigate molecular pathways involved with Parkinson's disease. Dev Dyn 239:1282–1295
13. Zhang Y, Ma C, Delohery T, Nasipak B, Foat BC, Bounoutas A, Bussemaker MJ, Kim SK, Chalfie M (2002) Identification of genes expressed in *C. elegans* touch receptor neurons. Nature 418:331–335
14. Von Stetina EV, Watson JD, Fox RM, Olszewski KL, Spencer WC, Roy PJ, Miller DM 3rd (2007) Cell-specific microarray profiling experiments reveal a comprehensive picture of gene expression in the *C. elegans* nervous system. Genome Biol 8:R135
15. Bianchi L, Driscoll M. Culture of embryonic *C. elegans* cells for electrophysiological and pharmacological analyses (September 30, 2006), WormBook, ed. The *C. elegans* Research Community, WormBook, doi/10.1895/wormbook.1.122.1, http://www.wormbook.org.
16. Schafer WR. Neurophysiological methods in *C. elegans*: an introduction (June 2, 2006), WormBook, ed. The *C. elegans* Research Community, WormBook, doi/10.1895/wormbook.1.111.1, http://www.wormbook.org.
17. Strange K, Christensen M, Morrison R (2007) Primary culture of *Caenorhabditis elegans* developing embryo cells for electrophysiological, cell biological and molecular studies. Nat Protoc 2:1003–1012
18. Fox RM, Watson JD, Von Stetina EV, McDermott J, Brodigan TM, Fukushige T, Krause M, Miller DM 3rd (2007) The embryonic muscle transcriptome of *Caenorhabditis elegans*. Genome Biol 8:R188
19. Rayes D, Flamini M, Hernanado G, Bouza C (2007) Activation of single nicotinic receptor channels from *Caenorhabditis elegans* muscle. Mol Pharmacol 71:1407–1415
20. Conway KA, Lee SJ, Rochet JC, Ding TT, Harper JD, Williamson RE, Lansbury PT Jr (2000) Accelerated oligomerization by Parkinson's Disease linked α-synuclein mutants. Ann N Y Acad Sci 920:42–45
21. Caldwell GA, Williams SN, Caldwell KA (2006) Integrated genomics: a discovery-based laboratory course. Wiley, Chichester, pp 1–225
22. Cao S, Gelwix CC, Caldwell KA, Caldwell GA (2005) Torsin-mediated protection from cellular stress in the dompaminergic neurons of *Caenorhabditis elegans*. J Neurosci 15:3801–3812
23. Polymeropoulos MH, Layedan C, Leroy E, Ide SE, Dehejia A, Dutra A, Pike B, Root H, Rubenstein J, Boyer R, Stenroos ES, Chandrasekharappa S, Athanassiadou A, Papapetropoulos T, Johnson WG, Lazzarini AM, Duvoisin RC, Di Lorio G, Golbe LI, Nussbaum RL (1997) Mutation in the alpha-synuclein gene identified in families with Parkinson's disease. Science 276:2045–2047

Chapter 7

Modelling the Blood–Brain Barrier

Marie-Pierre Dehouck, Elodie Vandenhaute, Lucie Dehouck, Emmanuel Sevin, Anne-Marie Lenfant, Yannick Delplace, Dorothée Hallier-Vanuxeem, Maxime Culot, and Roméo Cecchelli

Abstract

Located at the level of brain capillaries, the blood–brain barrier (BBB) is a crucial component of the neurovascular unit, since its highly regulated properties are needed to maintain optimal conditions for proper neuronal and glial functions. Therefore, understanding BBB features and behaviours in physiological and pathological conditions is a key issue in neurobiology. Since the BBB controls the exchanges between the blood and brain compartments, it also represents a major hurdle for molecules to reach the brain parenchyma. Given the localisation and complexity of the BBB in vivo, modelling the BBB in vitro can help to investigate cellular and molecular mechanisms, as well as evaluate the ability of compounds to cross the BBB. In this chapter, three in vitro BBB models will be described; all the methods and materials needed to design and to use each one will be detailed. The first model, comprising a coculture of bovine brain capillary endothelial cells and rat glial cells, is a powerful and robust system for studying mechanistic aspects and biological processes. To go further in immunological and molecular aspects, a syngenic mouse model based on a coculture of mouse microvessel endothelial cells and glial cells will be useful. The last model was designed to generate BBB toxicity and permeability data at a large scale, which is helpful in the development of central nervous system compounds. Ready after only 4 days of culture, it is suitable for a high throughput screening of molecules.

Key words: Blood–brain barrier, *In vitro* models, Cell culture, Endothelial cells, Glial cells, Permeability

1. Introduction

1.1. Understanding and Modelling the BBB: A Key Issue in Neurobiology

The blood–brain barrier (BBB) is a dynamic interface localised at the level of brain capillaries, comprising three major actors: endothelial cells, astrocytes and pericytes. The BBB is known to regulate exchanges between blood and brain parenchyma, because of absence of fenestration, presence of continuous tight junctions, metabolising enzymes, specific transporters (such as GLUT-1,

Michael Aschner et al. (eds.), *Cell Culture Techniques*, Neuromethods, vol. 56,
DOI 10.1007/978-1-61779-077-5_7, © Springer Science+Business Media, LLC 2011

for glucose transport) and efflux pumps (such as P-glycoprotein, Multi-Resistance Proteins family). Given these features, the BBB maintains optimal conditions for neuronal and glial function, but it also represents a major hurdle for blood-borne molecules to reach the brain, and many neuropharmaceutical compounds have proved unable to reach their central target.

Since *in vivo* complexity makes cellular and molecular mechanisms difficult to apprehend, modelling the BBB is necessary for understanding its functions and behaviour. In this purpose, in early 1990s, our group did pioneering work in establishing an *in vitro* model of the BBB. It consists in a coculture of bovine brain capillary endothelial cells and rat glial cells (1); this model is currently considered as one of the most powerful alternatives to *in vivo* studies of the BBB (2). It can be used routinely in industrial drug discovery and development programmes, but also provides a valuable tool for studying mechanistic aspects of transport as well as biological processes related to the BBB (3). Indeed, brain capillary endothelial cells in this model exhibit most of the features of the *in vivo* situation such as complex tight junctions, low permeability to small hydrophilic molecules, presence of metabolising enzymes, transporters and active efflux pumps. The BBB is also implicated in pathologies such as neurodegenerative disorders (e.g., Alzheimer's disease and multiple sclerosis), stroke, infectious processes and inflammatory pain; these pathological processes can be studied thanks to the same model. For example, it has proved useful in understanding BBB response to ischaemia (4,5).

However, the use of such a bovine/rat system could appear invaluable for the study of inflammatory events, and the help of a syngenic in vitro model is more appropriate in this case. The laboratory has therefore undertaken the establishment of a mouse BBB model, using primary endothelial cells coming from murine cerebral capillaries cocultivated with murine glial cells. This coculture model is worth using for immunological aspects (6). Moreover, molecular tools can be used for unravelling some molecular mechanisms, such as knock-out mice (7).

Obviously these models can be subjected to modification and/or complexification in order to closely mimic the in vivo situation closer; for instance pericytes – the least studied of BBB components – can be added to the original coculture system, to create a three-cell culture model where the three actors of the BBB are represented. This model set up is part of the EUSTROKE programme (*European Stroke Network*, FP7 2007–2013).

Despite much progress made by the pharmaceutical industry over the last few years, the number of products launched to treat central nervous system (CNS) diseases has not yet met neither with expectation nor demand. One reason is that more than 50% of compounds fail during late stage due to a pharmacokinetic deficit or to toxicological problems. Indeed, as explained previously, the CNS is highly protected by the BBB, which

regulates and controls the selective and specific transport of both exogenous and endogenous materials from the blood to the brain. In this context, there are increasingly higher demands on satisfactory ADME (adsorption, distribution, metabolism and excretion) and toxicological profiles in drug discovery and development processes. In order to increase the throughput of the first model and to adapt it to automation, some parts of the procedures have been modified. The main changes involved the reduction of experimental format (24-well plates instead of 6–well plates) and the replacement of glial cells with the "BBB inducing medium". This new model is ready to use after only 4 days of culture and shows the typical expression and localisation of tight junction proteins. The function of P-glycoprotein and other efflux transporters has also been demonstrated. Based on the ECVAM (*European Centre for the Validation of Alternative Methods*) workshop 50 (8) recommendations, the development and validation of this model were undertaken within the European ACuteTox project. It aims at assessing BBB toxicity and making risk assessment of potentially toxic compounds according to their predicted ability to reach the CNS compartment. This new BBB model (High Throughput Screening model, HTS model) has proven to be a relevant tool for assessing brain toxicity and BBB permeability in a high throughput screening mode. It allows to considerably increase the rate at which BBB permeability data are generated, and could be included in neurotoxicity testing strategy for large sets of chemicals, as in the frame of REACH (*Registration, Evaluation and Authorisation of Chemicals*) program (9).

All of the three models (bovine/rat, syngenic murine and HTS models) will be further described in the following sections, where their design will be detailed.

1.2. Principle of the Models

1.2.1. Isolating Brain Endothelial Cells

The very first step consists in isolating primary brain endothelial cells, and to cultivate them. The starting material is always brain microvessels from the cortex. Brain endothelial cells can be isolated thanks to several techniques: mechanical dispersion, enzymatic digestion or both (Fig. 1).

On the one hand, the bovine model does not use any enzymatic digestion step. Since only capillaries adhere on the corneal extracellular matrix, we are sure of getting brain capillary endothelial cells. On the other hand, the murine model needs an enzymatic digestion for endothelial cells growth out from the microvessels.

In the case of the murine syngenic model, each experiment needs primary cells extraction. As for the bovine model, endothelial cells can be subcultured as soon as they reach confluence (Cecchelli *et al.*, 1999), which allows providing large quantities of endothelial monolayers. Indeed, the lifespan of the culture is about 50 cumulative population doublings.

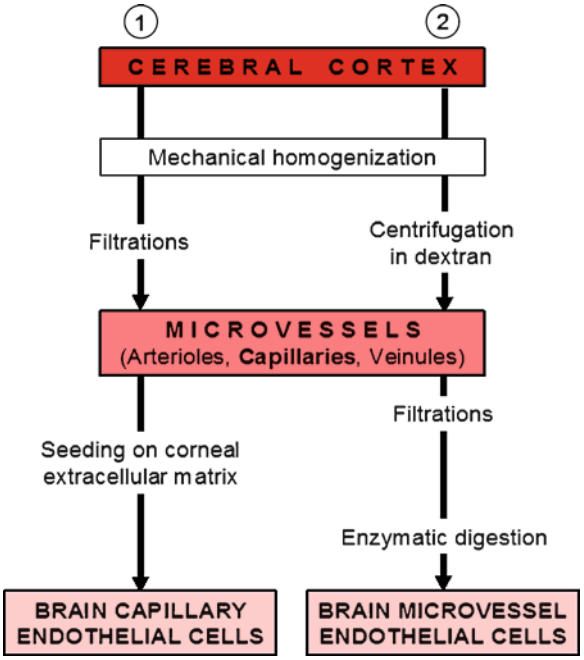

Fig. 1. Isolation of brain microvessel endothelial cells for the bovine/rat model ① (Protocol from Méresse *et al.* (16)) and the syngenic murine model ② (Protocol from Coisne *et al.* (6)).

1.2.2. Differentiating Brain Endothelial Cells

Environment is crucial for differentiating endothelial cells. In order to get endothelial cells with BBB features, they are cocultivated with other cell types – glial cells – which are known to induce the BBB phenotype in endothelial cells (Fig. 2) (11). Here primary glial cells are used; they are mainly composed of astrocytes (see Fig. 2c), but also contain oligodendrocytes and microglial cells.

Murine endothelial cells are ready after 5 days of coculture with glial cells. Bovine endothelial cells are fully differentiated after 12 days of coculture with rat glial cells. In these conditions, endothelial cells exhibit most features of *in vivo* BBB: they form a regular monolayer of nonoverlapping cells (Fig. 2a), show a high paracellular restriction because of functional tight junctions (Fig. 2b) and a low transcellular permeability. The relevant BBB efflux transporters (P-gp, MRPs) are expressed. Bovine endothelial cells retain their functional BBB properties for several days in culture.

Some could prefer to use immortalised endothelial cells, but should remember that they do not necessarily meet the requirements in terms of restrictive paracellular permeability (12).

In the same way, one could prefer using immortalised glial cells, for instance C6 cell line. In presence of these cells, endothelial cells show a low electrical resistance, a high permeability to integrity markers, and do not exhibit their common morphology, demonstrating a poor BBB differentiation. Moreover this cell line was shown to

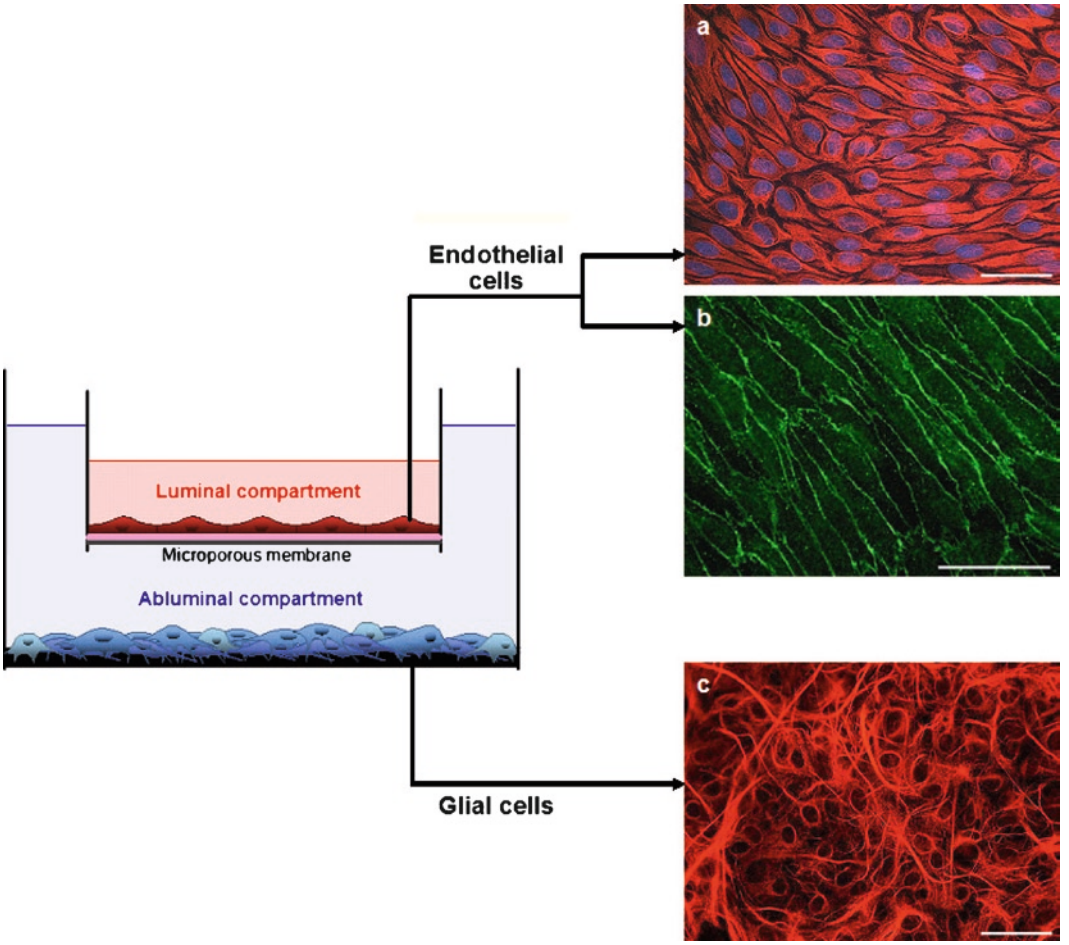

Fig. 2. General scheme of the *in vitro* blood–brain barrier model. Endothelial cells are seeded on the upper side of the filter. Here they were immunostained for vimentin (**a**) and for occludin (**b**), a tight junction protein. Glial cells are seeded at the bottom of the well, mainly composed of astrocytes (glial fibrillary acidic protein staining), (**c**) Bar = 50 μm.

secrete high rates of VEGF, inducing a permeability increase in endothelial monolayers (13). Therefore, C6 cells failed in replacing primary glial cells to get a reliable BBB *in vitro* model under our experimental conditions.

To gather both cell populations, a double compartment system is used (Fig. 2). It is composed of an insert – on which endothelial cells are seeded – adapted over a well, containing the glial cells. The insert mimics the blood compartment (luminal compartment), whereas the well corresponds to the parenchyma (abluminal compartment).

1.2.3. Permeability Studies

The above-mentioned system with two compartments provides a practical device for studying the transport of compounds from the blood compartment to the cerebral compartment and vice versa. By using known nonpermeant molecules (Lucifer Yellow,

sucrose) for these transport experiments, it allows verifying monolayer integrity. Coincubating these integrity markers with a compound (e.g. a pharmaceutical compound) will give information about its toxic effect towards the BBB. The permeability of a compound is given as an endothelial permeability coefficient (noted Pe).

Set up of each model and calculation of the permeability coefficient will be detailed in the following sections.

2. Materials

The products used are listed below for all models described in this chapter. Refer to the text in the following section for further details according to the model.

Cells are cultivated in incubators at 37°C, in a humidified atmosphere with 5% CO_2/95% air. Before incorporating any serum in culture media, it is previously heat-inactivated (incubated at 58°C for 30 min).

2.1. Material for Media Preparation

Basal medium: Dulbecco's modified eagle's medium (DMEM), Ref: 31600-083, Gibco

Sera:

- Calf Serum (CS), Ref: 7316368D, InvitroGen
- Horse Serum (HS), Ref: 7399488D, InvitroGen
- Fetal Calf Serum (FCS), Ref: K002603F, Integro

Antibiotics:

- Gentamicin, Ref: A2712, Biochrom AG
- Amphotericin B (Fungizone®)

Growth factor: bFGF (basic Fibroblast Growth Factor), Ref: F0291, Recombinant Human bFGF, Sigma-Aldrich

Amino acid: L-glutamine, Merck Chemicals

2.2. Material for Cells Isolation and Culture

2.2.1. Animals:

- Freshly slaughtered calf (for bovine endothelial cells extraction)
- Newborn Sprague–Dawley rats (Centre d'Elevage Roger Janvier, Le Genest Saint Isle, France) (for rat glial cells extraction)
- Newborn OF1 mice (Centre d'Elevage Roger Janvier, Le Genest Saint Isle, France) (for mouse glial cells extraction)
- Four- to five-week-old OF1 mice (Centre d'Elevage Roger Janvier, Le Genest Saint Isle, France) (for mouse endothelial cells extraction)

2.2.2. Material for Cell Extraction

To remove meninges:

- Dry cotton swabs, Ref: 115-2524, VWR (for removing mouse brain meninges)
- Moria Ultra Fine Tipped Forceps (Straight model, Item n° 11370-40) (for removing rat brain meninges)

To homogenate suspensions:

- 40-mL glass homogeniser
- Glass pestles (152, 76 μm clearance)
- Dounce homogeniser with a large clearance pestle: 0.06–0.08 mm

To sieve suspensions:

- Nylon sieves, pore size: 180, 60, 59 μm (endothelial cells), 82 μm (rat glial cells), Blutex®, Saati, France

To digest vessels and trypsinise cells:

- Collagenase/dispase, Ref: 10 269 638 001, Roche Diagnostics
- DNase I, Ref: 11 284 932 001, Roche Diagnostics
- TLCK (Tosyl-L-LYSINE Chloromethyl Ketone), Ref: T7254, Sigma-Aldrich
- Trypsine/EDTA, 0.05%/0.02% (w/v) in Phosphate Buffered Saline – Calcium and Magnesium Free (PBS-CMF), Ref: L2143, Biochrom AG

Buffers:

- PBS-CMF (8.0 g L^{-1} NaCl, 0.2 g L^{-1} KCl, 0.2 g L^{-1} KH_2PO_4 and 2.87 g L^{-1} $Na_2HPO_4(12H_2O)$ at pH 7.4)

To seed cells:

- 60-mm Petri dishes, Ref: 430166, Corning, Corning Incorporated
- 35-mm Petri dishes, Ref: 430165, Corning, Corning Incorporated

To coat dishes:

- Gelatine Type A (from Porcine skin), Ref: G2500, Sigma-Aldrich
- Growth Factor Reduced BD Matrigel™ Matrix, Ref: 354230, BD Biosciences
- Rat tail collagen type I, Ref: 354236, BD Biosciences
- Bovine corneal extracellular matrix

Specific needs for the mouse model:

- Hanks Balanced Salt Solution (HBSS) 1×, Ref: H8264, Sigma-Aldrich (mouse model)
- Bovine Serum Albumin, Ref: A4161, Sigma-Aldrich
- HEPES 1 M, Ref: H0887, Sigma-Aldrich
- Amino acids 50×, Ref: B6766, Sigma-Aldrich
- Vitamins 100×, Ref: B6891, Sigma-Aldrich
- Dextran from *Leuconostoc mesenteroides*, average molecular weight 100,000–200,000, Ref: D4876, Sigma-Aldrich

2.3. Material for Model Set Up: Plates and Filters

Plates:

- 6-multiwell dishes, Ref: 3506, Costar, Corning Incorporated (bovine model)
- 12-multiwell dishes, Ref: 3512, Costar, Corning Incorporated (mouse model)

Filters:

- CM, diameter 30 mm, pore size 0.4 μm, Millicell-CM, Millipore Corporation (bovine model) or Transwell, diameter 24 mm, polyester membrane, pore size 0.4 μm, Ref: 3450, Costar, Corning Incorporated (bovine model)
- Transwell, diameter 12 mm, polyester membrane, pore size 0.4 μm, Ref: 3460, Costar, Corning Incorporated (mouse model)

Assemblies:

- 24-well cell culture plate assemblies, Ref: PSHT010R5, Millicell 24, Cell Culture Plate PCF 0.4 μm, Millipore Corporation (HTS model)

2.4. Material for Transport Experiment

- 24-well receiver tray, Ref: PSMW010R5, Millicell®24, 24-well receiver tray, Millipore Corporation
- 6-multiwell dishes, Ref: 3506, Costar, Corning Incorporated
- 12-well dishes, Ref: 3512, Costar, Corning Incorporated
- Ringer-HEPES (RH) buffer (150 mM NaCl; 5.2 mM KCl; 2.2 mM $CaCl_2$; 0.2 mM $MgCl_2 \cdot 6H_2O$; 6.0 mM $NaHCO_3$; 5.0 mM HEPES; 2.8 mM de glucose, pH 7.4)
- High-Pressure Liquid Chromatography (HPLC) (ThermoFinigan, San Jose, CA, USA) and/or liquid scintillation counter (Perkin Elmer, Courtaboeuf, France) and /or fluorometer (Fluoroscan Ascent, Thermolabsystems OY, Helsinki, Finland)

2.5. Material for Calculation of Permeability Data

- Spreadsheet programme

2.6. Material for Analysis of Permeability Data

– Statistical analysis Software (Ex: GraphPad Prism, GraphPad Software)

3. Methods

3.1. The Bovine/Rat BBB Model (12 Days/6 Wells)

Primary cultures of mixed glial cells (comprising astrocytes, oligodendrocytes and microglial cells) are prepared from the cerebral cortex of newborn rats according to the method of Booher and Sensenbrenner (14) (see Fig. 3).

3.1.1. Glial Cells Isolation and Culture

1. Thanks to the straight forceps, remove all meninges from the brain tissue.
2. Force the resulting tissue gently through the nylon sieve.
3. Seed glial cells suspension in 6-multiwell dishes at a concentration of 1.2×10^5 cells/mL. Each well is filled with 2 mL of DMEM supplemented with 10% FCS, 2 mM L-glutamine and 50 µg/mL gentamycin. This medium is the same as the one used for dissociating the cerebral tissue.
4. Before putting plates in the incubator, shake them gently by circular motions in order to homogenise the culture.
5. The medium is renewed 24 h after seeding, and then twice a week (2 mL per well). After 3 weeks in culture, glial cells can be used for setting up the BBB model, until 6 weeks.

3.1.2. Isolation and Culture of Bovine Brain Capillary Endothelial Cells

Bovine brains are removed from freshly slaughtered calves.

1. Cut the brain cortex into 2 mm^3 fragments and wash them twice with PBS.
2. Resuspend tissue fragments in 2 volumes of PBS and homogenise them by 15 up-and-down strokes in a 40 mL-glass homogeniser fitted with a 152 µm clearance glass pestle.
3. Pass the homogenate through a 180-µm-nylon sieve to get a filtrate containing microvessels.
4. Homogenise again with a second glass pestle (76 µm clearance).
5. Collect capillaries on a 60-µm nylon sieve and wash them with PBS.
6. Resuspend capillaries in DMEM supplemented with 20% CS, 50 µg/mL gentamycin and 2.5 µg/mL Amphotericin B.
7. The resulting freshly isolated microvessels suspension proves to be mainly composed of capillaries as assessed by light and phase-contrast microscopy.

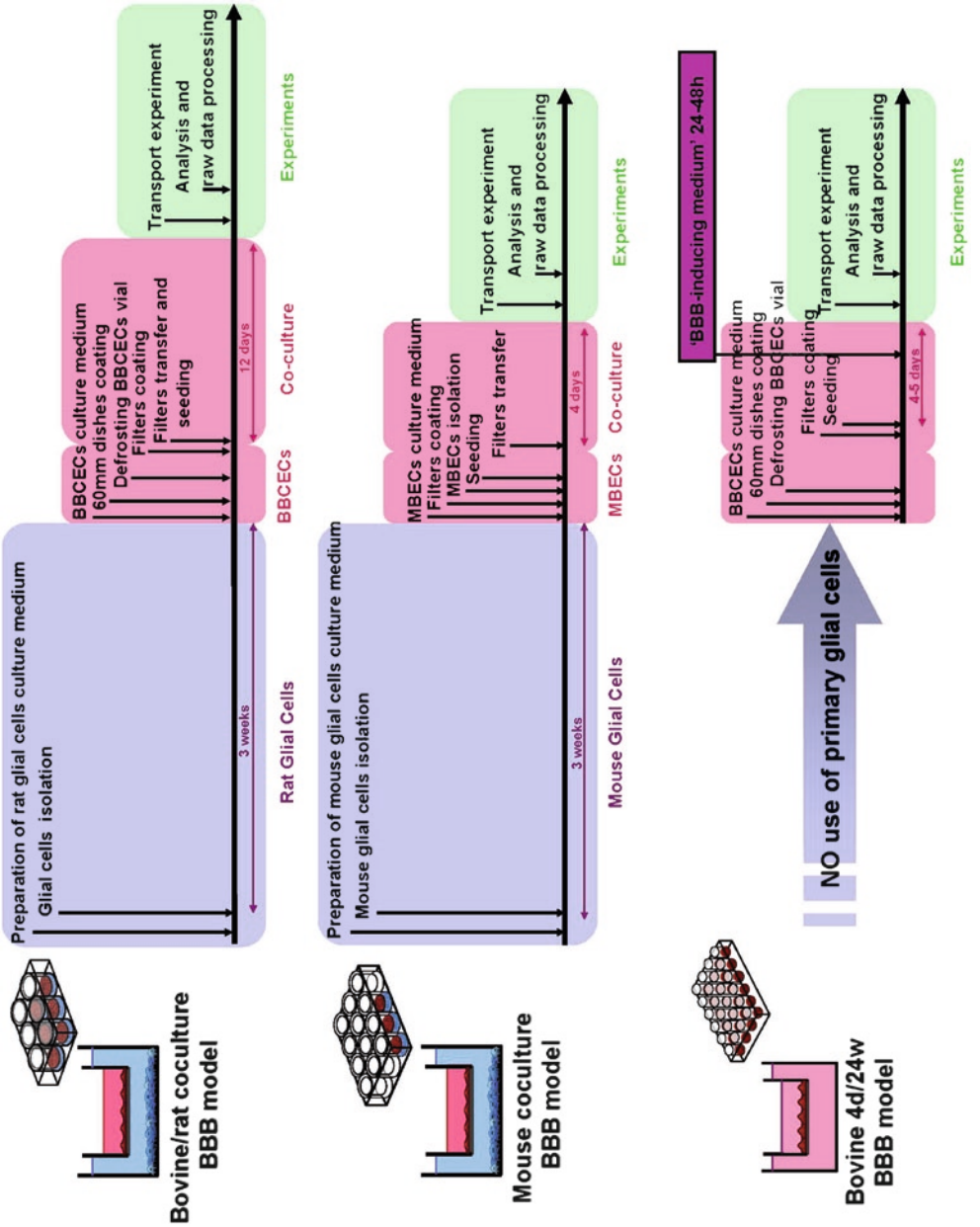

Fig. 3. General scheme resuming the time course for setting up the three BBB models. *BBECs* bovine brain capillary endothelial cells; *MBECs* mouse brain endothelial cells; *ECs* endothelial cells.

8. Immediately seed microvessels preparation at a density of 5–10 fragments/cm^2 into corneal extracellular matrix-coated dishes containing DMEM supplemented with 20% CS.
9. Incubate in a humidified incubator with 5% CO_2/95% air at 37°C. Most capillaries adhere to the corneal extracellular matrix.
10. Renew the medium in order to remove nonadherent microvessels.
11. From 4 to 5 days after seeding, the first endothelial cells migrate out from the capillaries and begin to form microcolonies: change the medium and add 1 ng/mL of bFGF (bFGF is then added every other day).
12. As soon as endothelial cell colonies are sufficiently large for cloning (from 50 to 100 cells), trypsinise them (with PBS containing 0.05% trypsin and 0.02% EDTA) and seed them onto 35-mm-diameter gelatine-coated dishes (one clone per dish) in the presence of DMEM supplemented with 15% CS, 2 mM L-glutamine, 50 µg/mL gentamicin, 2.5 µg/mL Amphotericin B and bFGF (1 ng/mL, added every other day).
13. Incubate cells in a humidified incubator (37°C, 5% CO_2/95% air).

Endothelial cells from one 35-mm-diameter gelatine-coated dish are harvested at confluence and seeded onto 60-mm-diameter gelatine-coated dishes. After 6–8 days, confluent cells are subcultured at the split ratio 1:15. Cells at the third passage can be stored in liquid nitrogen.

Frozen at passage 3, brain capillary endothelial cells are thawed into 60-mm-diameter gelatine-coated dishes, and trypsinised at confluence for seeding in the BBB model.

3.1.3. Bovine/Rat Coculture BBB Model Set-Up

1. As soon as glial cell are ready (3 weeks), coat 6-well-plate filters on the upper side with rat tail collagen prepared by a modification of the method of Bornstein (1). Otherwise, rat tail collagen is commercially available (see References list in Sect. 2).
2. Set these filters in 6-well dishes containing glial cells.
3. Plate brain capillary endothelial cells on the upper side of the filters, at a concentration of 4×10^5 cells/mL. The coculture medium is composed of DMEM supplemented with 10% CS, 10% HS, 2 mM L-glutamine, 50 µg/mL gentamicin and 1 ng/mL bFGF, renewed every other day. Under these conditions, brain capillary endothelial cells form a confluent monolayer within 5 days. After 12 days of coculture the cells are differentiated and are ready for experiments.

3.2. HTS BBB Model (4 Days/24 Wells)

As said previously, this model is a modification of the coculture model of Dehouck *et al.* (1). Therefore, endothelial cell isolation

and culture is identical to the protocol described in the previous Section (3.1.2). Unlike the original coculture model, glial cells are replaced by the coculture conditioned medium and the cell density at seeding is higher, in order to reduce culture time and increase model throughput.

1. Place filter inserts of 24-well-plate filters previously coated with rat tail collagen into a single-well feeding cell culture plate.
2. Fill filter inserts with 0.4 mL of brain capillary endothelial cell medium (DMEM supplemented with 10% CS, 10% HS, 2 mM L-glutamine, 50 µg/mL gentamicin and 1 ng/mL bFGF) and 24 mL in the lower compartment.
3. Seed 6×10^5 endothelial cells/mL on the upper side of each 24-well-plate insert.
4. Three days later, replace the medium by a "BBB inducing medium", developed in collaboration with *Cellial Technologies* (Lens, France). This conditioned medium is harvested 48 h after refreshing the original coculture system medium, and is frozen until further use.
5. Experiments are carried out 24 h later.

3.3. Syngenic Mouse BBB Model

Primary cultures of glial cells (astrocytes, oligodendrocytes and microglial cells) are prepared from newborn OF1 mouse cerebral cortices.

3.3.1. Mouse Glial Cells Isolation and Culture

1. Carefully remove meninges with dry cotton swabs.
2. Force the brain tissue gently through a nylon sieve as described by Booher and Sensenbrenner (14). Mixed glial cell cultures are obtained by plating the cells (12,500 cells/cm^2) in 12-well plates, in DMEM supplemented with 10% FCS, 2 mM L-glutamine and 50 µg/mL gentamicin. The medium is changed twice a week. Three weeks after seeding, the cultures can be used for coculture with endothelial cells.

3.3.2. Mechanical Isolation of Brain Microvessels from Adult Mice Cortices

1. Isolate the brain cortices from 4- to 5-week-old OF1 mice by removing cerebellum, striatum, optic nerves and brain white matter.
2. Remove outer vessels and meninges using dry cotton swabs.
3. Pool and grind the preparations using a Dounce homogeniser (with a large clearance pestle: 0.06–0.08 mm) in HBSS containing 10 mM HEPES and 0.1% BSA.
4. Mix the resulting homogenate with 30% dextran (v/v, molecular weight 100,000–200,000) in HBSS supplemented with 10 mM HEPES and 0.1% BSA (called "washing buffer").
5. Centrifuge this suspension at 3,000×*g* for 25 min at 4°C.

6. Discard the neural component and the dextran layer, and resuspend the pellet containing the vascular component in the washing buffer. The resulting suspension contains the vascular component.
7. Filter the resulting suspension through a 59-μm nylon mesh, in order to retain large vessels on the mesh surface, whereas capillaries will pass through.
8. Centrifuge the capillary-enriched filtrate at 1,000×*g* for 7 min at room temperature.
9. Digest the pellet in collagenase/dispase (2 mg/mL) diluted in DMEM supplemented with 10 μg/mL DNase I and 0.147 μg/mL TLCK, for 30 min at 37°C in a shaking water bath.

3.3.3. Seeding of Digested Brain Microvessels

1. After several washes, seed the resulting digested capillary suspension at 51,000 digested capillaries/cm^2 onto Matrigel-coated inserts. Culture medium is DMEM supplemented with 20% FCS, 50×amino acids, 100×vitamins, and 50 μg/mL gentamicin.
2. 24 h after plating, remove red blood cells, cell debris and nonadherent cells by washing with medium. Afterwards, change the medium every other day and supplement it with 1 ng/mL bFGF.

3.3.4. Coculture Between Endothelial and Glial Cells

1. The day of mouse endothelial cell isolation, place Matrigel-coated-12-mm-Transwell filters in the 12-multiwell dishes containing glial cell cultures.
2. Directly plate digested capillaries on the upper side of Matrigel-coated inserts. Under such conditions, endothelial cells migrate from digested capillaries and reach confluence within 2 days after plating.
3. Use these cultures 3 days after confluence, in order to enhance mouse brain capillary endothelial cells differentiation by glial cells. Coculture medium is the same as the one used for endothelial cells growth and is changed every other day.

4. Permeability Calculation and Data Interpretation

4.1. Transport Experiment

1. Transfer confluent brain capillary endothelial monolayer inserts into plates containing RH buffer (abluminal compartment) (see Table 1 for volume).
2. The medium of the apical chambers (luminal compartment) is removed and replaced by RH buffer containing radiolabelled (inulin, sucrose, urea, vincristine, etc.), unlabelled (caffeine,

Table 1
Transport experiment parameters for the three different systems. Note that these data are only valuable if you use the references listed in Sect. 2

Model	Plate	RH volume (μL)		Membrane surface (cm^2)
		Insert (luminal)	Well (abluminal)	
Bovine model	6-well	1,500	2,500	CM filters: 4.2 TW filters: 4.67
Murine model	12-well	500	1,500	1.13
HTS model	24-well	400	800	0.70

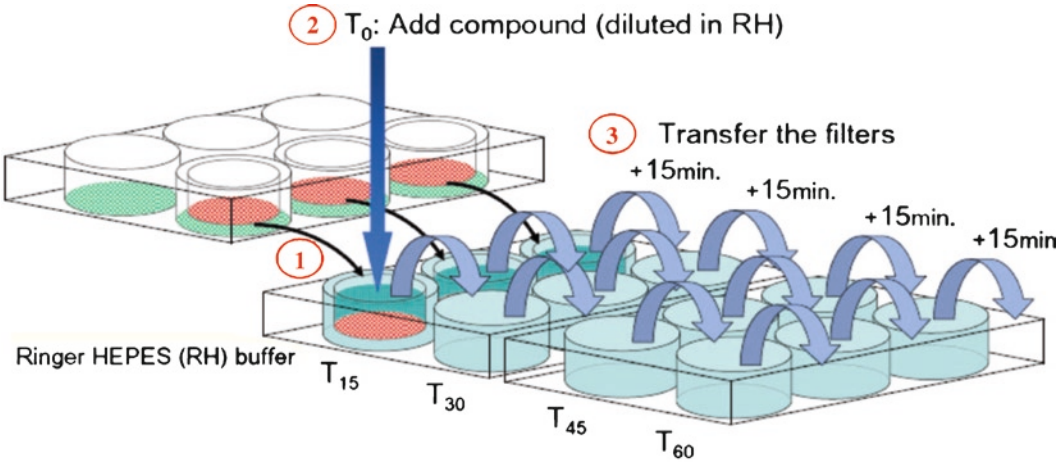

Fig. 4. Transport experiment steps. First the filters have to be transferred in wells containing RH buffer ①, and then the drug (and/or the integrity marker) is deposed in the insert ②. Afterwards, to reduce transport from the abluminal to the luminal compartment, the filters are regularly transferred into new wells containing RH ③. In the example 15-min intervals are used.

antipyrine, cimetidine, etc.) compounds (see Table 1) or fluorescent molecules (Lucifer Yellow, Rhodamine 123, etc.)

3. At different time points, each insert is transferred in another well containing RH buffer (to minimise an eventual flux of compounds from the abluminal to the luminal compartment) (Fig. 4).
4. At the end of the experiment, the amount of molecules in the abluminal compartments is measured using a liquid scintillation counter, HPLC or fluorometer.

4.2. Permeability Calculation

Permeability calculations are performed as described by Siflinger-Birnboim et al. (15). To get a concentration-independent transport parameter, the clearance principle is used.

1. Calculate the increment in cleared volume between successive sampling events by dividing the amount of solute transport during the interval (in the example of Fig. 4: 15 min) by the donor chamber concentration.
2. Calculate the total cleared volume at each time point by summing the incremental cleared volume up to the given time point thanks to the following formula:

$$\text{Clearance}\left(\text{noted Cl, in mL}\right) = X / \text{Cd}$$

   where X = amount of drug in the receptor chamber
   and Cd = the donor chamber concentration at each time point
3. Note that during the whole (45 min) experiment, the clearance volume increases linearly with time.
4. Plot the average cleared volume versus time, and estimate the slope by linear regression analysis. The slope of clearance curves is denoted PS_t, where

$$\text{PS} = \text{permeability} \times \text{surface area product}\left(\text{in mL/min}\right)$$

5. The slope of the clearance curve with the control insert (i.e., filter coated with collagen only, without endothelial cells) is denoted PS_f.
6. The PS value for the EC monolayer (noted PS_e) is calculated thanks to the following formula:

$$1/\text{PS}_e = 1/\text{PS}_t - 1/\text{PS}_f$$

7. Divide PS_e value by the surface area of the filter porous membrane (see Table 1), in order to generate the endothelial permeability coefficient (noted Pe, expressed in cm/min).

Acknowledgments

The authors greatly thank the European Stroke Network (EUSTROKE, FP7) as well as the European ACuteTox project (FP6). Elodie Vandenhaute has received a doctoral fellowship from the French Ministry of Research.

References

1. Dehouck MP, Meresse S, Delorme P, Fruchart JC, Cecchelli R (1990) An easier reproducible, and mass-production method to study the blood–brain barrier in vitro. J Neurochem 54:1798–1801
2. Mertsch K, Maas J (2002) Blood–brain barrier penetration and drug development from an industrial point of view. Curr Med Chem 2:187
3. Cecchelli R, Berezowski V, Lundquist S, Culot M, Renftel M, Dehouck MP, Fenart L (2007) Modelling of the blood–brain barrier in drug discovery and development. Nat Rev Drug Discov 6:650–661

4. Brillault J, Berezowski V, Cecchelli R, Dehouck MP (2002) Intercommunications between brain capillary endothelial cells and glial cells increase the transcellular permeability of the blood–brain barrier during ischaemia. J Neurochem 83:807–817
5. Culot M, Mysiorek C, Renftel M, Roussel BD, Hommet Y, Vivien D, Cecchelli R, Fenart L, Berezowski V, Dehouck MP, Lundquist S (2009) Cerebrovascular protection as a possible mechanism for the protective effects of NXY-059 in preclinical models: an in vitro study. Brain Res 1294:144–152
6. Coisne C, Dehouck L, Faveeuw C, Delplace Y, Miller F, Landry C, Morissette C, Fenart L, Cecchelli R, Tremblay P, Dehouck B (2005) Mouse syngenic in vitro blood–brain barrier model: a new tool to examine inflammatory events in cerebral endothelium. Lab Invest 85:734–746
7. Mysiorek C, Culot M, Dehouck L, Derudas B, Staels B, Bordet R, Cecchelli R, Fenart L, Berezowski V (2009) Peroxisome-proliferator-activated receptor-alpha activation protects brain capillary endothelial cells from oxygen-glucose deprivation-induced hyperpermeability in the blood–brain barrier. Curr Neurovasc Res 6:181–193
8. Gennari A, van den Berghe C, Casati S, Castell J, Clemedson C, Coecke S, Colombo A, Curren R, Dal Negro G, Goldberg A, Gosmore C, Hartung T, Langezaal I, Lessigiarska I, Maas W, Mangelsdorf I, Parchment R, Prieto P, Sintes JR, Ryan M, Schmuck G, Stitzel K, Stokes W, Vericat JA, Gribaldo L (2004) Strategies to replace in vivo acute systemic toxicity testing. The report and recommendations of ECVAM Workshop 50. Altern Lab Anim 32:437–459
9. Hallier-Vanuxeem D, Prieto P, Culot M, Diallo H, Landry C, Tahti H, Cecchelli R (2009) New strategy for alerting central nervous system toxicity: integration of blood–brain barrier toxicity and permeability in neurotoxicity assessment. Toxicol In Vitro 23:447–453
10. Cecchelli R, Dehouck B, Descamps L, Fenart L, Buee-Scherrer VV, Duhem C, Lundquist S, Rentfel M, Torpier G, Dehouck MP (1999) In vitro model for evaluating drug transport across the blood–brain barrier. Adv Drug Deliv Rev 36:165–178
11. Dehouck B, Dehouck MP, Fruchart JC, Cecchelli R (1994) Upregulation of the low density lipoprotein receptor at the blood–brain barrier: intercommunications between brain capillary endothelial cells and astrocytes. J Cell Biol 126:465–473
12. Prieto P, Blaauboer BJ, de Boer AG, Boveri M, Cecchelli R, Clemedson C, Coecke S, Forsby A, Galla HJ, Garberg P, Greenwood J, Price A, Tahti H (2004) Blood–brain barrier in vitro models and their application in toxicology. The report and recommendations of ECVAM Workshop 49. Altern Lab Anim 32:37–50
13. Boveri M, Berezowski V, Price A, Slupek S, Lenfant AM, Benaud C, Hartung T, Cecchelli R, Prieto P, Dehouck MP (2005) Induction of blood–brain barrier properties in cultured brain capillary endothelial cells: comparison between primary glial cells and C6 cell line. Glia 51:187–198
14. Booher J, Sensenbrenner M (1972) Growth and cultivation of dissociated neurons and glial cells from embryonic chickrat and human brain in flask cultures. Neurobiology 2:97–105
15. Siflinger-Birnboim A, Del Vecchio PJ, Cooper JA, Blumenstock FA, Shepard JM, Malik AB (1987) Molecular sieving characteristics of the cultured endothelial monolayer. J Cell Physiol 132:111–117
16. Meresse S, Dehouck MP, Delorme P, Bensaid M, Tauber JP, Delbart C, Fruchart JC, Cecchelli R (1989) Bovine brain endothelial cells express tight junctions and monoamine oxidase activity in long-term culture. J Neurochem 53:1363–1371

Chapter 8

In Vitro Models of the Blood–Cerebrospinal Fluid Barrier and Their Use in Neurotoxicological Research

Nathalie Strazielle and Jean-François Ghersi-Egea

Abstract

The choroid plexus epithelium forms the interface between the blood and the cerebrospinal fluid. In addition to its barrier function resulting from the presence of tight junctions sealing the epithelial cells together, the choroid plexus epithelium fulfills vectorial transport (influx and efflux), neuroprotective, antioxidant and secretory functions, all relevant to different aspects of neurotoxicological sciences. To investigate these choroidal functions without the interference of the blood–brain barrier proper and brain parenchyma, in vitro cellular models of the blood–cerebrospinal fluid barrier, retaining the differentiated phenotype of the choroidal epithelium, have been established, taking advantage of the advent of refined culture methods and availability of permeable membranes.

This chapter provides information to help investigators to set up and characterize choroid plexus epithelial cells in culture in bicameral devices. It first describes the factors that are critical to isolate the cells and select the culture conditions, and provides a survey of available cell lines with their advantages and limitations. Then the primordial specific choroidal features that can be examined within a validation scheme are discussed, emphasizing the need for a careful interpretation of their significance. In a third part, selected examples of studies performed with these models are presented, highlighting their potential applications in the field of neurotoxicology.

Key words: Choroid plexus, Blood–brain barrier, Cerebrospinal fluid, In vitro models, Cell culture, Transport, Drug metabolism, Tight junction, Neurotoxicology, Metal

1. Introduction

The choroid plexuses (CPs) which form the blood–cerebrospinal fluid (CSF) barrier (BCSFB) are, in conjunction with the blood–brain barrier, responsible for maintaining the appropriate microenvironment required by the brain. The CPs, located in the lateral, third and fourth ventricles of the brain, secrete a major part of the CSF which circulates from the ventricles into the subarachnoid

Michael Aschner et al. (eds.), *Cell Culture Techniques*, Neuromethods, vol. 56,
DOI 10.1007/978-1-61779-077-5_8,

spaces and the spinal canal, and as such, exert a considerable influence on the composition of the medium bathing the central nervous system. The CP functions include the selective blood-to-CSF entry of required molecules such as inorganic anions, nutrients and hormones, as well as the CSF-to-blood export of toxic compounds and metabolites (1, 2). The major influence of the CP on brain development has been highlighted (3). The site of the BCSFB is the choroidal epithelium proper (Fig. 1). CP functions require the presence of numerous transport systems distributed in a polarized pattern between the apical or brush border (CSF facing) and the basolateral (stroma facing) membrane domains of the choroid plexus epithelial (CPE) cells. They also depend on the existence of interepithelial tight junctions (TJ), which strongly restrict the paracellular pathway for small lipid insoluble compounds (1, 2). More recently a specific role in neuroimmune surveillance and neuroinflammation has been attributed to the

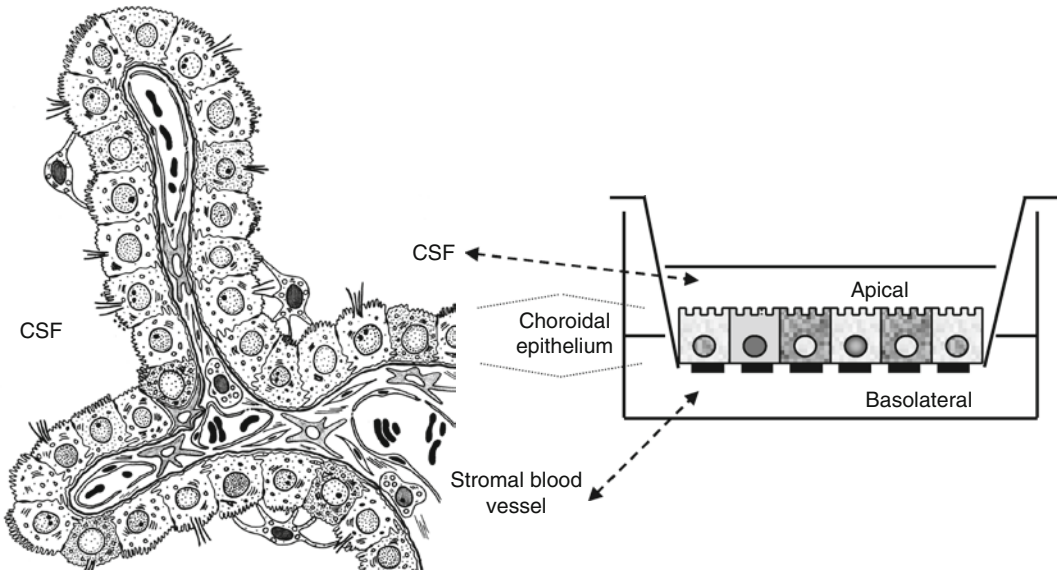

Fig. 1. In vitro model of the blood–cerebrospinal fluid barrier. Located in the ventricles of the brain, and folding into numerous villi, the CPs are formed by a choroidal epithelium delimiting an inner conjonctive stroma, which contains permeable capillaries and cells of the myeloid lineage. Epiplexuel macrophages, or Kolmer cells, locate at the CSF-facing membrane of the epithelium (*left*).The site of the BCSFB is the choroidal epithelium proper. The tight regulation of the transepithelial permeability required to maintain brain homeostasis implies a passive blockade of the paracellular pathway, and an active control of the transcellular pathway. The former is achieved by the presence of tight junctional complexes sealing the intercellular clefts between epithelial cells and restricting the passage of ions and small lipid-insoluble nonelectrolytes. The control of the transcellular pathway involved both in the secretion of fluid, ions, essential nutrients and hormones, and in the reabsorption of endogenous toxic metabolites from the CSF, occurs via a machinery of channels, pumps and transport systems distributed in a polarized pattern between the apical and basolateral membrane domains of the CPE cells. To reproduce the BCSFB in vitro, CPE cells are grown on a permeable membrane (*right*). The monolayer separates two compartments, the upper one containing the apical fluid which represents the CSF and the lower chamber, containing the basolateral fluid assimilated to the stromal blood (reprinted from (24), with permission).

CP, based on evidence for the capacity of the choroidal cells to produce chemokine/cytokine and for immune cell migration from blood to CSF (4, 5).

Defining the role of this epithelium in solute transport between the blood and the CSF, or in polarized secretion processes, by analyzing CSF in vivo is complicated by the flow and constant renewal of CSF, and by the contribution of the blood–brain barrier and the nervous tissue to the composition of this fluid. Diffusion from the interstitial fluid into the CSF of material secreted by neural cells or exchanged across the cerebral capillaries occurs across the nonrestrictive permeable ependyma or to a lesser extent across the glia limitans. Alternatively, CSF-borne molecules diffuse into the parenchyma. These different parameters cannot be easily taken into consideration when CP-specific processes are investigated by in vivo techniques such as ventriculocisternal perfusion, in situ brain perfusion, or microdialysis. The development of ex vivo or in vitro techniques was therefore mandatory to study CP physiology and transport functions without the interference of the blood–brain barrier and brain parenchyma. The in situ perfused CP can be used to estimate transcellular transport from CSF to blood as well as from blood to CSF (6). However, perfusion of the choroidal vasculature requires a large animal and the technique has been carried mainly on sheep and goats. The isolated CP and isolated apical and basolateral membrane vesicles prepared from epithelial cells provide – relatively – simpler and convenient systems. Isolated CPs in particular have been extensively used to characterize choroidal uptake, but obviously are not adequate to study transepithelial transfer or polarized transport and secretion mechanisms, as they do not offer easy and separate access to the stromal facing membrane of the CPE cells. One exception concerns fluorescent compounds whose apical to basolateral movement can be visualized by confocal microscopy. Other limitations shared by these different ex-vivo techniques are (a) the limited survival time of the choroidal tissue, precluding pretreatments and studies related to regulated phenomena or toxicity, and (b) the coexistence of other cells in the choroidal tissue that may contribute to protein/polypeptide synthesis and secretion.

For these reasons, establishing in vitro cellular models of the BCSFB, retaining the differentiated phenotype of the choroidal epithelium, became a challenge a few decades ago. With the advent of refined culture methods and availability of permeable membranes, cultured monolayers of CPE cells have now become an appropriate tool to demonstrate transcellular transport and vectorial secretion by the BCSFB. Recently, immortalized cell lines have been generated to overcome the time-consuming aspect inherent to primary culture in general, and the difficulty to carry on certain studies such as long-term toxicity studies.

Our aim in this chapter is to provide useful information to help investigators to set up and characterize their own CPE cell culture system on bicameral devices. For that purpose, we will discuss the factors that are critical to isolate the cells and select the culture conditions, and describe primordial specific choroidal features that can be examined within a validation scheme, emphasizing the need for a careful interpretation of their significance. A survey of available cell lines, with their advantages and limitations, will also be provided. Finally, selected studies performed with these models will be presented, highlighting the potential usefulness of such models in the field of neurotoxicology.

2. Methods

2.1. Establishment of Choroidal Epithelial Cells in Primary Culture

2.1.1. Animals and CP Isolation

Primary cultures of CPE cells can be established from various animal species. The care paid to CP dissection will influence the degree of purity of the cell monolayer, and this step should be performed using stereotaxic microscope, in particular for small animals such as rodents. CP from bovine pig and sheep species can also be used to obtain primary cultures of CPE cells.

2.1.2. Cell Isolation, Seeding and Culture Conditions

2.1.2.1. Cell Dissociation Techniques

CPE cells are closely associated in vivo by junctional complexes, and a general observation in CPE cell culture is that these cells survive better as clusters, which calls for a rather mild dissociation technique. Various dissociation conditions have been compared (e.g., (7)), and pronase (at a concentration of 0.5–1 mg/mL), showing better performance over collagenase, dispase, or collagenase/dispase on the basis of cell viability and plating efficiency, has been widely used (8–14). We and others found that further dissociation of the large cell clumps by trypsin digestion was useful for homogeneous subsequent plating of rat CPE cells (10–12, 15). An alternative to pronase digestion is the use of trypsin alone (at a concentration of 0.25%) (16–18). DNAse I is classically added to the dissociating enzymes, to digest the genomic DNA released from damaged cells. This prevents an increase in viscosity of the cellular suspension that would interfere with the tissue disaggregation. Owing to their cluster organization, the released epithelial cells can be collected by allowing them to sediment more rapidly through the more dispersed stromal cells, but the accurate determination of the number of cells in the suspension is thereby impeded. The seeding density is therefore better adjusted on the basis of the initial weight or number of CPs.

2.1.2.2. Preparation of Permeable Culture Membranes

Permeable membranes may be selected from a large panel of inserts, available from various manufacturers, made of different materials and offering variable porosities. The choice of the insert

depends on the application (Note 1). Permeable inserts should be coated beforehand, and the nature of the matrix component has been shown to considerably influence the attachment, growth and purity of the cultured cells. A number of investigations have designated laminin as the most appropriate matrix component for culturing CPE cells. Rat choroidal cells would also attach efficiently on inserts coated with rat tail collagen (12). However, collagen promotes the adhesion and growth of the fibroblasts present in the cell suspension, thus impairing the purity of the cultures. By favoring the adhesion and proliferation of epithelial cells over that of fibroblast-like cells, laminin permits the formation of rat CPE cell monolayers with a good purity on permeable membranes (12, 18, 19).

2.1.2.3. Culture Medium

While CPE cells are customarily grown in DMEM or a mix of DMEM and Ham's F-12, an important variability in the culture supplements is noticeable among the different in vitro models. Various combinations of the following growth factors, hormones and culture additives, i.e., hydrocortisone, insulin, selenite, epidermal growth factor, basic fibroblast growth factor, prostaglandin E1, triiodothyronine, hypoxanthine, forskolin and progesterone have been applied to CPE cell cultures. In the absence of a detailed investigation of the influence of each of these compounds taken alone or in combination, it is difficult at present to delineate the exact contribution of individual supplements to the cultured cell characteristics.

By contrast, it is a general agreement that addition of serum to the medium is a prerequisite for efficient adhesion of the CPE cells on the culture membranes. At the time of seeding, and thereafter during proliferation, fetal bovine serum is classically used at a 10% concentration. Calf serum may not always allow attachment, as reported by Tsutsumi et al. (15) for rat cells, in contrast to results from other investigators who used it successfully (20). Removal of serum after 3–4 days can be applied without affecting epithelial cell characteristics of confluent and differentiated rat CPE cell monolayers for specific studies such as protein secretion analysis, or to prepare conditioned medium (14, 21, 22). By contrast to CPE cell cultures in other species, serum withdrawal on porcine CPE cell cultures appears necessary for a complete morphological and functional differentiation (active transport processes) of the cells (23, 24).

2.1.3. Means to Achieve Pure Epithelial Cell Cultures

A recurrent problem encountered in epithelial cell culture in general arises from the contaminating stromal cells, in particular fibroblasts, as the latter usually proliferate more rapidly in serum-supplemented medium, and tend to overgrow the epithelial cells. Methods to overcome or limit fibroblast contamination may have a limited success when used separately, but can be of value when combined. The following approaches have been found efficient for CPE cells.

2.1.3.1. Differential Attachment

This approach takes advantage of the more or less developed tendency that various cell types display to adhere on a given support. It can be first applied to enrich the cell suspension in epithelial cells, by promoting the adhesion of stromal elements. Fibroblasts, and to a greater extent macrophages, attach rapidly onto plastic within the first couple of hours, while epithelial cells remain in suspension and are easily recovered for further plating on the appropriate substrate. This technique has proved very useful for CPE cells, in particular for rat cells (11–13, 17, 18, 25). This principle of selective attachment is also exploited when permeable filters are coated with laminin that favors the adhesion of CPE cells as mentioned above. These rather simple steps proved sufficient to prevent fibroblast contamination for several groups, while others have found it necessary to associate them with selective culture techniques.

2.1.3.2. Selective Culture

D-Valine selective culture media, based on substitution of L-valine for the D-isomer, was shown to selectively inhibit human and rodent fibroblast proliferation (26). This effect is based upon the lack in fibroblast cells of D-amino acid oxidase activity, which in other cell types such as epithelial cells, can convert the D-amino acid into its essential L-isomer. It is important to note that using this technique requires to dialyze the serum or to omit it from the culture media, because the serum contains endogenous L-valine that negates the advantage of D-valine selective media. D-valine strongly impedes the overgrowth of the CPE cell cultures initiated from rat tissue by fibroblasts (13, 27–29). However, the effect of D-valine selective medium did not prove to be reproducible when used in bovine CPE cell cultures by Crook et al. (7).

Instead, this group observed on the same bovine cultures a more reliable effect of cis-4-hydroxy-L-proline (cis-OH-proline), a growth inhibitor which, by decreasing the production of extracellular collagen (30), limits the rate of fibroblast proliferation. Cis-OH-proline is also active in rodent cultures (14), but whichever the animal species, this inhibitor also affects the epithelial cells to some extent. Both cis-OH-proline concentration and time of addition need thus to be tested in each cell culture protocol to achieve an optimal efficiency and selectivity toward fibroblasts (7, 14).

Supplementation of the media with 20 μM cytosine arabinoside (Ara-C), a S phase-specific blocking agent, appears as the method of choice to achieve purity of porcine CPE cells (16, 31). The specificity of the compound toward fibroblasts remains unclear, as, at least in rabbit, Ara-C is taken up by isolated CPs via a saturable facilitating carrier, and is phosphorylated (32), suggesting that the active metabolite is indeed synthesized within the CPE cells. However, by treating the cells with 20 μM Ara-C for the first 5 days of culture, Gath et al. reported a complete inhibition

of all contaminating cells, without affecting the growth of epithelial cells. It is possible that nucleoside transporters in these cells differ from those of the rabbit, or are rapidly down-regulated in culture.

2.1.4. Life Span and Subculture

Another consensus has emerged from the various attempts to culture CPE cells, in that these cells passage poorly. Subculturing rodent choroidal cells induces a loss of differentiated functions or a rapid cell death ((14, 33), personal observation). Furthermore, subculture results in progressive fibroblast enrichment (7). As a consequence, CPE cells are used mostly as primary cultures proper, with the exception of porcine cells which appear to be subcultured once at the time of seeding on permeable membranes (34). The cells grown as monolayers on permeable filters have a life span varying between 1 and 2 weeks, during which differentiated functions are retained. Thereafter, dedifferentiation is expected to occur as illustrated by the decrease in Na^+-dependent taurine transport observed in 30-day-old cultures of rabbit CPE cells (35).

2.2. Available Choroidal Epithelial Cell Lines

Either spontaneous or laboratory-engineered cell lines originating from CP are available.

The s-called "SCP" (sheep CP) cells which are widely cultured in virology laboratories to support the propagation of Maedi-visna virus strains, cannot be used to develop BCSFB models as they display a fibroblastic appearance and are likely to be of mesenchymal rather than epithelial origin.

The American Type Culture Collection (ATCC) offers a cell line also designated SCP (CRL 1700), prepared from brain CP of *Ovis aries* and susceptible to visna virus, strain 1514. These cells may be of choroidal epithelial origin as they express mRNAs for transthyretin (TTR) and IGF-II (36). The ATCC SCP cell line might represent a potential tool, at least for the study of certain neuroendocrine functions of the CP, or some aspects of the regulation of CSF secretion (37–40), but the establishment of junctional complexes and diffusion barrier properties necessary to the set-up of a BCSFB model remains undetermined.

Other cell lines were generated from human CP carcinoma or papilloma. The HIBSPP cell line derived from a CP papilloma (resected from a 29-year-old female patient) and forms heterogeneous multilayers without cell contact inhibition (41), and therefore appears as an unlikely in vitro model of the BCSFB. By contrast, other cells derived from a fragment of a fourth-ventricle CP papilloma (resected from a 28-year-old male patient) were shown to form on plastic a monolayer with a pavement-like appearance (42), and displayed ultrastructural features similar to those of the papilloma epithelial cells, retaining in particular microvilli, cilia and interdigitations. A CP carcinoma cell line,

CPC-2, was established from the resected tumor of a 2-month-old boy. It produces adrenomedullin, a potent vasodilatator peptide shown by immunocytochemistry to localize in human CP (43). As for the ATCC cell line, whether these two latter spontaneous cell lines grown on bicameral devices will adopt a tight phenotype remains unknown. While mRNAs for tight and adherens junction proteins were detected in CPC-2 cells, the proteins themselves were either not detected or mislocated (44), suggesting that these cells may not form an impermeable monolayer.

Several laboratories have engineered immortalized cell lines from transgenic animals. In transgenic mice harboring the viral SV40 large T oncogene under the transcriptional control of an intronic enhancer region from the human immunoglobulin heavy chain gene, the oncogene expression was restricted to the lymphocytes and unexpectedly to the CP. ECPC-3 and ECPC-4 are two morphologically distinct cell lines cloned from cultures of the resected CP carcinoma that developed in these mice (45, 46). These cells proliferate with a doubling time of 7–9 h, and displayed a good stability in culture over a 1-year period. The SV11 mouse CP cell lines have also been prepared from transgenic mice engineered to express SV40 T antigen in the CP (47).

Five rat CPE cell lines, TR-CSFB 1–5, were produced from a transgenic rat harboring a temperature-sensitive mutant of the SV40 large T antigen, expressed ubiquitously under the control of its own promoter (48). At the permissive temperature of 33°C, the TR-CSFB cell lines grow with a doubling time of 35–40 h and contact inhibition is observed after 7 days. Finally, a cell line called Z310 has been produced by immortalization of rat CPE cells in primary culture using both SV40 small and large tumor (T) antigens, followed by a cytotoxic selection (49). It grows with a doubling time of 20–22 h and up to the 110th subculture, did not display variability in TTR expression or in its growth rate. The RCP cell line generated using a very similar strategy, i.e., primary cultures of rat CPE cells transduced with the TSOri minus adenovirus harboring the SV40 large T antigen (50) cannot be used to establish a BCSFB model as it actually shows endothelial characteristics.

The SV11 lines have not been characterized with respect to their choroidal differentiation status. The ECPC, Z310, and TR-CSFB cell lines have been shown to display at least some specific properties indicative of their epithelial origin, and to retain some differentiated features of the CP epithelium (45, 48, 49, 51). However, they apparently do not maintain to a high degree the structural diffusion properties that would be mandatory in order to study transepithelial transport processes and polarized phenomena. Several tight and adherens junction proteins are missing or weakly expressed in TR-CSFB3 and Z310 cells (44). When cultured on permeable filters, TR-CSFB cells do not allow

reliable transcellular studies as stated by the authors (52), and the paracellular diffusion barrier formed by Z310 cells is poor as compared to that of rat or pig CPE cells in primary culture (reviewed in (24)).

2.3. Characterization of the Cellular Models of the Blood–CSF Barrier

Evaluating the extent to which the cultured CPE cells retain their epithelial phenotype and the differentiated functions, they exert in vivo in the choroidal tissue, is a prerequisite for their use as in vitro models of the BCSFB. We list and discuss below the main criteria which have been used by different groups and proved useful as validation markers for such models.

2.3.1. General Morphology, Ultrastructure and Epithelial Phenotype

The morphology and the structural organization of cells in culture assessed by light and electron microscopy are good indices of their epithelial nature. Following adhesion to the membrane and proliferation, clumps of epithelial cells should consistently give rise to monolayers with a classical tight pavement-like appearance, which can be easily distinguished from the elongated fibroblasts that grow in the absence of appropriate inhibitors or on inadequate substratum (12).

Ultrastructure studies by transmission electron microscopy can confirm the single layer structure and several features characterizing the choroidal epithelium in vivo and indicative of cell polarity can be assessed, among which (a) junctional complexes located near the apical end of the lateral membrane domains, (b) complex invaginations of the basolateral membrane creating large intercellular lateral spaces, and (c) an apical membrane domain bearing microvilli and occasionally cilia. The number of microvilli displayed by the cells in vitro varies among the models, but never appears to thoroughly match the abundance of this structure in vivo (12, 13, 16–18).

Other cell types at high density may present a cobblestone epithelial-like pattern. Therefore, the phenotype of the cultured cells should also be assessed with epithelial markers, the most frequently used in general culture of epithelial cells being the epithelial-specific cytoskeletal intermediate filaments, namely the cytokeratins. The use of pan-cytokeratin antibodies, which recognize epitopes of many cytokeratins are appropriate for that purpose. Of note, there is a switch in intermediate filament expression in rodent CP epithelium around birth, from a vimentin positivity during fetal life, that is abolished by the 4th postnatal day, to a cytokeratin positivity that first appears in some cells at embryonic day 18 and extends to most cells by the 4th postnatal day (53). When using CP from developing animals, immunostaining with pan-cytokeratin antibodies reveals cell-to-cell variation in staining intensity (12), which likely reflects the more or less advanced stage of individual cells in this intermediate filament switch process. Immunostaining of desmosomal proteins can also be used to

identify desmosomal junctions that are specific to epithelial cells at confluence (discrete spots found only at the cell boundaries of cultured cells (16)).

Exclusive markers to test for the possible presence of contaminating cells are also useful to assess the purity of the epithelial cells in culture. Vimentin, constituting the specific mesenchymal intermediate filament, is an appropriate marker for fibroblasts when coupled to the morphology analysis showing the typically elongated morphology of the positive cells. Endothelial cells, also displaying an elongated shape, can be searched by indocarboxythionine-conjugated acetylated low-density lipoprotein staining, or immunoreactivity of factor VIII-associated antigen or of MESA-1 (mouse endothelial surface antigen-1) (7, 9, 54). Stromal myeloid cells are unlikely to be contaminating cells, particularly when differential attachment on plastic is included in the cell preparation protocol, as they will adhere very rapidly to the membrane. Furthermore, culture conditions selected to favor CPE cells do not support their in vitro proliferation. Phenotypic markers can be used to detect these cells in culture by immunostaining (55).

2.3.2. Assessing the Choroidal Differentiation

The degree of choroidal differentiation achieved in vitro by the CPE cells needs to be defined by analyzing tissue-specific features.

TTR is considered a highly specialized feature of CPs. It is a carrier protein for thyroid hormones in biological fluids which is not synthesized in mammalian brain parenchyma, but is produced by the choroidal epithelium and secreted almost exclusively into the CSF, at least in adult mammals (56, 57). TTR mRNA is expressed early during development (58). TTR mRNAs or immunoreactive protein can be used therefore as an index of cell differentiation in various models of the BCSFB. The secretion of TTR in the medium can be analyzed by immunoprecipitation, but the in vivo polarity of TTR secretion is apparently not maintained in vitro, even in models in which polarity of secretion was demonstrated for other proteins (18).

Na^+, K^+-ATPase plays a major role in the highly differentiated function of the CP epithelium that is CSF production, as well as in secretory and absorptive processes. This pump displays a specific apical distribution in the CP epithelium, which contrasts with other epithelia in which it is found on the basolateral membrane. The apical distribution of the pump can be assessed by ultrastructural immunochemistry or fluorescent immunocytochemistry to evaluate the degree of choroidal differentiation and also of polarization of CPE cells in culture (13, 16, 54).

Drug metabolizing enzymes and transporters are also differentiation markers of interest. CPs have a high, liver-like, capacity for drug metabolism, involving hydrolysis, reduction or conjugation enzymes.

Preservation of microsomal epoxide hydrolase, 1-naphtol-UDP-glucuronosyl transferase, or chloro-dinitro-benzene glutathione-*S*-transferase enzymatic activities at levels comparable to those determined in the initial choroidal tissue can be assessed as an index of choroidal differentiation. Protocols for enzymatic measurements are available in (12, 59). Among drug transporters, MRP1 (ABCC1) has been shown to be highly expressed in the CP in comparison to the cerebral capillaries forming the blood–brain barrier or to the neuropil, and is restricted to the basolateral membrane of the choroidal epithelium (60). Therefore, it also represents a good marker of both cell differentiation and polarization which can be assessed by Western blot and immunocytochemistry, respectively.

Other less specific differentiation markers have been used, such as insulin-like growth factor-II (IGF-II) and insulin-like growth factor binding protein-2, which are widely expressed in the whole brain during development but become more CP-specific in the adult brain (8), or else transferrin, a carrier protein involved in iron transport and synthesized at high levels and secreted by the rat CP epithelium (15). However, the latter cannot be used for all species as transferrin mRNA was not detected in pig, sheep, cow or human CPs (61).

2.3.3. Monitoring the Diffusion Barrier Properties

CP epithelium function as a diffusion barrier toward electrolytes, polar organic compounds and macromolecules requires apically located TJ (*Zonula occludens* (ZO)), which seal the paracellular pathway between apposing membranes of adjacent cells. Analyzing the diffusion barrier properties of CPE cells cultured in bicameral devices can be approached structurally by investigating the reconstitution of TJs, and functionally by measuring the transepithelial resistance and the flux of inert paracellular markers.

2.3.3.1. Structural Investigations

The investigation of the molecular composition of choroidal epithelial TJs, that was conducted mostly in rats, mice and pigs, indicates that occludin, claudin 1, claudin 2, claudin 3 and possibly claudin 11, are integral constituents of TJ strands (16, 62, 63). The different claudin species associate in an heterotypic manner within individual strands, but can interact as hetero- or homodimers between adjacent strands, and the combination and mixing ratios of claudin species appear to be important factors that determine the tightness of individual strands and their ion selectivity (64, 65). Like in other epithelia, these transmembrane proteins interact with the cytoskeleton protein actin, through cytoplasmic TJ-associated proteins such as the ZO proteins. Another integral membrane protein with a single spanning domain, JAM, also localizes at TJs. The distribution of these TJ components, assessed by immunocytochemistry in confluent CPE cells cultured on permeable membranes for 7 days, should present a continuous honey

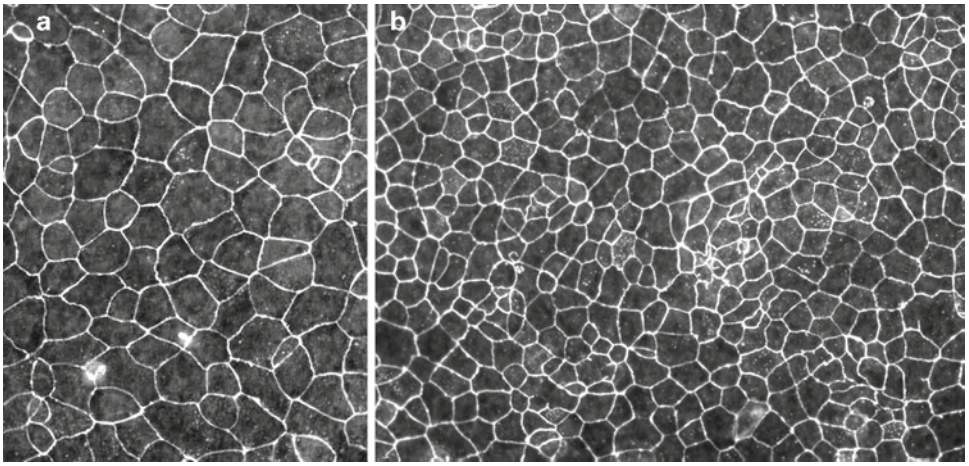

Fig. 2. Immunocytochemical localization of tight junction-associated proteins in a rat choroidal epithelial cell monolayer. Cells were cultured for 7 days on microporous filters. The images obtained by conventional fluorescent microscopy illustrate the continuous, circumferential distribution of claudin 1 (**a**, high magnification, Zymed 51-9000 antibody), and claudin 2 (**b**, low magnification, Zymed 51-6100 antibody). The allover staining of the epithelial apposing membranes is an index of the cellular barrier integrity (Note 2).

comb-shaped immunoreactivity pattern, comparable to in vivo (e.g., Fig. 2, and (66)). Components of TJ strands such as claudins are better markers of TJ integrity and continuity than is ZO1 or actin (Note 2). Freeze-fracture and electron microscopy techniques also are interesting approaches to study TJs in CPE cell culture, but are more time-consuming and difficult to interpret, and do not provide an overall picture of the TJ network throughout the monolayer.

2.3.3.2. Functional Investigations

While the expression and continuous pericellular distribution of TJ proteins in cultured CPE cells are prerequisite to the existence of a diffusion barrier, the efficacy of the latter needs be assessed further by functional studies. This obviously implies the use of permeable filters, and is classically achieved by evaluating the transepithelial electrical resistance (TEER) or the flux of inert paracellular markers across the cell monolayer, both of which should ideally be comparable to values measured in vivo when available. It is worth mentioning that these two parameters are not equivalent. TEER reflects the passive conductance of the TJ to small inorganic electrolytes, and the paracellular flux represents the permeability of the cells to lipid insoluble organic compounds with much higher molecular weights. They are neither strictly correlated, nor do they always vary concomitantly in response to cell treatment.

A first criterion reflecting the tightness of the monolayer is the ability of the cells to establish a hydrodynamic barrier, i.e., to

maintain unbalanced medium levels in the upper and lower compartment over a 48-h period, which is readily assessed visually.

The measurement of the TEER of cell monolayers grown on permeable filters, using alternative current techniques, has become a nondestructive routine method to monitor the growth of cell cultures. TEER measurements on CPE cell monolayers has been performed by impedance spectroscopy (16), or more often with commercially available resistance meter instruments, i.e., the Millicell-ERS™ or EVOM™ equipped with chopstick electrodes, which are widely used for their convenience. The more recent Endohm™ chambers, which provide a more uniform current and an improved accuracy, may be preferred to the chopstick device. The resistance should be measured in parallel on blank filters (coated with matrix, but without cells), and subtracted from the resistance value of the cell-covered filters in order to determine the resistance of the cell monolayer proper (Note 3).

For technical reasons, in vivo TEER values for the choroidal epithelium are scarce. They have been determined mostly on amphibian or elasmobranch posterior CPs, but also in cats, and range from 100 to 200 Ωcm^2 (67–69), thus designating the CP epithelium as a "leaky" epithelium in contrast with "tight" epithelia such as the urinary bladder epithelium which displays values of 1,200–2,000 Ωcm^2 (70). TEER values reported for CPE cells cultured in serum-containing medium reach 100–200 Ωcm^2, whichever the animal species from which the CP tissue originated (11, 12, 14, 16–18).

Small polar inert compounds such as radiolabeled mannitol (MW 182 Da), sucrose (MW 342 Da), polyethylene glycol (MW ~4,000 Da), inulin (MW ~5,000 Da), or fluorescent dextrans (with a large range of MWs) are useful markers of the paracellular pathway. They can be used to (1) monitor the time-dependent establishment of barrier properties of CPE cells cultured on permeable membranes, (2) provide a quality index of the BCSFB model, and assess the reproducibility of successive cell preparations, (3) estimate, in drug transport studies, the relative contribution of the paracellular vs. transcellular pathways to the overall permeability of a compound of interest (providing the paracellular marker is chosen appropriately to match the size of the latter), and (4) monitor possible adverse effects generated upon addition of potentially toxic molecules on the epithelial monolayer.

The transfer of paracellular markers can be measured indifferently in the CSF-to-blood direction, or in the blood-to-CSF direction. The marker is added in the donor compartment and its appearance in the acceptor compartment is monitored on a time-dependent multi-sampling scheme. Flux measurements on both filters with cells and blank filters (without cells) allow to generate permeability coefficients (Pe) for the epithelial monolayer proper

(Note 4). In vivo transchoroidal permeability coefficients for a number of solutes of different molecular weights have been determined in rabbit by Welch and Sadler (71), and were in 10^{-3} cm min^{-1}, 0.324 ± 0.084, 0.219 ± 0.060 and 0.102 ± 0.042 for the paracellular markers mannitol, sucrose and inulin, respectively. Typical Pe values obtained for sucrose with in vitro models of the BCSFB should be in the range of $0.1–0.3 \times 10^{-3}$ cm min^{-1} (e.g., (11, 66)), and the interpretation of transport and polarity studies performed on cell monolayers with a sucrose Pe higher than 0.6×10^{-3} cm min^{-1} is difficult and hazardous.

The paracellular permeability of cell monolayers grown on polycarbonate filters (known to promote higher cell-substrate resistance, see (72)) may be slightly lower than on other membranes, as cell-substrate contact space can influence to some extent the flux of paracellular tracers across cell-covered filters.

2.3.4. Functional Index of Cell Transport Polarity

Active transport of organic anions such as phenol red (PR, phenolsulfonphtalein, present in culture media as a pH indicator) from the CSF to the blood through the CP was demonstrated by Papenheimer, using a sophisticated technique of ventriculocisternal perfusion in goats (73). It represents a useful functional index of the unidirectional transport capacity of the choroidal epithelium in vitro. The accumulation of PR present in the culture medium, uphill its building concentration gradient, from the apical into the basolateral chamber of the cell culture bicameral device across CPE cell monolayers can be measured by spectrophotometric analysis of the media (6, 22). Based on data generated using well-differentiated porcine and rat in vitro BCSFB models, with an initial PR concentration of ~20 μM (corresponding to the PR concentration in a basic DMEM/F12 1/1 medium), the initial clearance rate (Note 5) should reach 20 and 30 μL cm^{-2} h^{-1} for serum-fed and serum-starved cells, respectively, the difference between the two conditions being accounted for by the binding of PR to serum proteins (24).

2.3.5. Other Choroidal Functions

The validation scheme of a newly developed in vitro BCSFB model will also include parameters more specifically related to the application envisioned for the model. For example for transport studies, whenever possible, the expression and localization of relevant carrier proteins will be analyzed in comparison to the choroidal epithelium in situ. This type of approach, aiming at characterizing the cultured cells and verifying that they retain the specific properties of the in vivo BCSFB, is extendable to receptors, enzymes, secreted proteins or polypeptides, adhesion molecules, etc. Additional validation criteria should be chosen accordingly to one's personal experimental goal.

3. Applications of In Vitro Models of the Blood–CSF Barrier for Neurotoxicological Studies

The BCSFB cellular models have already proven useful for a better understanding of various CP functions related to choroidal protein secretion, transport and enzymatic activities, or else receptor-mediated signaling/regulation mechanisms at the CPE cells. The examples given below aim at illustrating the potential contribution of these models to the advancement of neurotoxicological sciences.

3.1. Evaluation of Influx/Efflux of Drugs and Neurotoxins Across the Blood–CSF Barrier

Influx into the CNS and efflux from the CSF across the BCSFB are important factors to consider when determining brain susceptibility to potentially neurotoxic or pharmacologic molecules. Functional BCSFB cellular models obtained by cultivating cells in a bicameral device allow to generate true transcellular transfer measurement data and vectorial information, and, also to study nonradioactive compounds, as culture medium can be easily analyzed by HPLC or by other analytical procedures. Furthermore, by opposition to studies conducted in transfected cell systems which generally overexpress one particular transporter, the relative contribution of the different native coexisting choroidal transport proteins to the permeability of a given compound can be approached. Such models have been used to study transport mechanisms of molecules belonging to several chemical families.

Peptide transporter substrates. The implication of the peptide transporter PEPT2 in vectorial CSF-to-blood transfer has been revealed by transcellular transfer measurements of the model dipeptide substrate glycylsarcosine (GlySar), across rat CPE cell cultures. The results showed a clear vectorial transport in favor of the apical to basolateral direction. Affinity constant determination showed that the apical uptake of GlySar was characterized by a higher affinity than that of the basolateral uptake (11). PEPT2, present at the apical membrane of the choroidal epithelium, is known to accept as another substrate 5-aminolevulinic acid (ALA), a precursor of porphyrins and heme involved in neuropsychiatric symptoms caused by hereditary porphyrias. Uptake experiments on rat CPE cells cultured on porous filters showed a much greater ALA saturable uptake at the apical vs. the basolateral membrane (74). This suggested that an apical transport, possibly mediated by PEPT2, keeps ALA concentration in the CSF to a low level. Overall, the data indicated the potential role of choroidal PEPT2, not only in endogenous peptide removal from CSF, but also in the biodisposition of the peptidomimetic drugs sharing an affinity for the transport system.

Nucleoside transporter substrates. Using a sheep cellular model of the BCSFB, Redzic et al. (75) showed that adenosine transport across the epithelial monolayer was significantly impaired by both

intracellular phosphorylation and metabolic degradation pathways. Uptake studies realized separately at the apical or basolateral side of the monolayer indicated that nucleoside transporters are unevenly distributed between the two membranes. Hypoxanthine, the main metabolic degradation product of purine, was also transported from the CSF side, and in part could enter the nucleotide salvage pathway within the epithelial cells (76).

Anti-infectious drugs. In aids treatment, targeting the CSF itself is important to allow the antiretroviral drugs to reach the ventricular, meningeal and perivascular macrophages which are the main infected and replicative cells in the brain. Using an in vitro cellular model of the BCSFB coupled to HPLC analysis, a classification based on the relative ability of clinically used antiretroviral nucleoside analogs such as azidothymidine, to distribute into the CSF through the choroidal epithelium, was produced (66). This study also confirmed that azidothymidine influx was independent from thymidine transporters. Most compounds tested had an apical to basolateral efflux rate higher than the basolateral to apical influx rate. This efflux was shown to be governed by an apical transport system belonging to the solute carrier Slc22 (organic anion transporter OAT) subfamily, and could be reversed by therapeutic concentrations of uricosuric compounds (66). These data on nucleoside analogs illustrate the usefulness of in vitro BCSFB models in screening compounds for their ability to reach the CSF, and in testing strategies which aim at increasing or decreasing drug entry into the CSF.

An elegant way to distinguish an unidirectional, active transport process from simple diffusion across cell membranes or from a facilitated (equilibrative) transport is to add the compound of interest at the same concentration to both sides of CPE cells cultured on porous filters. The appearance of an imbalance in the concentration between both compartments over time will indicate the involvement of an active transport system. Hakvoort et al. (77) used this approach with porcine CPE cells to demonstrate that the antibiotic drug benzylpenicillin undergoes vectorial active transport. The transepithelial active transport was in the apical to basolateral direction. The kinetic analysis revealed affinity constants which were close to those measured in isolated CPs.

As a general advice, during or immediately following unidirectional flux measurements and imbalanced concentration measurements, the tightness of the monolayer needs to be ascertained with paracellular markers (especially when very high doses of substrates are used for kinetic analysis purposes), as the back diffusion via an augmented paracellular pathway would counteract active transport systems which work uphill a concentration gradient, or an increased paracellular diffusion may mask a decrease in active transport measured downhill the concentration gradient.

Immortalized cell line-based transport investigations. The characteristics of choroidal uptake of estrone-3-sulfate, a metabolite formed within the brain, have been investigated in the immortalized cells TR-CSFB (51). The results were fairly consistent with known data generated using isolated CPs and implicated both Slc21A5 (oatp2) and Slc21A7 (oatp3) in the uptake process. This indicates that the cell line may be a practical, easy-to-use tool to investigate uptake at the CP. However, vectorial information could not be drawn from this uptake-based approach as Slc21A7and Slc21A5 are differently distributed, i.e., on the apical and basolateral membranes, respectively, in the choroidal epithelium in situ.

3.2. Understanding Neuroprotective Mechanisms Associated with the BCSFB

In addition to their drug efflux transport properties, the CPs have a high capacity to metabolize xenobiotic compounds, especially through conjugation pathways. The ability of the choroidal epithelium to act as an enzymatic barrier preventing lipophilic compounds to reach the CSF has been addressed using an in vitro rat BCSFB model and performing HPLC analysis of the media. The cells efficiently prevented the entry of phenolic compounds into the CSF compartment by conjugating these xenobiotics via a UDP-glucuronosyltransferase-dependent pathway (12). The CPE cells could also prevent 1-chloro-2,4-dinitrobenzene, a model molecule for electrophilic toxic compounds, from reaching the CSF compartment by enzymatically conjugating this toxic agent with reduced glutathione (59). Furthermore, a strong basolateral, i.e., blood-facing polarity of the efflux of both the glucurono- and glutathione-conjugates was demonstrated. The involvement of the multidrug-resistant protein MRP1 (ABCC1), present at the basolateral membrane of the CPE cells, or other members of the MRP family, was suggested by efflux inhibition studies (12, 59). These data demonstrate an efficient neuroprotective function of the choroidal epithelium, through coupled metabolic and transport processes, and further indicate that the in vitro cellular model of the BCSFB is an adequate tool to evaluate strategies reinforcing the neuroprotective antioxidant capacities of the choroidal epithelium (59).

3.3. Alteration of Blood–CSF Barrier Functions by Toxic Compounds

Effect of lead on TTR regulation. Exposure of the organism to lead (Pb) results in the accumulation of this metal in the CP, and also in a decrease in TTR concentration in the CSF. Using rat CPE cells cultivated onto permeable filters, Southwell et al. (18) showed that the extent of transfer of the thyroid hormone T4 from the blood side to the brain side was influenced by choroidal TTR synthesis and secretion in the CSF. The effect of Pb on TTR synthesis and secretion, as well as on T4 partitioning across the epithelial monolayer was investigated using rat CPE cells in culture (78). The authors demonstrated that Pb exposure induces a

decrease in the secretion of TTR from cells grown on solid supports, and observed in parallel a reduction in the CSF-favoring polarity of T4 partition across the cells cultured in a bicameral device. These results provide a link between Pb accumulation in CPs during Pb intoxication and the decrease in CSF-borne TTR, and hint at a possible T4-related mechanism to explain mental retardation observed in children exposed to this metal.

Effect of cytokine exposure on organic anion efflux. The PR active clearance index (see above) was used in a rat CPE cell model to demonstrate that active, vectorial apical-to-basolateral organic anion transport capacity of the BCSFB is impaired in inflammatory conditions (22), thus indicating that some of the neuroprotective properties of the CP can be altered in pathological situations.

3.4. Involvement of the Blood–CSF Barrier in Neuroinflammation

Most neurotoxic insults initiate an inflammatory reaction, and the CPs which are rapidly activated when exposed to pro-inflammatory mediators, can participate in the propagation of this process. In vitro BCSFB models have been used to decipher these mechanisms.

Matrix metalloproteases. These enzymes, referred to as MMPs, catalyze the proteolytic cleavage of basal lamina components, and thus are involved in extracellular matrix remodeling and in cellular migration. They also participate to the maturation by cleavage of various membrane receptors and ligands. A dysregulation of the balance between MMPs and their endogenous inhibitors appears to play an important role in the pathophysiology of neuroinflammation. The basal secretions of MMP-2 and MMP-9 by CPs can be reproduced in rat CPE cells cultured on bicameral devices (22). A strong up-regulation and a polarization of MMP secretion, especially of MMP-9, were induced upon exposure of the cultured cells to pro-inflammatory cytokines. These data show that the CP can contribute at least partially to the increased levels of MMP-9 observed in the CSF in both neuroinflammatory diseases in human and in experimental neuroinflammation. Basolaterally secreted MMPs may play a role in the invasion of immune cells that accompanies these pathologies.

Adhesion molecules and chemokines. The induction of cellular adhesion molecules such as ICAM-1, VCAM-1, or MadCAM-1 was investigated on mouse CPE cells cultured on solid supports. Their expression was increased in some of the epithelial cells following treatment for up to 16 h with pro-inflammatory molecules such as TNFα, IL-1β, IFNγ, or a lipopolysaccharide preparation (79). In a rat BCSFB model set up on a bicameral device, the up-regulation and polarity of secretion of the chemokine Cinc-1, involved in neutrophile recruitment, was shown to be dependent on the concentration in the medium of IL-1β (5).

These examples illustrate various areas of the current research in neurotoxicology that can benefit from the in vitro BCSFB

technology. The role of the BCSFB in controlling the cerebral bioavailability of toxic molecules can be evaluated in differentiated cultures of the choroidal epithelium with regard to the contribution of influx, efflux mechanisms as well as metabolic detoxification processes. Furthermore, deleterious effects caused by a given toxic insult on the barrier per se can be investigated using these cellular models. The impact of acute and to a certain extent chronic toxicological exposure may be assessed owing to the availability of both primary cultures and cell lines, although applications of the latter are dependent on their degree of differentiation and are currently limited by their higher rate of paracellular diffusion.

4. Notes

1. The microporous membrane of the insert and the extracellular matrix components (laminin, ±collagen) coated to favor attachment of CPE cells, may lead to the nonspecific absorption and the retention of some compounds. Different devices can be tested among which the transparent polyester or translucent polycarbonate Transwell inserts (Costar), the polyethylene terephtalate (PET) transparent low pore density or the PET translucent high pore density membranes (Falcon). Inserts are also available from Millipore and Nunc. However, in our hands, CPE cells from newborn rats did not attach to laminin-coated inserts from Millipore, and we have not tested inserts from Nunc. Laminin-coated inserts from Costar and Falcon yield similar results in terms of cell attachment, cell differentiation and transport properties. The use of collagen precoated Transwell-COL™ membranes (Costar) did not improve any of those criteria, even when treated with laminin. By providing a good cell visibility under phase contrast microscopy, transparent membranes advantageously allow to follow cell growth and to assess the formation of monolayers.

   The 0.4 μm porosity is well suited to study transfer of solutes as such pores will allow free diffusion of chemicals or even proteins across the filter. In theory, restricted diffusion will not occur if the pore diameter is greater than 20 times the effective diameter of the solute (80). As an example, for a medium size protein such as albumin (MW 700,000 Da), this effective diameter is about 6 nm.

2. With regard to fluorescent immunocytochemistry on CPE cell monolayers, the use of a confocal microscope should be preferred as it allows, through image stacking, to correct unfocussed labeling due to the undulation of the cell-covered membranes often seen following fixation, and to avoid the background due to the autofluorescence of the membranes.

This is particularly crucial for TJ protein localization studies to assess the allover staining of the monolayer.

3. The electrical resistance is inversely proportional to the surface area covered by the cells. The latter is taken into account by calculating a resistance × surface area product, in Ω cm^2 (and not a resistance to surface area ratio, in Ω cm^{-2} as it may sometimes be reported in the cell culture literature).
4. Experimental conditions for measurement of flux across the in vitro BCSFB and Pe calculation can be found in details in (6). Permeability × surface area (PS) products, in µL min^{-1} filter^{-1}, are generated from the clearance curves obtained for cell-covered filters and filters without cells. From these data, a permeability coefficient Pe can be calculated for the cell monolayer only. Flux data expressed as per cent values of the initial amount in the donor compartment should be avoided. If full information related to the initial tracer concentration, the surface area available for exchange, and the fluid volumes on both sides of the cells at the time of the experiment is not specified, percentages are not fully interpretable and cannot be used to compare in vitro systems or cell preparations. In addition, a number of factors such as agitation (orbital shaker, 200 rpm/min recommended) or fluid balance can influence the permeability measurement and should be standardized. Finally, when the flux of a compound results from an unidirectional active transport, then the resistance to flux of the filter alone becomes rapidly negligible, and reporting data as permeability coefficient Pt for the cell-covered filter is preferred. Details are given in the discussion section of (81).
5. The active unidirectional transport component of PR clearance (in µL) can be calculated using the following equation

$$Cl = [(C_a - C_d) \times V_a \times V_d) / [C_a \times V_a + C_d \times V_d],$$

where C_a and C_d are the differences in optical density measured at 558 nm (maximal absorption of PR in its basic form) and 700 nm for the acceptor and donor medium, respectively, at the time of sampling, and V_a and V_d are the volumes of media in the acceptor and donor compartments, respectively. Sample media are basified by addition of sodium hydroxide to a final concentration of 0.375 M.

Acknowledgements

This work was supported by the European Union (HEALTH-F2-2009-241778).

References

1. Davson H, Segal MB (1996) Physiology of the CSF and the blood–brain barriers. CRC Press, Boca Raton
2. Strazielle N, Ghersi-Egea JF (2000) Choroid plexus in the central nervous system biology and physiopathology. J Neuropathol Exp Neurol 59:561–574
3. Johansson PA, Dziegielewska KM, Liddelow SA, Saunders NR (2008) The blood–CSF barrier explained: when development is not immaturity. Bioessays 30:237–248
4. Charo IF, Ransohoff RM (2006) The many roles of chemokines and chemokine receptors in inflammation. N Engl J Med 354:610–621
5. Szmydynger-Chodobska J, Strazielle N, Zink BJ, Ghersi-Egea JF, Chodobski A (2009) The role of the choroid plexus in neutrophil invasion after traumatic brain injury. J Cereb Blood Flow Metab 27:1503–1516
6. Strazielle N, Preston JE (2003) Transport across the choroid plexuses in vivo and in vitro. Methods Mol Med 89:291–304
7. Crook RB, Kasagami H, Prusiner SB (1981) Culture and characterization of epithelial cells from bovine choroid plexus. J Neurochem 37:845–854
8. Holm NR, Hansen LB, Nilsson C, Gammeltoft S (1994) Gene expression and secretion of insulin-like growth factor-II and insulin-like growth factor binding protein-2 from cultured sheep choroid plexus epithelial cells. Brain Res Mol Brain Res 21:67–74
9. Mayer SE, Sanders-Bush E (1993) Sodium-dependent antiporters in choroid plexus epithelial cultures from rabbit. J Neurochem 60:1308–1316
10. Plotkin MD, Kaplan MR, Peterson LN, Gullans SR, Hebert SC, Delpire E (1997) Expression of the Na(+)-K(+)-2Cl-cotransporter BSC2 in the nervous system. Am J Physiol 272:C173–C183
11. Shu C, Shen H, Teuscher NS, Lorenzi PJ, Keep RF, Smith DE (2002) Role of PEPT2 in peptide/mimetic trafficking at the blood–cerebrospinal fluid barrier: studies in rat choroid plexus epithelial cells in primary culture. J Pharmacol Exp Ther 301:820–829
12. Strazielle N, Ghersi-Egea JF (1999) Demonstration of a coupled metabolism-efflux process at the choroid plexus as a mechanism of brain protection toward xenobiotics. J Neurosci 19:6275–6289
13. Villalobos AR, Parmelee JT, Pritchard JB (1997) Functional characterization of choroid plexus epithelial cells in primary culture. J Pharmacol Exp Ther 282:1109–1116
14. Zheng W, Zhao Q, Graziano JH (1998) Primary culture of choroidal epithelial cells: characterization of an in vitro model of blood–CSF barrier. In Vitro Cell Dev Biol Anim 34:40–45
15. Tsutsumi M, Skinner MK, Sanders-Bush E (1989) Transferrin gene expression and synthesis by cultured choroid plexus epithelial cells. Regulation by serotonin and cyclic adenosine 3′, 5′-monophosphate. J Biol Chem 264:9626–9631
16. Gath U, Hakvoort A, Wegener J, Decker S, Galla HJ (1997) Porcine choroid plexus cells in culture: expression of polarized phenotype, maintenance of barrier properties and apical secretion of CSF-components. Eur J Cell Biol 74:68–78
17. Ramanathan VK, Hui AC, Brett CM, Giacomini KM (1996) Primary cell culture of the rabbit choroid plexus: an experimental system to investigate membrane transport. Pharm Res 13:952–956
18. Southwell BR, Duan W, Alcorn D, Brack C, Richardson SJ, Kohrle J, Schreiber G (1993) Thyroxine transport to the brain: role of protein synthesis by the choroid plexus. Endocrinology 133:2116–2126
19. Haselbach M, Wegener J, Decker S, Engelbertz C, Galla HJ (2001) Porcine choroid plexus epithelial cells in culture: regulation of barrier properties and transport processes. Microsc Res Tech 52:137–152
20. Sanders-Bush E, Breeding M (1991) Choroid plexus epithelial cells in primary culture: a model of 5HT1C receptor activation by hallucinogenic drugs. Psychopharmacology (Berl) 105:340–346
21. Hoffmann A, Gath U, Gross G, Lauber J, Getzlaff R, Hellwig S, Galla HJ, Conradt HS (1996) Constitutive secretion of beta-trace protein by cultivated porcine choroid plexus epithelial cells: elucidation of its complete amino acid and cDNA sequences. J Cell Physiol 169:235–241
22. Strazielle N, Khuth ST, Murat A, Chalon A, Giraudon P, Belin MF, Ghersi-Egea JF (2003) Pro-inflammatory cytokines modulate matrix metalloproteinase secretion and organic anion transport at the blood–cerebrospinal fluid barrier. J Neuropathol Exp Neurol 62:1254–1264
23. Hakvoort A, Haselbach M, Wegener J, Hoheisel D, Galla HJ (1998) The polarity of

choroid plexus epithelial cells in vitro is improved in serum-free medium. J Neurochem 71:1141–1150

24. Strazielle N, Ghersi-Egea JF (2005) In vitro investigation of the blood–cerebrospinal fluid barrier properties: primary cultures and immortalized cell lines of the choroidal epithelium. In: Zheng W, Chodobski A (eds) The blood–cerebrospinal fluid barrier. Taylor and Francis, Boca Raton, pp 553–593
25. Nilsson C, Hultberg BM, Gammeltoft S (1996) Autocrine role of insulin-like growth factor II secretion by the rat choroid plexus. Eur J Neurosci 8:629–635
26. Gilbert SF, Migeon BR (1975) D-valine as a selective agent for normal human and rodent epithelial cells in culture. Cell 5:11–17
27. Chang M, Zhang L, Tam JP, Sanders-Bush E (2000) Dissecting G protein-coupled receptor signaling pathways with membrane-permeable blocking peptides. Endogenous 5-HT(2C) receptors in choroid plexus epithelial cells. J Biol Chem 275:7021–7029
28. Esterle TM, Sanders-Bush E (1992) Serotonin agonists increase transferrin levels via activation of 5-HT1C receptors in choroid plexus epithelium. J Neurosci 12:4775–4782
29. McGrew L, Chang MS, Sanders-Bush E (2002) Phospholipase D activation by endogenous 5-hydroxytryptamine 2C receptors is mediated by Galpha13 and pertussis toxin-insensitive Gbetagamma subunits. Mol Pharmacol 62:1339–1343
30. Kao WW, Prockop DJ, Berg RA (1979) Kinetics for the secretion of nonhelical procollagen by freshly isolated tendon cells. J Biol Chem 254:2234–2243
31. Peiser C, McGregor GP, Lang RE (2000) Binding and internalization of leptin by porcine choroid plexus cells in culture. Neurosci Lett 283:209–212
32. Spector R (1982) Pharmacokinetics and metabolism of cytosine arabinoside in the central nervous system. J Pharmacol Exp Ther 222:1–6
33. Gabrion JB, Herbute S, Bouille C, Maurel D, Kuchler-Bopp S, Laabich A, Delaunoy JP (1998) Ependymal and choroidal cells in culture: characterization and functional differentiation. Microsc Res Tech 41: 124–157
34. Hartter S, Huwel S, Lohmann T, Abou El Ela A, Langguth P, Hiemke C, Galla HJ (2003) How does the benzamide antipsychotic amisulpride get into the brain? – An in vitro approach comparing amisulpride with clozapine. Neuropsychopharmacology 28:1916–1922
35. Ramanathan VK, Chung SJ, Giacomini KM, Brett CM (1997) Taurine transport in cultured choroid plexus. Pharm Res 14:406–409
36. Gee P, Rhodes CH, Fricker LD, Angeletti RH (1993) Expression of neuropeptide processing enzymes and neurosecretory proteins in ependyma and choroid plexus epithelium. Brain Res 617:238–248
37. Albert O, Ancellin N, Preisser L, Morel A, Corman B (1999) Serotonin, bradykinin and endothelin signalling in a sheep choroid plexus cell line. Life Sci 64:859–867
38. Angelova K, Fralish GB, Puett D, Narayan P (1996) Identification of conventional and novel endothelin receptors in sheep choroid plexus cells. Mol Cell Biochem 159:65–72
39. Dickinson KE, Baska RA, Cohen RB, Bryson CC, Smith MA, Schroeder K, Lodge NJ (1998) Identification of [3H]P1075 binding sites and P1075-activated K+ currents in ovine choroid plexus cells. Eur J Pharmacol 345:97–101
40. Thornwall M, Chhajlani V, Le Greves P, Nyberg F (1995) Detection of growth hormone receptor mRNA in an ovine choroid plexus epithelium cell line. Biochem Biophys Res Commun 217:349–353
41. Ishiwata I, Ishiwata C, Ishiwata E, Sato Y, Kiguchi K, Tachibana T, Hashimoto H, Ishikawa H (2005) Establishment and characterization of a human malignant choroids plexus papilloma cell line (HIBCPP). Hum Cell 18:67–72
42. Nakashima N, Goto K, Tsukidate K, Sobue M, Toida M, Takeuchi J (1983) Choroid plexus papilloma. Light and electron microscopic study. Virchows Arch A Pathol Anat Histopathol 400:201–211
43. Takahashi K, Satoh F, Hara E, Murakami O, Kumabe T, Tominaga T, Kayama T, Yoshimoto T, Shibahara S (1997) Production and secretion of adrenomedullin by cultured choroid plexus carcinoma cells. J Neurochem 68:726–731
44. Szmydynger-Chodobska J, Pascale CL, Pfeffer AN, Coulter C, Chodobski A (2007) Expression of junctional proteins in choroid plexus epithelial cell lines: a comparative study. Cerebrospinal Fluid Res 4:11
45. Enjoji M, Iwaki T, Hara H, Sakai H, Nawata H, Watanabe T (1996) Establishment and characterization of choroid plexus carcinoma cell lines: connection between choroid plexus and immune systems. Jpn J Cancer Res 87:893–899

46. Enjoji M, Iwaki T, Nawata H, Watanabe T (1995) IgH intronic enhancer element HE2 (mu B) functions as a cis-activator in choroid plexus cells at the cellular level as well as in transgenic mice. J Neurochem 64:961–966
47. Schell TD, Mylin LM, Georgoff I, Teresky AK, Levine AJ, Tevethia SS (1999) Cytotoxic T-lymphocyte epitope immunodominance in the control of choroid plexus tumors in simian virus 40 large T antigen transgenic mice. J Virol 73:5981–5993
48. Kitazawa T, Hosoya K, Watanabe M, Takashima T, Ohtsuki S, Takanaga H, Ueda M, Yanai N, Obinata M, Terasaki T (2001) Characterization of the amino acid transport of new immortalized choroid plexus epithelial cell lines: a novel in vitro system for investigating transport functions at the blood–cerebrospinal fluid barrier. Pharm Res 18:16–22
49. Zheng W, Zhao Q (2002) Establishment and characterization of an immortalized Z310 choroidal epithelial cell line from murine choroid plexus. Brain Res 958:371–380
50. Battle T, Preisser L, Marteau V, Meduri G, Lambert M, Nitschke R, Brown PD, Corman B (2000) Vasopressin V1a receptor signaling in a rat choroid plexus cell line. Biochem Biophys Res Commun 275:322–327
51. Ohtsuki S, Takizawa T, Takanaga H, Terasaki N, Kitazawa T, Sasaki M, Abe T, Hosoya K, Terasaki T (2003) In vitro study of the functional expression of organic anion transporting polypeptide 3 at rat choroid plexus epithelial cells and its involvement in the cerebrospinal fluid-to-blood transport of estrone-3-sulfate. Mol Pharmacol 63:532–537
52. Terasaki T, Ohtsuki S, Hori S, Takanaga H, Nakashima E, Hosoya K (2003) New approaches to in vitro models of blood–brain barrier drug transport. Drug Discov Today 8:944–954
53. Miettinen M, Clark R, Virtanen I (1986) Intermediate filament proteins in choroid plexus and ependyma and their tumors. Am J Pathol 123:231–240
54. Peraldi-Roux S, Nguyen-Than Dao B, Hirn M, Gabrion J (1990) Choroidal ependymocytes in culture: expression of markers of polarity and function. Int J Dev Neurosci 8:575–588
55. Nataf S, Strazielle N, Hatterer E, Mouchiroud G, Belin MF, Ghersi-Egea JF (2006) Rat choroid plexuses contain myeloid progenitors capable of differentiation toward macrophage or dendritic cell phenotypes. Glia 54:160–171
56. Sousa JC, Cardoso I, Marques F, Saraiva MJ, Palha JA (2007) Transthyretin and Alzheimer's disease: where in the brain? Neurobiol Aging 28:713–718
57. Richardson SJ (2009) Evolutionary changes to transthyretin: evolution of transthyretin biosynthesis. FEBS J 276:5342–5356
58. Thomas T, Stadler E, Dziadek M (1992) Effects of the extracellular matrix on fetal choroid plexus epithelial cells: changes in morphology and multicellular organization do not affect gene expression. Exp Cell Res 203:198–213
59. Ghersi-Egea JF, Strazielle N, Murat A, Jouvet A, Buenerd A, Belin MF (2006) Brain protection at the blood–cerebrospinal fluid interface involves a glutathione-dependent metabolic barrier mechanism. J Cereb Blood Flow Metab 26:1165–1175
60. Gazzin S, Strazielle N, Schmitt C, Fevre-Montange M, Ostrow JD, Tiribelli C, Ghersi-Egea JF (2008) Differential expression of the multidrug resistance-related proteins ABCb1 and ABCc1 between blood–brain interfaces. J Comp Neurol 510:497–507
61. Tu GF, Achen MG, Aldred AR, Southwell BR, Schreiber G (1991) The distribution of cerebral expression of the transferrin gene is species specific. J Biol Chem 266:6201–6208
62. Lippoldt A, Jansson A, Kniesel U, Andbjer B, Andersson A, Wolburg H, Fuxe K, Haller H (2000) Phorbol ester induced changes in tight and adherens junctions in the choroid plexus epithelium and in the ependyma. Brain Res 854:197–206
63. Lippoldt A, Liebner S, Andbjer B, Kalbacher H, Wolburg H, Haller H, Fuxe K (2000) Organization of choroid plexus epithelial and endothelial cell tight junctions and regulation of claudin-1, -2 and -5 expression by protein kinase C. Neuroreport 11:1427–1431
64. Furuse M, Sasaki H, Tsukita S (1999) Manner of interaction of heterogeneous claudin species within and between tight junction strands. J Cell Biol 147:891–903
65. Tsukita S, Furuse M (2002) Claudin-based barrier in simple and stratified cellular sheets. Curr Opin Cell Biol 14:531–536
66. Strazielle N, Belin MF, Ghersi-Egea JF (2003) Choroid plexus controls brain availability of anti-HIV nucleoside analogs via pharmacologically inhibitable organic anion transporters. AIDS 17:1473–1485
67. Saito Y, Wright EM (1983) Bicarbonate transport across the frog choroid plexus and its control by cyclic nucleotides. J Physiol 336:635–648
68. Welch K, Araki H (1975) Features of the choroid plexus of the cat studied in vitro. In:

Cserr HF, Fenstermacher JD, Fencl V (eds) Fluid environment of the brain. Academic, New York, pp 157–165

69. Wright EM (1972) Mechanisms of ion transport across the choroid plexus. J Physiol 226:545–571
70. Claude P, Goodenough DA (1973) Fracture faces of zonulae occludentes from "tight" and "leaky" epithelia. J Cell Biol 58:390–400
71. Welch K, Sadler K (1966) Permeability of the choroid plexus of the rabbit to several solutes. Am J Physiol 210:652–660
72. Lo CM, Keese CR, Giaever I (1999) Cell-substrate contact: another factor may influence transepithelial electrical resistance of cell layers cultured on permeable filters. Exp Cell Res 250:576–580
73. Papenheimer JR (1961) Active transport of Diodrast and phenolsulfonphtalein from cerebrospinal fluid to blood. Am J Physiol 200:1–10
74. Ennis SR, Novotny A, Xiang J, Shakui P, Masada T, Stummer W, Smith DE, Keep RF (2003) Transport of 5-aminolevulinic acid between blood and brain. Brain Res 959:226–234
75. Redzic ZB, Isakovic AJ, Misirlic Dencic ST, Popadic D, Segal MB (2006) Uneven distribution of nucleoside transporters and intracellular enzymatic degradation prevent transport of intact [14C] adenosine across the sheep choroid plexus epithelium as a monolayer in primary culture. Cerebrospinal Fluid Res 3:4
76. Isakovic AJ, Dencic SM, Segal MB, Redzic ZB (2008) Transport of [14C]hypoxanthine by sheep choroid plexus epithelium as a monolayer in primary culture: Na+-dependent and Na+-independent uptake by the apical membrane and rapid intracellular metabolic conversion to nucleotides. Neurosci Lett 431:135–140
77. Hakvoort A, Haselbach M, Galla HJ (1998) Active transport properties of porcine choroid plexus cells in culture. Brain Res 795:247–256
78. Zheng W, Blaner WS, Zhao Q (1999) Inhibition by lead of production and secretion of transthyretin in the choroid plexus: its relation to thyroxine transport at blood–CSF barrier. Toxicol Appl Pharmacol 155:24–31
79. Steffen BJ, Breier G, Butcher EC, Schulz M, Engelhardt B (1996) ICAM-1, VCAM-1, and MAdCAM-1 are expressed on choroid plexus epithelium but not endothelium and mediate binding of lymphocytes in vitro. Am J Pathol 148:1819–1838
80. Pappenheimer JR, Renkin EM, Borrero LM (1951) Filtration, diffusion and molecular sieving through peripheral capillary membranes; a contribution to the pore theory of capillary permeability. Am J Physiol 167:13–46
81. Khuth ST, Strazielle N, Giraudon P, Belin MF, Ghersi-Egea JF (2005) Impairment of blood–cerebrospinal fluid barrier properties by retrovirus-activated T lymphocytes: reduction in cerebrospinal fluid-to-blood efflux of prostaglandin E2. J Neurochem 94: 1580–1593

Chapter 9

Introducing Cloned Genes into Cultured Neurons Providing Novel In vitro Models for Neuropathology and Neurotoxicity Studies

Marcelo Farina, Jordi Berenguer, Sebastián Pons, João Batista Teixeira da Rocha, and Michael Aschner

Abstract

Recent advances in techniques to introduce nucleic acids into cultured cells have significantly contributed to understanding the roles of genes (and their encoded proteins) in maintaining cellular homeostasis. The objective of this chapter is to provide methodological strategies for gene introduction specifically into cultured neuronal cells. This approach has been used to study the role of specific proteins in neurodegenerative and neuroprotective events, as well as in neurotransmission, antioxidant defenses, energetic metabolism, and several other physiological phenomena related to the neuronal homeostasis. The chapter starts with a description of the most important vectors currently available for neuronal transfections. A particular emphasis is directed at plasmid vectors, and a simple but useful protocol to isolate plasmids from bacteria is presented. This is followed by a discussion on the fundamentals of gene manipulation emphasizing the basics on how to isolate a DNA fragment, as well as modify and insert it into a vector. Since bacteria can be transfected with the cloning vector, it is possible to achieve high levels of the vector during bacterial growth. The purified vector can be inserted into a eukaryotic cell, such as a neuron, which uses its transcriptional machinery to overexpress the protein of interest. The chapter also presents discussions and protocols on delivering nucleic acids into cultured neuronal cells (primary and cell lines), with a particular emphasis on lipid-based (lipofection) and electroporation-based transfection. At the end of the chapter, we discuss recent applications of gene transfection to study neuropathology and neurotoxicity. The use of strategies to overexpress specific proteins into cultured neuronal cells has been useful to study neurodegenerative diseases (i.e., Parkinson disease vs. alpha-synuclein or parkin) and neurotoxicity events (i.e., methylmercury-induced neurotoxicity vs. glutathione peroxidase). In this regard, studies point to the fact that genetically-modified cultured neuronal cells may help neurotoxicologists in the difficult task of screening environmental toxicants with potential hazard for predisposition to neurodegenerative diseases.

Key words: Cultured neuronal cells, Cloning techniques, Vectors, Plasmids, Transfection, Protein overexpression, Neuropathology, Neurotoxicity

Michael Aschner et al. (eds.), *Cell Culture Techniques*, Neuromethods, vol. 56,
DOI 10.1007/978-1-61779-077-5_9,

1. Introduction

The introduction of nucleic acids into cultured cells has been widely used to study the gene-specific function. With the advent of novel techniques for molecular cloning and cultured cell transfection, innovative approaches have provided relatively rapid and efficient ways to elucidate the effects of genes (and their encoded proteins) in the living cells. With particular emphasis on cultured neuronal cells, the transfection of nucleic acids can be used to overexpress genes that encode proteins involved in neurodegenerative and neuroprotective events, as well as in neurotransmission, antioxidant defenses, energetic metabolism, and several others physiological phenomena related to the neuronal homeostasis.

Books have been written on manipulating gene expression in cultured cells derived from different sources. Given space limitations, this chapter cannot treat the subject in depth; rather, it discusses the fundamentals of dealing with vectors (especially plasmids), bacterial transformation, plasmid maximization and purification, and transfection of cultured neuronal cells. For additional topics and details on protocols concerning molecular cloning and cultured cell transfection, the reader is referred to an excellent text listed at the end of the chapter (Sect. Recommended Reading).

2. Cloning Techniques

Molecular cloning techniques describe how to isolate a DNA fragment (i.e., a complete gene, part of it or a promoter), modify it, and insert it into another DNA molecule. This receiver DNA molecule is generally called vector, which allows producing high amounts when transfected into bacteria (cloning vectors). Some vectors may also use the transcriptional machinery of a eukaryotic cell, like a neuron, and can be used to study the function of the inserted DNA sequence. Due to their many different applications in the neuroscience field, in this section, we will focus on their generation and handling.

2.1. Vectors

Vectors are DNA molecules derived from natural extrachromosomal DNA molecules found in bacteria and yeast (plasmids, which are double-stranded generally circular DNA) or from bacteriophages and other viruses. Since the 1970s, thousands of vectors have been created by cutting and joining sequences from different sources (other vectors, prokaryotic, or eukaryotic sequences) in an attempt to provide them useful features. Some of these features are common between the majority of vectors, such as (1) the replication origin (ori), required to be propagated into the host cell, (2) an antibiotic

resistance to eliminate bacteria that have not been transformed (commonly ampicillin resistance (Amp^r), kanamycin resistance (Km^r), or cloramphenicol resistance (Cm^r)), and (3) a multiple cloning site (MCS), used to open the circular molecule and insert the sequence of interest. Other features will depend on the particular application of the vector.

2.1.1. Overexpression Vectors

Overexpression vectors are designed to produce high quantities of a protein encoded by the cloned sequence. Of particular importance, the overexpression of the specific protein allows for predicting its role in neurotoxic/neuroprotective events (1). Figure 1 shows an example of the overexpression vector (pCIG). These vectors need to have a strong promoter in an upstream position to the MCS, as well as a polyadenylation signal at a downstream position, which must be recognized by the transcriptional machinery of the transfected eukaryotic cell. Common promoters used for overexpression in eukaryotic cells are the human cytomegalovirus (CMV)

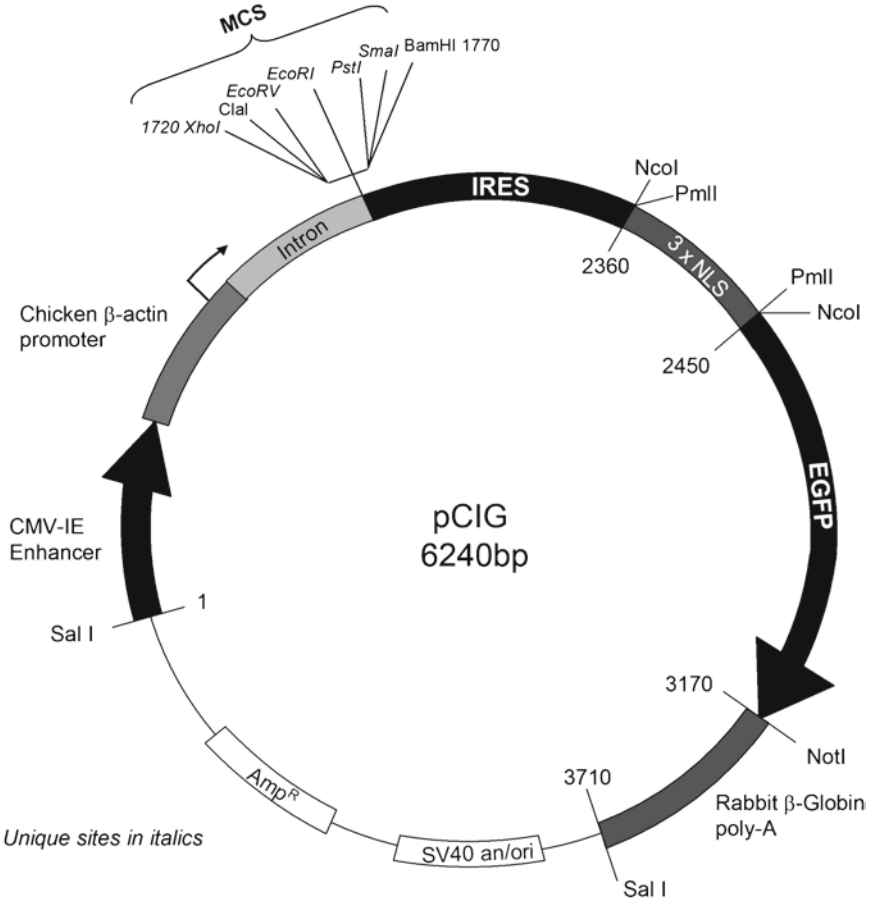

Fig. 1. pCIG overexpression vector map. Main features and restriction sites are shown. Unique restriction sites useful for cloning are shown in *italics*. *MCS* multiple cloning site; *Amp*^{R} gene encoding ampicillin resistance.

immediate-early promoter/enhancer (2–4) and the Simian virus 40 early promoter/enhancer (5). It is important to note that the activity of a promoter depends on the transfected cell type (6). According to our experience, the chicken β-actin promoter, in combination with the CMV immediate-early promoter–enhancer, represent a good choice when working with cultured neuronal cells. Particularly, the vector depicted in Fig. 1 presents a specific region that confers ampicillin resistance (Amp^r).

As discussed later, the process by which a vector enters the eukaryotic cell (transfection) never reaches a complete efficiency. Accordingly, after a transfection, a mixture of transfected and non-transfected cells is obtained. Overexpression vectors often have specific features allowing for distinction between transfected and non-transfected cells. One of such features is characterized by the use of reporter genes, such as green fluorescent protein (GFP) or its derivatives. GFP is a protein cloned from the jellyfish *Aequorea victoria* that emits green fluorescent light when exposed to blue or ultraviolet light. Interestingly, GFP does not alter normal cellular homeostasis. Consequently, its use as well as similar vectors allow for distinction between transfected and non-transfected neurons by irradiating them with blue light in a fluorescence microscope. Another way to identify transfected cells is the fusion of the cloned sequence to an epitope-Tag that is inserted in specific commercial vectors. Epitope-tag sequences (like myc-Tag or Flag-Tag) encode epitopes easily identifiable with the commercially available antibodies.

Overexpression vectors can also be used to decrease the function of a specific protein. In fact, it is possible to mutate a gene and convert it into a dominant-negative form that, when overexpressed, blocks the function of the wild-type gene (7, 8). This strategy takes advantage of the fact that the mutated overexpressing protein can compete for specific substrates of the non-mutated protein.

2.1.2. Luciferase Vectors

Luciferase vectors are designed to clone regulatory regions of the genomic DNA (i.e., promoters, enhancers, or transcription factor binding sites) to evaluate their function from a quantitative point of view. In these vectors, the MCS is located upstream a sequence encoding for luciferase protein, driving its expression. Luciferase, which is a protein derived from the firefly *Photinus pyralis*, catalyzes the reaction in which luciferin is oxidized to oxyluciferin and light (9, 10), usually in the green to yellow region, typically 550–570 nm. Thus, the relative activity of a regulatory sequence cloned into a luciferase vector and transfected into cells can be measured through the luciferase reaction (light emission) (11, 12).

2.1.3. Other Purpose Vectors

There are four different types of vectors (plasmids, bacteriophages and other viruses, cosmids, and artificial chromosomes) with several properties that make them useful in molecular biology. Of particular importance to neuroscience studies, inducible

promoter vectors can start transcription only in response to a concrete signal (i.e., an antibiotic or a naturally secreted molecule) and short interfering RNA (siRNA) vectors specifically downregulate the expression of a particular gene. Since the aim of this section is to provide a brief, simple, but comprehensible guide for gene manipulation and transfection into cultured neuronal cells, we describe only two of the most common vectors used in molecular biology. For more information about vectors in general, please check the Sect. Recommended Reading.

2.1.4. Plasmid Isolation Protocol

There are several methods for the isolation of plasmid DNA from bacteria. Many of them are based on alkaline lysis with sodium dodecyl sulphate (SDS). They are fast, simple, and provide good yield. The purification is performed in three steps. In the first step, bacteria are resuspended in a buffer containing ethylenediaminetetraacetic acid (EDTA). EDTA destabilizes the cell wall by chelation of divalent cations and inhibits DNAses. In the second step, a buffer at high pH containing NaOH and SDS is added. In this step, SDS breaks cell walls, disrupts cell membranes and proteins and chromosomal DNA are denatured while plasmid DNA is released into the supernatant. Base pairs of chromosomal and plasmid DNA are disrupted, but plasmid DNA remains topologically constricted. In the third step, –OH ions are replaced by potassium ions. This step renaturates plasmid DNA while precipitating chromosomal DNA. This protocol gives DNA of sufficient quality for many molecular cloning techniques, but purification steps can be added if needed (i.e., phenol:chlorophorm extraction, see Sect. Recommended Reading).

1. Pick a single colony of plasmid-transformed bacteria into 3 mL Luria–Bertani (LB) medium (1% bacterial peptone, 0.5% yeast extract, 1% NaCl) supplemented with the antibiotic whose resistance is encoded in the plasmid. Grow it overnight or until log phase is achieved (do not let it grow too long: If the antibiotic is fully processed by bacteria, the plasmid will be lost).
2. Transfer 1.5 mL of the culture to propylene tube and centrifuge at 13,000×*g* for 2 min. Store the rest of the culture at 4°C and pour off the supernatant.
3. Add 100 μL of buffer P1 (Resuspension buffer: 50 mM Tris–HCl – pH 8.0, 10 mM EDTA, 100 μg/mL RNAse A). Resuspend the pellet vigorously.
4. Add 100 μL of P2 buffer (Lysis buffer: 200 mM NaOH, 1% SDS). Mix by inversion 10 times.
5. Add 100 μL of P3 buffer (potassium acetate 3 M – pH 5.5). Mix by inversion 10 times. Centrifuge at 13,000×*g* for 5 min. Harvest supernatant.
6. Add to the supernatant 2 volumes (600 μL) of cold 100% ethanol. Mix by inversion 10 times. Centrifuge at 13,000×*g* for 5 min.

7. Pour off the supernatant and wash the pellet with 1 mL of 80% ethanol. Centrifuge at 13,000×*g* for 5 min. Pour off the supernatant and let the pellet dry.
8. Resuspend the pellet in 30 μL of water (stable at –20°C for several weeks).

2.2. Manipulating Genes: Cutting, Pasting, and Inserting into Bacteria

Recombinant DNA technology arose in the early of 1970s as a result of great advances in the field of the bacterial and bacteriophage's biology (13). These advances led scientists to isolate enzymes able to modify DNA: Restriction endonucleases (RE), which cut DNA in concrete positions, or DNA ligases, which join DNA molecules. The insertion of these DNA molecules into bacteria (transformation) allowed the production of large amounts of the inserted gene.

2.2.1. Restriction Endonucleases

Restriction endonucleases (or restriction enzymes; RE) are bacterial proteins involved in the recognition and elimination of foreign DNA sequences inside the cell, like bacteriophage's DNA (14–17). They recognize specific nucleotide sequences that are cleaved when unmethylated. To avoid cleavage of the own DNA, bacterial RE can methylate DNA to "label" it as its own molecule, protecting against cleavage (18–21).

There are at least three types of RE, based on their composition, the point of recognition, methylation and cleavage, and cofactor requirements (22).

Type I REs are composed of a single enzyme with different subunits for recognition, methylation, and cleavage. These enzymes cut at a site that differs, and is at some distance (at least 1,000 bp) away from their recognition site. They require several cofactors for catalytic activity, such as adenosine triphosphate (ATP), s-adenosyl methionine (AdoMet), and Mg^{2+}.

Type II REs are composed of two different enzymes with one subunit each, which recognize the same target site, usually a palindromic 4–8 bp long sequence. One of them methylates the sequence and the other one cuts it. Usually, the only cofactor required for their activity is Mg^{2+}, with no need for ATP or AdoMet. These facts (possibility to separate cleavage and modification activities, recognition and cleavage at the same specific sequence and requirement of only Mg^{2+} as a cofactor) render them very useful for molecular cloning. In the last several decades, dozens of type II REs have been isolated and several companies have commercialized them as useful tools to perform restriction reactions. Typically, a restriction reaction contains only the target DNA, a specific buffer, and the restriction enzyme. Furthermore, REs often have similar buffer requirements, making possible to cleavage the target DNA at two sites in only one step reaction.

Type II REs perform result in two types of cleavage in the double-strand (ds) DNA. Since the target sequence is generally palindromic, that is, both strands have the same sequence when ridden from 5′ to 3′, the RE makes a symmetric cleavage.

In the case of EcoRI cleavage, the enzyme recognizes the following sequence,

```
5′-G A T A T C-3′
   I I I I I I
3′-C T A T A C-3′
```

and cuts between the G and the first A. Then, after the cleavage, the new DNA ends generated will be,

```
5′-G-3′                    5′-A A T T C-3′
   I                                I
3′-C T T A A-5′                  3′-G-5′
```

which are cohesive or "sticky" ends, due to the 5′ "overhang." These regions can anneal to other DNA fragments cut by the same RE. Alternatively, some REs cut dsDNA at the middle of the recognition site. This is observed for EcoRV, whose recognition site is

```
5′-G A T-3′        5′-A T C-3′
   I I I              I I I
3′-C T A-5′        3′-T A G-5′
```

In this case, no "overhang" is created in the cleavage site and the created ends are called "blunt" ends.

```
5′-G A A T T C-3′
   I I I I I I
3′-C T T A A G-5′
```

Type III REs are composed of one enzyme with two different subunits: One that recognizes and methylates the same sequence and another that cleaves at 20–30 bp away from their recognition site. They need ATP and AdoMet for catalytic activity.

2.2.1.1. Restriction Protocol

Here, we describe a simple protocol to cut DNA using the RE EcoRI provided in the Fermentas® Five Buffer System. Where other REs are used, the buffer and temperature might differ. Other companies have similar systems.

1. In a clean tube, mix the target DNA (between 0.1 and 2 μg), 2 μL of 10× EcoRI buffer (final concentration: 50 mM Tris–HCl (pH 7.5 at 37°C), 10 mM $MgCl_2$, 100 mM NaCl, 0,02% Triton X-100, 0.1 mg/mL BSA), 0.5 μL EcoRI (5 U) and water to a final volume of 20 μL.
2. Incubate at 37°C/1 h.
3. Add 4 μL of 6× DNA loading buffer (0.09% bromophenol blue, 60% glycerol, 60 mM EDTA) and run the sample in agarose gel with DNA staining dye (i.e., ethidium bromide or SybrGreen) and a commercial DNA ladder (i.e., 1 kb plus DNA ladder from Invitrogen, Carlsbad, CA) to separate RE and verify the restriction. The concentration of agarose will depend on the fragments size. Typically, use 1.5–2% for fragments smaller than 1 kb and 0.5–1% for fragments larger than 1 kb.

2.2.2. DNA Ligases

DNA ligases are enzymes that close nicks in the phosphodiester backbone of DNA. They are found in eukaryotes, prokaryotes, and viruses, and are involved in important cellular processes, such as the sealing of Okazaki fragments during replication (23). Prokaryotic DNA ligases use NAD^+ as a cofactor while eukaryotic and viral DNA ligases (like T4 bacteriophage DNA ligase, the most used in recombinant DNA technology) use ATP (24, 25). The reaction catalyzed by DNA ligases occurs in two steps, where ATP is crucial for the formation of an AMP–DNA complex (Fig. 2).

When two DNA molecules are cut with the same RE, the sticky ends of the double chain can anneal by base-complementarities. Since the four generated nicks are substrates for DNA ligase, a new artificially recombinant DNA molecule can be generated after ligation (i.e., the overexpression vector with a human gene cloned in its MCS – Fig. 3a).

During the ligation reaction, another possibility is the closing of the pattern DNA molecule (Fig. 3a) with no addition of the insert (recircularization). This event is particularly undesired when working with vectors, because the empty recircularizated vector can be transformed and propagated into bacteria. Since recircularization of a vector is usually more frequent than insert–vector ligation, it is difficult to discriminate bacteria with the empty vector from those containing the insert–vector. There are some strategies to minimize this problem. Ligation reactions are usually performed at high DNA concentration and high insert:vector ratios (typically 4:1–6:1) to maximize intermolecular reactions rather than intramolecular ones. Another strategy to minimize the occurrence of recircularization is to cut both ends of the vector and insert with two different, incompatible REs (Fig. 3b). Consequently, one end of the molecule cannot hybridize with the other one, avoiding recircularization. When this approach is not possible, a vector dephosphorilation step is included in the cloning protocol, between restriction and ligation (Fig. 3c). Alkaline phosphatases, such as calf or shrimp alkaline phosphatases, are able to dephosphorylate 5′ phosphate ends of DNA. When a vector is dephosphorylated, it can no longer recircularize because DNA ligase needs 5′-phosphate

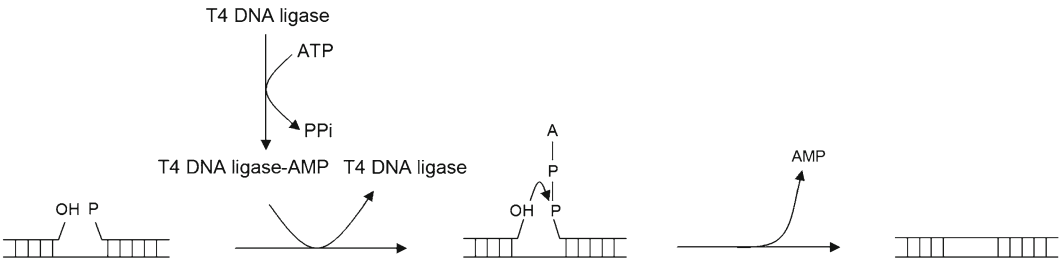

Fig. 2. Overview of the reaction catalyzed by DNA ligase. Firstly, a complex between the enzyme and the cofactor is formed, in a process in which ATP is hydrolyzed into AMP, and the complex binds the 5′-phosphate end of the nick. In a second step, the 3′-OH end of the nick attacks the AMP–DNA bond, releasing AMP and forming a new covalent bond in the phosphodiester chain.

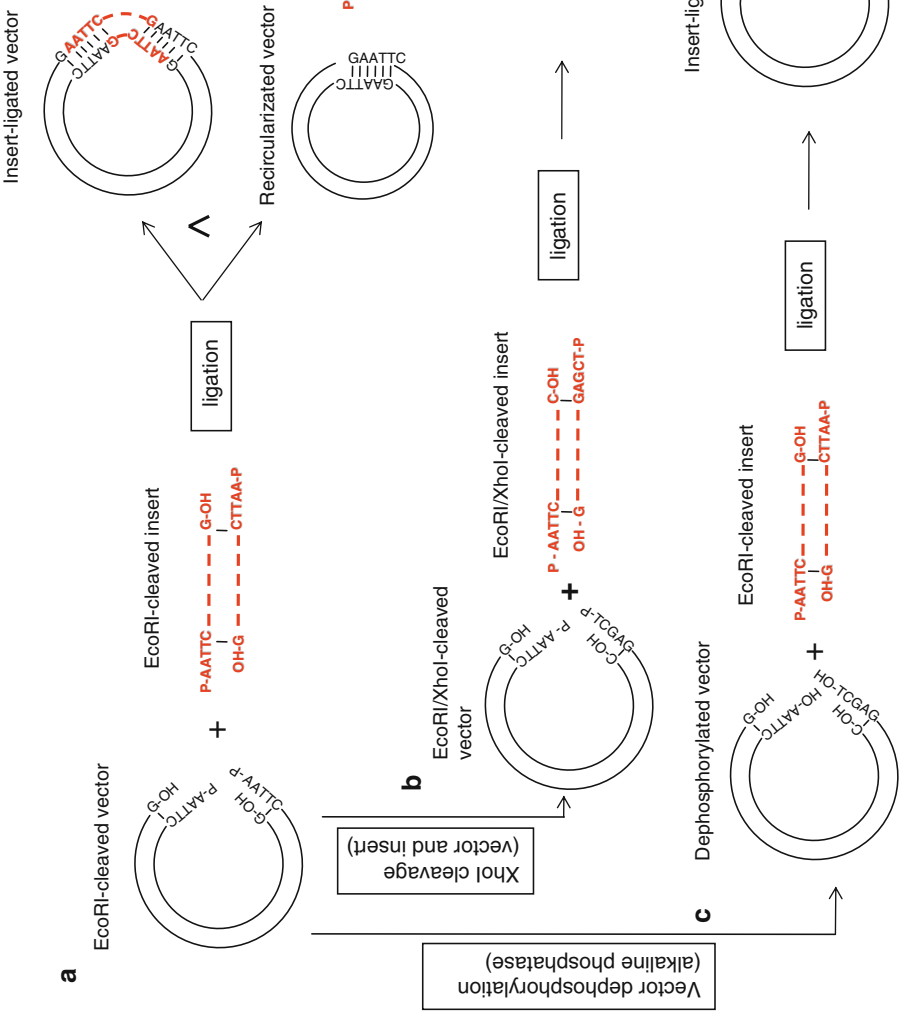

Fig. 3. Insert–vector ligation and strategies to avoid recircularization. (**a**) Ligation reaction of an EcoRI cleaved DNA fragment in an EcoRI cleaved vector without further treatment. Self-circularization of vector is highly favored. (**b**) Second cleavage of vector and insert with XhoI make incompatible both ends of the vector, avoiding self-circularization. (**c**) Vector dephosphorylation with alkaline phosphatase eliminates 5′ phosphate groups at the ends of the vector, necessary for recircularization. Note that in (**b**), as well as in (**c**), the only possible ligation reaction is between vector and insert.

residue to catalyze ligation reaction. This way, the only possible ligation reaction is between 5′ phosphate group of the insert and 3′-OH group of the vector, leaving a nick in each chain, which can be repaired in subsequent replications of the plasmid.

2.2.2.1. Ligation Protocol

In this section, we describe a protocol for ligation of a cohesive double-restricted insert into a vector with the Fermentas® system. Other companies have very similar protocols. For blunt-end ligation, see Sect. Recommended Reading.

1. Run a small sample of the vector and the insert in an agarose gel with DNA loading buffer (see Sect. 2.2.1.1).
2. Quantify the relative intensity of bands (visually or with the help of software (i.e., Bio-Rad's Quantity-One)).
3. Transform the relative intensity of the bands to relative quantity of DNA. Intensity will depend only on the amount of DNA and the size of the molecule (a band of 2 kb has double intensity than a band of 1 kb, if they are present in similar amounts).
4. In a clean tube, mix the vector and insert at a 1:4–1:6 ratio (if the amount of DNA is known, around 25–50 ng of vector are recommended). Add 2 μL of 10× T4 DNA ligase buffer (final concentration: 40 mM Tris–HCl, 10 mM $MgCl_2$, 10 mM DTT, 0.5 mM ATP), 0.5 μL T4-DNA ligase and water to a final volume of 20 μL. Repeat the ligation in another tube replacing the insert with water (negative control). Negative control-transformed cells will provide an estimate of the proportion of recircularized vector-transformed cells.
5. Incubate the reaction: The optimum temperature for DNA ligase is 37°C, but annealing of sticky ends is compromised at this temperature. Usually, 1 h at room temperature works best. For harder ligations, incubate overnight at 17°C.
6. Store at –20°C or proceed with bacterial transformation.

2.2.3. Competence and Transformation

The process by which bacteria remove free DNA from the extracellular environment is called transformation and the ability to be transformed is called competence. Bacteria naturally acquire competence and are transformed to transfer genetic information (such as antibiotic resistances) between individuals. This phenomenon was discovered by Griffith (26), but the techniques to generate competent and transform *E. coli* in vitro were developed only in the 1970s (27, 28). In molecular cloning, *E. coli* can be transformed by chemical transformation, electroporation, biolistic methods, or sonic transformation. In this section we describe a simple chemical method to make competent cells and transform them.

2.2.3.1. Preparation of Competent Cells and Transformation Protocol

This protocol is based on the ability of poliethylene glycol (PEG) to induce bacterial transformation (29, 30). It is very simple and provides good transformation efficiency.

Preparation of Competent Cells

1. Grow 5 mL of cells in Luria–Bertani (LB) medium without antibiotic, overnight, at 37°C (250 rpm).
2. Inoculate 1 mL of the culture into 250 mL of LB until the optic density at 600 nm reaches 0.6.
3. Pellet the cells by centrifugation at 1,000×*g* for 10 min. Pour off the supernatant and let the tube over paper to dry excess of medium.
4. Resuspend the cells in 25 mL filter-sterilized (0.22 μm) TSB (LB pH 6.1, 10% PEG (3,350 Da), 5% DMSO, 10 mM $MgCl_2$, 10 mM $MgSO_4$).
5. Let on ice during 10 min and aliquot in 0.5 pre-chilled tubes. Freeze in liquid N_2 or ethanol/dry ice bath. Store at –70°C.

Transformation

1. Thaw one aliquot of competent cells on ice.
2. Mix 20 μL KCM (KCl 0.5 M, $CaCl_2$ 0.15 M, $MgCl_2$ 0.25 M) with the ligation mixture (derived from protocol in Sect. 2.2.2.1) and add water to 100 μL.
3. Pipette 100 μL of competent cells to each tube of DNA/KCM and mix gently and leave it for 20 min on ice.
4. Leave 10 min at room temperature and add 800 μL of LB medium (without antibiotic).
5. Incubate for 1 h at 37°C under agitation
6. Centrifuge at 14,000×*g* during 15 seconds.
7. Remove 850 μL of LB, resuspend the cells and plate them in LB-Agar (LB with 1.5% Bacteriological Agar) with antibiotic.

2.3. DNA Amplification and Site-Directed Mutation by Polymerase Chain Reaction

Molecular cloning techniques had important limitations until the second half of 1980s. The discovery of RE and ligases allowed for novel methods for cloning DNA sequences into plasmids but, until the description and improvement of polymerase chain reaction (PCR), the only way was to construct DNA libraries. A DNA library is constructed by cutting (mechanically or by restriction) genomic DNA (gDNA) or complementary DNA (cDNA, which is DNA synthesized in vitro by reverse transcription) into thousands of unknown fragments that can be cloned into phagemid vectors. Once the library is constructed, it is necessary to identify the clones of interest by laborious screening strategies based on nucleic acid probe hybridization, functional studies, and immunological recognition of products by antibodies. The use of these techniques presented several difficulties and limitations. One of them was the fact that the fragments were randomly generated and then were frequently lost, incomplete, or contained undesired regulatory regions. On the other hand, sometimes there were no screening strategies to

find the sequence of interest. PCR technique abolished these problems. It allows to exponentially amplify a known DNA region with defined edges (amplicon) in such a way that can be considered a "purification" from the remainder DNA. Moreover, new sequences can be added at the end of the amplified sequence, enabling cloning into a vector and allowing for site-directed mutagenesis.

2.3.1. Overview of PCR Technique

PCR technique was first described in 1986, by Mullis (31). Basically, the reaction consists of repetitions of three defined steps, driven by temperature (Fig. 4). In the first step, both strands of DNA are separated by heat-denaturation. In the second step, the reaction medium is cooled to a temperature in which two chemically synthesized oligonucleotides anneal specifically to the flanks of the amplicon. In the third step, the reaction is set to a temperature in which purified DNA polymerase will synthesize complementary strands of the oligonucleotide-flanked region. DNA polymerases can only polymerize DNA in 5–3′ direction by adding nucleotides to a free 3′-OH group. For this reason, the oligonucleotides used in this technique are called "primers" (they "prime" polymerase reaction). At the second cycle of amplification (Fig. 5), two DNA molecules that comprise exactly the target region to be amplified are generated. As the reaction proceeds, these molecules are amplified geometrically in spite of other-length molecules that are arithmetically amplified (32).

The power of this technique is extraordinary: a very small amount of DNA (at the low nanogram range) can be amplified with high specificity to several micrograms. Since its inception multiple applications have been developed, which include DNA cloning and mutagenesis, DNA sequencing, DNA quantification and genotyping, just to name a few.

2.3.2. Factors Affecting PCR Specificity and Efficiency and Basic Reaction

2.3.2.1. DNA Polymerases

In the first description of the technique, the Klenow fragment of DNA polymerase I from *E. coli* was used. It was denatured in each denaturing step and fresh enzyme had to be added at every cycle. The use of thermophilic DNA polymerases (33) allowed for the automatization of the whole process. The first thermophilic DNA polymerase used in PCR was obtained from *Thermus aquaticus* (Taq DNA polymerase), an aerobic gram-negative bacteria isolated in Yellowstone National Park by Thomas Brock (34). Actually, several companies commercialize thermostable DNA polymerases from *Thermus aquaticus* and other organisms, such as *Pyrococcus furiosus*. Modern DNA polymerases for DNA cloning generally share two common features: (1) they have an improved proofreading activity to minimize misincorporation of nucleotides and (2) are reversibly inactivated by antibodies, which are inactivated in the first denaturation step (hot-start protocol). This strategy is used to prevent polymerase activity under temperatures lower than melting temperature (Tm, the temperature at which primers anneal to the flanks of the amplicon), that would give unspecific

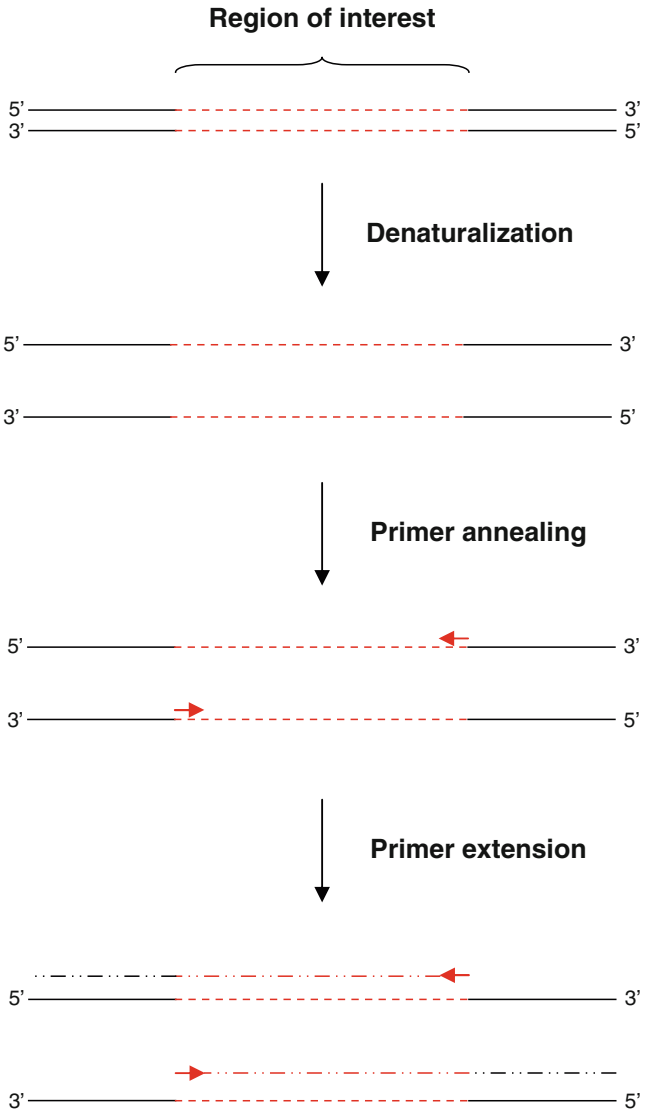

Fig. 4. Steps of the first cycle of a PCR (denaturation, annealing of primers, and primer extension). Target region to be amplified is shown as *dashed lines*. *Horizontal arrows* represent chemically synthesized oligonucleotides designed to anneal at the flanks of the amplicon. *Dash-dotted lines* represent newly synthesized DNA strand.

products. Two examples of commercial DNA polymerases suitable for cloning are Fast Start High Fidelity DNA polymerase from Roche and platinum Pfx DNA polymerase from Invitrogen.

In a PCR reaction, there are several factors that affect the specificity and efficiency of thermostable DNA polymerases. Among them, are (1) the polymerase used, (2) the buffer composition, (3) the template's source, (4) the amount of nucleotides and primers, and (5) the thermal cycler program. Accordingly, it is impossible to set conditions that work well for all PCRs. We recommend choosing the primers following instructions given below

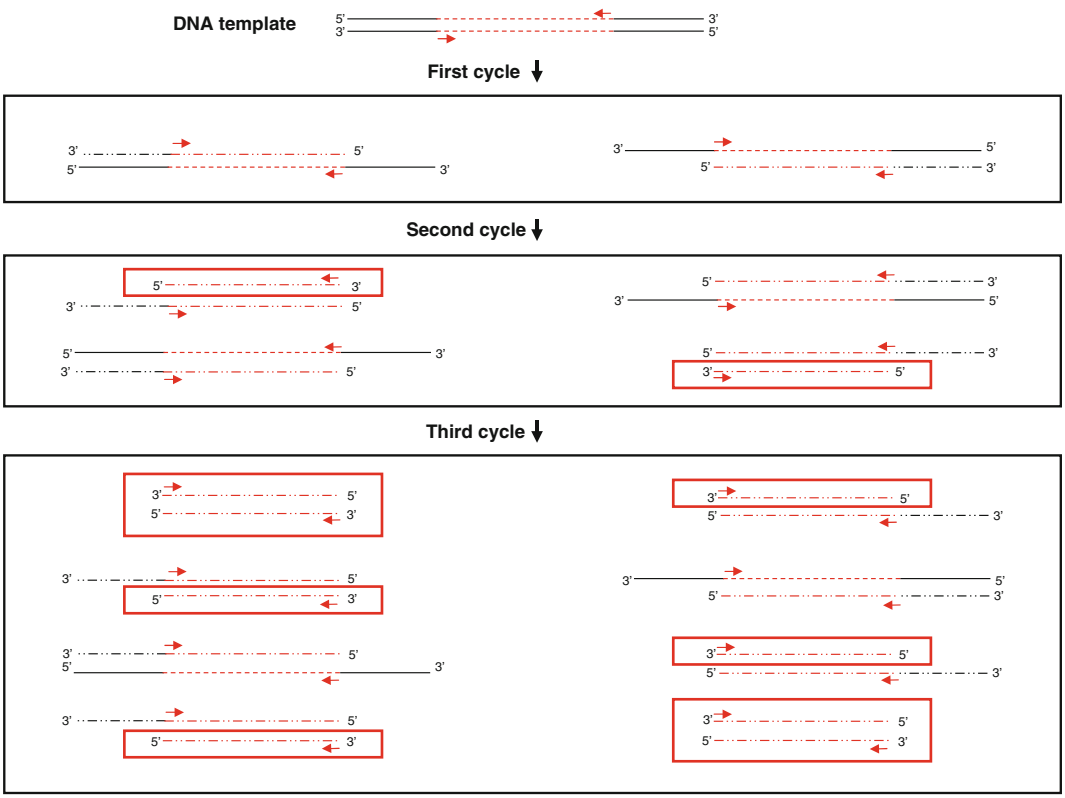

Fig. 5. First three cycles of a PCR and exponential amplification of the amplicon. Target region and oligonucleotides are shown as in Fig. 4. At the second cycle of amplification, two DNA molecules that comprise exactly the amplicon are generated (*boxed*). Progression of PCR amplifies these molecules exponentially.

and performing a basic PCR reaction. If this reaction does not work (mainly because of a poor efficiency or specificity), it is necessary to test the optimal condition for the reaction.

2.3.2.2. Primers

Several companies commercialize chemically synthesized oligonucleotides at a reasonable price. The choice of a good pair of primers is essential for PCR. There are several factors to consider. The length of the primers should be between 16 and 30 nucleotides and the G/C content should be around 50%. Both primers should have similar Tms and it is preferable to choose a longer primer than a low Tm primer. Tm depends on length and composition; there are several rules to calculate it. One of them, called "the Wallace rule" (35, 36) which is as follows:

$$\mathrm{Tm}\ (^{\circ}\mathrm{C}) = 2(\mathrm{A}+\mathrm{T}) + 4(\mathrm{C}+\mathrm{G}),$$

where (A + T) is the sum of the A and T residues in the oligonucleotide and (C + G) is the sum of C and G residues.

The sequence of the primer should avoid, as far as possible, mono and dinucleotide repetitions, as well as polypurine and polypyrimidine tracts. The 3′ last base of the primer must

preferably be a G or a C. There should not be secondary structure in the primers, and they should not anneal to each other, especially if this annealing leaves a 3′ end that can be a substrate for DNA polymerase. These factors are easily checked with the help of different programs. Among others, Oligo Explorer developed by Teemu Kuulasmaa (http://www.genelink.com/tools/gl-oe.asp) is a very simple and useful program freely available online.

Every molecule polymerized in a PCR is flanked by chemically synthesized primers of our choice. This feature allows for insertion of DNA sequences in the primer that will be present in the amplified DNA. One powerful application is the insertion of RE sites in the 5′ end of the primers, making much easier the cloning procedure. The addition of non-complementary sequences at the 5′ end does not significantly affect the Tm of the primer.

A typical PCR reaction contains equimolar amounts of each primer (around 0.2–0.4 μM). Anyway, the concentration of each primer can be increased or decreased (from 0.1 to 0.5 μM) to optimize the PCR reaction.

2.3.2.3. Deoxynucleoside Triphosphates (dNTPs)

In reactions containing $MgCl_2$ (generally 1.5 mM), a standard PCR mix has equimolar amounts of every deoxynucleoside triphosphate (dNTP), at concentrations around 200–250 μM. The concentrations of dNTPs and DNA molecules, as well as template and primers, must be related to $MgCl_2$ concentrations, taking into account the direct chemical interaction between phosphate groups of dNTPs or DNA with divalent cations, such as Mg^{2+}.

2.3.2.4. Divalent Cations

Thermostable DNA polymerases need free divalent cations to work. The most widely used cation for PCR is Mg^{2+} (its most common source is $MgCl_2$). As previously mentioned, the availability of free cations in a PCR reaction depends on the length and amount of primers, template, and nucleotides, because their phosphate groups sequester free cations from the medium. This fact makes it impossible to establish a cation concentration adequate for all PCRs. Commercial PCR kits usually contain two different 10× buffers: (1) one of them contains $MgCl_2$ at concentrations of 15–18 mM (final concentration 1.5–1.8 mM), which are suitable for most PCRs and (2) another one that does not contain divalent cations to allow for experimental determination of its optimal concentration.

2.3.2.5. Buffers

PCR reaction needs a buffer to maintain pH. Typically, 10 mM Tris–Cl (pH between 8.3 and 8.8, at room temperature) is used. At 72°C (primer extension temperature), pH falls to 7.2, near the optimal for Taq DNA polymerase. PCR buffer also contains 50 mM KCl. The salt concentration affects template denaturation and annealing of primers because it neutralizes the negative charges on the phosphate backbone of DNA, stabilizing the double-stranded DNA structure.

2.3.2.6. Template

PCR technique works with small amounts of DNA molecules from any source (either double or single stranded). Some natural sources contain natural inhibitors of the reaction, such as blood or feces (37), which can be easily eliminated through simple DNA purification procedures. Circular DNA amplifies slightly worse than linear, but generally plasmid DNA is shorter and cleaner, producing less unspecific amplifications than cDNA or gDNA. The ideal amount of template is around 5–250 ng for gDNA or cDNA and 100 pg–10 ng for plasmid DNA. Higher concentrations can increase non-specific amplification.

2.3.2.7. Enhancers

Some commercial kits include additives that can enhance PCR efficiency and/or specificity, like dimethylsulfoxide (DMSO), glycerol, ammonium sulfate, detergents, and other compounds. Although they are not usually necessary, we recommend following the manufacturer's instructions.

2.3.2.8. Thermal Cycling Program

As previously mentioned, PCR consists of repetitions of three steps. In the first step, DNA must be heated to be denatured and allow subsequent annealing of the primers. This step is generally performed at a maximum of 94°C during 30 s, because Taq DNA polymerase does not resist more than 30 cycles at higher temperatures. When the template is double-stranded, an initial 5′ denaturation step (to completely denature DNA sample) is generally added at the beginning of the program.

In the annealing step, temperature is generally set at a few degrees below the theoretical Tm (we recommend 1–3°C). A temperature too close to the Tm does not allow proper annealing, and a temperature too low decreases specificity of the product. Variations in buffer composition, Mg^{2+}, primer or template concentration will affect specificity, and the optimal Tm must be empirically determined.

The optimal temperature for the majority of thermostable DNA polymerases is between 68 and 78°C. Primer extension step for a PCR performed with Taq DNA polymerase is typically set at 72°C. At this temperature, Taq DNA polymerase can polymerize near to 2,000 nucleotides per minute. As a general rule, 1 min/1 kb of amplicon is necessary to perform accurate primer extension. After the last cycle, a long extension step (10 min) is commonly added to ensure that all the molecules have been properly polymerized. However, this step is not clearly necessary.

2.3.2.9. PCR Optimization

To amplify a DNA fragment, we recommend accurately choosing the primers and performing a basic PCR, following the recommendations given in this section (or in the manufacturer's instructions). If the result is not optimal (poor amplification, presence of unspecific or smeared bands), we recommend testing three to four different Mg^{2+} concentrations (from 1 to 5 mM) with three to four different Tms (from Tm to Tm –4°C), resulting in 9–16

conditions. This grid generally gives optimal Tm and Mg^{2+} concentration. If none of the different combinations give a suitable product, it is recommended to set the best couple of conditions and then test different concentrations of each primer. Optimal conditions for the majority of PCRs are established with this method. If it is not your experience, recheck your primers.

2.3.2.10. Basic PCR

Table 1 depicts a summary of the recommended conditions to perform PCR reaction. If the result is not satisfactory, change the used conditions according to recommendations in the previous section.

2.3.3. Site-Directed Mutagenesis by PCR

As mentioned above, the artificial sequences introduced in the 5′ end of a primer will be present in the amplified molecule. This fact allowed the development of techniques to introduce mutations in a defined position of the amplified sequence (site-directed mutations) (38). The development of site-directed mutagenesis had enormous applications in molecular biology. Point mutations can give information about the function of specific residues and domains in a protein. In this way, proteins can be mutated into inactive forms. Especially informative are the mutations with dominant-negative behavior (7, 8). Furthermore, the introduction of RE sites can be used to create chimeric fusions between two proteins.

Figure 6 shows a simple and effective method to perform PCR-based site-directed mutagenesis as described by Higuchi and co-workers (39). Two independent PCR reactions generate two DNA fragments that overlap in the point of the mutation. One reaction (PCR 1 in the picture) amplifies the amplicon from

Table 1
Recommended conditions to perform a PCR reaction

PCR MIX (50 µL) of final volume

	Stock concentration	Final concentration	Thermal program
5 µL Buffer	(10×) (with 18 mM $MgCl_2$)	1× 1.8 mM	94°C/5′
1 µL dNTPs	(10 mM each)	200 µM	94°C/30″
2.5 µL DMSO	(100%)	5%	(Tm–2°C)/30″
1 µL Fw primer	(10 µM)	200 nM	72°C/(1 min/Kb)
1 µL Rv primer	(10 µM)	200 nM	Go to step 2, 34 times
2 µL cDNA	(50 ng/µL)	2 ng/µL	72°C/10′
0.5 µL *Taq* DNA pol (High Fidelity)	(5 U/µL)	50 mU//µL	
37 µL H_2O			

Fw forward primer; *Rv* reverse primer

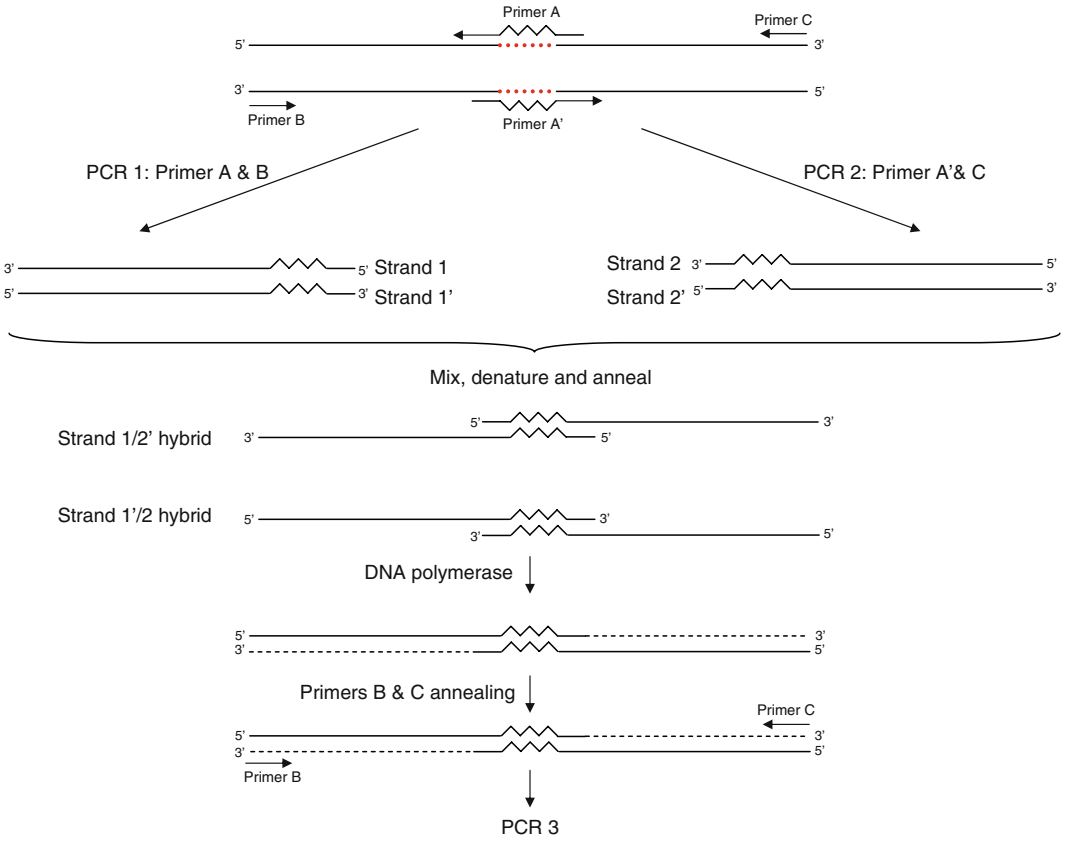

Fig. 6. PCR-based site-directed mutagenesis. Region to be mutated in the template is shown as a *dotted line*. Mutation point in the primers is shown as a *zigzag line*. Two independent PCRs (PCR 1 and PCR 2) generate two overlapping fragments of the amplicon that have incorporated the mutation (strand 1–1′ and strand 2–2′). Mixing of this fragments and a single round of polymerase reaction generate a template that incorporates the mutation and can be amplified in a third round of PCR (PCR 3).

its 5′ end to the mutation point, which is introduced in the primer. The other one (PCR 2) amplifies the amplicon from the point of the mutation to its 3′ end, also including the mutation in the primer. When the products of the two reactions are mixed and driven to the melting temperature of the overlapping zone, two kinds of hybrid molecules are formed, one of them hybridizes through the 5′ ends and consequently is not a substrate for DNA polymerase, but the second type hybridizes through the 3′ ends, leaving the free 3′-OH residues that can prime the polymerization of the rest of the amplicon. This strategy generates a template that has incorporated the mutation and can be amplified in another PCR (PCR 3) with the outer primers already used in PCR 1 and 2.

2.3.4. Protocol: Cloning of Mouse Myc Associated Factor X gene into pCIG Overexpression Vector

Specific approaches on cloning techniques (amplifying, cutting and pasting DNA, inserting DNA fragments into vectors, transforming bacteria) were detailed in the previous section. In order to summarize them, we present here a protocol to clone Myc

associated factor X (MAX) gene into pCIG vector. From initial challenges (such as primer selection) to latter stages (such as selecting positive bacteria colony), the protocol highlights the steps necessary prior to eukaryotic cell (neuronal) transfection, which are discussed in the third section of this chapter.

1. Primer selection.

   Murine MAX mRNA sequence (NCBI accession number: NM_008558) was pasted into Oligo Explorer software. A couple of 20 mer primers comprising exactly the coding sequence (CDS, bases 224–706) were tested. This primer approach presented several problems: The forward primer had a G/C content of 40% whereas the reverse primer had a G/C content of 60%. This difference in nucleotide composition was transduced to a Tm difference higher than 8°C. Furthermore, thermodynamical study of reverse primer self-annealing revealed the formation of a very stable dimmer, which was also a substrate for the polymerase reaction. To avoid this problem, different couples of primers were tested moving the annealing position of both primers few bases outside the amplicon. It is noteworthy that is not recommended to clone significant parts of untranslated regions (3′ or 5′ UTRs) of a gene for an overexpression experiment, because they could contain regulatory regions that could affect expression levels and give unexpected results. After few tests, a satisfactory primer couple was found: (1) The forward primer was shifted four bases upstream, giving better features (more G/C content, absence of secondary structures, and a G in its 3′ end) and (2) the reverse primer was shortened to 18 bp, allowing a new Tm of 58°C, avoiding the dangerous self-hybridizing structure observed in its 20 bp form. In order to investigate the potential occurrence of primer dimmers (two primers anneal one to the other instead of to the target DNA sequence to be amplified), dimerization calculations were performed. The primer couple did not provide important stable structure, suggesting no possibility of primer dimmer formation.

   Informatics restriction analysis of the amplicon was confronted with available restriction sites in the MCS of pCIG. XhoI and EcoRI are present in the MCS of pCIG and can be used in the same restriction reaction, because they share common buffer requirements. For this reason, this restriction sites were introduced in the 5′ end of the primers previously selected. Commonly, some nucleotides are added at the end of a primer when a RE site is introduced in it, because RE work better if they do not cut in the last bases of the chain. Finally, the chosen primers were:

   Fw MAX XhoI:

   GAA CTCGAG GGAAATGAGCGATAACGATG Tm: 58°C
   XhoI

Rv MAX EcoRI:

ACC GAATTC TTAGCTGGCCTCCATCCG Tm: 58°C
EcoRI

2. A basic PCR was performed using 100 ng of cerebellar granule neuron cDNA. Basic receipt and program given in Sect. 2.3.2.10 were followed. Melting temperature was set at 56°C and primer extension time at 30″ (amplicon size: 482 bp). Running of the product in a 1.5% Agarose gel revealed the presence of a moderate-intensity band in the correct weight, with no unspecific extra bands.
3. Band was excised from the gel and DNA was purified in a final volume of 40 μL with Qiagen's QiaQuick Gel Extraction Kit following the manufacturer's instructions.
4. 15 μL of the purified band and 1 μg of pCIG were double-restricted with EcoRI and XhoI with Fermenta's Tango 2× buffer (66 mM Tris–Acetate (pH 7.9 at 37°C), 20 mM Mg-acetate, 132 mM K-acetate, 0.2 mM BSA) and following instructions given in Sect. 2.2.1.1.
5. Bands were excised from the gel and purified again with QiaQuick Gel extraction kit. Again, elution was performed in a 40 μL volume.
6. 5 μL of the eluted bands were run on a 1% Agarose gel to quantify the relative quantity of each DNA (since purification procedure gives variable yield, quantification must be done). MAX band was one-third intense than pCIG one. As pCIG is 12.86 times larger than MAX, this means MAX is four times more concentrated (in molar terms) than pCIG (12.86/3 = 4.29).
7. Equal volumes of insert and vector represent a 4.29:1 molar ratio (see Sect. 2.2.2.1) then, ligation reaction was performed as follows: 2 μL of T4 DNA ligase buffer (final concentration: 40 mM Tris–HCl, 10 mM $MgCl_2$, 10 mM DTT, 0.5 mM ATP), 2 μL of purified restricted pCIG, 2 μL of purified restricted MAX, 0.5 μL T4-DNA ligase, and 13.5 μL of water were incubated at 17°C overnight. Ligation was repeated adding 2 μL of water instead of MAX protein (negative control).
8. Ligation reactions were transformed following instructions given in Sect. 2.2.3.1.2 and plates were incubated overnight at 37°C. Around 200 colonies grew in the insert-ligated plate, whereas around 20 colonies grew in negative control plate.
9. To asses insert ligation, eight colonies were picked. The plasmid DNA was isolated as described in Sect. 2.1.4 and SmaI restriction was performed as described in Sect. 2.2.1.1 (Buffer Tango 1×, 30°C/1 h). The presence of a 300 bp band confirmed insert ligation in all colonies (there is a SmaI site at 300 bp of MAX coding sequence end and at the pCIG's MCS).

10. DNA of a positive colony was large-scale produced and purified (for DNA maxipreparation, see Sect. Recommended Reading) and the presence of intact MAX CDS was confirmed by sequencing.

3. Introducing Cloned Genes into Cultured Neuronal Cells

There are numerous strategies to deliver nucleic acids into cultured cells. They include the transfection with Ca^{2+}-phosphate/DNA co-precipitates, lipid-based transfection protocols (lipofection), biolistics, microinjection, electroporation, as well as virus-based infection methods (40, 41). The choice of a specific transfection/infection method is determined by the experimental goal. With particular emphasis to the transfection of primary cultured neurons, which are post-mitotic cells, most methods remain relatively unsatisfactory with regard to either cytotoxicity or transfection/infection efficiency (42).

This section of the chapter describes the elementary basics and concepts involved in the strategies for delivering nucleic acids into cultured neuronal cells (primary and cell lines), as well as their advantages and drawbacks. A particular emphasis is directed to lipid-based (lipofection) and electroporation-based transfection protocols. For a more rigorous discussion of the topics mentioned here, see the Sect. Recommended Reading at the end of the chapter.

3.1. Transfection Methods

The methods to deliver nucleic acids into cultured cells fall into three classes: Transfection by chemical methods, transfection by physical methods, and virus-mediated infection.

3.1.1. Chemical Reagents

Diethylaminoethyl cellulose (DEAE)-dextran represents one of the first chemical reagents used to introduce nucleic acids into cultured mammalian cells (43, 44). It is a cationic polymer that associates with the negative charge of nucleic acids. The excess of positive charges allows the complex to come into closer association with the negatively charged cell membrane; its uptake is apparent by endocytosis. This method is useful for delivery of nucleic acids into cells for transient expression (see Sect. 3.2). However, this system is not normally useful for stable transfection studies, where integration of the transferred DNA into the chromosome is required (45). Other synthetic cationic polymers have been used for the transfer of DNA into cells, including polybrene (46), polyethyleneimine (47), and dendrimers (48, 49).

Calcium phosphate co-precipitation represents another interesting technique for the delivery of nucleic acids into cultured cells; it became exceedingly popular in the early 1970s (50). The protocol involves mixing DNA with calcium chloride, adding it to a

buffered saline/phosphate solution and allowing the mixture to incubate at room temperature. This procedure generates a precipitate that is dispersed onto the cultured cells. The precipitate is taken up by the cells through endocytosis or phagocytosis. The method is commonly used for both transient and stable transfections of a variety of cell types. Complete protocols based on the use of either cationic polymer or calcium phosphate co-precipitation for the delivery of nucleic acids into cultured cells are presented in the book by Sambrook and Russell (Sect. Recommended Reading).

Synthetic liposomes are also used to deliver DNA into cells (51). Particularly, the development of synthetic cationic lipids by Felgner and colleagues (52) was a significant progress in liposomal vehicles. The cationic head group of the lipid associates with the negative charges of phosphate groups on the nucleic acids. The methods based on this approach have several advantages such as relatively high efficiency of gene transfer and capability to transfect certain cell types that are resistant to calcium phosphate or DEAE-dextran, such as neuronal cells. Cells transfected by lipofection can be used for transient expression studies and long-term experiments that need the integration of the DNA into the chromosome.

A lipid positively charged at physiological pH is the most frequent synthetic lipid component of liposomes developed for gene delivery (Fig. 7). Generally, the cationic lipid is mixed with a neutral lipid such as l-dioleoyl phosphatidylethanolamine (DOPE; Fig. 7). The cationic part of the lipid associates with the negative charges of nucleic acids, resulting in compaction of the nucleic acid in a liposome/nucleic acid complex (53). For cultured cells, the positive charge of the liposome/nucleic acid complex allows closer association of the complex with the negatively charged cell membrane, resulting in higher transfection efficiencies. The entrance of the liposome complex into the cell may occur via endocytosis or fusion with the plasma membrane by the lipid moieties of the liposome (54). After cellular internalization, the complexes appear in the endosomes and later in the nucleus (55).

There is a great variety of transfection reagents that use cationic lipids for the delivery of nucleic acids to eukaryotic cells. These include the TransFast™, Tfx™ and Transfectam® Reagents (Promega), Lipofectamine™ LTX Reagent (Invitrogen), and the TransFectin Lipid Reagent (Bio-Rad). The best transfection reagent and conditions for a particular cell type must be determined, because the properties of a particular cell type influence the success of any specific transfection method. Detailed methods based on the use of cationic lipids to delivery of nucleic acids into cultured cells are presented in the Sect. Recommended Reading. A short lipofection-based protocol to transfect cultured neural cells is presented below.

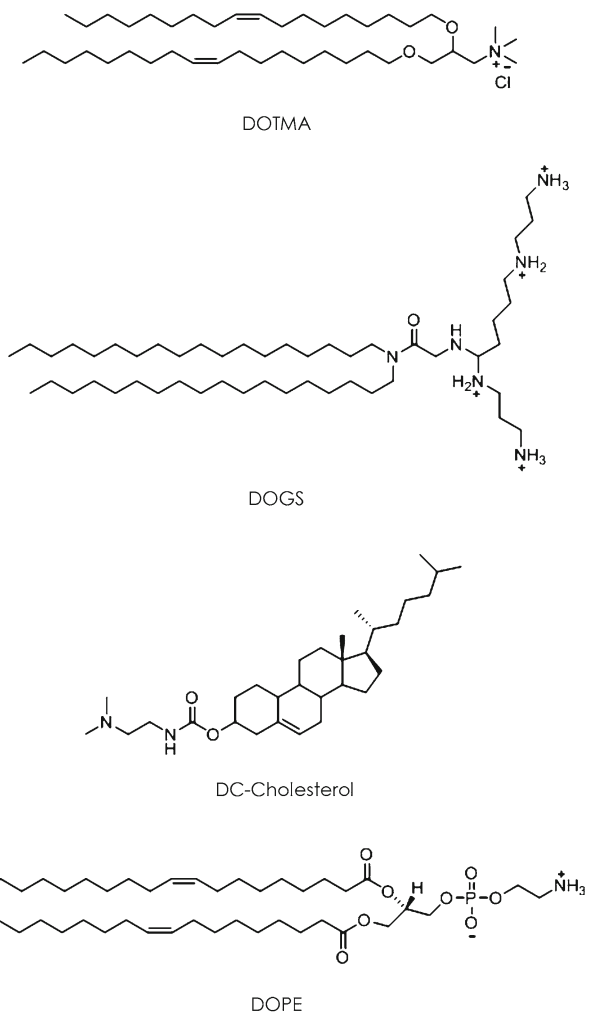

Fig. 7. Chemical structures of some lipids used in lipofection. DOTMA (N-[1-(2,3-dioleoyloxy)propyl)-N,N,N-trimethylammonium chloride); DOGS (Spermine-5-carboxy-glicine dioctadecyl-amide); DC-Cholesterol (3β[N-(N′,N′-dimethylaminoethane) carbamoyl)-cholesterol); DOPE (L-dioleoyl phosphatidylethanolamine).

3.1.1.1. Lipofection Protocol

Since many variables affect the efficiency of lipofection, it is suggested that the conditions outlined in the following protocol be used as an initial point for systematic optimization of the system. Alternatively, a protocol recommended by a commercial manufacturer of a particular lipofectant could be used to begin the standardization process. The following protocol is based on the methodologies described by Sambrook and Russell (Sect. Recommended Reading) and on the method provided by Invitrogen Corporation (56).

Introducing plasmid DNA into PC12 cells by lipofection

1. PC12 cells are maintained in neurobasal media supplemented with 1% l-Glutamine, 10% FBS (fetal bovine serum) and 5%

HS (horse serum), and antibiotics (mixture of penicillin (100 U/mL), streptomycin (100 μg/mL), and fungizone (0.25 μg/mL)) – in a 5% CO_2 environment.

- The cells should be around 40–75% confluent at the time of lipofection. If the cells are grown for fewer than 12 h before transfection, they will not be well anchored to the substratum and are likely to detach during exposure to the lipid.

2. For each transfection sample in 96-well format, dilute 100 ng of plasmid DNA into serum-free medium. Add 0.1 μL of PLUS™ Reagent (Invitrogen) and incubate for 5 min.
3. Lipofectamine™ LTX Reagent (Invitrogen) is then added (transfection should be optimized by titrating the amount of the lipofection reagent) and gently mixed by pipetting up and down, and the lipid/DNA complex is allowed to form by incubating at room temperature for 30 min.
4. 20 μL of the DNA–lipid complex is added to each well of the 96-well plates containing cells, which should be in a serum-free medium.
   - It is very important to rinse the cells free of serum before the addition of the lipid–DNA complex. In some cases, serum is a very effective inhibitor of transfection process (57).
5. Incubate the cells for 1–24 h at 37°C in a 5% CO_2 environment.
6. After the cells have been exposed to the DNA for the appropriate time, wash them three times with serum-free medium. Feed the cells with complete medium and return them to the incubator.

As already mentioned, several variables affect the efficiency of lipofection. Thus, the presented protocol should be used as an initial point for systematic optimization. It is recommended to take into consideration:

(a) The density of the culture: Cell monolayers should be in mid-log phase and should be between 40 and 75% confluent.

(b) Amount of DNA added per dish: Depending on the concentration of the sequences of interest, as little as 50 ng and as much as 40 μg of DNA might be required to obtain maximum signal for a reporter gene.

(c) Time of exposure of cells to the cationic lipid–DNA complex: Varies from 0.1 to 24 h.

(d) Purity of the DNA preparation: Whenever possible, the DNA should be dissolved in water rather than buffers containing EDTA. Plasmid preparations used for lipofection should be free of bacterial lipopolysaccharides.

All of these variables must be optimized in order to establish optimal transfection frequencies for a target cell line. Although the

current lipofection methods/reagents allow for good transfection efficiencies in neural cell lines, the transfection efficiencies obtained with primary neuronal cells are still low.

3.1.2. Viral Methods

Adenoviral vectors are also useful for gene transfer due to a number of characteristics: (1) they infect a wide range of human cells and can achieve high levels of gene transfer compared to other vectors; (2) they accommodate relatively large segments of DNA (up to 7.5 kb) and transduce these transgenes in non-proliferating cells, such as neurons; and (3) adenoviral vectors are simple to manipulate using recombinant DNA techniques (58). Other vectors of interest (adeno-associated virus, herpes simplex virus, retroviruses) can infect quiescent cells, and can integrate into the host cell genome to allow stable, long-term expression. Of particular importance, recombinant lentiviral vectors have been described as powerful tools for gene transfer in the central nervous system, showing great potential as a gene therapy strategy for neurological disorders (59).

3.1.3. Physical Methods

Physical methods for delivering nucleic acids were developed in the early 1980s. Direct microinjection into cultured cells is an effective although laborious technique (60). Since the apparatus is costly and the technique extremely laborious, it is not an appropriate method for studies that require a great number of transfected cells.

Another physical method is biolistic particle delivery: Particle bombardment. This method is based on high velocity delivery of nucleic acids on microprojectiles to recipient cells by membrane penetration (61). This method has been successfully employed to deliver nucleic acid to cultured cells as well as to cells in vivo (62–64).

Electroporation was initially reported for gene transfection into mouse cells (65). This technique is normally used for cell types that are difficult to transfect by other methods. The method is based on perturbing the cell membrane by an electrical pulse, which forms transient pores that allow the entrance of nucleic acids into the cell (66). The technique needs optimization for duration and strength of the pulse for each type of cell used. In addition, electroporation generally requires more cells than chemical methods because of considerable cell death; it is necessary to balance transfection efficiency against cell viability.

To ascertain whether electroporation is a useful method of transfection for a particular cell type/line, it is important to use a range of field strengths and pulse lengths and thus establish conditions that generate the maximal number of transfectants. Several companies that sell electroporation devices offer lists of optimized conditions. However, because of variation in properties between different cultivars of the same cell type/line, it is important for the investigators to confirm that the conditions described in the literature are optimal for cells grown in their laboratory.

Since transfection and cell death are dependent on the field strength (67), it is recommendable to expose aliquots of cells to electric fields of increasing strength with time constants between 20 and 200 ms. For each field strength, measure (1) the number of cells that express the transfected reporter gene and (2) the proportion of cells that survive exposure to the electric field. Platting efficiency is a more accurate measure of cell survival than staining with vital dyes since, after electroporation, cells can remain permeable to vital dyes such as trypan blue for 1–2 h. There are other variables that affect the efficiency of electroporation.

(a) The temperature: Electroporation is usually carried out on cells that have been pre-chilled to 0°C. These cells are maintained at 0°C after electroporation (to maintain the pores in an open position) and are diluted into warm medium for plating (68).

(b) The concentration and the conformation of the DNA: Linear DNA is preferred for stable transformation and circular DNA is preferred for transient transfection (69, 70).

(c) The state of the cells: Best transfections are achieved with cell cultures in the mid-log phase of growth. This represents a limitation for primary cultured neurons.

3.1.3.1. Electroporation Protocol

A transfection protocol by electroporation (microporation) in mouse primary cerebellar granule cells follows next. Microporation is an electroporation technology in which a pipette tip is used to provide an electroporation space. Transfections were carried out using a Microporator Pipet-type Electroporation System device (Digital Bio Technology) and the optimal transfection efficiency was achieved by using a single pulse of 1,700 V during 20 ms.

1. Primary cerebellar granule cells are obtained from mice according to previously described methods (71).
2. After counting, cells are resuspended in buffer R medium (Digital Bio Technology) at a density of 3×10^7 cells/mL and placed on ice.
3. The plasmid DNA (pCIG-GFP) is added at a concentration of 50 μg/mL (5 μg/3×10^6 cells).
4. After mixing, the cell suspension remains on ice and an aliquot of 100 μL (3×10^6 cells) is taken for electroporation, using the pipette device.
5. The microporator pipette is inserted into pipette station and the electroporation is performed using a single pulse of 1,700 V for 20 ms.
    - For optimization, it is important to use a range of field strengths and pulse lengths and thereby establish conditions that generate the maximum number of transfectants for your conditions.

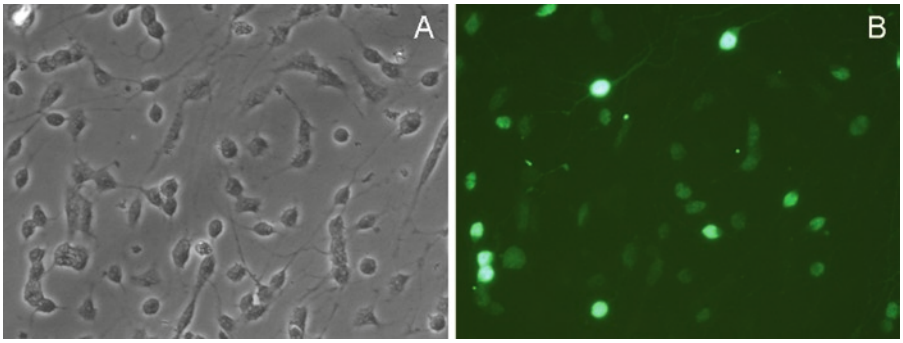

Fig. 8. Transfection of mouse cerebellar granule cells by electroporation. Mouse cerebellar granule cells were transfected by electroporation (microporation) with 5 μg of a plasmid encoding the EGFP. Forty-eight hours post-microporation, the cells were analyzed by phase contrast (**a**) and fluorescence microscopy (**b**).

6. After microporation with optimized electric parameter, the cells are immediately transferred into pre-warmed complete medium – Dulbecco's Modified Eagle Medium (DMEM) (25 mM KCl, 31 mM glucose and 0.2 mM glutamine) supplemented with *p*-aminobenzoate, insulin, penicillin, and 10% fetal calf serum.
7. The cell suspension (3.2×10^6 cells/mL) is seeded in multi-well plates precoated with poly-d-lysine and incubated at 37°C in a 5% CO_2 environment.
   - A mixture of 5 μM 5-fluoro-2′-deoxyuridine and 20 μM uridine should be added at 24 h after seeding to prevent glial proliferation.
8. GFP (in this case, encoded by the pCIG-GFP) is used as gene reporter (see Fig. 8). Transfection efficiency was around 80% in living cells. Cell viability was around 60%.
   - The number of electroporations depends on the number of required plates/wells. Consider to plate cells at a density of 3.2×10^6 cells/mL of the complete medium.
   - As already mentioned, several variables (temperature, DNA concentration, cell type) affect the efficiency of electroporation. Thus, the above protocol should be used as an initial point for systematic optimization.

3.2. Stable and Transient Transfection

Following the review of the most common transfection methods, next, we will discuss two different approaches for the delivery of nucleic acids into cultured neuronal cells: Transient transfection and stable transfection. In transient transfection, recombinant DNA is introduced in a recipient cell in order to obtain a temporary, but high-level expression of the target gene. The transfected DNA is not necessarily integrated into the host chromosome. Transient transfection is practical when a large number of samples are to be

analyzed within a short period of time. In general, the cells are harvested at few days after transfection and the resulting lysates can be assayed for expression of the target gene. This approach has been used to overexpress, at few days after transfection, genes that encode proteins involved in neurodegenerative (72) and neuroprotective events (73), as well as neurotransmission (74), antioxidant defenses (75), energetic metabolism (76), and several others physiological events related to the neuronal homeostasis.

Permanent or stable transfection is used to obtain cell lines in which the transfected gene is integrated into chromosomal DNA, allowing for the synthesis of moderate quantities of the target protein. In general, up to 90% of a population of cells expresses the transfected gene in a transient manner. At some point within the first hours after transfection, the transfected DNA undergoes non-homologous intermolecular recombination and ligation events in order to form a large structure that may integrate into the cellular chromosome (77).

Since the uptake, integration, and expression of DNA are infrequent events, *stable transformants* are generally isolated by selection of the cells that have acquired a new phenotype. This is commonly achieved by co-transfection with a second marker gene, which offers a selectable advantage, such as resistance against a certain antibiotic or drug. In the presence of the toxin in the cell culture, only those cells with the marker gene integrated into their genomes will proliferate and the other cells will die.

The most commonly used selection agent in permanent transfection experiments is Geneticin, also known as G418, which is a toxin that can be neutralized by the product of the neomycin resistant gene (aminoglycoside phosphotransferase) (78). In addition to aminoglycoside phosphotransferase, there are several other selection markers, such as hygromycin-B phosphotransferase (resistance to hygromycin-B) (79) and puromycin-*N*-acetyl transferase (resistance to puromycin) (80). Detailed methods for stable transfection are presented in the book by Sambrook and Russell (Sect. Recommended Reading).

3.2.1. Stable Transfectant Protocol

Here, we present an example of a stable transfectant protocol using PC12 cells and G418. The protocol is based on the study by Gollapudi and collaborators (81), which delves into the use of stable transfection of PC12 cells with the estrogen receptor (ERα) in order to detect protective effects.

1. PC12 cells are maintained in a "complete medium" – DMEM (Dulbecco's modified Eagle medium) containing 5% FBS (fetal bovine serum) and 10% HS (horse serum), 5 mM glutamine, and antibiotics (mixture of penicillin (100 U/mL), streptomycin (100 μg/mL), and fungizone (0.25 μg/mL)) – in a 5% CO_2 environment.
2. The cells are seeded at a concentration of 1.5×10^6 cells per well into collagen-polylysine-coated 6-well culture dishes.

They are allowed to adhere overnight, and the next day washed twice with serum-free DMEM.

3. The introduction of the plasmid DNA is mediated by lipofection. Transfection solution containing lipofection reagent and DNA (vector alone or vector ligated with ER cDNA) is carefully overlaid and incubated with the cells for 5 h.
   - For details on DNA transfection mediated by lipofection, please see Sect. 3.1.2.
   - The used plasmid DNA (vector pcDNA3) encodes the aminoglycoside phosphotransferase gene, which confers resistance to geneticin (G418).
4. After lipofection, cells are washed three times with serum-free medium. Next, complete medium is added and the cells are incubated for 4 days, with media being replaced every day.
5. To isolate stable transfectants, cells are trypsinized and replated in the selective medium (complete medium containing 500 μg/mL of G418).
6. Change this medium every 2–4 days for 2–3 weeks to remove the debris of death cells and to allow colonies of resistant cells to grow.
7. Individual colonies can be isolated by cloning cylinders, selected and transferred to multiwell plates for further propagation in the presence of selective medium.
   - Individual cells that survive the drug treatment expand into clonal groups that can be individually propagated and characterized.
   - To standardize a protocol, it is necessary to determine the killing concentration (kill curve) of the selective drug prior to transfection (82).

3.3. Analysis of Transfection Efficiency

As already mentioned, after transfection of cultured neuronal cells with a specific DNA sequence, it is important to determine the percentage of cells that have received and are expressing the foreign DNA. In addition, it is important to quantify the relative or absolute increases in the expression of the protein encoded by the transfected gene in the whole sample.

To quantify the expression of a given protein encoded by the transfected gene, semi-quantitative and quantitative methods can be used. Immunocytochemistry (83), western blot (1), flow cytometric analyses (84), and protein activity (85) can give a general view of the expression of the transfected gene.

In order to determine the percentage of transfected cells that have received and are expressing the foreign DNA sequence, a reporter gene can be used. The reporter gene can be present on the same vector as the gene of interest or it can be localized on a separate plasmid. As already stated, a convenient reporter for monitoring transfection efficiency is the GFP (see Sect. 2.1.1).

The typical image of cultured cells expressing GFP is presented in Fig. 8. For quantitative evaluations on the transfection efficiency, counts of the number of nuclei (DAPI) and cells expressing GFP should be conducted, deriving a percentage of the transfection efficiency. Notably, there are specific antibodies for GFP which allow its detection in cells even when low expression rates are achieved.

4. Applications of Gene Transfection to Study Neuropathology and Neurotoxicity

Advances in molecular cloning techniques have revolutionized over the last two to three decades, resulting in an explosion in the number of both in vitro and *in vivo* studies on the consequences of overexpression or deletion of specific proteins and their role in neurodegeneration or neurotoxicity (86–90). It is noteworthy that in contrast to the huge number of studies on the role of specific proteins in pathways that lead to cell death or dysfunctioning in chronic neurodegenerative diseases (i.e., Alzheimer and Parkinson's diseases), the number of studies on the modulatory role of specific proteins in neurotoxicity elicited by environmental neurotoxicants is relatively limited (1, 91, 92). The tools/protocols described in the previous sections of this chapter and the illustrative studies cited herein intend to provide basic information on how these techniques can potentially be used to advance the knowledge in the neuroscience field. We suggest that the use of the aforementioned techniques can simplify the task of studying complex signaling pathways upon exposure to different toxicants in the whole cell (neuronal) milieu. With a particular emphasis on the neurotoxicity induced by xenobiotics, genetically transformed neuronal cells can be considered a powerful tool for screening and identifying specific molecular targets and deciphering complex cascades of molecular events involved in either neurotoxic or neuroprotective events (1, 91).

4.1. Neurodegenerative Diseases

Several laboratories have taken advantage of genetically modifying different types of organisms, specific mammalian brain areas and/or cultured neuronal cells to clarify the role of putative key proteins as modulatory factors of different neuropathological conditions (73–75, 81, 86–90, 93). Next, we illustrate several examples on how the transfection of cultured neuronal cells can assist in elucidating the role played by specific proteins in neurodegenerative diseases and neurotoxicity induced by environmental neurotoxicants. Because of the large number of studies on these topics and due to space limitations, particular emphasis on Parkinson's disease and methylmercury-induced neurotoxicity is presented.

4.1.1. The Case of Parkinson's Disease (PD)

The intracellular deposition of misfolded proteins is believed to participate in age-related neurodegenerative diseases (93–95). For

instance, PD is associated with degeneration of dopaminergic neurons located in the *substantia nigra* and with the presence of inclusion bodies containing alpha-synuclein (89, 95). The exact role of alpha-synuclein misfolding in the neurotoxicity of PD is still unknown. However, in vitro and in vivo transfection models of neuronal cells overexpressing wild type or mutated alpha-synuclein have indicated that its aggregation can modify different intracellular processes and contribute to neuronal death (89, 96). Consistent with these observations, Lee and co-workers (97) have demonstrated that dorsal root ganglia neurons overexpressing alpha-synuclein exhibit microtubule dysfunction, neuritic degeneration, trafficking defects, and Golgi fragmentation, which are common features in other human neurodegenerative diseases. Hsu et al. have investigated the effects of alpha-synuclein overexpression in a hypothalamic neuronal cell line and in an analogous fashion observed that its overexpression resulted in formation of alpha-synuclein-immunopositive aggregates and mitochondrial dysfunction associated with increased formation of reactive oxygen species. They have also demonstrated that pretreatment with vitamin E ameliorated the alpha-synuclein-induced neuronal toxicity (98).

Another protein that is involved in PD etiology is parkin (89, 96) and data obtained with transfected neuronal cells have been fundamental in elucidating the antagonistic effect of wild-type parkin and the stimulatory effect of its mutants to PD development. For instance, Hyun et al. (99) have reported that neuronal toxicity and oxidative stress caused by different factors (serum withdrawal, H_2O_2, MPP(+), or 4-hydroxy-2-trans-nonenal) were attenuated by wild-type parkin overexpression. In contrast, overexpression of the mutant parkins increased cell death and oxidative stress markers in response to these stressors. Consequently, it was concluded that parkin mutation in *substantia nigra* in PD may increase neuronal vulnerability to a range of toxic insults, which could facilitate disease initiation and progression (99). In line with this in vitro study, in vivo rodent transgenic models have indicated a neuroprotective role for wild-type parkin, where overexpression of the gene decreased the responsiveness to alpha-synuclein-induced neuropathology (100).

4.2. Mechanisms of Neurotoxicity

Neurodegeneration is a complex process and represents a hallmark in a variety of acute and chronic human diseases (94). Although the cascade of events that occur in each disease can be unique, from the point of view of gross behavioral, cellular and molecular outcomes, the pathways that lead to the various diseases can have overlapping molecular mechanisms. For instance, oxidative stress is believed to underlie neuronal dysfunction in many neurodegenerative disorders (100–102), including those caused by environmental toxicants (91, 103). In this regard, a variety of studies have taken advantage of neuronal transfection with potentially toxic or protective key proteins to demonstrate that oxidative

stress and apoptosis can be a common modulators of neurodegeneration. For instance, primary cultures of neocortical neurons obtained from transgenic mice overexpressing human Bcl-2 under the control of neuron-specific enolase promoter were more resistant to the pro-oxidant and dopaminergic neurotoxin 6-OHDA than neurons from normal mice (104). These results indicate that the antiapoptotic Bcl-2 protein can modulate oxidative stress and dopaminergic cell death. In the same vein, overexpression Bcl-2 protects PC12 cells from 3-nitropropionic acid-induced hydrogen peroxide production, mitochondrial DNA damage, and cell death (105). However, Bcl-2 protection against apoptotic cell death and increased oxidative stress in dopaminergic PC12 cells was dependent on a definite level of expression. In fact, induction of high-level expression of Bcl-2 in PC12 cells resulted in generation of oxidative stress and cessation of growth by cell cycle arrest, suggesting that Bcl-2 expression is beneficial only in a limited range and that its high-level expression can cause neurotoxicity (106).

The relationship between environmental toxicants and neuropathological conditions represents an important topic that deserves particular consideration when neurotoxicity and neuropathology are analyzed from a mechanistic point of view. In fact, although genetic research has shown that particular gene variations predispose some individuals to neuropathologies, the role of the environment in the etiology of such conditions has become clearer (107). Of particular importance, the exposure of brain to environmental toxicants can trigger the activation of cytotoxic pathways that partially overlaps with those triggered by neurodegenerative diseases (108–110). Environmental toxicants, such as MPPT, 3-nitropropionic acid and toxic metals can cause oxidative stress and mitochondrial dysfunction (103, 108–111). In this regard, methylmercury (MeHg) is an environmental neurotoxicant that seems to cause neurotoxicity via disruption of multiple targets, which will culminate in mitochondrial dysfunction and oxidative stress (103). However, the exact role of specific targets in MeHg neurotoxicity is still not fully defined. We have observed that MeHg-induced neuronal cell death in cultured mouse cerebellar granule cells was preceded by a marked inhibition of the antioxidant enzyme glutathione peroxidase 1 (GPx1) (1) and that the overexpression of GPx1 prevented MeHg-induced neuronal death. These results indicate that GPx1 is an important molecular target involved in MeHg-induced neurotoxicity and reinforce the view that peroxides and oxidative stress are fundamental factors in MeHg toxicity. In accordance with this, Nrf2 overexpression attenuated MeHg-induced cytotoxicity in SH-SY5Y cells (112), which is in line with data showing a protective role for Nrf2 activation in astrocytes exposed to MeHg (113). Collectively, these data can help to explain the earlier demonstration that overexpression of metallothionein in cultured astrocytes affords

protection against the cytotoxic effects of MeHg (114), particularly, in view of the demonstration that metallothionein protected SH-SY5Y cells from the neurotoxic effects caused by 6-OHDA via activation of the Nrf-2 signaling pathway (115).

The illustrative and simplified examples presented above support an important role for oxidative stress and apoptosis in cell death caused by different neurotoxic agents and also an important role for antioxidant or antiapoptotic proteins as antagonists of neuropathology in different in vitro models. The development of transgenic cells that overexpress key proteins, such as GPx1, parkin and alpha-synuclein, among others, is a valuable tool for determining the molecular mechanisms involved in different neuropathological conditions. Furthermore, transgenic cells could be used to help neurotoxicologists in the difficult task of screening environmental toxicants with potential hazard for predisposition for neurodegenerative diseases in humans (116).

Acknowledgments

The authors would like to thank the agencies that support their research activities (in alphabetical order): Conselho Nacional de Desenvolvimento Científico e Tecnológico – CNPq and INCT for Excitotoxicity and Neuroprotection-MCT/CNPq, Brazil (Marcelo Farina and João B. T. Rocha); Fundação de Amparo à Pesquisa do Estado de Santa Catarina, Brazil (Marcelo Farina); NIH ES10563 and ES 07331 (Michael Aschner); Spanish Ministry of Education Grant BFU2008-02424/BFI (Sebastián Pons). Jordi Berenguer is a FPI fellow in Sebastián Pons laboratory (fellowship also supported by the Spanish Ministry of Education Grant BFU2008-02424/BFI).

References

1. Farina M, Campos F, Vendrell I, Berenguer J, Barzi M, Pons S, Suñol C (2009) Probucol increases glutathione peroxidase-1 activity and displays long-lasting protection against methylmercury toxicity in cerebellar granule cells. Toxicol Sci 112:416–26
2. Anderson S, Davis DL, Dahlbäck H, Jörnvall H, Russell DW (1989) Cloning, structure and expression of the mitochondrial cytochrome p-450 sterol 26-hydrolase, a bile acid biosynthethic enzyme. J Biol Chem 264:8222–29
3. Boshart M, Weber F, Jahn G, Dorsch-Häsler K, Fleckenstein B, Schafner W (1985) A very strong enhancer is located upstream of an immediate early gene of human cytomegalovirus. Cell 41:521–30
4. Nelson JA, Reynolds-Kohler C, Smith BA (1987) Negative and positive regulation by a short segment in the 5′ flanking region of the human cytomegalovirus major immediate-early gene. Mol Cell Biol 7:4125–29
5. Cereghini S, Herbomel P, Jouanneau J, Saragosti S, Katinka M, Bourachot B, de Crombrugghe B, Yaniv M (1983) Structure and function of the promoter-enhancer region of Polyoma and SV40. Cold Spring Harb Symp Quant Biol 47:935–44
6. Cheng L, Ziegelhoffer PR, Yang NS (1993) In vivo promoter activity and transgene expression in mammalian somatic tissues evaluated by particle bombardment. Proc Nat Acad Sci USA 90:4455–59

7. Herskowitz I (1987) Functional inactivation of genes by dominant negative mutations. Nature 329:219–22
8. Sheppard D (1994) Dominant negative mutants: tools for the study of protein function in vitro and in vivo. Am J Respir Cell Mol Biol 11:1–6
9. Wood KV, de Wet JR, Dewji N, DeLuca M (1984) Synthesis of active firefly luciferase by in vitro translation of RNA obtained from adult lanterns. Biochem Biophys Res Commun 124:592–6
10. de Wet JR, Wood KV, Helinski DR, DeLuca M (1985) Cloning of firefly luciferase cDNA and the expression of active luciferase in *Escherichia coli*. Proc Natl Acad Sci USA 82:7870–3
11. Vieites JM, Navarro-García F, Pérez-Diaz R, Pla J, Nombela C (1994) Expression and in vivo determination of firefly luciferase as gene reporter in Saccharomyces cerevisiae. Yeast 10:1321–27
12. Gailey PC, Miller EJ, Griffin GD (1997) Low-cost system for real-time monitoring of luciferase gene expression. Biotechniques 22:528–34
13. Cohen SN, Chang AC, Boyer HW, Helling RB (1973) Construction of biologically functional bacterial plasmids in vitro. Proc Nat Acad Sci USA 70:3240–4
14. Dussoix D, Arber W (1962) Host specificity of DNA produced by *Escherichia coli*. I. Host controlled modification of bacteriophage lambda. J Mol Biol 5:18–36
15. Dussoix D, Arber W (1962) Host specificity of DNA produced by *Escherichia coli*. II. Control over acceptance of DNA from infecting phage lambda. J Mol Biol 5:37–49
16. Boyer H (1964) Genetic control of restriction and modification in *Escherichia coli*. J Bacteriol 88:1652–60
17. Meselson M, Yuan R (1968) DNA restriction enzyme from *E. coli*. Nature 217:1110–14
18. Arber W, Linn S (1969) DNA modification and restriction. Ann Rev Biochem 38:467–500
19. Smith HO, Wilcox KW (1970) A restriction enzyme from *Haemophilus influenzae*. I. Purification and general properties. J Mol Biol 51:379–91
20. Kelly TJ, Smith HO (1970) A restriction enzyme from *Haemophilus influenzae*. II. Base sequence of the recognition site. J Mol Biol 51:393–409
21. Hattman S, Brooks JE, Masurekar M (1978) Sequence specificity of the P1 modification methylase (M.Eco P1) and the DNA methylase (M.Eco dam) controlled by the Escherichia coli dam gene. J Mol Biol 126:367–80
22. Wilson GG (1991) Organization of restriction-modification systems. Nucleic Acids Res 19:2539–66
23. Tomkinson AE, Vijayakumar S, Pascal JM, Ellenberger T (2006) DNA ligases: structure, reaction mechanism, and function. Chem Rev 106:687–99
24. Olivera BM, Hall ZW, Lehman IR (1968) Enzymatic joining of polynucleotides. V. A DNA adenylate intermediate in the polinucleotide joining reaction. Proc Nat Acad Sci USA 61:237–44
25. Gumport RI, Lehman IR (1971) Structure of the DNA ligase-adenylate intermediate: lysine (epsilon-amino)-linked adenosine monophosphoramidate. Proc Nat Acad Sci USA 68:2559–63
26. Griffith F (1928) The significance of pneumococcal types. J Hyg 27:113–159
27. Mandel M, Higa A (1970) Calcium-dependent bacteriophage DNA infection. J Mol Biol 53:159–62
28. Cohen SN, Chang ACY, Hsu L (1972) Nonchromosomal antibiotic resistance in bacteria: genetic transformation of Escherichia coli by R-Factor DNA. Proc Nat Acad Sci USA 69:2110–14
29. Klebe RJ, Harriss JV, Sharp ZD, Douglas MG (1983) A general method for polyethyleneglycol-induced genetic transformation of bacteria and yeast. Gene 25:333–41
30. Chung CT, Miller RH (1988) A rapid and convenient method for the preparation and storage of competent bacterial cells. DNA 7:609–15
31. Mullis KB, Faloona F, Scharf S, Saiki R, Horn G, Erlich H (1986) Specific enzymatic amplification of DNA in vitro: the polymerase chain reaction. Cold Spring Harb Symp Quant Biol 51:263–73
32. Mullis KB, Faloona FA (1987) Specific synthesis of DNA in vitro via a polymerase-catalyzed chain reaction. Methods Enzymol 155:335–50
33. Saiki RK, Gelfand DH, Stoffel S, Scharf SJ, Higuchi R, Horn GT, Mullis KB, Erlich HA (1988) Primer-directed enzymatic amplification of DNA with a thermostable DNA polymerase. Science 29:487–91
34. Brock TD, Freeze H (1969) *Thermus aquaticus* gen. n. and sp. n., a nonsporulating extreme thermophile. J Bacteriol 98:289–97
35. Suggs SV, Wallace RB, Hirose T, Kawashima EH, Itakura K (1981) Use of synthetic oligonucleotides as hybridization probes: isolation

of cloned cDNA sequences for human beta 2-microglobulin. Proc Natl Acad Sci USA 78:6613–7

36. Thein SL, Wallace RB (1986) The use of synthetic oligonucleotides as specific hybridization probes in the diagnosis of genetic desorders. In: Davies KE (ed) Human genetic diseases: a practical approach. IRL, Oxford, pp 33–50
37. Bickley J, Hopkins D (1999) Inhibitors and enhancers of PCR. Quality and Validation, eds Saunders, G.C., and Parkes, H.C., Royal Society of Chemistry, London, Chapter in Analytycal Molecular Biology, pp 81–102
38. Kunkel TA, Roberts JD, Zakour RA (1987) Rapid and efficient site-specific mutagenesis without phenotypic selection. Methods Enzymol 154:367–82
39. Higuchi R, Krummel B, Saiki RK (1988) A general method of in vitro preparation and specific mutagenesis of DNA fragments: study of protein and DNA interactions. Nucleic Acids Res 16:7351–67
40. Washbourne P, McAllister AK (2002) Techniques for gene transfer into neurons. Curr Opin Neurobiol 12:566–73
41. Dahm R, Zeitelhofer M, Gotze B, Kiebler MA, Macchi P (2008) Visualizing mRNA localization and local protein translation in neurons. Methods Cell Biol 85:293–327
42. Goetze B, Grunewald B, Baldassa S, Kiebler M (2004) Chemically controlled formation of a DNA/calcium phosphate coprecipitate: application for transfection of mature hippocampal neurons. J Neurobiol 60:517–25
43. Pagano JS, Vaheri A (1965) Enhancement of infectivity of poliovirus RNA with diethylaminoethyl-dextran (DEAE-D). Arch Gesamte Virusforsch 17:456–64
44. McCutchan JH, Pagano JS (1968) Enchancement of the infectivity of simian virus 40 deoxyribonucleic acid with diethylaminoethyl-dextran. J Natl Cancer Inst 41:351–7
45. Gluzman Y (1981) SV40-transformed simian cells support the replication of early SV40 mutants. Cell 23:175–82
46. Kawai S, Nishizawa M (1984) New procedure for DNA transfection with polycation and dimethyl sulfoxide. Mol Cell Biol 4:1172–4
47. Boussif O, Lezoualc'h F, Zanta MA, Mergny MD, Scherman D, Demeneix B, Behr JP (1995) A versatile vector for gene and oligonucleotide transfer into cells in culture and in vivo: polyethylenimine. Proc Natl Acad Sci USA 92:7297–301
48. Haensler J, Szoka FC Jr (1993) Polyamidoamine cascade polymers mediate efficient transfection of cells in culture. Bioconjug Chem 4:372–9
49. Kukowska-Latallo JF, Bielinska AU, Johnson J, Spindler R, Tomalia DA, Baker JR Jr (1996) Efficient transfer of genetic material into mammalian cells using Starburst polyamidoamine dendrimers. Proc Natl Acad Sci USA 93:4897–902
50. Graham FL, van der Eb AJ (1973) A new technique for the assay of infectivity of human adenovirus 5 DNA. Virology 52:456–67
51. Fraley R, Papahadjopoulos D (1982) Liposomes: the development of a new carrier system for introducing nucleic acid into plant and animal cells. Curr Top Microbiol Immunol 96:171–91
52. Felgner PL, Gadek TR, Holm M, Roman R, Chan HW, Wenz M, Northrop JP, Ringold GM, Danielsen M (1987) Lipofection: a highly efficient, lipid-mediated DNA-transfection procedure. Proc Natl Acad Sci USA 84:7413–7
53. Labat-Moleur F, Steffan AM, Brisson C, Perron H, Feugeas O, Furstenberger P, Oberling F, Brambilla E, Behr JP (1996) An electron microscopy study into the mechanism of gene transfer with lipopolyamines. Gene Ther 3:1010–7
54. Gao X, Huang L (1995) Cationic liposome-mediated gene transfer. Gene Ther 2:710–22
55. Farhood H, Bottega R, Epand RM, Huang L (1992) Effect of cationic cholesterol derivatives on gene transfer and protein kinase C activity. Biochim Biophys Acta 1111:239–46
56. Invitrogen Corporation. BioTechniques Protocol Guide (2009) Transfection of PC12 Cells with lipofectamine™ LTX does not affect their ability to differentiate upon NGF stimulation. 33, doi: 10.2144/000113028
57. Felgner PL, Holm M, Chan H (1989) Cationic liposome mediated transfection. Proc West Pharmacol Soc 32:115–21
58. Vorburger SA, Hunt KK (2002) Adenoviral gene therapy. Oncologist 7:46–59
59. Lundberg C, Björklund T, Carlsson T, Jakobsson J, Hantraye P, Déglon N, Kirik D (2008) Applications of lentiviral vectors for biology and gene therapy of neurological disorders. Curr Gene Ther 8:461–73
60. Capecchi MR (1980) High efficiency transformation by direct microinjection of DNA into cultured mammalian cells. Cell 22:479–88
61. Ye GN, Daniell H, Sanford JC (1990) Optimization of delivery of foreign DNA into higher-plant chloroplasts. Plant Mol Biol 15:809–19
62. Klein TM, Fromm M, Weissinger A, Tomes D, Schaaf S, Sletten M, Sanford JC (1988)

Transfer of foreign genes into intact maize cells with high-velocity microprojectiles. Proc Natl Acad Sci USA 85:4305–4309

63. Burkholder JK, Decker J, Yang NS (1993) Rapid transgene expression in lymphocyte and macrophage primary cultures after particle bombardment-mediated gene transfer. J Immunol Methods 165:149–56
64. Ogura R, Matsuo N, Wako N, Tanaka T, Ono S, Hiratsuka K (2005) Multi-color luciferases as reporters for monitoring transient gene expression in higher plants. BMC Biotechnol 22:151–5
65. Wong TK, Neumann E (1982) Electric field mediated gene transfer. Biochem Biophys Res Commun 107:584–7
66. Shigekawa K, Dower WJ (1988) Electroporation of eukaryotes and prokaryotes: a general approach to the introduction of macromolecules into cells. Biotechniques 6:742–51
67. Chu G, Hayakawa H, Berg P (1987) Electroporation for the efficient transfection of mammalian cells with DNA. Nucleic Acids Res 15:1311–26
68. Rabussay D, Uher L, Bates G, Piastuch W (1987) Electroporation of mammalian and plant cells. Focus (Life Technol) 9:1–3
69. Neumann E, Schaefer-Ridder M, Wang Y, Hofschneider PH (1982) Gene transfer into mouse lyoma cells by electroporation in high electric fields. EMBO J 1:841–5
70. Potter H, Weir L, Leder P (1984) Enhancer-dependent expression of human kappa immunoglobulin genes introduced into mouse pre-B lymphocytes by electroporation. Proc Natl Acad Sci USA 81:7161–5
71. Alvarez-Rodriguez R, Barzi M, Berenguer J, Pons S (2007) Bone morphogenetic protein 2 opposes Shh-mediated proliferation in cerebellar granule cells through a TIEG-1-based regulation of Nmyc. J Biol Chem 282:37170–80
72. Ting JT, Kelley BG, Lambert TJ, Cook DG, Sullivan JM (2007) Amyloid precursor protein overexpression depresses excitatory transmission through both presynaptic and postsynaptic mechanisms. Proc Natl Acad Sci USA 104:353–8
73. Monje ML, Phillips R, Sapolsky R (2001) Calbindin overexpression buffers hippocampal cultures from the energetic impairments caused by glutamate. Brain Res 911:37–42
74. Rintoul GL, Raymond LA, Baimbridge KG (2001) Calcium buffering and protection from excitotoxic cell death by exogenous calbindin-D28k in HEK 293 cells. Cell Calcium 29:277–87
75. Haque ME, Asanuma M, Higashi Y, Miyazaki I, Tanaka K, Ogawa N (2003) Overexpression of Cu-Zn superoxide dismutase protects neuroblastoma cells against dopamine cytotoxicity accompanied by increase in their glutathione level. Neurosci Res 47:31–7
76. Gimenez-Cassina A, Lim F, Cerrato T, Palomo GM, Diaz-Nido J (2009) Mitochondrial hexokinase II promotes neuronal survival and acts downstream of glycogen synthase kinase-3. J Biol Chem 284:3001–11
77. Perucho M, Hanahan D, Wigler M (1980) Genetic and physical linkage of exogenous sequences in transformed cells. Cell 22:309–17
78. Maisonhaute C, Echalier G (1986) Stable transformation of Drosophila Kc cells to antibiotic resistance with the bacterial neomycin resistance gene. FEBS Lett 197:45–9
79. Blochlinger K, Diggelmann H (1984) Hygromycin B phosphotransferase as a selectable marker for DNA transfer experiments with higher eukaryotic cells. Mol Cell Biol 4:2929–31
80. Vara JA, Portela A, Ortin J, Jimenez A (1986) Expression in mammalian cells of a gene from *Streptomyces alboniger* conferring puromycin resistance. Nucleic Acids Res 14:4617–24
81. Gollapudi L, Oblinger MM (1999) Stable transfection of PC12 cells with estrogen receptor (ERalpha): protective effects of estrogen on cell survival after serum deprivation. J Neurosci Res 56:99–108
82. Ausubel FM, Brent R, Kingston RE, Moore DD, Seidman JG, Smith, JA, Struhl K (1999) Short protocols in molecular biology, 4th edn (Paperback). John Wiley & Sons, Inc. New York
83. Domingues A, Almeida S, da Cruz e Silva EF, Oliveira CR, Rego AC (2007) Toxicity of beta-amyloid in HEK293 cells expressing NR1/NR2A or NR1/NR2B *N*-methyl-D-aspartate receptor subunits. Neurochem Int 50:872–880
84. Chong KW, Lee AY, Koay ES, Seet SJ, Cheung NS (2006) pH dependent high transfection efficiency of mouse neuroblastomas using TransFectin. J Neurosci Methods 158:56–63
85. Huang RQ, Qu YH, Ke WL, Zhu JH, Pei YY, Jiang C (2007) Efficient gene delivery targeted to the brain using a transferrin-conjugated polyethyleneglycol-modified polyamidoamine dendrimer. FASEB J 21:1117–25
86. Gabizon R, Taraboulos A (1997) Of mice and (mad) cows-transgenic mice help to understand prions. Trends Genet 13:264–9

87. Kirik D, Björklund A (2003) Modeling CNS neurodegeneration by overexpression of disease-causing proteins using viral vectors. Trends Neurosci 26:386–92
88. Kobayashi Y, Sobue G (2001) Protective effect of chaperones on polyglutamine diseases. Brain Res Bull 56:165–8
89. Moore DJ, West AB, Dawson VL, Dawson TM (2005) Molecular pathophysiology of Parkinson's disease. Annu Rev Neurosci 28:57–87
90. Rockenstein E, Crews L, Masliah E (2007) Transgenic animal models of neurodegenerative diseases and their application to treatment development. Adv Drug Deliv Rev 59:1093–102
91. Kitazawa M, Anantharam V, Kanthasamy AG (2003) Dieldrin induces apoptosis by promoting caspase-3-dependent proteolytic cleavage of protein kinase Cδ in dopaminergic cells: Relevance to oxidative stress and dopaminergic degeneration. Neuroscience 119:945–64
92. Thiruchelvam M, Prokopenko O, Cory-Slechta DA, Richfield EK, Buckley B, Mirochnitchenko O (2005) Overexpression of superoxide dismutase or glutathione peroxidase protects against the paraquat plus maneb-induced Parkinson disease phenotype. J Biol Chem 280:22530–9
93. Zoghbi HY, Botas J (2002) Mouse and fly models of neurodegeneration. Trends Genet 18:463–71
94. Jellinger KA (2009) Recent advances in our understanding of neurodegeneration. J Neural Transm 116:1111–62
95. Lee SJ (2003) Alpha-synuclein aggregation: a link between mitochondrial defects and Parkinson's disease? Antioxid Redox Signal 5:337–48
96. Di Napoli M (2009) New molecular avenues in Parkinson's disease therapy. New molecular avenues in Parkinson's disease therapy. Curr Top Med Chem 9:913–48
97. Lee HJ, Khoshaghideh F, Lee S, Lee SJ (2006) Impairment of microtubule-dependent trafficking by overexpression of alpha-synuclein. Eur J Neurosci 24:3153–62
98. Hsu LJ, Sagara Y, Arroyo A, Rockenstein E, Sisk A, Mallory M, Wong J, Takenouchi T, Hashimoto M, Masliah E (2000) alpha-synuclein promotes mitochondrial deficit and oxidative stress. Am J Pathol 157:401–10
99. Hyun DH, Lee M, Halliwell B, Jenner P (2005) Effect of overexpression of wild-type or mutant parkin on the cellular response induced by toxic insults. J Neurosci Res 82:232–44
100. Lo Bianco C, Schneider BL, Bauer M, Sajadi A, Brice A, Iwatsubo T, Aebischer P (2004) Lentiviral vector delivery of parkin prevents dopaminergic degeneration in an alpha-synuclein rat model of Parkinson's disease. Proc Nat Acad Sci USA 101:17510–5
101. Reynolds A, Laurie C, Mosley RL, Gendelman HE (2007) Oxidative stress and the pathogenesis of neurodegenerative disorders. Int Rev Neurobiol 82:297–325
102. Moreira PI, Zhu X, Wang X, Lee H-g, Nunomura A, Petersen RB, Perry G (2010) Mitochondria: a therapeutic target in neurodegeneration. Biochim Biophys Acta 1802:212–20
103. Aschner M, Syversen T, Souza DO, Rocha JBT, Farina M (2007) Involvement of glutamate and reactive oxygen species in methylmercury neurotoxicity. Braz J Med Biol Res 40:285–91
104. Offen D, Beart PM, Cheung NS, Pascoe CJ, Hochman A, Gorodin S, Melamed E, Bernard R, Bernard O (1998) Transgenic mice expressing human Bcl-2 in their neurons are resistant to 6-hydroxydopamine and 1-methyl-4-phenyl-1, 2, 3, 6-tetrahydropyridine neurotoxicity. Proc Nat Acad Sci USA 95:6789–94
105. Mandavilli BS, Boldogh I, Van Houten B (2005) 3-Nitropropionic acid-induced hydrogen peroxide, mitochondrial DNA damage, and cell death are attenuated by Bcl-2 overexpression in PC12 cells. Mol Brain Res 133:215–23
106. Seyfried J, Evert BO, Schwarz CS, Schaupp M, Schulz JB, Klockgether T, Wüllner U (2003) Gene dosage-dependent effects of bcl-2 expression on cellular survival and redox status. Free Radic Biol Med 34:1517–30
107. Schmidt CW (2007) Environmental connections: a deeper look into mental illness. Environ Health Perspect A404:A406–10
108. Kotake Y, Ohta S (2003) MPP plus analogs acting on mitochondria and inducing neurodegeneration Cur. Med Chem 10:2507–2516
109. do Nascimento JLM, Oliveira KRM, Crespo-Lopez ME, Macchi BM, Maues LAL, Pinheiro MDN, Silveira LCL, Herculano AM (2008) Methylmercury neurotoxicity and antioxidant defenses. Ind J Med Res 128:373–82
110. Quintanilla RA, Johnson GVW (2009) Role of mitochondrial dysfunction in the pathogenesis of Huntington's disease. Brain Res Bull 80:242–47

111. Valko M, Rhodes CJ, Moncol J, Izakovic M, Mazur M (2006) Free radicals, metals and antioxidants in oxidative stress-induced cancer. Chem Biol Interact 160:1–40
112. Toyama T, Sumi D, Shinkai Y, Yasutake A, Taguchi K, Tong KI, Yamamoto and M, Kumagai Y (2007) Cytoprotective role of Nrf2/Keap1 system in methylmercury toxicity. Biochem Biophys Res Commun 363:645–50
113. Wang L, Jiang HY, Yin ZB, Aschner M, Cai JY (2009) Methylmercury toxicity and Nrf2-dependent detoxification in astrocytes. Toxicol Sci 107:135–43
114. Yao CP, Allen JW, Conklin DR, Aschner M (1999) Brain Res 818:414–20
115. Hwang YP, Kim HG, Han EH, Jeong HG (2008) Metallothionein-III protects against 6-hydroxydopamine-induced oxidative stress by increasing expression of heme oxygenase-1 in a PI3K and ERK/Nrf2-dependent manner. Toxicol Appl Pharmacol 231:318–27
116. Forsby A, Bal-Price AK, Coecke S, Fabre N, Gustafsson H, Honegger P, Kinsner-Ovaskainen A, Pallas M, Rimbau V, Rodriguez-Farre E, Sunol C, Vericat JA, Zurich MG (2009) Neuronal in vitro models for the estimation of acute systemic toxicity. Toxicol In Vitro 23:1564–69

Recommended Reading

Sambrook J, Russell D (2001) Molecular cloning: a laboratory manual (Hardcover), 3rd edn. Cold Spring Harbor Laboratory, New York

Primrose SB, Twyman RM (2007) Principles of gene manipulation and genomics, 7th edn. Blackwell Publishing, Oxford, UK

Glick BR, Pasternak JJ (2003) Molecular biotechnology. Principles and applications of recombinant DNA, 3rd edn. ASM Press, Washington DC

Brown TA (2008) Gene cloning and DNA analysis, 5th edn. Blackwell Publishing, Oxford, UK

Chapter 10

P19 Embryonic Carcinoma Cell Line: A Model To Study Gene–Environment Interactions

Joseph Bressler, Cliona O'Driscoll, Cathleen Marshall, and Walter Kaufmann

Abstract

In studies on pluripotency and differentiation, teratocarcinoma cell lines have been used as alternatives to mouse embryonic stem cell lines. Teratocarcinoma cell lines cost less to maintain and they are easier to genetically manipulate. Their disadvantage, of course, is being derived from a tumor, which prevents their use in certain types of studies such as in implantation and proliferation. The P19 cell line is one of the better studied teratocarcinoma cell lines, being first introduced in 1982. The cells express the same transcription factors for pluripotency maintenance as embryonic stem cells but do not require specialized media or feeder cells. Dimethylsulfoxide induces P19 cells to smooth muscle cells and beating cardiomyocytes, whereas, retinoic acid causes P19 cells to differentiate into functional neurons complete with synapses with specific neurotransmitter phenotypes. Excellent transfection efficiencies can be achieved with the less expensive calcium phosphate method though the more expensive commercially developed reagents also work well. Consequently, transient expression of genes or knocking down gene expression with siRNA is straightforward. Furthermore, establishing stable cell lines with these changes in gene expression is also quite feasible. The procedures for taking advantage of these properties of P19 cells in studies on differentiation and toxicology will be discussed in this chapter.

Key words: Pluripotency, Differentiation, P19 cells, Neurons, Muscle

1. Introduction

Embryonic stem cell lines are a versatile and exciting tool, because of their pluripotency, but they have distinct disadvantages namely cost, time, and difficulty to establish. In order to overcome these disadvantages without losing all the benefits of pluripotent stem cells, we have been using the P19 embryonic carcinoma cell lines as a model for studying gene environment interactions. The P19 embryonic carcinoma cell line, first derived in 1983, displays pluripotency in an easy to manipulate cell line. In this chapter, the advantages and disadvantages of the P19 cell line and other model

Michael Aschner et al. (eds.), *Cell Culture Techniques*, Neuromethods, vol. 56,
DOI 10.1007/978-1-61779-077-5_10,

systems will be discussed. Our interests in gene–environment interactions come from the need to better understand neurodevelopmental disorders. While there are few reports on the effect of toxicants on gene expression during human neurodevelopment, the contribution of environmental factors and genetics in autism and schizophrenia has been documented (1–3). The importance of gene–environment interactions has been extensively documented in cancer but only recently have studies demonstrating its importance in neurological diseases. For example, the risk of Parkinson's disease increases in agricultural workers who harbor certain polymorphisms in the dopamine transporter (4, 5). Phenylketonuria, an inability to metabolize proteins resulting in neurodevelopmental deficits, is yet another example of how the environment can have far reaching consequences (6).

Our specific interests have been determining sensitivity to environmental factors in individuals harboring mutations and polymorphisms in the *MECP2* gene. Mutations in *MECP2* are known to cause Rett syndrome (RTT) and abnormal expression of Mecp2 have been found in the brain of autistic children (7). Several polymorphisms and over 200 mutations have been identified throughout the *MECP2* gene though seven recurrent mutations accounting for more than two-thirds (70%) of RTT cases in whom an *MECP2* gene mutation is characterized (8, 9). Clinically, different mutations are associated with phenotypes of differing profile and severity (9–11), which is thought to be due to effects on specific functional domains and overall protein function. Mecp2 is composed of three domains: the methyl-CpG binding domain, the transcriptional repression domain, and a C-terminal domain with two nuclear localization signals. The methyl-CpG binding domain specifically binds to methylated CpG dinucleotides, with preference for CpG sequences with adjacent A/T-rich motifs though binding to unmethylated DNA has been observed. The transcriptional repression domain is involved in transcriptional repression through recruitment of corepressors and chromatin remodeling complexes. The C-terminus facilitates MeCP2 binding to naked DNA and to the nucleosomal core, and it also contains evolutionarily conserved poly-proline runs that can bind to group II WW domain splicing factors (12, 13).

In the CNS, MECP2 expression coincides with the later stages of neuronal differentiation. Furthermore, several lines of evidence, including pattern of induction, induction of brain-derived neurotrophic factor, and obvious clinical manifestation after age 6 months, suggest that Mecp2 is involved in synaptic plasticity (12, 14). The fact that the phenotype in Mecp2 null mice can be rescued by reintroduction of Mecp2 supports its' role in neuronal plasticity (15, 16). Nonetheless, *MECP2* mutations and/or polymorphisms could also affect earlier

developmental processes. Indeed, Mecp2 inhibits astrocyte differentiation and promotes neuronal differentiation in neural precursor cells when ectopically expressed (17). Furthermore, *MECP2* mutations could have indirect effects on brain development by affecting the immune response. Indeed, nuclear factor kappa B cell signaling, which regulates cytokine responses, is affected by Mecp2 expression in the liver (18) and increased autoimmune reactions have been shown in individuals harboring *MECP* mutations (19).

2. Cell Lines

2.1. Neural-Derived Cell Lines to Study Mecp2

A number of approaches can be taken to study the functional consequences of *MECP2* mutations and polymorphisms; the choice depends largely on the question being addressed. Mouse models are helpful for studying neurobehavior and complex cell interactions but are expensive and time consuming to develop. Cell lines are more commonly employed because they are generally less expensive and techniques are readily available to manipulate gene expression. Conceptually, a human cell line should be considered because of possible species differences. Many human cell lines are available to study neural differentiation in response to differentiating factors such as retinoic acid (RA), soluble second messages, and neurotrophic factors. A consideration, often overlooked, is the embryological and anatomical origin of cell lines. Many human neuronal cell lines are derived from neuroblastomas, tumors of the peripheral nervous system, and may not be able to express properties of neurons in the central nervous system (CNS). Many also fail to express the properties of mature neurons such as action potentials, neurotransmitter biosynthesis, and receptors. Even many rodent neuroblastoma cell lines, which were derived from chemically induced brain tumors, fail to express properties of mature neurons even after undergoing differentiation. More recently, human neuronal cell lines have been developed by transducing human neural stem cells with viral vectors carrying the gene for myc transcription factor (20), or mutated myc that has lost its' transforming ability, resulting in highly differentiated neurons. For example, overexpressing myc in human primary cells from developing cortex and mesencephalon has produced stable neural stem cell lines that differentiate into dopaminergic neurons capable of firing action potentials (21). Furthermore, a stable neural human stem cell line has been developed with a myc viral construct that displays self-renewal ability and can be induced to well-differentiated oligodendrocytes, astrocytes, and neurons (22).

2.2. Embryonic Stem Cell Lines

Pluripotent embryonic stem cell lines are a good choice if the goal is to examine the progression of events starting prior to commitment to a neural lineage and ending in neurotransmitter specific neurons forming synapses. Techniques have been developed to induce well-differentiated neurons from mouse and human embryonic stem cell lines. Indeed, glutamatergic, dopaminergic (23, 24), and cholinergic (25) derived neurons capable of forming synapses can be studied. These pluripotent stem cells derived from the blastocyst provide a model for studying the progression of events that take place from early stages of embryogenesis to well-differentiated neurons. Unlike conventional cell lines, pluripotent cell lines are difficult to derive, and require culture conditions designed to maintain growth and pluripotency. To uniformly overexpress or knockdown gene expression, viral vectors need to be constructed to introduce the gene to the cell population (26). Alternatively, induced pluripotent stem (IPS) cells can be derived directly from patients harboring mutations. Similar to embryonic stem cells, IPS cells can be stimulated to undergo differentiation to neuronal subtypes that are capable of expressing action potentials (27). Thus, it is not necessary to genetically manipulate IPS cell line if the study's objective is to study mutations in patients. IPS cells are, however, not completely similar to human embryonic stem cells. For example, a recent study found that the DNA methylation pattern of IPS cells differs both from those of the parent somatic cells and from those of the human embryonic stem cells (28). The maintenance of pluripotent embryonic and IPS cell lines is time-consuming and costly, due to growth requirements and the tendency of the cells to undergo spontaneous differentiation. New advances in culture techniques and vector construction could potentially make it easier and bring down the cost (29).

2.3. Human Teratocarcinoma Cell Lines

Teratocarcinomas are another potential source of pluripotent stem cell lines. Teratocarcinomas are comprised of a heterogenous group of cells (somatic, extraembryonal and small quantities of embryonic carcinoma (EC) cells) of which the EC is considered to be the cancer stem cell (30, 31). The human pluripotent clonal TERA-1 cell line was derived by cloning the embryonic carcinoma cells from a teratocarcinoma (32). The EC cells have a high potential for self-renewal, and are capable of forming a new tumor if injected into a host. Most importantly, the cell lines do not require the strict growth conditions needed for embryonic stem cells and clonal cell lines can be established. Pluripotency is demonstrated by the presence of cell types from the different embryological layers, endoderm, mesoderm, and ectoderm, in tumors formed by injecting the cells in nude mice. The demonstration of pluripotency in vivo has been the hallmark of pluripotent cell lines, though biomarkers such as the expression of transcription

factors, such as Oct4 or Nanog, can also be considered valid. Little work has been published demonstrating pluripotency of the TERA-1 cell line in vitro. Rather, the NT2 cell line was cloned from the TERA-1 cell line and has been mostly used for studying neuronal differentiation in response to RA (33). Although NT2 cell line is derived from a clone, NT2-derived neurons are heterogeneous. These neurons express glutamate (34) and gamma-amino-butyric acid receptors (GABA) (35) as well as synthesize acetylcholine (36) and GABA. However, a dopaminergic phenotype has not been observed (37, 38). Most interesting, differentiated neurons derived from the NT2 cells make synapses and display pre-synaptic vesicles and synaptic vesicle-associated proteins such as synaptobrevin, synaptophysin, and synapsin (39). NT2-derived neurons also express L, N, P/Q, and R-type Ca^{2+} channels that are recruited for neurotransmission (40, 41) and generate low-amplitude slow-action potentials, with characteristics that are nearly identical to those of primary neurons in the CNS (42).

A distinct advantage of the NT2 cell line is that pure neurons are easily obtainable. Because an enriched neuronal population is derived, it is possible to study interactions with oligodendrocytes and astrocytes. Interestingly, co-culture with astrocytes enhances synapse formation (42). A major disadvantage of the NT2 cell line had been the length of time needed to differentiate into neurons, which is about 4 weeks and similar to human embryonic stem cells (43). In contrast, 2 weeks are required to differentiate mouse embryonic stem cells to neurons (44). In recent years, however, this rather lengthy differentiation method was significantly reduced by employing a cell aggregate culture method (45). A cautionary consideration is whether the NT2 cell line is truly pluripotent or rather is committed to a neural lineage. In developing the NT2 cell line, clones were selected from the parental TERA cell line that best differentiated to a neuronal lineage after treatment with RA.

2.4. Rodent Teratocarcinoma Cell Lines

Several rodent teratocarcinoma cell lines with different tissue origins are available. Two rodent teratocarcinoma cell lines that retain pluripotency have been well-characterized, the F9 and P19 cell lines. The P19 cell line was derived from a teratocarcinoma that was initiated by implanting a 7.5 day embryo into the testes. The objective of the study was to develop cell lines from female mice that were heterozygous for X-linked alleles. The embryo was derived by mating a male mouse carrying a feral X chromosome with a female C3H mouse (46). Similar to TERA cell lines, the cells were grown in the absence of a feeder layer. The pluripotential of the P19 cell line was verified by injection into blastocysts of a different mouse strain. P19-derived cells were found in tissues of all three germ layers in the resulting chimeric mice, even

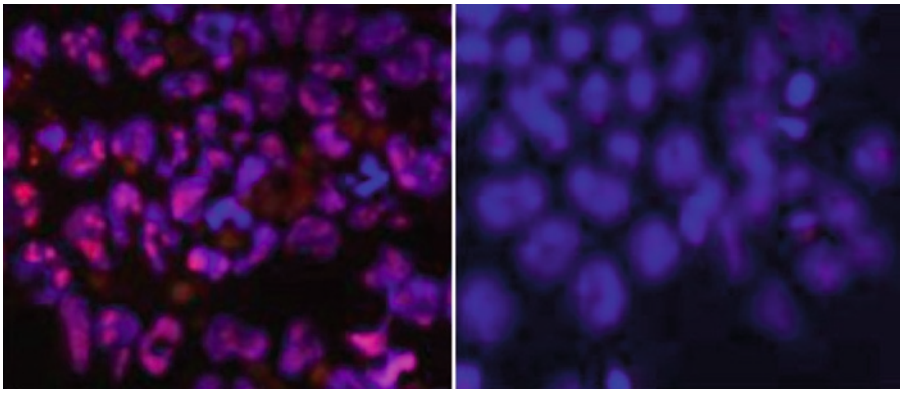

Fig. 1. *Oct4 expressed in P19 cells.* Non-treated (*left*) and two old RA treated P19 cells (*right*) were fixed and solubilized with 4% paraformaldehyde and 0.5% Triton-X 100 and stained with a rabbit antibody against mouse Oct4 followed by a secondary rhodamine labeled goat anti-rabbit antibody.

when only a single P19 cell was injected (47). P19 cells express pluripotent transcription factors such as Oct4, which is lost after cells begin to differentiate (Fig. 1). P19 cells will also form a teratocarcinoma when injected into an immunologically compromised host. In contrast, mouse embryonic cell lines form a benign teratoma when injected into a host. Although P19 cells form carcinomas, they are euploid as long as the laboratory maintains them properly.

Many teratocarcinoma-derived cell lines are derived from tumors in the testis and ovary and others, like P19, were developed from grafted embryos. Many are found to be aneuploid and therefore are not capable of proceeding through meiosis and producing mature sex cells (48). Another popular cell line for studying differentiation is the F9 cell line. Similar to P19 cells, but unlike most other embryonic carcinoma cell lines, F9 cells do not undergo spontaneous differentiation in culture. The F9 cell line has been used to understand the molecular mechanism underlying the development of the parietal and visceral endoderm, which are major components of the yolk sack in the early embryo. F9 cells, grown as aggregates in bacterial dishes, form embryoid bodies, which morphologically resemble early mouse embryos at the two-layered stage. The formation of embryoid bodies has been useful as a three-dimensional model of some of the processes occurring in early embryogenesis, such as endoderm differentiation, cavitation, and epithelial layer formation (49). Endoderm formation can also be studied in monolayer cultures of F9 cells. RA induces differentiation to primitive endoderm, while treatment with both RA and dibutyryl cyclic AMP causes differentiation to parietal endoderm. These parietal endoderm cells express high levels of plasminogen activator, laminin, and type IV collagen along with very low levels of alkaline phosphatase and lactate dehydrogenase, (50) typical of parietal endoderm in vivo.

2.4.1. P19 Cells Differentiation to Neurons

Induction of neural differentiation by RA is commonly used to induce pluripotent embryonic stem cells and P19 cells to a neural lineage and also to differentiate neuroblastoma cells. The biological effects of RA are primarily mediated through the action of two classes of specific receptors, RARs and RXRs (51). RA is generally considered a morphogen in the development of the posterior hindbrain and anterior spinal cord. P19 cells undergo a developmental time course that can be monitored by examining transcription factors, as well as axonal, dendritic, and synaptic proteins. In the early stages of neuronal differentiation of P19 cells, transcriptional regulatory mechanisms are very similar to those found in the developing brain. For example, repressor element silencing transcription factor binding to the neuron restrictive silencer element decreases (52) and the expression of the basic helix–loop–helix transcription factors, Mash-1 and Ngn-1 (53), and NeuroD are upregulated (54). The expression of β III tubulin begins early but the expression of synaptic proteins is not observed until later (Fig. 2). Axons and dendrites can be distinguished by staining for neurofilaments and microtubule-associated protein 2 (Fig. 2). The neurons also express neurotransmitter receptors. Within 2–3 weeks after induction by RA, P19 formed excitatory synapses, mediated by glutamate receptors, or inhibitory synapses, mediated by receptors for GABA or glycine (55).

Whole-cell recordings from P19-derived neurons, grown on glial cells and differentiated with RA, display inward currents in response to *N*-methyl D aspartate (NMDA) or kainate. The pharmacological responses of the NMDA receptor were similar to responses displayed by primary cultures of neurons. The NMDA-induced currents exhibit voltage-dependent blockade by magnesium, require glycine for maximal activation, and were blocked by the NMDA antagonist dizocilpin (56). Similarly, kainate-induced

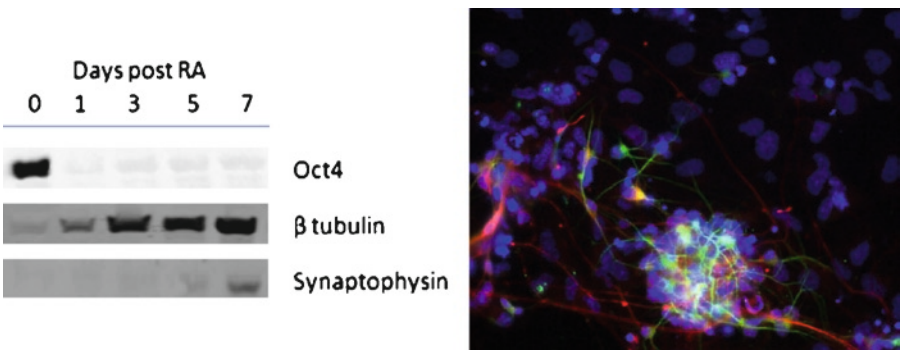

Fig. 2. Expression of neuronal proteins in P19-derived neurons. Western blot analysis of Oct4, β III tubulin, and synaptophysin at different days after treatment with after RA (*left*). At 10 days after treatment with RA, cells were fixed as described in Fig. 1 and stained with rabbit antibody against neurofilament 200 kDa and a mouse antibody against map2 followed by a fluorescein labeled goat anti-mouse antibody and a rhodamine labeled rabbit anti-neurofilament antibody (*right*).

currents were blocked by the AMPA/kainate receptor antagonist CNQX. P19 cells treated with NMDA and kainate results in widespread death that was blocked by their respective antagonists and is likely due to calcium influx (57). Interestingly, the EC_{50} for the NMDA response was 70 μM, which is lower than responses for most cell lines and within the range observed for primary cultures of neurons. Conditions can be established to promote a cholinergic phenotype in P19 cells, as evident by their ability to form contacts with a muscle cell-line – C2 and undergo depolarization-dependent acetylcholine release (58). P19 cells can also be used in studies on drug abuse because P19-derived neurons express functional opioid (59) and cananinboid receptors (60).

Most studies on differentiating P19 cells have examined RA only, despite the importance of many other factors in neural differentiation. For example, dehydroepiandrosterone (DHEA) is a neurosteroid that was shown to have protective effects in various models of neuronal cell death. In mice treated with the dopaminergic toxicant MPT, for example, DHEA prevents decreases in dopaminergic neurons (61). DHEA enhances differentiation into dopaminergic neurons when it is added with RA to P19 cell cultures though DHEA had no effect alone (62). Neuronal induction can also be induced in the absence of RA in cultures of P19 cells by growing reaggregates in the presence of a combination of the chemically defined media N2 and B27 media (discussed below). The N2B27-derived neurons express the cholinergic neuronal markers choline acetyltransferse, the dopaminergic neuron marker tyrosine hydroxylase, the glutamatergic neuron marker vesicular glutamate transporter, and the serotonergic neuron markers tryptophan hydroxylases 1 and 2 as well as the GABA marker glutamic acid decarboxylase 67 (63).

2.4.2. Muscle Cell Differentiation

Traditionally muscle cell cultures have been achieved through hanging drop cultures, these cultures require the suspension of a cell culture in an inverted drop of media for a period of a week, but although these cultures provide uniform sized embryoid bodies (unlike suspension cultures which produce a wide variety of sizes) they are difficult and time consuming to maintain. An alternative is to maintain the cells in bacteriological plates to discourage adherence. To obtain muscle cultures, aggregates are treated with 0.5–1% dimethylsulfoxide (DMSO) for 4 days. After replating into tissue culture dishes, about 10–25% of the cells become cardiomyocytes by day 6 and approximately 5–15% of the cells are skeletal myocytes by day 9. The rhythmic beating of the P19-derived cardiomyoctyes demonstrates the existence of a fully operational contraction apparatus (64), which can be observed in cultures by 3 weeks. P19-derived cardiomyocytes express sodium and potassium ion channels, and the L type calcium channel similar to cardiomyocytes (65). Additionally, P19-derived cardiomyocytes also

express coupled alpha- and beta-adrenergic receptors. The stage of differentiation, however, is similar to the heart of the developing fetus (66). Cells are mononucleated rather than binucleated and many of the early transcription factors, such as myocyte enhancer factor 2C and Nkx2-5 (67), and the zinc-finger protein GATA binding protein 4 are expressed (68). Additionally, the organization of the actin and myosin filament is more similar to the developing heart than the mature heart (66).

Although DMSO is not a physiological inducer, it has been used in several protocols to differentiate cells. Most notably, DMSO had been used to differentiate the Friend leukemic cell line into erythrocyte-like cells (69). The effect is quite effective because two-thirds of the cells display hemoglobin. The observation was unexpected because the intent of the investigators was to use DMSO to "soften" the cells for transfection (70). DMSO prevents crystallization of water and had been used previously in medium to freeze cells down. This observation prompted further investigations to develop small-molecule polar solvents to induce differentiation. More recent studies have provided evidence indicating that DMSO and other small molecule polar solvents induce differentiation by changing the epigenome. In an embryonic stem cell line, DMSO was shown to modify DNA methylation of different genes (71). DMSO and several other small polar chemicals also inhibit histone deacetylation. Other chemicals capable of differentiating P19 cells into cardiomyocytes include the DNA methyl transferase 1 inhibitor 5-azacytidine (72).

Oxytocin and DMSO appear to induce differentiation through a similar pathway. DMSO increases the expression of oxytocin receptor on the differentiating P19 cells and differentiation is inhibited by oxytocin receptor antagonists (73). Possibly, DMSO induces P19 differentiation by increasing oxytocin receptor, which is activated by oxytocin in the fetal bovine serum. Interestingly, the variability of serum lots to support differentiation of P19 cells into cardiomyocytes might be due to the levels of oxytocin. Because no study has yet reported whether oxytocin alone induces differentiation, it is likely that serum contains additional factors for cardiomyocyte differentiation.

2.4.3. Trophoblast Differentiation

The trophectoderm gives rise to all the trophoblast cell types of the fetal part of the placenta (74). Very similar to embryonic stem cell lines, P19 cells can be induced to differentiate into trophoblasts. Embryonic stem cells have been induced to differentiate to trophoblasts by deleting the expression of Oct4 (75) or the methyl DNA binding protein 3 (76). P19 differentiate into large multinucleated trophoblasts after treatment with hydralazine (Fig. 3). Similar to mouse embryonic stem cells, there is loss of Oct4, expression of trophoblast transcription factors and the trophoblast intermediary filament Troma-1. Also, differentiation requires

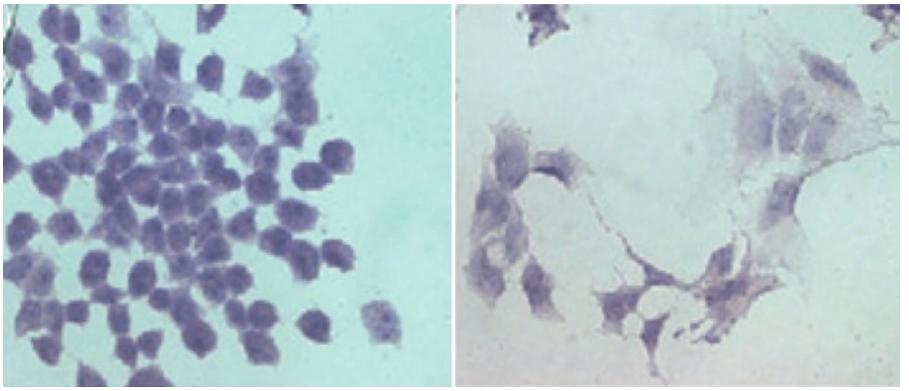

Fig. 3. Hydralazine induces P19 to differentiate to trophoblasts. Cells were fixed and stained with hematoxylin and eosin in controls (*left*) and at 5 days of treatment with hydralazine (*right*).

the expression of the TEAD4 transcription factor in P19 cells and embryonic stem cells. Interestingly, differentiation to trophoblasts is not observed when embryonic stem cells are introduced back into early embryos (77).

3. Culture Conditions for Promoting Differentiation

3.1. Chemically Defined Media

The response of P19 cells to RA is not 100%. Consequently, steps have been developed to increase the purity of neurons after treatment with RA. Because neurons do not proliferate (in contrast to glia and other cells), procedures very often include the addition of a mitotic inhibitor such as cytosine arabinoside (AraC) (a selective DNA synthesis inhibitor) 48 h post plating. The inhibitor inhibits proliferating cell allowing neurons to survive and dominate the culture. Other approaches include killing non-neuronal cells with antibody and complement and selective media. Early approaches used media with no or little serum or horse serum. Alternative sources of serum provide neuronal survival factors but lower amounts of mitogens. Many laboratories have been using chemically defined media to support neurons. A defined media used in our laboratory is Neural Basal Media supplemented with B27 (discussed above). Neural Basal Media and B27 were specifically formulated to optimize neuronal survival (78), eliminating the need for AraC addition. This growth media has lower osmolarity than most growth media and glutamine was eliminated because it is unstable at physiological pH in liquid media, breaking down to ammonium and pyroglutamate that could induce excitotoxicity. Instead, dipeptide forms, such as alanyl-L-glutamine and glycyl-L-glutamine should be used in neuronal cultures. B27 is a complex mixture of hormones, growth factors, and anti-oxidants. It can be

purchased with or without vitamin A or anti-oxidants. B27 has been successfully used to culture neurons from different brain regions including cerebellum, striatum, and hippocampus. Another supplement that is often used is N2, which was formulated by grow the rat B104 neuroblastoma cell line without serum (79). It also contains several growth factors though no anti-oxidants.

3.2. Aggregation and P19 Differentiation

Most procedures for differentiating pluripotent cells require adding inducers to aggregating cultures. These aggregates are often induced by plating cells on a surface that is not conducive for adhesion like uncoated bacteriological plates. Early studies on F9 cell line found that the aggregates appeared similar to embryoid bodies because of their resemblance to the 2-layer stage of the mouse embryo (49). Aggregation is needed for DMSO-mediated muscles differentiation, but it is not absolutely needed for RA-mediated neuronal differentiation (80–82). Monolayer cultures with high cell densities could provide sufficient cell-to-cell contacts. Because high cell density increases metabolism of RA, higher RA concentration would be needed (81). Even at low concentration of RA up to 75% of cell die by apoptosis. Aggregation in the absence of RA will not result in neurons but rather causes P19 into differentiate to endoderm layer (83). Recent studies have suggested that aggregation promotes differentiation by repressing pluripotency in P19 cells. Bone morphogenic protein-mediated gene expression is needed to maintain pluripotency but was blocked in aggregating P19 cultures by a mechanism involving increased expression of FGF8 and subsequent activation of Erk1/2 signaling pathway (84). It is also possible to obtain neuronal P19 culture without aggregation or RA. Forced expression of cadherin (85) and Wnt-1 (53) have been demonstrates to induce P19s to differentiate to neurons.

4. P19 Cell Line Protocols

4.1. Materials

P19 cells line ATCC # CRL-1825
α MEM Invitrogen 11900-024
BCS Sigma 12133C
FBS Hyclone SH30088.03
All trans retinoic acid Sigma R2625
Neurobasal Invitrogen 21103049
B27 Invitrogen 17504044
DMSO Mediatech 25-950-CQC
Cytosine arabinosidase (AraC) Sigma C1768
Poly-D-lysine Sigma P6407
Puromycin Sigma P8833-25MG
G418 Mediatech 30-234-CR

4.2. Cell Line Maintenance

Notes. Our laboratory maintains P19 cells in the same media that was used to develop the cell line. We have not had experience with other types of media though other laboratories have used DMEM with FBS. P19 cells grow differently than most other cell types. They should not exceed 80% confluency and careful monitoring of passage number is important. At older passages, cell lines will lose their ability to transfect and differentiate. Passage number is determined empirically by the laboratory. Cells lose these abilities because of selection pressures caused by the cell culture environment and the number of cell divisions. To assure that each passage number accurately reflects the same number of cell divisions, cells must be plated at the same density and harvested after the same number of days after plating.

Growth media
αMEM
2.5% FBS
7.5% BCS

Thawing and culture

1. P19 cells should be rapidly thawed at 37°C. Transfer cell suspension to a 15 mL conical tube and bring up to 10 mL in growth media.
2. Centrifuge at 1,000 RPM for 5 min and remove supernatant, taking care not to disturb the pellet.
3. Resuspend in 8 mL of fresh media and transfer into a T25 culture flask. Place in 37°C-humidified incubator until 80% confluent.
   - Rapid removal of DMSO is important as its presence can cause differentiation.
   - P19s grow rapidly and die when they become over confluent (doubling time of 22 h).
   - P19s only differentiate efficiently for up to 16 passages, freeze down cells before continuing to do experiments
   - Culture confluence is very important seeding the cells at very low confluency causes them to spontaneously differentiate (as does exposure to stress).
   - P19 cells retain their ability to differentiate better when they are passed by scraping rather than by trypsin.
   - Maintance of the cells for over 6–8 weeks may result in loss of their karyotype and changes in cell behavior.
4. Remove old media, gently scrape cells to detach from the flask surface and resuspend in fresh media. Transfer to T75 or T150.
5. Culture until they reach 80% confluence. Split at 1:6–1:10.

Freezing

Freeze cells down in 95% growth media, 5% DMSO at a concentration of one million cells/mL.

4.3. Neuronal Differentiation

Notes. Retinoic acid should be prepared in DMSO and stored in frozen aliquots, under nitrogen if possible. RA is very light, air- and oxidation-sensitive and, for this reason, aliquots should be discarded after one use. Any molecular weight poly-D-lysine between 70,000 and 300,000 can be used. The higher weights are more viscous but provide more attachment sites. We use poly lysine in the 70,000–150,000, which provides a compromise between viscosity and attachment sites. Poly-D-lysine is used rather than Poly-L-Lysine to avoid l-lysine toxicity. If cells are plated in growth media after treatment with RA, add 10 μM AraC 48 h post plating to inhibit differentiation of glial cells. Terminal differentiation takes 7 days. The cells become more susceptible to stress after exposure to RA therefore it is important to minimize the time they are not in culture.

Either Growth Media or Neurobasal with B27

1. Harvest cells by scraping, transfer to a 15 mL tube and triturate to achieve a single cell suspension. Make a cell suspension of 2×10^5 cells per mL of growth media.
2. Transfer 10 mL of suspension to a 100 mm bacteriological plate (encourages suspension growth) and add retinoic acid to a final concentration of 500 nM.
3. Culture for 72 h, by 48 h you should see the formation of aggregates.
4. Harvest the aggregates by transferring all the media into a 50 mL conical tube, rinse the plate with growth media to ensure removal of all spheres.
5. Centrifuge at 600 rpm for 5 min, up to 70% of the cells may have died during exposure to retinoic acid the slow spin will allow separation of the aggregates from the cell debris.
6. Resuspend aggregates in 10 mL of differentiation media, to break up the aggregates triturating up to 100 times may be required. Count cells using a vital stain such as trypan blue.
7. Cells should be resuspended at a concentration of 500,000 per mL of Neural Basal Media/B27 and plate onto Poly-D-Lysine (0.1 μg/mL) coated plates. We coat for at least one hours and rinse twice in PBS before plating cells. Cells progressively differentiate to neurons and glial equally as well on glass or plastic. As shown in Fig. 1, cell clumps are formed in older cultures. The clumps prevent counting the number individual cells.

4.4. Differentiation to Trophoblasts

1. Plate P19s cells at a density of 1,500 cells/cm^2.
2. After an overnight incubation, add hydralazine at a concentration of 5–10 μM for a period of 4–5 days. Because hydralazine is a highly reactive nucleophile, it must be made fresh when it is used.

3. Trophoblast cells can be identified morphologically by staining with hematoxylin and eosin stain, by immunocytochemistry (Troma-1 staining) or by the presence of gene markers of trophoblast, e.g., Hand1 or Mash2.

4.5. Immunocy to chemistry

1. The cells should be plated on to Poly-D-Lysine coated coverslips. Once the cells have reached the required level of differentiation fix them with 4% paraformaldehyde.
2. Incubate the cells with the paraformaldehyde for 20 min, remove and wash with PBS. Coverslips can be stored refrigerated in PBS for up to 3 weeks.
3. The fixed cells were incubated in a block/permabilization solution of 1% BSA/0.5% tween-20 (for extracellular staining do not include tween) for 2 h.
4. Primary antibodies were prepared in the blocking solution at a dilution of 1:50–1:100 and were incubated on the coverslip overnight at 4°C, the coverslips were washed 3 times in PBS and incubated with secondary antibodies (1:200 in blocking solution) for 1 h at room temperature.
5. The coverslips were washed 3 times in PBS and mounted with room temperature Prolong with DAPI for visualization.

5. Generating Long-Term Cell Lines after Introducing New Genes

Notes. P19 cells are relatively easy to transfect in their naïve form, but it is recommended to use the least harsh method available to avoid unduly stressing the cells and causing spontaneous differentiation. One major advantage of the P19 system is the ability to develop stable clonal cell lines in the naïve cells and then differentiate them to determine the effect of the gene manipulation in the differentiating cell line. In general, it is possible to achieve 50% transfection efficiency using calcium phosphate. We use the calcium phosphate method for routine transfections because it is much less expensive than others. Reported efficiencies for other methods vary between 40 and 80% depending on method. Amaxa electroporation reported the highest efficiency. Transfection reagents that only work in the absence of serum would require a media change to serum-free media, which would cause an increase in cytotoxicity and could induce P19 differentiation due to stress. To generate long-term P19 cell lines with siRNA vectors, lipid based reagent from Ambion was used. Although it is more expensive, we decided to use it because of the special application. The concentration of siRNA or DNA to be used must be determined by the end user.

1. Plate undifferentiated P19s cells in uncoated plates at a density of 3,500/cm^2 in growth media. Allow to grow for 24 h before transfection.
2. At 24 h after transfection, expose cells to the antibiotic. Neomycin resistant cells can be selected with 300–400 ng/mL G418 for 14 days. Puromycin resistant cells can be selected with 1–2 μg/mL for 7 days. A complete media change every 2 days is needed in growth colonies and remove dead cells. After 1 week or as long as it takes to completely kill switch your selected cells to a lower dose (usually half the selection dose) of puromycin for maintenance.
3. Single cells are harvested and replated in 10 cm plates to achieve individual colonies. Maintain in media with half the puromycin used to select cells. It is very important to visually inspect the plate daily to verify the colonies had been derived from single cells and that individual colonies are easy to distinguish. Clones are identified by marking their position with a marker on the bottom outside of the plate. Soak a sterile cloning disc in trypsin (Sigma Aldrich Z374431-100EA) and apply it to the colony for approximately 3–5 min after the media was removed. Transfer the cloning disc to a well in a 96 well plate and add media. Do not remove cloning disc, but allow it to remain until cells are transferred to a 48 well plate.
4. Once the cells are confluent they can be transferred into a 6 well plate, and once confluent split into three plates and once confluent two can be frozen. Keep selected clones in culture with a low level of antibiotic to maintain clone stability. Very important, freeze down early passage cells.
5. In our experience, puromycin attenuates RA-mediated P19 cell differentiation. We routinely remove puromycin from the cells at least 1 week before differentiation is induced. Indeed, cell lines do not have to be routinely maintained in puromycin. Finally, be very careful with passage number, which is true for all cell lines.

References

1. Brown AS, Derkits EJ (2010) Prenatal infection and schizophrenia: a review of epidemiologic and translational studies. Am J Psychiatry 167(3):261–280
2. Muhle R, Trentacoste SV et al (2004) The genetics of autism. Pediatrics 113(5): e472–e486
3. Newschaffer CJ, Croen LA et al (2007) The epidemiology of autism spectrum disorders. Annu Rev Public Health 28:235–258
4. Kelada SN, Checkoway H et al (2006) 5' and 3' region variability in the dopamine transporter gene (SLC6A3), pesticide exposure and Parkinson's disease risk: a hypothesis-generating study. Hum Mol Genet 15(20):3055–3062
5. Ritz BR, Manthripragada AD et al (2009) Dopamine transporter genetic variants and pesticides in Parkinson's disease. Environ Health Perspect 117(6):964–969

6. Widaman KF (2009) Phenylketonuria in children and mothers: genes, environments, behavior. Curr Dir Psychol Sci 18(1):48–52
7. Nagarajan RP, Hogart AR et al (2006) Reduced MeCP2 expression is frequent in autism frontal cortex and correlates with aberrant MECP2 promoter methylation. Epigenetics 1(4):e1–e11
8. Miltenberger-Miltenyi G, Laccone F (2003) Mutations and polymorphisms in the human methyl CpG-binding protein MECP2. Hum Mutat 22(2):107–115
9. Bebbington A, Anderson A et al (2008) Investigating genotype-phenotype relationships in Rett syndrome using an international data set. Neurology 70(11):868–875
10. Carter P, Downs J et al (2010) Stereotypical hand movements in 144 subjects with Rett syndrome from the population-based Australian database. Mov Disord 25(3):282–288
11. Downs JA, Bebbington A et al (2008) Gross motor profile in rett syndrome as determined by video analysis. Neuropediatrics 39(4):205–210
12. Chahrour M, Zoghbi HY (2007) The story of Rett syndrome: from clinic to neurobiology. Neuron 56(3):422–437
13. Singh J, Saxena A et al (2008) MECP2 genomic structure and function: insights from ENCODE. Nucleic Acids Res 36(19):6035–6047
14. Kaufmann WE, Johnston MV et al (2005) MeCP2 expression and function during brain development: implications for Rett syndrome's pathogenesis and clinical evolution. Brain Dev 27(Suppl 1):S77–S87
15. Giacometti E, Luikenhuis S et al (2007) Partial rescue of MeCP2 deficiency by postnatal activation of MeCP2. Proc Natl Acad Sci USA 104(6):1931–1936
16. Jugloff DG, Vandamme K et al (2008) Targeted delivery of an Mecp2 transgene to forebrain neurons improves the behavior of female Mecp2-deficient mice. Hum Mol Genet 17(10):1386–1396
17. Tsujimura K, Abematsu M et al (2009) Neuronal differentiation of neural precursor cells is promoted by the methyl-CpG-binding protein MeCP2. Exp Neurol 219(1):104–111
18. Mann J, Oakley F et al (2007) Regulation of myofibroblast transdifferentiation by DNA methylation and MeCP2: implications for wound healing and fibrogenesis. Cell Death Differ 14(2):275–285
19. Webb R, Wren JD et al (2009) Variants within MECP2, a key transcription regulator, are associated with increased susceptibility to lupus and differential gene expression in patients with systemic lupus erythematosus. Arthritis Rheum 60(4):1076–1084
20. Villa A, Liste I et al (2009) Generation and properties of a new human ventral mesencephalic neural stem cell line. Exp Cell Res 315(11):1860–1874
21. Donato R, Miljan EA et al (2007) Differential development of neuronal physiological responsiveness in two human neural stem cell lines. BMC Neurosci 8:36
22. De Filippis L, Ferrari D et al (2008) Immortalization of human neural stem cells with the c-myc mutant T58A. PLoS ONE 3(10):e3310
23. Perrier AL, Tabar V et al (2004) Derivation of midbrain dopamine neurons from human embryonic stem cells. Proc Natl Acad Sci USA 101(34):12543–12548
24. Schulz TC, Noggle SA et al (2004) Differentiation of human embryonic stem cells to dopaminergic neurons in serum-free suspension culture. Stem Cells 22(7):1218–1238
25. Heikkila TJ, Yla-Outinen L et al (2009) Human embryonic stem cell-derived neuronal cells form spontaneously active neuronal networks in vitro. Exp Neurol 218(1):109–116
26. Suter DM, Cartier L et al (2006) Rapid generation of stable transgenic embryonic stem cell lines using modular lentivectors. Stem Cells 24(3):615–623
27. Karumbayaram S, Novitch BG et al (2009) Directed differentiation of human-induced pluripotent stem cells generates active motor neurons. Stem Cells 27(4):806–811
28. Doi A, Park IH et al (2009) Differential methylation of tissue- and cancer-specific CpG island shores distinguishes human induced pluripotent stem cells, embryonic stem cells and fibroblasts. Nat Genet 41(12):1350–1353
29. Draper JS, Moore HD et al (2004) Culture and characterization of human embryonic stem cells. Stem Cells Dev 13(4):325–336
30. Pierce GB, Stevens LC et al (1967) Ultrastructural analysis of the early development of teratocarcinomas. J Natl Cancer Inst 39(4):755–773
31. Solter D, Dominis M et al (1979) Embryo-derived teratocarcinoma: I. The role of strain and gender in the control of teratocarcinogenesis. Int J Cancer 24(6):770–772
32. Andrews PW, Damjanov I et al (1984) Pluripotent embryonal carcinoma clones derived from the human teratocarcinoma cell line Tera-2. Differentiation in vivo and in vitro. Lab Invest 50(2):147–162
33. Lee VM, Andrews PW (1986) Differentiation of NTERA-2 clonal human embryonal carcinoma

cells into neurons involves the induction of all three neurofilament proteins. J Neurosci 6(2):514–521

34. Younkin DP, Tang CM et al (1993) Inducible expression of neuronal glutamate receptor channels in the NT2 human cell line. Proc Natl Acad Sci USA 90(6):2174–2178
35. Neelands TR, Zhang J et al (1999) GABA(A) receptors expressed in undifferentiated human teratocarcinoma NT2 cells differ from those expressed by differentiated NT2-N cells. J Neurosci 19(16):7057–7065
36. Zeller M, Strauss WL (1995) Retinoic acid induces cholinergic differentiation of NTera 2 human embryonal carcinoma cells. Int J Dev Neurosci 13(5):437–445
37. Guillemain I, Alonso G et al (2000) Human NT2 neurons express a large variety of neurotransmission phenotypes in vitro. J Comp Neurol 422(3):380–395
38. Podrygajlo G, Tegenge MA et al (2009) Cellular phenotypes of human model neurons (NT2) after differentiation in aggregate culture. Cell Tissue Res 336(3):439–452
39. Tegenge MA, Stern M et al (2009) Nitric oxide and cyclic nucleotide signal transduction modulates synaptic vesicle turnover in human model neurons. J Neurochem 111(6):1434–1446
40. Gao ZY, Xu G et al (1998) Retinoic acid induction of calcium channel expression in human NT2N neurons. Biochem Biophys Res Commun 247(2):407–413
41. Neelands TR, King AP et al (2000) Functional expression of L-, N-, P/Q-, and R-type calcium channels in the human NT2-N cell line. J Neurophysiol 84(6):2933–2944
42. Hartley RS, Margulis M et al (1999) Functional synapses are formed between human NTera2 (NT2N, hNT) neurons grown on astrocytes. J Comp Neurol 407(1):1–10
43. Zhang XQ, Zhang SC (2010) Differentiation of neural precursors and dopaminergic neurons from human embryonic stem cells. Meth Mol Biol 584:355–366
44. Gaspard N, Bouschet T et al (2009) Generation of cortical neurons from mouse embryonic stem cells. Nat Protoc 4(10):1454–1463
45. Paquet-Durand F, Tan S et al (2003) Turning teratocarcinoma cells into neurons: rapid differentiation of NT-2 cells in floating spheres. Brain Res Dev Brain Res 142(2):161–167
46. McBurney MW, Strutt BJ (1980) Genetic activity of X chromosomes in pluripotent female teratocarcinoma cells and their differentiated progeny. Cell 21(2):357–364
47. Rossant J, McBurney MW (1982) The developmental potential of a euploid male teratocarcinoma cell line after blastocyst injection. J Embryol Exp Morphol 70:99–112
48. Andrews PW (2002) From teratocarcinomas to embryonic stem cells. Philos Trans R Soc Lond B Biol Sci 357(1420):405–417
49. Grover A, Oshima RG et al (1983) Epithelial layer formation in differentiating aggregates of F9 embryonal carcinoma cells. J Cell Biol 96(6):1690–1696
50. Strickland S, Mahdavi V (1978) The induction of differentiation in teratocarcinoma stem cells by retinoic acid. Cell 15(2):393–403
51. Maden M (2007) Retinoic acid in the development, regeneration and maintenance of the nervous system. Nat Rev Neurosci 8(10):755–765
52. Park SY, Kim JB et al (2007) REST is a key regulator in brain-specific homeobox gene expression during neuronal differentiation. J Neurochem 103:2565–2574
53. Tang K, Yang J et al (2002) Wnt-1 promotes neuronal differentiation and inhibits gliogenesis in P19 cells. Biochem Biophys Res Commun 293(1):167–173
54. Seo S, Richardson GA et al (2005) The SWI/SNF chromatin remodeling protein Brg1 is required for vertebrate neurogenesis and mediates transactivation of Ngn and NeuroD. Development 132(1):105–115
55. Finley MF, Kulkarni N et al (1996) Synapse formation and establishment of neuronal polarity by P19 embryonic carcinoma cells and embryonic stem cells. J Neurosci 16(3):1056–1065
56. Turetsky DM, Huettner JE et al (1993) Glutamate receptor-mediated currents and toxicity in embryonal carcinoma cells. J Neurobiol 24(9):1157–1169
57. Canzoniero LM, Sensi SL et al (1996) Glutamate receptor-mediated calcium entry in neurons derived from P19 embryonal carcinoma cells. J Neurosci Res 45(3):226–236
58. Parnas D, Linial M (1995) Cholinergic properties of neurons differentiated from an embryonal carcinoma cell-line (P19). Int J Dev Neurosci 13(7):767–781
59. Park SW, Huq MD et al (2005) Retinoic acid-induced chromatin remodeling of mouse kappa opioid receptor gene. J Neurosci 25(13):3350–3357
60. Svensson AC, Johansson M et al (2006) Expression of functional CB1 cannabinoid receptors in retinoic acid-differentiated P19 embryonal carcinoma cells. J Neurosci Res 83(6):1128–1140

61. D'Astous M, Morissette M et al (2003) Dehydroepiandrosterone (DHEA) such as 17beta-estradiol prevents MPTP-induced dopamine depletion in mice. Synapse 47(1):10–14
62. Azizi H, Mehrjardi NZ et al (2010) Dehydroepiandrosterone stimulates neurogenesis in mouse embryonal carcinoma cell- and human embryonic stem cell-derived neural progenitors and induces dopaminergic neurons. Stem Cells Dev 19(6):809–818
63. Xia C, Wang C et al (2007) Induction of a high population of neural stem cells with anterior neuroectoderm characters from epiblast-like P19 embryonic carcinoma cells. Differentiation 75(10):912–927
64. Wobus AM, Kleppisch T et al (1994) Cardiomyocyte-like cells differentiated in vitro from embryonic carcinoma cells P19 are characterized by functional expression of adrenoceptors and Ca2+ channels. In Vitro Cell Dev Biol Anim 30A(7):425–434
65. Maltsev VA, Wobus AM et al (1994) Cardiomyocytes differentiated in vitro from embryonic stem cells developmentally express cardiac-specific genes and ionic currents. Circ Res 75(2):233–244
66. Rudnicki MA, Jackowski G et al (1990) Actin and myosin expression during development of cardiac muscle from cultured embryonal carcinoma cells. Dev Biol 138(2):348–358
67. Skerjanc IS, Petropoulos H et al (1998) Myocyte enhancer factor 2C and Nkx2-5 upregulate each other's expression and initiate cardiomyogenesis in P19 cells. J Biol Chem 273(52):34904–34910
68. Grepin C, Robitaille L et al (1995) Inhibition of transcription factor GATA-4 expression blocks in vitro cardiac muscle differentiation. Mol Cell Biol 15(8):4095–4102
69. Friend C, Preisler HD et al (1974) Studies on the control of differentiation of murine virus-induced erythroleukemic cells. Curr Top Dev Biol 8:81–101
70. Marks PA, Breslow R (2007) Dimethyl sulfoxide to vorinostat: development of this histone deacetylase inhibitor as an anticancer drug. Nat Biotechnol 25(1):84–90
71. Iwatani M, Ikegami K et al (2006) Dimethyl sulfoxide has an impact on epigenetic profile in mouse embryoid body. Stem Cells 24(11):2549–2556
72. Choi SC, Yoon J et al (2004) 5-azacytidine induces cardiac differentiation of P19 embryonic stem cells. Exp Mol Med 36(6):515–523
73. Uchida S, Fuke S et al (2007) Upregulations of Gata4 and oxytocin receptor are important in cardiomyocyte differentiation processes of P19CL6 cells. J Cell Biochem 100(3):629–641
74. Thomas P, Beddington R (1996) Anterior primitive endoderm may be responsible for patterning the anterior neural plate in the mouse embryo. Curr Biol 6(11):1487–1496
75. Niwa H, Toyooka Y et al (2005) Interaction between Oct3/4 and Cdx2 determines trophectoderm differentiation. Cell 123(5):917–929
76. Zhu D, Fang J et al (2009) Mbd3, a component of NuRD/Mi-2 complex, helps maintain pluripotency of mouse embryonic stem cells by repressing trophectoderm differentiation. PLoS ONE 4(11):e7684
77. Beddington RS, Robertson EJ (1989) An assessment of the developmental potential of embryonic stem cells in the midgestation mouse embryo. Development 105(4):733–737
78. Brewer GJ, Torricelli JR et al (1993) Optimized survival of hippocampal neurons in B27-supplemented Neurobasal, a new serum-free medium combination. J Neurosci Res 35(5):567–576
79. Bottenstein JE, Sato GH (1979) Growth of a rat neuroblastoma cell line in serum-free supplemented medium. Proc Natl Acad Sci USA 76(1):514–517
80. Campione-Piccardo J, Sun JJ et al (1985) Cell-cell interaction can influence drug-induced differentiation of murine embryonal carcinoma cells. Dev Biol 109(1):25–31
81. Berg RW, McBurney MW (1990) Cell density and cell cycle effects on retinoic acid-induced embryonal carcinoma cell differentiation. Dev Biol 138(1):123–135
82. Pachernik J, Bryja V et al (2005) Neural differentiation of pluripotent mouse embryonal carcinoma cells by retinoic acid: inhibitory effect of serum. Physiol Res 54(1):115–122
83. Jones-Villeneuve EM, McBurney MW et al (1982) Retinoic acid induces embryonal carcinoma cells to differentiate into neurons and glial cells. J Cell Biol 94(2):253–262
84. Wang C, Xia C et al (2006) Cell aggregation-induced FGF8 elevation is essential for P19 cell neural differentiation. Mol Biol Cell 17(7):3075–3084
85. Gao X, Bian W et al (2001) A role of N-cadherin in neuronal differentiation of embryonic carcinoma P19 cells. Biochem Biophys Res Commun 284(5):1098–1103

Chapter 11

Signal Transduction and Neurotoxicity: What Can We Learn from Experimental Culture Systems?

Lucio G. Costa, Gennaro Giordano, and Marina Guizzetti

Abstract

Signal transduction is a key process to transmit information from the extracellular milieu, and to elicit changes in the biological activity of target cells. Several cell signaling pathways can be targeted by neurotoxicants and developmental neurotoxicants. This chapter focuses on the interactions of ethanol, a known human developmental neurotoxicant, with signal transduction pathways stimulated by acetylcholine through activation of muscarinic receptors. It shows how initial observations in vivo, upon developmental exposure to ethanol, have been followed-up by a series of studies in cell culture systems which have allowed the discoveries that ethanol, by interfering with muscarinic signaling in astroglial cells, inhibits their proliferation and their ability to foster neuronal differentiation. Such effects of alcohol may be related to microencephaly and abnormal neuronal development, two hallmarks of the fetal alcohol syndrome.

Key words: Signal transduction, Muscarinic receptors, Astroglial cells, Ethanol

1. Introduction: An Overview of Signal Transduction

The mechanisms by which extracellular signals are transferred to the cell cytosol and nucleus, commonly referred to as "cell signaling" or "signal transduction," are receiving much attention in all areas of biology and medicine. Neurotransmitters, hormones, and growth factors serve as first messengers to transfer information from one cell to another by binding to specific cell membrane receptors. This interaction results in activation or inhibition of specific enzymes and/or opening of ion channels, which lead to changes in intracellular metabolism and, in turn, to a variety of effects, including activation of protein kinases and transcription factors. These intracellular pathways can be activated by totally different receptors, and are very interactive or "cross-talking," so they can control and modulate each other. As the area of signal

Michael Aschner et al. (eds.), *Cell Culture Techniques*, Neuromethods, vol. 56,
DOI 10.1007/978-1-61779-077-5_11,

transduction is very broad, a review of all its aspects is well beyond the scope of this chapter, and only a few examples are discussed below, for illustrative purposes.

Some of the most studied signaling pathways are those activated by membrane receptors. These include for example enzyme-linked receptors and G-protein-linked receptors (1, 2). Enzyme-linked receptors (such those of insulin or of epidermal growth factor) are receptors in which the ligand-binding domain, the membrane-spanning region, and the effector enzyme are usually separate domains of the same protein. Binding of the ligand to the receptor activates the effector enzyme. The most widely studied of these receptors are those with tyrosine kinase activity. Tyrosine kinase autophosphorylates the receptor and also phosphorylates other substrate proteins. This initiates a cascade of processes whereby a large number of proteins are activated, including, for example, Ras, Raf-1, JAK-STAT, as well as mitogen-activated protein kinases (MAPK) and p70S6 kinase (1).

G-protein-linked receptors are activated by a wide variety of ligands, including neurotransmitters and hormones. These receptors have a seven-transmembrane domain, extracellular loops, with the ligand-binding domain, and intracellular loops, which interact with G-proteins. The G (for GDP/GTP binding)-proteins consist of three subunits, α, β, and γ. Upon interaction with the ligand, the GDP bound to the α subunit is replaced by GTP, and Gα dissociates from Gβγ. Gα-GTP then activates an effector enzyme, which starts a signal transduction cascade. Depending on the nature of the G-protein, a receptor can activate or inhibit the same enzyme (e.g., adenylate cyclase), or activate a totally different enzyme. Furthermore, in addition to Gα, Gβγ has also been shown to activate an array of effector enzymes, including those also activated by Gα (3). This model of G-protein-linked receptor is utilized for example by the adenylate cyclase system. Upon activation by Gα-GTP, adenylate cyclase catalyzes the conversion of ATP to cAMP; the latter acts as a second messenger by activating protein kinase A (PKA). This occurs via the binding of two cAMP molecules to each of the regulatory subunits of PKA, thus releasing the catalytic subunit. In turn, PKA phosphorylates, and thus changes the activity, of substrate proteins in the cytoplasm, in the membrane, as well as in the nucleus (e.g., the transcription factor CREB). If the Gα subunit is of the inhibitory type (Gi), then inhibition of adenylate cyclase and a decrease of cAMP levels will ensue.

Another pathway which utilizes this system is that regulating the metabolism of membrane phosphoinositides. In this case, Gα-GTP (Gq) activates the enzyme phospholipase Cβ (PLCβ) which catalyzes the breakdown of the membrane phospholipid phosphatidylinositol 4,5-bisphosphate to inositol 1,4,5 trisphosphate ($InsP_3$) and diacylglycerol (DAG), both of which act as second

messengers. It should be noted that PLCs can also be activated by other receptors (e.g., that of nerve growth factor), thus underlining the complex entangled web of interactions in signal transduction pathways (1). $InsP_3$ binds to specific receptors in the endoplasmic reticulum and mobilizes calcium from intracellular stores, thereby allowing activation of a variety of cellular enzymes. DAG, in concert with calcium and phosphatidylserine, activates certain subtypes of protein kinase C (PKC). In turn, PKC phosphorylates a number of cellular substrates, including transcription factors. Only classical PKCs (such as α and γ) are activated as indicated; novel PKCs (e.g., PKC ε) do not need calcium for activation, and atypical PKCs (e.g., PKC ζ) are activated by other means. In addition to DAG, other important lipid mediators can be generated in cells by G-protein-linked receptors through multiple pathways. An important pathway is represented by the hydrolysis of phosphatidylcholine, one of the major membrane phospholipids, by phospholipase D (PLD), to generate phosphatidic acid (PA), which can activate atypical PKC ζ. Activation of classical and novel PKCs stimulates PLD activity, thus generating PA; this can also be converted to DAG by a PA hydrolase, thus providing a mean for a prolonged stimulation of PKCs. Other important lipid mediators are arachidonic acid, the precursor of all prostanoids, which is generated by hydrolysis of membrane phospholipids by phospholipase A_2 (PLA_2), and ceramide, which is released from sphyngomyelin by sphyngomyelinase.

Phosphoinositide-3 (PI-3) kinase represents another important cell signaling pathway, which plays important roles in the control of cell growth, proliferation and survival (4). When activated by surface receptors or interaction with Ras, class I PI-3 kinases produce phosphatidylinositol (3,4,5)-trisphosphate ($PtdIns(3,4,5)P_3$). PI-3 kinase regulates cellular functions by recruiting $PtdIns(3,4,5)P_3$-binding proteins to the plasma membrane. The prototype of these molecules is protein kinase B (PKB), also known as Akt, which is activated by ligation of $PtdIns(3,4,5)P_3$ and by phosphorylation by 3 phosphoinositide-dependent kinase 1 (PDK1) (5). PDK also phosphorylates some PKC isoforms (e.g., PKC ζ) and downstream kinases (e.g., p70S6 kinase).

The ability of certain receptors to increase intracellular levels of cyclic GMP (cGMP) and the fact that such effect was indirect, i.e., it necessitated an additional second messenger, has been known for quite some time. Initial candidates for such role included calcium ions and arachidonic acid metabolites (see (6)). However, it was later discovered that nitric oxide (NO), synthesized from l-arginine by NO synthase (NOS), binds to a heme moiety attached to guanylate cyclase and stimulates the formation of cGMP (7, 8). The NOS family consists of three isoforms: neuronal NOS (nNOS) and endothelial NOS (eNOS) which are

constitutively expressed and require the formation of calcium–calmodulin complexes for their activation, and inducible NOS (iNOS), which exerts its activity in a calcium-independent manner (9). NO is involved in a wide array of cellular effects in the CNS, ranging from neuroprotection to neurotoxicity (10, 11). The diversity in response appears to be related to the steady-state concentration of NO. In general, low concentrations of NO (1–300 nM) would promote cell survival, whereas at higher concentrations (1 μM) nitrosative stress would prevail, leading to cell cycle arrest and apoptosis (12).

2. Signal Transduction as a Target for Neurotoxicants

In recent years, investigations on the molecular mechanisms of neurotoxicity have started to consider a variety of signal transduction pathways as potential targets for neurotoxicants. Such studies have followed three basic experimental approaches: the study of the direct effects of a chemical on a particular step in cell signaling (e.g., a protein kinase); the study of the direct effects of a neurotoxicant on second messenger responses activated by an endogenous compound (e.g., a neurotransmitter-induced activation of phospholipid hydrolysis); and, to a limited extent, the alterations in signal transduction resulting from other toxic actions (e.g., oxidative stress).

Interactions of neurotoxicants with signal transduction pathways may occur in neuronal or in glial cells, and may lead to inhibition or stimulation of cell proliferation and/or cell differentiation, to the direct induction of cell death, to inhibition of pathways that provide protection against cell death, or to other effects on cellular function. As such, such interaction may be relevant to neurotoxicity in adults, to developmental neurotoxicity, as well as to neuro-oncology. The relevance of interactions with signal transduction pathways in the neurotoxicity and developmental neurotoxicity of a number of chemicals (mostly lead, polychlorinated biphenyls, domoic acid, aluminum, cyanide, organotin compounds, certain pesticides) has been discussed in a number of reviews and book chapters in the past 15 years (6, 13–19). In this chapter, a selected example of such interactions will be discussed, related to mechanisms possibly underlying the developmental neurotoxicity of ethanol. In this example, initial studies were done in vivo or ex vivo in rodents; while these studies provided important clues for associating effects of alcohol on signal transduction to neurotoxicity, the exact cellular and molecular mechanisms remained elusive. A series of further investigations conducted in vitro in cells in culture and in co-culture have instead allowed an understanding of how disruption of signal transduction by

ethanol may lead to alterations of glial cell proliferation and of neuronal differentiation, which may underlie some of the effects seen in vivo following developmental ethanol exposure.

3. The Developmental Neurotoxicity of Ethanol

Offspring of alcoholics may be affected by the fetal alcohol syndrome (FAS), whose main features include facial dysmorphogenesis, growth retardation and, most importantly, a number of central nervous system (CNS) abnormalities (mental retardation, brain malformations, microencephaly) (20). The timing of ethanol exposure during brain development is of particular relevance for the type of effects that are manifest. Animal studies and human observations have shown that exposure to ethanol during the so-called brain growth spurt (the third trimester in humans and the first 2 postnatal weeks in rats or mice) causes microencephaly, which is present in more than 80% of FAS children (21). The brain growth spurt is characterized by proliferation and maturation of glial cells and by maturation of neurons and synaptogenesis. A large number of studies have also shown that alcohol abuse during pregnancy causes loss of certain neurons (hippocampal pyramidal neurons, cerebellar granule, and Purkinje cells), which may be due to a direct toxic effect of ethanol and/or may result from inhibition of the trophic action of neurotransmitters and growth factors (22, 23). Developmental exposure to ethanol has also been shown to affect neuronal differentiation, by causing alterations in the elongation of axons and neurites (24, 25). In addition to its toxic effects on neurons, ethanol has been also shown to affect glial cells, in particular astrocytes (26, 27). Evidence exists of abnormal glial migration in humans with FAS, as well as primates and rats exposed to ethanol during development (28). In children with FAS, hypoplasia of the corpus callosum and anterior commissure, two area originally formed by neuroglial cells, have been reported (29).

4. Effects of Ethanol on Cholinergic Muscarinic Receptors Signaling

Studies carried out during the past two decades have suggested that signal transduction pathways activated by the neurotransmitter acetylcholine via cholinergic muscarinic receptors may represent a relevant target for the developmental neurotoxicity of ethanol (see an earlier review (30)). There is growing evidence that acetylcholine may influence various aspects of brain development through activation of muscarinic receptors (30–34).

Muscarinic receptors can be detected in rats at day 15 of gestation, and increase slowly with age reaching a plateau at about postnatal day 28 (35). The activity of choline acetyltransferase in rat brain also increases slowly, as only 19% of activity is present at 1 week of age (36). In contrast, choline levels, which are considered the rate-limiting factor in the synthesis of acetylcholine, are actually higher in the neonatal than in the adult rat brain (36). This fact, together with the low activity of acetylcholinesterase in the neonatal rat brain, may explain why acetylcholine levels are high (80–90% of adult values) early postnatally (37). There are five distinct subtypes of muscarinic receptors, M1–M5 (38). The M2 and M4 subtypes are negatively coupled to adenylate cyclase, while the other three subtypes stimulate phospholipid hydrolysis. Inhibition of adenylate cyclase is not detected until postnatal week 3 in the rat, suggesting that M2 and M4 receptors are uncoupled from Gi at earlier ages (39). In contrast, muscarinic receptor-stimulated phosphoinositide metabolism was found to be much higher in brains from neonatal mice than in adult mice, despite a low expression of M1, M3, and M5 muscarinic receptors (35, 40). Though the exact mechanisms underlying such enhanced stimulation of phosphoinositide metabolism are still not fully understood (suggested explanations are a more efficient coupling and/or a lack of inhibitory feedback by PKC), this effect has been seen also in brain from neonatal mice (41) and human fetuses (42). Further in vitro studies in brain slices from rat at different ages indicated that muscarinic receptor-stimulated phosphoinositide metabolism gradually increased after birth, peaked on postnatal day 7, and gradually declined (35). Activation of PLD by muscarinic agonists is also enhanced in the neonatal rat brain (43).

These initial findings, and the fact that muscarinic receptor formation precedes the development of presynaptic markers, suggested that muscarinic receptors may play a role in the regulation of synaptogenesis, neurocytomorphogenesis, and glial proliferation (31–33). These considerations, together with a comparison of the postnatal developmental curves of the brain growth spurt (44) and of muscarinic receptor-induced phosphoinositide hydrolysis (35), led to the hypothesis that this signal transduction system may represent a possible target for developmental neurotoxicants, such as ethanol, which is most deleterious when exposure occurs during the growth spurt (21).

Initial studies done in vivo showed that administration of ethanol (4 g/kg/day) from postnatal day 4–10, i.e., during the brain growth spurt, caused microencephaly and inhibited muscarinic receptor-stimulated phosphoinositide metabolism in cerebral cortex and hippocampus (45). Further studies investigated the dose- and time-dependence of these effects. Microencephaly and a decreased muscarinic receptor-stimulated hydrolysis of phosphoinositides were found only when ethanol (4 g/kg) was administered at the peak of the growth spurt (PND 6–8 or

10–12), but not when it was given earlier (PND 2–4) or later (PND 13–15) despite comparable blood alcohol levels (46). Furthermore, a dose–response study indicated that only doses capable of causing microencephaly inhibited muscarinic receptor-stimulated phosphoinositide hydrolysis (47). Additional studies carried out in vitro in rat brain slices also showed that sensitivity of muscarinic receptor-stimulated phosphoinositide hydrolysis to ethanol inhibition was maximal at PND 7–10, that it increased with time of incubation, that it was more pronounced in cerebral cortex and hippocampus than in brainstem or cerebellum, that is was relatively specific for acetylcholine and muscarinic receptors compared to other neurotransmitters, that it was due to ethanol itself, rather than to its conversion to acetaldehyde, and that it also occurred in brain slices from mice (41, 48–50).

Overall, this initial series of studies indicated that exposure to ethanol at sufficient dose levels and in very specific postnatal periods caused microencephaly that was always accompanied by inhibition of muscarinic receptor-stimulated phosphoinositide hydrolysis. To further probe the significance of this association, it was necessary to switch to in vitro primary cultures. A first study, carried out in mixed cortical cultures, confirmed that ethanol could inhibit muscarinic receptor-stimulated phosphoinositide metabolism in a concentration- and age-dependent manner, and could also inhibit muscarinic receptor-induced calcium mobilization (51). These experiments served as confirmation that what observed in vivo and in brain slices could be seen also in primary cells in culture. However, the observed association between ethanol-induced microencephaly and inhibition of muscarinic receptor signaling still needed clarification, which was provided by studies discussed in the next section.

5. In Vitro Studies on Astrocyte Proliferation

An earlier study by Ashkenazy et al. (52) had suggested that acetylcholine, by activating phospholipase C-coupled muscarinic receptor subtypes (M1, M3, M5), may act as a mitogen in glial cells. This effect of acetylcholine may be relevant in terms of brain development, as proliferation of astrocytes is a major event occurring during the growth spurt, a period in which muscarinic signaling is particularly enhanced (35, 43). We hypothesized that ethanol, by interfering with muscarinic receptor signaling, would inhibit the mitogenic action of acetylcholine in astroglial cells, and that this would explain, at least in part, microencephaly seen upon ethanol exposure during the brain growth spurt (21, 45).

We first carried out a detailed characterization of acetylcholine-induced cell proliferation in rat cortical astrocytes and in a human astrocytoma cell line (53). These experiments indicated

that proliferation was due to stimulation of the M3 muscarinic receptor subtype, and that it involved activation of PKC (53). A subsequent study showed that ethanol, at concentrations of 10–100 mM, could inhibit acetylcholine-induced astroglial cell proliferation (54). Similar results were obtained in rat cortical astrocytes, human astrocytoma cells, and human fetal astrocytes (54, 55). Note in this regard that ethanol-induced microencephaly in vivo was observed at blood alcohol levels of about 50 mM (45, 47).

We then sought to determine the signaling pathway(s) activated by muscarinic receptors in astroglial cells and their involvement in the mitogenic action of acetylcholine, to identify the molecular target(s) of ethanol's antiproliferative action. Given the findings obtained in the in vivo experiments (45) and in the in vitro experiments in brain slices and in mixed cortical cultures (49, 51), initial experiments focused on the phospholipase C pathway, also because of its suggested role in cell proliferation (56). The acetylcholine analogue carbachol, by activating M3 muscarinic receptors, increased InsP3-mediated intracellular calcium release in rat cortical astrocytes and in human astrocytoma cells, and this effect was inhibited by ethanol at concentration of 100 mM or higher (57). Carbachol did not activate classical PKC α in human astrocytoma cells, but caused a rapid activation of novel PKC ε (58). This latter study concluded that PKC ε plays a minor role in the mitogenic action of acetylcholine, but that its activation was not sufficient for a full mitogenic action to be manifesting (58). Furthermore, inhibition of carbachol-stimulated PKC ε was only evident at concentrations of ethanol of 100 mM or higher (59). Activation of PKC ε by carbachol was also found to mediate subsequent activation of mitogen-activated protein kinase (MAPK) (60). This pathway appears to play a (minor) role in the mitogenic action of acetylcholine in astrocytes, and was not affected by ethanol (60).

Given the minor relevance of classical and novel PKCs in the mitogenic action of acetylcholine, and their relative insensitivity to inhibition by ethanol, research then focused on atypical PKCs, namely PKC ζ. By stimulating muscarinic M3 receptors, carbachol was found to induce a potent and long-lasting activation of PKC ζ (61). Such activation was most relevant for the mitogenic action of acetylcholine, as inactivation of PKC ζ with a specific pseudosubstrate abolished carbachol-induced DNA synthesis in astroglial cells (61). PKC ζ can be activated by PA, generated from phosphatidylcholine by hydrolysis catalyzed by PLD, and by PI-3 kinase. Carbachol was found to activate PI-3 kinase in astroglial cells, and inhibition of this pathway inhibited its mitogenic effect (62). Carbachol also stimulated PLD activity in astroglial cells (43, 63), and inhibition of PLD by 1-butanol was found to antagonize the mitogenic effect of acetylcholine (63).

Ethanol was a potent inhibitor of muscarinic receptor-induced activation of PKC ζ, with a concentration of 50 mM causing >80% inhibition (62). Activation by carbachol of two downstream effectors of PKC ζ, p70S6 kinase and nuclear factor-κB (NF-κB), were also inhibited by ethanol at concentrations of 25–50 mM (62, 64). Thus, the PKC ζ – p70S6 kinase/NF-κB pathway is inhibited by ethanol in the same range of concentrations which inhibit DNA synthesis.

Ethanol was further found to inhibit both upstream signals known to activate PKC ζ, i.e., PI-3 kinase and PLD. However, 100 mM ethanol was necessary for inhibiting PI-3 kinase (62), while PLD was inhibited at 25–50 mM ethanol (63).

The overall picture emerging from these studies is that acetylcholine, by activating muscarinic M3 receptors induces DNA synthesis in astroglial cells. This mitogenic effect is mediated by multiple pathways, as illustrated in Fig. 1. Ethanol inhibits the mitogenic effect of acetylcholine by inhibiting muscarinic receptor signal transduction, at the level of PLD. This interaction of ethanol with PLD, which consists of a transphosphatidylation reaction whereby ethanol substitutes for water, and phosphatidylethanol is formed instead of PA (63), inhibits the formation of PA, its activation of PKC ζ, and the subsequent downstream activation of p70S6 kinase and of NF-κB. In vitro cell culture systems have thus provided a tool for interpreting the initial in vivo finding, and have allowed the identification of the underlying mechanisms. As astrocytes represent the great majority of brain cells, inhibition of their proliferation, which occurs during the brain growth spurt, may explain, at least in part, the observed microencephaly caused by ethanol.

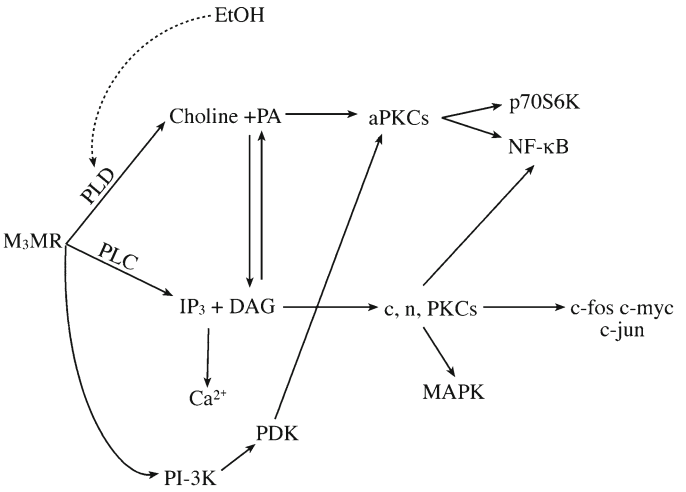

Fig. 1. Pathways activated by carbachol in astroglial cells and involved in acetylcholine-induced DNA synthesis. Shown is also the site of action of ethanol.

6. In Vitro Studies on Astrocyte–Neuron Interactions

The ability of ethanol to inhibit muscarinic receptor signaling in astrocytes has led to an additional hypothesis which involves the interactions of astrocytes and neurons, and the ability of astrocytes foster neuronal differentiation.

Glial cells exert a profound effect on neuronal development as they provide trophic support essential for neuronal survival, and are involved in neuronal migration, axon and dendritic outgrowth, and synaptogenesis (65–67). Astrocytes are known to express and release molecules that promote (e.g., fibronectin) or inhibit (e.g., neurocan) neurite outgrowth, thus playing an important role during brain development and regeneration after lesions (68, 69). We hypothesized that activation of muscarinic receptors in astrocytes may increase the expression and release of permissive factors leading to neuronal differentiation, most notably neuritogenesis. Incubation of rat cortical or hippocampal astrocytes with the cholinergic agonist carbachol, followed by a complete washout, was indeed found to increase the ability of astrocytes to induce neurite outgrowth in hippocampal neurons (70). Carbachol-"primed" astrocytes caused a two-three-fold increase in the length of the largest neurite, and a twofold increase in the minor neurites' length in hippocampal neurons. This effect of carbachol was also due to activation of M3 muscarinic receptors. Under the conditions of these experiments, carbachol did not cause an increase in DNA synthesis; thus, the effect of carbachol-stimulated astrocytes on hippocampal neurons neuritogenesis was not due to an increase in the number of astrocytes.

By means of shotgun proteomics, we analyzed the proteins present in rat astrocyte secretoma (71). One hundred and thirty three secreted proteins were identified. Extracellular proteins were classified based on their biological and molecular functions; most of the identified proteins were involved in neuronal development (71). As neurite outgrowth in CNS neurons is primarily dependent on extracellular matrix proteins that are produced and released by glial cells, the effects of carbachol on two of these proteins, fibronectin and laminin-1, were investigated. Activation of astrocytic M3 muscarinic receptors caused an increase in protein and mRNA levels of both fibronectin and laminin-1 in these cells, as well as in astrocyte conditioned medium. Carbachol also increased the levels of plasminogen activator inhibitor-1 (PAI-1), which inhibits degradation of fibronectin and of laminin-1, and has a neuritogenic action on its own (70). Thus, cholinergic muscarinic stimulation of astrocytes enacts a cascade of events that contribute to the creation of an

extracellular environment favorable to neuronal development, leading to neurite outgrowth and axonal differentiation in hippocampal neurons.

In vivo evidence indicates that ethanol affects neuronal differentiation (72, 73), and this effect has been ascribed to a direct action of ethanol on neurons. However, studies examining the effects of ethanol on neurite outgrowth in neuronal cell in culture have provided contrasting results, with both inhibition and augmentation of neurite outgrowth being reported (e.g., (74, 75)). An important variable in these culture models is the presence of astrocytes, which are obviously present together with neurons in an in vivo situation. Utilizing the co-culturing system described above, we investigated whether ethanol would inhibit the ability of carbachol-stimulated astrocytes to promote neuritogenesis in hippocampal neurons. We found that co-incubation of astrocytes with carbachol and ethanol (25–100 mM), followed by complete washout, inhibited their ability to promote neurite outgrowth in hippocampal neurons (76). As was the case for inhibition of astrocyte proliferation, the target for ethanol was shown to be PLD; indeed, the effect of ethanol was mimicked by 1-butanol, a PLD inhibitor, but not by tert-butanol, an inactive analogue (76). Furthermore, ethanol also inhibited carbachol-induced increases of fibronectin, laminin and PAI-1, substantiating a role for these mediators in astrocyte–neuron interactions leading to neuritogenesis (76).

7. Conclusions

In summary, these studies with ethanol indicate that signal transduction systems coupled to muscarinic M3 receptors in astrocytes represent a relevant target for the developmental neurotoxicity of this alcohol. By inhibiting PLD, ethanol impairs muscarinic receptor signaling in astrocytes leading to decreased proliferation of these cells, and to a decreased ability of astrocytes to promote neuronal maturation. This action of ethanol may underlie, at least in part, microencephaly and altered neuronal development, which are two important characteristics of FAS.

These studies also provide an example of how cell culture systems provide the means of investigating mechanism of action of neurotoxic chemicals affecting signal transduction systems. Indeed, the initial in vivo observation of an inhibition of muscarinic receptor signaling by ethanol has developed in a series of cell culture studies which have allowed identification of cellular and molecular substrates for the action of ethanol on the developing nervous system.

Acknowledgments

Studies by the authors were supported in part by grants from NIAAA (AA-08154) and NIEHS (P30ES07033).

References

1. Eyster KM (1998) Introduction to signal transduction: a primer for untangling the web of intracellular messengers. Biochem Pharmacol 55:1927–1938
2. Eyster KM (2007) New paradigms in signal transduction. Biochem Pharmacol 73:1511–1519
3. Smrcka AV (2008) G protein betagamma subunits: central mediators of G-protein coupled receptors signaling. Cell Mol Life Sci 65:2191–2214
4. Cantley LC (2002) The phosphoinositide 3-kinase pathway. Science 296:1655–1657
5. Wymann MP, Zvelebil M, Laffargue M (2003) Phosphoinositide 3-kinase signaling-which way to target? Trends Pharmacol Sci 24:366–376
6. Costa LG, Costa LG, Costa LG (1997) Role of cell signalling in neurotoxicity. In: Lowndes HE, Reuhl KR (eds) Comprehensive toxicology, vol. 11. Nervous system and behavioral toxicology. Elsevier, New York, pp 99–113
7. Moncada S, Palmer RMJ, Higgs EA (1991) Nitric oxide: physiology, pathophysiology and pharmacology. Pharmacol Rev 43:109–142
8. Southam E, Garthwaite J (1993) The nitric oxide-cyclic GMP signaling pathway in rat brain. Neuropharmacology 32:1267–1277
9. Guix FX, Uribesalgo I, Coma MA, Munoz FJ (2005) The physiology and pathophysiology of nitric oxide in the brain. Progr Neurobiol 76:126–152
10. Moncada S, Bolanos JP (2006) Nitric oxide, cell bioenergetics and neurodegeneration. J Neurochem 97:1676–1689
11. Calabrese V, Mancuso C, Calvani M, Rizzarelli E, Butterfield DA, Giuffrida-Stella AM (2007) Nitric oxide in the central nervous system: neuroprotection versus neurotoxicity. Nat Rev Neurosci 8:766–775
12. Thomas DD, Ridnour LA, Isenberg JS et al (2008) The chemical biology of nitric oxide: implications in cellular signaling. Free Rad Biol Med 45:18–31
13. Costa LG (1990) The phosphoinositide/protein kinase C system as a target for neurotoxicity. Pharmacol Res 22:393–408
14. Costa LG (1994) Cell signaling and neurotoxic events. In: Chang LW (ed) Principles of Neurotoxicology. Marcel Dekker, New York, pp 475–493
15. Costa LG (1994) Second messenger systems in developmental neurotoxicity. In: Harry J (ed) Developmental Neurotoxicology. CRC Press, Boca Raton, FL, pp 77–101
16. Costa LG (1994) Signal transduction mechanisms in developmental neurotoxicity: the phosphoinositide pathway. Neurotoxicology 15:19–28
17. Costa LG (1998) Signal transduction in environmental neurotoxicity. Annu Rev Pharmacol Toxicol 38:21–43
18. Costa LG, Guizzetti M, Lu H, Bordi F, Vitalone A, Tita B, Palmery M, Valeri P, Silvestrini B (2001) Intracellular signal transduction pathways as targets for neurotoxicants. Toxicology 160:19–26
19. Costa LG, Giordano G, Guizzetti M (2010) Cell signaling and neurotoxicity. In: Philbert M (ed) Comprehensive toxicology, vol 13. Nervous system and behavioral toxicology, 2nd edn. Elsevier, Oxford
20. Streissguth AP, Landesman-Dwyer S, Martin JC, Smith DW (1980) Teratogenic effects of alcohol in human and laboratory animals. Science 209:353–361
21. Samson HH (1986) Microcephaly and fetal alcohol syndrome: human and animal studies. In: West JR (ed) Alcohol and Brain Development. Oxford University Press, Oxford, pp 167–183
22. Ikonomidou C, Bittigau P, Ishimaru MJ et al (2000) Ethanol-induced apoptotic neurodegeneration and fetal alcohol syndrome. Science 287:1056–1060
23. Cui SJ, Terwai M, Schneider TA, Rubin R (1997) Ethanol promotes cell death by inhibition of the insulin-like growth factor I receptor. Alcohol Clin Exp Res 21:1121–1127
24. Miller MW (1997) Effects of prenatal exposure to ethanol on callosal projection neurons in rat somatosensory cortex. Brain Res 766:121–128
25. Miller MW, Astley SJ, Clarren SK (1999) Number of axons in the corpus callosum of the mature macaca nemestrina: increases caused by prenatal exposure to ethanol. J Comp Neurol 412:123–131

26. Guerri C, Pascual M, Renau-Piqueras J (2001) Glia and fetal alcohol syndrome. Neurotoxicology 22:65–81
27. Costa LG, Yagle K, Vitalone A, Guizzetti M (2004) Alcohol and glia in the developing brain. In: Aschner M, Costa LG (eds) The Role of Glia in Neurotoxicity, 2nd edn. CRC Press, Boca Raton, FL, pp 343–354
28. Miller MW, Robertson S (1993) Prenatal exposure to ethanol alters the postnatal development and transformation of radial glia to astrocytes in the cortex. J Comp Neurol 337:252–266
29. Riley EP, Mattson SN, Sowell ER, Jernigan TL, Sobel TF, Jones KL (1995) Abnormalities of the corpus callosum in children prenatally exposed to alcohol. Alcohol Clin Exp Res 19:1198–1201
30. Costa LG, Guizzetti M (1999) Muscarinic cholinergic receptor signal transduction as a potential target for the developmental neurotoxicity of ethanol. Biochem Pharmacol 57:721–726
31. Costa LG (1993) Muscarinic receptors and the developing nervous system. In: Zagon IS, McLaughlin PJ (eds) Receptors in the Developing Nervous System. Chapman and Hall, London, pp 21–42
32. Costa LG (1995) Effect of developmental neurotoxicants on muscarinic receptors and intracellular signalling pathways. In: Shaw CA (ed) Receptors Dynamics in Neural Development. CRC Press, Boca Raton, FL, pp 305–320
33. Costa LG (1998) Ontogeny of second messenger systems. In: Slikker W, Chang LW (eds) Handbook of Developmental Neurotoxicology. Academic Press, San Diego, pp 275–284
34. Lauder JM, Schambra U (1999) Morphogenetic roles of acetylcholine. Environ Health Perspect 107(suppl 1):65–69
35. Balduini W, Murphy SD, Costa LG (1987) Developmental changes in muscarinic receptor-stimulated phosphoinositide metabolism in rat brain. J Pharmacol Exp Ther 241:421–427
36. Ladinsky H, Consolo S, Peri G, Garattini S (1972) Acetylcholine, choline and choline acetyltransferase activity in the developing brain of normal and hypothyroid rats. J Neurochem 19:1947–1952
37. Coyle JT, Yamamura HI (1976) Neurochemical aspects of the ontogeny of cholinergic neurons in the rat brain. Brain Res 188:429–440
38. Hosey MM (1992) Diversity of structure, signaling, and regulation within the family of cholinergic muscarinic receptors. FASEB J 6:845–852
39. Lee W, Nicklaus KJ, Manning DC, Wolfe BB (1990) Ontogeny of cortical muscarinic receptor subtypes and muscarinic receptor-mediated responses in the rat. J Pharmacol Exp Ther 252:482–490
40. Heacock AM, Fisher SK, Agranoff BW (1987) Enhanced coupling of neonatal muscarinic receptors in rat brain to phosphoinositide turnover. J Neurochem 48:1904–1911
41. Tan XX, Costa LG (1995) Postnatal development of muscarinic receptor – stimulated phosphoinositide metabolism in mouse cerebral cortex: sensitivity to ethanol. Dev Brain Res 86:348–353
42. Larocca JN, Rodriguez-Gain AG, Rashbaum WK, Weidenheim KM, Lyman WD (1994) Muscarinic receptor-dependent activation of phospholipase C in the developing human fetal central nervous system. Brain Res 653:9–15
43. Costa LG, Balduini W, Renò F (1995) Muscarinic receptor stimulation of phospholipase D activity in the developing brain. Neurosci Res Comm 17:169–176
44. Dobbing J, Sands J (1979) Comparative aspects of the brain growth spurt. Early Hum Develop 3:79–83
45. Balduini W, Costa LG (1989) Effects of ethanol on muscarinic receptor-stimulated phosphoinositide metabolism during brain development. J Pharmacol Exp Ther 250:541–547
46. Balduini W, Renò F, Costa LG, Cattabeni F (1994) Developmental neurotoxicity of ethanol: further evidence for an involvement of muscarinic receptor – stimulated phosphoinositide metabolism. Eur J Pharmacol Mol Pharmacol Sect 266:283–289
47. Renò F, Tan XX, Balduini W, Costa LG (1994) Administration of ethanol during the rat's brain growth spurt causes dose – dependent microencephaly and inhibition of muscarinic receptor – stimulated phosphoinositide metabolism. Res Comm Alcoh Subst Abuse 15:141–150
48. Balduini W, Costa LG (1990) Developmental neurotoxicity of ethanol: in vitro inhibition of muscarinic receptor-stimulated phosphoinositide metabolism in brain from neonatal but not adult rats. Brain Res 512:248–252
49. Balduini W, Candura SM, Manzo L, Cattabeni F, Costa LG (1991) Time-, concentration-, and age- dependent inhibition of muscarinic receptor- stimulated phosphoinositide metabolism by ethanol in the developing rat brain. Neurochem Res 16:1235–1240
50. Tan XX, Castoldi AF, Manzo L, Costa LG (1993) Interaction of ethanol with muscarinic receptor – stimulated phosphoinositide

metabolism during the brain growth spurt in the rat: role of acetaldehyde. Neurosci Lett 156:13–16

51. Kovacs KA, Kavanagh TJ, Costa LG (1995) Ethanol inhibits muscarinic receptor – stimulated phosphoinositide metabolism and calcium mobilization in rat primary cortical cultures. Neurochem Res 20:939–949
52. Ashkenazy A, Ramachandran J, Capon DJ (1989) Acetylcholine analogue stimulates DNA synthesis in brain-derived cells via specific muscarinic receptor subtypes. Nature 340:146–150
53. Guizzetti M, Costa P, Peters J, Costa LG (1996) Acetylcholine as a mitogen: muscarinic receptor – mediated proliferation of rat astrocytes and human astrocytoma cells. Eur J Pharmacol 297:265–273
54. Guizzetti M, Costa LG (1996) Inhibition of muscarinic receptor – stimulated glial cell proliferation by ethanol. J Neurochem 67:2236–2245
55. Guizzetti M, Moeller T, Costa LG (2003) Ethanol inhibits muscarinic receptor-mediated DNA synthesis and signal transduction in human fetal astrocytes. Neurosci Lett 344:68–70
56. Stanimirovic DB, Ball R, Mealing G, Morley P, Durkin JP (1995) The role of intracellular calcium and protein kinase C in endothelin-stimulated proliferation of type I astrocytes. Glia 15:119–130
57. Catlin MC, Guizzetti M, Costa LG (2000) Effect of ethanol on muscarinic receptor-induced calcium responses in astroglia. J Neurosci Res 60:345–355
58. Guizzetti M, Wei M, Costa LG (1998) The role of protein kinase C α and ε isozymes in DNA synthesis induced by muscarinic receptors in a glial cell line. Eur J Pharmacol 359:223–233
59. Guizzetti M, Costa LG (2000) Muscarinic receptors, protein kinase C isozymes and proliferation of astroglial cells: effects of ethanol. Neurotoxicology 21:1117–1122
60. Yagle K, Lu H, Guizzetti M, Moller T, Costa LG (2001) Activation of mitogen-activated protein kinase by muscarinic receptors in astroglial cells: role in DNA synthesis and effect of ethanol. Glia 35:111–120
61. Guizzetti M, Costa LG (2000) Possible role of protein kinase C ζ in muscarinic receptor-induced proliferation of astrocytoma cells. Biochem Pharmacol 60:1457–1466
62. Guizzetti M, Costa LG (2002) Effect of ethanol on protein kinase C ζ and p70S6 kinase activation by carbachol: a possible mechanism for ethanol-induced inhibition of glial cell proliferation. J Neurochem 82:38–46
63. Guizzetti M, Thompson BD, Kim Y, VanDeMark K, Costa LG (2004) Role of phospholipase D signaling in ethanol induced inhibition of carbachol-stimulated DNA synthesis of 1321N1 astrocytoma cells. J Neurochem 90:646–653
64. Guizzetti M, Bordi F, Dieguez-Acuna FJ, Vitalone A, Madia F, Woods JS, Costa LG (2003) Nuclear factor kB activation by muscarinic receptors in astroglial cells: effect of ethanol. Neuroscience 120:941–950
65. Ullian EM, Christopherson KS, Barres BA (2004) Role for glia in synaptogenesis. Glia 47:209–216
66. Volterra A, Meldolesi J (2005) Astrocytes, from brain glue to communication elements: the revolution continues. Nat Neurosci 6:626–640
67. Seth P, Koul N (2008) Astrocyte, the star avatar: redefined. J Biosci 33:405–421
68. Pagani F, Zagato L, Vergani C, Cassari G, Sidoli A, Barale FE (1991) Tissue-specific splicing pattern of fibronectin messenger RNA precursor during development and aging rat. J Cell Biol 113:1223–1229
69. Rauch U, Feng K, Zhou XH (2001) Neurocan: a brain chondroitin sulfate proteoglycan. Cell Mol Life Sci 58:1842–1856
70. Guizzetti M, Moore NH, Giordano G, Costa LG (2008) Modulation of neuritogenesis by astrocyte muscarinic receptors. J Biol Chem 283:31884–31897
71. Moore NH, Costa LG, Shaffer SA, Goodlett DR, Guizzetti M (2009) Shotgun proteomics implicates extracellular matrix proteins and protease systems in neuronal development induced by astrocyte cholinergic stimulation. J Neurochem 108:891–908
72. Davies DL, Smith DE (1981) A Golgi study of mouse hippocampal CA1 pyramidal neurons following perinatal ethanol exposure. Neurosci Lett 26:49–54
73. Smith DE, Davies DL (1990) Effect of perinatal administration of ethanol on the CA1 pyramidal cell of the hippocampus and Purkinje cells of the cerebellum: an ultrastructural survey. J Neurocytol 19:708–719
74. Zou J, Rabin RA, Pentney RJ (1993) Ethanol enhances neurite outgrowth in primary cultures of rat cerebellar macroneurons. Brain Res Dev Brain Res 72:75–84
75. Bearer CF, Swick AR, O'Riordan MA, Cheng G (1999) Ethanol inhibits L1-mediated neurite outgrowth in postnatal rat cerebellar granule cells. J Biol Chem 274:13264–13270
76. Guizzetti M, Moore N, Giordano G, Costa LG (2010) Ethanol inhibits neuritogenesis induced by astrocyte muscarinic receptors. Glia 58(12):1395–1406

Chapter 12

Neurite Degeneration in Human Neuronal SH-SY5Y Cells as an Indicator of Axonopathy

Anna Forsby

Abstract

Neurotoxicological testing is mainly based on experimental animal models, but several cell and tissue culture models have been developed to study the mechanisms of neurotoxicity. In general, cells of human origin are attractive alternatives to the animal models for extrapolation of toxicity on humans. The characteristics, culture conditions and usefulness of the human neuroblastoma cell line SH-SY5Y as a model for axonopathy are presented in this chapter. It is described how the cell line can be differentiated to mature neurons by using serum-free "N2" medium supplemented with retinoic acid. Detailed protocols for the determination of neurite degeneration and general cytotoxicity are presented.

Key words: SH-SY5Y, Neuroblastoma cell line, Axonopathy, Neurite degeneration, General cytotoxicity

1. Introduction

1.1. Neuronal Cell Lines

The classical test systems for estimating neurotoxicity involve laboratory animal models. However, several alternative cell models have been developed to study the mechanisms, and attempts to find useful in vitro models for risk assessment have also been initiated. One approach is to use cloned neuronal cell lines, which can be obtained from cell and tissue banks (e.g., American Type Culture Collection (ATCC) and European Collection of Animal Cell Cultures (ECACC)). The main advantages of using cell lines over primary cells are summarized in Table 1. Although the cell lines have many benefits, one must be aware that they are immortalized by genomic transformation and may not be sufficiently organotypic. Furthermore, there is a risk that cell lines of neuroblastoma origin can behave as cancerous cell types.

Michael Aschner et al. (eds.), *Cell Culture Techniques*, Neuromethods, vol. 56,
DOI 10.1007/978-1-61779-077-5_12,

Table 1
Advantages and limitations of neuronal cell lines

Advantages	Limitations
Exponential growth of a continuous cell line provides almost indefinite source of cells	May transform with increased number of passages
Human cells can be used	Abnormal karyotype may appear
Homologous cell population and often well characterized	Abnormal tissue environment, often 2D cultures lacking glia cells
Can be genetically modified yielding (over)-expression or knock down of specific proteins of interest	Neuronal functions may be limited
Available on the market guarantees quality and supply	

1.2. The SH-SY5Y Neuroblastoma Cell Line

One of the advantages of neuroblastoma cell lines is that neuronal cells of human origin are readily available. The SH-SY5Y is a neuronal sub-clone of the SK-N-SH neuroblastoma cell line, which was isolated from a metastatic bone marrow tumor in the early 1970s (1). It is now well characterized and one of the most frequent neuroblastoma cell lines reported in the PubMed data base (http://www.ncbi.nlm.nih.gov/pubmed/). The native SH-SY5Y cells possess catecholamine-synthesizing enzyme and monoamine transporter activity (2, 3), and they are widely used as a dopaminergic cell model in the research on Parkinson's disease (4, 5) as well as in studies on molecular aspects of Alzheimer's disease (6–8). Furthermore, SH-SY5Y cells express muscarinic acetylcholine receptor signaling pathway systems and extracellular acetylcholine esterase activity (9). Because of their neurospecific properties and their uncomplicated culture requirements (see Sects. 2.1 and 3.1), they are also popular for neurotoxicity analyses.

The organotypic features of SH-SY5Y cells can be enhanced by culturing the cells in serum-free N2 medium, supplemented with all-trans retinoic acid (denoted N2-RA medium) (10), which induces biochemical, physiological and morphological neuronal differentiation (Fig. 1). The expression of nicotine- and muscarine-like acetylcholine receptors and downstream signaling pathways is increased, the resting membrane potential becomes more negative, and an extensive neuronal network of neurites is developed after a few days in culture with N2-RA medium (11, 12).

1.3. Neurite Degeneration as an Indicator for Neurotoxicity

Attenuated outgrowth or retraction of neuronal processes and axons are common features of neurotoxicity. Classical neurotoxic chemicals such as acrylamide and certain organophosphorous compounds induce degeneration of neuronal processes in brain as

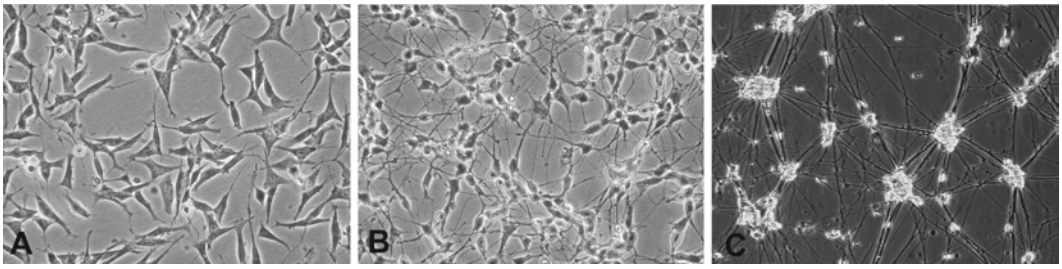

Fig. 1. Native and differentiated SH-SY5Y cells, (**a**) 24 h after plating, (**b**) 6 days in N2-RA medium and (**c**) 3 weeks in N2-RA medium (image taken at another occasion).

well as of peripheral nerves (axonopathy) (13, 14). Neurotoxicity testing for regulatory purposes comprises acute or repeated in vivo exposure of animals. The Organization for Economic Co-operation and Development (OECD) test guidelines for estimation of organophosphate-induced delayed neuropathy (OPIDN) recommend hens as the experimental animals (OECD TG 418 and 419). No specific test guidelines are developed for estimation of axonopathy caused by other chemicals, but this specific sign of neurotoxicity is included in OECD TG 424, which describes tests for biochemical, histological and behavioral effects associated with neurotoxicity in rodents.

A few in vitro assays have been developed for estimation of OPIDN (15–17), and in our laboratory we have studied acrylamide-induced axonopathy in vitro (18, 19). Axonopathy is an active, well-controlled process of axon segment self-destruction resembling the apoptosis-signaling pathways (20). The SH-SY5Y cells have been shown to constitute a convenient model for mechanistic research and quantitative analysis of degenerating neurites by determination of the number of processes per cell body during and after exposure (19, 21). By integrating neurite degeneration over time with a pharmacologically based biokinetic model of acrylamide, neurotoxic doses after acute and subchronic exposure could be estimated for rat (22).

The feasibility to use neurite degeneration as an endpoint for axonopathy has been demonstrated by the fact that the concentration of chemicals which affect axons and neuronal processes is significantly lower than the concentration that induces general cytotoxicity (i.e., reduced cell viability) of the same chemicals. Chemicals that are known *not* to induce axonopathy induce cytotoxicity at the same or lower concentration than neurite degeneration, if the neurites are affected at all. Hence, the difference between the concentration inducing 20% reduced viability (IC20) and the concentration inducing 20% neurite degeneration (ND20) determines whether a compound may induce axonopathy or not (18, 19).

The neurite degeneration assay has been used for studies on novel chemicals and complex mixtures as shown by *Aspergillus fumigatus*-produced mycotoxins with gliotoxin as a specific example (23). Furthermore, we have previously shown that SH-SY5Y cells which have been cultured for 6 days in differentiation medium become sensitive to increased glucose concentrations. The "hyperglycemic" in vitro model illustrates that the method is also useful in diabetes research as an indication of neuropathy (24).

2. Materials

2.1. Media

2.1.1. Medium for Culturing Native SH-SY5Y Cells

Complete minimal essential medium with Earle's salts (EMEM) is used for routine culture of the cells, for seeding of cells before experiments and as culture medium for the native cells that will be used in experiments.

1. Supplement the EMEM without L-glutamine (Invitrogen, cat no 21090-022) with 10% fetal bovine serum (FBS), South American, EC-approved (Invitrogen, cat no 10270-106), 2 mM L-glutamine (Invitrogen, cat no 25030-024), 100 µg streptomycin/mL, 100 U penicillin/ml (Invitrogen, cat no 15140-122) and 1% non-essential amino acids (Invitrogen, cat no 11140-035).
2. Store the complete EMEM at 4°C and use the medium within 2 weeks after mixing.
3. Pre-warm the medium to 37°C before adding it to the cells.

2.1.2. Medium for Differentiating SH-SY5Y Cells

Differentiate the cells in a mixture of Dulbeccos's Minimal essential medium (DMEM) and Ham's F12 medium with N2 supplements (10), and 1 µM all-trans retinoic acid (RA).

1. Supplement the DMEM:F12 medium containing L-glutamine and 15-mM HEPES (Invitrogen, cat no 31330-038) with 1-mM L-glutamine, 100-µg streptomycin/mL and 100-U penicillin/mL (denoted complete DMEM:F12 medium).
2. To make 100 mL complete DMEM:F12 medium with N2 supplements, add one aliquot of the concentrated N2 supplements (33× final concentration, see Sect. 2.1.2.1) to 97 mL complete DMEM:F12 medium.
3. Store the DMEM:F12 medium with N2 supplements in dark at 4°C and use the medium within 2 weeks after mixing.
4. On the day of addition to the cells, add 0.1% all-trans retinoic acid (RA, Sigma, cat no R2625, diluted to 1 mM in 99% ethanol and stored at −20°C in dark) to the complete DMEM:F12 medium with N2 supplements to give a final concentration of 1 µM.

5. Keep the complete DMEM:F12 medium with N2 supplements with RA (denoted N2-RA) in dark since RA is light sensitive.
6. Pre-warm the medium to 37°C before adding it to the cells.

2.1.2.1. N2 Supplement

Prepare the N2 supplement at 33.3× final concentration in complete DMEM:F12 medium:

1. Transfer 25 mL complete DMEM:F12 medium to a 50 mL centrifuge tube.
2. Add 100 mg apo-transferrin (bovine, ICN, cat no 152334). Allow the transferrin to dissolve slowly, do not shake.
3. Add 16.1 mg putrescine (Sigma, cat no P5780).
4. Add 1,000 µL insulin (bovine, Sigma, cat no I1882), prepared as 5 mg/mL in sterile 1% acetic acid.
5. Add 10 µL sodium selenite (Sigma, cat no S5261), prepared as 3 mM in ultra-pure H_2O.
6. Add 100 µL progesterone (Sigma, cat no P8783), prepared as 200 µM in ethanol).
7. Invert the tube slowly several times.
8. Adjust the pH by drop-wise addition of 1 M NaOH until the medium has retained its red color, indicating natural pH.
9. Adjust the medium volume to 30 mL by adding complete DMEM:F12 medium.
10. Sterile filter the N2 supplement concentrate through a nylon 0.22 µm filter.
11. Make 3 mL aliquots and store at –20°C for up to 6 months.

The final concentrations of the N2 supplements added to the cells are shown in Table 2.

Table 2
Final concentration of N2 supplements in the complete DMEM:F12 medium

Supplement	Final concentration
Insulin	5 µg/mL
Progesterone	20 nM
Sodium selenite	30 nM
Putrescine	100 µM
Apo-transferrin	100 µg/mL

2.2. Exposure to Chemicals or to Neurotoxic Conditions

Prepare the solutions of the test chemicals on the day of exposure.

2.2.1. Chemical Exposure

1. Dissolve polar chemicals in 37°C N2-RA medium and non-polar chemicals in DMSO or ethanol.
2. Make a stock solution in N2-RA medium at the highest soluble concentration or at approximately IC80, if the cytotoxicity of the chemical is known.
3. Sterile filter the stock solution through a 0.22 μm nylon filter.
4. Prepare a dilution series with 6–8 concentrations from the sterile stock solution (equal to the highest concentration) in 0.5log10 dilution steps for the initial dose-finding experiments.
5. For the repeated experiments, adjust the concentrations in the dilution series to cover the effect on cell viability and neurites from 0% of control (no effects) to at least 90% of control (total cell death or neurite degeneration).

Nota bene: The DMSO and ethanol concentration must not exceed 0.5 and 0.2%, respectively, in the solutions that are added to the cells. Control cells must be exposed to the same concentration of solvent.

2.2.2. Glucose Exposure

The standard D-glucose concentration in DMEM:F12 medium is 17 mM. To prepare N2 medium with lower concentration, manual preparation of the medium must be made:

1. Mix 250 mL DMEM with 1,000 mg (low) D-glucose/L (Invitrogen cat no 31885-023) and 250-mL Ham's F12 medium (Invitrogen cat no 21765-029). This will yield a final D-glucose concentration of 8 mM.
2. Adjust the concentrations of Hepes (free acid or sodium salt), L-glutamine, antibiotics and N2 supplements as described in Sect. 2.1.2 under sterile conditions.
3. Prepare stock solutions of 592 mM D-glucose in N2 medium and mix well. Do not consider the d-glucose concentration in the N2 medium.
4. Sterile filter through a 0.22 μm nylon filter.
5. Dilute the 592 mM D-glucose solution in N2 medium with 8 mM D-glucose to 5 (yielding 30 mM) and 10% (yielding 60 mM) D-glucose, simulating hyperglycemic conditions.
6. Use the N2 medium with 8 mM D-glucose concentration as control.

2.3. Materials for Determining Neurite Number and Neurite Elongation

Use an inverted phase contrast microscope at 150–200 times magnification. Depict the cells using a CCD camera (e.g., Olympus DP50) and the StudioLite (v. 3.0.1) and Viewfinder (v. 3.0.1) software (Pixera Corporation).

2.4. General Cytotoxicity

The general cytotoxicity caused by exposure to chemicals, mixtures or radiation is determined as reduction of the total cellular protein concentration, according to a modified version of Lowry et al. (25).

2.4.1. Reagents

Solution A: 20 g of Na_2CO_3.

4 g of NaOH.

Dilute to 1 L with ultra-pure H_2O and store in room temperature.

Solution B: Prepare at the day of experiment:

1 mL 1% $CuSO_4$*$5H_2O$ (1 g/100 mL ultra-pure H_2O) (store at 8°C)

1 mL 2% Na-tartrat (1.02 g/50 mL ultra-pure H_2O) (store at 8°C)

Solution C: Prepare at the day of experiment:

100 mL solution A + 2 mL solution B (B is also mixed on the day of experiment).

Folin reagent diluted 1:4 in ultra-pure H_2O (store at 8°C).

2.4.2. Standard Curve

Prepare a stock solution of bovine serum albumin (BSA) 1 mg/mL in 0.1 M NaOH to check the linear interval of the absorbance versus protein concentration correlation by dissolving 2–5 mg of BSA in 0.1 M NaOH and make a dilution series of 0.01, 0.05, 0.1, 0.2, 0.3, 0.4 and 0.5 mg/mL.

2.5. Determination of Toxic and Neurotoxic Parameters

The toxic effects are calculated as percent of control and concentration–effect curves can be prepared, e.g., in the GraphPad Prism software.

3. Methods

3.1. Cell Maintenance and Culture Procedures of SH-SY5Y

3.1.1. Routine Cell Culture

Plate 2×10^6 cells in single-cell suspension in 20 mL complete EMEM in a 75 cm^2 flask. Change the medium after 3–4 days to fresh complete EMEM. Keep the cell cultures in a humidified CO_2 (5% in air) incubator at 37°C. Subculture the cells every seventh day using 0.05% trypsin and 0.02% EDTA in Hank's balanced salt solution (Invitrogen cat no 25300-054):

1. Aspire the medium and rinse the cells rapidly but gently in 3 mL trypsin/EDTA solution (Invitrogen, cat no 25300-054). Aspire the trypsin/EDTA solution.
2. Detach the cells in 1 mL trypsin/EDTA solution for 5 min in 37°C (no CO_2).
3. Add 9 mL complete regular cell culture medium to the detached cells and prepare single-cell suspension by vigorous

flushing at least 20 times by a 10 mL pipette. Check under the microscope that the cells are in single-cell suspension.

3.1.2. Differentiating SH-SY5Y Cells

1. Plate $8–10 \times 10^3$ cells per square centimeter in complete EMEM in appropriate vessels, e.g., 9 cm^2 cell culture dishes, 6- or 24-well plates.
2. Change the complete EMEM the day after plating to N2-RA to induce differentiation. After 3–4 days in differentiation medium, cell proliferation has slowed down and a network of neurites has started to develop. The cultures are now regarded as "semi-differentiated."
3. The cells can be further differentiated after medium changes every third to fourth day and are regarded as terminally differentiated after 3 weeks in culture.

3.2. Exposure

The SH-SY5Y cells can be used at different stages of differentiation, depending on which neuronal developmental stage is desired. Exposure starts at the onset of differentiation for studies on neuroblast maturation and studies on neurite outgrowth. Semi-differentiated cultures are used for measurements of reduction of the number of neurites per cell, indicating neurite degeneration as well as attenuated neurite outgrowth. After 6 days in differentiation medium, the cells have developed an extensive neurite network and have also become sensitive to increased glucose concentrations, simulating a hyperglycemic condition (24). The procedures for the different applications are described below. All exposures are performed in a humidified cell incubator at 37°C and 5% CO_2 in air.

3.2.1. Effects of Chemicals and Complex Mixtures on the Number of Neurites per Cell

1. Inhibition of neurite outgrowth
   (a) Remove the complete EMEM medium the day after plating.
   (b) Start exposure of immature cells to chemicals diluted in N2-RA and to N2-RA medium for control cells. The exposure can proceed for hours up to 6 days.
   (c) Change the medium with test chemicals to fresh N2-RA medium after exposure.
   (d) Incubate the cells for up to 6 days after start of exposure and differentiation.
2. Neurite degeneration
   (a) Remove the N2-RA medium after 3 days of differentiation.
   (b) Start exposure of semi-differentiated cells to chemicals diluted in N2-RA and to N2-RA medium for control cells.
   (c) Expose the cells for 24–72 h.
   (d) For recovery, change exposure medium with test chemicals to fresh N2-RA medium and incubate for 4 days.

3.2.2. Diabetic Neuropathy Cell Model

1. To obtain glucose-sensitive neuronal cells, the SH-SY5Y cells must be differentiated for 6 days using N2-RA medium with one medium change after 3 days.
2. Depict the cultures before start of exposure at 150 times magnification using a phase contrast microscope with a CCD camera.
3. Remove the N2-RA medium and add:
   (a) N2-RA medium with reduced (8 mM) D-glucose concentration for control cultures (see Sect. 2.2.2).
   (b) N2-RA medium with 30 and 60 mM D-glucose for "hyperglycemic" conditions (see Sect. 2.2.2).
4. Expose the cells for 3 days.

3.3. Determination of the Number of Neurites per Cell

Neurite degeneration can be followed over time if the cells are depicted every 24 h (19).

1. The cells are depicted at the end of exposure in the N2-RA medium or in PBS after the exposure medium has been removed. Be aware that exposed cells may be loosely attached to the plastic surface and must be handled with care.
2. Every cell culture plate or dish is put under the phase-contrast microscope and four random areas per vessel are depicted at 150 times magnification using a CCD camera.
3. Count the numbers of cell bodies and the number of neurites with a length exceeding the diameter of the cell body per image manually (Fig. 2). Ramifications of the neurites are counted if they fulfill the criterion of the length. Dead cells and non-neuronal cells, i.e., epithelial-like neuroblastoma cells (26), when apparent, are not included.
4. Determine the effects on neurite outgrowth or induced neurite degeneration as an indication of impaired morphological differentiation or axonopathy, respectively, by comparing the number of neurites per cell in exposed cultures with that in control cultures.

3.4. Determination of General Cytotoxicity

1. Rinse the cells with cold PBS (containing Mg^{2+} and Ca^{2+} ions); 2 mL per 9 cm^2 dish and well in 6-well plates or 0.5 mL per well in 24-well plates. Be very careful since the cells easily detach from the plastic surface.
2. Lyse the cells in 0.1 M NaOH; 0.4 mL per 9 cm^2 dish and well in 6-well plates or 0.15 mL per well in 24-well plates.
3. Incubate for 1 h on shake at room temperature.
4. Suspend the cell lysates with an automatic pipette.
5. Take 4×50 µL from each well to 4 wells in a 96-well plate, *columns 6–11*.

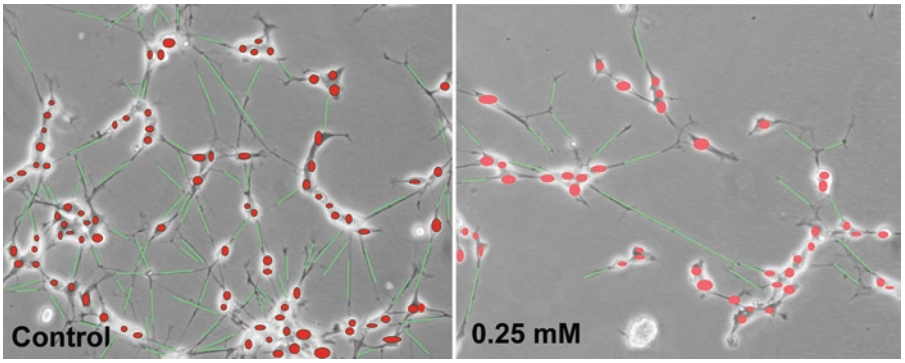

Fig. 2. Quantification of the number of neurites per cell in control and acrylamide-exposed cell cultures. The cells were differentiated in N2-RA medium for 72 h before 0.25 mM in N2-RA (0.25 mM) or just N2-RA (control) was added to the cells. The cell cultures were exposed for 72 h and depicted at originally 150× magnification by a phase contrast microscope equipped with an Olympus DP50 CCD camera. The cell bodies are marked in red and the neurites are marked in green using Adobe Photoshop CS2. The calculated number of neurites per cell is 0.95 in control and 0.47 in acrylamide-exposed cultures, indicating 50% neurite degeneration.

6. The first column should only contain 50 µL 0.1 M NaOH (blank). Distribute BSA standard (see Sect. 2.4.2) on columns 2–5; 50 µL/well, 4 wells/concentration.
7. Add 200-µL solution C per well, incubate exactly 10 min after addition of solution C in the first column and place the plate on shake.
8. Add 50 µL Folin reagent per well and incubate 30 min on shake.
9. Measure the absorbance at 690 nm or higher up to 750 nm in a spectrophotometer designed for 96-well plates.
10. Calculate the reduction in total protein content (cytotoxicity) as a percentage of decrease in absorbance, compared with control.

3.5. Evaluation of Neurotoxicity

1. Plot the total protein content (cytotoxicity) and number of neurites per cell (neurotoxicity) versus the test chemical concentration using the GraphPad Prism 5.0 curve fit program or equivalent software.
2. Determine the concentrations that induce 20 and 50% cytotoxicity (IC20 and IC50) and 20 and 50% neurotoxicity (ND20 and ND50) by using the equation for nonlinear sigmoid curve fit.

The criterion for judging if a chemical shall be regarded as potentially harmful for the axonal architecture by using this assay is that the neurites are significantly more sensitive than the general physiology of the cell, i.e., neurite degeneration occurs at lower concentrations than does the general cytotoxicity (Fig. 3).

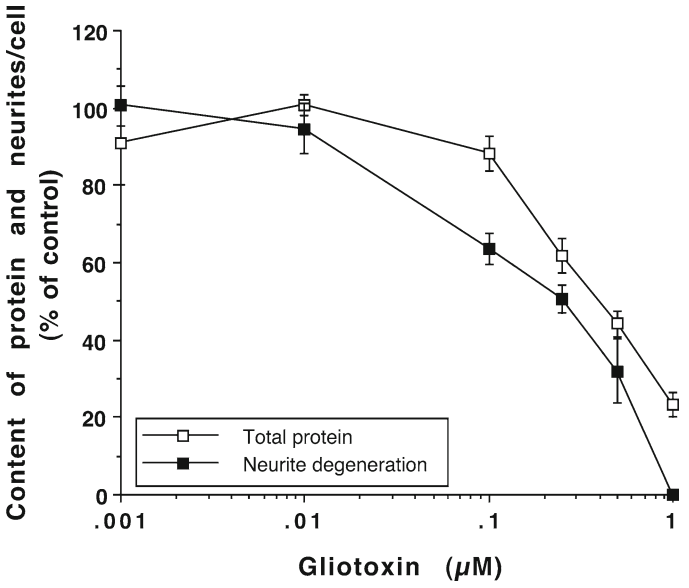

Fig. 3. Concentration-dependent effect on the total protein content and the number of neurites per cell in differentiated SH-SY5Y cells after exposure to gliotoxin for 72 h. (Reproduced from Wenehed et al. (23) with permission from Elsevier).

4. Notes

4.1. General

The SH-SY5Y cells may display at least two phenotypes, one neuronal-like and the other epithelial-like, but "intermediate" cell types may also occur (26). The neuronal phenotype is described in this chapter. Cultures with >5% epithelial-like cell types should not be used for the described experiments. However, routine cultures containing this unwanted cell type may "recover" with increased passages if the cultures are quickly trypsinated. By this method the neuronal phenotype is selected since the epithelial cells are more firmly attached and will therefore remain in the "old" culture flask. Also note that the SH-SY5Y cells must always be sub-cultured into new culture flask. Reuse of "old" flasks should be avoided.

The SH-SY5Y cells may lose differentiation and turn into a more tumor cell-like phenotype at high passages, with increased proliferation rate and lost contact inhibition as a consequence. These cultures will not recover and must be discarded. It is therefore important to keep track on the growth pattern of the cultures.

4.2. Sections

Section 2.1.1. The growth pattern and morphology of the SH-SY5Y cells may change with different batch numbers of FBS. It is therefore very important to establish growth curves and check for standardized (neurochemical) biomarkers when the serum batch needs to be changed.

Section 2.1.2.1. N2 supplements may be purchased from Invitrogen (cat no 17502-048), but this option is more expensive and is slightly different. However, we have not noted any differences in the differentiation process between the commercial and "home-made" N2 supplements.

Section 2.2.1. Acrylamide is neurotoxic as a monomer, but polymerized acrylamide has no specific effect on axons or neurites. It is therefore important to use fresh acrylamide when investigating neurotoxic effects.

Section 2.2.2. Higher concentration of d-glucose in the medium, more than 60 mM, will increase that osmolarity to non-physiological levels.

Section 3.1.2. To facilitate cell separation, the tip of the pipette can be pressed to the bottom of the flask during the preparation of the single-cell suspension.

Section 3.3. To our experience, the human neuroblastoma SH-SY5Y cells from ATCC respond to RA as described above, whereas the SH-SY5Y clone from ECACC does not develop the extensive neurite network.

Section 3.3. We have made attempts to quantify the numbers of cell bodies and neurites by using the SigmaScan Pro 5.0 image analysis software as an alternative to the manual counting. However, the automated counting requires optimized settings for the image capturing under the microscope. The cell bodies and the neurites have to be depicted in different gray scale tones and the cell bodies must be separated. To our experience, the manual counting generates very low variance between each experiment provided that the cells and neurites are counted in at least two images per duplicate culture (i.e., four images per situation/concentration).

Acknowledgements

I wish to thank Johanna EL Andaloussi-Lilja, PhD, for characterization of SH-SY5Y cell differentiation pattern, Viktoria Axelsson, PhD (maiden name Wenehed), for her extensive work on mycotoxin-induced neurotoxicity, Marika Nordin-Andersson, PhD, for the successful evaluation of the assay for risk assessment of acrylamide exposure, Helena Gustafsson, PhD, for showing that the assay is a valuable tool for diabetic neuropathy research and Prof. Erik Walum who invented the method and convinced me of its usefulness. The development and evaluation of the assay have been supported by the Swedish foundation for

research without animal experiments, the National board for laboratory animals, the European Centre for Validation of Alternative Methods, the Swedish farmer's foundation for agricultural research and the Åke Wiberg's foundation.

References

1. Biedler JL, Helson L, Spengler BA (1973) Morphology and growth, tumorigenicity, and cytogenetics of human neuroblastoma cells in continuous culture. Cancer Res 33:2643–2652
2. Biedler JL, Roffler-Tarlov S, Schachner M, Freedman LS (1978) Multiple neurotransmitter synthesis by human neuroblastoma cell lines and clones. Cancer Res 38:3751–3757
3. Perez-Polo JR, Tiffany-Castiglioni E, Ziegler MG, Werrbach-Perez K (1982) Effect of nerve growth factor on catecholamine metabolism in a human neuroblastoma clone (SY5Y). Dev Neurosci 5:418–423
4. Fang J, Zuo D, Yu PH (1995) Comparison of cytotoxicity of a quaternary pyridinium metabolite of haloperidol (HP+) with neurotoxin N-methyl-4-phenylpyridinium (MPP+) towards cultured dopaminergic neuroblastoma cells. Psychopharmacology (Berl) 121:373–378
5. Oyagi A, Oida Y, Hara H et al (2008) Protective effects of SUN N8075, a novel agent with antioxidant properties, in in vitro and in vivo models of Parkinson's disease. Brain Res 1214:169–176
6. Holback S, Adlerz L, Iverfeldt K (2005) Increased processing of APLP2 and APP with concomitant formation of APP intracellular domains in BDNF and retinoic acid-differentiated human neuroblastoma cells. J Neurochem 95:1059–1068
7. Uhrig M, Brechlin P, Jahn O et al (2008) Upregulation of CRABP1 in human neuroblastoma cells overproducing the Alzheimer-typical Abeta42 reduces their differentiation potential. BMC Med 6:38
8. Wang H, Xu Y, Yan J et al (2009) Acteoside protects human neuroblastoma SH-SY5Y cells against beta-amyloid-induced cell injury. Brain Res 1283:139–147
9. Gustafsson H, Runesson J, Lundqvist J, Lindegren H, Axelsson V, Forsby A (2010) Neurofunctional endpoints assessed in human neuroblastoma SH-SY5Y cells for estimation of acute systemic toxicity. Toxicol Appl Pharmacol 245(2):191–202
10. Bottenstein JE, Sato GH (1979) Growth of a rat neuroblastoma cell line in serum-free supplemented medium. Proc Natl Acad Sci USA 76:514–517
11. Pahlman S, Ruusala AI, Abrahamsson L, Mattsson ME, Esscher T (1984) Retinoic acid-induced differentiation of cultured human neuroblastoma cells: a comparison with phorbolester-induced differentiation. Cell Differ 14:135–144
12. El Andaloussi-Lilja J, Lundqvist J, Forsby A (2009) TRPV1 expression and activity during retinoic acid-induced neuronal differentiation. Neurochem Int 55:768–774
13. Spencer PS, Schaumburg HH (1974) A review of acrylamide neurotoxicity. Part II. Experimental animal neurotoxicity and pathologic mechanisms. Can J Neurol Sci 1:152–169
14. Lotti M (1991) The pathogenesis of organophosphate polyneuropathy. Crit Rev Toxicol 21:465–487
15. Ehrich M, Correll L, Veronesi B (1994) Neuropathy target esterase inhibition by organophosphorus esters in human neuroblastoma cells. Neurotoxicology 15: 309–313
16. Hong MS, Hong SJ, Barhoumi R et al (2003) Neurotoxicity induced in differentiated SK-N-SH-SY5Y human neuroblastoma cells by organophosphorus compounds. Toxicol Appl Pharmacol 186:110–118
17. Cho T, Tiffany-Castiglioni E (2004) Neurofilament 200 as an indicator of differences between mipafox and paraoxon sensitivity in Sy5Y neuroblastoma cells. J Toxicol Environ Health A 67:987–1000
18. Forsby A, Pilli F, Bianchi V, Walum E (1995) Determination of critical neurotoxic concentrations in human neuroblastoma (SH-SY5Y) cells. Altern Lab Anim 23: 800–811
19. Nordin-Andersson M, Walum E, Kjellstrand P, Forsby A (2003) Acrylamide-induced effects on general and neurospecific cellular functions during exposure and recovery. Cell Biol Toxicol 19:43–51
20. Saxena S, Caroni P (2007) Mechanisms of axon degeneration: from development to disease. Prog Neurobiol 83:174–191

21. Axelsson V, Holback S, Sjogren M, Gustafsson H, Forsby A (2006) Gliotoxin induces caspase-dependent neurite degeneration and calpain-mediated general cytotoxicity in differentiated human neuroblastoma SH-SY5Y cells. Biochem Biophys Res Commun 345:1068–1074
22. DeJongh J, Nordin-Andersson M, Ploeger BA, Forsby A (1999) Estimation of systemic toxicity of acrylamide by integration of in vitro toxicity data with kinetic simulations. Toxicol Appl Pharmacol 158:261–268
23. Wenehed V, Solyakov A, Thylin I, Haggblom P, Forsby A (2003) Cytotoxic response of Aspergillus fumigatus-produced mycotoxins on growth medium, maize and commercial animal feed substrates. Food Chem Toxicol 41:395–403
24. Gustafsson H, Soderdahl T, Jonsson G, Bratteng JO, Forsby A (2004) Insulin-like growth factor type 1 prevents hyperglycemia-induced uncoupling protein 3 down-regulation and oxidative stress. J Neurosci Res 77:285–291
25. Lowry OH, Rosebrough NJ, Farr AL, Randall RJ (1951) Protein measurement with the Folin phenol reagent. J Biol Chem 193:265–275
26. Ciccarone V, Spengler BA, Meyers MB, Biedler JL, Ross RA (1989) Phenotypic diversification in human neuroblastoma cells: expression of distinct neural crest lineages. Cancer Res 49:219–225

Chapter 13

The Use of Differentiating N2a and C6 Cell Lines for Studies of Organophosphate Toxicity

Alan J. Hargreaves, Magda Sachana, and John Flaskos

Abstract

A major goal of our cellular toxicology research has been the identification of novel targets of organophosphorous compounds (OPs), to which end we have studied the effects of sub-lethal concentrations of OPs on morphological and molecular end points in differentiating mammalian cell lines. This chapter describes the key practical approaches that we use to monitor OP toxicity in mouse N2a neuroblastoma and rat C6 glioma cell lines. These cell lines are easy to maintain and are useful for the study of short-term, potentially reversible, effects of OPs on the outgrowth and maintenance of neurites and associated regulatory proteins.

The main topics covered include (a) the basic maintenance of cells and the induction and morphological assessment of cell differentiation in various experimental scenarios, (b) the measurements of key enzyme activities, and (c) the detection of molecular changes using a targeted proteomic approach focussed on immunofluorescence staining of fixed cells and western blotting analysis of cell extracts with antibodies to proteins known to be important in the regulation of cell differentiation.

This approach can also be used for the study of other neurotoxins and is amenable to the measurement of a wide range of end points.

Key words: N2a neuroblastoma, C6 glioma, Neural differentiation, Neurotoxicity, Organophosphorous compound

1. Introduction

Organophosphorous compounds (OPs) have applications in agriculture and the aviation industry (1). They are still the most widely used group of pesticides, exerting their acute toxicity via inhibition of acetylcholinesterase (AChE) in target organisms. Over exposure to such OPs can, however, be problematic to non-target organisms where severe irreversible inhibition of AChE can lead to respiratory failure. Moreover, while certain OPs used as aviation fluid additives/lubricants tend to be relatively weak

Michael Aschner et al. (eds.), *Cell Culture Techniques*, Neuromethods, vol. 56,
DOI 10.1007/978-1-61779-077-5_13,

inhibitors of AChE, they can still induce neurodegenerative effects (1, 2).

Sub-acute levels of several OPs cause various forms of delayed toxicity in nontarget organisms including humans (3–10). For example, clinical symptoms of OP-induced delayed neuropathy (OPIDN) may appear up to 3 weeks after exposure to OPs such as tricresyl phosphate (TCP) (3, 4, 7). OPIDN has been studied in animal models including rodents and hens (11, 12). However, little is known about the molecular basis of OPIDN, although impairment of neuropathy target esterase (NTE) and disruption of the axonal cytoskeleton are known to precede its onset (3, 4, 7, 13). Some OPs cause developmental toxicity (9, 10), intermediate syndrome (8) and neuropsychological complications (5, 6), underlining the possibility of multiple protein targets (14). As increasing worldwide use of OPs is a major public health concern, further work is needed to elucidate the molecular events associated with sub-acute exposure to OPs, which may help to identify novel biomarkers of effect.

In an attempt to develop an in vitro alternative to animal models to study the direct effects of OPs on neural cells, we have used differentiating rodent cell lines to identify noncholinergic biomarkers of OP toxicity, with special emphasis on the characterization of molecular events following exposure to sub-lethal concentrations of a number of OPs (15–24). Sub-lethal concentrations of all OPs tested inhibit the outgrowth of axon-like processes by differentiating mouse N2a neuroblastoma, although some of them (e.g., TOCP, PSP and chlorpyrifos) were effective within 4 h of exposure (17–20), whereas others (e.g., diazinon, TCP and TPCP) required longer incubation times (18, 21). Some OPs (e.g., chlorpyrifos, chlorpyrifos oxon and diazinon oxon (23, 24)) inhibited the outgrowth of extensions by differentiating rat C6 glioma cells, whereas others (e.g., TCP and diazinon) did not (16, 18, 21). These findings are consistent with the view that there may be both common and compound-specific specific cellular targets in the two cell types, in agreement with the proposal of Richards et al. (14) that multiple OP targets exist.

Of course, sub-lethal inhibition of neurite outgrowth is not a specific biomarker of OP toxicity, as many other agents are able to inhibit this process through different molecular pathways. In order to characterize the molecular events that follow exposure to sub-lethal neurite inhibitory levels of OPs, we have used a targeted proteomic approach to identify likely protein targets. As altered cell morphology implies disruption of the cytoskeleton, which plays a key in cell differentiation, we have focussed mainly on the analysis of cytoskeletal and associated proteins known to be important in this process. Indeed, western blotting analysis has shown that the neurite inhibitory effects of all OPs in N2a cells were associated with reduced levels or altered phosphorylation

state of the axon enriched cytoskeletal protein neurofilament heavy chain (NFH) (16–22).

This approach has also highlighted differences between the modes of action of certain OPs. For example, the inhibition of glial cell differentiation by chlorpyrifos oxon and diazinon oxon, but not chlorpyrifos, is associated with reduced levels of α-tubulin (23, 24). Furthermore, exposure to neurite inhibitory concentrations of chlorpyrifos and leptophos is associated with increased levels of the heat shock protein HSP-70 (17, 19), whereas the opposite is the case following exposure to diazinon (21). Differences between the molecular effects of the OPs tested may represent important biomarkers of toxicity in vivo. Thus, a more detailed study of these phenomena would help to elucidate the mechanisms of toxicity more fully and to establish toxicity profiles for different OPs.

The aim of this review is to present a detailed account of the cell culture and targeted proteomic approaches that we use for the analysis of the mechanisms of toxicity of OPs by differentiating N2a and C6 cells, emphasizing potential problems and points of good practice in the application of our system in studies of sublethal OP toxicity.

2. Cell Culture and Differentiation

2.1. Materials and Reagents

Unless otherwise stated, all reagents mentioned in this chapter are from Sigma Aldrich Co Ltd (Poole, UK). Dulbecco's modified Eagle's medium (DMEM; with 4.5-g/L glucose, without L-glutamine) is purchased from Lonza (Viviers, Belgium). Cell culture plastic ware is obtained from Scientific Laboratory Supplies (SLS, Wilford, UK).

Cell lines: Both C6 and N2a cell lines are available from ATCC or ECACC (see Note 1).

OP working stock solutions: Working stock solutions are prepared in dimethyl sulfoxide (DMSO) at 200× the desired final concentration (stored at –20°C or lower), giving a 0.5% v/v final concentration of DMSO (see Note 2). We have used a number of suppliers for different OPs (see Note 3) including: Sigma Aldrich for TCP, triphenyl phosphite, paraoxon and trichlorfon; ICN (Thane, UK) for purified isomers of TCP; Riedel de Haen (Seelze, Germany) for leptophos, chlorpyrifos and chlorpyrifos-methyl; Greyhound Chromatography (Birkenhead, UK) for diazinon and diazinon oxon.

Growth medium (GM): DMEM supplemented with 10% v/v fetal bovine serum (FBS), 2-mM L-glutamine, penicillin (100 units/mL) and streptomycin (100 µg/mL). Store at 4°C.

Serum-free medium (SFM): GM without FBS. Store at 4°C.

To induce differentiation, supplement with either 0.3-mM

dibutyryl cAMP (for N2a cells) or 2-mM sodium butyrate (for C6 cells). Prepare both inducers as 100-fold stocks in DMEM, filter sterilize using sterile 0.22-μm filters (Millipore) and store in 1-mL aliquots at –20°C for up to several months.

Tris buffered saline (TBS): A 10-mM Tris base in 140-mM NaCl (pH 7.4). Prepare as a 10× concentrate, which can be stored in large dispensers at room temperature and diluted to working concentration as required (see Note 4).

BSA/TBS: 3% (w/v) bovine serum albumin (BSA) in TBS. Store at 4°C, adding 0.01% (w/v) sodium azide for longer-term storage.

Coomassie blue staining solution: Coomassie Brilliant Blue R250 (0.25% w/v) in a solution of 10% (v/v) acetic acid and 50% w/v methanol. Filter and store at room temperature.
Gloves should be worn at all times.

2.2. Methods

2.2.1. Maintenance of Cell Lines

1. Maintain both cell lines as monolayers in T25 flasks with 10-mL GM, using a humidified incubator at 37°C and an atmosphere of 5% CO_2/95% air. Cells should be passaged at regular intervals on reaching approximately 80% confluence (see Note 5).
2. When ready for sub-culture, detach N2a cells by removing all but 1–2 mL of GM then blowing the remaining GM repeatedly with GM from a sterile Pasteur pipette (or equivalent) across the monolayer. To detach C6 monolayers, remove all GM, rinse the monolayer gently with sterile phosphate-buffered saline (PBS) then add 1 mL of 1× trypsin/EDTA (add 4 mL for a T75 flask) and incubate for 5 min at 37°C until all cells are rounded. Remove cells from the flask surface with a pipette or cell scraper (see Note 5). Dilute detached cells into 10-mL GM and centrifuge at 300 × *g* for 5 min (see Note 6).
3. Resuspend cell pellets in 1-mL GM by 20 passes through a Pasteur pipette and transfer one-third to one-fifth of the resuspension into a new T25 flask containing 10-mL GM. Cells will be ready to passage again with 3–5 days and their level of confluence should be checked on a daily basis.

2.2.2. Induction of Cell Differentiation

1. Detach mitotic cells at 60–80% confluence, centrifuge and resuspend with a Pasteur pipette as described above. Then pass them six times through a syringe fitted with a 23-G needle. Take 20 μL of suspension and dilute to 200 μL in GM. Apply 10 μL of suspension to a hemocytometer chamber. Count the number of cells within five independent large squares (four corners and the central square) and take an average. The cell density is calculated as follows:

$$\text{Number of cells / mL} = \text{average cell count} \times 10^4 \times \text{dilution factor (usually 10).}$$

2. Prepare the cells for plating out by diluting the suspension to a density of 50,000 cells/mL of GM. Then add an appropriate volume of diluted cell suspension to the appropriate tissue culture vessel. For example, for assays of neurite outgrowth or cell viability seed 24-well culture dishes with 0.5 mL of this cell suspension per well, giving 25,000 cells/well. For SDS-PAGE, Western blotting or assays of AChE activity, use T25 or T75 flasks seeded with either 10 mL (500,000 cells) or 40 mL (two million cells) of cell suspension, respectively (see Note 7). Return the cells to the CO_2 incubator and allow 24-h recovery.
3. After recovery, carefully remove the GM and replace it with the same volume of filter sterilized SFM containing either 0.3-mM dibutyryl cAMP (N2a cells) or 2-mM sodium butyrate (C6 cells) with or without OP (see Note 2). If using 24-well dishes, process only 4 wells at a time to avoid cell damage as a result of drying out (see Note 7). Cells are then incubated for the desired period of time (4–48 h). However, the effects of OPs on preformed neurites can be studied by allowing cells to differentiate for 24 h before carefully replacing SFM with SFM-containing OPs or carrier only.

2.2.3. Morphological Analysis of Cell Differentiation

1. After the required incubation time, quickly remove medium from the wells by inverting over a bleach bowl and remove remaining traces of SFM by pipette. Apply 0.5 mL/well of fixing solution (90% v/v methanol in TBS; precooled to –20°C), cover and incubate at –20°C for 20 min.
2. Remove the fixative, replace with 0.5 mL of Coomassie blue staining solution and incubate at room temperature for 2 min.
3. Remove staining solution and wash the cells twice for 2 min with distilled water. Remove distilled water and allow to air

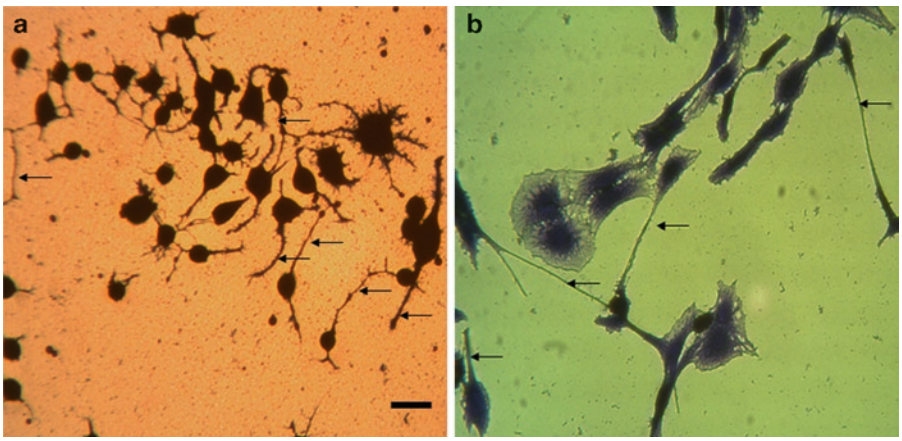

Fig. 1. Images of differentiating N2a and C6 cells. Typical images of (**a**) N2a (**b**) and C6 cells induce to differentiate for 24 h, followed by staining with Coomassie blue. *Arrows* indicate typical axon-like processes in N2a cells and extensions in C6 cells. Bar represents 20 μm.

dry, after which cells can be viewed by bright field illumination using an inverted light microscope (Fig. 1).

4. Record images from five areas from different parts of each well (upper, lower, right, left and center) with approximately 30–50 cells per field of view; too many cells in a field will make neurite counting difficult (see Note 8).
5. For N2a cells, in each field, count the total number of cells and axon-like processes (i.e., neurites longer than 2 cell body diameters in length, which we have found to be selectively affected by all OPs tested). Add the totals for the five fields in each well and express as axons/100 cells. Do the same for the remaining wells for each treatment and take an average for the experiment. For differentiating C6 cells, count the total number of cells and total number of outgrowths (all of which tend to be relatively long) in each field, and express the data as extensions/100 cells (see Note 9).

2.2.4. Immunohistochemical Staining of Cells

1. To assess the effects of OPs on the cellular distribution of an antigen, cells are plated out into LabTek 8-well chamber slides (Nalge Nunc International, New York, USA), at 50,000 cells/mL, adding 300 µL of medium per well.
2. After the desired exposure time, fix the cells in 90% methanol/TBS at –20°C for 10 min.
3. Remove the fixative, then incubate each sample for 5 min in 300-µL TBS containing 0.1% Triton X100 (extraction step), followed by three 5-min incubations with TBS to remove excess detergent. Then add 300-µL BSA/TBS and incubate at room temperature for 45 min (blocking).
4. The fixed and blocked cell monolayers are now ready to be incubated with primary antibody. We typically incubate with primary antibodies diluted in BSA/TBS overnight at 4°C in a humidified chamber (see Note 10).
5. After primary antibody incubation, wash monolayers with three changes of TBS at room temperature. Incubate with appropriate secondary antibodies conjugated with, for example, fluorescein isothiocyanate (FITC) or tetramethyl rhodamine isothiocyanate (TRITC) for 1–2 h at room temperature (see Note 11).
6. Wash the monolayers three times with 300-µL TBS, then remove all of the final TBS wash, dismantle the chamber assembly, apply four drops of anti-fade mountant solution (Vectashield or DakoCytomation) and mount the stained sample under a large glass cover slip, taking care to avoid air bubbles.
7. Gently remove excess liquid from under the cover slip by contacting its edges with tissue paper, then carefully seal around its edges with colorless nail varnish or rubber glue. Once the sealant has dried, specimens can be viewed using an epifluorescence microscope.

2.3. Notes on Cell Culture and Differentiation

1. To revive cells from liquid N_2, rapidly thaw cryovials at 37°C, dilute the cell suspension into 20-mL GM at ambient temperature, centrifuge at 300 × *g* for 5 min and resuspend the pellet in 1-mL GM by gentle trituration with a pipette. Apply all of this to a single T25 flask and allow the cells to recover by incubating them in the CO_2 incubator until approximately 80% confluent, feeding the monolayer with fresh GM after 2 days. At this point sub-culture the cells (Sect. 2.2.1) by dividing equally between five new flasks and culture as above until 80% confluent, at which point they can each be sub-cultured again until 20–30 new cultures are ready for cryopreservation. Resuspend each centrifuged cell pellet in ice cold cryopreservation medium (GM containing 5% v/v DMSO) and wrap tightly in two pieces of tissue paper, which allows them to freeze slowly at –80°C overnight. Frozen cryovials are then transferred to the gas phase of a liquid N_2 storage unit for long-term storage.
2. The same concentration of DMSO must be added to the control cell cultures. Always add OPs and DMSO freshly to SFM shortly before its application to the cell monolayers, making sure that the OP is well mixed by inversion as soon as it is added to the SFM.
3. Unless a study of the toxicity of a commercial formulation (which contains at least one other component) is of specific interest, obtain the highest purity of OP available, as contaminants may influence the cellular response.
4. At its working concentration, TBS should be stored at 4°C. PBS can be used instead.
5. T75 flasks containing 40-mL GM can be used for scaling up. However, cells that become over-confluent or exceed 20 passages are discarded to reduce the influence of genetic drift.
6. Incubation of monolayers with ice cold PBS or PBS/EDTA (versene) and detachment with a cell scraper also work well.
7. All of operations for plating out should be carried out within 15 min of removal of cells from the incubator to minimize the effects of stress caused by cooling. Handle only one plate or flask at a time, thus avoiding long periods at room temperature. SFM should be prewarmed to 37°C before use.
8. To avoid overcrowded areas of cells, which hinder visualization of neurites, scan the stained cell monolayers with the objective lens slightly out of focus so that the neurites are not discernible but cell bodies are. This will avoid the temptation to pick an area where lots of neurites can be seen. Having found a suitable field, the image can then be brought into focus and data recorded for morphological analysis.
9. A range of other parameters can be measured. For example, the average lengths of extensions or neurites can be determined using an eye piece graticule or image analysis software packages.

However, we find that counting of axon-like processes is a more sensitive indicator of sub-lethal effects of OPs. Likewise, the shape of cell bodies can be monitored to determine the percentage of cells with flat, round or extended cell bodies, though such parameters are not significantly affected by the OPs tested thus far.

Important: Calculating the mean for each treatment on the same plate gives only a measure of intra-experimental variation and is therefore equivalent to $n = 1$. At least four independent experiments should be performed so that the final average takes into account inter-experimental variation. If (as is usual) the distributions of values for all treatments and controls do not deviate significantly from normality, the statistical significance of differences between control and treatments can be determined using paired *t* tests or ANOVA, as appropriate. Otherwise, use an appropriate nonparametric test.

10. As there is flexibility in incubation times, 1-h incubation at 37°C or up to 4 h at room temperature can be used, depending on the antibodies used.
11. It is important to centrifuge the diluted secondary antibodies for 30 min at 10,000 × *g* prior to use, in order to remove fluorescent aggregates that would otherwise be seen as background on the specimen slide.

3. Measurement of Cellular Enzyme Activities

3.1. Measurement of N2a and C6 Cell Viability by the MTT Reduction Assay

3.1.1. Materials

Substrate stock solution: 5 mg/mL 3-[4, 5-dimethylthiazol-2-yl]-2, 5-diphenyl tetrazolium bromide (MTT) in SFM. Filter sterilize and store in 1-mL aliquots at –20°C for up to several months. Thaw and warm up to 37°C before use but avoid repeat freeze/thaw cycles. MTT solution is an irritant; wear gloves and avoid contact with skin and eyes.

3.1.2. Method (MTT Reduction Assay)

The MTT assay provides an easy, time- and cost-effective measurement of growth and survival in adherent cell lines and is well suited to our cell lines (21–23). This colorimetric assay was first proposed by Mosmann (25) and is based on the reduction of MTT by succinate dehydrogenase in metabolically active cells, to purple formazan crystals. The assay has been extensively described in the literature, modified or compared to other viability assays (see Note 1). Our adaptation of the assay for N2a and C6 cells is presented here:

1. Incubate 24-well plates containing N2a or C6 cells in the presence and absence of OPs or vehicle only (control cells) as described in Sect. 2.2.2.

2. Thirty minutes before the completion of exposure times, 50 µL of MTT stock solution is aseptically added to each well and, after slight agitation, plates are returned to the incubator.
3. After termination of the required exposure time, medium is carefully removed and 1 mL of DMSO added (see Note 2). Dissolve the formazan product by gently agitating the plate on a platform shaker for up to 10 min.
4. Finally, check for complete solubilization of crystals and transfer 200 µL from each well to the wells of 96-well microtiter plate (see Note 3). Read absorbance at 570 nm within 1 h, using a microtiter plate reader connected to a computer that allows efficient data collection, analysis and report. An absorbance correction should be made to take into account the background value from wells containing DMSO alone.
5. Repeat the experiment on at least three separate occasions, each experiment involving a different initial cell population, with four replicate wells for each compound and condition tested. Thus, $n = 1$ is an average of 4 wells from a single plate.
6. Results are expressed as the average absorbance from at least three independent experiments ±SEM and/or as a percentage of the corresponding control value.

3.2. Measurement of Acetylcholinesterase Activity in N2a and C6 Cells

3.2.1. Materials

Buffers: A 0.25-M phosphate buffer (pH 7.4). Store at 4°C, stable for several weeks.

Substrate and detection reagents: Dithiobisnitrobenzoate (DTNB) is prepared at a concentration of 1.25 mM in 0.25-M phosphate buffer (pH 7) containing 1.5 mg/mL $NaHCO_3$ and stored at 4°C for up to a week, protected from light with aluminum foil (see Note 4). Acetylthiocholine iodide (2.5 mM) is freshly prepared in distilled water immediately before use and stored on ice.

Protein assay: Cell protein measurement is carried out in 96-well plates applying the bicinchoninic acid assay (BCA) according to the kit's instructions (Pierce Chemical Company, Rockford, Illinois, USA). Protein standards are prepared with BSA and range from 0.2 to 1 mg/mL. Gloves should be worn at all times.

AChE: Electric eel AChE (Type VI-S: Sigma). Prepare master stock solutions of enzyme at 1 mg/mL in 0.25-M phosphate buffer. Store in 5-µL aliquots at –20°C, stable for at least 12 months. This can be diluted to 0.0001 mg/mL or lower prior to the assay and used as a positive control or to confirm the biological activity of existing OP stock solutions.

3.2.2. Method (AChE Assay)

AChE, the enzyme responsible for the degradation of the neurotransmitter acetylcholine and a known target of OP pesticides, is routinely assayed in our laboratory. Activity is measured in both N2a and C6 cells to investigate whether OP-induced morphological or cytoskeletal alterations are associated with its

inhibition (21, 22, 24) (see Note 5). This spectrophotometric approach relies on the hydrolysis of the substrate acetylthiocholine by AChE to thiocholine and acetate. Thiocholine combines with DTNB and the yellow product 5-thio-2-nitrobenzoate formed is measured spectrophotometrically. Our assay is based on the method of Ellman et al. (33) with minor adjustments to make it suitable for a microtiter plate format.

1. N2a and C6 cells are plated out in T75 culture flasks as described in Sect. 2.2.2 (see Note 6).
2. After completion of experimental exposure to OPs, harvest the cells as described in Sect. 2.2. Remove the supernatant from the centrifuged cell pellet, resuspend the cells in 1-mL ice cold PBS and transfer to an Eppendorf tube on ice.
3. Centrifuge at 1,200×*g* for 10 min at 4°C using a bench top microcentrifuge. Discharge the buffer and either use the pellets immediately or store at −20°C for up to 24 h (see Note 7).
4. Resuspend the cell pellets in ice cold 0.25-M phosphate buffer pH 7.4 by trituration. Then sonicate all samples for 30 s, keeping the tube on ice, using a probe sonicator set at half of its maximum amplitude. Finally, vortex mix the cell sonicates to ensure that cell pellets are completely dispersed just before dispensing.
5. Add 100 µL of sonicated cell sample to 4 wells of the microtiter plate followed by 50 µL of acetylthiocholine iodide solution and 50 µL of DTNB solution. Tap plate briefly to allow mixing of the solutions. Always include substrate and enzyme (cell) blanks (see Note 8).
6. Load the plate in an appropriate scanning microplate reader set to 415 nm wavelength, which is connected to a computer and record absorbance of the samples at 1-min intervals for a total of 10 min.
7. Enzymatic hydrolysis of acetylthiocholine iodide is monitored by the change in absorbance, which is linear for cell extracts over a 10-min period.
8. After determining the protein in all samples (BCA assay), AChE activity can be expressed as the average absorbance change ±SEM per minute per milligram of sample protein.
9. Repeat the experiment on at least three separate occasions, with quadruplicate wells for each compound and condition tested.

3.3. Notes on MTT and AChE Assays

1. The formazan product forms water insoluble crystals that must be dissolved in an adequate solvent, resulting in a blue solution that is measured spectrophotometrically. The MTT assay has used a number of different solvents such as propanol

(26) acid/2-propanol, DMSO, 10–20% SDS or 20% SDS in 0.02-M HCl (27, 28). However, DMSO is the solvent of choice for N2a and C6 cells because interference by protein precipitation is averted by using SFM, leaving only traces of serum proteins that are unlikely to affect assay measurements (7).

Several cytotoxicity assays are available. Among the most popular viability assays that have been compared to MTT are: Trypan blue exclusion, ATP measurement (29), neutral red uptake or release, kenacid blue staining (30), membrane integrity/LDH release, macromolecular synthesis, glutathione depletion (31), alamar blue assay (32) and ^{3}H-labeled thymidine incorporation into cellular DNA.

A potential disadvantage of the MTT assay is that cells with reduced metabolic activity cannot be distinguished from dead cells (22) and that cells used for this assay cannot be subsequently used for most other assays. However, as the cell monolayers remain after removal of DMSO, it is possible to carry out a modified Kenacid blue assay by staining the cells subsequently with Coomassie brilliant blue.

2. Take special care not to damage cell monolayers with the tip of the pipette. Alternatively, aspiration of the medium avoids fatigue from extensive pipetting in large-scale experiments. At this stage, take the opportunity to observe the purple crystals in the cells with the aid of an inverted light microscope to get a rough idea about the survival status of treated cells compared with the controls.
3. The MTT assay is performed in 24-well plates because the reproducibility of the experimental data is superior compared with the use of 96-well plates.
4. $NaHCO_3$ is added to facilitate the solubilization of DTNB. Otherwise, vortex mix or sonicate to achieve complete solubilization of the reagent.
5. Although adequate metabolic activation of OPs is a problem in cell lines, our data suggest that both N2a and C6 cells are capable of metabolizing protoxicants to the more toxic forms responsible for the inhibition of AChE (21, 22).
6. As high numbers of N2a and C6 cells are required to determine AChE activity, it is advisable to use T75 flasks.
7. If medium remains in contact with the pellet (pink appearance), resuspend the pellet in PBS and re-centrifuge as before.
8. Alternatively, freshly prepare a substrate mixture comprising equal volumes of acetylthiocholine iodide solution and DTNB solution and use a multi-channel pipettor to add 100 µL of the substrate mixture to individual wells.

4. Analysis of Cell Extracts by SDS-PAGE and Western Blotting

In order to perform targeted proteomic analyses, proteins from cell extracts are separated by polyacrylamide gel electrophoresis in the presence of sodium dodecyl sulfate (SDS-PAGE) and then transferred electrophoretically by western blotting onto nitrocellulose membrane filters to make them more accessible to antibody probing. This section covers the main practical aspects of the techniques used, showing a schematic example of targeted proteomic analysis using a specific selection of antibodies.

4.1. Materials

Antibodies: Primary antibodies are stored at +4 or –20°C, as recommended by the manufacturers. Details of all commercial primary antibodies we have used to study cytoskeletal effects of OPs on our cell lines are shown in Table 1. All secondary antibodies are from DakoCytomation (Ely, UK) or from Santa Cruz Biotechnology (Santa Cruz, CA, USA) and stored at 4°C.

The following solutions are required:

4% (w/v) SDS, 20% (v/v) glycerol, 10% (v/v) 2-mercaptoethanol, 0.004% (w/v) bromophenol blue, 0.125-M Tris–HCl pH 6.8 (Laemmli 2× concentrated sample buffer).

1.5-M Tris–HCl, pH 8.8 (resolving gel buffer).

0.5-M Tris–HCl, pH 6.8 (stacking gel buffer).

25-mM Tris, 192-mM glycine, 0.1% (w/v) SDS, pH 8.3 (electrophoresis running buffer).

25-mM Tris, 192-mM glycine, 20% (v/v) methanol, pH 8.3 (transfer buffer).

0.2-M glycine, 0.5-M NaCl, pH 2.8 (stripping buffer).

0.15-M Tris, pH 9.5 (alkaline-phosphatase substrate buffer).

These buffers together with TBS (or PBS), 0.05% (v/v) Tween 20 in TBS (TBS/Tween) and BSA/TBS are all kept at 4°C.

Acrylamide/bisacrylamide solution (40% w/v, 29:1, and ultra pure) and buffer stock solutions for SDS-PAGE are purchased from Gene Flow (Fradley, UK). Acrylamide/bisacrylamide is particularly toxic and kept at 4°C.

10% w/v SDS: store at room temperature (stable for several weeks).

Catalysts: 10% w/v ammonium persulfate (APS) is aliquoted and kept at –20°C. TEMED is kept in a dark bottle at room temperature. Both APS and TEMED are available from BioRad (Hemel Hempstead, UK) or Sigma.

A 0.05% (w/v) copper pthalocyanine in 12-mM HCl is stored at room temperature.

Alkaline phosphatase (*AP*) *substrates*: 5-Bromo-4-chloro-3 indolyl phosphate (BCIP: 50 mg/mL in dimethyl formamide) and nitroblue

Table 1
Commercially available antibodies used in our cytoskeletal studies of OP toxicity in N2a and C6 cells

Supplier	Antigen	Cellular location/ properties	Antibody type	Clone/other name	Applications	Dilution for probing blots[a]
Sigma Aldrich Co. Ltd.	α-Tubulin	Total microtubules	McAb	B512	WB, IFA	1/1,00–1/5,000
	Tyrosinated α-tubulin	Labile microtubule sub-domains	McAb	T1A2	WB	1/1,00–1/2,000
	NFH	Neurofilaments (phosphorylation independent epitope)	McAb	N52	WB, IFA	1/20–1/500
	Actin	Microfilaments	PcAb (R)	AA20-33	WB, IFA	1/500
	GAP-43	Membrane-cytoskeleton linker	McAb	GAP7B10	WB, IFA	1/50–1/1,000
	HSP-70	Cytoplasm (chaperone)	McAb	BRM-22	WB	1/1,00–1/5,000
Abcam	Cofilin	Microfilament-binding protein	PcAb (R)	ab11062	WB, IFA	1/50–1/1,000
Santa Cruz Biotechnology	ERK	Total MAP kinase (ERK 1/2-phosphorylation independent epitope)	PcAb (R)	K-23: sc94	WB	1/1,00–1/2,000
	p-ERK	Activated MAP kinase (ERK 1/2-phosphorylation-dependent epitope)	McAb	E-4: sc7383	WB	1/50–1/1,000
	MAP 1B	Microtubule-associated protein	PcAb(R)	H-130: sc25729	WB	1/25–1/500

(continued)

Table 1
(continued)

Supplier	Antigen	Cellular location/ properties	Antibody type	Clone/other name	Applications	Dilution for probing blots[a]
	MAP 2c	Microtubule-associated protein	PcAb(R)	H-300: sc20172	WB	1/25–1/500
	GFAP	Astrocyte-specific intermediate filament	PcAb(G)	C-19: sc6170	WB	1/25–1/500
	GAPDH	Cytosolic (household protein)	PcAb (R)	6C5: sc32233	WB	1/50–1/1,000
	Cofilin	Microfilament-binding protein	PcAb (G)	N19: sc8441	WB, IFA	1/50–1/1,000
	p-Cofilin	Microfilament-binding protein in its inactivated (phosphorylated) form	PcAb (R)	(mSer 3)-R Sc21867-R	WB	1/25–1/500
Chemicon Europe Ltd.	p-NFH	NFs (phosphorylation-dependent epitope)	McAb (rat)	Ta51	WB, IFA	1/200–1/500
Sternberger monoclonals Inc.	p-NFH	NFs (phosphorylation-dependent epitope)	McAb	SMI34	WB, IFA	1/500–1/1,000

Shown are details of the main commercially available antibodies used in our targeted proteomic studies on differentiating rodent cell lines. McAb signifies a mouse monoclonal antibody, McAb (rat), a rat monoclonal antibody, PcAb (R), a rabbit polyclonal antibody, and PcAb (G), a goat polyclonal antibody

WB Western blotting; *IFA* immunofluorescence staining

[a]Dilutions used for indirect immunofluorescence assays range from 1/20 to 1/200

tetrazolium (NBT: 75 mg/mL in 70% v/v dimethylformamide) are stored in working aliquots at –20°C, stable for several months.

Gloves should be worn at all times and especially during the preparation of the resolving and the stacking gel mixture as well as during handling of the nitrocellulose membrane and the preparation of the blotting sandwich. Lids of all tubes incubated in the heating block should be clamped with Eppendorf clips.

4.2. Methods

4.2.1. Sample Preparation

1. For proteomic analysis we routinely prepare cell lysates from monolayers induced to differentiate in T25 or T75 flasks in the presence and absence of OPs, as described in Sect. 2.2.2.
2. In a typical analysis, following the required experimental exposure, monolayers are gently rinsed with sterile PBS (preheated to 37°C) to remove traces of SFM.
3. Remove the PBS and immediately add either 1 mL (for a T25 flask) or 4 mL (for a T75 flask) of 0.5% w/v SDS preheated in a heating block to 100°C.
4. Tilt the flasks to allow lysates to drain to the bottom. Transfer lysates to Eppendorf tubes and incubate at 100°C in a heating block for 5 min. Lysates can be used directly or stored at –20°C, thawing thoroughly before use.
5. Once cooled, the protein content of the cell lysates can be determined using the BCA assay (Sect. 3.2.1), to ensure equal protein loadings on electrophoresis gels.
6. To prepare a sample for SDS-PAGE, it is mixed with an equal volume of Laemmli 2× concentrate and incubated in a heating block at 100°C for 5 min. After cooling, an appropriate volume can be loaded in to the sample wells of an SDS-PAGE gel. Alternatively, samples prepared in this way can be stored at –20°C, thawing thoroughly before use.

4.2.2. Casting and Running the Electrophoresis Gel

For SDS-PAGE we use the BioRad Mini Protean 3 or the more recently introduced Mini Protean Tetra Cell. We commonly run two or four 1.5-mm-thick gels at a time.

1. Assemble the glass cassette sandwich and the casting stand, as indicated in the instruction manual. Use a spacer glass plate suitable for 1.5-mm-thick gels (see Note 1).
2. Wearing gloves, prepare the resolving gel mixture solution by mixing the reagents in a small beaker as shown in Table 2. The volumes given are for two 1.5-mm-thick, 7.5% (w/v) polyacrylamide resolving gels (see Note 2).
3. Once TEMED has been added, swirl gently and without delay pour the resolving gel mixture smoothly (to avoid bubble formation) between the two glass plates with a 1-mL Gilson pipette, leaving sufficient space at the top for a stacking gel. Immediately overlay the gel solution with distilled water

Table 2
Composition of a typical polyacrylamide gel

	Volume (mL)	
Reagent	**7.5% resolving gel**	**4% stacking gel**
40% w/v acrylamide/ bisacrylamide (29:1)	3.75	1.0
1.5-M Tris–HCl (pH 8.8)	5.0	–
0.5-M Tris–HCl (pH 6.8)	–	2.5
Distilled water	11	6.4
10% (w/v) SDS	0.2	0.1
10% (w/v) ammonium persulfate	0.1	0.05
TEMED	0.04	0.02

Shown are the volumes of stock reagents required to produce two 7.5% (w/v) polyacrylamide gels overlaid with a 4% polyacrylamide stacking gel. Gels of different polyacrylamide concentrations are obtained by changing the volume of acrylamide stock and distilled water only, retaining the same final volume

applied gently and evenly along its whole surface. Allow to polymerize for at least 1 h and 30 min (see Note 3).

4. After polymerization, as evidenced by the presence of a sharp interface between the polymerized gel and the water overlay, tilt the assembly to pour off the overlay and remove any excess water from the edges of the gel using a piece of tissue paper.
5. Prepare the stacking gel solution by mixing the components in a small beaker as indicated in Table 2. Again, these volumes are sufficient for two 1.5-mm-thick, 4% (w/v) polyacrylamide stacking gels.
6. Once the TEMED has been added, swirl the stacking gel mixture gently. Without delay, using a Gilson pipette, pour it smoothly (to avoid bubble formation) almost to the top of the glass plate. Immediately insert an ethanol cleaned, 1.5-mm-thick, 10-well comb between the glass plates and into the stacking gel solution. Take special care that air bubbles are not trapped beneath the comb. Leave to polymerize for at least 45 min.
7. After polymerization, carefully remove the comb, rinse out the wells with running buffer and gently remove any remaining liquid from each well of the stacking gel with a Gilson micropipette fitted with a gel-loading tip.

8. Once prepared, load the samples into each of the wells of both gels using Gilson micropipettes fitted with gel-loading tips. Samples can be loaded into wells filled with running buffer, as the sample buffer has a higher density than the running buffer and can be seen falling to the bottom of the well and leveling off. You may choose to load larger volumes into empty sample wells; if so, carefully overlay with running buffer to the top of the well (see Note 4). At least one of the wells (first left) in each 10-well gel is normally reserved for loading 3–5 μL of BioRad Precision Plus Protein Dual Color or All Blue Standards (see Note 5).
9. After loading the standards and the samples on all gels, place the two gel sandwiches attached to the electrode assembly unit into the electrophoresis tank. Fill the inner and outer tanks with the recommended volumes of running buffer and place the lid on the tank. Insert the electrical leads to a suitable power supply (e.g., BioRad "PowerPac") with the correct polarity and perform electrophoresis at room temperature initially at a constant voltage of 50 V till the descending dye front has entered the stacking gel. Then, continue electrophoresis at a constant voltage of 150 V till the dye front is about to leave the bottom of the gel. The total run time is 50–70 min.

4.2.3. Western Blotting

1. During electrophoresis prepare materials for Western blotting. We use a BioRad Mini Trans-Blot Cell (see Note 6). Wearing gloves throughout, add to a glass dish sufficient transfer buffer to cover the blot assembly. For two blots, cut two pieces of nitrocellulose membrane (approximately 7×9 cm, 0.45-μm pore size) and eight slightly larger pieces of filter paper (approximately 7.5×10 cm) and immediately immerse and soak them, together with the four clean fiber pads provided, in the transfer buffer in the tray for a few minutes.
2. After turning off the SDS-PAGE power supply, pour off the running buffer (see Note 7) and remove the gel cassettes from the electrode assembly. Carefully separate the two glass plates then cut off and discard the stacking gel. Gently detach the resolving gel from the glass plate surface with the aid of a broad plastic spatula, lifting it carefully with both hands to transfer it to equilibrate in the transfer buffer in the tray. Repeat the above with the second gel.
3. Place the two blot cassettes into the tray, clear side down with the black side against the side of the tray. Put one presoaked fiber pad on to the clear side of the cassette, then two pieces of filter paper and then the nitrocellulose membrane on top. Then, carefully align the equilibrated gel on the membrane and cover it with two more pieces of filter paper (see Note 8)

and complete the sandwich by adding a second fiber pad on top. Close the cassette and, firmly holding it with one hand, lock it with the white latch. Place the cassette vertically into the electrode module so that the nitrocellulose membrane side of the sandwich (clear side) is facing toward the anode (+). Repeat the above with the other gels and cassettes.

4. Fill the tank completely with transfer buffer. Put on the lid and attach the electrical leads with the correct polarity to a BioRad PowerPac Basic Power Supply. Carry out electrophoresis at 30 V overnight at room temperature.
5. After transfer is complete, switch off the power supply, discard the transfer buffer and disassemble the blotting sandwiches. With a pair of blunt ended blotting tweezers, transfer the two blots (nitrocellulose membrane pieces) into two clean recipients (approximately 12 × 12 cm) containing distilled water. Separated colored bands of loaded standards are now evident on the blots.
6. Wash each blot twice with distilled water (see Note 9), and then reveal proteins on the blot by staining with copper pthalocyanine. If desired, record an image of the staining pattern (see Note 10). After approximately 2 min, remove the copper stain (see Note 11) and destain by adding 12-mM NaOH. When all blue sample protein bands disappear from the blots, remove destain solution and wash blots briefly in TBS (see Note 12).
7. Then, block each blot in the tray by incubating with BSA/TBS (see Note 13) on a rotary shaker for at least 1 h at room temperature (see Note 14).
8. Meanwhile, prepare appropriate primary antibody dilutions (Table 1) in total volumes of 20-mL BSA/TBS (see Note 15). After incubation with BSA/TBS, remove the trays from the shaker and with a pair of scissors carefully cut across the whole length of each of the two blots at the level just below the 100-kDa reference band and well above the 75-kDa reference band of the standards used (see Note 16).
9. With the aid of blot tweezers, place the resultant four blot segments into four more separate trays. Mark each tray on its side with the name of the antibody to be added and then add the appropriately diluted primary antibodies. The example in Fig. 2 illustrates how blot segments of two N2a cell lysates could be probed with antibodies specific for total NFH, phosphorylated NFH, MAP 1B, GAP-43, HSP-70, tubulin and ERK (relative to which results can be expressed) (see Note 17). Leave the blots in primary antibodies overnight or over the weekend at 4°C (see Note 18).
10. Wash the blots six times (10 min each wash) on a rotary shaker with TBS/Tween. Meanwhile, prepare the horseradish

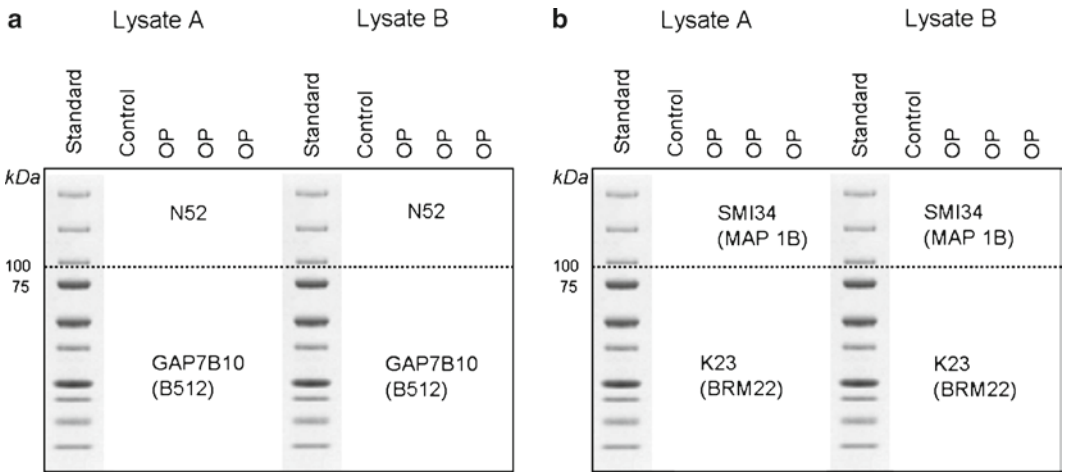

Fig. 2. Schematic representation of how blots are divided for antibody probing. The diagram of two blots (**a**, **b**) shows the position of the standards to the left of the samples, the level at which the two blots are cut for probing/reprobing with the antibodies shown for the purposes of this illustration (reprobing antibodies are shown in parentheses). Note the simultaneous treatment of two different N2a cell lysates (lysates A and B), each of which has been exposed to three different organophosphate concentrations (OPs), and which are separated by a second set of standards.

peroxidase (HRP)-conjugated secondary antibody solutions diluted 1:1,000 to 1:2,000 in BSA/TBS (see Note 19), making sure that the secondary antibody matches the primary antibody species and Ig class. Incubate with secondary antibody for 2–4 h at room temperature, before giving the blots five 10-min washes with TBS/Tween, followed by a final 10-min wash with TBS only.

11. Antibody reactivity is detected with an enhanced chemiluminescence (ECL) detection system, using ECL reagents (from Santa Cruz or GE Healthcare), in a Fuji LAS-3000 or Syngene G:BOX ECL camera system (see Note 20). Antibody reactivity is then quantified by densitometric scanning of the blots using Advanced Image Data Analyzer (AIDA) (version 4.03) or Quantiscan (Version 3, BIOSOFT®) software. The band densities for each antigen are normalized to the band density for ERK, which is used as internal control (see Note 21).
12. Following ECL detection, blots can be reprobed with different antibodies. For instance, in the example shown in Fig. 1a, b, the blot pieces for reprobing are washed in TBS and stored at 4°C for further analysis (see Note 22).
13. To reprobe the blots, remove TBS and incubate with stripping buffer (see Note 23) on a rotary shaker at room temperature for 2–5 min. Then wash each blot twice with TBS for approximately 5 min, before adding BSA/TBS to block nonspecific binding. Continue with the rest of the procedure as described previously (see Note 24).

4.3. Notes on SDS-PAGE and Western Blotting

1. After assembly of the casting stand and prior to gel casting, check for leaks by pouring distilled water into the space between the spacer and the short glass plate. If leaks occur, dismantle the casting assembly, clean the glass plates thoroughly and reassemble.
2. If high molecular weight proteins (e.g., NFH and MAP 1B) are not of interest, a 10 or 12% w/v polyacrylamide resolving gel can be used. The latter is particularly useful for resolving very low molecular weight cytoskeletal proteins such as cofilin (14–18 kDa).
3. Exploit this time to prepare solutions needed later in the day (e.g., electrophoresis running buffer, transfer buffer, etc.).
4. In 10-well, 1.5-mm-thick mini gels, the maximum volume of sample that can be loaded per well is 50 μL and the amount of total protein loaded into each well should ideally be 20–30 μg. If protein levels are too low to allow such loadings, samples can be concentrated prior to SDS-PAGE by precipitation overnight (−20°C) in nine volumes of acetone. Centrifuge precipitated protein at 10,000 × *g* for 30 min. Remove the supernatant and resuspend air dried acetone pellets by boiling in a smaller volume of sample buffer.
5. Sample overflow into adjacent sample wells may sometimes occur. To minimize this risk, start with loading the lower volume samples and continue with loading the higher volume samples.
6. If high molecular weight proteins are not of interest to the analysis, a semi-dry blotter can be used, which offers the advantages of rapid transfer (<90 min) and economy (only minimal amounts of transfer buffer are required). Moreover, manipulations are easier, as there are no fiber pads, cassettes or buffer tanks. We use Gene Flow SD20 or V10/V20-SDB Blotting Units but equipment from other suppliers meets the same standards. For the electrophoretic transfer of proteins from gels, we use a current of 0.8 mA/cm^2 or approximately 60 mA per mini gel.
7. Electrophoresis running buffer can be reused once, but in the outer tank only (not recommended).
8. To ensure full contact between the gel and the membrane, which is necessary for efficient transfer, squeeze out trapped air bubbles by rolling a glass rod in both directions over the surface of the filter papers.
9. Throughout all manipulations blots should be entirely covered in liquid and not allowed to dry out.
10. This staining step is important in order to check for efficient transfer of proteins onto the blot. The presence of blank, unstained circles on the blots, swirls or missing bands indicate the presence of air bubbles and poor contact between the gel

and the blot. Staining also confirms whether equal amounts of cell lysate protein were loaded.

11. The copper stain solution can be reused a few times. Do not stain the blots for more than 2 or 3 min, otherwise complete destaining may be impossible.
12. Alternatively, PBS can be used throughout with equal success.
13. If the BSA/TBS solution prepared is not be used immediately, it should be stored at 4°C, after adding sodium azide (0.01% w/v).
14. It is important to minimize binding of antibody to nonspecific sites on the nitrocellulose membrane. Instead of BSA/TBS, we often use a solution of 3% (w/v) nonfat milk powder in TBS. Marvel is widely available from supermarkets, dissolves more easily and is considerably cheaper than BSA. However, Marvel may contain phosphatase enzymes and is therefore unsuitable for the detection of phosphorylated epitopes.
15. Even when Marvel is used instead of BSA to block nonspecific binding, all primary antibody dilutions are made in BSA/TBS. The appropriate dilution for each antibody varies, depending on the secondary antibody conjugate and detection system used. For example, the sensitivity of the color development system for AP conjugates (see Note 19) is lower than for HRP conjugates using ECL.
16. The exact position of the cut varies; it must be made in such a way as to ensure inclusion of the desired antigen in the probed blot segment.
17. For protein analysis of C6 cell lysates, primary antibodies for total and phosphorylated NFH would not be used, as this protein is neuron-specific.
18. Some primary antibody solutions (e.g., B512 and anti-ERK) can be reused if the signal strength was high at previous use. Such solutions should be stored at 4°C in BSA/TBS containing 0.01% (w/v) sodium azide.
19. Alternatively, AP-conjugated antibodies can be used.
20. For AP conjugated secondary antibodies, antibody binding is revealed by incubation at room temperature in freshly prepared substrate buffer, comprising:
    - 33-µL BCIP.
    - 44-µL NBT.
    - 20-mL 0.15-M Tris buffer (pH 9.5).

Incubate until colored bands appear on the blots with an acceptable background. Prevent overdevelopment by washing the blots extensively with distilled water and dry blots using filter paper.

21. Alternatively, glyceraldehyde-3-phosphate dehydrogenase reactivity can be used as internal control.
22. Reprobing is carried out within 1 or 2 days after ECL detection.
23. Using this buffer normally achieves adequate antibody stripping. However, a more severe stripping procedure can be employed, involving incubation for 30 min at 50°C in 62-mM Tris, pH 6.7, 2% w/v SDS and 100-mM mercaptoethanol, followed by four 10-min washes with TBS/Tween, prior to blocking with BSA/TBS.
24. Dilutions of primary antibodies in BSA/TBS are as shown in Table 2. Use appropriate secondary antibodies diluted 1:1,000 in BSA/TBS.

References

1. Chambers H (1992) Organophosphate compounds: an overview. In: Chambers JE, Levi PE (eds) Organophosphates: chemistry, fate and effects. Academic Press, New York, pp 3–17
2. Aldridge WN (1954) Tricresyl phosphates and cholinesterase. Biochem J 56:185–189
3. Abou Donia MB, Lapadula DM (1990) Mechanisms of organophosphorous ester induced delayed neurotoxicity: Type I and II. Ann Rev Pharmacol Toxicol 30:405–440
4. Lotti M (1992) The pathogenesis of organophosphate polyneuropathy. Crit Rev Toxicol 21:465–487
5. Nutley BP, Crocker J (1993) Biological monitoring of workers occupationally exposed to organophosphorous pesticides. Pesticide Sci 39:315–322
6. Pilkington A, Buchanan D, Jamal GA, Gillham R, Hamsen S, Kidd M, Hurley JF, Soutar CA (2001) An epidemiological study of the relations between exposure to organophosphate pesticides and indices of chronic peripheral neuropathy and neuropsychological abnormalities in sheep farmers and dippers. Occup Environ Med 58:702–710
7. Abou Donia MB (2003) Organophosphorus ester induced chronic neurotoxicity. Arch Env Health 58:484–497
8. Karalliedde L, Baker D, Marrs TC (2006) Organophosphate-induced intermediate syndrome: aetiology and relationships with myopathy. Toxicol Rev 25:1–14
9. Slotkin TA, Seidler FJ (2008) Developmental neurotoxicants target differentiation into the serotonin phenotype: chlorpyrifos, diazinon, dieldrin and divalent nickel. Toxicol Appl Pharmacol 233:211–219
10. Slotkin TA, Ryde TI, Levin ED, Seidler FJ (2008) Developmental neurotoxicity of low dose diazinon exposure of neonatal rats: effects on serotonin systems in adolescence and adulthood. Brain Res Bull 75: 640–647
11. Lotti M, Johnson MK (1978) Neurotoxicity of organophosphorus pesticides: predictions can be based on in vitro studies with hen and human enzymes. Arch Toxicol 41:215–221
12. Ehrich M, Jortner BS, Padilla S (1995) Comparison of the relative inhibition of acetylcholinesterase and neuropathy target esterase in rats and hens given cholinesterase inhibitors. Toxicol Sci 24:94–101
13. Glynn P (1999) Neuropathy target esterase. Biochem J 344:625–631
14. Richards P, Johnson M, Ray DE, Walker C (1999) Novel targets for organophosphorus compounds. Chem Biol Interact 119–120: 503–511
15. Flaskos J, McLean WG, Hargreaves AJ (1994) The toxicity of organophosphate compounds towards cultured PC12 cells. Toxicol Lett 70:71–76
16. Flaskos J, McLean WG, Fowler MJ, Hargreaves AJ (1998) Tricresyl phosphate inhibits the formation of axon-like processes and disrupts neurofilaments in cultured mouse N2a and rat PC12 cells. Neurosci Lett 242:101–104
17. Sachana M, Flaskos J, Alexaki E, Glynn P, Hargreaves AJ (2001) The toxicity of chlorpyrifos towards differentiating mouse N2a neuroblastoma cells. Toxicol In Vitro 15:105–108
18. Fowler MJ, Flaskos J, Mc Lean WG, Hargreaves AJ (2001) Effects of neuropathic

and non-neuropathic isomers of tricresyl phosphate and their microsomal activation on the production of axon-like processes by differentiating mouse N2a neuroblastoma cells. J Neurochem 76:671–678

19. Sachana M, Flaskos J, Alexaki E, Hargreaves AJ (2003) Inhibition of neurite outgrowth in N2a cells by leptophos and carbaryl: effects on neurofilament heavy chain, GAP-43 and HSP-70. Toxicol In Vitro 17:115–120
20. Hargreaves AJ, Fowler MJ, Sachana M, Flaskos J, Bountouri M, Coutts IC, Glynn P, Harris W, McLean WG (2006) Inhibition of neurite outgrowth in differentiating mouse N2a neuroblastoma cells by phenyl saligenin phosphate: effects on neurofilament heavy chain phosphorylation, MAP kinase (ERK 1/2) activation and neuropathy target esterase activity. Biochem Pharmacol 71:1240–1247
21. Flaskos J, Harris W, Sachana M, Munoz D, Tack J, Hargreaves AJ (2007) The effects of diazinon and cypermethrin on the differentiation of neuronal and glial cell lines. Toxicol Appl Pharmacol 219:172–180
22. Sidiropoulou E, Sachana M, Flaskos J, Harris W, Hargreaves AJ, Woldehiwet Z (2009) Diazinon oxon affects the differentiation of mouse N2a neuroblastoma cells. Arch Toxicol 83:373–380
23. Sidiropoulou E, Sachana M, Flaskos J, Harris W, Hargreaves AJ, Woldehiwet Z (2009) Diazinon oxon interferes with differentiation of rat C6 glioma cells. Toxicol In Vitro 23:1548–1552
24. Sachana M, Flaskos J, Sidiropoulou E, Yavari CA, Hargreaves AJ (2008) Inhibition of extension outgrowth in differentiating rat C6 glioma cells by chlorpyrifos and chlorpyrifos oxon. Toxicol In Vitro 22:1387–1391
25. Mosmann Y (1983) Rapid colorimetric assay for the cellular growth and survival: application to proliferation and cytotoxic assays. J Immunol Meth 65:55–63
26. Denizot F, Lang R (1986) Rapid colorimetric assay for cell growth and survival. Modifications to the tetrazolium dye procedure giving improved sensitivity and reliability. J Immunol Meth 89:271–277
27. Rexen P, Emborg C (1992) Investigation of different modifications to the tetrazolium based colorimetric viability assay. Biotechnol Tech 6:255–260
28. Young FM, Phungtamdet W, Sanderson BJS (2005) Modification of MTT assay conditions to examine the cytotoxic effects of amitraz on the human lymphoblastoid cell line, WIL2NS. Toxicol In Vitro 19:1051–1059
29. Untch M, Sevin BU, Perras JP, Angiol R, Untch A, Hightower RD, Koechli O, Averette HE (1994) Evaluation of paclitaxel (taxol), cisplatin, and the combination paclitaxel-cisplatin in ovarian cancer in vitro with the ATP cell viability assay. Gynecol Oncol 53:44–49
30. Clothier RH (1995) The Frame cytotoxicity test (Kenacid Blue). In: O'Hare S, Atterwill CK (eds) Methods in molecular biology, vol 43, in vitro toxicity testing. Humana Press, Totowa, pp 109–114
31. Baker MA, Cerniglia GJ, Zaman A (1990) Microtiter plate assay for the measurement of glutathione and glutathione disulfide in large numbers of biological samples. Anal Biochem 190:360–365
32. Hamid R, Rotshteyn Y, Rabadi L, Parikh R, Bullock P (2004) Comparison of alamar blue and MTT assays for high through-put screening. Toxicol In Vitro 18:703–712
33. Ellman GL, Courtney KD, Andres V Jr, Featherstone RM (1961) A new and rapid colorimetric determination of acetylcholinesterase activity. Biochem Pharmacol 7:88–95

Chapter 14

Assessing Toxic Injuries of Experimental Therapeutics to the Crystalline Lens Using Lens Explant Culture

Michael D. Aleo

Abstract

Cataract formation during preclinical drug safety assessment studies can be a devastating safety finding during drug development based on the stage at which these findings usually occur. The lens explant culture models offer an extremely versatile and simple in vitro model to screen compound for such toxic liabilities or to study possible mechanisms of toxicity. The following chapter is designed to highlight numerous examples of cataract formation during the drug development process, techniques used to prepare the model and some approaches used to understand drug-induced cataract formation in vitro from a mechanistic, screening and species sensitivity perspective.

Key words: Lens explant culture, Cataract, Opacities, In vitro models, Mechanisms of toxicity, Drug discovery, Screening

1. Introduction

From a toxicology perspective, there are several different cell types within the mammalian eye that represent target tissues for a variety of therapeutic agents. Several marketed therapeutic agents have known effects on the human eye and can either manifest themselves as something innocuous such as temporary changes in visual acuity and color perception (like that caused by cGMP-specific phosphodiesterase type 5 inhibitors) or as serious as retinopathy (e.g., phenothiazines, aminoquinolines, and tamoxifen), optic neuropathy (e.g., amiodarone and ethambutol), or cataract formation (e.g., glucocorticoids and phenothiazines). These adverse findings in humans have been reviewed elsewhere (1). Such toxicities may or may not limit or restrict the use of these pharmaceuticals in medical practice depending upon many factors such as the costs and availability of alternative medicines in the

Michael Aschner et al. (eds.), *Cell Culture Techniques*, Neuromethods, vol. 56,
DOI 10.1007/978-1-61779-077-5_14, © Springer Science+Business Media, LLC 2011

market place and the risk/benefit consideration for the patient. A comprehensive review for discerning these potential adverse effects has been published by us and can be used as a practical guide for understanding the current pharmaceutical industry practice for examining and dealing with proposed therapeutic agents that were found to cause some form of ocular toxicity during animal testing (2). In this chapter the focus will be on presenting the pros and cons of a relatively simple in vitro technique we have successfully used in the past to assess the potential hazard of experimental therapeutics to the mammalian crystalline lens. An adverse finding in the lens (i.e., opacity formation) is only one of several types of adverse ocular events that can be discovered in animal safety assessment studies conducted during the development of potentially new therapeutic agents.

Several pharmaceuticals in use today have some or no apparent association with cataract formation in humans even though they caused lenticular opacities in animals at some point during animal testing. For example, simvastatin (3) and tamoxifen (4) caused lenticular opacities in chronic 2-year rat studies while lovastatin (5), simvastatin (3), cerivastatin (6), NK-104 (7) and fluvastatin (8) caused opacity formation in 3-month to 2-year dog studies depending upon the strength of the administered oral dose. The antipsychotic, quetiapine (9), reportedly caused lenticular opacities in dogs after 6–12 months of treatment or monkeys after 1 year. Tacrolimus (FK-506) was also shown to be cataractogenic in adult rats administered the drug for 13 weeks or more (10). In this particular case the etiology of cataract formation was related to pancreatic injury and the resultant rise in blood glucose levels. The ability to decrease sorbitol levels in lens and the incidence of cataract formation when administered in conjunction with an aldose reductase inhibitor confirmed that the etiology was related to osmotic stress in the lens. In contrast to the pharmaceutical agents listed above, several experimental therapeutics have been reported in the general literature as being discontinued from further development, either wholly or in part, due to cataract formation in preclinical animal species. For example, several 5-HT3 antagonists have been associated with either nuclear cataract formation in rats after in utero exposure to RG 12915 (11) or posterior subcapsular cataracts in adult rats after 6-month exposure to SDZ ICT 322 (12, 13). The peroxisome proliferator-activated receptor (PPAR)-γ agonist ciglitazone caused varying degrees of opacity formation (bilateral changes ranging from posterior cortical capsular cataracts with or without nuclear cataracts to mature complete cataracts during the conduct of 3-month rat studies) (14). Two 5-lipoxygenase inhibitors, CJ-12,918 and CJ-13,454, were associated with lenticular opacity formation in 1-month rat studies (15, 16). These two works demonstrated the value of understanding in vivo drug metabolism and

the design of structural modifications to block sites of metabolism in eventually producing an agent that did not cause opacity formation in rodents. Two antihyperlipidemic agents (ZD9720 and ZD7851) that disrupt cholesterol biosynthesis through inhibition of oxidosqualene cyclase were also shown to cause cataracts within less than 1 month of oral dosing in mouse and/or dog (17). Bencz and colleagues (18) were able to identify a common toxicophore (dimethyl- or diethyl-aminoethoxy group) among several experimental agents (RGH-6201, U-18666A, triparanol, and tilorone) that also disrupted cholesterol biosynthesis and caused cataract formation.

At the biochemical level lenticular opacities are caused by broad and overlapping mechanisms such as (a) oxidative stress (19) like that caused by the generation of a reactive metabolite (e.g., naphthalene) or osmotic stress (20) like that caused by the accumulation of active osmolytes such as polyols within the lens, (b) Ca^{2+}-dependent activation of calpains (21), (c) the inhibition or disregulation of normal bioenergetic processes (22–24) at the mitochondrial level, or (d) alterations in thiol status (24, 25) caused directly or indirectly by affecting glutathione metabolism or the regeneration of proper thiol status through inhibition of the pentose phosphate shunt. Many of these biochemical mechanisms are interdependent upon each other and therefore difficult to ascertain the true initiating event or sequence of events. Another important biochemical mechanism of cataract formation in animals appears to be the disruption of lenticular cholesterol biosynthesis. This mechanism has long been recognized as an another mechanism of cataract formation through clinical administration of triparanol in humans (26), but mostly through the effects of various statins administered to animals (27–30). Early work with the statins showed that opacity formation in dogs could be avoided by screening compounds for their ability to inhibit 3-hydroxy-3-methyl-glutaryl-CoA reductase (HMG-CoA reductase) activity in the liver without affecting the lens isoform (31). As an avascular structure, the lens relies on de novo cholesterol biosynthesis that is necessary to support continual growth and differentiation of lens epithelial cells into lens fiber cells. It is estimated that the developing lens fiber cell volume increases 1200-fold during this process. Because of the primary dependence upon cholesterol formation by the lens itself we have furthered this approach by developing a 2-day bioassay in rats. Using this approach we have demonstrated the potential of numerous potential therapeutic agents to inhibit lens cholesterol biosynthesis after in vivo administration (32) and the relative lack of specificity to chemicals such as naphthalene and galactose (33).

In many cases it is desirable to assess the cataractogenic potential of experimental agents or mechanisms of toxicity totally in vitro. The benefits of using the isolated lens compared to whole

animal models include the ability to control the extracellular milieu bathing the lens (e.g., drug or other treatment conditions) and the ability to quantitatively measure biochemical or molecular endpoints associated with the mechanisms of cataract formation (e.g., cholesterol biosynthesis, intracellular ion content or transport, adenosine triphosphate (ATP) content, glutathione redox status, calpain activation). For studying mechanisms of cataract formation caused by chemicals or pharmaceutical agents, the ability to directly expose isolated lenses to the insulting agent significantly reduces the time and amount of drug needed to conduct screening of potential drug candidates for cataractogenic potential. These latter factors are critically important early in the drug development process when quantities of drug available for testing are typically quite low or when the amount of time needed to produce the cataract in vivo is lengthy. Finally, the isolated lens model enables safety assessments of both intended disease targets and of unintended or off-target chemotype-related effects. Therefore the isolated rat lens is often used by us as an in vitro model to rank order compounds for cataract risk and to study mechanisms of cataractogenesis (14, 16, 22). The applications of these procedures will be presented to illustrate our experience in the use of this model in the pharmaceutical industry.

2. Experimental Protocols: Lens Isolation and Explant Culture

2.1. Materials

Reagents: Bicarbonate supplemented media TC-199 (295 ± 5 mOsm, final adjusted). Sigma M3769 is supplemented with 2.2 g sodium bicarbonate per liter according to product information sheet from the manufacturer.

Supplies: Scalpel blades (#11), filter paper forceps, fine scissors, 35 mm petri dish or 6–12 well plate, guitar pick, plastic tubing to cover forcep tips, iris scissors, and fine forceps.

2.2. Method: Rodent

1. Euthanize the animals according to accepted institutional and regulatory guidelines.
2. Grasp the connective tissue on the temporal side of the eye with forceps. Cut the tissue surrounding the eye with a pair of fine scissors. Once half of the perimeter is cut, make a cut deep in the eye socket to cut the optic nerve. This will leave you with at least 3 mm of optic nerve to manipulate the eyeball.
3. Clean the eye of any connective tissue, fat, or harderien gland and place corneal side down on a piece of filter paper.
4. While grasping the optic nerve, place a #11 scalpel blade gently against the eye next to the optic nerve and roll the eye

against the blade. If the incision is long enough, the lens can gently be pushed out of the eye. If tissue such as retina is still attached, the lens can be gently washed with media or rolled along the equator on premoistened filter paper. The ciliary body will still be attached.

5. NOTE: The rat lens occupies roughly 80% of the eye volume. It is imperative that the cut be superficial to avoid damaging the lens. Also, any contact with the rat lens made with metal will induce an artificial cataract as will storing the eye on ice or not prewarming the media. For our use, a guitar pick is used to roll the lens and forceps with tubing is used for picking up the eye.
6. Place the lens explant in appropriate volume of bicarbonate supplemented media TC-199 (295 ± 5 mOsm) and incubate overnight at 37°C in a 5% CO_2 humidified tissue culture incubator.

12 well plate (2 mL)	6 well plate (4 mL)
35 mm petri dish (4 mL)	20 × 150 mm tube (1 mL)

7. On the following day, check the lenses for visual clarity. This has been a sufficient measure for grading lens integrity within the lab although the amount of lactate dehydrogenase release into the media can also be used to check the lens integrity.
8. Rat lenses can usually be cultured for 1 week and possibly up to 2; however, it is not recommended to exceed more than 1 week. Media should be changed every 2–3 days. See Fig. 1 for representative example of explanted rat lens in culture.

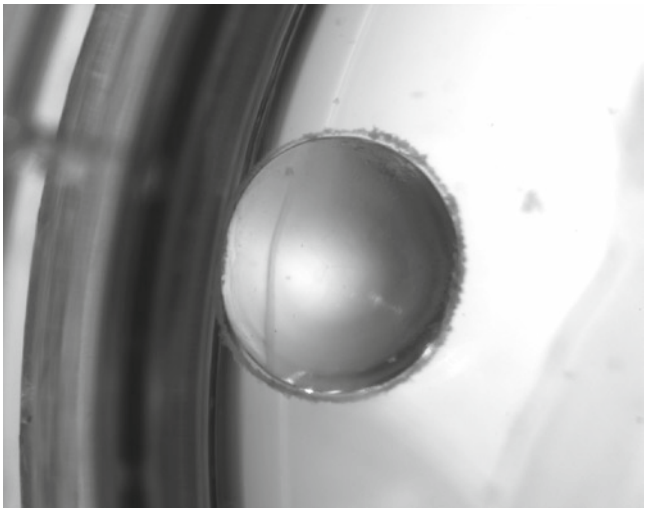

Fig. 1. Example of a single rat lens in explant culture for 7 days using 35 mm petri dish. Note the lens clarity even after 7 days in culture.

2.3. Method: Canine or Non-Human Primate

1. Eyes are received on ice or in prewarmed bicarbonate supplemented media TC-199 (295 ± 5 mOsm) from necropsy technicians.
2. NOTE: Canine and primate lenses do not appear as sensitive to the effects of storage on ice for up to 30 min after necropsy and contact with metal. However, it is not recommended to exceed 30 min on ice or contacting the lens with metal.
3. With the eye corneal side down and filter paper, gauze, or eye holder, make an incision anterior to the ora serrata. If using a scalpel blade, angle it pointing towards the posterior. Continue cutting with fine scissors around the ora serrata, taking care not to penetrate deep into the eye. Remove the posterior portion of the eye to reveal the lens. It may be necessary to cut the vitreous to remove the posterior. Cut the sclera posterior to anterior in 4–5 different places to aid in opening the eye cup the lens is sitting on. Free the lens by cutting the zonule fibers. This is achieved by gently pulling the ciliary body and cutting the fibers with iris scissors.
4. Note: This method can also be used for the rat lens. It is recommend to continually bathe the lens in media to avoid drying.
5. Place the lens explant in appropriate volume of bicarbonate supplemented media TC-199 (295 ± 5 mOsm) and incubate overnight at 37 °C in a 5% CO_2 humidified tissue culture incubator.

12 well plate (2 mL)	20 × 150 mm tube (2 mL)

6. On the following day, check the lenses for visual clarity. This has been a sufficient measure for grading lens integrity within the lab although lactate dehydrogenase release into the media can also be used to check lens integrity.
7. Canine or primate lenses can usually be cultured for 1 week and up to 2 weeks. Media should be changed every 2–3 days.

Note:

Although the lens represents a large portion of the rodent eye, it is fairly easily harvested from the rat eye and used as an explant culture for periods of at least 1 week. However, the development of this technique requires repeated practice to be able to routinely harvest lenses that are not damaged as a result of the extraction procedure. Extreme care should be taken in handling the lens in order to avoid producing a mechanically induced cataract. Cultured lenses that remain clear for ~24 h in vitro can be used for subsequent studies to evaluate the effects of candidate drugs on lens clarity. Figures 2–4 provide examples of opacification

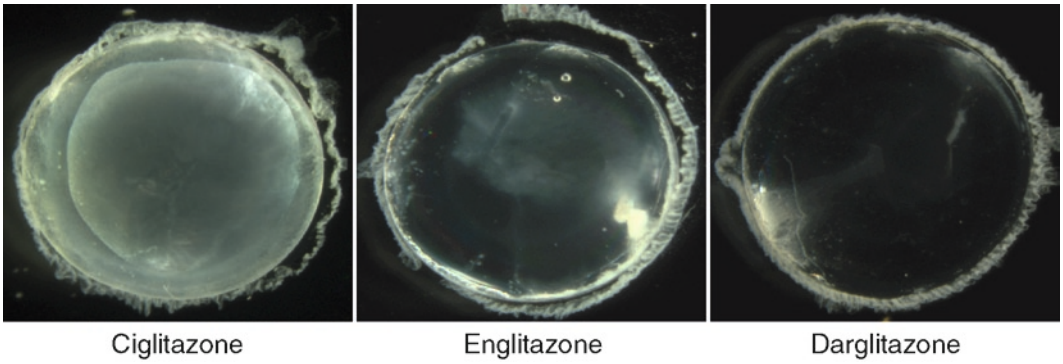

Fig. 2. Visual appearance of rat lenses in explant culture treated with the thiazolidinediones ciglitazone, englitazone, or darglitazone after 48 h of exposure (representative examples). Note the presence of stage 2 opacity in ciglitazone-treated lens. Other investigators have visualized opacity formation in explanted lenses using a grid to assess clarity and swelling by visual assessment or with other more sophisticated analyses tools and instruments such as that presented below in Fig. 3 by Bantseev et al. (43). Reprinted from Aleo et al. (16) with permission from Wiley (New York, NY).

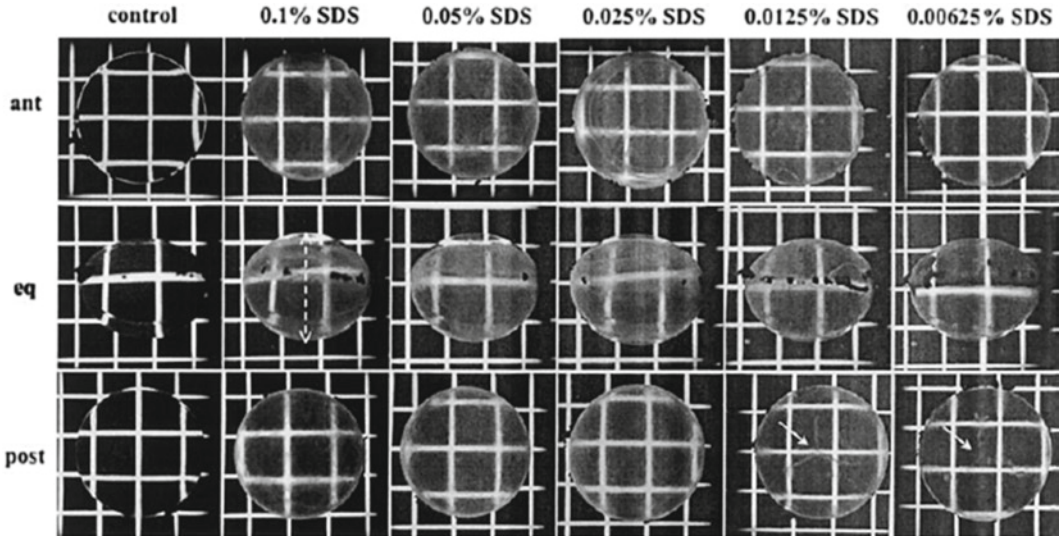

Fig. 3. Representative photographs of bovine lenses showing the effect of different concentrations of sodium dodecyl sulfate (SDS) on lens clarity and swelling. Lenses were treated with different concentrations of SDS (0.1–0.00625%) for 30 min and photographed at the end of the experiment. Axial swelling (*white dashed arrow*) was seen in lenses treated with higher SDS concentrations (0.025–0.1%). While severe opacities were seen in lenses treated with higher concentrations of SDS, fewer opacities were seen in lenses treated with 0.0125 and 0.00625% SDS. However, in lenses treated with 0.0125 and 0.00625% SDS opacities around posterior lens sutures were seen (*white arrows*). Figure and figure legend reprinted from Bantseev et al. (43) with permission from Oxford University Press (New York, NY).

of lenses in vitro in terms of assessment for screening compounds (Fig. 2). Some investigators have visualized opacity formation in explanted lenses using a grid to assess clarity and swelling by visual assessment or with other more sophisticated analytical tools and instruments for classifying grades of opacification using bovine lens (Fig. 3) while we have relied upon a simple visual classification system based on the examples presented in Fig. 4 using the rat lens.

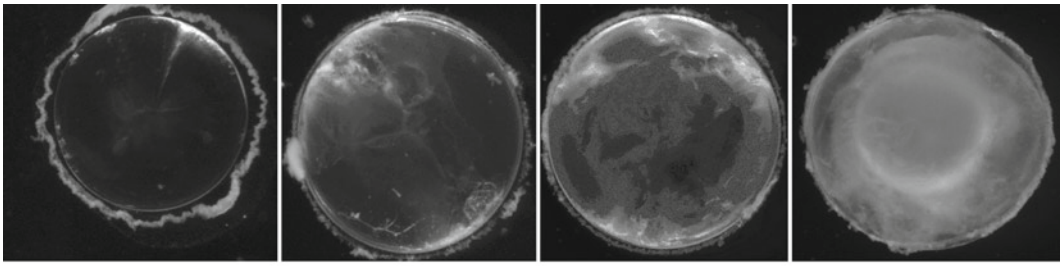

Fig. 4. Representative examples of the gradation of opacity formation in rat lenses in vitro. Progression of opacity formation from left to right. These in vitro representations are similar to those seen in lenses obtained from animals exposed to the same compound.

3. Applications

The lens explant culture model has been used by us to rank order and select alternative drug candidates based on their potential to cause opacity formation in vitro (14, 16) and to investigate mechanisms of cataract formation with various chemicals and drug candidates, such as *S*-(1,2-dichlorovinyl)-L-cysteine (22) and ciglitazone (14). Although the model is extremely versatile, a major limitation is the increased likelihood of identifying false positives (16). This is because the in vitro model allows direct access of compounds to the lens, even though these compounds may have limited ability to gain access to the inner chambers of the eye and penetrate the lens in vivo. In our experience, explant lenses exposed in vitro can achieve greater than 10× the amount of parent drug found in the lenses after in vivo exposure. Therefore, because of the high levels of parent drug achieved, a compound that has limited access to the lens in vivo may cause severe opacities in vitro.

Screening for back-up compounds. There have been several occasions when we have had a lead compound promote opacity formation in either rat or dog studies of 1–6 months in duration. For example, rat lens explant cultures were used to assess structural modifications for cataractogenic potential with the 5-lipoxygenase inhibitor CJ-12,918, despite the fact that the model was overly sensitive in predicting cataractogens (16). Because one can add exogenous sources of metabolic activation, this approach can demonstrate the possible involvement of biotransformation in the progression of cataract formation or the lack of involvement. For example, the presence of an aroclor-induced S9 microsomal fraction increases the rate and extent of opacity formation in rat lens explants. CJ-12,918 in the absence of S9 causes only slight opacification of lenses after 6 days in culture while addition of S9 microsomal fraction causes extreme opacification of lenses within

4 days of exposure. In contrast, we have seen examples with other compounds where the presence of S9 does not affect the rate or extent of opacification in lenses in vitro, suggesting that metabolic activation is not likely involved in the mechanism of cataract formation in vivo.

Mechanistic insights. Rat lens explant cultures can also be used to assess the mechanisms of toxicity as well. For example, through the use of various biochemical manipulations we showed that opacity formation by *S*-(1,2-dichlorovinyl)-L-cysteine (DCVC) in rodent and primate lenses in vitro is primarily mediated via lenticular β-lyase metabolism of DCVC to a reactive metabolite (22). Perturbations in mitochondrial Ca^{2+} homeostasis and increased poly(ADP-ribosylation) of nuclear proteins played a limited role in opacity formation while oxidative stress or calpain activation did not appear to play a role. A similar approach was used to examine possible mechanisms related to ciglitazone toxicity to the lens in which early and selective changes in lenticular ATP content as well as the protective effects of ruthenium red, a mitochondrial Ca^{2+} uniport inhibitor, suggested that alterations in lens bioenergetics could play an important role in ciglitazone-induced cataract formation (14).

At the molecular level we have also used rat lens explant culture to explore changes in microRNA (miRNA) expression (34). MiRNAs are a class of endogenously expressed small RNA molecules (20–25 nt long) that regulate one or more target mRNA through translational repression or cleavage. In this study both ciglitazone and ZD2138 differentially expressed three miRNAs (miR-31 and miR-99a/b) during the process of producing opacities in vitro. Using target predictive tools, miR-99a and 99b seem to regulate actin cytoskeleton and integrin signaling pathway while miR-31 appears to be involved in the regulation of cell cycle and proliferation, both of which are important in maintaining lens function and integrity. These results indicate that miRNA expression in the lens is altered during the process of opacity formation and that their differential expression may be used to understand toxicity pathways and/or as biomarkers of lens toxicity.

Others have used rat lens explant culture to explore the role of the Ras superfamily of small GTP-binding proteins (35–37). Here there is evidence that inhibition of the synthesis of nonsterol metabolites of mevalonate such as farnesyl pyrophosphate and geranylgeranyl pyrophosphate, and the resultant disruption of cytoskeletal organization rather than reductions in lens cholesterol biosynthesis per se is involved in the cataractogenic potential of certain statins. Although these findings were consistent with earlier results showing no apparent change in lens cholesterol levels in lovastatin-treated dogs (29) or the cholesterol to phospholipid molar ratio in the lenses of simvastatin-treated rats for 2 weeks

with opacities (38), de Vries et al. (39, 40) was able to demonstrate a 20–25% reduction in the cholesterol content of lenses from rat pups treated for 3 weeks with lovastatin and somvastatin, but not pravastatin. These mixed results suggest that these types of cataracts may be due to a mixture of perturbations at the molecular and biochemical levels.

Others have explored more basic mechanisms of cataract formation. Fukiage et al. (41) used cultured lenses from guinea pigs and rabbits to explore the contributions of calpain-induced proteolysis using the prototypic calcium ionophore A23187. Although lenses from both species developed outer cortical opacities, lenses from guinea pigs were more susceptible to nuclear cataract formation compared to the rabbit, suggesting differences in crystalline classes or structures between these two species.

Species differences in lens antioxidant capacity. At a biochemical level Slaughter et al. (42) investigated the antioxidant system between different laboratory animals used in nonclinical toxicology studies (beagle dog, Sprague–Dawley rats, marmosets and New Zealand white rabbits). This study was not designed as a lens explant culture study, but rather a biochemical characterization of freshly obtained lenses extracted from animals. They found substantial differences between species that may explain relative differences in species susceptibility to oxidative stress-mediated cataract formation. High levels of reduced glutathione and its corresponding maintenance system was found in the marmoset lens while the rat had the low levels of glutathione reductase, glutathione peroxidase and glutathione *S*-transferase.

In summary, the versatility of lens explant cultures should not be underrated. Its broad application has been demonstrated by us and many others for screening and exploring mechanisms of cataract formation of potentially new therapeutic agents at the biochemical and molecular level.

Acknowledgments

The author thanks the technical contributions of Jim Coutcher, Colleen Doshna and Dan Baltrukonis over the years in perfecting the in-house technique and protocol development.

References

1. Li J, Tripathi RC, Tripathi BJ (2008) Drug-induced ocular disorders. Drug Saf 31:127–141
2. Somps CJ, Greene N, Render JA, Aleo MD, Fortner JH, Dykens JA, Phillips G (2009) A current practice for predicting ocular toxicity of systemically delivered drugs. Cutan Ocul Toxicol 28:1–18
3. ZOCOR, NDA no. 019766, product label approved 6/11/2008. United States Food and Drug Administration. Accessed 12 Jan 2010. http://www.accessdata.fda.gov/drugsatfda_docs/label/2008/019766s076lbl.pdf
4. Greaves P, Goonetilleke R, Nunn G, Topham J, Orton T (1993) Two-year carcinogenicity

study of tamoxifen in Alderley Park Wistar-derived rats. Cancer Res 53:3919–3924

5. MEVACOR, NDA no. 019643, product label approved 3/9/2009. United States Food and Drug Administration, Accessed 12 Jan 2010. http://www.accessdata.fda.gov/drugsatfda_docs/label/2009/019643s080lbl.pdf
6. von Keutz E, Schluter G (1998) Preclinical safety evaluation of cerivastatin, a novel HMG-CoA reductase inhibitor. Am J Cardiol 82:11J–17J
7. Shibuta T, Kato Y, Amano Y, Kakishita T, Tanaka M, Takimoto M (1998) A 12-month oral toxicity study of (+)-monocalcium bis[(3R, 5S, 6E)-7-[2-cyclopropyl-4-(4-fluorophenyl)-3-quinolyl]-3,5-dihydroxy-6-heptenoate] (NK-104) in dogs followed by a 2-month recovery test. Oyo Yakuri Pharmacometrics 56:101–130
8. LESCOL, NDA no. 020261, product label approved 6/12/2007. United States Food and Drug Administration. Accessed 12 Jan 2010. http://www.accessdata.fda.gov/drugsatfda_docs/label/2007/020261s039,021192s013lbl.pdf
9. SEROQUEL, NDA no. 020639, product label approved 12/2/2009. United States Food and Drug Administration, Accessed 12 Jan 2010. http://www.accessdata.fda.gov/drugsatfda_docs/label/2009/020639s045s046lbl.pdf
10. Ishida H, Mitamura T, Takahashi Y, Hisatomi A, Fukuhara Y, Murato K, Ohara K (1997) Cataract development induced by repeated oral dosing with FK506 (tacrolimus) in adult rats. Toxicology 123:167–175
11. Lerman SA, Delongeas JL, Plard JP, Veneziale RW, Clark RL, Rubin L, Sanders JE (1995) Cataractogenesis in rats induced by *in utero* exposure to RG 12915, a 5-HT3 antagonist. Fundam Appl Toxicol 27:270–276
12. Langle UW, Wolf A, Kammuller ME (1993) Cataractogenic effects in rats following chronic administration of SDZ ICT 322, a selective 5-HT3 antagonist. Fundam Appl Toxicol 21:393–401
13. Langle UW, Wolf A, Cordier A (1997) Enhancement of SDZ ICT 322-induced cataracts and skin changes in rats following vitamin E- and selenium-deficient diet. Arch Toxicol 71:283–289
14. Aleo MD, Doshna CM, Navetta KA (2005) Ciglitazone-induced lenticular opacities in rats: in vivo and whole lens explant culture evaluation. J Pharmacol Exp Ther 312:1027–1033
15. Mano T, Okumura Y, Sakakibara M, Okumura T, Tamura T, Miyamoto K, Stevens RW (2004) 4-[5-Fluoro-3-[4-(2-methyl-1H-imidazol-1-yl)benzyloxy]phenyl]-3,4,5,6-tetrahydro-2H-pyran-4-carboxamide, an orally active inhibitor of 5-lipoxygenase with improved pharmacokinetic and toxicology characteristics. J Med Chem 47:720–725
16. Aleo MD, Avery MJ, Beierschmitt WP, Drupa CA, Fortner JH, Kaplan AH, Navetta KA, Shepard RM, Walsh CM (2000) The use of explant lens culture to assess cataractogenic potential. Ann NY Acad Sci 919:171–187
17. Pyrah IT, Kalinowski A, Jackson D, Davies W, Davis S, Aldridge A, Greaves P (2001) Toxicologic lesions associated with two related inhibitors of oxidosqualene cyclase in the dog and mouse. Toxicol Pathol 29:174–179
18. Bencz Z, Ivan E, Cholnoky E (1985) Analysis of cataract and keratotic damage induced by 4-diethylaminoethoxy-alpha-ethyl-benzhydrol (RGH-6201) in rats. Arch Toxicol Suppl 8:476–479
19. Spector A (2000) Review: oxidative stress and disease. J Ocul Pharmacol Ther 16:193–201
20. Chung SS, Ho EC, Lam KS, Chung SK (2003) Contribution of polyol pathway to diabetes-induced oxidative stress. J Am Soc Nephrol 14:S233–S236
21. Azuma M, Tamada Y, Kanaami S, Nakajima E, Nakamura Y, Fukiage C, Forsberg NE, Duncan MK, Shearer TR (2003) Differential influence of proteolysis by calpain 2 and Lp82 on in vitro precipitation of mouse lens crystallins. Biochem Biophys Res Commun 307:558–563
22. Walsh Clang CM, Aleo MD (1997) Mechanistic analysis of *S*-(1,2-dichlorovinyl)-L-cysteine-induced cataractogenesis *in vitro*. Toxicol Appl Pharmacol 146:144–155
23. Martynkina LP, Qian W, Shichi H (2002) Naphthoquinone cataract in mice: mitochondrial change and protection by superoxide dismutase. J Ocul Pharmacol Ther 18:231–239
24. Belusko PB, Nakajima T, Azuma M, Shearer TR (2003) Expression changes in mRNAs and mitochondrial damage in lens epithelial cells with selenite. Biochim Biophys Acta 1623:135–142
25. Lou MF (2003) Redox regulation in the lens. Prog Retin Eye Res 22:657–682
26. Kirby TJ (1967) Cataracts produced by triparanol (MER-29). Trans Am Ophthalmol Soc 65:494–543
27. MacDonald JS, Gerson RJ, Kornbrust DJ, Kloss MW, Prahalada S, Berry PH, Alberts AW, Bokelman DL (1988) Preclinical evaluation of lovastatin. Am J Cardiol 62:16J–27J
28. Gerson RJ, MacDonald JS, Alberts AW, Kornbrust DJ, Majka JA, Stubbs RJ, Bokelman

DL (1989) Animal safety and toxicology of simvastatin and related hydroxy-methylglutaryl-coenzyme A reductase inhibitors. Am J Med 87:28S–38S

29. Gerson RJ, MacDonald JS, Alberts AW, Chen J, Yudkovitz JB, Greenspan MD, Rubin LF, Bokelman DL (1990) On the etiology of subcapsular lenticular opacities produced in dogs receiving HMG-CoA reductase inhibitors. Exp Eye Res 50:65–78
30. Gerson RJ, Allen HL, Lankas GR, MacDonald JS, Alberts AW, Bokelman DL (1991) The toxicity of a fluorinated-biphenyl HMG-CoA reductase inhibitor in beagle dogs. Fundam Appl Toxicol 16:320–329
31. Mosley ST, Kalinowski SS, Schafer BL, Tanaka RD (1989) Tissue-selective acute effects of inhibitors of 3-hydroxy-3-methylglutaryl coenzyme A reductase on cholesterol biosynthesis in lens. J Lipid Res 30: 1411–1420
32. Aleo MD, Drupa CA, Fritz CA, Walsh CM, Whitman-Sherman JL, Fortner JH (2001) Alterations in lenticular sterol content precede CJ-12,918-induced cataract formation. Toxicol Sci 60(Suppl):101
33. Baltrukonis DJ, Fortner JH, Somps CJ, Ryan AM, Aleo MD, Verdugo ME (2003) Comparisons between U18666A, naphthalene, and galactose on lens cholesterol biosynthesis and evaluation of cataract progression by Scheimpflug and slit lamp exams *Invest.* Ophthalmol Vis Sci 44:3489
34. Simic D, Deng S, Somps CJ (2008) Drug-induced lens toxicity and differential expression of miRNA *Invest.* Ophthalmol Vis Sci 49:2780
35. Cheng Q, Gerald Robison W, Samuel Zigler J (2002) Geranylgeranyl pyrophosphate counteracts the cataractogenic effect of lovastatin on cultured rat lenses. Exp Eye Res 75: 603–609
36. Rao PV, Robison WG Jr, Bettelheim F, Lin LR, Reddy VN, Zigler JS Jr (1997) Role of small GTP-binding proteins in lovastatin-induced cataracts. Invest Ophthalmol Vis Sci 38:2313–2321
37. Maddala RL, Reddy VN, Rao PV (2001) Lovastatin-induced cytoskeletal reorganization in lens epithelial cells: Role of Rho GTPases. Invest Ophthalmol Vis Sci 42: 2610–2615
38. Cenedella RJ, Kuszak JR, Al-Ghoul KJ, Qin S, Sexton PS (2003) Discordant expression of the sterol pathway in lens underlies simvastatin-induced cataracts in Chbb: Thom rats. J Lipid Res 44:198–211
39. De Vries ACJ, Cohen LH (1993) Different effects of the hypolipidemic drugs pravastatin and lovastatin on the cholesterol biosynthesis of the human ocular lens in organ culture and on the cholesterol content of the rat lens *in vivo.* Biochim Biophys Acta 1167:63–69
40. De Vries ACJ, Vermeer MA, Bredman JJ, Bär PR, Cohen L (1993) Cholesterol content of the rat lens is lowered by administration of simvastatin, but not by pravastatin. Exp Eye Res 56:393–399
41. Fukiage C, Azuma M, Nakamura Y, Tamada Y, Shearer TR (1998) Nuclear cataract and light scattering in cultured lenses from guinea pig and rabbit. Curr Eye Res 17:623–635
42. Slaughter MR, Thakkar H, O'Brien PJ (2003) Differential expression of the lenticular antioxidant system in laboratory animals: A determinant of species predilection to oxidative stress-induced ocular toxicity? Curr Eye Res 26:15–23
43. Bantseev V, McCanna D, Banh A, Wong WW, Moran KL, Dixon DG, Trevithick JR, Sivak JG (2003) Mechanisms of ocular toxicity using the in vitro bovine lens and sodium dodecyl sulfate as a chemical model. Toxicol Sci 73:98–107

Chapter 15

Necrosis, Apoptosis, and Autophagy: Mechanisms of Neuronal and Glial Cell Death

Michael Fricker and Aviva M. Tolkovsky

Abstract

Most neurodegenerative diseases culminate in cell death, although it is not uncommon for signs of dysfunction to precede cell death in humans and animal models. There is considerable evidence that neuronal and glial cell death during development occurs through apoptosis but whether apoptosis occurs during degeneration is still a contentious issue. Apoptosis is a well-defined process with key steps that mark the progress of the process in individual cells. Necrosis and autophagy as primary causes of death are less well defined. Two issues need particular clarification: (1) when is necrosis deemed to be the death mechanism rather than a secondary outcome of another death mechanism, and (2) whether the autophagic process, or its deficiency, causes death, or whether autophagy is a bystander (or survival) effect. Here we present a framework for addressing how to discern when necrosis, apoptosis, and/or autophagy occur in primary cultures of neurons and glia.

Key words: Necrosis, Apoptosis, Autophagy, Neuron, Glia, Cell culture, Cell death

1. Introduction

Cell death in the nervous system is a common feature of early development. It occurs widely during neurogenesis (1), in post-mitotic neurons during target innervation (2), and is also used to control the number of glia, such as oligodendrocytes during myelination of the optic nerve (3). By looking at samples of dying neurons microscopically, Clarke defined three major neuronal cell death types with features that were "apoptotic," "autophagic," and "non-lysosomal vesiculate" (4). In the wider context of pathological neurodegeneration, however, a myriad of additional cell death morphologies have been described, not least those ascribed to having been mediated by autophagy or necrosis. Studies of purified cultured neurons dying after they express mutant proteins

Michael Aschner et al. (eds.), *Cell Culture Techniques*, Neuromethods, vol. 56,
DOI 10.1007/978-1-61779-077-5_15,

implicated in neurodegenerative conditions (e.g., (5, 6)) show that most of these deaths are not purely apoptotic, necrotic, or autophagic, although they may display some features of each. Likewise, astrocytes may die in a non-apoptotic, non-necrotic fashion in response to insults (7).

Despite the 20 years since Clarke's review was published, only apoptotic death is well understood at the molecular level. The molecules that mediate autophagy are also now quite well defined, but whether autophagy kills mammalian cells (as in "programmed autophagic death") is still under debate (8). For example, a recent study of death after hypoxic–ischaemic injury used mice deficient in brain-specific Atg7 ($Atg7^{flox/flox}$; nestin-Cre) (9) – a gene essential for constitutive autophagosome formation. It was shown that death after hypoxic–ischaemic injury was reduced in this mouse, implicating autophagy in the death (10). However, most evidence for autophagic cell death relies on changes in autophagosome numbers during death, rather than on demonstrating the autophagic process, and is thus inconclusive. Indeed, in mouse Atg5- and Atg7-null autophagy-deficient neurons (9, 11), cells accumulated polyubiquitinated protein inclusions, a hallmark of many degenerative conditions, and there was marked cell death in the cortex and cerebellum, as well as a marked axonopathy (12). Thus, autophagy may be protective or destructive. The answer regarding autophagy may lie in what exactly is being gotten rid of by autophagic degradation, or what is accumulating when autophagy is defective, rather than in autophagy as a cell death process per se.

Of the three mechanisms, necrosis is the easiest type of cell death to diagnose in vitro but least tractable in terms of its mechanism (see (13) for review). Not understanding the "alternative" mechanisms of death is hampering our understanding of the mechanisms of pathological neurodegeneration. In this quest, in vitro studies can help to identify death pathways without prejudice, with one possible caveat: in cultures of pure cell populations, as in developmental death, most cell deaths occur autonomously by activating intrinsic death-signalling pathways. However, there is now some thought that neurons (and glia?) are actively killed by their neighbours in neurodegenerative diseases (14). Hence, culturing mixed populations of cells (or brain slices) may reveal novel death pathways that would not be observed in purified cell populations.

Extensive recommendations for best practice in assessing cell death and its mechanisms (15), or autophagy (15, 16), have been published just recently. Therefore, this article concentrates on a more conceptual framework for dealing with the questions of how to discern when necrosis, apoptosis, and/or autophagy occur in primary cultures of neurons and glia. One area of emphasis is how to establish positive controls for each type of system.

Emphasis is also placed on how to diagnose whether cells at any point are committed to die, by removing the agent that promotes death and observing whether the cell goes on to live. Death commitment can precede observable features of cell death and is thus an important diagnostic feature in attempting to unravel the mechanisms and prevent degeneration. Although there is crossover or coincidence between the various forms of cell death, this review divides the field into three parts: necrosis, apoptosis, and autophagy.

2. Necrosis

The undisputed hallmark of necrosis is the early and sudden loss of plasma membrane integrity. Traditionally, this has been ascribed to profound loss of ATP leading to homeostatic ion imbalance and is often preceded by cell swelling without other notable changes occurring inside the cell. Sometimes, a phase-dark "balloon" protrudes from the membrane before the cells become phase dark; this seems to form between the inner and outer plasma membrane leaflets and occurs in particular with pro-oxidant insults or when excessive reactive oxygen/nitrogen species accumulate in the cell. Whether the cell is already committed to die at this point is not clear, since, as far as we know, attempts to prevent death after this phenotype has formed have not been described.

In cultured cells, as in vivo, necrosis can be the primary cause of death (making it of great interest) or a secondary feature that occurs in cells that have already been committed to die by apoptosis or other means. In vivo, many apoptotic cells may have disappeared by phagocytosis before secondary necrosis occurs, but in pure cultures lacking professional phagocytes, secondary necrosis is not uncommon (see Sect. 3 for further comments, and Chap. 10).

Since necrosis of cells is defined by increased permeability of the plasma membrane, reagents that do not cross the membrane unless its permeability barrier is disrupted are used to identify necrosis. Because any small metabolite that is soluble in the cytoplasm will diffuse out of the permeabilized cell as well as diffuse in (indeed producing holes in a controlled manner is a way to leach out nutrients, ions, and ATP without causing loss of proteins (17)), the dyes used to detect necrosis are commonly those that bind to nuclear DNA. A positive control for necrosis can be induced by profound inhibition of ATP production, for example using mitochondrial respiration poisons (oligomycin, cyanide (careful!), azide) together with inhibition of glycolysis (achieved by glucose removal or by adding a tenfold excess of a non-metabolisable glucose analogue such as 2-deoxyglucose) (7, 18). Exposure to excessive nitric oxide/peroxynitrite (NO/HNOO),

arsenite, or H_2O_2 may also cause rapid necrosis via plasma membrane lipid peroxidation, a possible cause of the 'balloon' phenotype. Notably, in the case of mild doses of NO treatment of astrocytes (7), cells activated a kinase whose inhibition switched the death from apoptosis to necrosis, perhaps due to loss of ATP (19). Other kinase inhibitors may also enhance necrosis in astrocytes under conditions of energy depletion (18).

2.1. Fluorescent Dyes

Necrotic cells can be distinguished from live and early apoptotic cells under phase microscopy. Live/apoptotic cells appear phase bright whereas necrotic cells usually appear granular and phase dark. An experienced user will be able to count necrotic cells based on this difference but a reliable measure of necrosis is to use dyes. One of the most common dyes used to measure necrosis is propidium iodide (PI) (see scheme in Fig. 1). PI does not permeate membranes of live cells but produces very bright fluorescence when it intercalates into double-stranded DNA. Therefore, it can be added together with a vital fluorescent nuclear dye such as

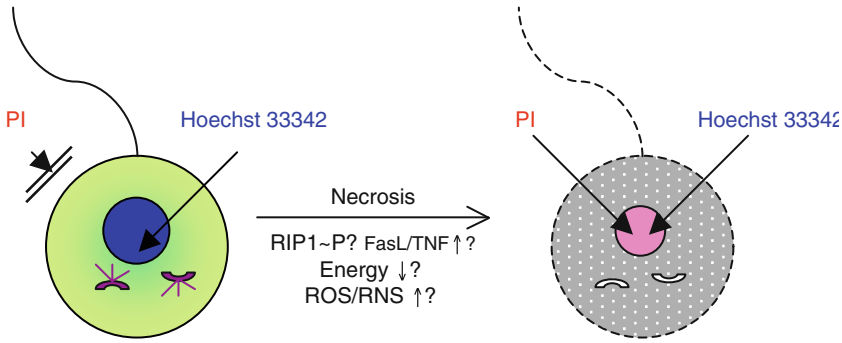

Nucleus	Well demarcated nucleus stains blue with Hoechst 33342 but does not stain with PI (or ethidium homodimer)	Can be slightly shrunken stains pink with Hoechst 33342 and PI or red when viewed under 'green' excitation
Mitochondria	Purple (reduced MTT) deposits rays irradiate out from mitochondria when viewed early (later, the entire cell fills with purple deposits and detail is lost)	No purple MTT deposits will not load with $\Delta\psi$m-dependent dyes
Cytoplasm	Filled with Calcein AM or BCECF (green under 'blue' excitation)	Calcein AM or BCECF AM do not load or they leak out if prefilled before necrosis.
Light microscope	Phase bright	Flat and Phase dark

Fig. 1. Testing for necrosis. Key markers of necrosis are indicated alongside the expected appearance of the cytoplasm, nucleus, and mitochondria, depending on the assay.

2′-(4-ethoxyphenyl)-5-(4-methyl-1-piperazinyl)-2,5′-bi-1H-benzimidazole trihydrochloride (Hoechst 33342) that will stain the nuclei of both live and dead cells. Using a "UV" filter for excitation/emission (ex/em) (ex/em ~350/450 nm) live cells will appear light blue whereas necrotic cells will appear pink. Without PI, necrotic, apoptotic, and live cells will stain with Hoechst 33342, hence its lack of value as a sole marker for necrosis unless there are structural changes in the nuclei that can be reliably discerned (see Sect. 3.1 on nuclear profiles in apoptosis for further comment). There are many additional nuclear dyes that only permeate the plasma membrane of dead cells (such as 4′,6-diamidino-2-phenylindole (DAPI), bisBenzimide, 2′-(4-hydroxyphenyl)-5-(4-methyl-1-piperazinyl)-2,5′-bi-1H-benzimidazole trihydrochloride hydrate (Hoechst 33528), 7-Amino-actinomycin, ethidium homodimer). Ethidium homodimer is a good (if expensive) alternative to PI and is used in a commercial live/dead fluorescent assay (see Sect. 2.3).

Under the "UV" filter, PI is only excited to 10% of its maximal emission. To see PI staining without interference from Hoechst 33342, one can switch to the "green" excitation/red emission filter (peak PI ex/em 536/617), whereupon nuclei will appear bright red. Hoechst 33342 staining will not be visible, however, so only the absolute number of dead cells can be counted.

Pink nuclei double-stained with PI and Hoechst 33342 may appear smaller than those in live cells, especially if pyknosis occurred due, for example, to an oxidative insult prior to necrosis. In cultured astrocytes, the live cell nucleus appears very flat and stretched, so if there is a slight detachment, the nucleus may appear smaller and more rounded. If apoptosis took place prior to necrosis, several pink or blue fragmented and condensed nuclear bodies per nucleus may also be observed. PI and Hoechst 33342 are used in culture at 1–5 μg/mL, diluted into medium from a stock (1 mg/mL) made up in water. Dyes are stable for years in the freezer if protected from light. The time of incubation should be determined empirically but is usually about 5 min at 37°C or 10–15 min at room temperature. Using the lowest amount of dye compatible with the microscopic system available, there is usually no need to wash the medium prior to observation, as background fluorescence is low.

Two points are worth noting: (1) although Hoechst 33342 penetrates membranes of both live and dead cells, it takes longer for the dye to stain the nuclei of live cells. This slower rate determines how long the incubation should last. Toxicity takes an hour or more to develop depending on culture type; thus, depending on how long it takes the user to count cells, one can stain up to 8 wells at the same time without loss of efficacy. (2) Since PI does not penetrate live cells, PI by itself is not usually toxic to living cells so it can be left in the incubation medium over hours to days

such that cumulative death can be measured by returning to the same area sequentially. Thus, for example, PI was present continually in a hippocampal slice culture system to detect cell death after oxygen/glucose deprivation (20). However, it is important to note that UV illumination under the microscope does cause release of toxic species so there may be bystander toxic effects. Should this occur, one finds that all the cells under view turn pink.

2.2. Colorimetric Detection of Dead Cells Using Trypan Blue Staining

Trypan blue is commonly used to count the number of living cells sampled onto a haemocytometer before plating. However, it can also be used to count the number of necrotic cells in attached cultures using light microscopy, because it is not toxic to living cells. We have noted that if one is using serum in the medium (or >1% BSA), a low amount of trypan blue (<0.1%) can be left in the medium after observation because the protein eventually adsorbs it, so that the medium becomes clear again in a few hours. This depends on how much trypan blue and albumin are present and should be assayed in the absence of cells to see whether this absorption is sufficient to remove trypan blue for further study. The advantage of using this dye is that the same culture can be observed repeatedly following successive additions of trypan blue.

2.3. Live/Dead Staining Based on Enzymatic Activity

The two methods described above do not actively demonstrate cell viability, they only demonstrate plasma membrane permeability change of the cells. The following assay is based on the trapping of a membrane-permeant fluorescent dye in the cytoplasm of live cells due to the activity of esterases. When the integrity of the plasma membrane is compromised, esterase activity is low/absent and if the dye was preloaded into living cells that subsequently die due to an experiment, the dye quickly leaks out into the medium where it is vastly diluted, giving rise to unstained cells. Thus, unlike Hoechst 33342 that looks at the structure of the nuclei, this assay demonstrates cytoplasmic viability. There are many commercial varieties of dyes available. In an assay to measure neurite production, we used 2′,7′-bis-(2-carboxyethyl)-5-(and-6)-carboxyfluorescein, acetoxymethyl ester (BCECF-AM), which was originally developed as a pH indicator, and can be visualised with a "blue" excitation filter (ex/em ~490/520) (21). It should be noted, however, that esterase activity might be altered by culture conditions/additives so a test run is necessary to make sure the dye is properly trapped inside the cell.

Another popular measure of viability is the MTT assay. This is a colorimetric assay that measures the reduction of yellow 3-(4,5-dimethythiazol-2-yl)-2,5-diphenyl tetrazolium bromide (MTT) by mitochondrial succinate dehydrogenase. A concentration of 0.5 mg/mL is sufficient, which can be achieved by adding

a 10× stock made up in water directly to the medium. MTT enters mitochondria where it is reduced to an insoluble, coloured (dark purple) formazan product. At early time points, one can observe purple mitochondria, which, in time, produce crystalline rays that look like small crowns. Hence, observing MTT reduction in cells at an early time point is a quick way to distinguish live from dead cells under the light microscope. Other reactions may also cause reduction of MTT at later time points. As time elapses, the crystals fill the cell and it becomes hard to observe single cells in this fashion. A bulk measurement of the relative number of live cells (comparing between cultures after growth or treatments) can be produced by solubilising the formazan in DMSO (or isopropanol). A bright blue solution is produced in DMSO, whose intensity is measured spectrophotometrically. However, it should be noted that neuronal cultures contain many mitochondria in their neurites, which also reduce MTT. Thus, depending on the proportion of mitochondria in neurites and the amount of neurites relative to cell bodies, it may be hard to discern small differences in the amount of soluble formazan produced between cultures in which there is 20–30% cell body loss. Other tetrazolium derivatives that give rise to soluble formazan are also available. Stock MTT (5 mg/mL in water) is stable for over a year in the refrigerator as long as it is protected from light.

2.4. Other Things to Test

Necrosis is emerging as being important in several forms of neurodegeneration, such as those induced by excitotoxicity and traumatic injury, since there is a class of drugs (termed necrostatins) that inhibit this non-apoptotic form of cell death (reviewed in (22)). The target of this drug has been identified as a kinase named receptor interacting protein (RIP1) (23, 24). RIP1 is activated by TNF or FasL, which are also involved in some types of neuronal death (25, 26). Consistent with necrosis using a different, but defined, pathway to that of apoptosis, RIP1 can trigger necrosis without the intervening caspases (27). Interestingly, RIP1 has also been implicated in one instance of "autophagic cell death" in non-neuronal L929 cells, where death ascribed to autophagy was actually caused by degradation of the antioxidant protein catalase, following which emergent reactive oxygen species (ROS) caused profuse lipid peroxidation and necrosis (28). Originally, when death was surprisingly induced in living L929 cells simply by adding the pan-caspase inhibitor zVAD.FMK (thereby deactivating any potential apoptosis in the process), autophagic removal of catalase explained the death. However, now it appears that zVAD.FMK causes these cells to produce necrosis-inducing amounts of TNF (24), thus explaining the involvement of RIP1 and its downstream consequences. Indirectly, therefore, both aborted apoptosis and autophagy can lead to execution of death by necrosis.

Other than implication of RIP1, there are no definitive markers for the myriad forms necrosis (although there is rather a profusion in death terminology what with autophagic cell death, necroptosis (29), aponecrosis (30) and paraptosis (31), parthanatos (32) or unnamed (33)). Recently, a few late necrotic features that are shared between three types of necrotic stimuli (TNF, H_2O_2, Fas) were described including oxidative burst, mitochondrial membrane hyperpolarization, and lysosomal membrane permeabilisation. In each case, different signalling mechanisms preceded the common characteristics of death (34). A similar profusion of upstream pathways is likely to take place even when mitochondrial membrane permeabilisation is the common attribute upon which different forms of death in neurons converge (34, 35).

What is worth testing in vitro in case one wants to confirm some mechanisms underlying necrosis? First, one might use a pan-caspase inhibitor to eliminate the possibility that apoptosis is mediating the death. In all cases of apoptosis that we have studied, addition of Boc-Asp(*O*-methyl) fluoromethyl ketone (FMK) (or Q-VD-OPH, both inhibitors being rapidly cell-permeant in neurons and astrocytes with little evident toxicity) inhibits apoptotic manifestations due to caspases and greatly delays secondary necrosis as well (36). If cells began by inducing apoptosis, the delay in cell death will not last forever since loss of cytochrome c will compromise cellular ATP levels to the point where glycolysis can no longer sustain homeostasis. Application of the commercially available RIP1 inhibitor necrostatin1 and investigation of catalase levels could be next on the list. Inhibition of autophagic induction (crudely using 3-methyladenine (3MA), see Sect. 4) may be informative, although this assay is not completely diagnostic, especially as 3MA may inhibit some kinases involved in cell survival and cell death (37). Some forms of necrosis involve lysosomal proteases and cell acidification (at least in *C. elegans* (38, 39)). Investigating whether lysosomal numbers have changed, or whether lysosomal membranes have been permeabilized or altered their internal pH is quite easy using Lysotracker™ dyes or staining for lysosomal markers such as CD63 (40). Inhibition of autophagic flux is discussed in Sect. 4.

3. Apoptosis

As discussed, apoptosis is the most studied and perhaps best understood mode of cell death. Two apoptotic signalling pathways, the intrinsic (or mitochondrial) and extrinsic (or death receptor), converge upon the activation of caspases-3 and -7 which in turn cleave numerous protein substrates to initiate a complex molecular demolition process (see schemes in Figs. 2 and 3).

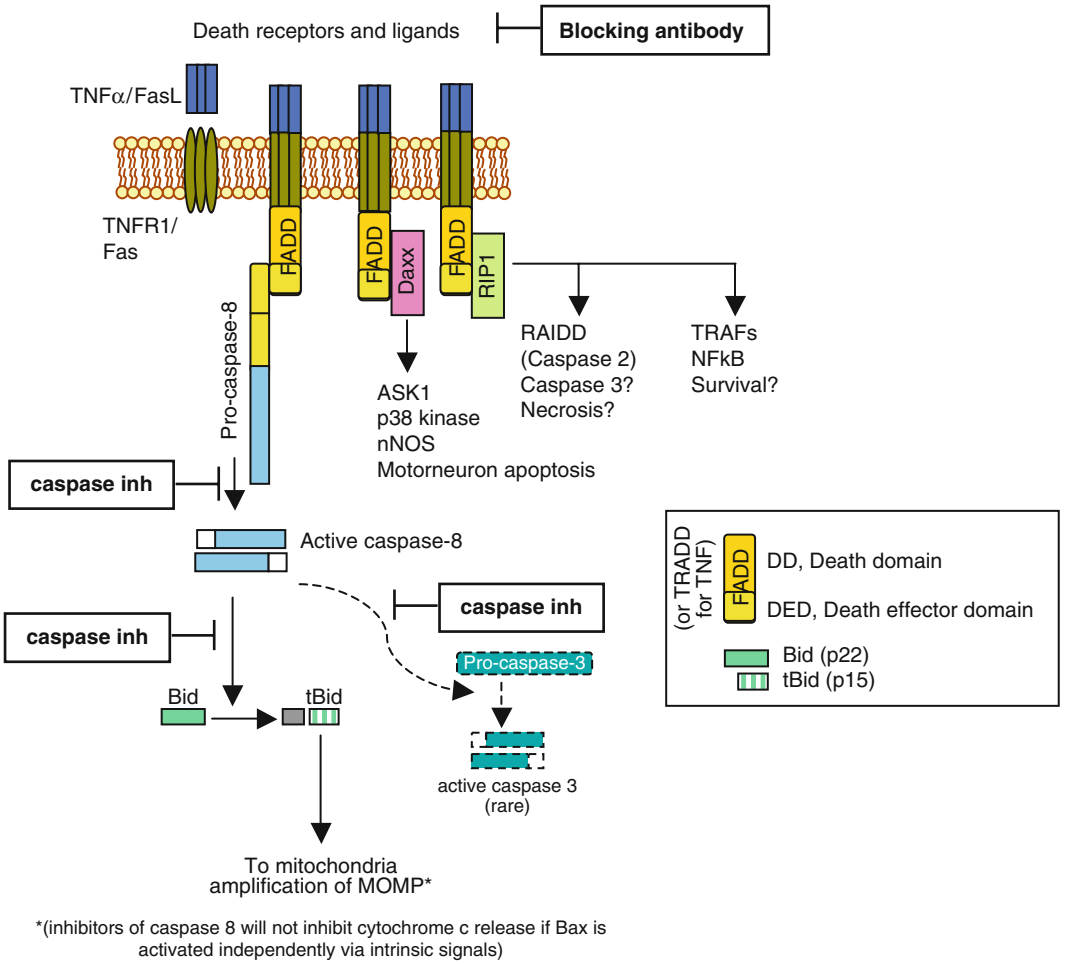

Fig. 2. Testing for apoptosis – the extrinsic pathway. Apoptosis is initiated via insults that activate Bax (known as the intrinsic pathway) or via death receptors (known as the extrinsic pathway). In most cell types, the death receptor pathway, which primarily activates caspase 8, links into the intrinsic pathway via cleavage of Bid to tBid, which amplifies the effects of Bax on MOMP. We found that in cortical neurons, tBid appeared after caspase-3 activation, and it is known that Bid can be activated by cleavage via calpains, so presence of tBid does not always indicate caspase 8 activation. Death receptors also activate many other pathways via recruitment of specific adaptors to the receptor death domains, some of which are indicated here. The Daxx-dependent pathway has been suggested to mediate developmental death of motor neurons (26). Also shown are other pathways implicated in necrosis and survival (though NFκB may mediate survival or death depending on cell context).

The extrinsic mode of cell death is mediated by the binding of an extracellular death ligand to a death receptor of the tumour necrosis factor (TNF) family, resulting in the assembly of a death-inducing signal complex (DISC) bringing inactive caspase-8 zymogens into close proximity to allow autoprocessing and activation (41). Active caspase-8 belongs to the sub-family of initiator caspases, so-called because they cleave and activate the

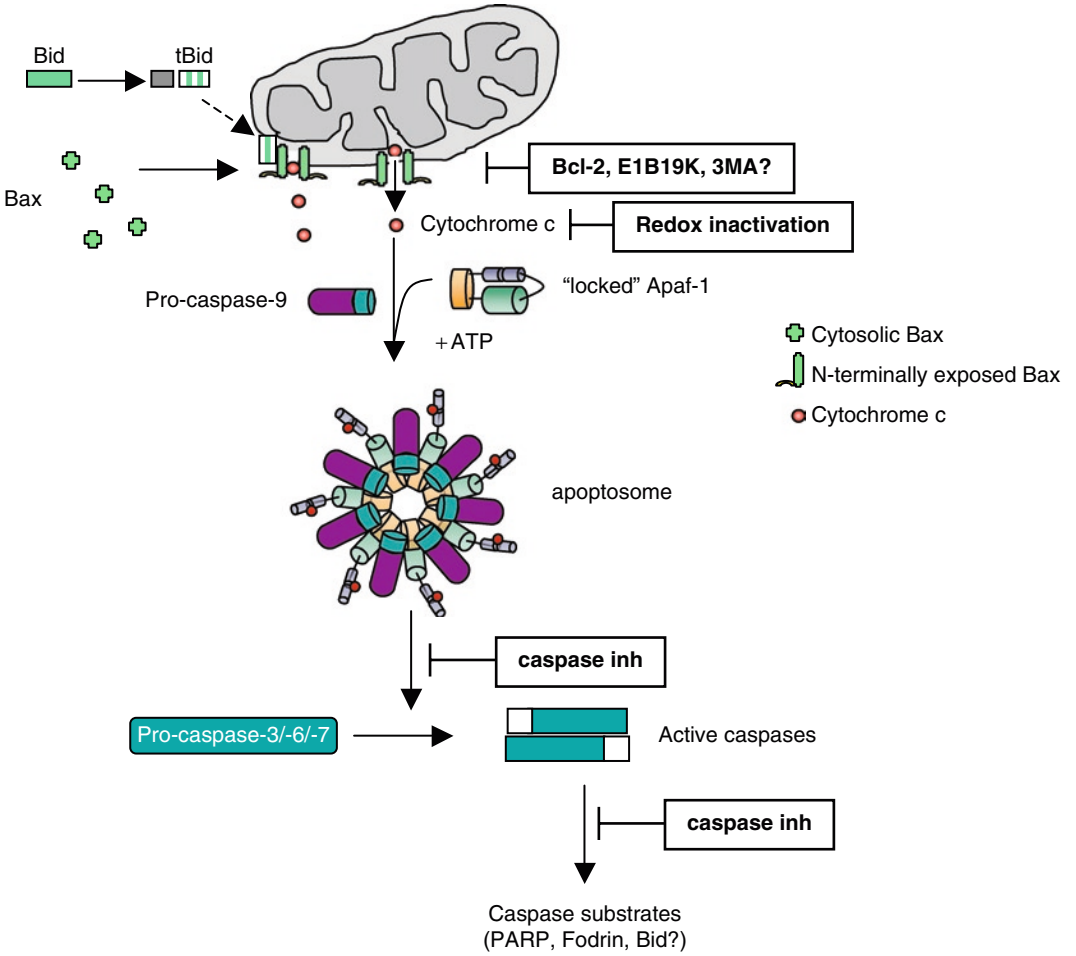

Fig. 3. Testing for apoptosis – the intrinsic pathway of apoptosis. The key steps that would indicate that apoptosis is occurring are: Bax activation (recruitment to mitochondria, exposure of the N-terminus, oligomerisation and MOMP), cytochrome c release, requirement for caspase activation, and cleavage of caspase substrates (only two of which are indicated; of interest, the substrates that are cleaved that are thought to lead to chromatin condensation and fragmentation are named ICAD (inhibitor of caspase activated DNase, also known as DFF45) and acinus). Other than caspase inhibitors (or expressing dominant negative forms of caspases that might show more specificity (25)), one should be able to interrupt this pathway by overexpressing anti-apoptotic members of the Bcl-2 family, or by keeping cytochrome c in its reduced form.

downstream executioner caspase-3. The intrinsic apoptotic pathway centres on the control of mitochondrial outer membrane permeabilisation (MOMP) mediated by the combined actions of pro- and anti-apoptotic Bcl-2 family proteins. MOMP results in the release of pro-apoptogenic proteins including cytochrome c from the mitochondrial intermembrane space to the cytosol. Once in the cytosol, cytochrome c complexes with apaf-1 to form a molecular scaffold termed the apoptosome upon which caspase-9 forms active dimers. Caspase-9, once activated, cleaves and activates caspase-3 and other caspases (caspase-6, -7).

The dissipation of the mitochondrial (inner) membrane potential ($\Delta\Psi m$), which often accompanies MOMP, along with the release of DNases EndoG and AIF from mitochondria, can result in the induction of caspase-independent death processes. Even in the absence of EndoG and AIF release, however, a necrotic phenotype will emerge. Thus, permeabilisation of the mitochondria represents an important commitment point in the death process and treatment of apoptotic neurons with pan-caspase inhibitors often only results in a temporary reprieve from their demise, except in the rare cases where cytochrome c can refill and repair the mitochondria (36). Extrinsic apoptotic pathways may also link into the intrinsic pathway, as the pro-apoptotic Bcl-2 protein Bid can be cleaved and activated by caspase-8 resulting in MOMP and amplification of the initial signal provided at the death receptor. This basic apoptotic framework provides one with multiple molecular steps to monitor the type and extent of apoptosis in neuronal/glial cultures.

Two important controls are needed: every experiment that studies apoptosis should include a control conducted in the presence of a pan-caspase inhibitor such as boc-aspartyl(*O*-methyl)-fluoromethylketone (BAF, ≤100 μM) or the more potent quinolyl-valyl-*O*-methylaspartyl-[-2,6-difluorophenoxy]-methyl ketone (Q-VD-OPh ≤50 μM). This is especially important when using caspase-dependent reporters such as nuclear morphology to distinguish apoptotic cells. A positive control is necessary as well. One of the most reliable types of inducers of apoptosis in neurons and glia are DNA damaging agents such as cytosine arabinoside or camptothecin (42, 43). Although postmitotic neurons do not replicate, signalling induced by DNA damaging agents dominate over those of survival factors and so will invariably induce apoptosis in living cultures without a huge overlap with necrosis. Staurosporine is also widely used but DNA damaging agents can be withdrawn to assess death commitment point, whereas we have never succeeded in removing staurosporine and rescuing cells.

3.1. Analysis of Nuclear Morphology

Observation of nuclear condensation and fragmentation during apoptosis is one of the easiest and fastest methods available to diagnose death by apoptosis. It does not by itself constitute proof of caspase-dependent processes unless a parallel assay is conducted in the presence of a pan-caspase inhibitor, which should prevent nuclear condensation. Apoptotic nuclear morphology can be quantified using the same dyes used to study necrosis – staining live cultures with Hoechst 33342 and using PI if one needs to record or exclude necrosis, as discussed above. Nuclei of apoptotic cells are fragmented or highly condensed and display bright blue fluorescence due to intense Hoechst 33342 staining of the packed DNA and/or increased uptake/retention of the dye (Fig. 4).

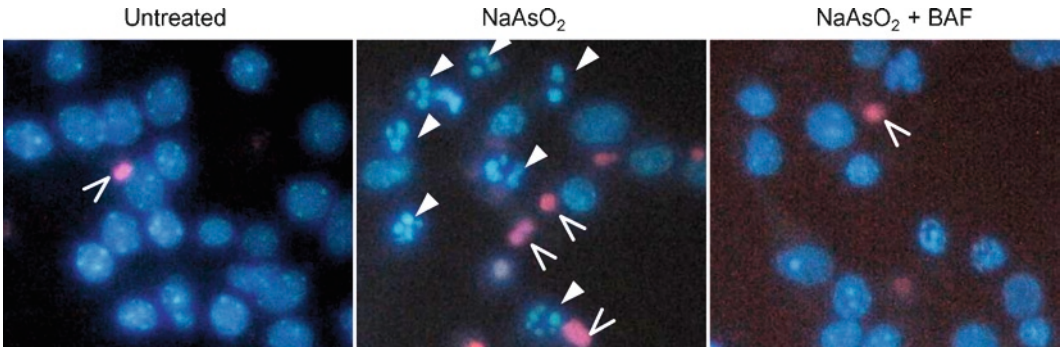

Fig. 4. Micrographs showing nuclear morphology of Hoechst 33342- and PI-stained DIV7 cortical neurons that were left either untreated (*left*) or treated with 6 μM sodium arsenite (*centre* and *right*) in the absence (*centre*) or presence (*right*) of 100 μM Boc-Asp-FMK (BAF). *Filled arrowheads* indicate condensed and fragmented apoptotic nuclei, V-shaped arrowheads indicate pink pyknotic nuclei.

At longer time points, if PI is included, condensed and fragmented nuclei will occasionally appear pink indicating that the plasma membrane is becoming permeable. This is due partly to the prolonged exposure to Hoechst, which can be toxic to neurons, and after ≥1 h of staining at room temperature, the cells start to lose plasma membrane integrity and can thus appear as necrotic during counts. It may be worth confirming DNA fragmentation using TUNEL or ISEL labelling, but neither labelling method constitutes proof that apoptosis occurred.

It should be noted that chromatin condensation and nuclear shrinkage and fragmentation occur downstream of MOMP and caspase activation, and thus their use as a measure of cell death may result in an underestimation of the number of cells undergoing apoptotic death. Hence, assays that measure death commitment point (such as removal of the death stimulus and addition of survival factors that rescue the cells) are useful although, as mentioned above, it is easier to replace a trophic factor (such as NGF) after its deprivation than ensure that a drug that was used to induce apoptosis was removed sufficiently so that survival can resume in uncommitted cells.

In mixed neuronal-glial cultures, with some experience and parallel immunocytochemical (ICC) studies using appropriate markers, it is possible to distinguish live neurons, astrocytes, and microglia from one another by examining nuclear morphology stained with Hoechst 33342. For example, in cultures of mixed cerebellar granule cultures, Hoechst 33342-stained neuronal nuclei appear round and speckled, astrocyte nuclei are larger, flatter, and exhibit relatively dim uniform fluorescence, while microglial nuclei often display an irregular "kidney bean" shape as well as existing in a slightly different plane of focus. Thus, cell staining with Hoechst 33342 can provide a more comprehensive view of

how individual cell types within a mixed neuronal–glial culture react in response to a stimulus, although this is only possible when using live cells, as nuclear morphology is often altered following fixation processes. Once a nucleus has condensed or fragmented, it is not possible to tell from its morphology what cell type it corresponds to.

3.2. Monitoring Bax activation

Bax and Bak are functionally redundant pro-apoptotic Bcl-2 family members absolutely required for the induction of MOMP and apoptosis via the mitochondrial pathway. In neurons, full length Bak does not seem to be expressed and thus apoptotic stimuli converge upon activation of Bax as the sole means of inducing MOMP and subsequent apoptosis (1, 44–46). Work on the peripheral nervous system and motoneuron cell death has established that the pivotal player in neuronal apoptosis during development is Bax. Hence Bax KO mice and Bax KO neurons in culture show delays in cell death of sympathetic, DRG, and motoneurons, and Bcl-2 transgenesis (which sequesters Bax) protects against these forms of death (47). In the cerebellum, in the case of non-apoptotic Purkinje cell death in the Lurcher mouse due to intrinsic gain of function of the glutamate receptor GluR2δ, the death of the majority of granule neurons that depend on the Purkinje cells for their trophic support was prevented in the $Bax^{-/-}$ mouse as well (48). However, it is interesting to note that there are many populations of neurons that die even during development whose mechanism of death is apoptotic but does not just rely solely on Bax (47).

In healthy primary cells, the majority of Bax molecules exist as cytosolic monomers in which the N-terminal alpha helix α1 and the C-terminal α9 are constrained and embedded within the protein structure. Upon receipt of an apoptotic stimulus both the α1 and α9 helices become exposed. Exposure of the C-terminal α9 mediates targeting of Bax to the outer mitochondrial membrane. Following mitochondrial translocation, Bax projects its N terminus and forms homo-oligomers that result in MOMP and cytochrome c release (49). A number of experimental methods have been developed which allow monitoring of these events.

Antibodies directed against the exposed N-terminal α1 helix are commercially available, including those developed in R Youle's lab (50) (6A7 (human, mouse), 2D2 (human) and 1D1 (rat)). There are also some polyclonal antibodies that work across species. Because non-ionic detergents may alter the conformation of Bax from the soluble to the N-terminally exposed form (50), it is safest to use an ionic detergent such as CHAPS (0.1%) to permeabilise paraformaldehyde-fixed cells prior to immunostaining. We also use CHAPS in all the antibody solutions as a precautionary measure. Tween-20 may also be used but Triton X-100 should be avoided. Antibodies should show little staining in unstimulated

cells, whereas intense mitochondrially localised punctate staining will be observed in apoptotic cells. Mitochondrial localisation can be verified using antibodies against stable proteins (such as ATP synthase β, HSP 60, prohibitin). It is also possible to preload dyes that enter the mitochondria in live cells and retain their fluorescence even in dying cells after fixation (some dyes of the MitoTracker® series, see Sect. 3.3.2). Immunostaining for N-terminally exposed Bax is a good assay because it can be correlated in many cases with the appearance of apoptotic nuclear morphology, for example (42).

Other assays that can be used to monitor the translocation of endogenous Bax from the cytosol to the mitochondria include immunoblot analysis of crude subcellular fractions containing mitochondria (often called heavy membranes) and the post-mitochondrial supernatant. This assay works best when plenty of cells are available but it works even if the cultures are not very dense (51). Immunoprecipitation of Bax using an N-terminally directed antibody (if there is enough material) followed by probing the blot with a total Bax antibody is also possible. Finally, fusion of GFP to the N terminus of Bax and subsequent expression of this fusion protein in cells allows monitoring of Bax translocation to the mitochondria in live cells via time lapse fluorescence microscopy (52). Care must be taken to optimise expression levels of such a construct, as high levels of GFP-Bax expression will induce MOMP and apoptosis before the apoptotic stimulus is applied. In addition, controls should always be included as the base-line ratio of cells displaying diffuse GFP-Bax vs mitochondrial GFP-Bax staining will likely differ somewhat between experiments.

It is important to note that in general, Bax translocation to mitochondria is a caspase-independent event, and so should occur in caspase-inhibited cells. This control helps define the sequence of steps and corroborate that classical apoptosis has occurred. Another way of showing that Bax induced apoptosis is to prevent its translocation by expression of anti-apoptotic members of the Bcl-2 family. A particularly strong inhibitor is the adenoviral Bcl-2 homologue E1B19K (53), though it is rarely used.

3.3. Monitoring MOMP and Cytochrome c Release

3.3.1. Cytochrome c Release

Cytochrome c release may be monitored using an identical ICC protocol to that described for Bax above, employing an appropriate anti-cytochrome c antibody. Note that antibodies for ICC detection of cytochrome c are not compatible with those used to detect cytochrome c on immunoblots (and vice versa). In healthy neurons, cytochrome c localized to mitochondria displays a punctate staining pattern. Upon MOMP induction and release from the mitochondrial intermembrane space into the cytosol, cytochrome c staining becomes diffuse and in neurons often disappears altogether (36, 91). It is also possible to detect cytochrome

c release from mitochondria biochemically using the subcellular fractionation protocol described above for Bax and detection of cytochrome c by immunoblot (released cytochrome c will appear in the supernatant). Cytochrome c-GFP can also be used to follow release in live cells (54). Of note, evidence of cytochrome c release alone does not represent proof that a neuron is destined to die by caspase-dependent apoptosis. In neurons, for example, pro-survival signals provided by trophic factors and synaptic activity can lower susceptibility to cytochrome c release by increasing the activity of endogenous caspase inhibitors such as XIAP or by lowering the amount of apoptosome components apaf-1 (55) and caspase-9 (91). Furthermore, there are forms of death where there is release of cytochrome c but no detectable caspase activation (5), or caspase activation but no release of cytochrome c (25). It has been proposed that cytochrome c needs to be oxidised to activate apaf-1 and this may be a good point of intervention to reveal non-apoptotic consequences of unregulated MOMP (56, 57). Thus, one should also seek to demonstrate activation of caspases and their requirement for cell death as a proof of caspase-dependent apoptosis.

3.3.2. Loss of Mitochondrial Membrane Potential (ΔΨm)

Mitochondrial membrane potential is often dissipated as a result of Bax-mediated MOMP and itself represents an important death commitment step during apoptosis. However, ΔΨm is also dissipated in nonapoptotic cells by drugs or ROS so this assay in itself does not constitute proof that apoptosis occurred, though it is more likely if Bax was translocated to the mitochondria. A number of fluorescent dyes are available allowing one to monitor ΔΨm. The dyes JC-1 (5,5′,6,6′-tetrachloro-1,1′,3,3′-tetraethylbenzimidazolylcarbocyanine iodide) and TMRM (tetramethylrhodamine methyl ester) are relatively non-toxic reversible dyes used to probe ΔΨm. JC-1 exists as a green-fluorescent monomer in mitochondria with low (polarized) ΔΨm (the normal situation in live cells) but forms red fluorescing aggregates in mitochondria with high (depolarized) ΔΨm. The green monomeric and red aggregated forms may be separately detected using optical filters designed for fluorescein and tetramethyrhodamine detection, respectively. Quantitive assessment of ΔΨm is extremely difficult using reversible dyes because these dyes load into mitochondria depending on both the plasma membrane potential and the mitochondrial membrane potential (58), and plasma membrane potential can change depending on drug treatment. Certain MitoTracker® dyes contain a thiol-reactive chloromethyl moiety that allows retention of the dye in mitochondria following fixation with paraformaldehyde and subsequent membrane permeabilisation as for ICC studies. Importantly, MitoTrackers® will not be taken up by mitochondria in which ΔΨm is dissipated. These agents are therefore used at the end-point

of the assay, where the number of cells that contain MitoTracker® is scored and presented as a percentage of control cells that were loaded with the dye. Preliminary assays should assess the lowest concentration of MitoTracker® (50–500 nM) and time of loading that can be visualised since overloading mitochondria causes toxicity depending on cell type.

3.4. Measuring Caspase Activation

All caspases are produced as inactive zymogens. Cleavage of executioner caspases (caspase-3, -7 and -6) at an internal aspartate residue by an upstream initiator caspase results in the production of catalytically active mature caspase homodimers composed of two monomers each comprising a large and small subunit (59). Once activated, executioner caspases (in particular caspase-3) mediate the cleavage of a plethora of target proteins, mediating the systematic disassembly of cells undergoing apoptosis (60). It is possible to detect caspase-3 activation by ICC methods using antibodies raised against the processed and active form of caspase-3. Cells in which caspase-3 has been cleaved and activated should display a robust increase in fluorescent signal throughout the cytoplasm. Anti-active caspase-3 antibodies are not exclusive to the cleaved form, they only have a higher affinity; so if total caspase-3 is very high, there may be positive staining in non-apoptotic cells. The best test for the presence of active caspase-3 due to apoptosis is to inhibit its production with pan-caspase inhibitors that will inhibit caspase-9.

It is also possible to monitor cleavage and activation of caspase-3, caspase-8, and caspase-9 through immunoblotting, by detecting a decrease in the amount of the pro-caspase zymogen (~35–40 kDa) and appearance of the lower molecular weight cleavage products (~15–18 kDa, the other subunit being ~12 kDa). In practice, so much protein has to be loaded to observe a cleaved caspase-3 that it is hard to observe a decrease in pro-caspase-3. It should also be noted that in some instances this approach is less useful in terms of monitoring caspase-9 activation as its cleavage is not required for activation, and appearance of cleavage products can be hard to detect due to their scarcity. Pro-caspase-9 can autoprocess in the apoptosome to give rise to shorter species that appear at 37 and 39 kDa.

It is also possible to detect caspase activation by monitoring the cleavage of known caspase substrates by immunoblotting, for example, cleavage of poly(ADP-ribose)polymerase (PARP) (61) by caspase-3 or α-fodrin. It is notable that both the substrates, along with many others, can also be cleaved by calpains which can be activated during both apoptotic and necrotic death in neurons; thus caution should be exercised in verifying that cleavage products are of the weight corresponding to caspase cleavage, and that cleavage is prevented by treatment of the neurons with a pan-caspase inhibitor (62).

Caspase activity can also be measured biochemically using fluorogenic or colorimetric caspase substrates that generate a signal once cleaved by caspases in vitro (61). Note it is important to include a control in which a pan-caspase inhibitor such as non-*O*-methylated Q-VD-OPh is added to parallel samples to rule out false-positive signals due to non-specific degradation. Note that the *O*-methylated forms of caspase inhibitors, modified so that the peptides with acidic groups will penetrate cells, have no inhibitory activity towards caspases. For use in vitro, unmodified inhibitors should be purchased or the O-methylated groups can be removed by mild hydrolysis under basic conditions. In cells, these groups are removed by esterase activity. Hence, aldehyde (-CHO) carrying inhibitors are used preferentially for biochemical assays. A number of fluorogenic or colorimetric peptide substrates are commercially available which are claimed to allow measurement of the activity of specific caspases. These fluorogenic substrates differ in the peptide sequence used, based on substrate specificity profiles. Thus, use of various fluorogenic caspase substrates with the goal of diagnosing the activity of individual caspases should be approached with extreme caution (63). Similarly, the use of supposed caspase-specific inhibitors (based on the same peptide sequences as those used in the fluorogenic substrates) to determine the contribution of individual caspases in apoptotic models should be performed in the knowledge that the majority show very little specificity between different caspase members (63, 64).

3.5. Monitoring PS Exposure

Apoptosis results in exposure of various "eat-me" signals at the cell surface, which direct the phagocytosis and subsequent destruction of the cellular corpse by neighbouring cells or professional phagocytes. Of the described eat-me signals, phosphatidylserine (PS) exposure is the best characterised, and molecular tools for study of this process are readily available commercially. In healthy cells PS is retained on the inner leaflet of the plasma membrane by the ATP-driven action of the aminophospholipid translocase. Frequently during the early stages of apoptosis, the asymmetrical distribution of PS is compromised resulting in the exposure of detectable amounts of PS at the cell surface. A variety of proteins bind to PS with a high specificity including Annexin V, which, when conjugated to fluorescent moieties, can be used to monitor exposure of PS in live cells. Note that Annexin V requires calcium in the medium in order to bind to PS. PS exposure is a commonly used method for detecting apoptotic death, but one should be aware of several caveats concerning circumstances of PS exposure, in particular when using neuronal systems. Necrotic cells may also expose PS, and PS exposure can be induced in neuronal cells in the absence of death or other apoptotic hallmarks by exposure to sublethal doses of amyloid-β peptide, oxidising agents, or nitrosative stress as well as during excitotoxic stress-induced

death (65–68). Thus, demonstration of PS exposure alone is insufficient proof of apoptosis in neuronal cell types without further controls demonstrating the requirement of downstream apoptotic components (e.g., inhibition by caspase inhibitors or overexpression of anti-apoptotic Bcl-2).

4. Autophagy

Autophagy has been the focus of many recent studies, especially those devoted to the study of degenerative diseases (69). What is notable is that diseases or injury may recruit novel death pathways that are not part of normal developmental death. For example, Oppeneheim and colleagues (70) found that the absence of Apaf-1 (in apaf-1 KO mice) instigated a non-apoptotic death in postmitotic neurons that was inhibited by crossing the animals with Atg7-KO animals. However, death of this neuronal population in wildtype animals was not inhibited by Atg7-KO.

Autophagy occurs via three methods: macroautophagy, microautophagy, and chaperone-mediated autophagy (CMA) (71, 72). Most cell deaths have been linked to macroautophagy, the focus here, although some thoughts about CMA will be addressed in the end. The framework for demonstrating macroautophagy (referred to here as autophagy) in action is now well defined (16), but showing that autophagy is occurring productively is still a major challenge, especially in the CNS (see (69) for a comprehensive analysis of autophagy in the nervous system). There are two assays that are the key to demonstrating that productive autophagy is occurring in response to treatment in cells: (1) inhibition of autophagosome formation, and (2) inhibition of autophagosome degradation. In the former, no new autophagosomes should be observed, and in the latter, autophagosomes should accumulate in stimulated cells above the number per cell that accumulate in unstimulated cells. Two adjunct assays are necessary: (a) EM evidence for autophagosome formation, and (b) a flux assay showing that increased protein degradation occurs during steady state autophagy induction. The following sections describe how these assays can be performed.

4.1. LC3

Tracing the location of Atg8/MAP1B-LC3 (named LC3 hereafter), and its lipidation by phosphatidylethanolamine (PtdEth) have been the methods of choice for demonstrating the activation of autophagosome formation: LC3 becomes associated with autophagosomes (via its covalent PtdEth tail) when autophagy is induced, and is largely digested inside lysosomes when the autophagic process reaches completion (see scheme in Fig. 5). Hence, if one inhibits autophagosome formation, LC3 will not be modified and will remain diffuse in the cytoplasm

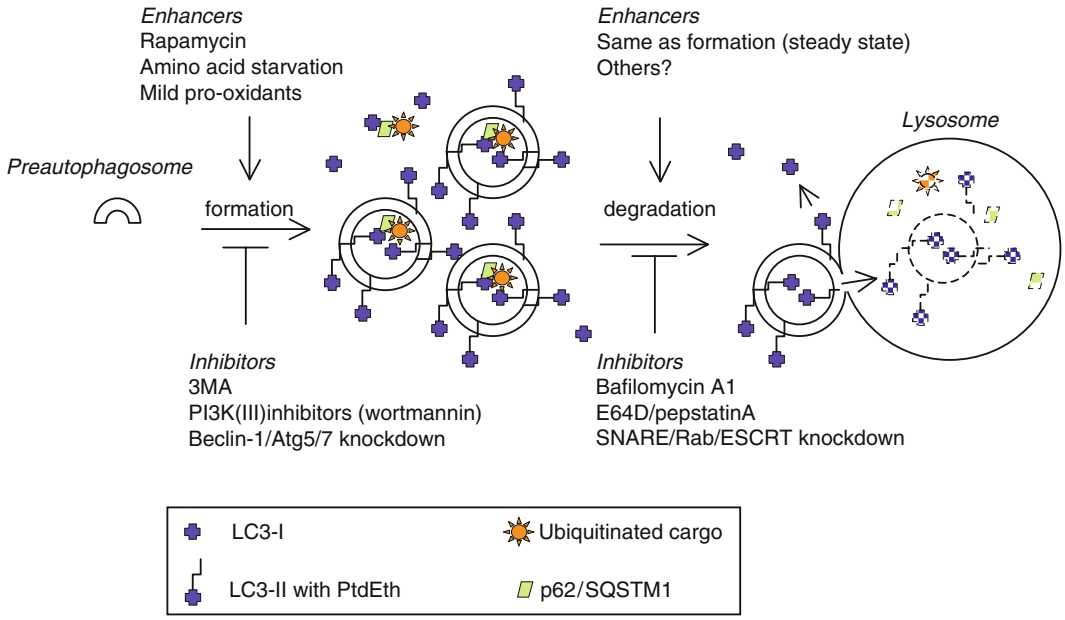

Fig. 5. Testing for autophagy. Formation and degradation of autophagosomes and their cargos. An autophagosome is expected to carry lipidated LC3-II, and depending on the cell type, it should deliver LC3, p62, and an associated misfolded ubiquitinated ligand to the lysosome for destruction. Note that LC3-II can also revert to LC3-I prior to fusion with lysosomes through the activity of the Atg4 that also cleaved the C terminus of LC3 and coupled the lipid to it.

despite activation of autophagy, whereas when the autophagic processing is inhibited, LC3/PtdEth-positive puncta will accumulate. In SDS-PAGE, LC3/PtdEth runs faster than unmodified LC3 and the same occurs for GFP-LC3 transfected into cells (40). Using immunoblotting for LC3, the prediction from the two assays is that in the former there will be no increase in LC3/PtdEth while in the latter LC3/PtdEth will accumulate. Tracing the amount of LC3/PtdEth as evidence for enhanced autophagy is precarious without using these two inhibition modes, as LC3/PtdEth may accumulate or be even lower than basal LC3/PtdEth itself depending on the rate of formation and degradation of autophagosomes (73).

Although there are two other molecules that are similarly modified by PtdEth (GABARAP1 and GATE-16), their widespread occurrence is less well documented. In mouse CNS neurons, experience suggests that the present commercial antibodies against LC3 appear to be generally poor at immunocytochemical detection, although there is a higher success rate in rat brain tissue, and some groups have produced good discriminating antibodies for mouse studies (70, 74). In culture, the advantage is that one can use biochemical methods to complement the immunocytochemistry, such as transfecting GFP-LC3 (or other derivatives of LC3) but it is important to note that these are not completely complementary methods.

4.2. Inhibition of Autophagy at the Formation and Degradation Steps

What kind of autophagy inducers, and inhibitors, are available? The key steps and markers have been set by what happens in cells and tissues during starvation. In the brain, however, systemic starvation does not appear to induce a lot of autophagy (69). Rapamycin has been used as an autophagy inducer in vitro but its efficacy again depends on the cell type (75). Expression of Beclin 1 has also been used as an inducer of autophagy, but its efficacy may depend on how much Beclin 1 is already expressed (76, 77). The best approach is to initiate starvation by incubating cells in a balanced salt solution (buffered by sodium bicarbonate) lacking glucose and amino acids and/or adding rapamycin (perhaps together with starvation) for a few hours in the first instance and following a time course of autophagic activation.

To prevent autophagosome formation, 3-methyladenine has been most widely used. While this drug is efficacious in blocking autophagosome formation, its actions are not exclusive to inhibition of the PtdIns 3-kinase Type III subunit of Beclin-1. It targets many other cellular processes that are implicated in autophagy as well as those implicated in survival (Akt) and death (JNK, mitochondrial permeability transition pore), at least in some neurons (37, 78). Another possibility is to express Atg4C47A, an inactive mutant form of Atg4 (the enzyme that cleaves the C terminus of LC3 and also removes the LC3 from the surface of the autophago/lysosome). The protein seems to prohibit LC3 lipidation and targeting to autophagosomes very effectively (79).

Until now, inhibition of autophagy by genetic ablation of the key genes Atg5 and Atg7, which are part of the LC3/PtdEth lipid conjugating pathway, has been thought to be definitive in inhibiting macroautophagy genetically (80, 81). As far as one can tell, there are no LC3/PtdEth-positive autophagosomes in Atg5- or Atg7-null cells. However, a recent paper reports on autophagy occurring in Atg5- and Atg7- null cells independent of LC3 modification (82). Hence, even this critical step can be bypassed in response to some insults or during reticulocyte maturation, making a definitive proof of autophagic induction, let alone autophagic activity, extremely difficult. It is interesting to note that Beclin-1 was still implicated in the Atg5/7-independent autophagy (82), thus suggesting that perhaps gene silencing of Beclin-1 is the target of choice.

How would one block lysosomal degradation? There are very good inhibitors of key lysosomal proteases that have been used extensively to inhibit this step. A common combination is to use E64d and pepstatin A (73). These target a subset of proteases in the lysosome and yet are very efficacious in blocking degradation of LC3/PtdEth (and LC3 itself). Another very specific inhibitor is Bafilomycin A1 (83), an inhibitor of vacuolar H+ ATPase, without which lysosomes cannot acidify their contents. In neurons this drug will inhibit other vesicular H+ ATPases, however, and it

can be quite toxic even at concentrations below 100 nM; so testing its toxicity/efficacy dose ratio in initial assays is important. Bafilomycin A1 has been claimed to inhibit fusion of lysosomes with autophagosomes but the evidence for this is scant (84).

Having used inhibitors of autophagosome formation and degradation it is important to analyse the veracity of autophagosome increases deduced by inspecting cells under the electron microscope. There are good anti-GFP antibodies that can be used for immuno-EM, if GFP-LC3 was used for indicating autophagy. Quantitative data are essential (16).

4.3. Autophagic Flux

The last vexing question is that of measuring autophagic flux. In general terms, it has been customary to label a random pool of proteins in cells metabolically, wash away any free label and chase short-lived proteins by incubating the cells over 1–2 h (85, 86). Then, one measures the amount of labelled amino acids/peptides that are released from cells that cannot be precipitated with trichloroacteic acid (TCA), and expresses this as a percentage of total label incorporated (TCA precipitated + non-precipitated). Previously, low-level labelling with ^{14}C amino acids or [^{35}S]methioinine has been used as tracers (85, 86). Ideally, however, one would want to follow a protein that is known to be degraded via the autophagosomal pathway. p62/SQSTM1 (hereafter p62) is one such possible protein. p62 is a polyubiquitin binding protein that also binds to LC3-PtdEth on autophagosomes (69). In cells in which p62 is a good reporter of autophagy, p62 accumulates when the autophagosomal degradation is blocked and is lower when autophagic flux is enhanced. Of note, crossing Atg7-KO mice with p62-KO mice, ameliorated the accumulation of ubiquitinated inclusions induced by the absence of Atg7, but did not prevent overall neuronal death or the appearance of behavioural deficits found in $Atg5^{Fl/Fl}$:nes-cre mice (87). Detailed methodology for studying p62 can be found in Reference (88).

4.4. Other Comments

The cardinal question that stumps most investigations is whether the autophagosomes that accumulate are there due to an activation of autophagy or a block in degradation (or both). Unlike genes that will block autophagosome production (like absence of Beclin-1 or Atg5/7), there are no genes that will specifically prevent resolution of autophagosomes. Perturbation of lysosomal function or autophagosome trafficking will perturb the balance between vesicular trafficking generally. Indeed, LC3-positive vesicles can be found colocalising with markers for early and late endosomes (40), as well as lysosomes. There may be a possibility to exclude CMA, though, as in this mechanism, the specific lysosomal receptor Lamp2a, is responsible for the delivery of cargo to the lysosomes (72, 89). Here also, however, perturbation of this receptor may lead to an accumulation of proteins that cause cell

toxicity. Additionally, when studying protein degradation, it is important to exclude the possibility that proteasomes are responsible for the degradation observed (although there may be confounding relationships between proteasome activity and autophagy due to a shared role of p62 in both mechanisms, especially if one or the other is perturbed (90)). Altogether, the gap between our understanding of autophagy and its involvement in cell death is still immense. Work in this area requires fastidious testing and openness to other interpretations.

References

1. Kuan CY, Roth KA, Flavell RA, Rakic P (2000) Mechanisms of programmed cell death in the developing brain. Trends Neurosci 23:291–297
2. Raff MC, Barres BA, Burne JF, Coles HS, Ishizaki Y, Jacobson MD (1994) Programmed cell death and the control of cell survival. Philos Trans R Soc Lond 345:265–268
3. Barres BA, Jacobson MD, Schmid R, Sendtner M, Raff MC (1993) Does oligodendrocyte survival depend on axons? Curr Biol 3:489–497
4. Clarke PG (1990) Developmental cell death: morphological diversity and multiple mechanisms. Anat Embryol 181:195–213
5. King MA, Goemans CG, Hafiz F, Prehn JH, Wyttenbach A, Tolkovsky AM (2008) Cytoplasmic inclusions of Htt exon1 containing an expanded polyglutamine tract suppress execution of apoptosis in sympathetic neurons. J Neurosci 28:14401–14415
6. Zhou W, Hurlbert MS, Schaack J, Prasad KN, Freed CR (2000) Overexpression of human alpha-synuclein causes dopamine neuron death in rat primary culture and immortalized mesencephalon-derived cells. Brain Res 866:33–43
7. Yung HW, Bal-Price AK, Brown GC, Tolkovsky AM (2004) Nitric oxide-induced cell death of cerebrocortical murine astrocytes is mediated through p53- and Bax-dependent pathways. J Neurochem 89:812–821
8. Debnath J, Baehrecke EH, Kroemer G (2005) Does autophagy contribute to cell death? Autophagy 1:66–74
9. Komatsu M, Waguri S, Chiba T, Murata S, Iwata J, Tanida I, Ueno T, Koike M, Uchiyama Y, Kominami E, Tanaka K (2006) Loss of autophagy in the central nervous system causes neurodegeneration in mice. Nature 441:880–884
10. Koike M, Shibata M, Tadakoshi M, Gotoh K, Komatsu M, Waguri S, Kawahara N, Kuida K, Nagata S, Kominami E, Tanaka K, Uchiyama Y (2008) Inhibition of autophagy prevents hippocampal pyramidal neuron death after hypoxic-ischemic injury. Am J Pathol 172:454–469
11. Hara T, Nakamura K, Matsui M, Yamamoto A, Nakahara Y, Suzuki-Migishima R, Yokoyama M, Mishima K, Saito I, Okano H, Mizushima N (2006) Suppression of basal autophagy in neural cells causes neurodegenerative disease in mice. Nature 441:885–889
12. Komatsu M, Wang QJ, Holstein GR, Friedrich VL Jr, Iwata J, Kominami E, Chait BT, Tanaka K, Yue Z (2007) Essential role for autophagy protein Atg7 in the maintenance of axonal homeostasis and the prevention of axonal degeneration. Proc Natl Acad Sci USA 104:14489–14494
13. Nagley P, Higgins GC, Atkin JD (1802) and Beart. P. M. Multifaceted deaths orchestrated by mitochondria in neurones, Biochimica et biophysica acta, pp 167–185
14. Ilieva H, Polymenidou M, Cleveland DW (2009) Non-cell autonomous toxicity in neurodegenerative disorders: ALS and beyond. J Cell Biol 187:761–772
15. Galluzzi L, Aaronson SA, Abrams J, Alnemri ES, Andrews DW, Baehrecke EH, Bazan NG, Blagosklonny MV, Blomgren K, Borner C, Bredesen DE, Brenner C, Castedo M, Cidlowski JA, Ciechanover A, Cohen GM, De Laurenzi V, De Maria R, Deshmukh M, Dynlacht BD, El-Deiry WS, Flavell RA, Fulda S, Garrido C, Golstein P, Gougeon ML, Green DR, Gronemeyer H, Hajnoczky G, Hardwick JM, Hengartner MO, Ichijo H, Jaattela M, Kepp O, Kimchi A, Klionsky DJ, Knight RA, Kornbluth S, Kumar S, Levine B, Lipton SA, Lugli E, Madeo F, Malomi W, Marine JC, Martin SJ, Medema JP, Mehlen P, Melino G, Moll UM, Morselli E, Nagata S, Nicholson DW, Nicotera P, Nunez G, Oren M, Penninger J, Pervaiz S, Peter ME,

Piacentini M, Prehn JH, Puthalakath H, Rabinovich GA, Rizzuto R, Rodrigues CM, Rubinsztein DC, Rudel T, Scorrano L, Simon HU, Steller H, Tschopp J, Tsujimoto Y, Vandenabeele P, Vitale I, Vousden KH, Youle RJ, Yuan J, Zhivotovsky B, Kroemer G (2009) Guidelines for the use and interpretation of assays for monitoring cell death in higher eukaryotes. Cell Death Differ 16:1093–1107

16. Klionsky DJ, Abeliovich H, Agostinis P, Agrawal DK, Aliev G, Askew DS, Baba M, Baehrecke EH, Bahr BA, Ballabio A, Bamber BA, Bassham DC, Bergamini E, Bi X, Biard-Piechaczyk M, Blum JS, Bredesen DE, Brodsky JL, Brumell JH, Brunk UT, Bursch W, Camougrand N, Cebollero E, Cecconi F, Chen Y, Chin LS, Choi A, Chu CT, Chung J, Clarke PG, Clark RS, Clarke SG, Clave C, Cleveland JL, Codogno P, Colombo MI, Coto-Montes A, Cregg JM, Cuervo AM, Debnath J, Demarchi F, Dennis PB, Dennis PA, Deretic V, Devenish RJ, Di Sano F, Dice JF, Difiglia M, Dinesh-Kumar S, Distelhorst CW, Djavaheri-Mergny M, Dorsey FC, Droge W, Dron M, Dunn WA Jr, Duszenko M, Eissa NT, Elazar Z, Esclatine A, Eskelinen EL, Fesus L, Finley KD, Fuentes JM, Fueyo J, Fujisaki K, Galliot B, Gao FB, Gewirtz DA, Gibson SB, Gohla A, Goldberg AL, Gonzalez R, Gonzalez-Estevez C, Gorski S, Gottlieb RA, Haussinger D, He YW, Heidenreich K, Hill JA, Hoyer-Hansen M, Hu X, Huang WP, Iwasaki A, Jaattela M, Jackson WT, Jiang X, Jin S, Johansen T, Jung JU, Kadowaki M, Kang C, Kelekar A, Kessel DH, Kiel JA, Kim HP, Kimchi A, Kinsella TJ, Kiselyov K, Kitamoto K, Knecht E, Komatsu M, Kominami E, Kondo S, Kovacs AL, Kroemer G, Kuan CY, Kumar R, Kundu M, Landry J, Laporte M, Le W, Lei HY, Lenardo MJ, Levine B, Lieberman A, Lim KL, Lin FC, Liou W, Liu LF, Lopez-Berestein G, Lopez-Otin C, Lu B, Macleod KF, Malorni W, Martinet W, Matsuoka K, Mautner J, Meijer AJ, Melendez A, Michels P, Miotto G, Mistiaen WP, Mizushima N, Mograbi B, Monastyrska I, Moore MN, Moreira PI, Moriyasu Y, Motyl T, Munz C, Murphy LO, Naqvi NI, Neufeld TP, Nishino I, Nixon RA, Noda T, Nurnberg B, Ogawa M, Oleinick NL, Olsen LJ, Ozpolat B, Paglin S, Palmer GE, Papassideri I, Parkes M, Perlmutter DH, Perry G, Piacentini M, Pinkas-Kramarski R, Prescott M, Proikas-Cezanne T, Raben N, Rami A, Reggiori F, Rohrer B, Rubinsztein DC, Ryan KM, Sadoshima J, Sakagami H, Sakai Y, Sandri M, Sasakawa C, Sass M, Schneider C, Seglen PO, Seleverstov O, Settleman J, Shacka JJ, Shapiro IM, Sibirny A, Silva-Zacarin EC, Simon HU, Simone C, Simonsen A, Smith MA, Spanel-Borowski K, Srinivas V, Steeves M, Stenmark H, Stromhaug PE, Subauste CS, Sugimoto S, Sulzer D, Suzuki T, Swanson MS, Tabas I, Takeshita F, Talbot NJ, Talloczy Z, Tanaka K, Tanaka K, Tanida I, Taylor GS, Taylor JP, Terman A, Tettamanti G, Thompson CB, Thumm M, Tolkovsky AM, Tooze SA, Truant R, Tumanovska LV, Uchiyama Y, Ueno T, Uzcategui NL, van der Klei I, Vaquero EC, Vellai T, Vogel MW, Wang HG, Webster P, Wiley JW, Xi Z, Xiao G, Yahalom J, Yang JM, Yap G, Yin XM, Yoshimori T, Yu L, Yue Z, Yuzaki M, Zabirnyk O, Zheng X, Zhu X, Deter RL (2008) Guidelines for the use and interpretation of assays for monitoring autophagy in higher eukaryotes. Autophagy 4:151–175

17. Dekker LV, De Graan PN, Pijnappel P, Oestreicher AB, Gispen WH (1991) Noradrenaline release from streptolysin O-permeated rat cortical synaptosomes: effects of calcium, phorbol esters, protein kinase inhibitors, and antibodies to the neuron-specific protein kinase C substrate B-50 (GAP-43). J Neurochem 56:1146–1153

18. Yung HW, Wyttenbach A, Tolkovsky AM (2004) Aggravation of necrotic death of glucose-deprived cells by the MEK1 inhibitors U0126 and PD184161 through depletion of ATP. Biochem Pharmacol 68:351–360

19. Nicotera P, Leist M, Fava E, Berliocchi L, Volbracht C (2000) Energy requirement for caspase activation and neuronal cell death. Brain Pathol 10:276–282

20. Laake JH, Haug FM, Wieloch T, Ottersen OP (1999) A simple in vitro model of ischemia based on hippocampal slice cultures and propidium iodide fluorescence. Brain Res 4:173–184

21. Tolkovsky AM (1987) Newly synthesized catalytic and regulatory components of adenylate cyclase are expressed in neurites of cultured sympathetic neurons. J Neurosci 7:110–119

22. Christofferson DE (2009) and Yuan, J. Necroptosis as an alternative form of programmed cell death, Current opinion in cell biology

23. Degterev A, Hitomi J, Germscheid M, Ch'en IL, Korkina O, Teng X, Abbott D, Cuny GD, Yuan C, Wagner G, Hedrick SM, Gerber SA, Lugovskoy A, Yuan J (2008) Identification of RIP1 kinase as a specific cellular target of necrostatins. Nat Chem Biol 4:313–321

24. Hitomi J, Christofferson DE, Ng A, Yao J, Degterev A, Xavier RJ, Yuan J (2008) Identification of a molecular signaling network that regulates a cellular necrotic cell death pathway. Cell 135:1311–1323

25. Yu LY, Saarma M, Arumae U (2008) Death receptors and caspases but not mitochondria are activated in the GDNF- or BDNF-deprived dopaminergic neurons. J Neurosci 28: 7467–7475
26. Haase G, Pettmann B, Raoul C, Henderson CE (2008) Signaling by death receptors in the nervous system. Curr Opin Neurobiol 18:284–291
27. Holler N, Zaru R, Micheau O, Thome M, Attinger A, Valitutti S, Bodmer JL, Schneider P, Seed B, Tschopp J (2000) Fas triggers an alternative, caspase-8-independent cell death pathway using the kinase RIP as effector molecule. Nat Immunol 1:489–495
28. Yu L, Wan F, Dutta S, Welsh S, Liu Z, Freundt E, Baehrecke EH, Lenardo M (2006) Autophagic programmed cell death by selective catalase degradation. Proc Natl Acad Sci USA 103:4952–4957
29. Li Y, Yang X, Ma C, Qiao J, Zhang C (2008) Necroptosis contributes to the NMDA-induced excitotoxicity in rat's cultured cortical neurons. Neurosci Lett 447:120–123
30. Formigli L, Papucci L, Tani A, Schiavone N, Tempestini A, Orlandini GE, Capaccioli S, Orlandini SZ (2000) Aponecrosis: morphological and biochemical exploration of a syncretic process of cell death sharing apoptosis and necrosis. J Cell Physiol 182:41–49
31. Sperandio S, Poksay K, de Belle I, Lafuente MJ, Liu B, Nasir J, Bredesen DE (2004) Paraptosis: mediation by MAP kinases and inhibition by AIP-1/Alix. Cell Death Differ 11:1066–1075
32. David KK, Andrabi SA, Dawson TM, Dawson VL (2009) Parthanatos, a messenger of death. Front Biosci 14:1116–1128
33. Castro-Obregon S, Del Rio G, Chen SF, Swanson RA, Frankowski H, Rao RV, Stoka V, Vesce S, Nicholls DG, Bredesen DE (2002) A ligand-receptor pair that triggers a non-apoptotic form of programmed cell death. Cell Death Differ 9:807–817
34. Berghe TV, Vanlangenakker N, Parthoens E, Deckers W, Devos M, Festjens N, Guerin CJ, Brunk UT, Declercq W, Vandenabeele P (2009) Necroptosis, necrosis and secondary necrosis converge on similar cellular disintegration features. Cell Death Differ 17(6):922–30
35. Galluzzi L, Blomgren K, Kroemer G (2009) Mitochondrial membrane permeabilization in neuronal injury. Nat Rev Neurosci 10:481–494
36. Fletcher GC, Xue L, Passingham SK, Tolkovsky AM (2000) Death commitment point is advanced by axotomy in sympathetic neurons. J Cell Biol 150:741–754
37. Xue L, Fletcher GC, Tolkovsky AM (1999) Autophagy is activated by apoptotic signalling in sympathetic neurons: an alternative mechanism of death execution. Mol Cell Neurosci 14:180–198
38. Artal-Sanz M, Samara C, Syntichaki P, Tavernarakis N (2006) Lysosomal biogenesis and function is critical for necrotic cell death in *Caenorhabditis elegans*. J Cell Biol 173:231–239
39. Syntichaki P, Xu K, Driscoll M, Tavernarakis N (2002) Specific aspartyl and calpain proteases are required for neurodegeneration in C. elegans. Nature 419:939–944
40. Bampton ET, Goemans CG, Niranjan D, Mizushima N, Tolkovsky AM (2005) The dynamics of autophagy visualized in live cells: from autophagosome formation to fusion with endo/lysosomes. Autophagy 1:23–36
41. Bao Q, Shi Y (2007) Apoptosome: a platform for the activation of initiator caspases. Cell Death Differ 14:56–65
42. Wyttenbach A, Tolkovsky AM (2006) The BH3-only protein Puma is both necessary and sufficient for neuronal apoptosis induced by DNA damage in sympathetic neurons. J Neurochem 96:1213–1226
43. Anderson CN, Tolkovsky AM (1999) A role for MAPK/ERK in sympathetic neuron survival: protection against a p53-dependent. JNK independent induction apoptosis by cytosine arabinoside. J Neurosci 19:664–673
44. Sun YF, Yu LY, Saarma M, Timmusk T, Arumae U (2001) Neuron-specific Bcl-2 homology 3 domain-only splice variant of Bak is anti-apoptotic in neurons, but pro-apoptotic in non-neuronal cells. J Biol Chem 276:16240–16247
45. Uo T, Kinoshita Y, Morrison RS (2005) Neurons exclusively express N-Bak, a BH3 domain-only Bak isoform that promotes neuronal apoptosis. J Biol Chem 280: 9065–9073
46. Deckwerth TL, Easton RM, Knudson CM, Korsmeyer SJ, Johnson EM Jr (1998) Placement of the BCL2 family member BAX in the death pathway of sympathetic neurons activated by trophic factor deprivation. Exp Neurol 152:150–162
47. Lindsten T, Zong WX, Thompson CB (2005) Defining the role of the Bcl-2 family of proteins in the nervous system. Neuroscientist 11:10–15
48. Doughty ML, De Jager PL, Korsmeyer SJ, Heintz N (2000) Neurodegeneration in

Lurcher mice occurs via multiple cell death pathways. J Neurosci 20:3687–3694

49. Kim H, Tu HC, Ren D, Takeuchi O, Jeffers JR, Zambetti GP, Hsieh JJ, Cheng EH (2009) Stepwise activation of BAX and BAK by tBID. BIM, and PUMA initiates mitochondrial apoptosis. Mol Cell 36:487–499
50. Hsu YT, Youle RJ (1998) Bax in murine thymus is a soluble monomeric protein that displays differential detergent-induced conformations. J Biol Chem 273:10777–10783
51. Wong HK, Fricker M, Wyttenbach A, Villunger A, Michalak EM, Strasser A, Tolkovsky AM (2005) Mutually exclusive subsets of BH3-only proteins are activated by the p53 and c-Jun N-terminal kinase/c-Jun signaling pathways during cortical neuron apoptosis induced by arsenite. Mol Cell Biol 25:8732–8747
52. Wolter KG, Hsu YT, Smith CL, Nechushtan A, Xi XG, Youle RJ (1997) Movement of Bax from the cytosol to mitochondria during apoptosis. J Cell Biol 139:1281–1292
53. Martinou I, Fernandez PA, Missotten M, White E, Allet B, Sadoul R, Martinou JC (1995) Viral proteins E1B19K and p35 protect sympathetic neurons from cell death induced by NGF deprivation. J Cell Biol 128:201–208
54. Goldstein JC, Waterhouse NJ, Juin P, Evan GI, Green DR (2000) The coordinate release of cytochrome c during apoptosis is rapid, complete and kinetically invariant. Nat Cell Biol 2:156–162
55. Wright KM, Smith MI, Farrag L, Deshmukh M (2007) Chromatin modification of Apaf-1 restricts the apoptotic pathway in mature neurons. J Cell Biol 179:825–832
56. Borutaite V, Brown GC (2007) Mitochondrial regulation of caspase activation by cytochrome oxidase and tetramethylphenylenediamine via cytosolic cytochrome c redox state. J Biol Chem 282:31124–31130
57. Vaughn AE, Deshmukh M (2008) Glucose metabolism inhibits apoptosis in neurons and cancer cells by redox inactivation of cytochrome c. Nat Cell Biol 10:1477–1483
58. Ward MW (2010) Quantitative analysis of membrane potentials. Methods Mol Biol 591:335–351
59. Shi Y (2002) Mechanisms of caspase activation and inhibition during apoptosis. Mol Cell 9:459–470
60. Timmer JC, Salvesen GS (2007) Caspase substrates. Cell Death Differ 14:66–72
61. Ciechomska IA, Goemans CG, Tolkovsky AM (2008) Molecular links between autophagy and apoptosis. Methods Mol Biol 445: 175–193
62. Wang KK (2000) Calpain and caspase: can you tell the difference? Trends Neurosci 23:20–26
63. Pereira NA, Song Z (2008) Some commonly used caspase substrates and inhibitors lack the specificity required to monitor individual caspase activity. Biochem Biophys Res Commun 377:873–877
64. Berger AB, Sexton KB, Bogyo M (2006) Commonly used caspase inhibitors designed based on substrate specificity profiles lack selectivity. Cell Res 16:961–963
65. Chong ZZ, Kang J, Li F, Maiese K (2005) mGluRI targets microglial activation and selectively prevents neuronal cell engulfment through Akt and caspase dependent pathways. Curr Neurovasc Res 2:197–211
66. Cocco RE, Ucker DS (2001) Distinct modes of macrophage recognition for apoptotic and necrotic cells are not specified exclusively by phosphatidylserine exposure. Mol Biol Cell 12:919–930
67. Hirt UA, Gantner F, Leist M (2000) Phagocytosis of nonapoptotic cells dying by caspase-independent mechanisms. J Immunol 164:6520–6529
68. White AR, Guirguis R, Brazier MW, Jobling MF, Hill AF, Beyreuther K, Barrow CJ, Masters CL, Collins SJ, Cappai R (2001) Sublethal concentrations of prion peptide PrP106-126 or the amyloid beta peptide of Alzheimer's disease activates expression of proapoptotic markers in primary cortical neurons. Neurobiol Dis 8:299–316
69. Yue Z, Friedman L, Komatsu M, Tanaka K (2009) The cellular pathways of neuronal autophagy and their implication in neurodegenerative diseases. Biochim Biophys Acta 1793:1496–1507
70. Oppenheim RW, Blomgren K, Ethell DW, Koike M, Komatsu M, Prevette D, Roth KA, Uchiyama Y, Vinsant S, Zhu C (2008) Developing postmitotic mammalian neurons in vivo lacking Apaf-1 undergo programmed cell death by a caspase-independent, non-apoptotic pathway involving autophagy. J Neurosci 28:1490–1497
71. Mizushima N, Levine B, Cuervo AM, Klionsky DJ (2008) Autophagy fights disease through cellular self-digestion. Nature 451:1069–1075
72. Ventruti A, Cuervo AM (2007) Autophagy and neurodegeneration. Curr Neurol Neurosci Rep 7:443–451
73. Tanida I, Minematsu-Ikeguchi N, Ueno T, Kominami E (2005) Lysosomal turnover, but

not a cellular level, of endogenous LC3 is a marker for autophagy. Autophagy 1:84–91

74. Shacka JJ, Klocke BJ, Young C, Shibata M, Olney JW, Uchiyama Y, Saftig P, Roth KA (2007) Cathepsin D deficiency induces persistent neurodegeneration in the absence of Bax-dependent apoptosis. J Neurosci 27: 2081–2090
75. Iwamaru A, Kondo Y, Iwado E, Aoki H, Fujiwara K, Yokoyama T, Mills GB, Kondo S (2007) Silencing mammalian target of rapamycin signaling by small interfering RNA enhances rapamycin-induced autophagy in malignant glioma cells. Oncogene 26: 1840–1851
76. Spencer B, Potkar R, Trejo M, Rockenstein E, Patrick C, Gindi R, Adame A, Wyss-Coray T, Masliah E (2009) Beclin 1 gene transfer activates autophagy and ameliorates the neurodegenerative pathology in alpha-synuclein models of Parkinson's and Lewy body diseases. J Neurosci 29:13578–13588
77. Pickford F, Masliah E, Britschgi M, Lucin K, Narasimhan R, Jaeger PA, Small S, Spencer B, Rockenstein E, Levine B, Wyss-Coray T (2008) The autophagy-related protein beclin 1 shows reduced expression in early Alzheimer disease and regulates amyloid beta accumulation in mice. J Clin Investig 118:2190–2199
78. Xue L, Borutaite V, Tolkovsky AM (2002) Inhibition of mitochondrial permeability transition and release of cytochrome c by anti-apoptotic nucleoside analogues. Biochem Pharmacol 64:441–449
79. Fujita N, Noda T, Yoshimori T (2009) Atg4B(C74A) hampers autophagosome closure: a useful protein for inhibiting autophagy. Autophagy 5:88–89
80. Kuma A, Hatano M, Matsui M, Yamamoto A, Nakaya H, Yoshimori T, Ohsumi Y, Tokuhisa T, Mizushima N (2004) The role of autophagy during the early neonatal starvation period. Nature 432:1032–1036
81. Komatsu M, Waguri S, Ueno T, Iwata J, Murata S, Tanida I, Ezaki J, Mizushima N, Ohsumi Y, Uchiyama Y, Kominami E, Tanaka K, Chiba T (2005) Impairment of starvation-induced and constitutive autophagy in Atg7-deficient mice. J Cell Biol 169:425–434
82. Nishida Y, Arakawa S, Fujitani K, Yamaguchi H, Mizuta T, Kanaseki T, Komatsu M, Otsu K, Tsujimoto Y, Shimizu S (2009) Discovery of Atg5/Atg7-independent alternative macroautophagy. Nature 461:654–658
83. Xue L, Fletcher GC, Tolkovsky AM (2001) Mitochondria are selectively eliminated from eukaryotic cells after blockade of caspases during apoptosis. Curr Biol 11:361–365
84. Klionsky DJ, Elazar Z, Seglen PO, Rubinsztein DC (2008) Does bafilomycin A1 block the fusion of autophagosomes with lysosomes? Autophagy 4:849–950
85. Kochl R, Hu XW, Chan EY, Tooze SA (2006) Microtubules facilitate autophagosome formation and fusion of autophagosomes with endosomes. Traffic 7:129–145
86. King MA, Hands S, Hafiz F, Mizushima N, Tolkovsky AM, Wyttenbach A (2008) Rapamycin inhibits polyglutamine aggregation independently of autophagy by reducing protein synthesis. Mol Pharmacol 73:1052–1063
87. Komatsu M, Waguri S, Koike M, Sou YS, Ueno T, Hara T, Mizushima N, Iwata J, Ezaki J, Murata S, Hamazaki J, Nishito Y, Iemura S, Natsume T, Yanagawa T, Uwayama J, Warabi E, Yoshida H, Ishii T, Kobayashi A, Yamamoto M, Yue Z, Uchiyama Y, Kominami E, Tanaka K (2007) Homeostatic levels of p62 control cytoplasmic inclusion body formation in autophagy-deficient mice. Cell 131:1149–1163
88. Waguri S, Komatsu M (2009) Biochemical and morphological detection of inclusion bodies in autophagy-deficient mice. Methods Enzymol 453:181–196
89. Bandyopadhyay U, Cuervo AM (2007) Chaperone-mediated autophagy in aging and neurodegeneration: lessons from alpha-synuclein. Exp Gerontol 42:120–128
90. Korolchuk VI, Menzies FM, Rubinsztein DC (2009) A novel link between autophagy and the ubiquitin-proteasome system. Autophagy 5:862–863
91. Léveillé F, Papadia S, Fricker M, Bell KF, Soriano FX, Martel MA, Puddifoot C, Habel M, Wyllie DJ, Ikonomidou C, Tolkovsky AM, Hardingham GE (2010) Suppression of the intrinsic apoptosis pathway by synaptic activity. J Neurosci 30(7):2623–2635.

Chapter 16

Inflammation and Reactive Oxygen/Nitrogen Species in Glial/Neuronal Cultures

Jonas J. Neher, Guy C. Brown, Agnieszka Kinsner-Ovaskainen, and Anna Bal-Price

Abstract

Inflammation contributes to a wide variety of brain pathologies. In this chapter methods are described for using microglia and astrocytes in culture to investigate inflammatory processes and inflammatory neurodegeneration, including the use of neuronal/glial co-cultures and transwells. Methods for detecting and characterising inflammatory activation in culture include changes in microglial phenotype, microglial phagocytosis and expression of pro-inflammatory cytokines. The protocols for how to determine cellular production of superoxide, hydrogen peroxide, peroxynitrite and nitric oxide in culture are described.

Key words: Inflammation, Microglia, Pro-inflammatory cytokines, Cell specific immunocytochemistry, Nitric oxide, Peroxynitrite, Reactive nitrogen species, Reactive oxygen species

1. Introduction

There is now significant evidence that brain inflammation contributes to the pathology of neurodegenerative diseases (Alzheimer's, Parkinson's, multiple sclerosis, and AIDS dementia), as well as more acute brain pathologies such as stroke, brain trauma and meningitis (1–6). These pathologies have different causes and courses, but they all involve brain inflammation, and there is evidence that blocking inflammation can either prevent onset or reduce symptoms for each of these pathologies (1–6). However, there are different types or modes of inflammation, and it is important to understand why inflammation is sometimes protective and at other times damaging, so that interventions can be designed to prevent one but not the other.

Brain inflammation may also occur at the level of the blood–brain barrier (BBB), leading to increased BBB permeability as a

Michael Aschner et al. (eds.), *Cell Culture Techniques*, Neuromethods, vol. 56,
DOI 10.1007/978-1-61779-077-5_16,

consequence of a progressive opening of tight junctions (7). This process is mainly mediated by glia activation (microglia and astrocytes) and their pro-inflammatory response.

During brain inflammation there is relative low leucocyte recruitment, and the major inflammatory cells are microglia. Microglia are resident brain macrophages, and are the key cells in brain inflammation and inflammatory neurodegeneration (5). Brain inflammation may be divided into three phases (acute, chronic and resolution), in which the microglia are largely found in three different morphologies (resting, activated and amoeboid/phagocytic). The healthy, non-inflamed brain contains almost entirely "resting" microglia, which are highly ramified, with a small, static cell body, but with dynamic and branched processes actively seeking out: (1) pathogens, and (2) damaged cells, in the brain (5). Pathogen receptors ("pattern recognition receptors") include: the toll-like receptors (TLRs) and the NOD-like receptors (NLRs), and generally recognise cell wall components or RNA/DNA of pathogens. Damage (or "danger") receptors include: scavenger receptors, purinergic receptors, receptor for advanced glycation endproducts (RAGE), and TLRs, and these recognise components released from stressed or damaged host cells, including ATP, aggregated β-amyloid and heat shock proteins (5). Engagement of these receptors induces signal cascades that will (after several hours) produce the "chronically activated" state due to expression of new proteins, including iNOS, COX-II and MHC-II. MHC-II enables activated microglia to present antigens derived from phagocytosed material to T cells. Activation is accompanied by partial rounding up and mobility of microglia, proliferation, and the expression and release of pro-inflammatory cytokines, including TNF-α, IL-1β and IL-6. These cytokines activate other microglia and astrocytes. Most of the expression changes are a result of activation of the transcription factor NF-κB via phosphorylation-induced activation of IκB kinase (IKK).

Prior to the induction of gene expression, the microglia are in the "acute" phase of activation triggered by receptor ligation. Receptor stimulation induces PKC activity causing rapid activation of the phagocyte NADPH oxidase (PHOX), which in turn contributes to NF-κB activation. After induced gene expression the microglia are in a chronic state of activation, which may be maintained by the pro-inflammatory cytokine release and the continued presence of pathogen/damage. However, the chronic state of activation may progress to a "resolution" phase, where microglia are amoeboid, highly phagocytic and produce anti-inflammatory cytokines (including IL-10 and TGF-β) in order to resolve the inflammation and clear up the mess. This three phase division (acute, chronic and resolution) of microglial inflammation is simplistic, as there are alternative modes of activation and alternative ways of classifying microglial activation (8).

Activated microglia can kill and/or remove pathogens, but they may also kill neurones. The mechanisms by which they induce neuronal cell death are complex (5), but may include: (1) reactive oxygen and nitrogen species derived from glial NADPH oxidase and inducible NO synthase, (2) glutamate from glia (and neurones) causing excitotoxicity to neurones, (3) proteases released from glia or MMPs, and/or (4) TNF-α and FasL released from glia causing apoptosis of neurones.

2. Cells: Types, Isolation, Characterisation, Co-Cultures and Transwells

At early stages, inflammation in the CNS is predominantly mediated by the innate immune system, which is comprised of astrocytes and microglia. Therefore, to assess their contribution to neuronal death, a culture model consisting of neurones, astrocytes and microglia is a useful tool for investigating inflammatory neurodegeneration in vitro. The culture and manipulation of cell types for delineating inflammatory effects in vitro will be described in the following.

2.1. Primary Mixed Neuronal/Glial Culture from Postnatal Rat/Mouse Cerebellum

Primary mixed neuronal/glial cultures can be obtained from rat or mouse pups at postnatal day 5–7. Briefly, pups are killed by decapitation after terminal anaesthesia. Brains are removed in ice-cold Hanks Buffered Salt Solution (HBSS, Invitrogen) containing antibiotics. To obtain cultures of cerebellar granule neurones (CGNs), cerebella are separated from the brainstem, and meninges are removed. The tissue is then transferred into pre-warmed Versene solution (37°C, Invitrogen), cut into small pieces and incubated for 5 min at 37°C, 5% CO_2. Cells are separated by trituration with fire-polished glass pasteur-pipettes of decreasing aperture size, transferring the supernatant to pre-warmed CGN medium (DMEM supplemented with 5% of heat-inactivated horse serum, 5% heat-inactivated foetal calf serum, 5 mM HEPES, 20 mM KCl, 2 mM L-glutamine, 13 mM glucose and 10 µg/mL gentamicin) in-between trituration steps. The cell suspension is then centrifuged at 150 g, 7 min, room-temperature (RT), resuspended in CGN medium and passed through a 40 µm cell-strainer (BD Bioscience). Cells are seeded at a density of $2–2.5 \times 10^5$ cells/cm^2 into poly-L-lysine (0.001%, Sigma)-coated culture vessels appropriate for the assay to be performed. The culture medium (e.g., 500 µL/24-well) is only exchanged once after 24 h and cultures are incubated for 7–9 days to allow for maturation (changing the medium after this will induce glial proliferation and neuronal death; if required, medium can be replaced with conditioned medium from sister cultures).

2.2. Primary Glial Cultures

Mixed microglial/astrocytic cultures can be obtained as part of the same preparation as CGNs, but from the cerebral hemispheres of rat/mouse pups at postnatal day 5–7. The cortical hemispheres are dissected, and meninges removed. The tissue is transferred into HBSS containing 0.18% trypsin (Invitrogen), minced thoroughly and incubated for 15 min, 37°C, 5% CO_2, with occasional shaking. The tissue is then allowed to settle down and the trypsin solution is removed as completely as possible without losing tissue. Cells are then resuspended in DMEM supplemented with 10% heat-inactivated foetal calf serum (glia medium) and 0.02 mg/mL deoxyribonuclease I (DNase I, Sigma) and triturated (as described in Sect. 2.1) in the same medium. Cells are centrifuged at 150 g, 7 min, 4°C, followed by resuspension in prewarmed glia medium and filtering first through a 100 μm cell strainer, and subsequently through a 40 μm cell strainer (BD Bioscience). Cells are plated at a density of 10^5 cells/cm^2 into appropriate culture vessels coated with 0.0005% poly-L-lysine and medium is exchanged after 24 h, preceded by careful tapping of plates/flasks to dislodge and remove cell debris. Cultures are grown in a humidified atmosphere of 5% CO_2/95% air, and left to mature for 8–10 days. Medium is exchanged every 2–3 days.

2.3. Microglial Isolation from Mixed Glial Cultures

To obtain pure microglial cultures, mixed glial cultures grown in culture flasks to confluence (around 14–16 days in vitro) are gently vortexed (level 2–3) for ~1 min to selectively dislodge microglial cells from the underlying astrocyte monolayer. Alternatively, cells can be shaken on a rotary shaker for ~5 h. The cell suspension is then collected and spun down at 150 g, 7 min, RT. The supernatant is removed, cells are counted and plated (at density, e.g., 2.0×10^5 cells/cm^2) into appropriate culture vessels coated with 0.0005% poly-L-lysine. The microglial cells should be cultured in astrocyte-conditioned media (medium collected from astrocytic cultures at least after 2 days in vitro and spun down) mixed 1:2 (v/v) with fresh DMEM medium (containing 10% foetal calf serum). The purity of cell population can be evaluated by immunostaining with anti-GFAP antibody (astrocytic marker) and anti-OX-42 antibody (microglial marker, an anti-CR3 complement receptor antibody).

2.4. Selective Microglial Elimination and Transwell-Experiments

Microglia are the brain's primary immune effector cells. However, astrocytes can contribute to neuroprotection as well as neurotoxicity and their absence (e.g., in enriched neuronal cultures) might therefore change the experimental outcome. Instead of performing experiments on enriched neuronal cultures, microglia can be selectively eliminated from mixed neuronal/astrocytic/microglial cultures leaving an astrocytic/neuronal culture for investigation.

Selective elimination of microglia is achieved by treating mature cerebellar cultures (7–8 days in vitro) with L-leucine-methyl-ester (LME, 50 mM, Sigma) for 4 h at 37°C, 5% CO_2. LME is a

lysosomotropic reagent, i.e., it leads to osmotic lysis of microglia due to their high lysosomal activity and consequent intracellular accumulation of L-leucine. After LME incubation, cultures are washed gently with prewarmed PBS and the neuronal/astrocytic cultures are grown in conditioned medium from sister cultures (NB: since LME treatment leads to cell lysis and release of chromatin, staining for necrotic cells does not truly reflect the number of necrotic cells in LME-treated cultures).

Sometimes it is important to distinguish the influence of soluble mediators released by microglia from contact-mediated effects. The selective elimination of microglia from mixed cultures by LME treatment allows the separation of these effects by culturing microglia on membrane transwell inserts. This allows for the signalling of soluble mediators to occur while preventing the physical interaction of the microglia and neurones/astrocytes. For transwell experiments in 24-well plates for example, 2.5×10^4 microglia from glial cultures are added either back to the neuronal/astrocytic cultures (as a control condition) or plated onto a poly-L-lysine (0.001%)-coated membrane transwell insert (pore-size 0.4 μm, Corning; the small pore size is essential to prevent microglial migration through the membrane) and left to adhere for 24 h. These cultures are then stimulated in the same way as mixed cultures (NB: often, the volume of culture medium needs to be increased to allow for complete submersion of the transwell microglia; the amount of stimulant added then needs to be adjusted accordingly).

The activation of transwell microglia can often be assessed by investigating their proliferation on the transwell. This can be achieved by staining the transwell microglia with a nuclear dye (such as Hoechst 33342), cutting out the bottom of the transwell insert and placing it upside down onto the lid of a culture plate. The nuclei can then be counted by fluorescence microscopy. Alternatively, measurement of soluble inflammatory mediators can be performed in the same way as for mixed cultures (see Sect. 4) to confirm inflammatory activation. If analysis of the neuronal/astrocyte layer is desired, these cells can be cultured on poly-L-lysine-coated glass coverslips, which can be imaged by conventional fluorescent or confocal microscopy.

As an additional step of analysis, this system can further be utilised to investigate the interaction between neurones/microglia after exposure to the inflammatory environment in transwell cultures (in which direct cell–cell contact is prevented). To this end, transwells are removed after an incubation time appropriate for the experiment and microglia from pure microglial cultures are added back to the neurones/astrocytes. For pre-treatment/stimulation of microglia, 5×10^5 cells are plated into poly-L-lysine-coated (0.0005%) 6-wells and left to adhere for 24 h. Cells are then stimulated for a desired amount of time and carefully washed twice with PBS. Conditioned neuronal medium is added and microglia are detached by mechanical agitation. Then, for

example in a 24-well, 2.5×10^4 microglia are added directly to neuronal/astrocytic cultures and incubated for 6 h, 37°C, 5% CO_2 (keeping the incubation time short is essential for preventing the microglia from significantly changing the inflammatory environment in the culture, thus allowing to distinguish soluble from contact-mediated effects).

This system allows for the investigation of the effects of prestimulation of either the neuronal/astrocytic cultures or the pure microglial cultures with inflammatory activators (or other substances). Thus, the effects on microglia and neurons/astrocytes can be disseminated. Furthermore, this system also allows for the selective application of inhibitors either to the microglial cultures or the neuronal/astrocytic cultures, thus helping to avoid artefacts due to action of the inhibitor on all cell types.

3. Characterisation of Neuronal and Glial Cultures (Immunocytochemistry and Morphology)

Immunostaining using antibodies directed against cell-specific antigens is commonly used to identify and quantify the different cell types in mixed neuronal–glial cultures, as well as to check the purity of microglial and astrocytic cultures.

The methods for staining of each cell type (neurones, astrocytes and microglia) are described below. Double-staining of mixed neuronal/glial cultures with more than one antibody can also be performed, provided that primary antibodies from two different species (e.g., mouse and rabbit) are used and that the secondary antibodies are labelled with fluorescent markers of different excitation/emission wavelengths (e.g., green FITC and red Cy3).

3.1. Neurones

Neurones can be identified in culture using several different markers. The most commonly used are neurofilaments (NF), microtubule-associated proteins-2 (MAP-2) or NeuN (neuronal nuclei).

Neurofilaments are a type of intermediate filament that serve as major elements of the cytoskeleton supporting the axon cytoplasm and are the most abundant fibrillar components of the axon (9). Three types of neurofilament proteins (68/70 kDa NF-L, 160 kDa NF-M and 200 kDa NF-H) are co-assembled in vivo forming heteropolymers. The neurofilament triplet proteins (68/70, 160 and 200 kDa) occur in both the central and the peripheral nervous system and are usually neurone-specific.

MAP-2 is one of several high molecular weight proteins that play an important role in microtubule assembly and is a stringent marker for neurones. In the central nervous system, MAP-2 is confined to neuronal cell bodies and dendrites, but exceptions were found where axons stained positive for small amounts of

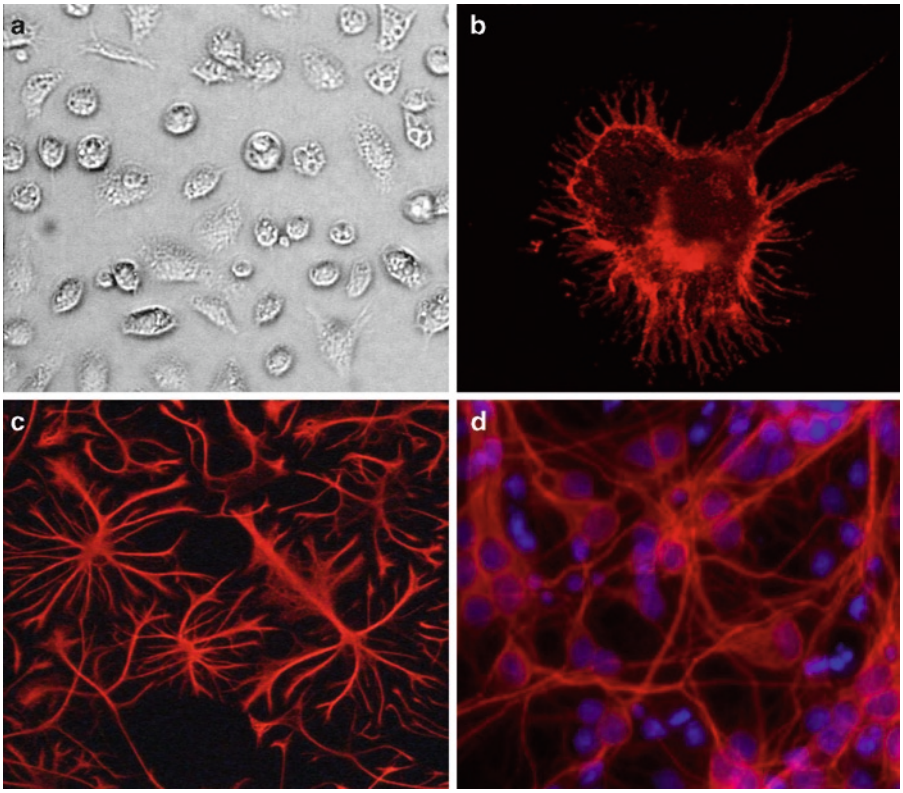

Fig. 1. Immunocytochemical staining of neuronal and glial cells in primary culture: (**a**) Pure culture of microglia (rat cortex) isolated from mixed astrocytes/microglia cell population (phase contrast microscope): (**b**) Microglial cell stained with the OX-42 antibody; (**c**) Pure astrocytic culture (rat cortex) stained with antibodies against GFAP; (**d**) A culture of rat cerebellar granule cells stained with antibodies against MAP-2 to visualise neuritres (the cell nuclei are stained with Hoechst 33342). In all immunocytochemical stainings (**b–d**) the secondary antibodies were labelled with Cy3 (ex. 550 nm/em. 572 nm).

MAP-2 (10). MAP-2 is uniformly distributed throughout the cell when first expressed in cultured neurones (Fig. 1d) but becomes selectively localised as dendritic development proceeds.

The anti-NeuN antibody reacts with a neuronal-specific nuclear protein in vertebrates, which has recently been identified as the gene product of Fox-3, a member of the RNA-binding protein Fox-1 gene family (11, 12). Antibodies against NeuN react with most neuronal cell types throughout the nervous system, in post-mitotic neurones. The NeuN antibody is an excellent marker for neurones in primary culture. The immunocytochemical staining is primarily localised in the nucleus of the neurones with lighter staining in the cytoplasm.

To identify neurones in culture, the cells can be grown on, e.g., 24-well plates or in 8-well chamber slides coated with poly-L-lysine (as described in Sect. 2.1) The culture should first be washed for 5 min with 10 mM phosphate buffered saline (PBS) followed by the fixation using 4% paraformaldehyde for 30 min

and then washed three times for 5 min each with PBS. The fixed cells are permeabilised for 10 min with 0.25% Triton X-100 in PBS. After washing (3×5 min), the unspecific binding is blocked by treatment with 10% goat serum for 30 min and then incubated with, e.g. anti-NF-200 (usually at 1:500–1:1,000), anti-MAP-2 (1:500) or anti-NeuN (1:100–1:1,000) antibodies overnight at 4°C. The dilution of each antibody has to be determined experimentally to reduce the unspecific binding (background). Subsequently, the cells are abundantly washed with 1% Triton X-100 in PBS and incubated for 2 h at room temperature with secondary antibodies (around 1:1,000–1:2,000) conjugated with fluorescent markers (e.g., FITC, Cy3, etc.) diluted in 1% goat serum in PBS. After removal of the secondary antibody and washing with 1% Triton X-100 in PBS, the cells are co-stained for 10 min with 5 μg/mL Hoechst 33342 reagent to identify cell nuclei of all cells present in the culture. The staining is analysed using a fluorescent microscope.

3.2. Astrocytes

Immunostaining with antibodies against glial fibrillar acidic protein (GFAP) is frequently used to identify astrocytes in culture. GFAP is an intermediate filament cytoskeletal protein expressed primarily by astrocytes (Fig. 1c) and it is commonly considered as the marker of astrocytes (13).

The cells grown on, e.g., 24-well plates or in 8-well chamber slides coated with poly-L-lysine (as described in Sect. 2.2) are washed with 10 mM PBS for 5 min and fixed with 4% paraformaldehyde for 1 h at 4°C. The cells are then rinsed with PBS (2×5 min), permeabilised with 0.3% Triton X-100 in PBS, followed by incubation with 10% goat serum in PBS to block unspecific binding sites. Primary anti-GFAP antibodies (around 1:500–1:1,000), diluted in 1% goat serum in PBS, are applied to the cells overnight at 4°C. After extensive washing with 0.1% Triton X-100 in PBS (4×5 min each time), cells are incubated for 2 h at room temperature with secondary antibodies conjugated with a fluorescent marker (e.g., FITC, Cy3) diluted in 1% goat serum in PBS. Cells are extensively washed with 1% Triton X-100 in PBS and subsequently stained for 10 min with 5 μg/mL Hoechst 33342 to visualise cell nuclei. The staining is observed under a fluorescent microscope.

3.3. Microglia

Microglia (Fig. 1a) can be identified in culture using histochemical staining with Isolectin B_4 from *Griffonia simplicifolia* (14, 15), which recognises α-galactose-containing glycoconjugates on the surface of microglial cells or using immunostaining with OX42, an antibody that recognises type 3 complement receptors (C3) in mononuclear phagocytes (Fig. 1b),

Histochemical staining of microglia with Isolectin B_4 is relatively quick and simple. The cells, isolated as described in Sects. 2.3–2.4 and grown, e.g., on 24-well plates, are gently

rinsed with PBS and incubated with fluorescein (FITC)- or rhodamine-labelled Isolectin B_4 (10 ng/mL in PBS) for 60 min at room temperature. After gentle washing (3×2 min with PBS), the cells are left in PBS and observed with a fluorescent microscope. At this point microglia can also be fixed with 4% paraformaldehyde, then mounted, covered with a coverslip and preserved for later examination with protection from light.

For immunostaining of microglia with the OX-42 antibody (16), the cells are fixed with 4% paraformaldehyde for 30 min at 4°C, followed by cold 100% methanol for 3–5 min. Methanol is then removed and cells washed with PBS twice for 5 min. Subsequently, the cells are incubated for 2 h at room temperature (or overnight at 4°C) with the OX-42 antibody (1:500–1:1,000) in 0.5% Triton X-100 in PBS. Following 3×5 min washes with PBS, secondary antibodies (1:1,000–1:2,000) conjugated with a secondary marker are added for 45 min, then cells are washed with PBS 3×5 min. At the end of the experiment, a co-staining performed with 5 μg/mL Hoechst 33342 for 10 min identifies nuclei of all cells present in the culture and enables to assess the purity of the microglial culture. The staining is viewed using a fluorescent microscope.

3.4. Microglia Morphology (Resting, Activated and Phagocytic Cells)

Microglial cells have several morphological forms depending on their functional state (Fig. 1). As mentioned earlier the healthy brain contains almost entirely "resting" microglia, which are also called ramified microglia. These cells have a small (5–10 μm) oval cell body with a large nucleus and only a little amount of cytoplasm, as well as numerous long, branched processes. Ramified microglia have been characterised as down-regulated (or inactive) macrophages (lack of phagocytic and endocytic activity, low expression of leukocyte common antigen (CD45), low levels of membrane ligands and receptors that are essential for mediating or inducing typical macrophage functions) (17).

One of the most remarkable properties of microglia is to react to stress signals coming from, e.g., necrotic cells as well as from the presence of various pathogens. Such pathological conditions may lead to microglia (and astrocyte) activation that can aid cell repair and protective immune responses. However, chronically activated microglia can release harmful molecules (ROS, RNS, pro-inflammatory cytokines, etc.) inducing neuronal damage. Following the stimulus (e.g., neuronal injury) microglia migrate to the damaged sites of the CNS where they proliferate and become activated. During this process microglia undergo maturation, leading to the acquisition of macrophage differentiation markers of two distinct forms – activated and reactive microglia. Activated microglia appear like swollen ramified cells and are characterised by a larger cell body with short processes. They are partially activated macrophages, as they express CR3 complement receptors and class I major histocompatibility complex (MHC) antigens.

Reactive microglia are typically small, spherical cells and lack ramified processes. They are fully active macrophages (further increased expression of CR3 receptor, class I and II MHC); thus they posses the ability to present antigens to T cells. These various microglial cell morphologies can be observed under in vitro conditions using phase-contrast and fluorescent microscopy. It can serve as an additional tool to characterise the microglial state (resting or activated).

4. Measurement of Cytokine Release

In the CNS, cytokines are key regulators of innate and adaptive immune responses. In the presence of pro-inflammatory cytokines, microglia and astrocytes become activated and subsequently produce both pro-inflammatory (e.g., IL-1α, IL-1β, IL-2, IL-6, IL-8 and TNF-α) and anti-inflammatory cytokines (e.g., TGF-β or IL-10). The levels of cytokines released by activated glia into the cell culture medium can be measured by ELISA assay or Luminex technology.

4.1. ELISA Assay

Quantification of cytokine levels in the medium of the control glial culture (pure microglial or astrocytic or mixed: microglia and astrocyte) and after activation (e.g., an exposure to LPS, the Gram-negative bacterial endotoxin lipopolysaccharide, as a positive control) can be performed by a sandwich ELISA, using commercially available antibody pairs (18). The plates have to be specifically designed for ELISA measurement, e.g., Nunc Maxisorp ELISA plates (Nunc).

Such plates should be coated overnight with the antibodies of interest. As typical markers of the pro-inflammatory response of activated glial cells, the levels of, e.g., TNF-α, IL-1β or IL-6 are usually measured. The anti-TNF-α, anti-IL-1β or anti-IL-6 antibodies should be diluted in 100 mM $NaHCO_3$, pH 8.3 at 4°C. These antibody dilutions as well as recombinant proteins (used as standards) should be prepared at the same time. After overnight incubation, the plates should be rinsed with PBS followed up by blocking with 3% BSA/PBS for 2 h. Then the samples of media and standard solutions (prepared in 3% BSA/PBS) are added for 3 h followed by incubation for 45 min with biotinylated anti-TNF-α, anti-IL-1β or anti-IL-6 antibodies and incubation with streptavidin-peroxidase (Biosource, Nivelles, Belgium) for 30 min. Detection of bound cytokines is carried out using TMB (3,3′,5,5′-tetramethylbenzidine, Sigma-Aldrich). The reaction is stopped using 1 M H_2SO_4 and the absorption is measured at 450 nm in a multiwell spectrophotometer (e.g., Spectra Max, Molecular Devices, Sunnyvale, CA, USA). The cytokine

concentrations are calculated using standard solutions of recombinant TNF-α, IL-1β or IL-6 and expressed in pg/mL/10^6 cells.

4.2. Luminex Technology

Luminex 100 (xMAP) platform is a flexible analyzer based on the principle of flow cytometry that allows quantifying the concentrations of various cytokines released into the medium or the content of intracellular kinases (both non- or phosphorylated, etc.). The colour-coded tiny beads (microspheres) are arranged into 100 distinct sets. Each bead set can be coated with a reagent specific to a particular bioassay, allowing the capture and detection of specific analytes from a sample. Many readings are made on each bead set allowing multiplexing of up to 100 unique assays within a single sample. This technology can be applied to non-activated culture of glial cells (non-treated control culture, e.g., in 25 cm^2 flasks) or activated cells, exposed to, e.g., LPS (positive control). The flasks with the cultured cells are placed on ice and medium collected into Eppendorf tubes. Then the cells are rinsed with PBS (at least three times) and after completely removing PBS the cells are lysed using a commercially available Bio-Plex cell lysis kit (BioRad, Hercules, CA, USA). The medium can be directly used as a sample. The cells are scraped and the flasks are agitated on a microplate shaker at 300 rpm for 20 min at 40°C. The cell lysates are colleted in 1.5 mL Eppendorf tubes and centrifuged at 4500 rpm for 20 min at 4°C. The supernatant is collected and the protein content in lysates determined using Bradford assay. Samples can be stored at –80°C until further analysis.

Analysis of the samples is performed according to the instructions supplied by the Bio-Plex phosphoprotein assay (BioRad, Hercules, CA, USA) kit. The assay is usually performed on 96-well filter plates (Millipore, Bedford, MA, USA). The samples and the provided controls are incubated with capturing beads coupled with antibodies against various cytokines or against various kinases (e.g., total-p38, total-ERK1/2, phospho-p38 (Thr^{180}/Tyr^{182}) and phospho-ERK1/2 (Thr^{202}/Tyr^{204}, Thr^{185}/Tyr^{187}) overnight, at room temperature, agitated on a microplate shaker at 300 rpm. As the beads are light sensitive, the plates should be covered with aluminium foil. On the next day the wells are washed three times with 100 μL wash buffer, using a filter plate vacuum manifold at 2 psi (Millipore, Bedford, MA, USA) and 25 μL of detection antibodies are added. The plate is left on the shaker for 30 min at room temperature (300 rpm) and subsequently washed three times with 100 μL wash buffer, followed by incubation with 50 μL streptavidin-PE for 10 min at room temperature. After washing the beads are resuspended in 125 μL resuspension buffer for analysis. Immediately before analysis, the plates are shaken again to ensure complete resuspension of beads. The fluorescence intensity readings for

100 beads/kinase (or cytokines) are determined and analysed using a Luminex 100 system (Luminex Corp., Austin, TX, USA) and the results are calculated as the mean fluorescence intensity.

5. Measurement of RONS

Reactive oxygen and nitrogen species (RONS) are molecules derived from oxygen or nitric oxide that are reactive, i.e., they react directly with other molecules without requiring catalysis by enzymes. RONS include superoxide (O_2^-), hydrogen peroxide (H_2O_2), nitric oxide (NO) and peroxynitrite ($OONO^-$). RONS are both regulators and effectors of inflammation. Inflammatory agents (such as LPS, β-amyloid, ATP and cytokines) and/or phagocytosis acutely activate the phagocytic NADPH oxidase (PHOX, found mainly in microglia, but also in astrocytes and some neurones) to produce superoxide, which then dismutates to hydrogen peroxide. This hydrogen peroxide causes inflammatory activation of the glia through NF-kB, resulting in the expression of inflammatory proteins such as inducible nitric oxide synthase (iNOS) in microglia and astrocytes. iNOS when expressed produces high levels of NO, which may react with oxygen to produce nitrite and nitrate, or react with superoxide to produce peroxynitrite. Thus measurements of ROS can be used as a measure of acute activation of glia (seconds to minutes), while measurements of iNOS, NO or its relatively stable product nitrite can be used as measurements of chronic activation of glia (hours to days).

5.1. Superoxide Production Measured with NBT

Superoxide production within cells can be assessed by nitro blue tetrazolium reduction, leading to the formation of a dark formazan precipitate (6, 7). At specific time-points after stimulation of cells, nitro-blue tetrazolium (Sigma) in HBSS (Invitrogen) is mixed with 200 µL of medium taken from individual 24-wells of cultures to avoid local concentration differences (final concentration 1 mg/mL). This solution is then added to the respective wells after removal of the remaining medium and incubated for 30 min, 37°C, 5% CO_2. Cultured cells are washed with HBSS, fixed with 4% PFA for 15 min, and kept in HBSS thereafter. The total number of formazan-positive cells/well or microscopic field is then counted under a light microscope.

5.2. Superoxide Production Measured with Cytochrome c

Extracellular superoxide production from activated cells can be assessed by adding cytochrome *c* to the medium and following its reduction (19). Superoxide directly reduces oxidised (Fe^{3+}) cytochrome *c* to reduced (Fe^{2+}) cytochrome *c* (which absorbs light at 550 nm, while oxidised cytochrome *c* does not). This reduction can be followed continuously in a spectrophotometer or using a

plate reader. If possible the absorbance at 540 nm should be subtracted from the absorbance at 550 nm to correct for any absorbance changes not due to cytochrome *c* reduction. Cells at a density of about 10^6 cells/mL are suspended in any medium that is not coloured (i.e., no phenol red), does not scatter light, and will not scavenge superoxide and will not reduce cytochrome *c* (no ascorbate), e.g., buffered salt solutions such as KREBS-Hepes or HBSS supplemented with glucose. Cytochrome *c* (50 μM final concentration, Sigma) is added and the cells are stirred before or during measurements in a spectrophotometer or plate reader, which ideally is thermostated at 37°C. At this density the cells may run out of oxygen after a few minutes – it may be an idea to saturate the medium with 95/100% oxygen, but bear in mind that superoxide production may depend on the oxygen level. It is also advisable to include in the medium 100 U/mL catalase, which prevents reoxidation of reduced cytochrome c by H_2O_2 (but remember that catalase is also a haemprotein). Measurements should be made with and without 50 U/mL superoxide dismutase (SOD, Sigma), to check the dependence of the signal on extracellular superoxide. If using a plate reader, adherent cells may be used, and the rate of increase in absorbance at 550 nm followed.

5.3. Cellular H_2O_2 Production Measured by Amplex Red Assay

Extracellular production of H_2O_2 by cells can be measured continuously using Amplex Red reagent and horse radish peroxidise (HRP). H_2O_2 passes rapidly through membranes, so extracellular H_2O_2 reflects both extracellular and intracellular production and breakdown. HRP catalyses H_2O_2 oxidation of Amplex Red to fluorescent resorufin. For example, the rate of hydrogen peroxide formation by isolated microglia can be measured in a continuous fluorometric assay. The reaction mixture contains 100 μM Amplex Red (Molecular Probes), 10 U/mL horseradish peroxidase and 3.5×10^5 microglia/mL resuspended in HBSS supplemented with glucose (5 mM). The rate of hydrogen peroxide production is measured in a stirred cuvette in a spectrofluorophotometer at excitation 560 nm and emission 587 nm, or in a plate reader (using black plates to avoid reading fluorescence from adjacent wells). The rate needs to be measured plus and minus cells, and plus and minus catalase to ensure that the change in fluorescence is due to H_2O_2 production only.

5.4. Direct Measurement of NO Generation Using a NO Electrode

NO can be measured directly from cells expressing iNOS using a Clark-type NO electrode (World Precision Instruments) (19). This is difficult or impossible for cells expressing nNOS or eNOS, but relatively easy for any cell expressing iNOS, simply because the latter produces a lot more NO continuously. The best way to do this is to get the cells (e.g., astrocytes or microglia or macrophages) into suspension (e.g., with trypsin) between 8 and 24 h after activation (e.g., with LPS and IFN-γ – you will get a lot

more iNOS expression with IFN-γ) when iNOS expression peaks. Note it may be advisable to use arginine-free culture media for the activation (or add arginase to the media), because the NO released by iNOS may damage the cells and limit iNOS expression. Between 10^5 and 10^6 cells are incubated in 1 mL, and put in a stirred, thermostated incubation chamber (WPI can supply this) with the NO electrode. It may be advisable to combine the measurement with an oxygen electrode (Rank Brothers can supply an electrode and chamber, then you need to drill a 2 mm hole through the chamber top to allow the NO electrode in, because the chamber needs to be gas tight and bubble free). It is best to use a relatively simple incubation medium such as KREBS buffer rather than a cell culture medium such as DMEM, as components of the latter including riboflavin react with NO in the presence of light. L-arginine, the substrate for iNOS, needs to be added in order to see NO generation, and glucose should be present for the cells to produce NADPH. The cells obviously need to be happy and healthy; NO readily passes through membranes and is therefore easily measurable by this method.

5.5. Assessment of NO Generation Through Nitrite Levels

Levels of nitrite (a stable break-down product of nitric oxide) can be measured using the Griess reaction, which visualises nitrite through the formation of a red azo dye that can be measured spectrometrically (20). In a 96-well plate (Nunc) 50 µL of cell-culture supernatants is mixed with an equal volume of freshly prepared ice-cold sulfanilamide (2 mM) in hydrochloric acid (1.2 M), and incubated for 10 min, RT, protected from light. Fifty microlitres of *N*-1-(1-naphtyl)ethylenediamine (3 mM) is then added and the mixture incubated for another 10 min, RT, in the dark. The absorbance is measured at 550 nm in a plate-reader. Nitrite concentrations are calculated using standards prepared from a nitrite standard solution (Sigma) in culture medium.

Alternatively, nitrite in cell-conditioned medium can be measured by the fluorometric DAN assay described in (21), which is about tenfold more sensitive than the Griess assay above. Briefly, the samples are diluted 1:50 in the 0.06 M HCl containing 5 mg/mL 2,3-diaminonaphthalene (DAN) that reacts with nitrite in acidic conditions to form 1-(*H*)-naphthotriazole, a fluorescent product, and incubated for 10 min at room temperature in dark. Then, 0.3 M NaOH is added to stop the reaction, and fluorescence intensity measured in a spectrofluorophotometer (or plate reader) at $\lambda_{ex} = 363$ nm and $\lambda_{em} = 426$ nm. Nitrite concentration in the samples is calculated according to a calibration curve constructed using known concentrations of nitrite.

5.6. Diaphorase Staining as Measure of iNOS Expression

NADPH diaphorase staining can be used to visualise iNOS expression in cultured glia and nNOS expression in neurones (20). Nitric oxide synthase (NOS) is an NADPH diaphorase, and using a chromogen (nitroblue tetrazolium, NBT), and NADPH

as the reductant, diaphorase staining can be used to detect cells with NOS activity. Following treatment (with cytokines or untreated) the neuronal/glial cultures are fixed with 4% paraformaldehyde in phosphate buffer for 30 min at 4°C. After fixation, cells are incubated with 0.3% Triton X-100 (in phosphate buffer) for 5 min. Cells are then incubated for 2 h at 37°C with 0.3% Triton X-100 containing 1 mg/mL NADPH and 0.2 mg/mL NBT. Cells are washed once and then viewed using an inverted light microscope (Leica). nNOS-expressing neurones give a light staining, but iNOS-expressing glia can be very dark.

5.7. Peroxynitrite Production Measured by Dihydrorhodamine Oxidation

The cellular formation of peroxynitrite ($ONOO^-$) can be determined from the peroxynitrite-mediated oxidation of non-fluorescent dihydrorhodamine-1,2,3 (DHR) to fluorescent rhodamine-1,2,3 (19). Dihydrorhodamine can enter cells so it will measure both intra- and extracellular oxidants. The product rhodamine will accumulate in mitochondria. For example, a suspension of 10^6 cells/mL of LPS/IFN-γ-activated microglia in Krebs–HEPES buffer (at 37°C) was stirred in a cuvette/plate with 5 μm dihydrorhodamine in a spectrofluorophotometer or plate reader (excitation wavelength of 500 nm, emission wavelength of 536 nm), the rate of fluorescence increase being equal to the rate of peroxynitrite production (19). Peroxynitrite production may be stimulated by adding PMA (10 ng/mL, to activate the NADPH oxidase) and L-arginine (1 mM, substrate for NOS), or inhibited by adding urate (100 μM, peroxynitrite scavenger) or L-NAME (1 mM, NOS inhibitor) or 1400W (100 μM, iNOS inhibitor). Note that other oxidants can oxidise dihydrorhodamine, so it is important to include controls with specific peroxynitrite scavengers.

5.8. Peroxynitrite Production Measured by 3-Nitrotyrosine Immuno-Cytochemistry

Peroxynitrite reacts with tyrosine residues in proteins to yield 3-nitrotyrosine (3-NT) residues, and there are antibodies that bind specifically to this protein modification, which thus enables visualisation of where peroxynitrite has been produced and reacted (20). Cultures are fixed with 4% paraformaldehyde and then incubated with 10 μg/mL of anti-nitrotyrosine monoclonal antibody (Upstate). The primary antibody may be detected, e.g., using a Cy3-conjugated secondary antibody (Jackson ImmunoResearch Laboratories). 3-NT-positive cells are visualised using a fluorescence microscope (excitation 546 nm, emission 590 nm). 3-NT immunostaining can be combined with staining for markers of specific cell types (see Sect. 3) to determine the site of production/action of peroxynitrite.

5.9. Phagocytosis Assays

The phagocytic activity of microglia can be followed by measuring the uptake of fluorescent beads or fluorescently labelled cells. For example, pure microglia isolated from glial cultures are plated at a density of 5×10^4 cells on poly-L-lysine coated 24-well plates.

Cells are left to adhere overnight and then stimulated with 100 ng/mL LPS or 50 ng/mL GM-CSF for 24 h. Three microlitres of a 1:10 dilution of carboxylate-modified microspheres (1 μm Fluospheres, Invitrogen) are added to the wells and incubated with the cells for 2 h, 37°C, 5% CO_2. The medium is removed, and cells are detached by mechanical agitation after addition of ice-cold culture medium to arrest uptake. Cells are spun down at 150 g, 7 min, RT, the supernatant is removed as completely as possible and cells are resuspended in 50 μL DMEM containing isolectin-B4 and Hoechst 33342 (to stain microglia and all nuclei, respectively). After staining, the number of beads per cell is counted using a fluorescence microscope.

Acknowledgements

Relevant research in our laboratory has been funded by the Wellcome Trust, Medical Research Council, British Heart Foundation, Alzheimer's Research Trust (UK) and European Commission Joint Research Centre (Italy).

References

1. Klegeris A, McGeer EG, McGeer PL (2007) Therapeutic approaches to inflammation in neurodegenerative disease. Curr Opin Neurol 20:351–357
2. Zipp F, Aktas O (2006) The brain as a target of inflammation: common pathways link inflammatory and neurodegenerative diseases. Trends Neurosci 29:518–527
3. Lucas SM, Rothwell NJ, Gibson RM (2006) The role of inflammation in CNS injury and disease. Br J Pharmacol 147(Suppl 1): S232–S240
4. Brown GC, Bal-Price A (2003) Inflammatory neurodegeneration mediated by nitric oxide, glutamate, and mitochondria. Mol Neurobiol 27:325–355
5. Block ML, Zecca L, Hong JS (2007) Microglia-mediated neurotoxicity: uncovering the molecular mechanisms. Nat Rev Neurosci 8:57–69
6. Wyss-Coray T (2006) Inflammation in Alzheimer disease: driving force, bystander or beneficial response? Nature Medicine 12:1005–1015
7. Boveri M, Kinsner A, Berezowski V, Lenfant AM, Draing C, Cecchelli R, Dehouck MP, Hartung T, Prieto P, Bal-Price A (2006) Highly purified lipoteichoic acid from gram-positive bacteria induces in vitro blood–brain barrier disruption through glia activation: role of pro-inflammatory cytokines and nitric oxide. Neuroscience 137(4):1193–1209
8. Ransohoff RM, Perry VH (2009) Microglial physiology: unique stimuli, specialized responses. Microglial physiology: unique stimuli, specialized responses. Annu Rev Immunol 27:119–145
9. Kirkpatrick LL, Brady ST (1999) In Basic Neurochemistry: molecular, cellular and medical aspects. (Siegel G. J. et al., eds). Lippincott Williams and Wilkins, Philadelphia, pp 155–173
10. Binder LI, Frankfurter A, Rebhun LI (1986) Differential localization of MAP-2 and tau in mammalian neurons in situ. Ann N Y Acad Sci 466:145–166
11. Mullen R, Buck C, Smith A (1992) NeuN, a neuronal specific nuclear protein in vertebrates. Development 116:201–211
12. Kim KK, Adelstein RS, Kawamoto S (2009) Identification of neuronal nuclei (NeuN) as Fox-3, a new member of the Fox-1 gene family of splicing factors. J Biol Chem 284(45):31052–61
13. Raine CS (1999) In Basic Neurochemistry: molecular, cellular and medical aspects. (Siegel G. J. et al., eds). Lippincott, Williams & Wilkins, Philadelphia, pp 3–30

14. Streit WJ (1990) An improved staining method for rat microglial cells using the lectin from Griffonia simplicifolia (GSA I-B4). J Histochem Cytochem 38:1683–1686
15. Colton C, Abel C, Patchett J, Keri J, Yao J (1992) Lectin staining of cultured CNS microglia. J Histochem Cytochem 40:505–512
16. Milligan CE, Cunningham TJ, Levitt P (1991) Differential immunochemical markers reveal the normal distribution of brain macrophages and microglia in the developing rat brain. Comp Neurol 314:125–135
17. Davis EJ, Foster TD, Thomas WE (1994) Cellular forms and functions of brain microglia. Brain Res Bull 34:73–78
18. Kinsner A, Pilotto V, Deininger S, Brown GC, Coecke S, Hartung T, Bal-Price A (2005) Inflammatory neurodegeneration induced by lipoteichoic acid from Staphylococcus aureus is mediated by glia activation, nitrosative and oxidative stress and caspase activation.J Neurochem 95: 1132–1143
19. Bal-Price A, Matthias A, Brown GC (2002) Stimulation of the NADPH oxidase in activated rat microglia removes nitric oxide but induces peroxynitrite production. J Neurochem 80:73–80
20. Mander PK, Brown GC (2005) Activation of microglial NADPH oxidase is synergistic with glial iNOS expression in inducing neuronal death: a dual-key mechanism of inflammatory neurodegeneration. Journal of Neuroinflammation 2:20–25
21. Misko TP, Schilling RJ, Salvemini D, Moore WM, Currie MG (1993) A fluorometric assay for the measurement of nitrite in biological samples. Anal Biochem 214:11–16

Chapter 17

Neuronal Oxidative Injury and Biomarkers of Lipid Peroxidation

Dejan Milatovic and Michael Aschner

Abstract

Oxidative stress is implicated as one of the major underlying mechanisms in a variety of human diseases. Reactive radicals, derived primarily from molecular oxygen, readily attack a variety of critical biological molecules, including DNA, cellular proteins, and lipids. Since lipid peroxidation is a central feature of cerebral oxidant injury, measurements of peroxidation products, such as F_2-isoprostanes (F_2-IsoPs) and F_4-neuroprostanes (F_4-NeuroPs), represent the most accurate approaches to identify oxidative injury in vivo. Our laboratory uses a gas chromatography/mass spectrometry negative ion chemical ionization with select ion monitoring for quantification of these biomarkers of oxidative stress in a plethora of biological media. This review summarizes state-of-the-art methodology for F_2-IsoPs and F_4-NeuroPs analyses and discusses the utility of these prostaglandin-like compounds as in vivo biomarkers of neuronal oxidative injury.

Key words: F_2-isoprostanes, F_4-neuroprostanes, Oxidative damage, Lipid peroxidation, Neuronal tissue

1. Introduction

Oxidative stress is implicated as one of the major underlying mechanisms in a variety of human diseases including cardiovascular and neurodegenerative diseases and even normal aging processes. Excess formation of free radicals may overwhelm the capacity of endogenous cellular antioxidant defense mechanisms, cause alterations in normal cell and organ physiology, and even activate and/or accelerate disease processes. Increased generation of free radicals derived primarily from molecular oxygen can attack a variety of critical biological materials, including DNA, essential cellular proteins, and lipids. The brain is especially susceptible to oxidative damage because of its great consumption of oxygen,

Michael Aschner et al. (eds.), *Cell Culture Techniques*, Neuromethods, vol. 56,
DOI 10.1007/978-1-61779-077-5_17,

glucose, and energy, as well as relatively low levels of antioxidants (1, 2). In addition, the high content of unsaturated lipids in the brain leads to pronounced lipid peroxidation, the central feature of oxidant injury in the brain.

Lipid peroxidation is the mechanism by which lipids are attacked by chemical species that have sufficient reactivity to abstract a hydrogen atom from a methylene carbon in their chain. Lipid peroxidation in vivo, through a free radical pathway, requires a polyunsaturated fatty acid (PUFA) and a reactant oxidant inducer that together form a free radical intermediate. The free radical intermediate subsequently reacts with oxygen to generate a peroxyl radical, which with unpaired electrons may additionally abstract a hydrogen atom from another PUFA. Greater number of double bonds in the molecule and higher instability of hydrogen atom adjacent to the double bond explain why unsaturated lipids are particularly susceptible to peroxidation (3, 4). Therefore, lipids are readily attacked by free radicals, resulting in the formation of a number of peroxidation products. F_2-isoprostanes (F_2-IsoPs) are one group of these compounds, which are derived by the free radical peroxidation of arachidonic acid (AA, C20:4, ω-6).

The measurement of the F_2-IsoPs, prostaglandin (PG)-like compounds, is one of the most accurate approaches to measure oxidative injury in vivo (5). Initially, their formation involves the generation of four positional peroxyl radical isomers of arachidonate, which undergo endocyclization to PGG_2-like compounds. These intermediates are reduced to form four F_2-IsoP regioisomers, each of which can consist of eight racemic diastereomers (6). In contrast to cyclooxygenase (COX)-derived PGs, nonenzymatic generation of F_2-IsoPs favors the formation of compounds in which the stereochemistry of the side chains has a *cis* orientation in relation to the prostane ring. A second important difference between F_2-IsoPs and PGs is that F_2-IsoPs are formed primarily in situ, esterified to phospholipids, and subsequently released by a phospholipases (7, 8), whereas PGs are generated only from free AA (6).

F_2-IsoPs analogs may be formed by peroxidation of other PUFA substrates, such as eicosapentaenoic acid (EPA, C20:5, ω-3) that leads to the production of F_3-IsoPs, and docosahexaenoic acid (DHA, C22:6, ω-3) that generates F_4-IsoPs. The latter compounds are also termed neuroprostanes (F_4-NeuroPs), due to the high levels of their precursor in brain (9). In contrast to AA, which is evenly distributed in all cell types in all tissues, DHA is highly concentrated in neuronal membranes (10). DHA is obtained mainly through dietary means as the human body can only minimally synthesize this fatty acid. DHA deficiency has been linked to slow mental development (11), while DHA supplementation has been linked to a variety of health benefits including decreased rates of neurodegenerative diseases (12). DHA can

undergo oxidation both in vitro and in vivo, and increased units of unsaturation suggest its higher susceptibility to lipid peroxidation than AA. Thus, while the measurement of F_2-IsoPs provides an index of global oxidative damage in the brain, integrating data from both glial and neuronal cells, determination of F_4-NeuroPs permits the specific quantification of oxidative damage to neuronal membranes in vivo. In fact, to our knowledge, F_4-NeuroPs are the only quantitative in vivo marker of oxidative damage that is selective for neurons. This is particularly important because of the implication of oxidative damage and lipid peroxidation being causative factors in numerous neurodegenerative diseases (13, 14).

Several methods have been developed to quantify the F_2-IsoPs from biological materials (15). Our laboratory uses a gas chromatography/mass spectrometry (GC/MS) to quantify the F_2-IsoPs, methodology which was originally established at our University (by the pioneering work of Dr. Roberts and Dr. Morrow, Vanderbilt University Medical School) (6, 7). More specifically, after isolation and derivatization of the F_2-IsoPs, we take advantage of stable isotope dilution, negative ion chemical ionization (NICI) GC/MS with select ion monitoring (SIM) for quantification. This methodology allows the lower limit of detection of the F_2-IsoPs to be in the low picogram range. These properties, along with the assay's high sensitivity and specificity, allow the F_2-IsoPs to be excellent biomarkers of and the most robust and sensitive measure of oxidative stress in vivo. In addition, we will outline the difference in methodology for quantification of F_4-NeuroPs. Accordingly, we highlight these methods in the present review and address its advantages and shortcomings. Description of the methodologies for quantification of these biomarkers of oxidative injury is followed by concrete examples of measurements of F_2-IsoPs and F_4-NeuroPs in studies conducted by our laboratory.

2. Materials

1. Tissue samples, fresh or frozen. It is important to process tissue samples immediately after isolation or assure their immediate storage at −80°C for later quantification.
2. Blade homogenizer (e.g., Kinematica Polytron® PT 10-35; Brinkmann Instruments, Westbury, NY) and sonicator (e.g., Utrasonic Bath, Fisher Scientific) are used for tissue processing.
3. Folch solution: 2:1 (v/v) chloroform/methanol, ice-cold, containing 0.005% (w/v) butylated hydroxytoluene (BHT; Sigma-Aldrich, cat. no. B1378). Free radical scavenging agent

such as BHT is added to the organic solvent during extraction of phospholipids (18) to prevent oxidation and formation of F_2-IsoPs.

4. Solution of NaCl (0.9%, w/v). Stored at room temperature.
5. Organic solvents including ethyl acetate, heptane, chloroform, ethanol, acetonitrile, and methanol, with and without 0.005% (v/v) BHT. Solutions are prepared as volume/volume ratio.
6. Fifteen percent potassium hydroxide solution (KOH, w/v) is used to release esterified isoprostanes.
7. One molar hydrochloric acid (1 M HCl) and pH 3 water, adjusted by adding 1 N HCl, is used to acidify the sample before solid-phase extraction (SPE) (see Note 3).
8. Deuterated standard, deuterium-labeled isoprostane, [$^2H_4$]15-F_{2t}-IsoP (8-iso-$PGF_2\alpha$) (Cayman Chemical, Ann Arbor, MI, cat. no. 316351) (see Note 4).
9. Anhydrous Na_2SO_4 is used to dry ethyl acetate/heptane eluate from the C18 Sep-Pak (see Note 5).
10. Sep-Pak Plus C18 cartridge (Waters Associates, Milford, MA, cat. no. WAT03657), Silica Sep-Pak cartridge (Waters, Milford, MA, cat. no. WAT036580), and 10-ml plastic syringe (Laboratory Supply; SMJ512878) are used for normal-phase SPE.
11. Pentafluorobenzyl bromide (PFBB; Sigma-Aldrich, cat. no. 10105-2) and *N,N*-diisopropylethylamine (DIPE; Sigma-Aldrich, cat. no.D3887) are prepared as 10% solutions (v/v) in anhydrous acetonitrile.
12. Thin-layer chromatography (TLC) plates, 5 × 20 cm glass plates covered with a 250-μm layer of silica gel particles 60 Å in diameter (Partisil LK6D; Whatman, Maidstone, England, cat. no. WC486562IV) and TLC developing chamber (e.g., VWR).
13. TLC standard, prostaglandin $F_2\alpha$ ($PGF_2\alpha$) methyl ester is diluted in methanol (Cayman Chemical, Ann Arbor, MI, cat. no. 16011).
14. Ten percent phosphomolybdic acid in ethanol (Sigma Chemical Co., St. Louis, MO, cat. no. P4869) is used to visualize sample migration on TLC plates wormed with hot plate (e.g., Corning, cat. no. 6795-200).
15. Dimethylformamide (DMF, Sigma-Aldrich, cat. no. 6407) and undecane are stored over calcium hydride to prevent water accumulation (see Note 8).
16. *Bis*(trimethylsilyl)trifluoroacetamide (BSTFA, Supelco, cat. no. 33084) is stored at room temperature.

17. 15-ml polypropylene culture tube with cap, 20-ml scintillation vial, 5-ml glass Reacti-Vial with Teflon-lined cap (e.g., Supelco, cat. No.33299) and 1.5-ml microcentrifuge tube are used for sample processing/chemical reactions.
18. Nitrogen gas and methane are used for sample evaporations and mass spectrometry.
19. Temperature-controlled water bath, centrifuge, 95°C oven and hair dryer.
20. 15-m, 0.25-mm diameter, 0.25-μm film thickness, DB1701-fused silica capillary GC column (Fisons, Folsum, CA) and GC/MS system (e.g., Hewlett Packard 5982A interfaced with an IBM Pentium computer).

3. Methods

Measurement of F_2-IsoPs has revolutionized our ability to quantify oxidative injury in vivo. F_2-IsoPs are stable, robust molecules and are detectable not only in neuronal tissues, but also in other tissues and biological fluids, such as plasma, urine, cerebrospinal fluid (CSF), and bronchoalveolar lavage fluid. As F_2-IsoPs can be readily generated ex vivo in biological materials containing arachidonoyl-containing lipids, it is important to process the samples immediately after isolation or assure their immediate storage at −80°C for later quantification. Formation of F_2-IsoPs does not occur if a free radical scavenging agent like BHT is added to the organic solvent during extraction of phospholipids (16) or if the samples are rapidly frozen in liquid nitrogen prior to placement at −80°C.

3.1. Lipid Extraction and Hydrolysis of F_2-IsoPs-Containing Phospholipids in Tissue Samples

Formation of F_2-IsoPs occurs in situ in the phospholipid bilayer and then subsequently released in free form. This creates two forms of F_2-IsoPs, one that remains esterified in the membrane and a second that is hydrolyzed and released in free form. To quantify total F_2-IsoPs formation, both free and esterified F_2-isoPs are analyzed. It is necessary to extract the phospholipids from the tissue and release the F_2-isoPs from the phospholipids via base hydrolysis (Fig. 1).

1. Fresh or frozen samples (0.05–0.25 g) are added in ice-cold 5 ml of Folch solution (chloroform:methanol, 2:1, v/v) containing 0.005% BHT in a polypropylene culture tube with cap. The tissue is then homogenized with a blade homogenizer for approximately 30 s. The second aliquot of ice-cold Folch solution, added to a separate culture tube, is used to wash the blade homogenizer and to ensure that all sample

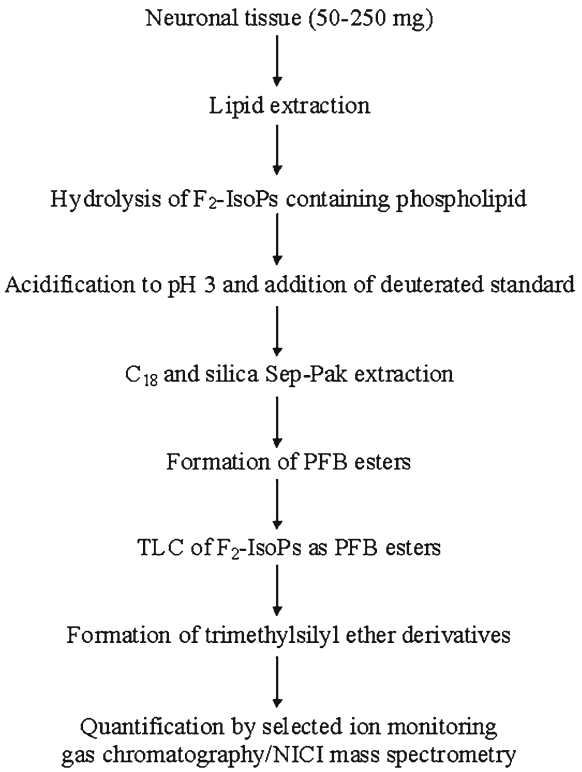

Fig. 1. Schematic representation of the procedure for the extraction, purification, derivatization, and mass spectrometric analysis of F_2-IsoPs from neural tissues.

tissue is recovered as tissue can adhere to or become lodged inside the blade of the homogenizer. The two aliquots are then combined, covered with a nitrogen blanket, and mixed every 10 min over 30 min at 25°C to allow maximal extraction of lipids from homogenized tissue.

Note 1: Presence of BHT during extraction and hydrolysis is important in order to inhibit ex vivo formation of F_2-IsoPs; since polystyrene is not resistant to chloroform and its subsequent interference with the analytical procedures, it is recommended that lipid extraction be carried out in polypropylene tubes kept on ice.

2. The lipid extracts are mixed vigorously with 2.0 ml NaCl (0.9%, w/v), and the phases separated by centrifugation at $800 \times g$ for 10 min at 25°C. After centrifugation, the upper aqueous layer is discarded and the lower organic layer is carefully separated from the intermediate semisolid proteinaceous layer. The organic layer is then evaporated to dryness under a stream of nitrogen.

Note 2: The organic layer and the proteinaceous layer can be readily separated by carefully pouring off the organic layer

into a new culture tube. If the proteinaceous layer is small, because of the type and size of the tissue sample, it is often easier to remove the aqueous and proteinaceous layers simultaneously via suction. However, care must be taken not to compromise the organic phase if this approach is used.

3. Total lipids are dissolved in 0.5 ml methanol containing BHT (0.005%), stored at −80°C or, if further processed, 0.5 ml of aqueous KOH (15%) added to the residue, and thus lipid extracts are saponified to release esterified isoprostanes. The mixture is sonicated and mixed vigorously until thoroughly suspended and heated at 37°C for 30 min to affect hydrolysis and release of the F_2-IsoPs. The mixture is then acidified to pH 3 with 1 M HCl (~1.2 ml) and diluted to a final volume of 10 ml with pH 3 water in preparation for purification of F_2-IsoPs with SPE.

   Note 3: It is important to dilute the methanol in this solution to 5% or less to ensure proper column extraction of free F_2-IsoPs in the subsequent purification procedure.

3.2. Sample Purification for Mass Spectrometric Analysis

1. Following acidification of the sample to pH 3 with 1 M HCl, 200–1,000 pg of deuterated standard is added. The mixture is vortexed and F_2-IsoPs isolated using reversed-phase and normal-phase SPE.

   Note 4: The internal standard is a deuterium-labeled isoprostane, [$^2H_4$]15-F_{2t}-IsoP (8-iso-$PGF_{2\alpha}$). The amount of internal standard added depends on the levels of F_2-IsoPs in the sample as well as the sensitivity of the mass spectrometer. For low-level samples such as CSF, less internal standard needs to be added. Samples that consist of a particularly large amount of tissue will require more internal standard. This is because complex tissues such as brain, despite our best purification efforts, will still contain some unwanted compounds that may potentially have the same *m/z* (mass-to-charge) ratio as the internal standard when analyzed by GC/MS. Increasing the amount of internal standard to 1,000 pg in these samples minimizes the variability in the internal standard ion channel due to contamination in the tissue sample.

2. A 10-ml plastic syringe is used to elute the sample and subsequent solvents through the Sep-Pak cartridge. For reverse phase, Sep-Pak Plus C18 columns (each cartridge contains 500 mg of C18) are preconditioned with 5 ml methanol (flow rate, ~1.0 ml/min) and 7.0 ml H_2O (adjusted to pH 3.0 with 1.0 N HCl). Once the sample has been added, the column is washed sequentially with 10 ml of water (pH 3) and 10 ml of heptane, which removes nonpolar contaminates including unoxidized AA. The F_2-IsoPs are eluted with 10 ml of ethyl acetate/heptane (50:50, v/v) into a 20-ml scintillation vial.

3. The ethyl acetate/heptane eluate from the C18 Sep-Pak is then dried over anhydrous Na_2SO_4 and applied to a silica Sep-Pak cartridge (each cartridge contains 500 mg of silica), which has been preconditioned with 5 ml of ethyl acetate. Once the sample has been added, the column is washed with 5 ml of ethyl acetate and the F_2-IsoPs are eluted with 5 ml of ethyl acetate/methanol (50:50, v/v) into a 5-ml glass reacta-vial (with Teflon-lined cap). For normal-phase SPE, Sep-Pak Plus Silica columns are used with a flow rate of ~0.5 ml/min throughout.

   Note 5: Drying of ethyl acetate/heptane eluate should be completed promptly, as Na_2SO_4 has been shown to adsorb lipids to some degree. Care must be taken not to transfer any Na_2SO_4 to the silica Sep-Pak cartridge.

3.3. Conversion of F_2-IsoPs to Corresponding Pentafluorbenzyl Esters

1. Isoprostanes isolated in ethyl acetate/methanol eluate by SPE are dried at 37°C under a nitrogen stream and derivatized to pentafluorbenzyl (PFB) esters. Samples are vigorously mixed with 40 µl PFBB:anhydrous acetonitrile (10:90, v/v) plus 20 µl diisopropylethylamine:anhydrous acetonitrile (10:90, v/v). Following reaction at 37°C for 20 min, the esters are dried under a nitrogen stream and dissolved in 50 µl chloroform:methanol (2:3, v/v).

   Note 6: Do not work outside of a well-ventilated hood because PFBB is a potent lachrymator.

3.4. Tin Layer Chromatography

1. TLC is accomplished with 5 × 20 cm glass plates covered with a 250 µm layer of silica gel particles 60 Å in diameter. Just before use, the plates are washed with ethyl acetate:ethanol (90:10, v/v), activated at 95°C for 20 min, and cooled in a dessicator. A TLC chamber is lined with filter paper and conditioned 30 min with 100 ml chloroform:ethanol (93:7, v/v).
2. Dissolved samples in chloroform:methanol (50 µl) are applied to the upper half of preadsorbent in four prescored lanes and dried 5–10 s with a hair dryer. Sample plates are added to both ends of the chamber. In contrast, TLC standard (5 µg of the methyl ester of $PGF_2\alpha$/5 µl CH_3OH) is applied to a separate plate that is positioned towards the center of the TLC chamber. After the chamber is rapidly closed, solvent is allowed to migrate 13 cm, and the plates removed.
3. Samples are scraped from silica plates in the region of the TLC standard and visualized by spraying with a 10% solution of phosphomolybdic acid in ethanol followed by heating. The areas 1 cm below and 1 cm above $PGF_2\alpha$ (R_f ~ 0.15) are scraped and extracted from the silica with 1 ml of ethyl acetate.
4. Following centrifugation at 13,000 × *g* for 3 min at 4°C, isoprostane pentafluorobenzyl esters in the ethyl acetate are

transferred into a virgin microcentrifuge tube and stored at –80°C or samples further processed for the GC-MS analysis.

Note 7: Ethyl acetate should be carefully removed without disrupting the silica pellet in the bottom of the tube (silica may affect the instrument's sensitivity). Avoid applying samples to the first 1 cm of the plate and do not spray the sample plate.

3.5. Formation of Trimethylsilyl Ether Derivatives and Quantification of F_2-IsoPs

1. Once dried under a nitrogen stream, samples are dissolved in 8 µl DMF and mixed with 20 µl *bis*(trimethylsilyl) trifluoroacetamide (BSTFA) to covert the residue to the trimethylsilyl ether derivatives.
2. After heating for 5.0 min at 37°C, silylated samples are dried at 37°C under a nitrogen stream, redissolved in 20 µl of undecane, which has been dried over calcium hydride, and transferred into autosampler vial for GC-MS analysis.

   Note 8: DMF should be stored over calcium hydride to prevent water accumulation. Similarly to the amount of internal standard that is added to a sample, consideration should be given to the amount of undecane that is used to dissolve the derivatized sample. The amount added will depend on the levels of F_2-IsoPs. Samples that are rich in F_2-IsoPs will require greater amounts of undecane to keep them from overloading the column during GC. Likewise, low-level samples will require less undecane in order for the GC/MS signal to be of sufficient intensity for optimal quantification.
3. For quantification of F_2-IsoPs, we routinely use a Hewlett Packard 5982A GC/MS system interfaced with an IBM Pentium computer. GC is performed using a 15-m, 0.25-mm diameter, 0.25-µm film thickness, DB1701-fused silica capillary column. The column temperature is programmed from 190 to 290° at 20°/min. Methane is used as the carrier gas for NICI at a flow rate of 1 ml/min. Ion source temperature is 250°C, electron energy is 70 eV, and the filament current is 0.25 mA.

   The major ions generated in the NICI mass spectra of the pentafluorobenzyl ester, tris-trimethylsilyl ether derivatives of F_2-IsoP are *m/z* 569 and corresponding ion for the $[^2H_4]15$-F_{2t}-IsoP internal standard, *m/z* 573 (Fig. 2). For quantification purposes, we compare the height of the pick containing derivatized F_2-IsoPs (*m/z* 569) with the height of the deuterated internal standard peak (*m/z* 573). Quantification of the F_2-IsoPs levels may be also achieved by comparing the areas of the appropriate peaks in the *m/z* 569 SIM chromatogram of the F_2-IsoPs to that of the peak of the internal standard in the *m/z* 573 SIM chromatogram (Fig. 2).

   The coefficient of variance for the assay is routinely less than 8%.

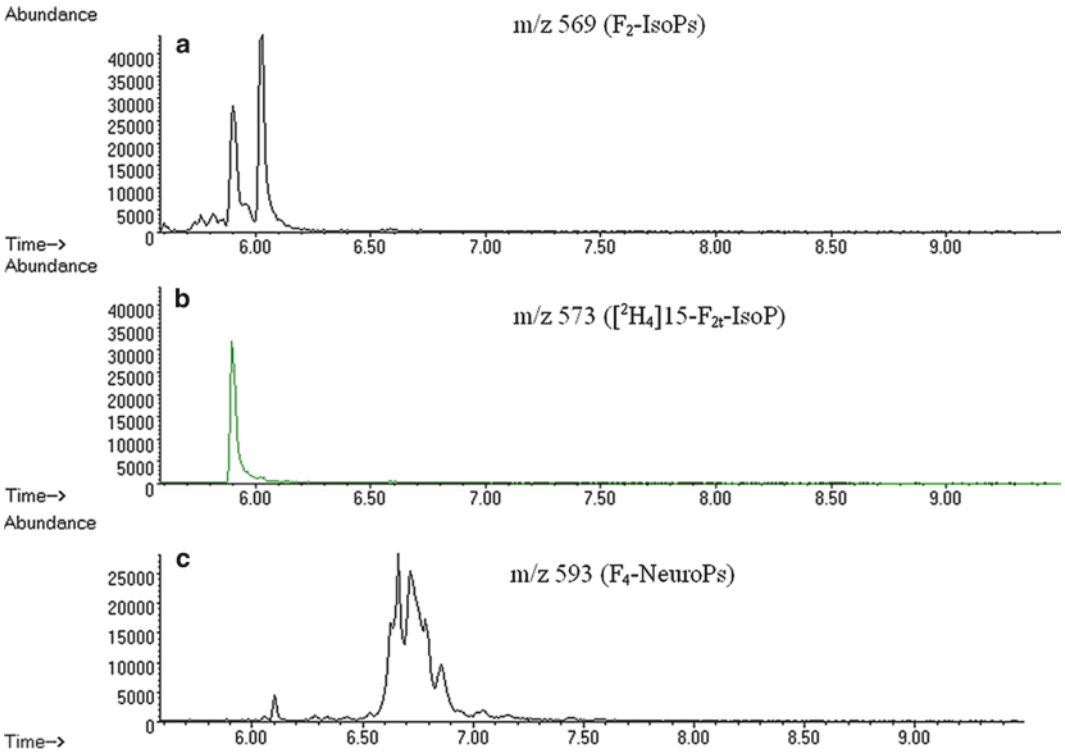

Fig. 2. Chromatograms of F_2-IsoPs and F_4-NeuroPs from mouse cerebrum. Chromatograms plot abundance vs. time (min) with *m/z* 569 chromatogram showing F_2-IsoPs, *m/z* 593 chromatogram showing F_4-NeuroPs, and *m/z* 573 chromatogram showing internal standard.

3.6. Simultaneous Quantification of F_2-IsoPs and F_4-NeuroPs

1. When dealing with brain tissue, we often analyze our biological samples for lipid peroxidation products derived from both AA and DHA simultaneously. Similarity between two assays and the use of a common internal standard allow us to use a single sample to measure both families of compounds by splitting the sample before TLC step. In this case, sample is dissolved in twice the amount of chloroform:methanol (100 µl) after conversion to PFB esters. Then 50 µl are spotted on two separate lanes and the TLC plates are scraped accordingly, 1 cm above and below the methyl ester $PGF_2\alpha$ standard for the F_2-IsoPs and 1 cm below and 4 cm above the standard for the F_4-NeuroPs. This effectively splits a biological sample into two, allowing for individual analysis of both F_2-IsoPs and F_4-NeuroPs.
2. For quantification of F_4-NeuroPs, we evaluate ions generated in the NICI mass spectra as *m/z* 594 and corresponding ion for the $[^2H_4]$15-F_{2t}-IsoP internal standard, *m/z* 573 (Fig. 2). However, for quantification purposes, we compare the area of the pick containing derivatized F_4-NeuroPs (*m/z* 593) with the area of the internal standard peak (*m/z* 573).

4. Timing and Troubleshooting

In general, 12 samples can be assayed for F_2-IsoPs and/or F_4-NeuroPs in approximately 12 h by an experienced investigator. Homogenization, lipid extraction, and hydrolysis of this number of samples require ~3 h; Sep-Pac purifications takes ~2 h; drying, derivatization, and TLC purification requires ~4 h; and drying and silylation requires ~3 h. Though compared to other assays of oxidative stress the time requirement for this assay is relatively large, it is noteworthy that the present assay has the greatest sensitivity and specificity for the detection of lipid peroxidation. Mass spectrometric analysis is automated and each sample requires ~10 min of instrument time. If the peak signal is low or if no peaks are detected by the mass spectrometer, the samples should be removed from the auto sampler vial, washed by ethyl acetate, dried under nitrogen, and the conversion procedure to silylether derivative should be repeated. If the internal standard is detected at *m/z* 573, but there is low or nonexistent peak at 569 or 593, then levels of F_2-IsoPs or F_4-NeuroPs are below the limit of detection. The limit of detection for the assay is ~5 pg.

5. F_2-IsoPs or F_4-NeuroPs Levels in Neuronal Tissues

We have explored cerebral oxidative damage in several models of neurodegeneration including excitotoxicity generated by kainic acid (KA) (14, 17), neurotoxicity associated with anticholinesterase agents (18–20), metals (21, 22), and innate immune activation by lipopolysaccharide (LPS) (23, 24). For glial innate immune response, we have used a single intracerebroventricular (ICV) injection of LPS, a major component of Gram negative bacterial cell walls. We have previously shown that LPS-activated glial innate immune response leads to indirect neuronal oxidative damage and synaptodendritic degeneration exclusively through a CD14-dependent mechanism free of behavioral or febrile response, and that LPS itself has no direct toxic effect on neurons (24, 25). Control mice received ICV PBS, which led to no change in cerebral F_2-IsoPs over 24 h following ICV PBS vehicle; average (+S.D.) basal F_2-IsoPs = 3.2 + 0.3 ng/g. ICV LPS generated delayed cerebral oxidative damage with no significant increase in cerebral F_2-IsoPs, even 10 h after injection. However, following this delay, cerebral oxidative damage peaked at 24 h after ICV LPS administration, returning to near baseline levels by 36 h (14).

In contrast to indirect neuronal damage induced with ICV LPS, there was a rapid onset of detectable oxidative damage upon ICV KA administration which was greatest at the earliest time

point (30 min) following injection, returned to baseline by 60 min, and remained at baseline levels 24 h after injection (17). Kainate is a rigid analog of glutamate and is a very potent stimulant of a subset of ligand-gated ion channels called KA receptors (14, 26). While mice entered status epilepticus within a minute of ICV KA injection, KA-induced seizures did not lead to activated resident inflammatory cells in brain until several days (>4) after exposure, outside of the time frame used in our experiments. Thus, cerebral oxidative damage from these two toxins followed very different temporal profiles. KA led to the rapid onset of cerebral oxidative damage, while LPS led to delayed oxidative damage. In both instances, the magnitude of cerebral oxidative damage achieved in these two models was equivalent and comparable to that observed in diseased regions of brain from patients with Alzheimer's disease (27).

Rat in vivo study with anticholiesterases showed that exposure to diisopropylphosphorofluoridate (DFP), a model compound for organophosphorus (OP) insecticides or nerve agents, induced significant increase in F_2-IsoPs (142%) and F_4-NeuroPs (225%) as early as 30 min after a single acute exposure to DFP (1.25 mg/kg, s.c.) (20) (Fig. 3). Time-course analysis of these cerebral biomarkers of oxidative damage showed transient increase that reached maximum at the time of the most intensive seizure activity (i.e., 1 h after DFP) and returned toward basal levels by 6 h (Fig. 3). The selective increase in F_4-NeuroPs indicates that neurons are specifically targeted by this mechanism (Fig. 3b). Thus, a one-time challenge with DFP produced a transient increase in both F_2-IsoPs and F_4-NeuroPs, which are sensitive and specific in vivo biomarkers of oxidative damage to AA and DHA, respectively.

We have also evaluated metal-induced alterations in biomarker of oxidative damage, F_2-IsoPs, in primary astrocytes and neuronal cultures, as well as the nervous system in vivo. Our data show that primary rat cortical neurons exposed to 1 mM of manganese for 2 h showed structural damage to neurons and twofold increase in F_2-IsoPs levels compared to controls (40.74 ± 5.4 pg/mg protein) (22). Following the same experimental condition, primary astrocytes cultures showed 233% increase in F_2-IsoPs levels compared to control (137.3 pg/mg protein) (21). We have also investigated cerebral oxidative damage in a mouse model of Mn neurotoxicity. Results from this study corroborated in vitro findings and revealed that one-time challenge with Mn (100 mg/kg, i.p.) was sufficient to produce significant increase in mice cerebral biomarkers of oxidative damage, F_2-IsoPs (22). Our previous study also showed that *N*,*N*-diethyldithiocarbamate (DEDC) mediates lipid oxidation and elevation of total copper in peripheral nerve. F_2-isoprostane levels in rat sciatic nerve were significantly elevated in the 2-week DEDC-exposed group (1.9 ng/g of

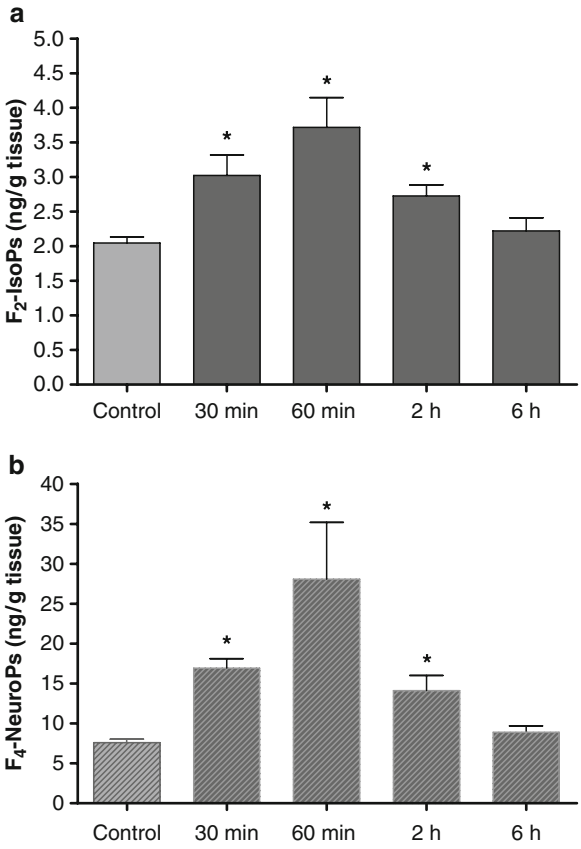

Fig. 3. Cerebral concentrations of F_2-IsoPs (**a**) and F_4-NeuroPs (**b**) following DFP (1.25 mg/kg, s.c.) exposure in rats. Values represent mean ± SEM ($n = 4–6$). *Asterisk* One-way ANOVA had $p < 0.001$ with Bonferroni's multiple comparison tests showing significant difference ($p < 0.05$) for vehicle-injected control vs. DFP treatment.

sciatic nerve) over controls (1.2 ng/g of sciatic nerve) (28). This relationship is consistent with copper-mediated oxidative stress contributing to the myelinopathy.

Combined, quantification of F_2-IsoPs and F_4-NeuroPs has extended our understanding of the role of free radicals in physiological processes and has established the occurrence of oxidative stress in a wide variety of research models and disease states. The method is reproducible and reliable and serves as an excellent platform for future studies on the role of oxidative stress in mediating human disease. Furthermore, the sensitivity of the method offers unique potential for surveying F_2-IsoPs and F_4-NeuroPs concentrations as potential biomarkers of early disease, as they can be reliably and accurately measured in a plethora of biological media.

Acknowledgments

This study was supported by grants from NIH NS057223 (DM), NIEHSES007331,NIEHS10563,andDoDW81XWH-05-1-0239 (MA).

References

1. Floyd RA (1997) Protective action of nitrone-based free radical traps against oxidative damage to the central nervous system. Adv Pharmacol 38:361–378
2. Simonian NA, Coyle JT (1996) Oxidative stress in neurodegenerative diseases. Annu Rev Pharmacol Toxicol 36:83–106
3. Pratico D, Rokach J, Lawson J, FitzGerald GA (2004) F_2-isoprostanes as indices of lipid peroxidation in inflammatory diseases. Chem Phys Lipids 128:165–171
4. Gao L, Yin H, Milne GL, Porter NA, Morrow JD (2006) Formation of F-ring isoprostane-like compounds (F_3-isoprostanes) in vivo from eicosapentaenoic acid. J Biol Chem 281:14092–14099
5. Kadiiska MB, Gladen BC, Baird DD, Germolec D, Graham LB, Parker CE, Nyska A, Wachsman JT, Ames BN, Basu S, Brot N, Fitzgerald GA, Floyd RA, George M, Heinecke JW, Hatch GE, Hensley K, Lawson JA, Marnett LJ, Morrow JD, Murray DM, Plastaras J, Roberts LJ II, Rokach J, Shigenaga MK, Sohal RS, Sun J, Tice RR, Van Thiel DH, Wellner D, Walter PB, Tomer KB, Mason RP, Barrett JC (2005) Biomarkers of oxidative stress study II: are oxidation products of lipids, proteins, and DNA markers of CCl_4 poisoning? Free Radic Biol Med 38:698–710
6. Morrow JD, Hill KE, Burk RF, Nammour TM, Badr KF, Roberts LJ II (1990) A series of prostaglandin F2-like compounds are produced in vivo in humans by a non-cyclooxygenase, free radical-catalyzed mechanism. Proc Natl Acad Sci USA 87:9383–9387
7. Morrow JD, Awad JA, Boss HJ, Blair IA, Roberts LJ II (1992) Non-cyclooxygenase derived prostanoids (F_2-isoprostanes) are formed in situ on phospholipids. Proc Natl Acad Sci USA 89:10721–10725
8. Famm SS, Morrow JD (2003) The isoprostanes: unique products of arachidonic acid oxidation – a review. Curr Med Chem 10:1723–1740
9. Roberts LJ II, Montine TJ, Markesbery WR, Tapper AR, Hardy P, Chemtob S, Dettbarn WD, Morrow JD (1998) Formation of isoprostane-like compounds (neuroprostanes) in vivo from docosahexaenoic acid. J Biol Chem 273:13605–13612
10. Salem N, Kim HY, Lyergey JA (1986) Docosahexaenoic acid: membrane function and metabolism. In: Martin RE (ed) Health effects of polyunsaturated acids in seafoods. Academic, New York, pp 263–317
11. Connor WE, Neuringer M, Reisbick S (1992) Essential fatty acids: the importance of n-3 fatty acids in the retina and brain. Nutr Rev 50:21–29
12. Schaefer EJ, Bongard V, Beiser AS, Lamon-Fava S, Robins SJ, Au R, Tucker KL, Kyle DJ, Wilson PW, Wolf PA (2006) Plasma phosphatidylcholine docosahexaenoic acid content and risk of dementia and Alzheimer disease: the Framingham Heart Study. Arch Neurol 63:1545–1550
13. Montine KS, Quinn JF, Zhang J, Fessel JP, Roberts LJ II, Morrow JD, Montine TJ (2004) Isoprostanes and related products of lipid peroxidation in neurodegenerative diseases. Chem Phys Lipids 128:117–718
14. Milatovic D, VanRollins M, Li K, Montine KS, Montine TJ (2005) Suppression of cerebral oxidative damage from excitotoxicity and innate immune response in vivo by α- or γ-tocopherol. J Chromatogr B 827:88–93
15. Basu S (2008) F_2-isoprostanes in human health and diseases: from molecular mechanisms to clinical implications. Antioxid Redox Signal 10:1405–1434
16. Morrow JD, Roberts LJ (1999) Mass spectrometric quantification of F_2-isoprostanes in biological fluids and tissues as a measure of oxidant stress. Methods Enzymol 300:3–12
17. Zaja-Milatovic S, Gupta RC, Aschner M, Montine TJ, Milatovic D (2008) Pharmacologic suppression of oxidative damage and dendritic degeneration following kainic acid-induced excitotoxicity in mouse cerebrum. Neurotoxicology 29: 621–627

18. Milatovic D, Gupta RC, Aschner M (2006) Anticholinesterase toxicity and oxidative stress. Scientific World J 6:295–310
19. Gupta RC, Milatovic S, Dettbarn W-D, Aschner M, Milatovic D (2007) Neuronal oxidative injury and dendritic damage induced by carbofuran: protection by memantine. Toxicol Appl Pharmacol 219:97–105
20. Zaja-Milatovic S, Gupta RC, Aschner M, Milatovic D (2009) Protection of DFP-induced oxidative damage and neurodegeneration by antioxidants and NMDA receptor antagonist. Toxicol Appl Pharmacol 240:124–131
21. Milatovic D, Yin Z, Gupta RC, Sydoryk M, Albrecht J, Aschner JL, Aschner M (2007) Manganese induces oxidative impairment in cultured rat astrocytes. Toxicol Sci 98:198–205
22. Milatovic D, Zaja-Milatovic S, Gupta RC, Yu Y, Aschner M (2009) Oxidative damage and neurodegeneration in manganese-induced neurotoxicity. Toxicol Appl Pharmacol 240:219–226
23. Milatovic D, Zaja-Milatovic S, Montine KS, Horner PJ, Montine TJ (2003) Pharmacologic suppression of neuronal oxidative damage and dendritic degeneration following direct activation of glial innate immunity in mouse cerebrum. J Neurochem 87:1518–1526
24. Milatovic D, Milatovic S, Montine K, Shie FS, Montine TJ (2004) Neuronal oxidative damage and dendritic degeneration following activation of CD14-dependent innate immunity response in vivo. J Neuroinflamm 1:20
25. Montine TJ, Milatovic D, Gupta RC, Morrow JD, Breyer R (2002) Neuronal oxidative damage from activated innate immunity in EP_2 receptor-dependent. J Neurochem 83: 463–470
26. Ben-Ari Y, Cossart R (2000) Kainate, a double agent that generates seizures: two decades of progress. Trends Neurosci 23:580–587
27. Reich EE, Markesbery WR, Roberts LJ II, Swift JD, Morrow JD, Montine JT (2001) Brain regional quantification of F-ring and D-/E-ring isoprostanes and neuroprostanes in Alzheimer's disease. Am J Pathol 158:293–297
28. Viquez OM, Valentine HL, Amarnath K, Milatovic D, Valentine WM (2008) Copper accumulation and lipid oxidation precede inflammation and myelin lesions in N, N-diethyldithiocarbamate peripheral myelinopathy. Toxicol Appl Pharmacol 229: 77–85

Chapter 18

Analysis of Protein Targets by Oxidative Stress Using the OxyBlot and Biotin–Avidin-Capture Methodology

Jeannette N. Stankowski, Simona G. Codreanu, Daniel C. Liebler, and BethAnn McLaughlin

Abstract

Carbonyl group formation on protein side chains is a common biochemical marker of oxidative stress and is frequently observed in a variety of acute and chronic neurological diseases including stroke, Alzheimer's disease, and Parkinson's disease. Given that proteins are often the immediate targets of cellular oxidative stress, it is of utmost importance to determine how adductions by reactive electrophiles and other oxidative reactions can irreversibly alter protein structure and function. Previously, protein adduction was thought to be a random process, but recently it has become increasingly clear that these protein modifications are specific and selective. In this work, two methodological approaches are presented which allow for the detection of protein carbonyl groups. While the OxyBlot methodology allows for the evaluation of general oxidative stress, the use of the novel and powerful biotin–avidin-capture methodology allows for the identification of specific proteins that have been targeted by oxidative stress.

Key words: Oxidative stress, Ischemic stroke, Biotin–avidin-capture methodology, OxyBlot, Reactive oxygen species, Protein carbonyl groups, Glutamate

1. Introduction

The mitochondrion is the primary cellular site for the generation of reactive oxygen species (ROS), such as superoxide anions ($O_2^{\bullet -}$), hydrogen peroxide (H_2O_2), and hydroxyl radicals ($OH^{\bullet}$). Complex I of the electron transport chain is thought to be the major source of ROS generation within mitochondria (1). Low concentrations of ROS are important for normal cellular function, triggering a variety of physiological events including apoptosis, proliferation, and senescence (1–3). Exposure to ionizing or ultraviolet radiation, growth factors, and cytokines as well as pathological metabolic processes can lead to the production of ROS (4). ROS can damage nucleic acids, proteins, and lipids and

Michael Aschner et al. (eds.), *Cell Culture Techniques*, Neuromethods, vol. 56,
DOI 10.1007/978-1-61779-077-5_18,

the overproduction of ROS has been associated with cellular dysfunction (2, 3).

Cells are equipped with robust cellular antioxidant defense mechanisms that prevent the damaging effects of ROS (4). The major cellular antioxidant is the low molecular weight thiol glutathione (GSH), which scavenges free radicals, conjugates with electrophilic compounds, and reduces peroxides (5). The disruption of this cellular homeostasis is referred to as oxidative stress (6), and it has been identified as a common theme in a variety of acute and chronic neurological diseases, including stroke, Alzheimer's disease, and Parkinson's disease (7–10).

Proteins are oftentimes involved in catalyzing cellular reactions, which renders proteins to be one of the major and most immediate targets of cellular oxidative stress. The loss of function of a protein due to adduction by reactive electrophiles has an overall larger impact on cellular function than any damage conferred to stoichiometric mediators (11). While amino acid residues such as cysteines, histidines, and lysines are solvent-exposed nucleophiles that are readily available for adduction by reactive electrophiles, thereby representing the most common target of ROS, structural features of proteins are also important in conferring susceptibility to damage by electrophiles (12, 13).

A common biochemical marker of oxidative stress is the formation of protein carbonyl groups (aldehydes and ketones) on protein side chains, particularly of prolines, arginines, lysines, and threonines (11, 12, 14–16). Carbonyl groups are composed of a carbon atom double-bonded to an oxygen atom and are formed primarily from lipid electrophiles generated under conditions of oxidative stress (11, 14–17). Electrophile adduction and other oxidative reactions can irreversibly alter protein structure and function (12). The accumulation of oxidatively modified and damaged proteins is a desirable means to evaluate cell stress and novel techniques have been advanced to allow investigators to determine the identity of adducted proteins. This is particularly salient given that, until recently, protein adduction by lipid electrophiles was thought to be a random process (12). It has, however, become increasingly clear that protein adduction by electrophiles is a selective and specific process and that 80% of all proteins can be modified at a single cysteine residue (12). One example of the impact of this subtle posttranslational modification is the adduction of heat shock protein 72 (HSP72) on cysteine 267 (Cys267) by the cytotoxic aldehyde 4-hydroxy-2-nonenal (4-HNE) (12, 18). The primary amino acid targets of 4-HNE on proteins are cysteines, histidines, and lysines, yet 4-HNE can also disrupt protein function via its ability to form Michael adducts and Schiff base products (18). Given that the cysteine residue of interest in HSP72 is located in the ATPase domain of this molecular chaperone,

adduction of Cys267 by free radicals results in the inhibition of HSP72's ATPase activity, thereby rendering this protein non-functional (12, 18).

This observation underscores the importance of identifying the relationship between specific protein modifications by ROS and the changes in protein function that result from these biochemical changes. Understanding how the adduction of a single protein residue can lead to toxicity and cell death will allow us to better understand the pathways triggered by and involved in stress signaling. It will also assist in identifying more effective targets for the development of clinically relevant and effective therapeutics for neurological diseases as well as other diseases. In approaching problems of ROS stress and protein oxidation, investigators have a wide variety of analytical tools available to them. In this work, we present two very different methodological approaches to evaluate general oxidative stress, using the OxyBlot methodology, as well as a powerful new technology which can be used to identify specific proteins targeted by oxidative stress.

2. Principles of the OxyBlot Methodology

The chemical reaction underlying the OxyBlot methodology was initially described by Shacter's group in 1994 (16) and has been extensively employed thereafter (11, 14, 17). Carbonylated proteins are relatively stable, thereby allowing the derivatization of carbonyl groups with 2,4-dinitrophenylhydrazine (DNPH), which leads to the formation of a stable dinitrophenyl (DNP) hydrazone product (Fig. 1). The subsequent separation of oxidatively modified proteins by electrophoresis followed by the identification of the DNP moiety of the protein (Fig. 1) using the Western blot technology and anti-DNP antibodies allows for the rapid and highly sensitive determination of total protein carbonyl formation (11, 14, 16, 17).

The use of the derivatization control solution (negative control, NC) allows for a side-by-side comparison of proteins that have and have not been oxidatively modified. Specifically, bands that are present in the derivatization reaction (DR), but absent in the NC reaction, have undergone modifications. Moreover, with the use of proper controls, the overall intensity of the bands is a correlation to the overall degree of protein oxidation. That is, the more intense the bands are, the more oxidized proteins are present in a given sample.

2.1. Materials for OxyBlot Procedure

All materials required for the OxyBlot procedure are listed below. It should be noted that similar products and equipments may be used from alternate vendors at the user's discretion.

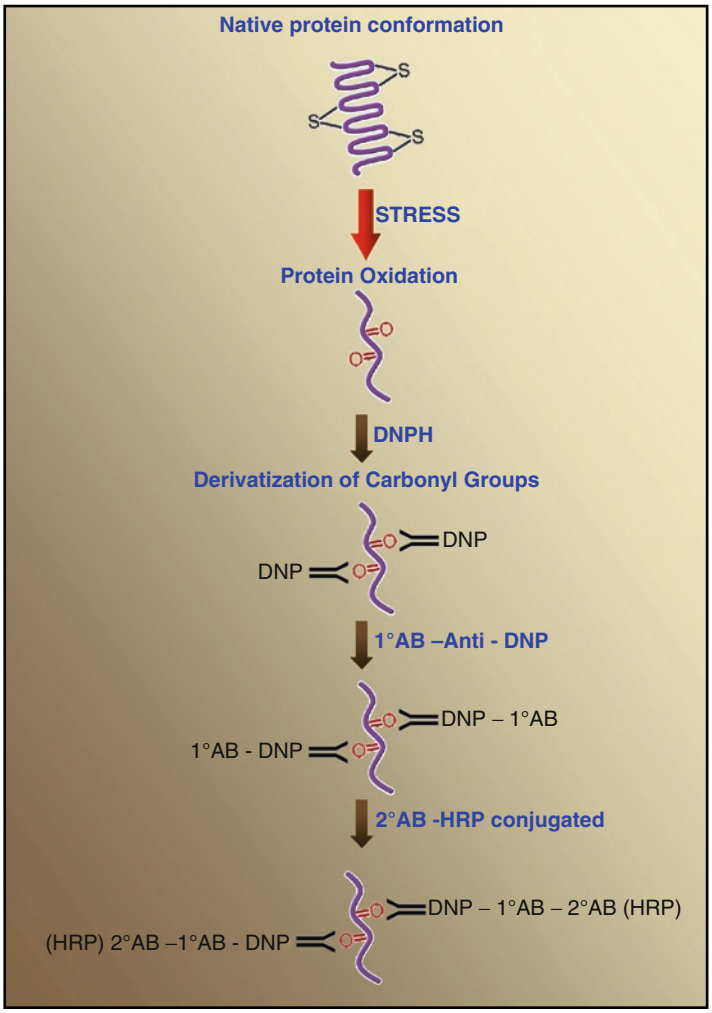

Fig. 1. Schematic of the derivatization of protein carbonyl groups. Cellular exposure to stress results in protein damage characterized by the formation of protein carbonyl groups (side chains). The OxyBlot methodology uses 2,4-dinitrophenylhydrazine (DNPH) to derivatize protein carbonyl groups leading to the formation of a stable dinitrophenyl (DNP) hydrazone product. The primary antibody is directed against the DNP moiety of the protein. The secondary, HRP-conjugated antibody allows for the use of chemiluminescent reagent to visualize bands of oxidized proteins upon exposure to film.

1. The OxyBlot Protein Oxidation Detection Kit (S7150) will be purchased from Chemicon International (Temecula, CA). The mixture of standard proteins with attached DNP residues should be stored at –20°C after the first use. All other reagents can be stored at 4°C.
2. 6-well tissue culture plates.
3. 1.5 ml Eppendorf tubes. For each condition, the following prelabeled Eppendorf tubes are needed:

(a) Sample for protein assay.
(b) Sample for Western blotting.
(c) Sample for OxyBlot.
(d) Derivatization reaction for OxyBlot.
(e) Negative control for OxyBlot.

4. Ice cold 1× PBS (100 ml 10× PBS; 900 ml milliQ H_2O).
5. TNEB (50 mM Tris–HCl, 2 mM EDTA, 100 mM NaCl, and 1%NP-40; pH 7.8) with added protease inhibitor cocktail (P8340, Sigma-Aldrich, St. Louis, MO).
6. Dithiothreitol (DTT; D9779, Sigma-Aldrich, St. Louis, MO). Prepare a 1 M stock solution in milliQ H_2O and store at –20°C. The working concentration of DTT is 50 mM and should not be stored for more than 6 h.
7. Laemmeli buffer (Cat # 161-0737, Bio-Rad Laboratories, Hercules, CA) with β-mercaptoethanol (M7154, Sigma-Aldrich, St. Louis, MO) at a ratio of 1:19.
8. 12% Sodium dodecyl sulfate made in milliQ H_2O (SDS; L3771, Sigma-Aldrich, St. Louis, MO).
9. Bio-Rad D_c Protein Assay kit (Bio-Rad Laboratories, Hercules, CA).

2.2. Materials for the Western Blot Procedure

1. 4–12% Criterion Bis-Tris gels (Cat # 345-0123, Bio-Rad Laboratories, Hercules, CA).
2. Precision Plus Protein Standard All Blue Molecular Weight Marker (Cat # 161-0373, Bio-Rad Laboratories, Hercules, CA).
3. XT-MOPS running buffer (Cat # 161-0788, Bio-Rad Laboratories, Hercules, CA).
4. 1× Tris/Glycine transfer buffer (Cat # 161-0772, Bio-Rad Laboratories, Hercules, CA).
5. Hybond P polyvinylidene difluoride (PVDF) membrane (Cat # RPN303F, GE Healthcare, Piscataway, NJ).
6. Western Lightning Chemiluminescence Reagent Plus (Cat # NEL105, Perkin Elmer Life Sciences, Inc., Boston, MA).
7. Gel Code Blue Stain Reagent (Cat # 24592, Thermo Scientific, Rockford, IL).
8. Methanol (439193, Sigma-Aldrich, St. Louis, MO).
9. Tween 20 (P7949, Sigma-Aldrich, St. Louis, MO).
10. 1× PBS-Tween 20 (0.05% Tween 20).
11. Blocking/dilution buffer (1%BSA/1xPBS-Tween 20).
12. Primary Antibody: Rabbit Anti-DNP antibody (provided in OxyBlot kit).

13. Secondary antibody: Goat Anti-Rabbit IgG (HRP-conjugated) antibody (provided in OxyBlot kit).

2.3. Methods

User-friendly versions of all of the protocols and procedures can be found on our website at http://www.mc.vanderbilt.edu/root/vumc.php?site=mclaughlinlab&doc=17838.

2.3.1. OxyBlot Procedure Using 5 µl of Each Sample

1. Start by scraping cells from the dish using a rubber policeman in 350 µl TNEB with added protease inhibitor cocktail. For each condition, cells grown in two wells of a 6-well plate are combined. A protein concentration of 1 mg/ml is recommended for the OxyBlot methodology.
2. Of this cell suspension, save 50 µl for the determination of protein concentrations (see Note 1), and resuspend 150 µl in an equal volume of Laemmeli Buffer with β-mercaptoethanol, heat sample to 95°C for 10 min, and store at −20°C.
3. Add the remaining 150 µl of the cell suspension into a new Eppendorf tube containing DTT (50 mM) and vortex sample briefly. For longer storage options of samples containing DTT, see Note 2.
4. For the OxyBlot procedure, follow the flow chart outlined in Fig. 2. In brief, 5 µl of the cell lysate designated for the OxyBlot procedure as well as 5 µl 12% SDS should be added into two new Eppendorf tubes, of which one is designated for the DR and the other one for the NC. Next, add 10 µl of 1× DNPH or 1× derivatization control solution into the 1.5 ml Eppendorf tubes designated for the DR or NC, respectively. The sample for the DR will take on an orange color following the addition of DNPH. For the derivatization of larger volumes of cell lysates, see Note 3. For important information about the exposure time of samples in the derivatization solution, see Note 4.
5. Allow samples to incubate at room temperature for 15 min after which 7.5 µl of the neutralization solution should be added to each sample.
6. Store samples at 4°C and run samples on a gel within 7 days of protein derivatization. For longer storage options of samples, see Note 5.

2.3.2. Western Blotting

1. Allow OxyBlot samples to reach room temperature prior to loading samples on a gel. Do not heat samples.
2. For best results, use a gradient gel (e.g., 4–12%).
3. Start loading the gel by adding 10 µl of the Precision Plus Protein Standard All Blue Molecular Weight Marker.
4. Assuring equal protein concentrations of all samples, load the appropriate volume of the OxyBlot samples so that the sample

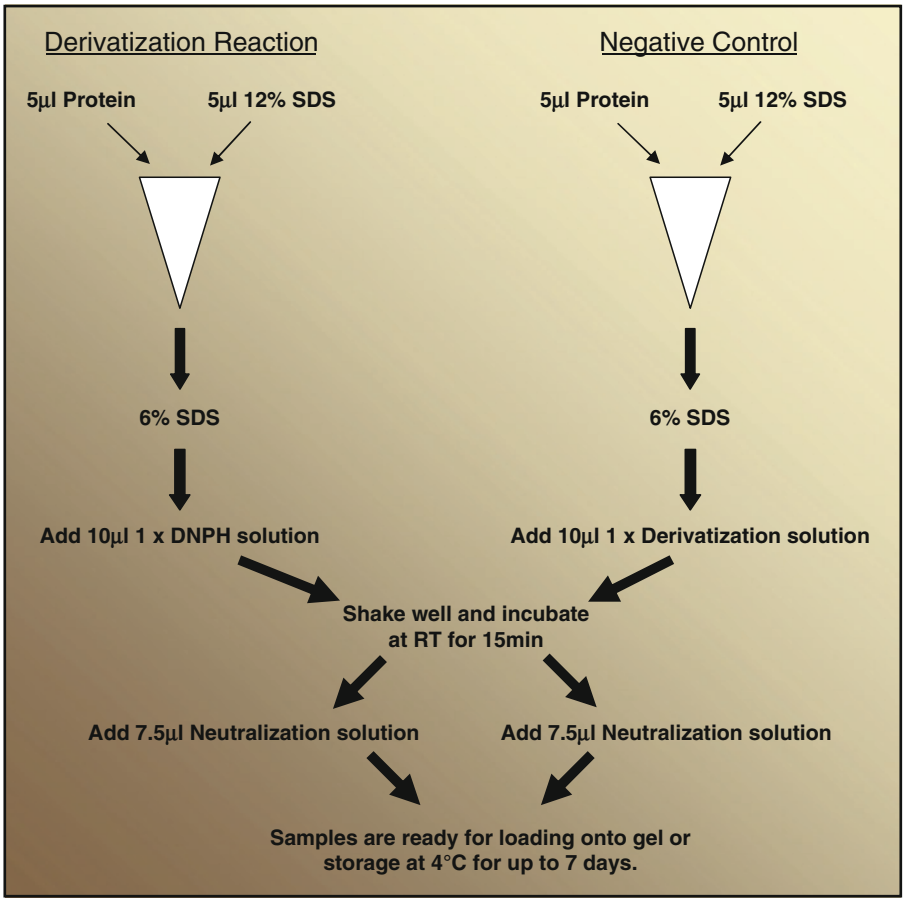

Fig. 2. OxyBlot methodology flow chart. 5 µl sample are added to two prelabeled 1.5 ml Eppendorf tubes, of which one is designated for the derivatization reaction (DR) and the second one for the negative control (NC). 5 µl of 12% SDS are added to each sample to obtain a final concentration of 6% SDS. 10 µl of 1× DNPH or 1× derivatization control solution should be added to samples designated for the DR or NC, respectively. Samples are allowed to incubate for 15 min at room temperature, after which 7.5 µl neutralization solution should be added to each sample. Samples are ready to be processed using gel electrophoresis.

of the DR is next to the sample of the NC. This will allow for a more efficient comparison of bands during analysis. For information about assuring equal protein loading, see Note 6.

5. Follow manufacturer's directions to run the gel.
6. Transfer proteins onto a PVDF membrane by following manufacturer's directions for the used transfer apparatus.
7. Block nonspecific primary antibody binding by placing the membrane into methanol for 5 min.
8. Allow membrane to dry for 15–20 min before placing it into primary antibody.
9. Prepare 15 ml of a 1:150 dilution of the primary antibody provided in the OxyBlot kit in blocking/dilution buffer. For

important information about the primary antibody provided in the OxyBlot kit, see Note 7.

10. Incubate the membrane in the primary antibody overnight at 4°C while shaking on an orbital shaker.
11. Using multiple changes of 1× PBS-Tween 20, wash membrane for a total of 30 min before adding the secondary antibody.
12. Prepare 15 ml of a 1:300 dilution of the secondary antibody provided in the OxyBlot kit in blocking/dilution buffer.
13. Incubate membrane for 1 h at room temperature while shaking on an orbital shaker.
14. Using multiple changes of 1× PBS-Tween 20, wash membrane for a total of 30 min before adding the chemiluminescent reagent according to manufacturer's specifications and exposing the membrane to film.

2.3.3. Interpretation of Data

1. All biological samples will have oxidized proteins with higher levels of total protein oxidation in samples following biological stress.
2. The final result of the OxyBlot procedure will show several bands in the DR sample of each condition (Fig. 3). Bands that are present in the DR but not in the NC have undergone oxidative modifications. For information about exposure times pertinent to the NC samples, see Note 8.

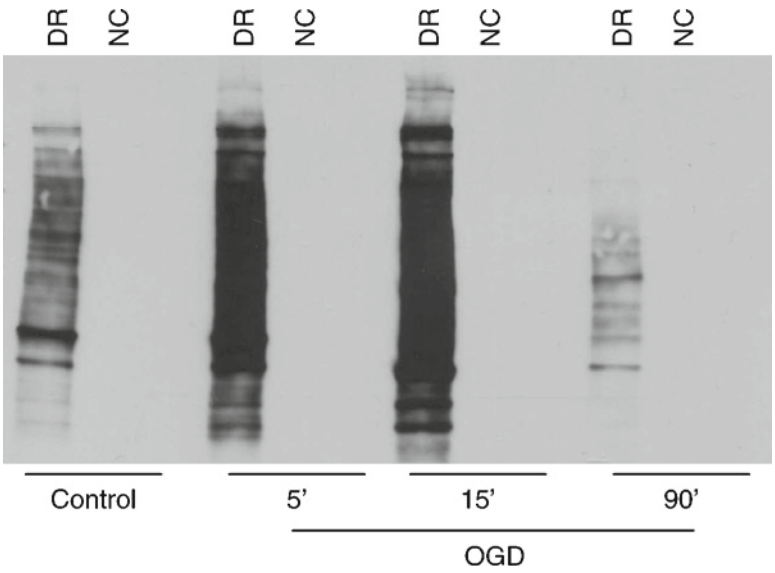

Fig. 3. Neuronal exposure to oxygen glucose deprivation (OGD) results in protein oxidation. Mature neuron-enriched primary forebrain cultures were exposed to OGD for various durations of time (5′, 15′ or 90′) and protein oxidation was determined using the OxyBlot methodology 24 h following termination of OGD. Levels of total oxidized proteins increased robustly following mild (5′) or moderate (15′) OGD, but decreased strongly following exposure to lethal (90′) OGD.

3. The degree of protein oxidation can be identified by the intensity of the bands. That is, the more intense the bands are, the higher is the degree of stress-specific protein oxidation.

3. Principles of the Biotin–Avidin-Capture Methodology

The biotin–avidin-capture methodology combined with immunoblotting is a powerful new technology that allows for the detection of *specific* proteins that have been modified by oxidative stress. This methodology uses biotin hydrazide to covalently label carbonyl groups that have formed on protein side chains upon exposure to oxidative stress (Fig. 4). Using immunoprecipitation, adducted proteins bound to biotin hydrazide are pulled down allowing for the elution of oxidatively modified proteins. The subsequent immunoblotting analysis allows for a rapid screening of proteins of interest to determine if these proteins have been oxidized (Fig. 5) (19).

3.1. Materials for the Biotin–Avidin-Capture Methodology

1. 1.5 ml Clear Eppendorf tubes.
2. Ice cold 1× PBS (100 ml 10× PBS; 900 ml milliQ H_2O).
3. TNEB (50 mM Tris–HCl, 2 mM EDTA, 100 mM NaCl and 1%NP-40; pH 7.8) with added protease inhibitor cocktail (P8340, Sigma-Aldrich, St. Louis, MO).
4. Bio-Rad D_c Protein Assay kit (Bio-Rad Laboratories, Hercules, CA).
5. MilliQ H_2O.
6. Dimethyl sulfoxide (DMSO; D8418, Sigma-Aldrich, St. Louis, MO).
7. Biotin hydrazide (B3770, Sigma-Aldrich, St. Louis, MO). Prepare a 50 mM stock solution in DMSO and prepare freshly before every experiment. The final concentration of biotin hydrazide per sample is 5 mM.
8. Sodium borohydride (213462, Sigma-Aldrich, St. Louis, MO). Prepare a 500 mM stock solution in milliQ H_2O and prepare freshly before every experiment. The final concentration of sodium borohydride is 50 mM.
9. NuPAGE LDS Sample Buffer (4×) (NP0007, Invitrogen, Carlsbad, CA).
10. Amicon Ultra Centrifugal Filter Devices (UFC801024, Millipore, Billerica, MA).
11. Streptavidin Sepharose High-Performance beads (17-5113-01, GE Healthcare, Uppsala, Sweden).

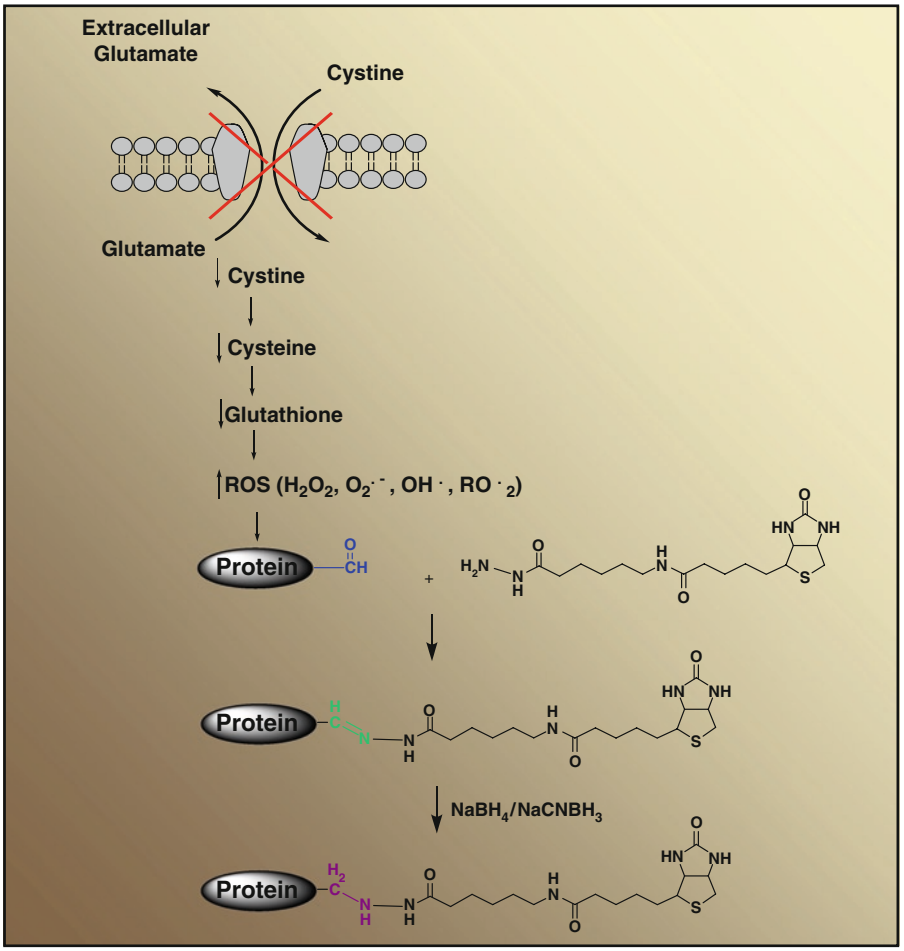

Fig. 4. Schematic of the biotin–avidin-capture methodology. Exposure of HT-22 cells to extracellular glutamate results in the depletion of the main intracellular antioxidant glutathione and the elevation of ROS levels. Protein damage by ROS results in the formation of carbonyl groups on protein side chains (top example) which are derivatized with biotin hydrazide (formation of double bond; middle example). The addition of sodium borohydride reduces the initial Schiff base formed between the carbonyl and biotin hydrazide (formation of single bond; bottom example), thus preventing the reversion of the adduct. The oxidative status of proteins of interest can then be analyzed by using the Western blot methodology. Although the addition of extracellular glutamate is used to induce oxidative stress in the HT-22 model system, interfering with glutathione synthesis at any other step or directly adding reactive oxygen species to the cells are equally effective means to induce oxidative stress.

12. 1% Sodium dodecyl sulfate (SDS; L3771, Sigma-Aldrich, St. Louis, MO).
13. 1 M sodium chloride (NaCl; S9525, Sigma-Aldrich, St. Louis, MO).
14. Dithiothreitol (DTT; D9779, Sigma-Aldrich, St. Louis, MO). Prepare a 1 M stock solution and store at –20°C. The working concentration of DTT is 50 mM and should not be stored for more than 6 h.
15. 4 M urea (U6504, Sigma-Aldrich, St. Louis, MO). Urea has to be freshly prepared before every experiment.

3.2. Materials for the Western Blot Procedure

1. 4–12% Criterion Bis-Tris gels (Cat # 343-0123, Bio-Rad Laboratories, Hercules, CA).
2. Precision Plus Protein Standard All Blue Molecular Weight Markers (Cat # 161-0373, Bio-Rad Laboratories, Hercules, CA).
3. XT-MOPS running buffer (Cat # 161-0788, Bio-Rad Laboratories, Hercules, CA).
4. 1× Tris/Glycine transfer buffer (Cat # 161-0772, Bio-Rad Laboratories, Hercules, CA).
5. Hybond P polyvinylidene difluoride (PVDF) membrane (Cat # RPN303F, GE Healthcare, Piscataway, NJ).
6. Western Lightning Chemiluminescence Reagent Plus (Cat # NEL105, Perkin Elmer Life Sciences, Inc., Boston, MA).
7. Gel Code Blue Stain Reagent (Cat # 24592, Thermo Scientific, Rockford, IL).
8. Methanol (439193, Sigma-Aldrich, St. Louis, MO).
9. Tween 20 (P7949, Sigma-Aldrich, St. Louis, MO).
10. 1× TBS-Tween 20 (100 ml 10× TBS, 900 ml milliQ H_2O, 0.05% Tween 20).
11. Carnation Instant Nonfat Dry Milk Powder (Nestlé, Vevey, Switzerland).
12. Primary antibodies: Rabbit Anti-HSC70 (SPA-816; Stressgen, Ann Arbor, MI); Rabbit Anti-Tau (A0024; DaykoCytomation, Glostrup, Denmark); Mouse Anti-GAPDH (AM4300; Ambion, Inc., Austin, TX).
13. Secondary antibodies: Anti-rabbit IgG HRP-linked antibody (7074; Cell Signaling, Danvers, MA); Anti-mouse IgG HRP-linked antibody (7076; Cell Signaling, Danvers, MA).

3.3. Methods

3.3.1. Biotin–Avidin-Capture Methodology

1. Start by harvesting cells and determining protein concentrations by using the Bio-Rad D_c Protein Assay kit.
2. Adjust protein concentrations to 2 mg/ml for each sample. The final volume of each sample should be 1 ml.
3. Remove 50 µl sample from each tube and transfer into a new prelabeled 1.5 ml Eppendorf tube. Add DTT (50 mM) and NuPage Sample buffer (4×) to each sample, heat samples for 10 min at 95°C, and store at –20°C. This sample is referred to as the *whole cell lysate*.
4. Add biotin hydrazide (5 mM) into the remainder of each sample and incubate samples for 2 h in the dark while rotating on a tube rotator.
5. Following the termination of the incubation time, add sodium borohydride (50 mM) to each sample and allow samples to incubate for 30 min at room temperature. The formation of

bubbles indicates the reduction of double bonds into single bonds. Do not close Eppendorf tubes during this process.

6. During the 30 min incubation time, prepare Amicon Ultra Centrifugal Filter Devices. One filter device per sample is needed. Add 1 ml 1× PBS into the filter device followed by a 20 min centrifugation at 2,472 × *g*.
7. Upon termination of the 30 min incubation, add the entire sample and 2.5 ml cold 1× PBS into the filter device. Spin samples at 2,472 × *g* for 20 min. Remove the flow through upon termination of centrifugation. Add another 2.5 ml 1× PBS into the filter device and centrifuge the sample at 2,472 × *g* for 20 min. Remove the flow through upon termination of centrifugation and repeat washes for a total of three times.
8. During the last spin, start to prepare a bead slurry composed of 250 µl Streptavidin Sepharose High-Performance beads and 250 µl 1× PBS.
9. Wash the beads for a total of three times by following the subsequent steps:
   (a) Vortex bead slurry.
   (b) Centrifuge bead slurry on bench top centrifuge at 2,282 × *g* for approximately 1 min.
   (c) Carefully discard supernatant.
   (d) Add 1 ml 1× PBS.
   (e) Repeat steps a–d.
10. Upon termination of the three washes of the beads, add 500 µl 1× PBS to prevent the drying out of the beads until samples are ready to be added.
11. After termination of the final centrifugation, the approximate volumes of each sample have to be estimated. Prepare a new 1.5 ml Eppendorf tube for each sample and estimate the approximate amount of the sample that did not flow through the filter by pipetting this volume into the designated prelabeled 1.5 ml Eppendorf tube, thereby paying attention to the volumes that are transferred.
12. Adjust all samples to an equal volume by adding the appropriate amount of 1× PBS to the samples. For information about the volume adjustment of samples, see Note 9. Transfer 100 µl of each sample into a new prelabeled 1.5 ml Eppendorf tube, followed by the addition of DTT (50 mM) and NuPage Sample buffer (4×). Heat the samples for 10 min at 95°C and store at –20°C. This sample is referred to as the *input*.
13. Centrifuge bead slurry on bench top centrifuge at 2,282 × *g* for approximately 1 min and carefully remove the entire supernatant.

14. Add the remainder of each sample to the appropriate prelabeled 1.5 ml Eppendorf tube containing washed Streptavidin Sepharose High-Performance beads and carefully mix the beads with the sample.
15. Allow samples to incubate at 4°C overnight while rotating on a tube rotator.
16. The following day, prepare 1% SDS, 1 M NaCl, and 4 M urea. Note that the urea has to be freshly prepared before every experiment.
17. Centrifuge samples on bench top centrifuge at 2,282 × *g* for approximately 1 min.
18. Transfer 100 µl of the supernatant into a new prelabeled 1.5 ml Eppendorf tube. Add DTT (50 mM) and NuPage Sample buffer (4×) to each sample. Heat samples for 10 min at 95°C and store at –20°C. This sample is referred to as the *flow through*. Transfer the remainder of the supernatant into another 1.5 ml Eppendorf tube and store at –20°C.
19. Follow steps a–e listed below for the following washes. Wash the beads twice with 1% SDS. Then wash beads with 4 M urea. Next, beads should be washed 1 M NaCl and finally with 1× PBS. (Example uses 1% SDS, which is the solution used for the first 2 washes. Save the supernatant after the first wash only. All other supernatants may be discarded):
    (a) Add 1 ml of 1% SDS to the beads.
    (b) Vortex.
    (c) Manually invert tubes approximately 20 times.
    (d) Centrifuge samples on bench top centrifuge at 2,282 × *g* for approximately 1 min.
    (e) Discard supernatant.
20. Elute beads in 90 µl NuPage Sample buffer (4×) and DTT (50 mM). This sample is referred to as the *eluate*.
21. Vortex all samples and heat for 10 min at 95°C. Store at –20°C.

3.3.2. Western Blotting

1. Heat input, eluate, and flow through samples of each experimental condition for 10 min at 95°C.
2. Dedicate one lane of your gel to the protein standard by adding 10 µl of the Precision Plus Protein Standard All Blue Molecular Weight Marker.
3. Load 10 µl of the samples to the gel. Add samples in the following order: input, eluate, flow through. This will allow for a more efficient comparison of bands during analysis. For information on protein concentrations and number of proteins that can be detected from each sample, see Notes 10 and 11, respectively.

4. Follow manufacturer's directions to run the gel.
5. Transfer proteins onto a PVDF membrane by following manufacturer's directions for the used transfer apparatus.
6. Block nonspecific primary antibody binding by placing the membrane into methanol for 5 min.
7. Allow membrane to dry for 15–20 min before placing the membrane into the primary antibody.
8. Prepare primary antibodies of interest in dilution buffer (5% nonfat dry milk, 1× TBS-Tween 20).
9. Incubate the membrane in primary antibody overnight at 4°C while shaking on an orbital shaker.
10. Using multiple changes of 1× TBS-Tween 20, wash membrane for a total of 30 min before adding the secondary antibody.
11. Prepare appropriate secondary antibodies in dilution buffer (5% nonfat dry milk, 1× TBS-Tween 20).
12. Incubate membrane for 1 h at room temperature while shaking on an orbital shaker.
13. Using multiple changes of 1× TBS-Tween 20, wash the membrane for a total of 30 min before adding the chemiluminescent reagent according to manufacturer's specifications and exposing the membrane to film.

3.3.3. Interpretation of Data

1. Proteins that have undergone modifications following exposure to oxidative stress will be identified as a band in the eluate lane (see Fig. 5, Tau). The absence of bands in the lane

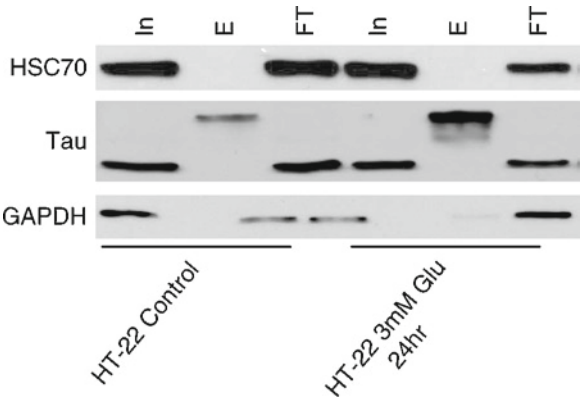

Fig. 5. Tau is oxidized in HT-22 cells. To induce oxidative stress, HT-22 cells were exposed to glutamate (3 mM) for 24 h after which cells were harvested, protein concentrations were determined, and oxidized proteins were immunoprecipitated using the biotin–avidin-capture methodology. Neither HSC70 nor GAPDH is oxidized in this cell line even after prolonged exposure to glutamate. The microtubule-associated protein tau is oxidized at baseline and is even further oxidized following exposure to glutamate for 24 h (band in "eluate" lane).

designated for the eluate sample indicates the absence of oxidative modifications of the protein of interest.

4. Notes

1. During preliminary experiments, it was noted that the concentration of DTT used for the OxyBlot procedure was not compatible with most standard protein assays. As a result, we decided to remove a 50 µl aliquot from the cell suspension for the determination of protein concentrations.
2. Ideally, it is best to perform the OxyBlot reaction (Fig. 2) directly after lysing the cells. However, samples containing 50 mM DTT may be frozen at –20°C. For best results, do not store samples for more than 1 month.
3. For the OxyBlot procedure, more than 5 µl of cell lysate per reaction tube may be treated, but the volumes of the other reagents have to be adjusted accordingly.
   - Example: if 10 µl of cell lysate are used, double all reagent volumes (i.e., 10 µl 12% SDS, 20 µl 1× DNPH solution, 20 µl 1× derivatization control solution, 15 µl neutralization solution). This will allow for running two Western blots probing for oxidized proteins from the same sample.
4. In order to prevent an artificial increase in protein carbonyl content in the samples, do not allow samples to stand in the derivatization solution for more than 15–20 min (16).
5. Once the OxyBlot procedure (Fig. 2) has been terminated, samples can be stored at 4°C or, alternatively, samples can be aliquated and stored at –20°C. Samples should be allowed to reach room temperature prior to immunoblotting.
6. To assure equal protein loading, use samples prepared for Western blot analysis and run gels probing for HSC70, GAPDH, or any other commonly used loading control.
7. Preliminary experiments determined that the primary antibody provided in the OxyBlot kit cannot be reused. For best results, prepare new primary antibody for each Western blot.
8. It has been determined that longer exposure times of the membrane are required in order for bands in the NC reaction to appear. Exposure times of up to 15 min have been required in order to see bands in the NC reactions.
9. Volumes of samples have to be adjusted in order to facilitate the balancing of the samples on the tube rotator overnight.
10. Given that exact protein concentrations cannot be determined following the elution of oxidized proteins from the

beads, we run Western blots assuming equal protein concentrations in the samples. As a result, these results should not be used for quantification purposes, but instead for the determination of the oxidative status of a protein only.

11. When using 10 μl of each input, eluate, and flow through from each sample, a total of 10 gels can be run. However, stripping the membrane following transfer will allow for the probing of one membrane with several different antibodies against proteins of varying molecular weights, thereby increasing the number of proteins that can be analyzed.

Acknowledgments

This work was supported by NIH grants NS050396 (BM), ES013125 (DL), and the Vanderbilt Neuroscience Predoctoral Training Fellowship T32 MH064913 (JS). Statistical and graphical support was provided by P30HD15052 (Vanderbilt Kennedy Center). The authors wish to express their gratitude to the members of the McLaughlin lab.

References

1. Chen C-L et al (2007) Site-specific S-glutathiolation of mitochondrial NADH ubiquinone reductase. Biochemistry 46(19):5754–5765
2. Sykes MC, Mowbray AL, Jo H (2007) Reversible glutathiolation of caspase-3 by glutaredoxin as a novel redox signaling mechanism in tumor necrosis factor-alpha-induced cell death. Circ Res 100(2):152–154
3. Ying J et al (2007) Thiol oxidation in signaling and response to stress: detection and quantification of physiological and pathophysiological thiol modifications. Free Radic Biol Med 43(8):1099–1108
4. Shackelford RE et al (2005) Cellular and molecular targets of protein S-glutathiolation. Antioxid Redox Signal 7(7–8):940–950
5. Maher P (2005) The effects of stress and aging on glutathione metabolism. Ageing Res Rev 4(2):288
6. Klatt P, Lamas S (2000) Regulation of protein function by S-glutathiolation in response to oxidative and nitrosative stress. Eur J Biochem 267(16):4928–4944
7. Brouns R, De Deyn PP (2009) The complexity of neurobiological processes in acute ischemic stroke. Clin Neurol Neurosurg 111(6):483–495
8. Mattsson N, Blennow K, Zetterberg H (2009) CSF biomarkers. Ann N Y Acad Sci 1180:28–35
9. Niizuma K, Endo H, Chan PH (2009) Oxidative stress and mitochondrial dysfunction as determinants of ischemic neuronal death and survival. J Neurochem 109(s1):133–138
10. Martin HL, Teismann P (2009) Glutathione-a review on its role and significance in Parkinson's disease. FASEB J 23(10): 3263–3272
11. Dalle-Donne I et al (2003) Protein carbonyl groups as biomarkers of oxidative stress. Clin Chim Acta 329(1–2):23
12. Liebler DC (2008) Protein damage by reactive electrophiles: targets and consequences. Chem Res Toxicol 21(1):117–128
13. Dennehy MK et al (2005) Cytosolic and nuclear protein targets of thiol-reactive electrophiles. Chem Res Toxicol 19(1):20–29
14. Robinson CE et al (1999) Determination of protein carbonyl groups by immunoblotting. Anal Biochem 266(1):48–57
15. Levine RL et al (1990) Determination of carbonyl content in oxidatively modified proteins. In: Lester P, Alexander NG (eds) Methods in enzymology. Academic, New York., pp 464–478

16. Levine RL et al (1994) Carbonyl assays for determination of oxidatively modified proteins. In: Lester P (ed) Methods in enzymology. Academic, New York, pp 346–357
17. Shacter E et al (1994) Differential susceptibility of plasma proteins to oxidative modification: examination by Western blot immunoassay. Free Radic Biol Med 17(5):429–437
18. Carbone DL et al (2004) Inhibition of Hsp72-mediated protein refolding by 4-hydroxy-2-nonenal. Chem Res Toxicol 17(11):1459–1467
19. Codreanu SG et al (2009) Global analysis of protein damage by the lipid electrophile 4-hydroxy-2-nonenal. Mol Cell Proteomics 8(4):670–680

Chapter 19

Catecholaminergic Cell Lines for the Study of Dopamine Metabolism and Neurotoxicity

Juan Segura-Aguilar

Abstract

The selective loss of melanin-containing dopaminergic neurons in the substantia nigra pars compacta and locus coeruleus has motivated a large number of preclinical studies aimed at understanding the molecular mechanisms involved in the neurodegeneration of dopaminergic neurons in Parkinson's disease. To perform these preclinical studies with catecholaminergic neurotoxins such as 6-hydroxydopamine, MPTP (1-methyl-4-phenyl-1,2,3,6-tetrahydropyridine), rotenon, paraquat, aminochrome, etc. requires to select cell model that expresses dopaminergic features such as dopamine transport, formation of neuromelanin, release of dopamine, and monoamine oxidase. The most used model cell lines are PC12 and SH-SY5Y cell lines due to their catecholaminergic properties, but we review several other cell lines that can be useful.

Key words: Dopamine, Parkinson's disease, MPTP (1-methyl-4-phenyl-1,2,3,6-tetrahydropyridine), Rotenone, Paraquat, Aminochrome, Neuromelanin, PC12, SH-SY5Y

1. Introduction

Parkinson's disease is a progressive neurodegenerative disease that is characterized pathologically by the selective loss of melanin-containing dopaminergic neurons in the substantia nigra pars compacta and locus coeruleus. This finding has motivated a large number of preclinical studies aimed at understanding the molecular mechanisms involved in the neurodegeneration of dopaminergic neurons in Parkinson's disease. Several neurotoxins have been used in these studies, most commonly 6-hydroxydopamine and MPTP (1-methyl-4-phenyl-1,2,3,6-tetrahydropyridine). Preclinical studies have used PC12 and SH-SY5Y cell lines due to their catecholaminergic properties. The cell line selected is an important

Michael Aschner et al. (eds.), *Cell Culture Techniques*, Neuromethods, vol. 56,
DOI 10.1007/978-1-61779-077-5_19,

factor to consider when interpreting data about the molecular mechanism underlying the cell death of melanin-containing neurons in the neurodegenerative process in Parkinson disease.

2. Dopaminergic Neurons Features

The correct selection of a suitable catecholaminergic cell line is a very important step for studying dopamine metabolism or neurotoxicity. A cell line should be as similar as possible to dopaminergic neurons. The most important features of dopaminergic neurons that we must take into account when selecting the most suitable catecholaminergic cell line are the following: synthesis of dopamine, expression of VMAT-2, neuromelanin formation, expression of dopamine transporter (DAT), and expression of monoamine oxidase.

2.1. Synthesis of Dopamine

Dopaminergic neurons produce dopamine by converting the amino acid tyrosine into L-dihydroxyphenylalanine (L-dopa), the precursor of dopamine. This process occurs through a sequence of reactions that are initiated by tyrosine hydroxylase, an enzyme that catalyzes the formation of L-dopa and is present in cells producing catecholamines. The conversion of tyrosine to L-dopa is the rate-limiting step in the synthesis of dopamine. L-Dopa is subsequently decarboxylated to dopamine, which is catalyzed by the aromatic amino acid decarboxylase (see Fig. 1). Cells expressing dopamine β-hydroxylase are able to produce norepinephrine; cells producing epinephrine require the expression of phenylethanolamine-*N*-methyl transferase.

2.2. Expression of VMAT-2

The synthesized dopamine is efficiently transported by VMAT-2 into monoaminergic vesicles that are used for neurotransmission. This step is crucial to preventing oxidation of dopamine in the presence of dioxygen, given that the hydroxyl group's protons are dissociated once they reach a physiological pH. The monoaminergic vesicles contain a vesicular-ATPase that uses the hydrolysis of cytoplasmic ATP in order to promote the influx of protons into monoaminergic vesicles, thereby creating a proton gradient.

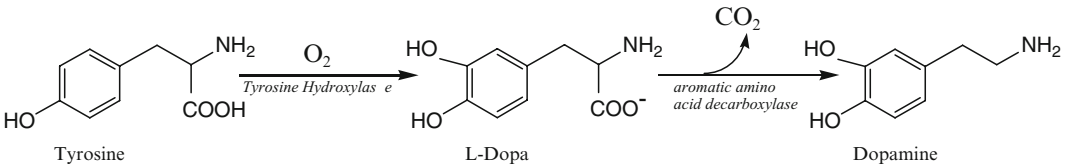

Fig. 1. Dopamine synthesis. The synthesis of dopamine is dependent on the availability of amino acid tyrosine and the enzyme tyrosine hydroxylase which catalyze the hydroxylation of tyrosine generating L-dopa. To form dopamine, the decarboxylation of L-dopa catalyzed by the enzyme aromatic amino acid decarboxylase is required.

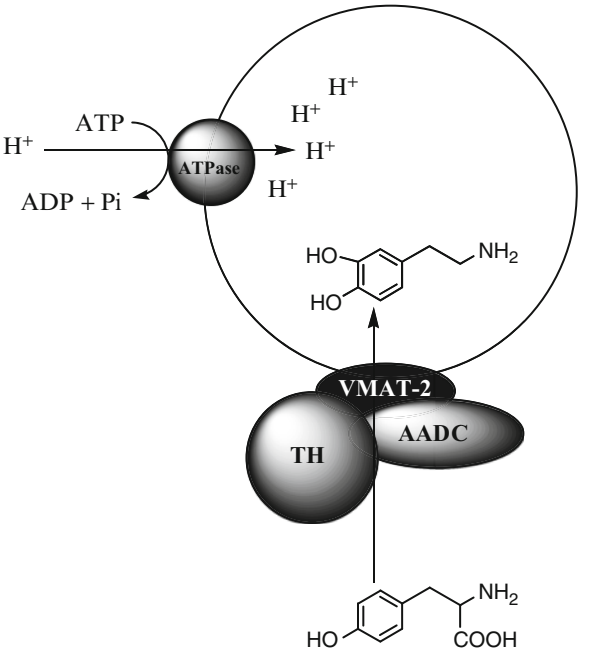

Fig. 2. Synthesis and dopamine uptake mediated by VMAT-2. The synthesis of dopamine is associated with VMAT-2 that is bound to monoaminergic vesicles, preventing the existence of free dopamine in the cytosol that can dissociate and autoxidize in the presence of oxygen. VAMT-2 drives dopamine transport by using vesicular-ATPase proton gradient.

VAMT-2 uses this proton gradient to drive dopamine transport into the monoaminergic vesicles. The high concentration of protons inside the monoaminergic vesicles creates a weak acid environment, with a pH around 5, thereby allowing the accumulation of a millimolar concentration of dopamine without risk of oxidation or polymerization to neuromelanin (Fig. 2).

2.3. Neuromelanin Formation

An important feature of dopaminergic neurons is the formation of neuromelanin. This process is particularly interesting when studying the mechanism of neurodegeneration in Parkinson's disease, given that neuromelanin-containing dopaminergic neurons from the nigrostriatal system are selectively lost in Parkinson's disease. In humans, neuromelanin naturally accumulates in the substantia nigra over time (1, 2). Neuromelanin-containing cells in the substantia nigra do not degenerate in healthy individuals, suggesting that neuromelanin formation is not a neurotoxic pathway, in and of itself, but rather neuromelanin formation is the result of dopamine oxidation. Dioxygen catalyzes dopamine one-electron oxidation to dopamine *o*-semiquinone (DAoSQ) radical with concomitant formation of one molecule of the superoxide radical (reaction 1). Dopamine one-electron oxidation can also be catalyzed by transition metals such as manganese(III) under both

aerobic and anaerobic conditions to aminochrome (3). Copper sulfate(II) and iron chloride(III) are both able to oxidize dopamine by forming a complex with dopamine prior to its oxidation to aminochrome (4–6). Peroxidases, such as lactoperoxidase, are also able to catalyze dopamine one-electron oxidation with the formation of the DAoSQ radical (reaction 1) (7). Other enzymes that catalyze dopamine oxidation act as peroxidases, including prostaglandin H synthase, cytochrome P450 forms, xanthine oxidase, tyrosinase, and dopamine β-monooxygenase (8–13). The DAoSQ radical can also be oxidized by dioxygen to dopamine *o*-quinone (reaction 2). However, DAoSQ is not particularly reactive with oxygen, given that its ESR-signal was stabilized by the presence of $ZnCl_2$ for more than 10 min (7). Therefore, it seems plausible that two DAoSQ radicals can react to each other (disproportionation reaction), resulting in the formation of one molecule of dopamine *o*-quinone and one molecule of dopamine (reaction 3). Dopamine can also be oxidized to dopamine *o*-quinone in one step that uses two electrons from tyrosinase, but does not form the DAoSQ radical, as evidenced by the fact that no ESR-signal was observed during this reaction (reaction 4; (7)). Tyrosinase is essential for melanin synthesis and is also found in the pigment epithelium of the retina. Moreover, tyrosinase mRNA was reportedly expressed in the human substantia nigra (14). However, it appears that the protein expression of tyrosinase is prevented by strict regulation, such that the formation of neuromelanin is a progressive event that takes place over the course of many years. Dopamine *o*-quinone cyclizes to form aminochrome in such a way that the amino chain spontaneously rearranges over several steps to finally form aminochrome at a physiological pH (reaction 5). Therefore, dopamine *o*-quinone acts as a transient molecule at physiological pH levels where it is stable with a pH lower than 2 (3). Aminochrome is the precursor of neuromelanin and is relatively stable at physiological pH 7.4, given that 50% of the decay was at 112 min (15). The formation of neuromelanin is a consequence of the rearrangement of aminochrome to 5,6-dihydroxyindole (reaction 6), thereby oxidizing indole-5,6-quinone (reaction 7) and finally producing polymerization and formation of the pigment that accumulates in double membrane vesicles (Fig. 3).

2.4. Expression of Dopamine Transporter

The DAT is a selective marker of dopaminergic neurons which plays an important role in terminating dopamine synaptic neurotransmission by catalyzing dopamine reuptake (16). DAT mRNA is restricted to dopaminergic neurons and is localized within cell bodies (17, 18). The DAT is a Na^+/Cl^--dependent neurotransmitter transporter that is similar to glycine, norepinephrine, serotonin, and GABA transporters (19). Dopamine uptake is driven by an electrochemical gradient that is energetically coupled to the

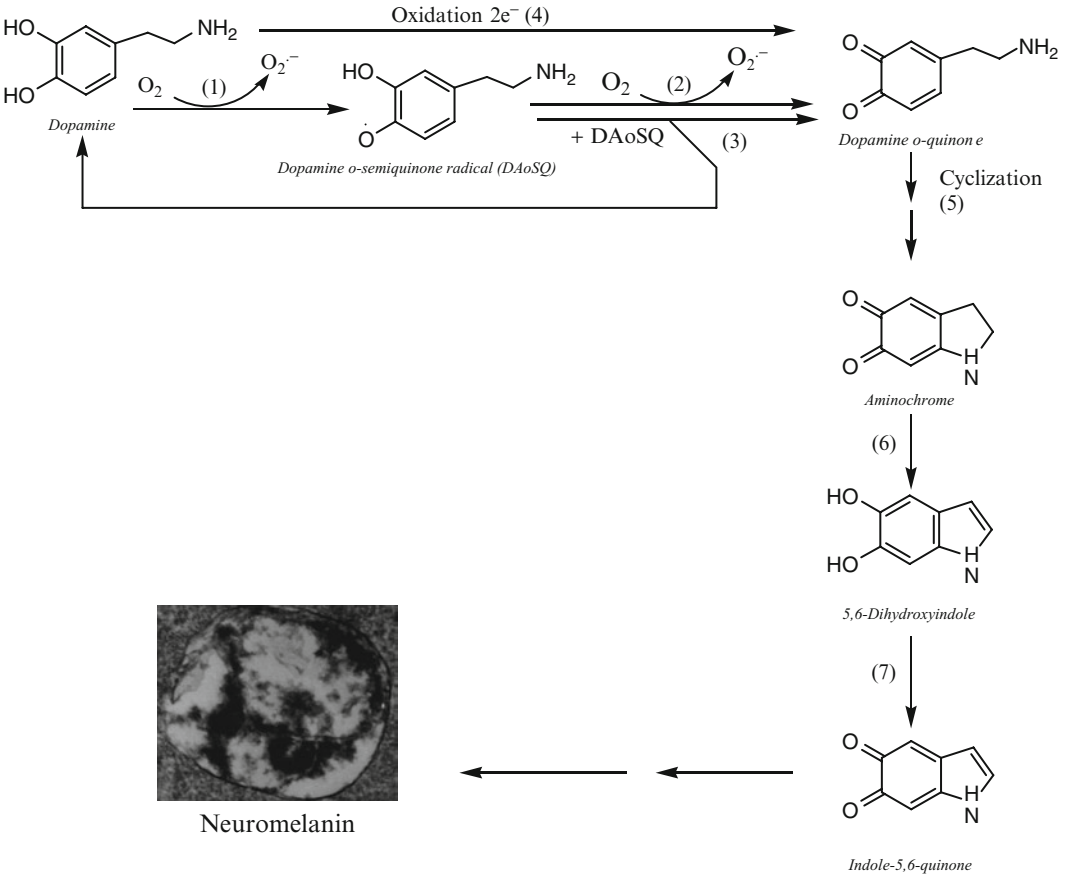

Fig. 3. Dopamine oxidation to neuromelanin. Dopamine can oxidize by two electrons to dopamine *o*-quinone or one electron with the formation of dopamine *o*-semiquinone (DAoSQ). Two molecules of DAoSQ radical disproportionate to form one molecule of dopamine and one molecule of dopamine *o*-quinone, which cyclize to aminochrome at physiological pH. Aminochrome can tautomerize to form indole-5,6-quinone.

transmembrane concentration gradient of Na^+, which is maintained by Na^+-K^+-ATPases (20). Dopamine uptake involves the translocation of one molecule of dopamine as well as two Na^+ and one Cl^- ions across the cell membrane. DAT is synthesized at the endoplasmic reticulum membrane; it is then glycosylated and transported to the plasma membrane (21). The regulation of DAT is mediated by several mechanisms including the following: (i) constitutive endocytosis that is dependent on PKC activation (22, 23); (ii) inhibition of ERK1/2 activity that results in down-regulation of DAT, suggesting that MAPK/ERK1/2 plays an important role in maximal localization of the DAT at the plasma membrane (24–26); (iii) DAT may be regulated by specific proteins that interact with the DAT. For example, alpha-synuclein is a negative modulator of human DAT activity (27). Wild-type alpha-synuclein facilitates DAT internalization, whereas mutated

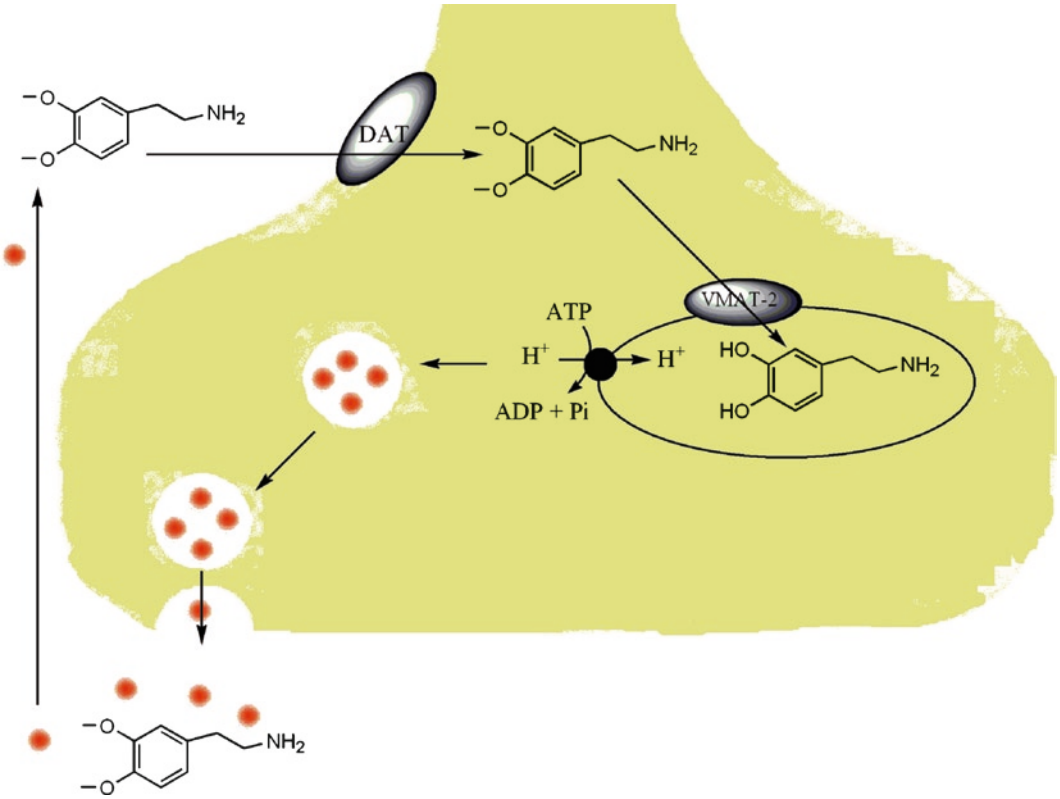

Fig. 4. Dopamine transporter (DAT). The reuptake of dopamine released during neurotransmission is mediated by DAT.

alpha-synuclein reduces DAT internalization (28); (iv) Psychostimulants that interact directly with DAT can regulate the number of DATs on cell surface. For example, amphetamines induce relatively long-term reversible down-regulation of DAT by reducing H^{3+}-dopamine uptake (29, 30). Conversely, cocaine increases dopamine uptake and the number of DAT on the cell surface (31). The selectivity of dopaminergic neurons is due to their ability to be transported by DAT. For example, DAT internalization reduces the toxic effects of MPP+ (28). Moreover, the inhibition of DAT by nomifensine prevents MPP+ neurotoxicity (32) and inhibits MPP+-induced DNA fragmentation (33) (Fig. 4).

2.5. Expression of Monoamine Oxidase

Monoamine oxidases (MAOs) A and B are flavoenzymes that catalyze the oxidative deamination of biogenic amines including neurotransmitters, such as dopamine. These enzymes are bound to the mitochondrial membrane in neurons, glial cells, and other cell types (34, 35). MAO function in dopaminergic neurons is involved with maintaining a low concentration of cytosolic dopamine. MAO-A mainly metabolizes monoaminergic neurotransmitters,

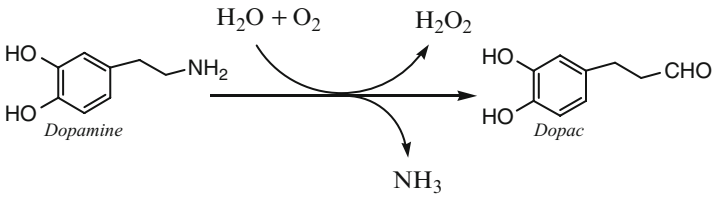

Fig. 5. Dopamine oxidative deamination. Dopamine excess is removed by monoamino oxidase that catalyzes oxidative deamination of dopamine to dopac and hydrogen peroxide.

such as serotonin, dopamine, noradrenaline, and adrenaline, whereas MAO-B mainly metabolizes trace amines, such as tyramine and phenylethylamine (36) (Fig. 5).

3. Catecholaminergic Cell Lines

PC12 and SH-SY5Y have been the most commonly used catecholaminergic cell lines used in preclinical experimental models for the neurodegeneration that occurs in Parkinson's disease. Neurodegenerative symptoms are modeled using neurotoxins such as 6-hydroxydopamine, 1-methyl-4-phenyl-1,2,3,6-tetrahydropyridine, or rotenone. Recently, other cell lines have been used to explore the activity of dopaminergic neurotoxins.

3.1. PC12 Cell Line

PC12 is a cell line that was originally derived from a pheochromocytoma (a tumor in the adrenal gland) that developed in an irradiated rat (37). Under standard culture conditions, these cells exhibit properties that are similar to those of immature rat adrenal chromaffin cells. When grown in the presence of nerve growth factor (NGF), PC12 cells extend neurites, eventually becoming electrically excitable, responding more efficiently to exogenously applied acetylcholine and increasing their expression of calcium channels as well as the biosynthesis of several neurotransmitters (38). PC12 cells grown in the presence of NGF resemble sympathetic neurons, and they have been widely used as an experimental model for preclinical studies on the mechanisms of neurodegeneration in Parkinson's disease. PC12 cells express dopamine, norepinephrine, and serotonin transporters (39–41), whereas only PC12 cells have been reported to transport serotonin (42).

3.1.1. Cell Culture Medium

The base medium for this cell line is F-12K Medium, (ATTC, Catalog No. 30-2004) supplemented with 2.5% (v/v) fetal bovine serum, 15% horse serum, and 1% (v/v) antibiotic/antimycotic mixture (Gibco).

3.1.2. Growth Conditions

PC12 cells are grown in suspension within an atmosphere composed of 95% air and 5% carbon dioxide (CO_2) at 37.0°C. Cells have a doubling time of 48 h under these conditions.

3.1.3. Subcultivation

The cells are recovered from the suspension using centrifugation between 180 and 225 × *g* for 8–15 min at room temperature. The cell pellet is resuspended in a small volume of fresh medium that contains the cell clusters. In order to break up cell clusters in the medium, an aliquot of 4–6 mL is then gently aspirated 5 times up and down with a new 20-mL syringe that is outfitted with needle. About 5×10^5 cells/mL are seeded in a new flask. The subcultivation ratio is 1:3 twice per week and media renewal is every 2–3 days.

3.1.4. Preservation

PC-12 cells can be frozen in F-12K medium supplemented with 2.5% (v/v) fetal bovine serum, 15% horse serum, 1% (v/v) antibiotic/antimycotic mixture, and 5% (v/v) DMSO. The cells can be stored in liquid nitrogen vapor phase.

3.1.5. Differentiation

In order to differentiate PC12 cells, 3.5 × 106 cells are seeded and the medium changed after 24 h to a medium that contains 50 ng/mL 50 ng/mL nerve growth factor (NGF-7S, Sigma-Aldrich, Inc., St Louis, MO) for 5–7 days.

3.1.6. Where to Obtain the Cells

This cell line can be obtained from ATTC catalogue number CRL-1721 (www.atcc.org).

3.2. SH-SY5Y Cell Line

The other cell line mentioned above, SH-SY5Y, is a third-generation neuroblastoma, cloned from SH-SY5. An important difference that distinguishes SH-SY5Y cells from PC12 cells is that this cell line is derived from human cells. The original cell line was isolated from a metastatic bone tumor in 1970. The cells possess an abnormal chromosome 1, exhibiting an additional copy of the 1q segment and thereby referred to as trisomy 1q. SH-SY5Y cells are known to be dopamine-β-hydroxylase active, cholinergic, glutamatergic, and adenosinergic. The dividing cells can form clusters that are reminiscent of their cancerous formation; however, treatment with retinoic acid or BDNF can force the cells to extend processes and differentiate. This cell line expresses dopamine and norepinephrine transporters (39–41), whereas PC12 cells have been reported to have serotonin transporters (42).

3.2.1. Cell Culture Medium

The cell culture medium is prepared by mixing Eagle's Minimum Essential Media (Gibco/Invitrogen) and F12 Media (Gibco/Invitrogen) at a ratio of 1:1. Each medium type is prepared independently and filtered using a sterile technique before adding 10% (v/v) fetal bovine serum, 2 mM L-glutamine (Gibco/

Invitrogen), and 1% (v/v) of the antibiotic/antimycotic mixture for the final media.

3.2.2. Growth Conditions

The cells are grown in glass or plastic petri dish in an atmosphere that is composed of 95% air and 5% carbon dioxide (CO_2) at a temperature of 37°C, and cells have a doubling time of 48 h.

3.2.3. Subcultivation

SH-SY5Y cells grow as a mixture of floating and adherent cells. The subcultivation is achieved by removing the media that contains the floating cells that are recovered during centrifugation. The adherent cells are incubated with a fresh solution of 0.3% (v/v) trypsin and 0.53 mM EDTA at room temperature, until the cells detach. The detached cells are recovered by centrifugation at 2,000 rpm, mixed with the floating cells recovered from the medium, and finally dispensed into a new petri dish. A subcultivation ratio between 1:20 and 1:50 is recommended and the medium should be changed every 4–7 days.

3.2.4. Preservation

SH-SY5Y cells can be frozen in media containing a mixture of Eagle's Minimum Essential Medium and F12 Medium at a ratio of 1:1, supplemented with 20% (v/v) fetal bovine serum and 5% (v/v) DMSO. The cells should be stored in liquid nitrogen vapor phase.

3.2.5. Differentiation

The differentiation was performed by seeding $6{\cdot}10^5$ SH-SY5Y cells in T75 flasks in the presence of cell culture medium that contains 10 μM retinoic acid (Sigma-Aldrich) dissolved in 0.01% DMSO (v/v) for 8 days. To assess the differentiated phenotype under retinoic acid treatment, cells were photographed using a phase contrast microscope.

3.2.6. Where to Obtain the Cells

This cell line can be obtained from ATTC catalogue number CRL-2266 (www.atcc.org).

3.3. RCSN-3 Cell Line

RCSN-3 is a cell line derived from the substantia nigra of a 4-month-old normal adult Fisher 344 rat (4, 43). An important feature of RCSN-3 cells is that under proliferating conditions, the cells express tyrosine hydroxylase, DAT, VMAT-2, norepinephrine transporters, and serotonin transporters and are able to release dopamine. Moreover, they contain MAO-A, but not MAO-B. The cells also express the divalent metal transporter 1 (DMT1) and the mRNA for dopamine receptor D1 and D5 (for review see ref (43)). The major advantage of using RCSN-3 cells as compared to PC-12 and SH-SY5Y cells is that catecholaminergic features can be achieved without using expensive or time-consuming protocols.

3.3.1. Cell Culture Medium

RCSN-3 cells grow in a mixture of Dulbecco's Modified Eagle's Medium (DMEM) and Ham's Nutrient Mixture F12 (HAM-F12, Sigma-Aldrich) in a ratio of 1:1, supplemented with 10% (v/v) bovine serum, 2.5% fetal bovine serum, and 40 mg/L gentamicin sulfate.

3.3.2. Growth Conditions

The cells grow in glass or plastic petri dish in a monolayer. The cells grow well under either an atmosphere composed of 90% air and 10% carbon dioxide (CO_2), or alternatively, 95% air and 5% CO_2. Cells are grown at a temperature of 37°C with a doubling time of 52 h, a plating efficiency of 21%, and a saturation density of 56,000 cells/cm^2.

3.3.3. Subcultivation

RCSN-3 cells grow as adherent cells in a monolayer. The subcultivation is achieved by incubating the cells with media containing 10% (v/v) trypsin for 15 min. The trypsin reaction is stopped by adding an equal volume of cell culture medium. The cells are subsequently collected by centrifugation at 2,000 rpm.

3.3.4 Preservation

RCSN-3 cells can be frozen in a medium containing a mixture of DMEM and HAM-F12 medium at a ratio of 1:1, with 10% (v/v) bovine serum, 2.5% fetal bovine serum, 40 mg/L gentamicine sulfate, and 10% glycerol. The cells are stored in liquid nitrogen vapor phase.

3.3.5. Where to Obtain the Cells

RCSN-3 cell line can be obtained by signing an MTA (Dr. Pablo Caviedes, e-mail: pablo.caviedes@cicef.cl).

3.4. SK-N-SH Cell Line

SK-N-SH is a human neuroblastoma cell line that has the ability to take up dopamine (44, 45) and noradrenaline (46). Furthermore, this cell line has been used in studies related to DATs (45) and norepinephrine transporters (47).

3.4.1. Cell Culture Medium

The cell culture medium is Eagle's Minimum Essential Medium (ATCC, Catalog No. 30-2003) supplemented with 10% (v/v) fetal bovine serum and 1% penicillin/streptomycin (10,000 U/10,000 µg).

3.4.2. Growth Conditions

SK-N-SH cells grow in a monolayer in an atmosphere composed of 95% air and 5% carbon dioxide (CO_2) at a temperature of 37°C.

3.4.3. Subcultivation

The cells will be incubated at room temperature with a medium containing 0.25% trypsin and 0.03% EDTA until the cells detach. For subcultivation, the collected cells will be seeded in a new flask with fresh medium using a ratio between 1:3 and 1:8 and the medium will be changed 1–2 times per week.

3.4.4. Preservation

SK-N-SH cells can be frozen in culture medium containing 5% (v/v) DMSO and stored in liquid nitrogen vapor phase.

3.4.5. Where to Obtain the Cells

This cell line can be obtained from ATTC catalogue number HTB-11 (www.atcc.org).

3.5. CATH.a Cell Line

CATH.a is a neuroblastoma cell line derived from a mouse that expresses tyrosine hydroxylase and dopamine β-hydroxylase and is able to synthesize dopamine and norepinephrine (48).

CATH.a cells display some of the properties that would be expected in a locus coeruleus neuron, i.e., expression of functional corticotrophin-releasing hormone receptors, α2-adrenoceptors, muscarinic cholinergic receptors, and bradykinin receptors (49). CATH.a cells express mRNA, encoding all three of the major subtypes of opioid receptors. Moreover, the pharmacological and functional data were in agreement with the results of RT-PCR (50).

3.5.1. Cell Culture Medium

The RPMI 1640 cell culture medium is used for CATH.a cells. It is supplemented with 2 mM L-glutamine, 1.5 g/L sodium bicarbonate, 4.5 g/L glucose, 10 mM HEPES, 1.0 mM sodium pyruvate, 8% (v/v) horse serum, 4% (v/v) fetal bovine serum, and 1% penicillin/streptomycin (10,000 U/10,000 µg).

3.5.2. Growth Conditions

CATH.a cells grow in suspension and in adherent conditions in an atmosphere composed of 95% air and 5% carbon dioxide (CO_2) at a temperature of 37°C. Biosafety level 2 should be used with CATH.a cells given that they contain SV-40 viral DNA sequences.

3.5.3. Subcultivation

CATH.a cells grow as a mixture of floating and adherent cells. The floating cells are recovered by centrifugation at 2,000 rpm, whereas the adherent cells are incubated with fresh 0.12% (v/v) trypsin in the cell culture medium at room temperature until the cells detach. The detached cells are then recovered by centrifugation at 2,000 rpm, mixed with the floating cells that are recovered from the media, and are finally dispensed into new petri dish of flask. A subcultivation ratio of 1:4 is recommended.

3.5.4. Preservation

CATH.a cells can be frozen in culture medium containing 10% (v/v) glycerol and stored in liquid nitrogen vapor phase.

3.5.5. Where to Obtain the Cells

This cell line can be obtained from ATTC catalogue number CRL-11179 (www.atcc.org).

3.6. CAD Cells

CAD cells are a mouse neuronal cell line that is derived from the CATH.a cell line. CAD cells undergo differentiation upon serum withdrawal. The differentiation is accompanied by the loss of the original immortalizing oncogene SV40 T antigen as well as the expression of neuron-specific proteins, such as class III β-tubulin, GAP-43, SNAP-25, synaptotagmin, and tyrosine hydroxylase, but not GFAP. Furthermore, CAD cells accumulate L-DOPA, suggesting that they are capable of dopamine transport. However,

CAD cells do not synthesize and secrete dopamine due to the absence of activity of the aromatic amino acid decarboxylase (for review, see ref (51)).

3.6.1. Cell Culture Medium

CAD cells grow in DMEM/F-12 media that is supplemented with 8% fetal bovine serum and 1% penicillin–streptomycin (100% stocks, 10,000 U/mL penicillin G sodium and 10,000 μg/mL streptomycin sulfate in 0.85% saline).

3.6.2. Growth Conditions

The cells grow under standard tissue culture conditions in an atmosphere of 95% air and 5% CO_2.

3.6.3. Subcultivation

CAD cells were passaged every 3–4 days by pipetting cells from a confluent plate and triturating them in 5 mL of fresh medium. Cells were replated at a 1:10 dilution (51).

3.6.4. Preservation

CAD cells can be frozen in a complete culture media that contain 10% glycerol and then stored in liquid nitrogen vapor phase.

3.6.5. Differentiation

The differentiation of CAD cells was induced by plating the cells in serum-containing DF12 medium and then switching to either serum-free medium or protein-free medium. Serum-free medium contained 20 μg/mL transferrin (Sigma, St. Louis, MO) and 50 ng/mL sodium selenite (Sigma) in DF12 medium. The protein-free medium contained only 50 ng/mL of sodium selenite. This differentiation protocol requires incubating CAD cells for at least 5 days in serum-free medium or protein-free medium.

3.6.6. Where to Obtain the Cells

CAD cell line consists of CATH.a cells that have been differentiated and can be obtained from ATTC catalogue number CRL-11179 (www.atcc.org).

3.7. RCHT Cell Line

The RCHT cell line was derived from the hypothalamus of a 4-month-old normal Fisher 344 rat. This cell line expresses norepinephrine, but not DATs or dopaminergic markers such as tyrosine hydroxylase and DOPA decarboxylase (52).

3.7.1. Cell Culture Medium

RCSN-3 cells grow in a mixture of DMEM and Ham's Nutrient Mixture F12 (HAM-F12, Sigma-Aldrich) at a ratio of 1:1, supplemented with 10% (v/v) bovine serum, 2.5% fetal bovine serum, and 40 mg/L gentamicine sulfate.

3.7.2. Growth Conditions

The cells grow in a glass or plastic petri dish in a monolayer. The cells grow well under either an atmosphere composed of 90% air and 10% carbon dioxide (CO_2), or alternatively, 95% air and 5% CO_2. Cells are maintained at a temperature of 37°C with a doubling time of 52 h, a plating efficiency of 21%, and a saturation density of 56,000 cells/cm^2.

3.7.3. Subcultivation

RCSN-3 cells grow as adherent cells in monolayer. The subcultivation is achieved by incubating the cells in a medium containing 10% (v/v) trypsin for 15 min. The trypsin reaction is stopped by adding an equal volume of cell culture medium and the cells are subsequently collected by centrifugation at 2,000 rpm.

3.7.4. Preservation

RCSN-3 cells can be frozen in a medium containing a mixture 1:1 of DMEM and HAM-F12 medium, 10% (v/v) bovine serum, 2.5% fetal bovine serum, 40 mg/L gentamicine sulfate, and 10% glycerol. The cells can be stored in liquid nitrogen vapor phase.

3.7.5. Where to Obtain the Cells

RCSN-3 cell line can be obtained by signing an MTA (Dr. Pablo Caviedes, e-mail: pablo.caviedes@cicef.cl).

3.8. N27 Cell Line

The N27 cell line is composed of tyrosine hydroxylase immortalized cells derived from mesencephalic tissue from 12-day-old rat fetuses; this cell line produces dopamine and its metabolites. These cells express the DAT, PKC isoforms, and adrenoreceptors (53) and have previously been used as a model to study neurotoxicity (54–57).

3.8.1. Cell Culture Medium

N27 cells were cultured in RPMI 1640 medium that was supplemented with 10% fetal bovine serum, penicillin (100 U/mL), streptomycin (100 μg/mL), and 2 mM glutamine.

3.8.2. Growth Conditions

N27 cells grow under standard tissue culture conditions in an atmosphere of 95% air and 5% CO_2. The doubling time of N27 cells is approximately 26 h.

3.8.3. Subcultivation

The subcultivation of N27 cells is complete when the 80% confluence is observed. These cells are then incubated in the cell culture medium with 0.25% trypsin for 20 min at room temperature. The cells will be collected by centrifugation (1,270 × *g*) for 4 min. The cells are finally seeded in a new flask (10,000 cells/cm^2).

3.8.4. Preservation

N27 cells can be frozen in the culture medium containing 10% DMSO. The cells can be stored in liquid nitrogen vapor phase.

3.8.5. Where to Obtain the Cells

N27 cell line was developed at the University of Colorado Health Sciences Center in Denver, CO, USA.

3.9. CV1-P Cell Line

CV1-P cell line was derived from the kidney of a male adult African green monkey. This nonneuronal cell line has been used in several studies with 6-hydroxydopamine due to the fact that CV1-P cells naturally express the DAT (58).

3.9.1. Cell Culture Medium

CV1-P cells are cultured in Dulbecco Eagle's Minimum Essential Medium with low glucose (1,000 mg/L, 0.11 g/L sodium pyruvate

and pyridoxine, 10% (v/v) fetal bovine serum, and 90 U/mL penicillin–streptomycin).

3.9.2. Growth Conditions

CV1-P cells grow adherently under standard tissue culture conditions in an atmosphere of 95% air and 5% CO_2.

3.9.3. Subcultivation

The subcultivation is achieved by incubating the cells in medium containing 1 mM EDTA and 2.5% (v/v) trypsin until the cells detached. The cells are collected by centrifugation at 240 × *g* for 4 min. A subcultivation ratio between 1:2 and 1:3 is recommended and the media should be changed 2–3 times per week.

3.9.4. Preservation

CV1-P cells can be frozen in the culture medium containing 10% glycerol. The cells can be stored in liquid nitrogen vapor phase.

3.9.5. Where to Obtain the Cells

CV1-P cells can be obtained from ATCC (ATTC catalogue number CCL-70; www.atcc.org).

3.10. NB69 Cell Line

NB69 is a human neuroblastoma cell line that can be differentiated into a catecholaminergic phenotype when in the presence of the nitric oxide donor *S*-nitroso-*N*-acetyl-D,L-penicillamine, thereby inducing an increase in catecholamine levels, ^{3}H-dopamine uptake, tyrosine hydroxylase activity, and monoamine metabolism (59).

3.10.1. Cell Culture Medium

NB69 cells are cultured in DMEM medium supplemented with 2 mM L-glutamine, 40 μg/mL gentamicin, and 15% (v/v) fetal bovine serum.

3.10.2. Growth Conditions

N27 cells grow semiadherently under standard tissue culture conditions in an atmosphere of 95% air and 5% CO_2 at 37°C.

3.10.3. Subcultivation

NB69 cells grow in aggregates as well as attached. A subcultivation ratio of 1:4 is recommended. The cells can be incubated for 20 min in cell culture medium containing 0.25% trypsin at room temperature or 37°C.

3.10.4. Differentiation

NB69 cells can be differentiated by incubating 50 μM *S*-nitroso-*N*-acetyl-D,L-penicillamine in serum-free culture medium for 24 h.

3.10.5. Preservation

NB69 cells can be frozen in the culture medium containing 10% glycerol. The cells will be stored in liquid nitrogen vapor phase.

3.10.6. Where to Obtain the Cells

NB69 cells can be obtained from European Collection of Cell Cultures, ECACC (no. 99072802) http://www.hpacultures.org.uk/collections/ecacc.jsp.

4. Methods to Measure Neurotoxicity

The measurement of cytotoxicity can been performed using several different principles and methods. (i) The measurement of cell viability is one alternative. Here, the viability of the cells that are not affected by the neurotoxin is quantified. Specific methods include the use of trypan blue, MTT, and XTT assays. (ii) Another option is to measure the membrane integrity by detecting the release of a cytosolic enzyme such as glucose 6-phosphate dehydrogenase, lactate dehydrogenase, or adenylate kinase from cells with a damaged cell membrane. (iii) A third option is to measure ATP level, given that all cells, especially neurons, are completely dependent on the formation of energy. For example, axonal transport of the DAT and VMAT-2 transporter are completely dependent on ATP. (iv) Finally, measurements of the number of both living and dead cells can be made using two compounds such calcein AM and ethidium homodimer-1.

4.1. Death and Live Method

This method is based on the ability of calcein AM to cross the cell membrane and then be enzymatically modified by intracellular esterase activity. This modification results in a metabolite that is no longer able to cross membranes and produces an intense uniform green fluorescence in living cells (ex/em ~495/515 nm). Conversely, ethidium homodimer-1 penetrates cells that have damaged membranes and undergoes a 40-fold enhancement of fluorescence upon binding to nucleic acids, thereby producing a bright red fluorescence in dead cells (ex/em ~495/635 nm).

4.1.1. Protocol

The cells must be seeded on a dish that contains cell culture medium. The cells should be attached to the dish after 24 h. The medium should then be replaced with a cell culture medium that does not contain bovine serum or phenol red. This replacement is considered time 0 h, at which point the different cell incubation treatments start.

The time of incubation with the treatment will depend on the mechanism of cell death that is induced by the neurotoxin. Therefore, it is suitable to do a time curve in order to determine the time until cell death. For example, necrotic cell death can take 2 h, whereas apoptotic cell death can take 24 or 48 h. Following treatment, the cell culture medium can be removed and washed with PBS. The cells can be incubated in the dark with a solution containing 0.5 M calceine AM and 1.5 μM ethidium homodimer-1 at room temperature for 45 min. The cells were counted using a phase contrast microscope equipped with fluorescence. Molecular Probe, Invitrogen suggests using ex/em ~495/515 nm for calceine Am and ex/em ~495/635 nm for ethidium homodimer-1. However, depending on the equipment and filter availability, we used the

following filters: Calcein AM, 510–560 nm (excitation) and LP-590 nm (emission); and ethidium homodimer-1, 450–490 nm (excitation) and 515–565 nm (emission).

4.2. MTT (XTT) Assay

The MTT (3-(4, 5-dimethyl-2-thiazolyl)-2, 5-diphenyl-2H-tetrazolium bromide) assay is based on the ability of a flavoenzyme to reduce MTT (yellow) to the water-insoluble purple formazan. The MTT assay is based on the conversion of tetrazolium salt by mitochondrial succinic dehydrogenases. This assay is used as marker of cell viability, and therefore, it is mentioned in the literature as a method for determining cell viability by measuring mitochondrial activity. However, we must remember that not only is MTT reduced by succinic dehydrogenases, but it is also reduced by a large number of flavoenzymes including DT-diaphorase NAD(P)H: quinone oxidoreductase. In addition, we should not use compounds than might interfere with this flavoenzyme activity, given that this use could lead to artifacts. Unlike the purple-colored formazan product of MTT, the extremely water-soluble, orange-colored formazan product of XTT (X6493, Molecular Probe, Invitrogen) does not require solubilization prior to quantification, thereby reducing the time required for several viability assays. Moreover, the sensitivity of the XTT reduction assay is reported to be similar to, or better than, that of the MTT reduction assay.

4.2.1. Protocol

After treatment, the cells should be washed with PBS and incubated with 0.5 mg/mL MTT dissolved in PBS for 4 h at 37°C. The media containing MTT is removed, and then the dark blue formazan crystals that formed in intact cells are solubilized by incubating the cells in DMSO for 15 min. The absorbance at 570 nm is then measured with microplate reader. The results are expressed as a percentage of MTT reduction, assuming that the absorbance of control cells was 100%.

4.3. Determination of Intracellular ATP

Adenosine 5′-triphosphate (ATP) is the chemical energy used for cellular metabolism. Dopaminergic neurons with a low level of ATP will collapse, given that essential functions, such as axonal transport, dopamine transport, and VMAT-2 transport, are dependent on ATP. The method is based on the catalytic activity of luciferase that uses ATP as substrate. This assay is extremely sensitive, as it can detect 0.1 picomole of intracellular ATP.

$$\mathrm{ATP + D\text{-}luciferin + O_2} \xrightarrow[\mathrm{Mg^{2+}}]{\text{Luciferase}} \text{oxyluciferin + AMP + PPi} + \mathrm{CO_2} + \text{light.}$$

4.3.1. Protocol

Prepare a standard reaction solution, which contains 8.9 mL dH_2O, 0.5 mL 20× Reaction Buffer, 0.1 mL 0.1 M DTT, and 0.5 mL of 10 mM D-luciferin (2.5 µL of firefly luciferase 5 mg/mL stock solution). Prepare low-concentration ATP standard

solutions by diluting 5 mM ATP solution in dH_2O. Typically, ATP concentrations ranging from 1 nM to 1 μM are appropriate. The same volume that was used in the standard curve should be used to measure the samples. Promega has a kit that is easier to work (http://www.promega.com/tbs/tb288/tb288.html).

4.4. Adenylate Kinase Release Assay

This assay measures the release of adenylate kinase from cells with damaged cell membranes. Adenylate kinase is present in all eukaryotic cells and is released into the culture medium when the cell membrane is damaged. This enzyme actively phosphorylates ADP, thereby forming ATP. The resultant ATP is then measured using the bioluminescent firefly luciferase reaction. A kit can also be purchased to measure adenylate kinase release (ToxiLight BioAssay, Lonza)

4.4.1. Protocol

When using ToxiLight BioAssay to determine toxicity in a 96-well plate, add 50 μL Tris acetate to treated cells and 50 μL of the ToxiLight® 100% lysis reagent to 100 μL of the culture controls. The cells are incubated for 10 min to complete the lysis of control cells. Add 100 μL AK Detection Reagent to all wells and incubate for 5 min before reading the luminescence.

4.5. Determination of Glucose 6-Phosphate Dehydrogenase Release

The release of the cytosolic enzyme glucose 6-phosphate dehydrogenase from damaged cells into cell culture medium can be determined by a two-step enzymatic process that leads to a reduction of resazurin, as measured by the red-fluorescent resorufin. The resulting signal is proportional to the amount of 6-phosphate dehydrogenase released into the cell medium, thereby correlating with the number of dead cells in the sample.

4.5.1. Protocol

Vybrant Cytotoxicity Assay Kit (Molecular probe, Invitrogen) can be used to determine whether this enzyme is present in the cell culture medium. Incubation of cells with the neurotoxins should not be for longer than 24 h because significant degradation of glucose 6-phosphate dehydrogenase will occur. Resazurin (15 mM) in reaction medium is added to treated cells and incubated at 37°C for 10–30 min (according kit protocol). The control cells will be incubated with cell lysis buffer in order to obtain 100% of the cell glucose 6-phosphate dehydrogenase content. Finally, the fluorescence can be measured with excitation and emission filters that are appropriate for resorufin (excitation 530–560 nm, emission 580–600 nm).

Acknowledgments

Supported by FONDECYT # 1100165.

References

1. Zecca L, Bellei C, Costi P, Albertini A, Monzani E, Casella L, Gallorini M et al (2008) New melanic pigments in the human brain that accumulate in aging and block environmental toxic metals. Proc Natl Acad Sci U S A 105:17567–17572
2. Zecca L, Fariello R, Riederer P, Sulzer D, Gatti A, Tampellini D (2002) The absolute concentration of nigral neuromelanin, assayed by a new sensitive method, increases throughout the life and is dramatically decreased in Parkinson's disease. FEBS Lett 510:216–220
3. Segura-Aguilar J, Lind C (1989) On the mechanism of Mn^{3+} induced neurotoxicity of dopamine: prevention of quinone derived oxygen toxicity by DT-diaphorase and superoxide dismutase. Chem Biol Interact 72:309–324
4. Paris I, Dagnino-Subiabre A, Marcelain K, Bennett LB, Caviedes P, Caviedes R, Olea-Azar C, Segura-Aguilar J (2001) Copper neurotoxicity is dependent on dopamine-mediated copper uptake and one-electron reduction of aminochrome in a rat substantia nigra neuronal cell line. J Neurochem 77:519–529
5. Paris I, Martinez-Alvarado P, Perez-Pastene C, Vieira MN, Olea-Azar C, Raisman-Vozari R, Cardenas S, Graumann R, Caviedes P, Segura-Aguilar J (2005) Monoamine transporter inhibitors and norepinephrine reduce dopamine-dependent iron toxicity in cells derived from the substantia nigra. J Neurochem 92:1021–1032
6. Paris I, Perez-Pastene C, Couve E, Caviedes P, Ledoux S, Segura-Aguilar J (2009) Copper dopamine complex induces mitochondrial autophagy preceding caspase-independent apoptotic cell death. J Biol Chem 284:13306–13315
7. Segura-Aguilar J, Metodiewa D, Welch C (1998) Metabolic activation of dopamine *o*-quinones to *o*-semiquinones by NADPH cytochrome P450 reductase may play an important role in oxidative stress and apoptotic effects. Biochim Biophys Acta 1381:1–6
8. Hastings TG (1995) Enzymatic oxidation of dopamine: the role of prostaglandin H synthase. J Neurochem 64:919–924
9. Segura-Aguilar J (1996) Peroxidase activity of liver microsomal vitamin D 25-hydroxylase and cytochrome P450 1A2 catalyzes 25-hydroxylation of vitamin D3 and oxidation of dopamine to aminochrome. Biochem Mol Med 58:122–129
10. Galzigna L, De Iuliis A, Zanatta L (2000) Enzymatic dopamine peroxidation in substantia nigra of human brain. Clin Chim Acta 300:131–138
11. Thompson CM, Capdevila JH, Strobel HW (2000) Recombinant cytochrome P450 2D18 metabolism of dopamine and arachidonic acid. J Pharmacol Exp Ther 294:1120–1130
12. Terland O, Flatmark T, Tangeras A, Gronberg M (1997) Dopamine oxidation generates an oxidative stress mediated by dopamine semiquinone and unrelated to reactive oxygen species. J Mol Cell Cardiol 29:1731–1738
13. Foppoli C, Coccia R, Cini C, Rosei MA (1997) Catecholamines oxidation by xanthine oxidase. Biochim Biophys Acta 1334:200–206
14. Xu Y, Stokes AH, Freeman WM, Kumer SC, Vogt BA, Vrana KE (1997) Tyrosinase mRNA is expressed in human substantia nigra. Brain Res Mol Brain Res 45:159–162
15. Paris I, Perez-Pastene C, Cardenas S, Iturriaga P, Muñoz P, Couve E et al (2010) Aminochrome induces disruption of actin, alpha-, and beta-tubulin cytoskeleton networks in substantia-nigra-derived cell line. Neurotox Res 18:82–92
16. Nirenberg M, Vaughan R, Uhl G, Kuhar M, Pickel V (1996) The dopamine transporter is localized to dendritic and axonal plasma membranes of nigrostriatal dopaminergic neurons. J Neurosci 16:436–447
17. Augood SJ, Westmore K, McKenna PJ, Emson PC (1993) Co-expression of dopamine transporter mRNA and tyrosine hydroxylase mRNA in ventral mesencephalic neurones. Brain Res Mol Brain Res 20:328–334
18. Lorang D, Amara SG, Simerly RB (1994) Cell-type-specific expression of catecholamine transporters in the rat brain. J Neurosci 14:4903–4914
19. Chen NH, Reith ME, Quick MW (2004) Synaptic uptake and beyond: the sodium- and chloride-dependent neurotransmitter transporter family SLC6. Pflugers Arch 447:519–531
20. Hitri A, Hurd YL, Wyatt RJ, Deutsch SI (1994) Molecular, functional and biochemical characteristics of the dopamine transporter: regional differences and clinical relevance. Clin Neuropharmacol 17:1–22
21. Zahniser NR, Sorkin A (2009) Trafficking of dopamine transporters in psychostimulant actions. Semin Cell Dev Biol 20:411–417
22. Melikian HE, Buckley KM (1999) Membrane trafficking regulates the activity of the human dopamine transporter. J Neurosci 19:7699–7710
23. Sorkina T, Hoover BR, Zahniser NR, Sorkin A (2005) Constitutive and protein kinase

C-induced internalization of the dopamine transporter is mediated by a clathrin-dependent mechanism. Traffic 6:157–170

24. Doolen S, Zahniser NR (2001) Protein tyrosine kinase inhibitors alter human dopamine transporter activity in *Xenopus* oocytes. J Pharmacol Exp Ther 296:931–938
25. Moron JA, Zakharova I, Ferrer JV, Merrill GA, Hope B, Lafer EM et al (2003) Mitogen-activated protein kinase regulates dopamine transporter surface expression and dopamine transport capacity. J Neurosci 23:8480–8488
26. Hoover BR, Everett CV, Sorkin A, Zahniser NR (2007) Rapid regulation of dopamine transporters by tyrosine kinases in rat neuronal preparations. J Neurochem 101:1258–1271
27. Wersinger C, Sidhu A (2003) Attenuation of dopamine transporter activity by alpha-synuclein. Neurosci Lett 340:189–192
28. Qian JJ, Cheng YB, Yang YP, Mao CJ, Qin ZH, Li K, Liu CF (2008) Differential effects of overexpression of wild-type and mutant human alpha-synuclein on MPP+-induced neurotoxicity in PC12 cells. Neurosci Lett 435:142–146
29. Fleckenstein AE, Metzger RR, Wilkins DG, Gibb JW, Hanson GR (1997) Rapid and reversible effects of methamphetamine on dopamine transporters. J Pharmacol Exp Ther 282:834–838
30. Sandoval V, Riddle EL, Ugarte YV, Hanson GR,FleckensteinAE(2001)Methamphetamine-induced rapid and reversible changes in dopamine transporter function: an in vitro model. J Neurosci 21:1413–1419
31. LittleM KY, ElmerM LW, Zhong H, Scheys JO, Zhang L (2002) Cocaine induction of dopamine transporter trafficking to the plasma membrane. Mol Pharmacol 61:436–445
32. Sundström E, Goldstein M, Jonsson G (1986) Uptake inhibition protects nigro-striatal dopamine neurons from the neurotoxicity of 1-methyl-4-phenylpyridine (MPP+) in mice. Eur J Pharmacol 131:289–292
33. Hirata Y, Suzuno H, Tsuruta T, Oh-hashi K, Kiuchi K (2008) The role of dopamine transporter in selective toxicity of manganese and rotenone. Toxicology 244:249–256
34. Weyler W, Hsu YP, Breakefield XO (1990) Biochemistry and genetics of monoamine oxidase. Pharmacol Ther 47:391–417
35. Shih JC, Grimsby J, Chen K (1997) Molecular biology of monoamine oxidase A and B: their role in the degradation of serotonin. In: Baumgarten HG, Gothert M (eds) Handbook of experimental pharmacology, vol 129, serotoninergic neurons and 5-HT receptors in the CNS. Springer, Berlin, pp 655–670
36. Strolin-Benedetti M, Dostert P, Tipton KF (1992) Developmental aspects of the monoamine-degrading enzyme monoamine oxidase. Dev Pharmacol Ther 18:191–200
37. Greene LA, Tischler AS (1976) Establishment of a noradrenergic clonal line of rat adrenal pheochromocytoma cells which respond to nerve growth factor. Proc Natl Acad Sci U S A 73:2424–2428
38. Greene LA, Tischler AS (1982) PC12 pheochromocytoma cells in neurobiological research. Adv Cellular Neurobiol 3:373–414
39. Hashimoto W, Kitayama S, Kumagai K, Morioka N, Morita K, Dohi T (2005) Transport of dopamine and levodopa and their interaction in COS-7 cells heterologously expressing monoamine neurotransmitter transporters and in monoaminergic cell lines PC12 and SK-N-SH. Life Sci 76:1603–1612
40. Jiang H, Jiang Q, Feng J (2004) Parkin increases dopamine uptake by enhancing the cell surface expression of dopamine transporter. J Biol Chem 279:54380–54386
41. Seitz G, Stegmann HB, Jäger HH, Schlude HM, Wolburg H, Roginsky VA et al (2000) Neuroblastoma cells expressing the noradrenaline transporter are destroyed more selectively by 6-fluorodopamine than by 6-hydroxydopamine. J Neurochem 75:511–520
42. King SC, Tiller AA, Chang AS, Lam DM (1992) Differential regulation of the imipramine-sensitive serotonin transporter by cAMP in human JAr choriocarcinoma cells, rat PC12 pheochromocytoma cells, and C33-14-B1 transgenic mouse fibroblast cells. Biochem Biophys Res Commun 183:487–491
43. Paris I, Lozano J, Cardenas S, Perez-Pastene C, Saud K, Fuentes P et al (2008) The catecholaminergic RCSN-3 cell line: a model to study dopamine metabolism. Neurotox Res 13:221–230
44. Bayer M, Kuçi Z, Schömig E, Gründemann D, Dittmann H, Handgretinger R et al (2009) Uptake of mIBG and catecholamines in noradrenaline- and organic cation transporter-expressing cells: potential use of corticosterone for a preferred uptake in neuroblastoma- and pheochromocytoma cells. Nucl Med Biol 36:287–294
45. Riherd DN, Galindo DG, Krause LR, Mayfield RD (2008) Ethanol potentiates dopamine uptake and increases cell surface distribution of dopamine transporters expressed in SK-N-SH and HEK-293 cells. Alcohol 42:499–508
46. Toyohira Y, Ueno S, Tsutsui M, Itoh H, Sakai N, Saito N, Takahashi K, Yanagihara N (2010) Stimulatory effects of the soy phytoestrogen genistein on noradrenaline transporter and

serotonin transporter activity. Mol Nutr Food Res 54:516–524

47. Bryan-Lluka LJ, Bönisch H (1997) Lanthanides inhibit the human noradrenaline, 5-hydroxytryptamine and dopamine transporters. Naunyn Schmiedebergs Arch Pharmacol 355:699–706
48. Suri C, Fung BP, Tischler AS, Chikaraishi DM (1993) Catecholaminergic cell-lines from the brain and adrenal-glands of tyrosine hydroxylase-SV40 T-antigen transgenic mice. J Neurosci 13:1280–1291
49. Bundey RA, Kendall DA (1998) Inhibition of receptor-mediated calcium responses by corticotrophin-releasing hormone in the CATH.a cell line. Neuropharmacology 38:39–47
50. Bouvier C, Avram D, Peterson VJ, Hettinger B, Soderstrom K, Murray TF, Leid M (1998) Catecholaminergic CATH.a cells express predominantly delta-opioid receptors. Eur J Pharmacol 348:85–93
51. Qi Y, Wang JK, McMillian M, Chikaraishi DM (1997) Characterization of a CNS cell line, CAD, in which morphological differentiation is initiated by serum deprivation. J Neurosci 17:1217–1225
52. Paris I, Martinez-Alvarado P, Cardenas S, Perez-Pastene C, Graumann R, Fuentes P, Olea-Azar C, Caviedes P, Segura-Aguilar J (2005) Dopamine-dependent iron toxicity in cells derived from rat hypothalamus. Chem Res Toxicol 18:415–419
53. Adams FS, La Rosa FG, Kumar S, Edwards-Prasad J, Kentroti S, Vernadakis A et al (1996) Characterization and transplantation of two neuronal cell lines with dopaminergic properties. Neurochem Res 21:619–627
54. Kaul S, Kanthasamy A, Kitazawa M, Anantharam V, Kanthasamy AG (2003) Caspase-3 dependent proteolytic activation of protein kinase C{Delta} mediates and regulates 1-methyl-4-phenylpyridinium (MPP+)-induced apoptotic cell death in dopaminergic cells: relevance to oxidative stress in dopaminergic degeneration. Eur J Neurosci 18:1387–1401
55. Kaul S, Anantharam V, Yang Y, Choi CJ, Kanthasamy A, Kanthasamy AG (2005) Tyrosine phosphorylation regulates the proteolytic activation of protein kinase C{Delta} in dopaminergic neuronal cells. J Biol Chem 280:28721–28730
56. Sun F, Anantharam V, Zhang D, Latchoumycandane C, Kanthasamy A et al (2006) Proteasome inhibitor MG-132 induces dopaminergic degeneration in cell culture and animal models. Neurotoxicology 27:807–815
57. Cunningham RL, Giuffrida A, Roberts JL (2009) Androgens induce dopaminergic neurotoxicity via caspase-3-dependent activation of protein kinase Cdelta. Endocrinology 150:5539–5548
58. Manakova S, Puttonen KA, Raasmaja A, Männistö PT (2004) The roles of dopamine transporter and Bcl-2 protein in the protection of CV1-P cells from 6-OHDA-induced toxicity. Toxicol Lett 154:117–123
59. Rodríguez-Martín E, Casarejos MJ, Bazán E, Canals S, Herranz AS, Mena MA (2000) Nitric oxide induces differentiation in the NB69 human catecholamine-rich cell line. Neuropharmacology 39:2090–2100

Chapter 20

^{13}C NMR Spectroscopy and Mass Spectrometry Analysis of Intermediary Metabolism in Cultured Neural Cells

Ursula Sonnewald, Arne Schousboe, and Helle S. Waagepetersen

Abstract

The use of ^{13}C and ^{15}N labeled precursors in combination with adequate analytical tools makes it possible to study metabolic pathways in cultured neural cells. The most commonly used precursors are ^{13}C labeled glucose, lactate, glutamate and acetate. For a dynamic evaluation of intermediary metabolism of cell cultures, incubation with ^{13}C containing substrates followed by nuclear magnetic resonance spectroscopy (NMRS) and mass spectrometry (MS) is excellent. NMRS can be used on cell extracts or living cells if a sufficient quantity of labeled atoms is present. MS is the more sensitive of the two methods but often it requires derivatization and separation of the components before analysis. The review provides descriptions of the basic and practical aspects of culturing neural cells, incubation and superfusion experiments and NMRS and MS analyses. It focuses on the analytical tools and the use of primary cultures of neurons and astrocytes for the elucidation of metabolic interactions between neurons and astrocytes.

Key words: Neurons, Cell culture, Nuclear magnetic resonance spectroscopy, Mass spectrometry, [1-^{13}C]glucose

1. Cell Cultures

Primary cultures of neural cells have been extensively used to study a large number of aspects of neuropharmacology and neurotransmission. Such studies have provided valuable knowledge regarding the roles of neurons and astrocytes in these processes and additionally, information about interactions between the two cell types has been obtained (reviewed by Hertz et al. (1)). During the past two decades such cultures have in combination with the use of energy substrates and amino acids labeled with isotopes (^{13}C and ^{15}N) been instrumental in providing detailed knowledge at the cellular level about energy metabolism and amino acid neurotransmitter biosynthesis and metabolism.

Michael Aschner et al. (eds.), *Cell Culture Techniques*, Neuromethods, vol. 56,
DOI 10.1007/978-1-61779-077-5_20,

1.1. Cultured Neurons

For studies concerning GABAergic and glutamatergic neurons, respectively two cell culture models have been extensively used. Cerebral cortical neurons in culture have been used to study GABAergic neurons and a detailed outline of the methodology for preparation and maintenance of such cultures is provided in an adjacent chapter (2). For studies of glutamatergic neurons, the culture system of cerebellar neurons originally described by Messer (3) has been frequently used. A detailed account of the procedure for preparation of such cultures is provided by Schousboe et al. (4) and summarized as follows:

Seven-day-old mice or rats are decapitated and the cerebellum removed aseptically and placed in Krebs' buffer containing 0.3% serum albumine and equilibrated with atmospheric air/CO_2 (95/5%). The tissue is subsequently cut into 0.4×0.4 mm cubes and minced using a Pasteur pipette. The minced tissue is incubated with shaking for 15 min in the Krebs' buffer containing 0.025% trypsin and this is terminated by adding Krebs' buffer containing 0.004% DNAse and 0.03% Soybean trypsin inhibitor. The cell suspension is centrifuged and the pellet triturated in the Krebs' buffer containing DNAse and the trypsin inhibitor. The dissociated cells are transferred to a centrifuge tube and subsequent to centrifugation at $200 \times g$ for 5 min, the pelleted cells are resuspended in neuronal culture medium containing 10% fetal calf serum (4, 5) and the cell density is adjusted to $2–3 \times 10^6$ cells/ml. The cells are seeded in poly-d-lysine coated plastic culture dishes. Astrocytic proliferation is prevented by addition of cytosine arabinoside at day 2 in culture to a concentration of 20 μM. Such cultures develop during 7–10 days in culture into functionally intact glutamatergic neurons (granule cells) which account for 80–90% of the cell population (6, 7). The remaining neurons are GABAergic stellate and Golgi neurons which can be functionally eliminated by exposing the cultures to 50 μM kainic acid (7, 8).

1.2. Cultured Astrocytes

Astrocytes are cultured either from dissociated cerebral cortex of newborn mice or cerebellum from 7-day-old mice. The procedure is essentially the same in the two cases and it is outlined in the adjacent chapter by Schousboe et al. (2).

1.3. Co-Cultures of Neurons and Astrocytes

For studies of metabolic interactions between neurons and astrocytes two different approaches have been taken to prepare suitable culture systems in which the two cell types can interact. One approach is based on the preparation of a confluent layer of astrocytes originating from either cerebral cortex or cerebellum as described above. Normally a culture period of 2 weeks is required to obtain such astrocyte cultures (9). In order to establish a co-culture system, either a suspension of dissociated cerebellum (see above) is seeded on top of a confluent layer of cerebellar astrocytes in a medium containing 20 μM cytosine arabinoside (9) or an analogous

suspension of dissociated cerebral cortex from 15-day-old embryos (see (2) for details) is seeded on top of confluent cerebral cortical astrocytes in a medium containing 20 μM cytosine arabinoside (10). In both cases a culture period of 1 week after seeding of the dissociated cells is required to obtain functionally intact glutamatergic neurons (cerebellum) or GABAergic neurons (cerebral cortex) as described by Westergaard et al. (9, 10).

Recently an alternative co-culture protocol for cerebral cortical neurons and astrocytes was developed (11). This is based on the procedure for preparation of cerebral cortical neurons (see (2) for details). Hence, cerebral cortices are aseptically dissected from 15 gestation day mouse embryos and exposed to trypsinization and trituration to produce a cell suspension in culture medium containing 10% fetal calf serum. The cell density is adjusted to 2.75×10^6 cells/ml in neuronal culture medium containing 10% fetal calf serum and seeded in plastic tissue culture dishes (11). In order to allow development of both neurons and astrocytes in these cultures during a 7–8 day culture period, cytosine arabinoside is not added to the cultures. This leads to a co-culture system exhibiting pronounced astrocytic metabolism, astrocyte-neuronal exchange of metabolites and a considerable GABA synthesis (11). Such cultures which are easily prepared and maintained have been successfully used for metabolic studies (11, 12).

2. Experiments: Superfusion, Incubation

Metabolic studies investigating energy and/or amino acid metabolism in neural cell cultures using stable isotopes such as ^{13}C and ^{15}N are performed either as incubations or superfusion studies. Several conditions have to be considered depending on the hypothesis to be examined.

2.1. Incubation Studies

An incubation experiment is uncomplicated to perform; however, plenty of parameters have to be considered to gain the best possible output.

Incubation experiments are often performed using a complete culture medium (5), however, without the addition of serum (from now on incubation medium). Change of medium is necessary since either the labeled substrate or metabolites of interest are often already present in the culture medium. Serum is not added to the medium since it makes the subsequent quantitative analyses more complicated. For the same reason the cultures are rinsed once in a phosphate buffered saline (PBS, without glucose) prior to the exposure to the incubation medium. The change of medium is a harsh procedure for the cell cultures and it has to be performed as gently as possible especially with regard to the neurons.

The PBS and incubation medium should be 37°C. The incubation is terminated by collecting the incubation medium quantitatively into an ice-cold tube. The cells are washed twice in ice-cold PBS (without glucose), after complete removal of the PBS the cells should either immediately be extracted or stored at –80°C until extraction. The extraction can be done with ice-cold 70% (v/v) ethanol or 7% perchloric acid, the former being the simplest procedure. The incubation experiment has been used in a series of studies for instance in the investigations of glucose, alanine and lactate metabolism in cerebellar granule neurons, cerebellar astrocytes and in co-cultures of these (13).

The incubation time is chosen on the basis of the type of cells, pathway of interest, labeled substrate, and analytical tools available. A short incubation period (≤1 h) requires that the labeled substrate is metabolized rather quickly into the metabolites that are analyzed and high sensitivity for detection of labeling. The amount of cells and cell culture matrix can of course be increased to circumvent this. When deciding on incubation periods one has to balance the wish to have maximal ^{13}C enrichment (long incubation time) with constant concentrations of substrate (short incubation). One should be aware of the fact that the concentration of the labeled substrate decreases and metabolites increase in the medium with time. This is of particular concern using substrates that are taken up and metabolized fast, such as investigations of glutamate metabolism in astrocytes. If a long incubation period is required the labeled substrate can be added several times at appropriate intervals. In such cases the concentration of the substrate should be monitored by taking samples from the medium prior to the addition of substrate. Particularly while using longer incubation periods (4 h) and/or while potential toxins are present in the incubation medium, one should consider examining cell survival.

2.2. Superfusion Studies

Metabolic studies have been performed using a superfusion system as that described by Drejer et al. (14). Although more complicated and expensive to use than the incubation approach, it provides a series of possibilities and benefits. The medium can be changed automatically during the experiment, thus it is possible to simulate in vivo conditions by repetitive exposure to a medium that induces neurotransmitter release. In a co-culture system, containing both glutamatergic neurons and astrocytes, metabolism can be investigated under conditions of an active glutamate-glutamine cycle (15).The flow should be kept high while attempting to imitate a narrow peak of neurotransmission. The actual flow to use is dependent on the cell culture matrix. Using 35 mm dishes 2 ml/min is recommended, however, using 25 or 80 cm^2 culture flasks, which is typical for metabolic studies, a flow of 4–5 ml/min is needed (16, 17). As mentioned above, investigating astrocytic glutamate metabolism in an incubation experiment is

hampered by the rapid decline in the concentration of glutamate in the medium. This can be overcome using the superfusion system at a constant low flow, being ≤2 ml/min for 25 and 80 cm^2 culture flasks (18). Alternatively, the exposure to glutamate could be performed in a repetitive fashion thus simulating the in vivo exposure of the astrocytes (19). Lactate is produced to a significant extent while studying energy metabolism employing ^{13}C labeled glucose. The superfusion system provides a way to avoid accumulation of lactate in the medium. Moreover, a more in vivo relevant concentration of glucose can be used due to the constant supply of fresh medium (18). One of the benefits of low flow is that you minimize the leak of metabolites which is promoted using a high flow of fresh medium.

Superfusion experiments may be performed using saline solution buffered with either HEPES (N-2-hydroxyethylpiperazine-N′-2-ethanesulfonic acid), tris (tris(hydroxymethyl) aminomethane) or phosphate. The reason for not using a complete culture medium is the complexity of the subsequent sample matrix which makes the analyses difficult. The concentration of the metabolites/analyte is much lower after a superfusion compared to the incubation design in which an accumulation occurs. However, if the medium is of no interest or the superfusion is performed at low flow a complete culture medium can be used.

The cells will detach from the matrix if they were not covered by a nylon mesh (80 μm) during the superfusion experiment. Prior to exposure to the labeled substrate the cells should adapt to the environment in the superfusion system by at least 15 min of superfusion in a buffered saline solution containing glucose in a range of 1–6 mM depending on conditions.

3. Mass Spectrometry and Nuclear Magnetic Resonance Spectroscopy

For a dynamic evaluation of intermediary metabolism of cell cultures, incubation with ^{13}C containing substrates followed by nuclear magnetic resonance spectroscopy (NMRS) and mass spectrometry (MS) is excellent. NMRS can be used on cell extracts or living cells if a sufficient quantity of labeled atoms is present. Typically cell cultures corresponding to 5–10 mg protein are used. It is difficult to give a precise number here since instruments, especially probes, are improving constantly. MS is the more sensitive of the two methods but it often requires derivatization and separation of the components before analysis. Using MS analysis of cells on 3 cm diameter dishes is possible. The following is a brief description of the basic and practical aspects of NMRS and MS analyses:

3.1. Mass Spectrometry, ^{15}N and ^{13}C Labeling

The following is by no means a comprehensive review of MS techniques but describes the methods used in the authors laboratories at present. Mass spectrometry is an analytical technique that identifies the chemical composition of a compound or sample based on the mass-to-charge (m/z) ratio of charged particles. A sample undergoes chemical fragmentation, thereby forming charged particles (ions). The ratio of charge to mass of the particles is calculated by passing them through electric and magnetic fields in a mass spectrometer (MS). In order to analyze the extent of ^{13}C or ^{15}N labeling in amino acids and organic acids, such as lactate, citrate, succinate and fumarate, gas chromatography-MS can be used if the analytes are derivatized employing MTBSTFA (-methyl--(tert-butyldimethylsilyl)-trifluoracetamide) thereby -butyldimethyl silylating active protic functions, i.e., hydroxyl, amino, carboxyl moieties as described by Mawhinney et al. (20). Alternatively liquid chromatography-mass spectrometry (LC-MS) can be used to determine the extent of ^{13}C or ^{15}N labeling in amino acids and organic acids. To obtain high accuracy and sensitivity the Phenomenex EZ:faast amino acid analysis kit combining solid phase extraction and derivatization is recommendable for a complex biological matrix (15). For analysis of extent of ^{13}C labeling in organic acids using LC-MS a derivatization procedure using TMPP, tris(trimethoxyphenyl)phosphonium can be employed (18, 21).

3.2. ^{1}H and ^{13}C Nuclear Magnetic Resonance Spectroscopy

The most sensitive nucleus for biological NMRS is ^{1}H. The carbon isotope that is most abundant, ^{12}C, does not have a nuclear spin. However, there is a naturally occurring carbon isotope that does have a nuclear magnetic moment and that is ^{13}C, which has a natural abundance of 1.1%. That together with the fact that ^{13}C has 4 times lower sensitivity than ^{1}H makes it difficult to obtain ^{13}C spectra of biological material. However, this gives the unique possibility to study cellular processes since ^{13}C enriched substrates can be administered and incorporation of ^{13}C into metabolites can be studied by ^{13}C NMRS.

When nuclei that have a magnetic moment (we will focus on ^{13}C and ^{1}H) are immersed in a static magnetic field and are exposed to pulses of radiofrequency, they can convert from a low- to a high-energy state. When relaxing back to the ground state the nuclei will release energy which gives rise to the NMRS signal. If a reference compound is present the amounts of the nuclei can be calculated from the area under relevant peaks. The reference compound added is typically ethylene glycol, a substance that gives only one ^{1}H and one ^{13}C peak (in the respective spectra). The peaks of organic compounds in the ^{13}C spectrum are due to the 1.1% naturally occurring ^{13}C. In the case of ethylene glycol this peak is in an area of the spectrum where no other peaks are located. The reference substance is added at a known concentration which gives ^{13}C peaks with a similar size as those expected from the sample.

One scan is seldom enough to obtain an adequate signal over noise (S/N) ratio. Thus, a new pulse can be given after the nuclei are fully relaxed and several pulses can be accumulated to increase the S/N ratio. For cell culture extracts the range of numbers of scans for a ^{13}C spectrum is approximately 10,000–30,000 and for a ^{1}H spectrum the number is typically 400. The time it takes for the nuclei to go back to their original energy level is called the relaxation time. Even though it complicates the issue further it has to be mentioned that the pulse angle which is applied to the nuclei and relaxation time are coupled. Signal is lost when the nucleus is not having the maximal pulse angle (90°) and the next pulse is given before the nucleus is fully relaxed. The smaller the pulse angle, the shorter the relaxation time and the smaller will be the signal. In the interest of experimental time (and thus often costs) it is important to optimize the number of scans, the pulse angle and the waiting time between pulses for optimum signal intensity. This is especially important in ^{13}C NMRS due to the low sensitivity and long acquisition times. Optimization experiments can be carried out to calculate which pulse angle and waiting time will provide the optimal signal in a given time period. However, when the waiting time between pulses is shorter than the time required for the nuclei to return to the ground state, correction factors have to be applied if accurate quantification of the signals is required (23). In the case of ^{13}C NMRS, an additional correction factor has to be used due to the phenomenon called nuclear Overhauser enhancement (NOE) which is caused by decoupling of ^{1}H. It is beyond the scope of this chapter to explain the physics behind decoupling and the NOE but the usefulness of combined relaxation and NOE correction factors for ^{13}C NMRS will be explained in the following. The spectrum of a sample with sufficient material for quantification within a reasonable period of time is taken with the pulse angle and relaxation delay that has been found to be optimal. A second spectrum is taken of the same sample with a relaxation delay of 20 s which is sufficient for relaxation of the nuclei of interest in the cell culture studies described in this chapter. Additionally, NOE is not applied to the nuclei since ^{1}H decoupling is only taking place during spectral acquisition and not during the relaxation delay. From the two sets of spectra correction factors can be obtained which have to be applied to the individual peaks. It should be noted that these factors are not NOE factors. They correct for the differential NOE and relaxation effects experienced by the reference compound and the compounds to be studied.

NMR spectra of biological material are complex and identification of compounds difficult. However, excellent reviews (for example (22)) have been published that make identification possible. This is the case since the so called “chemical shift” is constant if pH and temperature are controlled. The chemical shift differences are due to the fact that different types of nuclei and bonds in the molecule will be surrounded by various electron densities. Both,

the opposing field and the effective field can differ at each nucleus. This is described as the chemical shift phenomenon. The difference between the resonance frequency of the nucleus and a standard is the chemical shift of a nucleus. This quantity is stated in ppm (parts per million) and has the symbol delta (δ).

^{13}C Spectra are relatively easy to interpret due to the 200 ppm range over which they are distributed with only little peak overlap (22). Even though most organic molecules contain hydrogen, quantification by ^{1}H NMRS can be difficult due to overlapping signals. This is because the total spectral area is approximately 10 ppm and most peaks of interest cluster in the 1–4 ppm area. Furthermore, since the samples are usually dissolved in D_2O the HOD (deuterated water) peak generated from the non-covalently bound protons, can cause problems. If feasible, the samples should be lyophilized twice, the second time with D_2O, to minimize the HOD peak. However, it is usually necessary to suppress the residual water peak. This suppression can cause problems with the quantification of surrounding peaks as for example glucose. However, ^{13}C enrichment data can be obtained in spite of water suppression since protons on the ^{12}C and those on the ^{13}C are affected equally. ^{1}H NMR spectra are often used to calculate the ^{13}C enrichments in lactate and glucose. Furthermore, it is possible to quantify glutamate, glutamine, GABA, aspartate, acetyl aspartate, lactate, alanine and many more compounds. However, it should be noted that if ^{1}H spectra are used for quantification of metabolites the peaks have to be corrected for the number of ^{1}H, and where applicable ^{13}C enrichment (obtained from ^{13}C spectra). When the % ^{13}C enrichment is too large it is not possible to use ^{1}H spectra for quantification since ^{1}H coupled to the ^{13}C satellite peaks will overlap with ^{1}H on the ^{12}C.

4. Analysis of Results

In order to understand the results obtained by ^{13}C NMRS and MS it is necessary to understand the metabolic pathways that are to be studied. Below is a description of these pathways for [1-^{13}C]glucose (for other labeled precursors, see references (16, 23–26)).

4.1. Metabolism of [1-^{13}C]Glucose

[1-^{13}C]Glucose can be added to the incubation medium and is taken up by both neurons and astrocytes via their specific glucose transporters. It is, via glycolysis, converted to [3-^{13}C]pyruvate and one molecule of unlabeled pyruvate. Two molecules of [3-^{13}C]pyruvate and thus twice as much labeling can be obtained from [1,6-^{13}C]glucose. [3-^{13}C]Pyruvate can thereafter be converted into [3-^{13}C]lactate via the lactate dehydrogenase reaction or [3-^{13}C]alanine via the alanine aminotransferase reaction.

[3-^{13}C]Pyruvate can enter mitochondria and catalyzed by pyruvate dehydrogenase (PDH) or the anaplerotic pathway via pyruvate carboxylase (PC) in astrocytes enter the tricarboxylic acid (TCA) cycle (see Fig. 1.). [2-^{13}C]Acetyl CoA will be obtained in the oxidative pathway, and [3-^{13}C]oxaloacetate (OAA) in the anaplerotic pathway.

Figure 1 gives a schematic overview of the labeling patterns from [1-^{13}C]glucose in the first turn of the TCA cycle, both via the PDH route and the PC route. In neurons, [3-^{13}C]pyruvate enters the TCA cycle exclusively via [2-^{13}C]acetyl CoA formed by oxidative decarboxylation catalyzed by PDH. Acetyl CoA is metabolized in the cycle after condensation with unlabelled OAA to make citrate. This will in turn, after several steps, lead to the formation of [4-^{13}C]α-ketoglutarate (KG), which can leave the cycle to form [4-^{13}C]glutamate, and subsequently [2-^{13}C]GABA in GABAergic neurons. [4-^{13}C]Glutamine can be made via GS from [4-^{13}C]glutamate in the astrocytes. If [4-^{13}C]α-KG remains

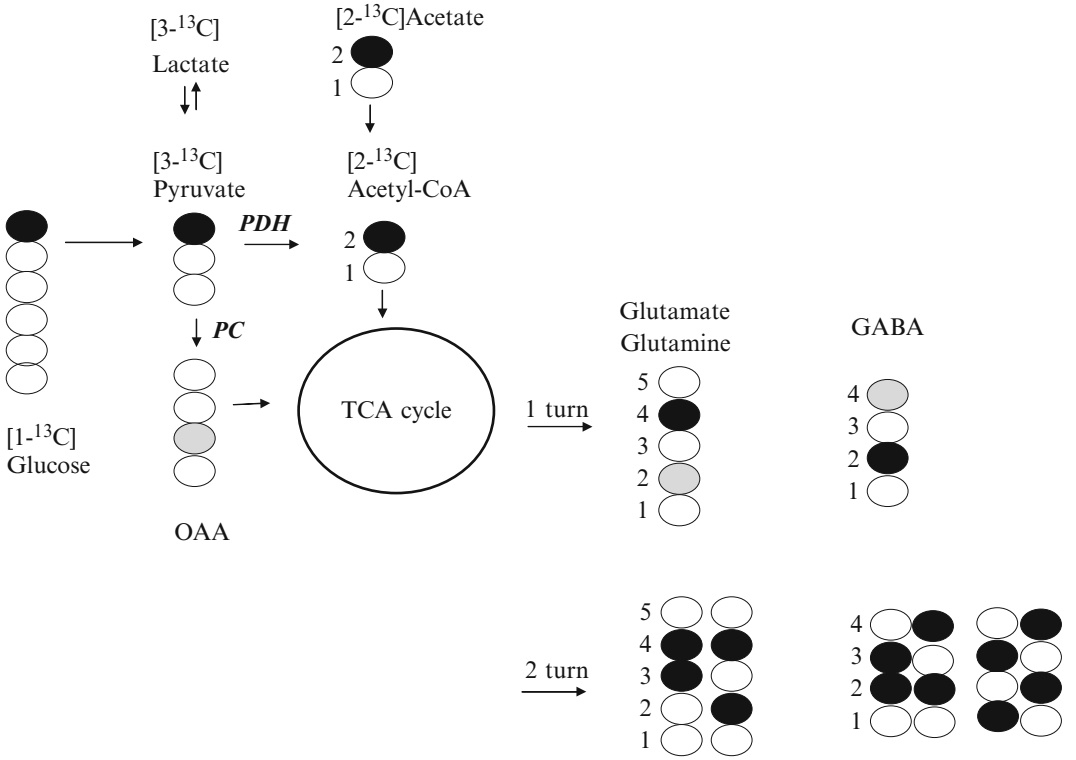

Fig. 1. A schematic overview of the metabolic fate of [1-^{13}C]glucose via the pyruvate decarboxylase (PDH) and the pyruvate carboxylase (PC) route (the latter only in astrocytes), and the first and second turn in the TCA cycle for both routes. [2-^{13}C] acetate labeling is also shown. After the initial transformation to [2-^{13}C]acetyl CoA labeling is as for [1-^{13}C]glucose. *Full black circles* represent ^{13}C from PDH, *full gray* ^{13}C from PC and *empty circles* ^{12}C. *PDH* pyruvate dehydrogenase; *PC* pyruvate carboxylase, *acetyl CoA* acetyl coenzyme A; *OAA* oxaloacetate; *TCA cycle* tricarboxylic acid cycle.

in the TCA cycle, however, it will be distributed equally between [2-^{13}C] and [3-^{13}C]succinate and fumarate and, subsequently between malate and OAA, due to the scrambling of the label in the symmetrical succinate-fumarate step. Through transamination of OAA by aspartate aminotransferase, [2-^{13}C] and [3-^{13}C]aspartate can be formed.

If [2-^{13}C]acetyl CoA condenses with labeled OAA in the second turn of the TCA cycle (Fig. 20.1), there will in addition to 1. turn labeling be an equal distribution in [2-^{13}C]/[3-^{13}C]glutamate and glutamine (the latter in astrocytes), [3-^{13}C]/[4-^{13}C]GABA, and in all carbon positions of aspartate. [3,4-^{13}C] or [2,4-^{13}C] glutamate/glutamine or [2,4-^{13}C] or [2,3-^{13}C]GABA will be formed in case [2-^{13}C] or [3-^{13}C]OAA condenses with [2-^{13}C] acetyl CoA. If α-KG remains in the cycle, [2,3-^{13}C] or [1,3-^{13}C]/[2,4-^{13}C]aspartate will be made from OAA.

In addition to the PDH route, as in neurons, in astrocytes [3-^{13}C]pyruvate can follow the anaplerotic pathway and be converted to [3-^{13}C]OAA by PC (Fig. 1). Thereafter, OAA can be aminated into [3-^{13}C]aspartate, or condense with unlabelled acetyl CoA and give [2-^{13}C]α-KG. Labeling from the anaplerotic pathway will further be detected as [2-^{13}C]glutamate and [2-^{13}C] glutamine. [4-^{13}C]GABA can then be formed in GABAergic neurons in co-culture after they have received glutamine from astrocytes and converted it to [2-^{13}C]glutamate. Following its scrambling in the symmetrical succinate step, the label will be distributed equally between [1-^{13}C] and [4-^{13}C]OAA and further in [1-^{13}C] and [4-^{13}C]aspartate (not shown in Fig. 1).

In ^{13}C NMR spectra of neurons and astrocytes incubated with [1-^{13}C]glucose labeling in glutamate, GABA (GABAergic neurons), glutamine (astrocytes), lactate, alanine and aspartate can be detected (27–29). From the multiplets around a peak it is possible to say something about the neighbors of the atom that is represented by this peak. If one neighbor has ^{13}C atoms this is represented by a doublet, if two neighbors have ^{13}C atoms it can either appear as a doublet of doublets or an apparent triplet (for details see (24)).

The advantage of ^{13}C NMR spectroscopy is that it is possible to quantify amounts of ^{13}C at specific positions in the molecule. Using MS, this is not possible (easily), and only the number of ^{13}C atoms in the molecule will be obtained. However, as stated above, sensitivity is superior to ^{13}C NMRS.

4.2. Metabolism of [2-^{13}C]Acetate

[2-^{13}C]Acetate can be added to the incubation medium and is taken up by astrocytes only since they in contrast to neurons possess transporters (29). Once taken up acetyl CoA synthetase converts [2-^{13}C]acetate to [2-^{13}C]acetyl CoA and the labeling patterns will be the same as from [1-^{13}C]glucose at the [2-^{13}C] acetyl CoA stage (Fig. 1).

5. What Are These Methods Used for?

In the following we give a few examples of what these methods can be used for. One of the major aims of the research carried out in the author's laboratories is to elucidate interactions between astrocytes and neurons. Figure 2 is a summation of some of the results obtained using the methods described.

5.1. Glutamine from Astrocytes as a Precursor for GABA in Neurons

Using [1-^{13}C]glucose or [2-^{13}C]acetate and incubation of cultures of cortical neurons (GABAergic) and astrocytes in the presence and absence of methionine sulfoximine (MSO), it was possible to demonstrate that glutamine from astrocytes is a direct precursor for GABA in neurons (28). Cortical neurons were incubated with either [1-^{13}C]glucose or [2-^{13}C]acetate and analysis of ^{13}C NMR spectra revealed that [1-^{13}C]glucose was able to label GABA in these neurons whereas [2-^{13}C]acetate was not. In astrocytes, metabolism of [1-^{13}C]glucose or [2-^{13}C]acetate led to labeling of glutamine, glutamate and others. Labeling experiments using co-cultures of neurons on astrocytes (28) revealed that GABA was labeled both by [1-^{13}C] glucose and [2-^{13}C]acetate. Thus, it was clear that a precursor from astrocytes was able to label GABA in the neurons. A possible candidate was glutamine and this hypothesis was tested by adding the

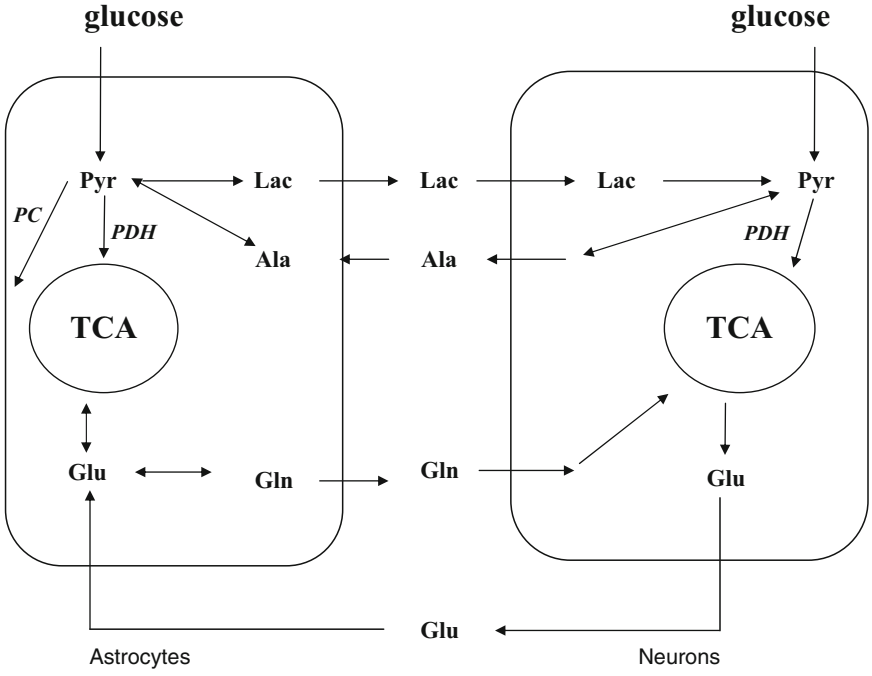

Fig. 2. A simplified overview of the "glutamate-glutamine cycle." Glutamine, formed from glutamate, is released by astrocytes and taken up by neurons. Neurons convert glutamine into glutamate which can be released by neurons and taken up by astrocytes. Lactate from astrocyte is also sent to neurons and alanine from neurons to astrocytes. *Ala* alanine; *Lac* lactate; *Gln* glutamine; *Glu* glutamate; *PC* pyruvate carboxylase; *PDH* pyruvate dehydrogenase; *Pyr* pyruvate; *TCA cycle* tricarboxylic acid cycle.

glutamine synthetase inhibitor MSO to the co-cultures to prevent glutamine synthesis and, sure enough, GABA labeling was abolished (28). This is an example of how ^{13}C NMR spectroscopy can answer questions about metabolic interaction and pathways.

References

1. Hertz L, Juurlink BHJ, Szuchet S (1985) Cell cultures. In: Lajtha A (ed) Handbook of neurochemistry, vol 8. Plenum, New York, pp 603–661
2. Schousboe A, Madsen KB, White HS (2010) Neurotransmitter transporters and anticonvulsant drug development. In: Aschner M, Sunol C (eds) chapter 22, this edition
3. Messer A (1977) The maintenance and identification of mouse cerebellar granule cells in mono layer culture. Brain Res 130:1–12
4. Schousboe A, Meier E, Drejer J, Hertz L (1989) Preparation of primary cultures of mouse (rat) cerebellar granule cells. In: Shahar A, De Vellis J, Vernadakis A, Haber B (eds) A dissection and tissue culture manual of the nervous system. Alan R. Liss, New York, pp 203–206
5. Hertz L, Juurlink BHJ, Fosmark H, Schousboe A (1982) Astrocytes in primary cultures. In: Pfeiffer SE (ed) Neuroscience approached through cell culture, vol 1. CRC, Boca Raton, FL, pp 175–186
6. Drejer J, Larsson OM, Kvamme E, Svenneby G, Hertz L, Schousboe A (1985) Ontogenetic development of glutamate metabolizing enzymes in cultured cerebellar granule cells and in cerebellum in vivo. Neurochem Res 10:49–62
7. Drejer J, Schousboe A (1989) Selection of a pure cerebellar granule cell culture by kainate treatment. Neurochem Res 14:751–754
8. Sonnewald U, Olstad E, Qu H, Babot Z, Cristofol R, Sunol C, Schousboe A, Waagepetersen HS (2004) First direct demonstration of extensive GABA synthesis in mouse cerebellar neuronal cultures. J Neurochem 91:796–803
9. Westergaard N, Fosmark H, Schousboe A (1991) Metabolism and release of glutamate in cerebellar granule cells co-cultured with astrocytes from cerebellum or cerebral cortex. J Neurochem 56:59–66
10. Westergaard N, Larsson OM, Jensen B, Schousboe A (1992) Synthesis and release of GABA in cerebral cortical neurons co-cultured with astrocytes from cerebral cortex or cerebellum. Neurochem Int 20:567–575
11. Leke R, Bak LK, Schousboe A, Waagepetersen HS (2008) Demonstration of neuron-glia transfer of precursors for GABA biosynthesis in a co-culture system of dissociated mouse cerebral cortex. Neurochem Res 33:2629–2635
12. Leke R, Bak LK, Anker M, Melø TM, Sørensen M, Keiding S, Vilstrup H, Ott P, Pertela LV, Sonnewald U, Schousboe A, Waagepetersen HS (2011) Detoxification of ammonia in mouse cortical GABAergic cell cultures increases neuronal oxidative metabolism and reveals an emerging role for release of glucose-derived alanine. Neurotox Res, submitted
13. Waagepetersen HS, Sonnewald U, Larsson OM, Schousboe A (2000) A possible role of alanine for ammonia transfer between astrocytes and glutamatergic neurons. J Neurochem 75:471–479
14. Drejer J, Honore T, Schousboe A (1987) Excitatory amino acid-induced release of 3H-GABA from cultured mouse cerebral cortex interneurons. J Neurosci 7:2910–2916
15. Bak LK, Sickmann HM, Schousboe A, Waagepetersen HS (2005) Activity of the lactate-alanine shuttle is independent of glutamate-glutamine cycle activity in cerebellar neuronal-glial cell cultures. J Neurosci Res 79:88–96
16. Bak LK, Schousboe A, Sonnewald U, Waagepetersen HS (2006) Glucose is necessary to maintain neurotransmitter homeostasis during synaptic activity in cultured glutamatergic neurons. J Cereb Blood Flow Metab 26:1285–1297
17. Bak LK, Walls AB, Schousboe A, Ring A, Sonnewald A, Waagepetersen HS (2009) Neuronal glucose but not lactate utilization is positively correlated with NMDA-induced neurotransmission and fluctuations in cytosolic Ca^{2+} levels. J Neurochem 109(suppl 1):87–93
18. Walls AB, Heimbürger CM, Bouman SD, Schousboe A, Waagepetersen HS (2009) Robust glycogen shunt activity in astrocytes: effects of glutamatergic and adrenergic agents. Neuroscience 158:284–292
19. Bak LK, Johansen ML, Schousboe A, Waagepetersen HS (2007) Among the branched-chain amino acids only valine metabolism is upregulated in astrocytes during glutamate exposure. J Neurosci Res 85:3465–3470

20. Mawhinney TP, Robinett RSR, Atalay A, Madson MA (1986) Analysis of amino acids as their tert.-butyldimethylsilyl derivatives by gas-liquid chromatography and mass spectrometry. J Chromatogr 358:231–242
21. Leavens WJ, Lane SJ, Carr RM, Lockie AM, Waterhouse I (2002) Derivatization for liquid chromatography/electrospray mass spectrometry: synthesis of tris(trimethoxyphenyl)phosphonium compounds and their derivatives of amine and carboxylic acids. Rapid Commun Mass Spectrom 16:433–441
22. Fana TW-M, Lane AN (2008) Structure-based profiling of metabolites and isotopomers by NMR. Prog Nucl Magn Reson Spectrosc 52:69–117
23. Badar-Goffer RS, Bachelard HS, Morris PG (1990) Cerebral metabolism of acetate and glucose studied by ^{13}C-n.m.r. spectroscopy. A technique for investigating metabolic compartmentation in the brain. Biochem J 266:133–139
24. Cerdan S, Kunnecke B, Seelig J (1990) Cerebral metabolism of [1, 2-$^{13}C_2$]acetate as detected by in vivo and in vitro 13C NMR. J Biol Chem 265:12916–12926
25. Sonnewald U, Qu H, Aschner M (2002) Pharmacology and toxicology of astrocyte-neuron glutamate transport and cycling. J Pharmacol Exp Ther 301:1–6
26. Qu H, Waagepetersen HS, van Hengel M, Wolt S, Dale O, Unsgard G, Sletvold O, Schousboe A, Sonnewald U (2000) Effects of thiopental on transport and metabolism of glutamate in cultured cerebellar granule neurons. Neurochem Int 37:207–215
27. Sonnewald U, Westergaard N, Hassel B, Muller TB, Unsgard G, Fonnum F, Hertz L, Schousboe A, Petersen SB (1993) NMR spectroscopic studies of ^{13}C acetate and ^{13}C glucose metabolism in neocortical astrocytes: evidence for mitochondrial heterogeneity. Dev Neurosci 15:351–358
28. Sonnewald U, Westergaard N, Schousboe A, Svendsen JS, Unsgard G, Petersen SB (1993) Direct demonstration by ^{13}CNMR spectroscopy that glutamine from astrocytes is a precursor for GABA synthesis in neurons. Neurochem Int 22:19–29
29. Waniewski RA, Martin DL (1998) Preferential utilization of acetate by astrocytes is attributable to transport. J Neurosci 18:5225–5233

Chapter 21

Culture Models for the Study of Amino Acid Transport and Metabolism

Marta Sidoryk-Węgrzynowicz and Michael Aschner

Abstract

Glutamine (Gln) plays an important role in satisfying brain metabolic demands and as a precursor for the synthesis of glutamate and γ-aminobutyric acid (GABA). In vitro cultured cell studies have shown that carrier-mediated Gln transport between astrocytes and neurons represents a key factor in the glutamate–GABA–glutamine cycle. Gln transport in astrocytes involves the following systems: sodium-dependent: system N; system ASC; system A and sodium-independent: system L, whereas in neurons only systems A and L are active. Gln-specific carriers primarily mediate not only inward transport, but can also largely contribute to outwardly transport. Therefore, both uptake and release studies are important for the investigation of Gln transport and metabolism. In this unit, methods are presented for radiolabel Gln uptake and efflux experiments in primary astrocyte cultures. These methods can be useful for the investigation of Gln transport by different systems in any tested conditions. We also review here the basic properties of the glutamate–GABA–glutamine cycle, including aspects of transport and metabolism. Furthermore, a section is devoted to the characteristics of the transport systems N, ASC, A and L and to the functional and molecular identifications of the Gln-specific carriers.

Key words: Glutamine, Transport system, Uptake assay, Efflux assay

1. Glutamine Uptake and Release by Primary Astrocytes

Glutamine (Gln) transport in mammalian cells is mediated by a variety of amino acid transporters (more details in the text below). Kinetic studies and substrate-specific inhibitory experiments in in vitro cultured cells have demonstrated that Gln transport in both in astrocytes and neurons mainly involves three sodium-dependent systems: A, ASC and N, and one sodium-independent system: L (1). Transporters belonging to these systems primarily mediate inward transport, but they can also function in outwardly Gln transport.

Michael Aschner et al. (eds.), *Cell Culture Techniques*, Neuromethods, vol. 56,
DOI 10.1007/978-1-61779-077-5_21,

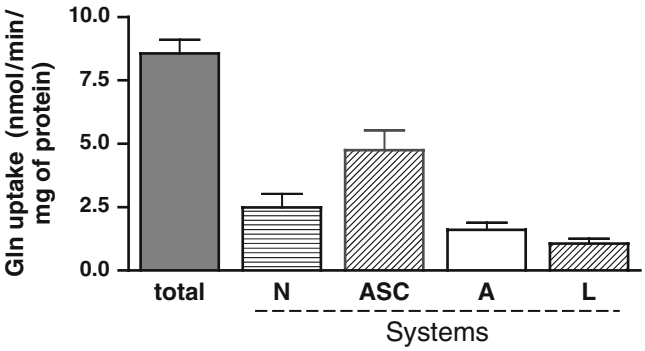

Fig. 1. A representative example of L-[G-^{3}H]-Gln uptake in primary astrocytes in control conditions. Experiments were performed in the presence of 32-fold excess of the following amino acids: MeAIB + Thr + Leu (selection for system N); MeAIB + His + Leu (selection for system ASC); Thr + His + Leu (selection for system A); MeAIB + Thr + His (selection for systems L). Results are mean ± SD of three independent experiments. *His* histidine; *Leu* leucine; *MeAIB* 2-(methylamino)isobutyric acid; *Thr* threonine.

Several questions relevant to the regulation of Gln transport in the CNS cells may be conveniently addressed by in vitro uptake and release assays. Studies in the presence of sodium-free or sodium-containing medium, as well as competitors specific for particular transporter families can dissect out the involvement of each system in Gln transport under the tested conditions. In this unit, protocols are presented for performing the uptake and release studies with radiolabeled Gln in primary astrocyte culture. These protocols can be easily modified for the investigation of Gln transport in other cultures and cell lines. A representative example of L-[G-^{3}H]-Gln uptake by primary astrocytes in control conditions is shown in Fig. 1.

2. Materials

2.1. Buffers and Reagents

1. Primary astrocytes culture grown to at least 75% confluence in 24-well culture plates.
2. L-[G-^{3}H] Gln (e.g., specific activity: 49.0 Ci/mmol; Amersham Biosciences, Piscataway, NJ).
3. L-Glutamine (Gln; e.g., Sigma, St. Louis, MO).
4. Incubation media (see recipe).
5. L-Histidine (His; e.g., Sigma, St. Louis, MO).
6. L-Threonine (Thr; e.g., Sigma, St. Louis, MO).
7. 2-Methylaminoisobutyric acid (MeAIB; e.g., Sigma, St. Louis, MO).
8. L-Leucine (Leu; e.g., Sigma, St. Louis, MO).

9. 6-Diazo-5-oxo-L-norleucine (DON; e.g., Sigma, St. Louis, MO).
10. 1 M NaOH.
11. Scintillation fluid (e.g., Fisher Scientific, Pittsburgh, PA).
12. DC Protein Assay Kit (Bio-Rad, Hercules, CA).

2.2. Equipment

1. Incubator suitable for mammalian tissue cultures (37°C, 5% CO_2).
2. Scintillation counter (e.g., 6500, Beckman Coulter, Fullerton, CA).
3. Scintillation vials and caps (e.g., Fisher Scientific, Pittsburgh, PA).
4. Equipments for measuring protein content: microplate reader set to 750 nm of excitation wavelength (e.g., FlexStation and SoftMax Pro Program, Molecular Devices, Sunnyvale, CA).

Note: When working with radioactivity, appropriate precautions must be taken to avoid contamination of personnel conducting the study and surroundings. The experiments must be performed in a designated area following the guidelines of the local radiation safety committee and the user must be authorized to use such materials.

3. Gln Uptake Assay Procedure

Each experimental treatment should be replicated in at least four wells in a minimum of three independently isolated cultures. Power analysis should be used a priori to determine the number of necessary replicates which will vary based on the variability of the results and the set alpha value.

1. Culture the cells in 24-well plates until they are >75% confluent.
2. Prepare incubation media (IM) (see Tables 1 and 2).
3. Adjust pH to 7.4.

3.1. Kinetic Analysis

1. Prepare stock of non-radioactive ("cold") 20 mM Gln in IM (±NaCl).
2. Prepare radioactive mixture: cold Gln + 1 μCi of radiolabeled ("hot") L-[G-^{3}H] Gln (1 tube per 4 wells) (see Table 3).
3. Remove culture medium.
4. Wash the cells three times using warm (37°C) IM (2 ml/well for each wash).
5. Preincubate culture with IM (250 μl/well) for 30 min at 37°C.

Table 1
Preparation of incubation medium for Gln uptake by both sodium-dependent and -independent carriers

+NaCl (pH 7.4)

IM volume (mM)		50 ml	100 ml	200 ml	300 ml	400 ml	500 ml	600 ml	1 l
150	NaCl (mg)	438	877	1.753	2.629	3.507	4.383	5.259	8.766
3	KCl (mg)	11.2	22.4	44.8	67.2	89.6	112	134	224
2	$CaCl_2$ (mg)	11.1	22.2	44.4	66.6	88.8	111	133	222
0.8	$MgCl_2$ (mg)	3.8	7.6	15.2	2.8	30.5	38.1	45.7	163
5	Glucose (mg)	45	90	180	270	360	450	540	900
10	HEPES (mg)	119	238	477	715	953	1.191	1.430	2.383

Table 2
Preparation of incubation medium for Gln uptake by sodium-independent carriers

–NaCl (pH 7.4)

IM volume (mM)		50 ml	100 ml	200 ml	300 ml	400 ml	500 ml	600 ml	1 l
150	Choline chloride (mg)	1.047	2.094	4.188	6.282	8.376	10.470	12.564	20.940
3	KCl (mg)	11.2	22.4	44.8	67.2	89.6	112	134	224
2	$CaCl_2$ (mg)	11.1	22.2	44.4	66.6	88.8	111	133	22
0.8	$MgCl_2$ (mg)	3.8	7.6	15.2	22.8	30.5	38.1	45.7	76.2
5	Glucose (mg)	45	90	180	270	360	450	540	900
10	HEPES (mg)	119	238	477	715	953	1.191	1.430	2.383

Table 3
Preparation of radioactive mixture for kinetic analysis

	Gln (μl)						
Gln (mM)	**0.158**	**0.5**	**1**	**2**	**4**	**8**	**10**
cold Gln	7.9	25	50	100	200	400	500
L-[G-^{3}H] Gln	1	1	1	1	1	1	1
IM (+ or – NaCl)	991.85	974.75	949.75	899.75	799.75	599.75	499.75

6. Remove IM and add radioactive mixture (250 µl/well).
7. Incubate for 5 min at 37°C.
8. Remove radioactive mixture into a radioactive waste container.
9. Terminate the reaction – wash the cells three times using ice-cold IM (2 ml/well for each wash).
10. Pour the washes into the radioactive waste container.
11. Add 450 µl of 1 M NaOH.
12. Incubate for 30 min at 37°C.
13. Transfer 400 µl of lysate to the scintillation vials and add 4 ml of scintillation fluid.
14. Prepare control for "hot" Gln: put 0.25 µl of L-[G-^{3}H] Gln into the scintillation vial and add 4 ml of scintillation fluid.
15. Measure ^{3}H activity using liquid scintillation counter.
16. Take 5 µl of lysate for protein concentration assay.
17. Measure protein content in the samples following the manufacturer's protocol.
18. Calculate the results using the following equation:

$$\frac{(1.125 * v_p / v_{iso}) * (C_{Gln} / 4)}{t * 90 * m_p} \quad [\text{nmol} / \text{min} / \text{mg}].$$

- v_p – activity in 400 µl of lysate [dpm]
- v_{iso} – activity in 0.25 µl of isotope [dpm]
- C_{Gln} – concentration of cold Gln [µM]
- t – time of incubation of cells in radioactive mixture [min]
- m_p – protein content in 5 µl of lysate [mg]

3.2. Competition Analysis

1. Prepare stock of cold 20 mM Gln in IM (+NaCl).
2. Prepare stocks of 20 mM amino acids (His, Thr, MeAIB, Leu) in IM (+NaCl).
3. Prepare radioactive mixture: cold Gln + 1 µCi of hot L-[G-^{3}H] Gln + combination of amino acid according to each System substrate specificity (1 tube per 4 wells) (see Table 4).
4. Remove culture medium.
5. Wash the cells three times using warm (37°C) IM (2 ml/well for each wash).
6. Preincubate culture with IM (250 µl/well) for 30 min at 37°C.
7. Remove IM and add radioactive mixture (250 µl/well).
8. Incubate for 5 min at 37°C.

Table 4
Preparation of radioactive mixture for competition analysis

	Final concentration	Investigated system (μl)			
		A	N	ASC	L
Cold Gln	0.158 mM	7.9	7.9	7.9	7.9
L-[G-^{3}H] Gln		1	1	1	1
His	5 mM	250	–	250	250
Thr	5 mM	250	250	–	250
MeAIB	5 mM	–	250	250	250
Leu	5 mM	250	250	250	–
IM (+ NaCl)		241.85	241.85	241.85	241.85

9. Remove the radioactive mixture into the radioactive waste container.
10. Terminate the reaction – wash the cells three times using ice-cold IM (2 ml/well for each wash).
11. Pour the washes into the radioactive waste container.
12. Add 450 μl of 1 M NaOH.
13. Incubate for 30 min. at 37°C.
14. Transfer 400 μl of lysate to the scintillation vial and add 4 ml of scintillation fluid.
15. Prepare control for "hot" Gln: put 0.25 μl of L-[G-^{3}H] Gln into the scintillation vial and add 4 ml of scintillation fluid.
16. Measure ^{3}H activity using liquid scintillation counter.
17. Take 5 μl of lysate for protein concentration assay.
18. Measure protein content in the samples following the manufacturer's protocol.
19. Calculate the uptake using the equation described above (point 18 of kinetic analysis protocol).

4. Gln Efflux Assay Procedure

IM used in efflux assays contains DON – an inhibitor of Gln-requiring enzymes, to prevent L-[G-^{3}H] Gln breakdown in the cells.

1. Prepare IM (±NaCl) with 50 μM DON.
2. Prepare stock of cold 20 mM Gln in IM (+NaCl).

3. Prepare stocks of 20 mM amino acids (His, Thr, MeAIB, Leu) in IM (+NaCl).
4. Prepare radioactive mixture: 0.5 µl of cold Gln + 4 µl of L-[G-^{3}H] Gln + 995.5 µl of IM (+NaCl) (1 tube per 4 wells).
5. Prepare efflux medium (1 tube per 4 wells) (see Table 5).
6. Remove culture medium.
7. Wash the cells three times using warm (37°C) IM (2 ml/well for each wash).
8. Preincubate culture with IM (250 µl/well) for 30 min at 37°C.
9. Pre-load the cells with radiolabeled Gln: remove IM and add radioactive mixture (250 µl/well).
10. Incubate for 30 min at 37°C.
11. Remove the radioactive mixture into the radioactive waste container.
12. Wash the cells three times using warm (37°C) IM (2 ml/well for each wash).
13. Pour the washes into the radioactive waste container.
14. Add warm efflux medium (250 µl/well).
15. Incubate for 10 min at 37°C.
16. Aspirate the medium and save it for scintillation counting.
17. Add 450 µl of 1 M NaOH.
18. Incubate for 30 min at 37°C.
19. Transfer 230 µl of efflux medium (point 16) to the scintillation vial and add 4 ml of scintillation fluid.
20. Transfer 400 µl of NaOH lysate to the scintillation vial and add 4 ml of scintillation fluid.

Table 5
Preparation of efflux medium

		Investigated systems (µl)					
	Final concentration (mM)	All	Na independent	A	N	ASC	L
His	5	–	–	250	–	250	250
Thr	5	–	–	250	250	–	250
MeAIB	5	–	–	–	250	250	250
Leu	5	–	–	250	250	250	–
IM (+ NaCl)		1.000	–	250	250	250	250
IM (– NaCl)		–	1.000	–	–	–	–

21. Measure ^{3}H activity using liquid scintillation counter.
22. Calculate the amount of Gln released from the cells in 10 min normalized to the amount of preloaded Gln (results should not be expressed in nmol of released Gln/min/mg of protein, because the concentration of intracellular Gln is not known) using the following equation:

$$[(1.087 * Ve) / (1.087 * Ve + 1.125 * Vi)] * 100\%$$

- *V*e – activity measured in 230 μl of efflux medium [dpm]
- *V*i – activity measured in 400 μl of lysate [dpm]

5. Background of Glutamine Transport in CNS

Active Gln transport across the plasma membrane is essential for the supply of this amino acid for cellular metabolism. In the CNS, Gln plays a key role in neuron–glia interactions predominantly via astrocyte-mediated control of the turnover of neuronally derived Glu and γ-aminobutyric acid (GABA), the principal excitatory and inhibitory neurotransmitters, respectively (2, 3). In addition to its specific role in neurotransmission, Gln also supports cellular energy requirements (4). A portion of Glu derived from Gln can be oxidized to an intermediate of tricarboxylic acid cycle (TCA) – alpha-ketoglutaric acid (αKG) (Fig. 2) (5).

Upon its synaptic release during neurotransmission, Glu is taken up largely by astrocytes (6, 7). In the astrocytes Glu is converted into Gln via a highly active and glia-specific enzyme, glutamine synthetase (GS) and subsequently released back into the extracellular space. Once taken up by juxtaposed neurons, Gln serves as a precursor for neurotransmitter synthesis, Glu or GABA in reactions catalyzed by phosphate-activated glutaminase (PAG) in glutamatergic neurons or by PAG and glutamic acid decarboxylase (GAD) in GABAergic neurons. Gln passage across the astrocytic and neuronal plasma membranes is mediated by specific transporting proteins and is a key factor in the so-called glutamine–glutamate–GABA cycle (Fig. 2) (8, 9).

Transporters are integral membrane proteins characterized by their ability to mediate movement of small molecules across the membranes by active transport or facilitated diffusion (10). Traditionally, mammalian amino acid transporters have been assigned to different transport systems, depending on their kinetic and regulatory properties, substrate specificity, pH sensitivity and ion dependence (11). Gln transport in mammalian tissues is mediated mainly by the sodium-dependent systems: A, ASC and N, and the sodium-independent system L (12). Table 6 summarizes

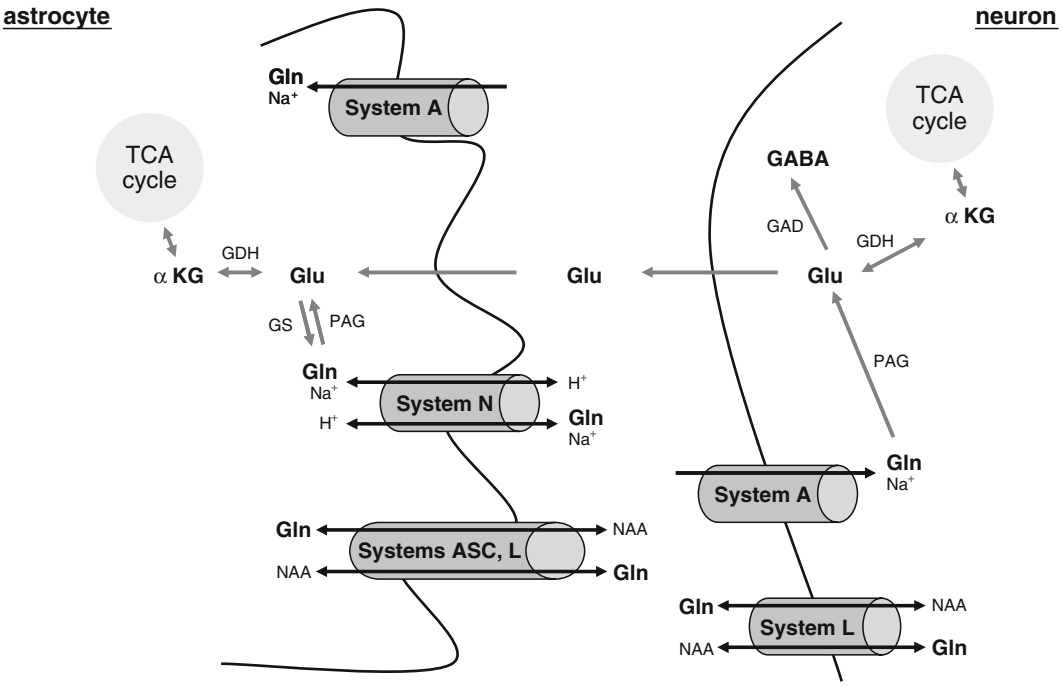

Fig. 2. Schematic representation showing the involvement of amino acid transporter systems in Gln–Glu–GABA cycle between astrocytes and neurons. Glutamate released from presynaptic terminals is transported to the astrocytes, where it is converted to Gln by the glutamine synthetase (GS). In turn, Gln is released into the extracellular space and taken up by neurons, where Glu is regenerated via phosphate-dependent glutaminase. Glu may then be subsequently converted into GABA. In both astrocytes and neurons some portion of Glu is utilized for the synthesis of alpha-ketoglutaric acid, which enters the tricarboxylic acid (TCA) cycle. For additional details please refer to the text above. *GAD* glutamic acid decarboxylase; *GDH* glutamate dehydrogenase; *GS* glutamine synthetase; *αKG* alpha-ketoglutaric acid; *PAG* phosphate activated glutaminase; *NAA* neutral amino acids; *TCA* tricarboxylic acid.

Table 6
Functional characteristic of the systems involved in Gln transport in mammalian CNS

	Systems			
Features	**A**	**ASC**	**N**	**L**
Neutral amino acids	Short chain	Short chain	Containing side-chain nitrogen	Bulky
Synthetic model substrates	MeAIB			BCH
Inhibition by low pH	+	–	+	–
Na^+ dependence	+	+	+	–

BCH 2-aminobicyclo [2,2,1]heptane-2-carboxylic acid; *MeAIB* 2-(methylamino)isobutyric acid

some of the properties that distinguish these four transport systems. Recently, several proteins belonging to these systems have been characterized at the molecular level. A list of Gln transporters is presented in Table 7.

Table 7
Glutamine transporters in the CNS

Transporter	Mechanism	Substrate specificity	Localization in brain
System ASC			
ASCT2	Antiport	Ala, Ser, Cys, Thr, Gln, Asn	Astrocytes
System N			
SNAT3	Cotransport with Na^+/ antiport with H^+	Gln, Asn, His	Astrocytes
SNAT5	Cotransport with Na^+/ antiport with H^+	Gly, Asn, Ala, Ser, Gln, Met, His	Astrocytes
System A			
SNAT1	Cotransport with Na^+	Gln, Asn, His	Neurons
SNAT2	Cotransport with Na^+	Gln, Asn, His	Astrocytes, neurons
System L			
LAT1	Antiport	Leu, Ala, Ser, Gln	Astrocytes, neurons
LAT2	Antiport	Leu, Ala, Ser, Gln	Astrocytes, neurons

Ala alanine; *Asn* asparagine; *Cys* cysteine; *Gln* glutamine; *Gly* glycine; *His* histidine; *Leu* leucine; *Ser* serine; *Thr* threonine

6. Functional Characteristics of the Systems Transporting Gln in the CNS

6.1. Sodium-Dependent Systems

6.1.1. System A (SNAT1 and SNAT2)

System A is widely expressed in mammalian cells and catalyzes Na^+-dependent transport of neutral short-chain amino acids with preference for alanine, glutamine and serine. It recognizes model substrate 2-(methylamino)isobutyric acid (MeAIB) and exhibits marked inhibition at low extracellular pH. System A transporters couple amino acid transport with the Na^+ electrochemical potential gradient with 1:1 stoichiometry (13). System A is able to mediate symport of amino acid and Na^+ ion without countertransporting an additional compound, while the majority of other transporters work as antiporters. Activity of system A can be stimulated by several factors, including amino acid starvation, hormones and growth factors (14–16).

System A transporter – SNAT1 (previously referred to as ATA1, GlnT, SA2, SAT1) is composed of 481 amino acids. SNAT1 transports all zwitterionic, aliphatic amino acids and displays high affinity for glutamine, alanine, asparagines and cysteine. In the CNS, SNAT1 is highly expressed in glutamatergic and GABAergic neurons in situ and in cultures (13, 17). This transporter was also found in dopaminergic neurons of the substantia nigra and in cholinergic motoneurons. SNAT1 is not expressed in

astrocytes but was found in other non-neuronal components, namely luminal membranes of the ependyma (18).

Another transporter belonging to the system A – SNAT2 (previously known as ATA2, SA1 or SAT2) is a protein consisting of 506 amino acids. This transporter operates by a mechanism similar to SNAT1, but differs from the latter in its substrate specificity as it shows high affinity for proline. The expression of SNAT2 is more widespread than SNAT1: this transporter has been found in all tested tissues. In the CNS, SNAT2 transporter is enriched in glutamatergic neurons and in spinal motoneurons (19). High levels of SNAT2 mRNA have also been found in glia and in endothelial cells comprising the blood–brain barrier (20).

6.1.2. System ASC (ASCT1, ASCT2)

System ASC was originally named for three of the preferred substrates, alanine, serine and cysteine (1). This system is known to function as an exchanger capable of mediating both influx and efflux of these amino acids. Distinguishing characteristics of system ASC from the other Na^+-dependent systems include insensitivity to pH changes. The first isolated isoform of system ASC from human brain, transporter ASCT1, is ubiquitously expressed, but does not recognize Gln (21, 22). The second isoform, ASCT2, was cloned from rat astrocyte cultures. This transporter is composed of 539 amino acids (23). ASCT2 accepts Gln with high affinity and is responsible for a highly efficient Gln uptake by cell lines and tumors (24–26). In astrocytes, this transporter is mainly responsible for Gln efflux by obligatory exchange with extracellular amino acids (27).

6.1.3. System N (SNAT3, SNAT5)

System N shows narrow substrate specificity to amino acids containing nitrogen in their side chain, such as Gln, histidine and asparagine. Other properties of system N include high sensitivity to pH and substitution for Li^+ in place of Na^+. In situ hybridization in brain sections and immunohistochemistry in primary cell cultures identified a glial localization of system N isoform – SNAT3 (previously referred to SN1). In humans, SNAT3 is composed of 504 amino acids (28). This transporter is responsible for the inward and outward transport of Gln, the direction depending on the Gln and pH gradients (27, 28). Marked immunoreactivity of SNAT3 was observed in glia adjacent to glutamatergic and GABAergic synapses and cell bodies, suggesting that this transporter is a major mediator of Gln efflux from astrocytes and supplies Gln for neurotransmitter synthesis in neurons (29).

Another system N isoform – SNAT5 (know also as a SN2) was found in a variety of tissues, including the brain. SNAT5 protein is composed of 471 amino acids and is 63% identical to SNAT3. Similar to SNAT3, SNAT5 mediates Na^+/amino acid cotransport and countertransport of H^+. These transporters differ in

their substrate profile: SNAT3 can recognize classic system N substrates, while SNAT5 favors serine (30, 31).

6.2. Sodium-Independent Systems

6.2.1. System L (LAT1 and LAT2)

System L catalyzes Na^+-independent transport of neutral amino acids with high affinity for leucine and is inhibited by synthetic model substrate 2-aminobicyclo (2,2,1)heptane-2-carboxylic acid (BCH). This system has been shown to be involved in efflux as well as in influx of amino acids (1). In the brain, system L is the major transport system of the blood–brain barrier (32). Low-affinity and high-capacity uptake of glutamine via this system was observed in both astrocytes and neurons. LAT1 and LAT2, two molecular isoforms belonging to the system L exist as heterodimers with the 4F2 heavy chain (33). LAT1 is a protein of 506 amino acids and has 12 transmembrane spanning domains. LAT2, which exhibits similar topology to LAT1, is composed of 535 amino acids. The mRNAs coding for both LAT1 and LAT2 are detectable in cultured astrocytes as well as cultured neurons (34). These transporters differ in substrate specificity; LAT1 has a narrow substrate profile, whereas LAT2 is capable of transporting many neutral amino acids. Studies have shown that LAT2 recognizes Gln with higher affinity than LAT1 (32).

7. Summary

Studies in the recent years have provided evidence that carrier-mediated glutamine transport between astrocytes and neurons is a key factor in the glutamate–glutamine–GABA cycle. The molecular basis of Gln passage in CNS has been investigated extensively over the last few years. Gln transport in CNS involves the following systems: (a) sodium-dependent: system N; system ASC; system A and (b) sodium-independent: system L. Here we are presenting protocols for performing the uptake and release studies of radiolabeled Gln by different systems in primary astrocyte culture. Moreover, in this unit, the basic properties of glutamine–glutamate–GABA cycle are discussed, including aspects of Gln transport and metabolism.

Acknowledgments

This chapter was supported by grants R01ES010563 (MA) and R01ES07331 (MA) from the National Institutes of Health and National Institute of Environmental Health Sciences; and grant W81XWH-05-0239 from the Department of Defense (MA).

References

1. Christensen HN (1990) Role of amino acid transport and countertransport in nutrition and metabolism. Physiol Rev 70:43–77
2. Bak LK, Schousboe A, Waagepetersen HS (2006) The glutamate/GABA-glutamine cycle: aspects of transport, neurotransmitter homeostasis and ammonia transfer. J Neurochem 98:641–653
3. Hamberger A, Chiang GH, Nylén G, Scheff SW, Cotman CW (1979) Glutamate as a CNS transmitter. Evaluation of glucose and glutamine as precursors for the synthesis of preferentially relased glutamate. Brain Res 168:513–530
4. Erecinska M, Zaleska M, Nelson D, Nissim I, Yudkoff M (1988) Glucose and the metabolism of [^{15}N] glutamate in synaptosomes. J Neurochem 51:892–902
5. Daikhin Y, Yudkoff M (2000) Compartmentation of brain glutamate metabolism in neurons and glia. J Nutr 130:1026S–1031S
6. Takanaga H, Tokuda N, Ohtsuki S, Hosoya K, Terasaki T (2002) ATA2 is predominantly expressed as system A at the blood-brain barrier and acts as brain-to-blood efflux transport for L-proline. Mol Pharmacol 61:1289–1296
7. Waniewski RA, Martin DL (1986) Exogenous glutamate is metabolized to glutamine and exported by rat primary astrocyte cultures. J Neurochem 47:304–313
8. Laake JH, Takumi Y, Eidet J, Torgner IA, Roberg B, Kvamme E et al (1999) Postembedding immunogold labelling reveals subcellular localization and pathway-specific enrichment of phosphate activated glutaminase in rat cerebellum. Neuroscience 88:1137–1151
9. Schousboe A, Hertz L, Svenneby G, Kvamme E (1979) Phosphate activated glutaminase activity and glutamine uptake in primary cultures of astrocytes. J Neurochem 32:943–950
10. Palacín M, Estévez R, Bertran J, Zorzano A (1998) Molecular biology of mammalian plasma membrane amino acid transporters. Physiol Rev 78:969–1054
11. Oxender D, Christensen H (1963) Distinct mediating systems for the transport of neutral amino acids by the Ehrlich cell. J Biol Chem 238:3686–3699
12. Christensen HN, Liang M (1965) An amino acid transport system of unassigned function in the Ehrlich ascites tumor cell. J Biol Chem 240:3601–3608
13. Chaudhry FA, Schmitz D, Reimer RJ, Larsson P, Gray AT, Nicoll R et al (2002) Glutamine uptake by neurons: interaction of protons with System A transporters. J Neurosci 22:62–72
14. Kilberg MS (1986) System A-mediated amino acid transport:metabolic control at the plasma membrane. Trends Biochem Sci 11:183–186
15. McGivan JD, Pastor-Anglada M (1994) Regulatory and molecular aspects of mammalian amino acid transport. Biochem J 15:321–334
16. Moule SK, McGivan JD (1987) Epidermal growth factor, like glucagon, exerts a short-term stimulation of alanine transport in rat hepatocytes. Biochem J 247:233–235
17. Armano S, Coco S, Bacci A, Pravettoni E, Schenk U, Verderio C et al (2002) Localization and functional relevance of system A neutral amino acid transporters in cultured hippocampal neurons. J Biol Chem 277:10467–10473
18. Mackenzie B, Schäfer MK, Erickson JD, Hediger MA, Weihe E, Varoqui H (2003) Functional properties and cellular distribution of the System A glutamine transporter SNAT1 support specialized roles in central neurons. J Biol Chem 278:23720–23730
19. Yao D, Mackenzie B, Ming H, Varoqui H, Zhu H, Hediger MA et al (2000) A novel System A isoform mediating Na^+/neutral amino acid cotransport. J Biol Chem 275:22790–22797
20. González-González IM, Cubelos B, Giménez C, Zafra F (2005) Immunohistochemical localization of the amino acid transporter SNAT2 in the rat brain. Neuroscience 130:61–73
21. Arriza JL, Kavanaugh MP, Fairman WA, Wu YN, Murdoch GH, North RA et al (1993) Cloning and expression of a human neutral amino acid transporter with structural similarity to the glutamate transporter gene family. J Biol Chem 268:15329–15332
22. Shafqat S, Tamarappoo BK, Kilberg MS, Puranam RS, McNamara JO, Guadano-Ferraz A et al (1993) Cloning and expression of a novel Na^+- dependent neutral amino acid transporter structurally related to mammalian Na^+/glutamate cotransporters. J Biol Chem 268:15351–15355
23. Sonnewald U, Westergaard N, Schousboe A, Svendes JS, Unsgard G, Petersen SB (1993) Direct demonstration by [^{13}C] NMR spectroscopy that glutamine from astrocytes is a precursor for GABA synthesis in neurons. Neurochem Int 22:19–29

24. Bode BP, Souba WW (1994) Modulation of cellular proliferation alters glutamine transport and metabolism in human hepatoma cells. Ann Surg 220:411–422
25. Fuchs BC, Bode BP (2005) Amino acid transporters ASCT2 and LAT1 in cancer: partners in crime? Semin Canc Biol 15:254–266
26. Wasa M, Wang HS, Okada A (2002) Characterization of L-glutamine transport by a human neuroblastoma cell line. Am J Physiol Cell Physiol 282:C1246–C1253
27. Bröer A, Brookes N, Ganapathy V, Dimmer KS, Wagner CA, Lang F et al (1999) The astroglial ASCT2 amino acid transporter as a mediator of glutamine efflux. J Neurochem 73:2184–2194
28. Chaudhry FA, Reimer RJ, Krizaj D, Barber D, Storm-Mathisen J, Copenhagen DR et al (1999) Molecular analysis of system N suggests novel physiological roles in nitrogen metabolism and synaptic transmission. Cell 99:769–780
29. Boulland JL, Osen KK, Levy LM, Danbolt NC, Edwards RH, Storm-Mathisen J et al (2002) Cell-specific expression of the glutamine transporter SN1 suggests differences in dependence on the glutamine cycle. Eur J Neurosci 15:1615–1631
30. Nakanishi T, Kekuda R, Fei YJ, Hatanaka T, Sugawara M, Martindale RG et al (2001) Cloning and functional characterization of a new subtype of the amino acid transport system N. Am J Physiol Cell Physiol 281:C1757–C1768
31. Nakanishi T, Sugawara M, Huang W, Martindale RG, Leibach FH, Ganapathy ME et al (2001) Structure, function, and tissue expression pattern of human SN2, a subtype of the amino acid transport system N. Biochem Biophys Res Commun 281:1343–13488
32. Segawa H, Fukasawa Y, Miyamoto K, Takeda E, Endou H, Kanai Y (1999) Identification and functional characterization of a Na+ – independent neutral amino acid transporter with broad substrate selectivity. J Biol Chem 274:23740–23745
33. Mastroberardino L, Spindler B, Pfeiffer R, Skelly PJ, Loffing J, Shoemaker CB et al (1998) Amino-acid transport by heterodimers of 4F2hc/CD98 and members of a permease family. Nature 395:288–291
34. Nagaraja TN, Brookes N (1996) Glutamine transport in mouse cerebral astrocytes. J Neurochem 66:1665–1674

Chapter 22

Neurotransmitter Transporters and Anticonvulsant Drug Development

Arne Schousboe, Karsten K. Madsen, and H. Steve White

Abstract

Excitatory and inhibitory neurotransmission mediated by glutamate and GABA, respectively, plays a major role in generation of seizures. So far, emphasis has been placed on the GABA system in attempts to develop antiepileptic drugs. Tiagabine, a selective inhibitor of GABA transporter 1 (GAT1), is marketed for treatment of certain seizure types and serves as a proof of principle that inhibitors of GABA transport may be interesting in this context. The chapter describes the methodology available to investigate in detail the pharmacology of GABA transporters and design of studies leading to identification of drug candidates. Emphasis is placed on a possible role of extrasynaptic GABA transporters in seizure control.

Key words: GABA, Transporters, Glutamate, Neurons, Astrocytes, Epilepsy

1. Introduction

Neurotransmission is based on release and subsequent inactivation of signaling molecules referred to as neurotransmitters. Stimulus-coupled release of classical neurotransmitters always involves coupling of neurotransmitter vesicles to the synaptic membrane and quantal release of the appropriate transmitter substance (1). The inactivation mechanism, however, may either rely on enzymatic degradation of the transmitter as in the case of acetylcholine or the mechanism involves the action of high-affinity plasma membrane transporters specific for certain transmitters (1). The present review will specifically deal with a discussion of the transporters involved in the inactivation of the excitatory and inhibitory amino acid neurotransmitters glutamate and GABA, respectively (2–5).

Michael Aschner et al. (eds.), *Cell Culture Techniques*, Neuromethods, vol. 56,
DOI 10.1007/978-1-61779-077-5_22,

2. Transporter Families

Two members of the solute carrier (SLC) families, the SLC1 and SLC6, are responsible for high-affinity transmembrane transport of the amino acid and monoamine neurotransmitters (3). The SLC1 family is selective for transport of glutamate and aspartate (4) and the SLC6 family includes transporters for GABA, glycine, norepinephrine, dopamine, and serotonin (3).

2.1. The SLC1 Family

Table 1 summarizes the members of the SLC1 family which are responsible for inactivation of glutamate and aspartate both of which have an excitatory action on neurons. The two most prominent of these transporters are EAAT1 and EAAT2; both of which are mainly expressed in astrocytes (6, 7). They are of great importance for the maintenance of low extracellular levels of glutamate (7, 8). Failure to carry out this function results in excitotoxic neuronal death (9, 10) and it has been shown that a number of neurodegenerative disorders are associated with malfunctioning astrocytic glutamate transporters (7, 11, 12).

2.2. The SLC6 Family

As mentioned earlier, the SLC6 family comprises a large number of neurotransmitter transporters (3) but in the context of anticonvulsant drugs, clearly the GABA transporters are the most interesting. Table 2 provides a summary of some of the basic characteristics of the GABA transporters. In the present review, the HUGO nomenclature has been used. The most abundantly expressed family member is GAT1 which is located presynaptically on GABAergic neurons throughout the central nervous system (13, 14). It is, however, also expressed in astrocytes (14).

Table 1
Basic characteristics of SLC1 transporters

Transporter		Substrate		Inhibitor
Systematic	Trivial	Endogenous	Synthetic	non-substrate
EAAT1	GLAST	L-glu/L-asp	THA, TMOA	TBOA
EAAT2	GLT-1	L-glu/L-asp	PDC, D-asp	TBOA·DHK
EAAT3	EAAC-1	L-glu/L-asp		TBOA
EAAT4	–	L-glu/L-asp		TBOA, TMG
EAAT5	–	L-glu/L-asp		TBOA

THA threo-β-hydroxy aspartate; *TMOA* threo-β-methoxyaspartate; *TBOA* threo-β-benzyloxyaspartate; *DHK* dihydrokaihate; *PDC* L-trans-pyrrolidine-2,4-dicarboxylate
From Gether et al. (3)

Table 2
Basic characteristics of GABA transporters in the SLC6 family

Transporter name				Substrate		
Mouse	**Rat**	**Human**	**HUGO**	**Endogenous**	**Synthetic**	**Inhibitor**
GAT1	GAT-1	GAT-1	GAT1	GABA	NIP/GUV	Tiagabine
GAT2	BGT-1	BGT-1	BGT1	Betaine/GABA	–	EF-1502
GAT3	GAT-2	GAT-2	GAT2	GABA/β-ala	NIP	SNAP-5114
GAT4	GAT-3	GAT-3	GAT3	GABA/β-ala	NIP	SNAP-5114

NIP nipecotic acid; *GUV* guvacine; *EF-1502* (*N*-[4,4-bis(3-methyl-2-thienyl)-3-butenyl]-4-(methylamino)-4,5,6,7-tetrahydrobenzo[*d*]isoxazol-3-ol); *SNAP-5114* 1-[2[tris(4-methoxyphenyl)mmethoxy]ethyl]-(*S*)-3-piperidine carboxylic acid

Expression of BGT1 is not restricted to the brain and it is found abundantly in the kidney (15). In the brain, BGT1 is located in both neurons and astrocytes and primarily in extrasynaptic regions (13, 16, 17). It may be of interest in relation to epilepsy and anticonvulsant drugs that the expression of BGT1 has been reported to be increased in the hippocampus after kainate-induced neuronal injury (18).

GAT2, like BGT1, is expressed in multiple organs, including the brain; however, its expression in the brain is limited and its highest expression level is seen neonatally (13, 19, 20). GAT3 expression is confined to the central nervous system with prominent expression in retina, brainstem, and diencephalon whereas it is less abundant in hippocampus and cortex. Its expression is most prominent in astrocytic processes often associated with GABAergic structures (21, 22). It should be noted that its expression seems to correlate with astrocyte sealing of synapses suggesting a perisynaptic localization matching that of GAT1 (23). Altogether, only GAT1, BGT1, and GAT3 may be of relevance in relation to being targets for anticonvulsant drugs. In this context, their perisynaptic or extrasynaptic localization may be of functional importance. This aspect will be discussed further later.

3. Transporters as Targets for Anticonvulsants

Among the members of the SLC1 and SLC6 transporter families presented earlier, the glutamate transporter family (SLC1) is generally not considered in this context. This does not in any way imply that glutamatergic excitatory transmission does not play a

role in seizure control. Quite to the contrary, hyperactivity of excitatory transmission will generate seizures (24) and it is interesting that β-lactam antibiotics, which have been shown to increase the expression of EAAT2 transporters (25), seem to ameliorate drug-induced seizure activity. Thus, a member of this β-lactam family, ceftriaxone reduced pentylenetetrazol-induced seizure in mice after prolonged treatment (26). It is, however, not clear that the treatment with the antibiotic actually led to increased expression of the EAAT2 glutamate transporter. In contrast, pharmacological agents which may inhibit glutamate transporters would be useless in this context as they would likely act as proconvulsants and neurotoxins (24).

Since seizure activity is associated with hypofunction of inhibitory GABAergic neurotransmission, strategies aimed at enhancing this function will often lead to anticonvulsant activity (24). It is therefore possible that inhibition of GABA transporters would constitute a promising strategy (24). Indeed the successful development of the antiepileptic drug tiagabine, which specifically inhibits GAT1, serves as an important proof of concept that supports this approach (24). To better understand this principle it is, however, necessary to elucidate the pharmacological properties of the different cloned GABA transporters of the SLC6 transporter family as well as that of neuronal and astroglial transport (27).

4. The Use of Cultured Neurons and Astrocytes as Well as Transfected HEK Cells to Study GABA Transporters

4.1. Cell Cultures

Primary cultures of cerebral cortical neurons and astrocytes are prepared as detailed by Hertz et al. (28, 29). An outline of the procedures is provided below. To prepare a neuronal culture consisting primarily of GABAergic neurons, the cerebral hemispheres are isolated aseptically from 15-day-old mouse embryos and placed in tissue culture medium (30) containing 10% fetal calf serum. The age of the embryos is critical as the period of peak neuronal production in cerebral cortex is around 4–6 days prenatally (31). Removal of the olfactory bulbs, hippocampus, basal ganglia, and meninges leads to a greater representation of GABAergic neurons in the cultures. The tissue is subsequently cut into small cubes and trypsinized for 15 min at 37°C in a Ca^{2+}- and Mg^{2+}-free salt solution containing 0.025% trypsin. The trypsinization is stopped by adding a trypsin inhibitor from soybeans and the cell suspension is triturated. To remove DNA, this medium contains additionally DNAse (75 IU/ml). Finally, the cells are suspended in culture medium at a density of 2×10^6 cell/ml (30) with 10% fetal calf serum, 25 mM KCl, 12 mM glucose, and 7 μM *p*-aminobenzoate, and seeded in poly-D-lysine coated plastic culture plates. Every 2 days the cultures receive aliquots of

1.2 M glucose to maintain a minimum glucose concentration of 12 mM. To minimize astrocytic contamination, the cultures are exposed to 20 μM cytosine arabinoside 48 h after seeding. The culture period is normally 1 week at which time the neurons are fully differentiated as GABAergic neurons (32).

Astrocytes from cerebral cortex are prepared using the technique originally described by Booker and Senserbrenner (33) and modified by Hertz et al. (29, 30). The cerebral hemispheres are removed aseptically from new born (0–24 h) mice at which age neuronal precursor cells have ceased proliferation and therefore develop poorly in culture (29). The tissue is placed in culture medium (30) containing 20% fetal calf serum and the neopallium is dissected, i.e., the olfactory bulbs, hippocampus, basal ganglia, and meninges are removed. Subsequently, the tissue is passed through a Nitex nylon mesh (80 μM) and the cell suspension (in culture medium) is seeded in plastic tissue culture dishes at a cell density of about 10^6 cells per 60 mm dish. After reaching confluency at 2 weeks in culture, the serum concentration is reduced to 10% and the culture medium supplemented with 0.25 mM dibutyryl cAMP for an additional week in culture. This procedure leads to well-differentiated astrocytes having morphological and biochemical properties corresponding to their in vivo counterparts (29, 30).

4.2. Transfected Cell Lines

Human embryonic kidney (HEK) cells stably or transiently expressing GABA transporters were generated as the cloned mouse cDNA of the four transporters were made available to us by Prof. Nathan Nelson (19). Construction of plasmids encoding the four mouse GABA transporters as well as a Blasticidine resistance coding region was carried out via standard molecular biology approaches (34). Generation of stable cell lines for each of the GABA-transporter clones was accomplished by introducing the antibiotic Blasticidine-S 48 h post-transfection at a concentration of 50 μM. At the time where a stable colony had been established, the concentration of Blasticidine-S was lowered to 5 μM to keep a constant selection pressure thereby ensuring the continued expression of the GABA transporter over multiple generations. The transfected HEK cells are kept in Dulbecco's culture medium supplemented with 10% fetal bovine serum, 1 U/mL penicillin, and 0.1 mg/mL streptomycin.

5. Pharmacology of Neuronal-, Astroglial-, and Cloned-GABA Transporters

More than 50 years ago, it was observed that slices from cerebral cortex were able to accumulate GABA from the incubation medium (35) but it took another 10 years to demonstrate a high-affinity transport system for GABA in cerebral cortical slices (36).

Most of the accumulated GABA was found associated with nerve terminals (37). It was unequivocally shown by Henn and Hamberger (38) that astroglial cells also possess a high-affinity transport system for GABA, a finding confirmed by the use of primary cultures of astrocytes (39). Primary cultures of cerebral cortical neurons and astrocytes have been used in detailed studies designed to characterize the pharmacological properties of these transporters (27, 40–43). Some of these results are given in Table 3. It is seen that only very few GABA analogs exhibit

Table 3
Inhibitory activities of various GABA analogs on cultured cortical neurons and astrocytes

	GABA uptake inhibition IC_{50} or $K_{m/i}$ (μM)	
Compound	**Neurons**	**Astrocytes**
GABA	8[a]	32[a]
Nipecotic acid	12	16
Guvacine	32	29
DABA	1,000	>5,000
ACHC	200	700
β-alanine	1,666[b]	843[b]
THPO	501[b]	262[b]
Exo-THPO	780	250
N-methyl-exo-THPO	405	48
N-ethyl-exo-THPO	390	301
N-2-hydroxyethyl-exo-THPO	300	200
N-4-phenylbutyl-exo-THPO	100	15
N-acetyloxyethyl-exo-THPO	200	18
(R/S)-EF1502	2	2
(R)-EF1502	1.5	0.65
(S)-EF1502	>100	>100
N-DPB-THPO	38[b]	26
N-DPB-Nipecotic acid	1.3[b]	2.0[b]
N-DPB-guvacine	4.9[b]	4.2[b]
N-DPB-exo-THPO	1.4	0.6
N-DPB-*N*-methyl-exo-THPO	5	2
NNC 05-2090	–	–
SNAP-5114	–	–
NNC-711	1.24	0.64
Tiagabine	0.45	0.18

Data summarized from (34, 39, 46, 47, 66–72)
[a]K_m
[b]K_i
[c]Human BGT-1

selectivity with regard to inhibition of neuronal and astrocytic GABA transport. The most selective analogs are those which are N-substituted derivatives of *exo*-THPO (3-hydroxy-4-amino-4,5,6,7-tetrahydro-1,2-benzisoxazol). As will be discussed below, these analogs have turned out to be important lead structures (Fig. 1) in designing drugs that have anticonvulsant properties.

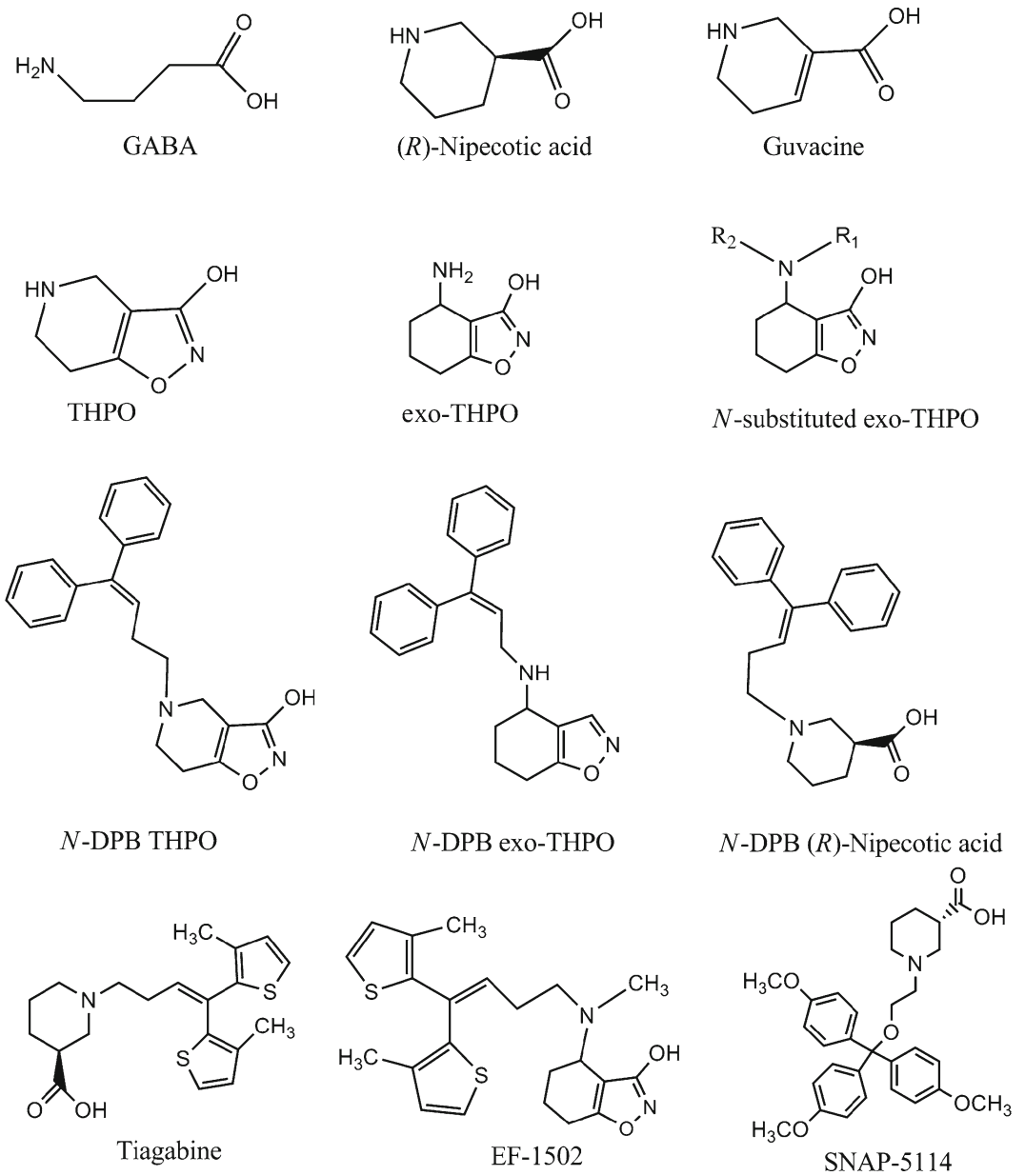

Fig. 1. Chemical structures of GABA and key GABA transport inhibitors mentioned in Tables 3 and 4.

The availability of the mouse clones of the four GABA transporters (Table 2) from the laboratory of Nathan Nelson (19, 44, 45) enabled us to create HEK cell lines transfected with those clones for either transient or stable expression of the transporters as described earlier (34, 46). Using these cell lines as tools it could be demonstrated that some of the GABA analogs and most prominently EF1502 (*N*-[4,4-bis(3-methyl-2-thienyl)-3-butenyl]-4-(methylamino)-4,5,6,7-tetrahydrobenzo[*d*]isoxazol-3-ol) (43) inhibited not only GAT1 but also the BGT1 carrier (47, 48). As shown in Table 4, the GABA analog SNAP-5114 ([(*S*)-(−)-1-[2-[tris-(4-methoxyphenyl)methoxy]ethyl]-3-piperidinecarboxylic

Table 4
Inhibitory activities of various GABA analogs on cloned GABA transporters

	GABA uptake inhibition IC_{50} or $K_{m/i}$ (μM)			
Compound	**GAT1**	**BGT1**	**GAT2**	**GAT3**
GABA	17[a]	51[a]	15[a]	17[a]
Nipecotic acid	24	>1,000	113	159
Guvacine	39	>1,000	228	378
DABA	128	528[c]	300	710
ACHC	132	1,070[c]	>1,000	>10,000
β-alanine	2,920	1,100[c]	66	110
THPO	1,300	3,000	800	5,000
Exo-THPO	1,000	3,000	>3,000	>3,000
N-methyl-exo-THPO	450	>3,000	>3,000	>3,000
N-ethyl-exo-THPO	320	>1,000	>1,000	>1,000
N-2-hydroxyethyl-exo-THPO	>500	>500	>500	>500
N-4-phenylbutyl-exo-THPO	7	>500	>1,000	>1,000
N-acetyloxyethyl-exo-THPO	550	>1,000	>1,000	>1,000
(R/S)-EF1502	7	26	>300	>300
(R)-EF1502	4	22	>150	>150
(S)-EF1502	120	34	>150	>150
N-DPB-THPO	30	200	>300	>1,000
N-DPB-Nipecotic acid	0.64	7,210[c]	550	4,390
N-DPB-guvacine	–	–	–	–
N-DPB-exo-THPO	6	100	>100	>100
N-DPB-*N*-methyl-exo-THPO	2	200	>100	>100
NNC 05-2090	19	1.4	41	15
SNAP-5114	>30	22	20	6.6
NNC-711	–	–	–	–
Tiagabine	0.11	>100	>100	800

Data summarized from (13, 34, 40–43, 46, 47, 73)
[a]K_m
[b]K_i
[c]Human BGT-1

acid] preferentially inhibits GAT3 (49). A more extensive summary of the ability of a number of the structural analogs of GABA to inhibit the cloned GABA transporters expressed in HEK cells is provided in Table 4. It is seen that the majority of these analogs are inhibitors of GAT1 while only some are inhibitors of either BGT1 or GAT2 and GAT3. The pharmacological basis for a number of these GABA analogs to act as potent anticonvulsants in animal models of epilepsy will be discussed in the following section. As several of these studies have utilized isobologram analysis, the principles underlying this analysis are described below.

6. Isobologram Analysis

Isobologram studies as described by Löewe (50) and further adapted by Tallarida (51) and Tallarida et al. (52) were performed on the combinations between tiagabin and EF1502 or SNAP-5114 and tiagabin or EF1502 in audiogenic seizure (AGS)-susceptible Frings mice and between tiagabin or EF1502 in corneal kindled CF no. 1 mice. Isobologram studies can identify the interaction of drugs in combination as being either purely additive, antagonistic, or synergistic. Drugs in combination theoretically follow the general equation of additivity $a/A + b/B = 1$ where a and b are the doses of the first and second drug, respectively, co-administered in a mixture exerting a desired effect. A and B are the doses of the drugs which exert the same desired effect when administered separately. The nature of a specific drug interaction for a pair of drugs is investigated at several fixed-ratio combinations, e.g., 3:1, 1:1, and 1:3. A requirement for isobologram analysis is parallelism of the slope function of drug A and B, which can be tested by doing a *t*-test on the slopes obtained by probit analysis of the dose–response curve as described by Finney (53).

A fixed-ratio combination of 1:3 means that the drug mixture is composed of $a = 1/4 * A$ and $b = 3/4 * B$ meaning that 25 and 75% of the action is mediated by drug A and B, respectively, regardless of the amounts of drugs in combination, hence the amount of a and b is fixed in respect to each other. The theoretical $ED_{50,add}$ dose of the 1:3 fixed-ratio combination is composed of $a = 1/4 * ED_{50}$ of drug A and $b = 3/4$ of the ED_{50} of drug B. Dose–response curves are then established for all three fixed-ratio combinations and the experimentally determined $ED_{50,exp}$ for each fixed-ratio combination is obtained by probit analysis. When determining the type of interaction resulting from the fixed-ratio combinations the theoretical $ED_{50,add}$ dose is compared to the experimentally derived $ED_{50,exp}$ using the Student's *t*-test. An $ED_{50,exp}$ that is found to be

significantly higher, equal, or lower than the $ED_{50,add}$ is considered to be either antagonistic, additive, or synergistic, respectively. The two drugs are injected in such a way that the time to peak effect coincides with the challenge stimulus to evoke a seizure, e.g., high-intensity sound stimulus used for the AGS-susceptible Frings mouse or corneal stimulation used for the corneal-kindled CF no.1 mice.

The data follow a normal distribution on the log scale, therefore the Student's *t*-test should also be performed on the log scale, hence $\log(ED_{50}) \pm SEM(\log ED_{50})$ of both the theoretical and experimental mixture needs to be obtained before a *t*-test can be performed. The $ED_{50,add}$ is calculated as described previously; however, the calculation of the $SEM(\log ED_{50,add})$ value is a bit more difficult and some assumptions need to be taken. $SEM(\log ED_{50})$ for drug A and B is established in (1a, 1b) and an approximation converts $SEM(\log ED_{50})$ to $SEM(ED_{50})$ from log to non-log scale in (2). The variance is obtained in (3) and the combined variance for the combination of drug A and B is finally calculated in (4). Going backwards through (3) and (2), the $SEM(\log ED_{50,add})$ is finally obtained. The upper 95% CI is used to calculate the $SEM(\log ED_{50,add})$ (1a) when evaluating an antagonistic interaction, and (1b) using the lower 95% CI is used when evaluating synergistic interactions. This is necessary if the 95% CI is not symmetric around the ED_{50} on the log scale.

$$SEM(\log ED_{50}) = (\log(\text{upper CI}) - \log(ED_{50}))/1.96, \quad (1a)$$

$$SEM(\log ED_{50}) = (\log(ED_{50}) - \log(\text{lower CI}))/1.96, \quad (1b)$$

$$SEM(ED_{50}) = 2.3 \times (ED_{50}) \times SEM[\log(ED_{50})], \quad (2)$$

$$V(ED_{50}) = SEM(ED_{50})^2, \quad (3)$$

$$V(ED_{50,add}) = f_A{}^2 \times V(ED_{50,\text{drug A}}) + (1 - f_A)^2 \times V(ED_{50,\text{drug B}}). \quad (4)$$

f_A corresponds to fraction of drug A in the mixture, hence, $f_A = ¼$ in the 1:3 fixed-ratio mixture. The degrees of freedom of $V(ED_{50,add})$ is given by $N_{add} = N_A + N_B - 4$. Likewise, the $SEM(\log ED_{50,exp})$ is obtained by (1a) or (1b) when evaluating synergistic or antagonistic interactions, respectively.

7. GAT Inhibitors as Anticonvulsants

Studies performed 3 decades ago by Horton et al. (54), Wood et al. (55, 56), Krogsgaard-Larsen et al. (57), Croucher et al. (58), and Schousboe et al. (59) demonstrated that inhibitors of GABA

uptake are, in general, able to act as anticonvulsants. It was shown that the mechanism for this action likely involves the ability of these compounds to increase the synaptic pool of GABA (55).

These GABA analogs are not able to cross the blood–brain barrier unless they are made less polar or more lipophilic by either converting the analogs to prodrugs (57) or placing a lipophilic side chain (see Fig. 1) at the nitrogen atom (60). The latter principle resulted in the synthesis of an enormous number of lipophilic GABA analogs during the subsequent decades (see (27) and (43) for references). An important outcome of these studies was the development of tiagabine, a selective GAT1 inhibitor as an antiepileptic drug (24). This unequivocally serves as a proof of principle for the mechanism by which GABA uptake inhibitors act as anticonvulsants.

It has been debated whether selective inhibition of astrocytic GABA uptake rather than neuronal GABA uptake might be a governing principle as suggested originally by Krogsgaard-Larsen et al. (57) and Schousboe et al. (59). Two observations seem to support this notion: (i) Diaminobutyric acid preferentially inhibiting neuronal GABA uptake (61) can act as a proconvulsant (54) and (ii) a close correlation exists between the affinity of a series of inhibitors of astroglial GABA transport and the potency of these compounds to act as anticonvulsants in the audiogenic Frings mice whereas no such correlation was found between the affinity for neuronal GABA transport and anticonvulsant potency (34).

The advent of the discovery using isobolographic analysis that the lipophilic GABA analog EF-1502 (Fig. 1), inhibiting equipotently GAT1 and BGT1 in combination with tiagabine (48) demonstrated a synergistic anticonvulsant action, has prompted investigations aimed at elucidating the role of BGT1 in seizure control. This has also led to the proposal that synaptic and extrasynaptic GABA acting at synaptic and extrasynaptic GABA receptors, respectively, may play different roles in seizure control (62–64). A recent study in which the GAT2/GAT3 inhibitor SNAP-5114 was combined with either tiagabine or EF-1502 in isobologram analysis using AGS-susceptible Fring's mice (65) has provided additional evidence in support of this hypothesis. Thus, tiagabine and SNAP-5114 exhibited an additive effect in this analysis whereas EF-1502 acted synergistically with SNAP-5114 when administered in combination. Since GAT1 and GAT2/GAT3 are located in close proximity in the synapse whereas BGT1 is located extrasynaptically this result is in perfect agreement with the notion that extrasynaptic GABA receptors are of particular interest in seizure management. Collectively, these observations demonstrate that drugs that act selectively to inhibit GABA transport by acting on the BGT1 transporter are potential drug candidates for seizure control.

8. Perspectives

Over the years, there has been much greater success in designing and synthesizing drugs that target GABA transporters than there has been in finding drugs that modulate (increase) expression of glutamate transporters. In this regard, it seems like there is a substantial opportunity for trying to modify hyperexcitability by enhancing the reuptake of the excitatory neurotransmitter substance glutamate.

The discovery of EF-1502 and SNAP-5114, both reasonably selective drugs that target non-GAT1 GABA transporters, has provided insight into the potential importance of extrasynaptic GABA transporters in the control of seizure disorders. However, the full potential of this class of GABA transport inhibitors will not be fully realized until a drug has been identified that is fully selective for each of the cloned transporters (much like tiagabine is for GAT1). Only then will we fully understand the therapeutic potential, safety, and adverse event profile of this class of drugs.

This brief review has focused on the potential therapeutic use of glutamate and GABA transport modulators as potential anticonvulsant compounds; however, glutamate and GABA also play extremely important roles in other neurological and psychiatric disorders including sleep, anxiety, depression, and neurodegenerative disorders (e.g., Parkinson's, Alzheimer's, Huntington's, etc.). In addition, drugs that modulate glutamate reuptake could be used to potentially enhance learning and memory and prevent excitotoxic cell death. The discovery and subsequent development of highly selective drugs that target glutamate and GABA transporters would potentially provide novel new approaches to treating these and other CNS disorders.

Acknowledgments

The expert secretarial assistance of Ms Hanne Danø is cordially acknowledged. The experimental work forming the basis of this review has been supported by grants from the Lundbeck Foundation (J.nr. 21/05 & R19-A2199).

References

1. McGeer PL, Eccles JC, McGeer EG (1987) Molecular neurobiology of the mammalian, 2nd edn. Plenum, New York, pp 109–150
2. Schousboe A (1990) Neurochemical alterations associated with epilepsy or seizure activity. In: Dam M, Gram L (eds) Comprehensive epileptology. Raven, New York, pp 1–16
3. Gether U, Andersen PH, Larsson OM, Schousboe A (2006) Neurotransmitter transporters: molecular function of important

drug targets. Trends Pharmacol Sci 27: 375–383

4. Gegelashvili G, Schousboe A (1997) High-affinity glutamate transporters: regulation of expression and activity. Mol Pharmacol 52:6–15
5. Fonnum F (1984) Glutamate: a neurotransmitter in mammalian brain. J Neurochem 42:1–11
6. Gegelashvili G, Schousboe A (1998) Cellular distribution and kinetic properties of high-affinity glutamate transporters. Brain Res Bull 45:233–238
7. Danbolt NC (2001) Glutamate uptake. Progr Neurobiol 65:1–105
8. Schousboe A (2003) Role of astrocytes in the maintenance and modulation of glutamatergic and GABAergic neurotransmission. Neurochem Res 28:347–352
9. Benveniste H, Drejer J, Schousboe A, Diemer NH (1984) Elevation of the extracellular concentrations of glutamate and aspartate in rat hippocampus during transient cerebral ischemia monitored by intracerebral microdialysis. J Neurochem 43:1369–1374
10. Choi DW, Rothman SM (1990) The role of glutamate neurotoxicity in hypoxic-ischemic neuronal death. Annu Rev Neurosci 13:171–182
11. Rothstein JD, Van Kammen M, Levey AI, Martin LJ, Kuncl RW (1995) Selective loss of glial glutamate transporter GLT-1 in amyotrophic lateral sclerosis. Ann Neurol 38:73–84
12. Schousboe A, Waagepetersen HS (2005) Role of astrocytes in glutamate homeostasis: implications for excitotoxicity. Neurotox Res 8:221–225
13. Borden LA (1996) GABA transporter heterogeneity: pharmacology and cellular localization. Neurochem Int 29:335–356
14. Conti F, Melone M, De Biasi S, Minelli A, Brecha NC, Ducati A (1998) Neuronal and glial localization of GAT-1, a high-affinity gamma-aminobutyric acid plasma membrane transporter, in human cerebral cortex: with a note on its distribution in monkey cortex. J Comp Neurol 396:51–63
15. Rasola A, Galietta LJ, Barone V, Romeo G, Bagnasco S (1995) Molecular cloning and functional characterization of a GABA/betaine transporter from human kidney. FEBS Lett 373:229–233
16. Borden LA, Smith KE, Gustasfson EL, Branchek TA, Weinshank RL (1995) Cloning and expression of a betaine/GABA transporter from human brain. J Neurochem 64:977–984
17. Zhu XM, Ong WY (2004) A light and electron microscopic study of betaine/GABA transporter distribution in the monkey cerebral neocortex and hippocampus. J Neurocytol 33:233–240
18. Zhu XM, Ong WY (2004) Changes in GABA transporters in the rat hippocampus after kainate-induced neuronal injury: decrease in GAT-1 and GAT-3 but upregulation of betaine/GABA transporter BGT-1. J Neurosci Res 77:402–409
19. Liu QR, Lopez-Corcuera B, Mandiyan S, Nelson H, Nelson N (1993) Molecular characterization of four pharmacologically distinct γ-aminobutyric acid transporters in mouse brain. J Biol Chem 268:2106–2112
20. Conti F, Zuccarello LV, Barbaresi P, Minelli A, Brecha NC, Melone M (1999) Neuronal, glial, and epithelial localization of gamma-aminobutyric acid transporter 2, a high-affinity gamma-aminobutyric acid plasma membrane transporter, in the cerebral cortex and neighboring structures. J Comp Neurol 409:482–494
21. Durkin MM, Smith KE, Borden LA, Weinshank RL, Branchek TA, Gustafson EL (1995) Localization of messenger RNAs encoding three GABA transporters in rat brain: an in situ hybridization study. Brain Res Molec Brain Res 33:7–21
22. Minelli A, DeBiasi S, Brecha NC, Zuccarello LV, Conti F (1996) GAT-3, a high-affinity GABA plasma membrane transporter, is localized to astrocytic processes, and is not confined to the vicinity of GABAergic synapses in the cerebral cortex. J Neurosci 16:6255–6264
23. Takayama C, Inoue Y (2005) Developmental expression of GABA transporter-1 and d3 during formation of the GABAergic synapses in the mouse cerebellar cortex. Brain Res Dev Brain Res 158:41–49
24. Schousboe A, White HS (2009) Modulation of excitability via glutamate and GABA transporters. In: Schwartzkroin P (ed) Encyclopedia of basic epilepsy research, vol 1. Elsevier, Oxford, UK, pp 397–401
25. Sheldon AL, Robinson MB (2007) The role of glutamate transporters in neurodegenerative diseases and potential opportunities for intervention. Neurochem Int 51:333–355
26. Jelenkovic AV, Jovanovic MD, Stanimirovic DD, Bokonjic DD, Ocic GG, Boskovic BS (2008) Beneficial effects of ceftriaxone against pentylenetetrazole-evoked convulsions. Exp Biol Med Maywood 233:1389–1394
27. Madsen K, White HS, Clausen RP, Frølund B, Larsson OM, Krogsgaard-Larsen P, Schousboe A (2007) Functional and pharmacological

aspects of GABA-transporters. In: Lajtha A, Reith M (eds) Handbook of neurochemistry and molecular neurobiology, 3rd edn, Neural membranes and transport. Springer, Berlin, pp 285–304

28. Hertz E, Yu ACH, Hertz L, Juurlink BHJ, Schousboe A (1989) Preparation of primary cultures of mouse cortical neurons. In: Shahar A, De Vellis J, Vernadakis A, Haber B (eds) A dissection and tissue culture manual of the nervous system. R. Liss, New York, pp 183–186
29. Hertz L, Juurlink BHJ, Hertz E, Fosmark H, Schousboe A (1989) Preparation of primary cultures of mouse (rat) astrocytes. In: Shahar A, De Vellis J, Vernadakis A, Haber B (eds) A dissection and tissue culture manual of the nervous system. R. Liss, New York, pp 105–108
30. Hertz L, Juurlink BHJ, Fosmark H, Schousboe A (1982) Astrocytes in primary cultures. In: Pfeiffer SE (ed) Neuroscience approached through cell culture, vol 1. CRC, Boca Raton, pp 175–186
31. Hertz L, Juurlink BHJ, Szuchet S (1985) Cell cultures. In: Lajtha A (ed) Handbook of neurochemistry, vol 8. Plenum, New York, pp 603–661
32. Hertz L, Schousboe A (1987) Primary cultures of GABAergic and glutamatergic neurons as model systems to study neurotransmitter functions. I. Differentiated cells. In: Vernadakis A, Privat A, Lauder JM, Timiras PS, Giacobini E (eds) Model systems of development and aging of the nervous system. M. Nijhoff, Boston, pp 19–31
33. Booher J, Sensenbrenner M (1972) Growth and cultivation of dissociated neurons and glial cells from embryonic chick, rat and human brain in flask cultures. Neurobiology 2:97–105
34. White HS, Sarup A, Bolvig T, Kristensen AS, Petersen G, Nelson N, Pickering DS, Larsson OM, Frølund B, Krogsgaard-Larsen P, Schousboe A (2002) Correlation between anticonvulsant activity and inhibitory action on glial GABA uptake of the highly selective mouse GAT1 inhibitor 3-hydroxy-4-amino-4, 5, 6, 7-tetrahydro-1, 2-benzisoxazole (exo-THPO) and its N-alkylated analogs. J Pharmacol Exp Therap 302:636–644
35. Elliott KA, van Gelder NM (1958) Occlusion and metabolism of gamma-aminobutyric acid by brain tissue. J Neurochem 3:28–40
36. Iversen LL, Neal MJ (1968) The uptake of [^{3}H]GABA by slices of rat cerebral cortex. J Neurochem 15:1141–1149
37. Iversen LL, Bloom FE (1972) Studies of the uptake of 3 H-gaba and (3 H)glycine in slices and homogenates of rat brain and spinal cord by electron microscopic autoradiography. Brain Res 41:131–143
38. Henn FA, Hamberger A (1971) Glial cell function: uptake of transmitter substances. Proc Natl Acad Sci USA 68:2686–2690
39. Schousboe A, Hertz L, Svenneby G (1977) Uptake and metabolism of GABA in astrocytes cultured from dissociated mouse brain hemispheres. Neurochem Res 2:217–229
40. Sarup A, Larsson OM, Bolvig T, Frølund B, Krogsgaard-Larsen P, Schousboe A (2003) Effects of 3-hydroxy-4-amino-4, 5, 6, 7-tetrahydro-1, 2-benzisoxazol (exo-THPO) and its N-substituted analogs on GABA transport in cultured neurons and astrocytes and by the four cloned mouse GABA transporters. Neurochem Int 43:445–451
41. Sarup A, Larsson OM, Schousboe A (2003) GABA transporters and GABA-transaminase as drug targets. Curr Drug Targ CNS Neurol Dis 2:269–277
42. Clausen RP, Madsen K, Larsson OM, Frølund B, Krogsgaard-Larsen P, Schousboe A (2006) Structure-activity relationship and pharmacology of γ-aminobutyric acid (GABA) transport inhibitors. Adv Pharmacol 54:265–284
43. Høg S, Greenwood JR, Madsen KB, Larsson OM, Frøund B, Schousboe A, Krogsgaard-Larsen P, Clausen RP (2006) Structure-activity relationships of selective GABA uptake inhibitors. Curr Top Med Chem 6:1861–1882
44. Liu QR, Mandiyan S, Nelson H, Nelson N (1992) A family of genes encoding neurotransmitter transporters. Proc Natl Acad Sci USA 89:6639–6643
45. Lopéz-Corcuera B, Liu QR, Mandiyan S, Nelson H, Nelson N (1992) Expression of a mouse brain cDNA encoding novel γ-aminobutyric acid transporter. J Biol Chem 267:17491–17493
46. Bolvig T, Larsson OM, Pickering DS, Nelson N, Falch E, Krogsgaard-Larsen P, Schousboe A (1999) Action of bicyclic isoxazole GABA analogues on GABA transporters and its relation to anticonvulsant activity. Eur J Pharmacol 375:367–374
47. Clausen RP, Moltzen EK, Perregaard J, Lenz SM, Sanchez C, Falch E, Frølund B, Sarup A, Larsson OM, Schousboe A, Krogsgaard-Larsen P (2005) Selective inhibitors of GABA uptake: synthesis and molecular pharmacology of 3-hydroxy-4-N-methylamino-4, 5, 6, 7-tetrahydro-1, 2-benzo[d]isoxazole analogues. Bioorg Med Chem 13:895–908
48. White HS, Watson WP, Hansen S, Slough S, Sarup A, Bolvig T, Petersen G, Larsson OM,

Clausen RP, Frølund B, Krogsgaard-Larsen P, Schousboe A (2005) First demonstration of a functional role for CNS betaine/GABA transporter (mGAT2) based on synergistic anticonvulsant action among inhibitors of mGAT1 and mGAT2. J Pharmacol Exp Therap 312:866–874

49. Borden LA, Dhar TGM, Smith KE, Branchek TA, Gluchowski C, Weinshank RL (1994) Cloning of the human homologue of the GABA transporter GAT-3 and identification of a novel inhibitor with selectivity for this site. Receptor Channels 2:207–213
50. Loewe S (1953) The problem of synergism and antagonism of combined drugs. Arzneimittelforschung 3:285–290
51. Tallarida RJ (1992) Statistical analysis of drug combinations for synergism. Pain 49:93–97
52. Tallarida RJ, Stone DJ Jr, Raffa RB (1997) Efficient designs for studying synergistic drug combinations. Life Sci 61:1–25
53. Finney DJ (1971) Probit analysis. Cambridge University Press, London
54. Horton RW, Collins JF, Anlezark GM, Meldrum BS (1979) Convulsant and anticonvulsant actions in DBA/2 mice of compounds blocking the reuptake of GABA. Eur J Pharmacol 59:75–83
55. Wood JD, Schousboe A, Krogsgaard-Larsen P (1980) In vivo changes in the GABA content in nerve endings (synaptosomes) induced by inhibitors of GABA uptake. Neuropharmacology 19:1149–1152
56. Wood JD, Johnson DD, Krogsgaard-Larsen P, Schousboe A (1983) Anticonvulsant activity of the glial selective GABA uptake inhibitor, THPO. Neuropharmacology 22:139–142
57. Krogsgaard-Larsen P, Labouta J, Meldrum B, Croucher M, Schousboe A (1981) GABA uptake inhibitors as experimental tools and potential drugs in epilepsy research. In: Morselli PL, Lloyd KG, Löscher W, Meldrum BS, Reynolds EM (eds) Neurotransmitters, seizures and epilepsy. Raven, New York, pp 23–33
58. Croucher MJ, Meldrum BS, Krogsgaard-Larsen P (1983) Anticonvulsant activity of GABA uptake inhibitors and their prodrugs following central or systemic administration. Eur J Pharmacol 89:217–228
59. Schousboe A, Larsson OM, Wood JD, Krogsgaard-Larsen P (1983) Transport and metabolism of GABA in neurons and glia: implications for epilepsy. Epilepsia 24:531–538
60. Yunger LM, Fowler PJ, Zarevics P, Setler PE (1984) Novel inhibitors of gamma-aminobutyric acid (GABA) uptake: anticonvulsant actions in rats and mice. J Pharmacol Exp Ther 288:109–115
61. Sutton I, Simmonds MA (1974) The selective blockade by diaminobutyric acid of neuronal uptake of [^{3}H]GABA in rat brain in vivo. J Neurochem 23:273–274
62. Dalby NO (2000) GABA-level increasing and anticonvulsant effects of three different GABA uptake inhibitors. Neuropharmacology 39:2399–2407
63. Mody I (2001) Distinguishing between GABA(A) receptors responsible for tonic and phasic conductances. Neurochem Res 26:907–913
64. Schousboe A, Larsson OM, Sarup A, White HS (2004) Role of the betaine/GABA transporter (BGT-1/GAT2) for the control of epilepsy. Eur J Pharmacol 500:281–287
65. Madsen KB, Clausen RP, Larsson OM, Krogsgaard-Larsen P, Schousboe A, White HS (2009) Synaptic and extrasynaptic GABA transporters as targets for anti-epileptic drugs. J Neurochem 109(suppl 1):139–144
66. Schousboe A (1979) Effects of GABA analogues on the high-affinity uptake of GABA. In: Mandel P, De Feudis FV (eds) Astrocytes in primary cultures in GABA – Biochemistry and CNS Function. Plenum, New York, pp 219–237
67. Larsson OM, Thorbek P, Krogsgaard-Larsen P, Schousboe A (1981) Effect of homo-β-proline and other heterocyclic GABA analogues on GABA uptake in neurons and astroglial cells and on GABA receptor binding. J Neurochem 37:1509–1516
68. Larsson OM, Johnston GAR, Schousboe A (1983) Differences in uptake kinetics of cis-3-aminocyclohexane carboxylic acid into neurons and astrocytes in primary cultures. Brain Res 260:279–285
69. Larsson OM, Griffiths R, Allen IC, Schousboe A (1986) Mutual inhibition kinetic analysis of (γ-aminobutyric acid, taurine, taurine and β-alanine high affinity transport into neurons and astrocytes: evidence for similarity between the taurine and β-alanine carriers in both cell types. J Neurochem 47:426–432
70. Larsson OM, Falch E, Krogsgaard-Larsen P, Schousboe A (1988) Kinetic characterization of inhibition of gamma-aminobutyric acid uptake into cultured neurons and astrocytes by 4, 4-diphenyl-3-butenyl derivatives of nipecotic acid and guvacine. J Neurochem 50:818–823
71. Falch E, Perregaard J, Frølund B, Søkilde B, Buur A, Hansen LM, Frydenvang K, Brehm L, Bolvig T, Larsson OM, Sanchez C,

White HS, Schousboe A, Krogsgaard-Larsen P (1999) Selective inhibitors of glial GABA uptake: synthesis, absolute stereochemistry, and pharmacology of the enantiomers of 3-hydroxy-4-amino-4, 5, 6, 7-tetrahydro-1, 2-benzisoxazole (exo-THPO) and analogues. J Med Chem 42: 5402–5414

72. Suzdak PD, Frederiksen K, Andersen KE, Sørensen PO, Knutsen LJ, Nielsen EB (1992) NNC-711, a novel potent and selective gamma-aminobutyric acid uptake inhibitor: pharmacological characterization. Eur J Pharmacol 224:189–198
73. Thomsen C, Sørensen PO, Egebjerg J (1997) 1-(3-(9H-carbazol-9-yl)-1-propyl)-4-(2-methoxyphenyl)-4-piperidinol, a novel subtype selective inhibitor of the mouse type II GABA-transporter. Br J Pharmacol 120: 983–985

Chapter 23

Ion Channel Electrophysiology in Cultured Neurons

Toshio Narahashi

Abstract

Studies of ion channel pharmacology have witnessed considerable developments during the past half a century. Whereas voltage clamp techniques were applied to neuropharmacology for the studies of some chemicals in the late 1950s, it was not until 1960s that cellular neuropharmacological studies started flourishing when tetrodotoxin was discovered to exert a selective and potent block of the sodium channels. The progress in this field was greatly accelerated when patch clamp techniques developed in the early 1980s. Incorporation of molecular biology into this area further promoted the development, and cellular neuropharmacology has now become one of the most important biomedical sciences.

A variety of cultured neurons are being used for research nowadays depending on the aims of study. In this chapter, variations of cell culture techniques are described in the former half of the chapter. The latter half is devoted to a few representative examples of our studies using cultured neurons.

Key words: Voltage clamp, Patch clamp, Dorsal root ganglion neuron, Hippocampal neuron, Cortical neuron, Cerebellar Purkinje neuron, Neuroblastoma cell, Alcohol, Pyrethroids, Fipronil, GABA receptor, Glutamate receptor, Glutamate-activated chloride current, Sodium channel

1. Introduction

Studies of ion channel pharmacology have witnessed considerable developments during the past half a century. In 1958, Shanes published two extensive review articles in *Pharmacological Reviews* (1, 2) not only summarizing the situation at that time but also pointing out possible future directions of cellular neuropharmacology especially with the use of voltage clamp technique (1, 2). Voltage clamp was originally developed by Cole (3) in 1949 and extensively used by Hodgkin, Huxley, and Katz (4–8) in 1952 to define the roles of ion channels in nerve excitation. This powerful technique was indeed applied in the late 1950s, albeit to the limited extent, for the study of the mechanism of action of some

Michael Aschner et al. (eds.), *Cell Culture Techniques*, Neuromethods, vol. 56,
DOI 10.1007/978-1-61779-077-5_23,

chemicals on sodium and potassium channels (9–11). However, it was not until the discovery of the selective tetrodotoxin (TTX) block of sodium channels (12, 13) in the early 1960s that toxins and chemicals made their debut as useful tools for the study of ion channels. The use of chemicals for this purpose has become explosively popular since that time breaking a dawn of cellular neuropharmacology. However, the preparations to which the voltage clamp technique was applicable were quite limited for technical reasons.

In 1976, Neher and Sakmann successfully recorded small currents flowing through the open single channels of nicotinic acetylcholine receptors (nAChRs) (14). A few years later, they developed this technique into what we now call patch clamp (15). Although the patch clamp is a variation of voltage clamp, it has become very popular for two reasons: (1) It is applicable practically to any type of cells including neurons, muscle cells, cardiac cells, lymphocytes, and mitochondria to mention a few as long as patch electrode is applicable. (2) Another reason is that single-channel currents which was impossible to measure before can now be recorded. Thus, patch clamp techniques are extensively used in combination with TTX and other chemical tools for the studies of physiology, pharmacology, and toxicology of ion channels. In spite of the current trend toward the molecular mechanism of ion channel studies, patch clamp is an indispensable part of integrated investigations.

This chapter gives some examples of ion channel studies using patch clamp techniques. Since the patch clamp techniques using single cells are now routine procedure, variations of these techniques as applied to various preparations are briefly described in the former half of the chapter, and a few examples of studies are given in the latter half. One of the most important points is to properly select cell preparations suitable for the purpose of the study.

2. Cell Culture and Patch Clamp Techniques

2.1. Dorsal Root Ganglion Neuron Cultures

Dorsal root ganglion (DRG) neurons are often used for the patch clamp study of voltage-gated sodium channels and GABA receptor channels. Neurons are acutely dissociated from rat DRG and maintained in a short-term primary culture to be used for patch clamp experiments within 1–3 days. A 1- to 7-day-old Sprague-Dawley rat is anesthetized with halothane (16, 17). The vertebral column is then removed and cut longitudinally, generating two hemisections, which are placed into sterile Ca^{2+}- and Mg^{2+}-free phosphate-buffered saline solution (PBS). The ganglia are isolated from the spinal lumen and enzymatically treated to weaken

the encapsulating tissue around the neuron bodies with PBS containing either a mixture of cysteine (0.5 mg/mL), papain (0.8 mg/mL), and collagenase-dispase (0.2 mg/mL), or trypsin alone (2.0–2.5 mg/mL). Cells are incubated with enzymes at 37°C for approximately 20 min and then rinsed twice with culture media (serum-free Dulbecco's Modified Eagle's Medium) containing gentamycin (0.08 mg/mL). By trituration using a sterile Pasteur pipette, neurons are mechanically isolated from extraneous tissues. The resulting cell suspension is evenly dispersed into cluster dish wells, with each containing a 12 mm poly-L-lysine (0.1 mg/mL)-coated glass coverslip and 1.0 mL of culture medium. Incubation for 1–2 h in 5–10% CO_2 with 100% humidity is necessary to allow cells to settle and adhere to the coverslips.

2.2. Cerebellar Purkinje Neuron Cultures

Cerebellar Purkinje neurons are used for the study of sodium channels. The methods for isolating and culturing cerebellar Purkinje neurons are described by Kay and Wong (18) and Song and Narahashi (19). Rats of 7–14 days old (postnatal) are anesthetized with halothane and decapitated. The brains are removed rapidly and immersed in ice-cold PIPES dissociation solution containing (in mM) NaCl 120, KCl 5, $CaCl_2$ 1, $MgCl_2$ 1, D-glucose 25 and PIPES 20 with pH 7.0 and 305 mOsm and equilibrated with 100% O_2. Cerebella are dissected out and cut into slices of 500 μm thickness using a tissue slicer. Slices are transferred into a dissociation chamber containing 10 mL PIPES dissociation solution added with 6 mg trypsin (Type XI, Sigma-Aldrich, St. Louis, MO). The solution containing slices is stirred gently for 50 min with a magnetic stirrer at a slow rate sufficient to prevent the cells from settling. The solution is continuously saturated with 100% O_2. The slices are then rinsed with PIPES dissociation solution, and individual cells are mechanically dissociated using a fire-polished Pasteur pipette in DMEM (GISCO-BRL, Grand Island, NY). Then cells are plated onto glass coverslips coated with poly-L-lysine and cultured in DMEM at 37°C. After 15 min medium is changed to DMEM supplemented with newborn calf serum (10%, v/v) and gentamicin (80 μg/mL). Cells can be used for electrophysiological experiments after 1–7 h of incubation in 10% CO_2 and 100% humidity. Cerebellar Purkinje neurons are distinguished by their large size (15–20 μm diameters) compared with granule, stellate, or basket cells.

2.3. Hippocampal Neuron Cultures

Hippocampal neurons are often used for the study of sodium channels and various ligand-gated receptor channels. Primary cultures of hippocampal neurons are prepared from 17-day-old embryos of a Sprague-Dawley pregnant rat under halothane anesthesia (20, 21). A transverse incision is made in the lower abdomen

of the pregnant rat and the fetuses are withdrawn from the abdomen. The heads of the fetuses are immediately cut-off and hippocampi are dissected and kept in a Ca^{2+}- and Mg^{2+}-free buffered saline solution (PBS). Neurons are then dissociated by repeated passages through a fire-polished Pasteur pipette containing Neurobasal Medium supplemented with B-27 and 2 mM L-glutamic acid (GIBCO/Life, Grand Island, NY). The final suspension is plated onto 12 mm poly-L-lysine-coated coverslips at a density of 200,000 cells/well. Cells are maintained in 10% CO_2 with 100% humidity at 37°C and are used for electrophysiological experiments within 3 weeks.

2.4. Cortical Neuron Cultures

Similar to hippocampal neurons, cortical neurons are used frequently for the study of sodium channels and various ligand-gated receptor channels. The methods for culture of cortical neurons are very similar to those for hippocampal neurons (22, 23). Embryos are removed from 17-day pregnant Sprague-Dawley rats under halothane anesthesia. Small wedges of frontal cortex are excised and subsequently incubated in phosphate buffer solution for 20 min at 37°C. The solution contains (in mM) NaCl 154, KH_2PO_4 1.05, $Na_2HPO_4 \cdot 7H_2O$ 3.0, 0.25% (w/v) trypsin (Type XI, Sigma-Aldrich, St. Louis, MO), pH 7.4, and with osmolarity of 287 mOsm. The digested tissue is then mechanically triturated by repeated passages through a Pasteur pipette and the dissociated cells are suspended in Neurobasal Medium with B-27 supplement (Invitrogen, Carlsbad, CA) and 2 mM glutamine. The cells are added to 35-mm culture wells at a concentration of 100,000 cells/well. Each well contains five 12-mm poly-L-lysine-coated coverslips overlaid with confluent glia that had been plated 2–4 weeks earlier. The cortical neuron/glia cultures are maintained in a humidified atmosphere of 10% CO_2 at 37°C. Cells cultured for 3–7 weeks are used in the experiments.

2.5. Cockroach Neurons

Cockroach neurons are used for the study of the mechanism of action of insecticides. As described later, they are particularly useful for the studies of selective toxicity and of glutamate-activated chloride channel (GluCl) currents which are not present in mammals. Glutamate-activated chloride currents can be recorded by patch clamp from the cockroach neurons (24–26). Adult cockroaches, *Periplaneta americana*, are maintained at room temperature (22–24°C) with free access to water and rat food. A cockroach is immobilized by pins with either dorsal side or ventral side up on a dissection dish coated with wax. The cuticle, gut, and some muscles are removed to gain access to the ventral nerve cord. Three thoracic ganglia are carefully dissected and placed in cockroach saline solution containing (in mM) NaCl 200, KCl 3.1, $MgCl_2$ 4, D-glucose 20, and HEPES acid 10 with pH adjusted to 7.3 with 1 mM NaOH. After removal of the remaining nerve

fibers and nerve sheets, the ganglia are incubated for 40 min at room temperature in the saline solution containing collagenase (Type A, 0.5 mg/mL, Roche Diagnostics, Mannheim, Germany) and hyaluronidase (Type I-S, 1 mg/mL, Sigma-Aldrich, St. Louis, MO). The ganglia are then rinsed twice in saline solution supplemented with 5 mM $CaCl_2$ and 5% (v/v) fetal calf serum and are immediately dissociated by gentle trituration through a fire-polished Pasteur pipette. The dissociated neurons, suspended in the supplemental saline solution, are allowed to settle on glass coverslips coated with poly-L-lysine. The neurons are used in 3–24 h for electrophysiological experiments.

2.6. Neuroblastoma Cell Cultures

Neuroblastoma cell line is used for the study of various voltage- and ligand-gated channels. NIE-115 neuroblastoma cells or NG108-15 neuroblastoma–glioma hybrid cells have been used often for patch clamp experiments (27–30). Cells are maintained in tissue cultures and grown in Dulbecco's modified Eagle's medium, supplemented with 10% newborn calf serum at 37°C in humidified air containing 10% CO_2. To facilitate development of ion channels and chemical sensitivity, 1 mM dibutyryl adenosine 3′, 5′-cyclic monophosphate could be added to the culture media. Three days to two weeks before use, cells are first grown on coverslips in media to which 2% (v/v) dimethylsulfoxide had been added to enhance cellular differentiation and expression of neuronal characteristics (31).

2.7. Patch Clamp Methods

Whole-cell currents or single-channels currents can be recorded by patch clamp techniques (15). Patch pipettes made from borosilicate glass capillary tubes with 1.5 mm inner diameter have a resistance of 5–10 megohm when filled with pipette solution.

Either inside-out or outside-out configuration of membrane patch to record single-channel currents can be used depending on the purpose of experiment. If a test compound is to be applied directly inside of the membrane, the inside-out configuration is more convenient. For external application of the chemical, the outside-out configuration is more convenient. Single-channel currents passing through the pipette are recorded by a patch clamp amplifier (e.g., Axopatch 200A, Molecular Devices, Sunnyvale, CA). The currents are filtered at 2–10 kHz with a four-pole Bessel filter, digitized at a rate of 10–50 kHz through an analog-to-digital converter (Digidata 1200, Molecular Devices), and stored on hard disk for later analysis. The baseline of current at the holding potential may be continuously recorded with a pen recorder. Programmed sequences of voltage pulses are applied using the software pClamp 6 (Molecular Devices) to the preparation from the computer using a digital-to-analog converter (Digidata 1200).

Whole-cell currents are recorded under patch clamp conditions by the method developed by Hamill et al. (15) using an Axopatch 200A amplifier. Currents are digitized with a 14-bit analog-to-digital converter, filtered with a Bessel filter at 5 kHz, and stored by a PC-based data acquisition system.

Two drug application methods can be used depending on situation (22, 26). Bath application and U-tube application methods are used separately or in combination. A U-tube is used for rapid application of external solution containing an agonist (e.g., acetylcholine or glutamate) alone or with test compounds. External solution containing agonist alone or with a test compound is fed through the U-tube by gravity from a container located above the bath. Closure of a computer-operated solenoid valve in the outlet side of the tube allows the U-tube solution to flow out of the hole located near the cell. Another valve controlling a suction tube with an opening on the other side of the cell is also opened, allowing the test solution to be sucked away quickly. The opening and closing of two solenoid valves are operated by ClampEX 6.0.4. With this method, the external solution surrounding the cell can be completely exchanged with a test solution in 20–30 ms.

3. Examples of Patch Clamp Studies of Cultured Neurons

3.1. Alcohol Modulation of Nicotinic Acetylcholine Receptors

Meyer–Overton's lipid theory has prevailed for nearly 90 years to explain the mechanism by which alcohol exerts paralysis and other actions on animals and humans (32–34). The theory says in essence that alcohol is dissolved in the lipid phase of the membrane thereby causing various effects. However, it has become increasingly clear that the major target site of alcohol is proteins, primarily those of neuroreceptors. Whereas alcohol (ethanol) interacts with a variety of neuroreceptors including, but not limited to, nAChRs, $GABA_A$ receptors, glutamate receptors, and $5\text{-}HT_3$ receptors (35–38), modulation of nAChRs is important not only because alcohol action on the receptor is potent but also because changes in the activity of nAChRs affect the release of various transmitters such as nor-epinephrine, GABA, glutamate, and ACh (39) leading to alterations of receptor's functions.

Whole-cell patch clamp technique was applied to rat cortical neurons in primary cultures (40). Neurons were used for patch clamp experiments after neuron/glia were co-cultured for 1–9 weeks. The standard external solution consisted of (in mM): NaCl 140, KCl 5, $CaCl_2$ 1.5, $MgCl_2$ 1, acid-HEPES 15, Na-HEPES 10, $LaCl_3$ 3 μM, TTX 0.2 μM, atropine sulfate 0.3 μM and pH 7.3. Two types of internal (pipette) solutions were used, one with high calcium buffering capacity, and the other with 5 mM

Mg-ATP added. These two solutions were used to evaluate the possible effects of internal calcium or energy processes on nAChR activity. The internal solution with high calcium-buffering capacity comprised (in mM): cesium gluconate 140, NaCl 15, potassium gluconate 5, acid-HEPES 15, Na-HEPES 10, cesium-BAPTA 35, Ca gluconate 12, and Mg gluconate 4. The ATP-containing internal solution consisted of (in mM); cesium gluconate 140, NaCl 15, K gluconate 5, $MgCl_2$ 1, acid-HEPES 15, Na-HEPES 10, EGTA 11, $CaCl_2$ 1, Mg-ATP 5, and Na-GTP 0.2.

In rat cortical neurons in primary cultures, applications of ACh through U-tube generated two types of current response. A fast desensitizing current with an EC_{50} of 300 μM ACh was blocked by α-bungarotoxin (α-BuTX) and a slowly desensitizing current with an ACh EC_{50} of 3 μM was not blocked by α-BuTX. The fast desensitizing current represented the activity of α7 nAChRs, whereas the slowly desensitizing current represented the activity of α4β2 nAChRs.

Alcohol slightly inhibited the α7 nAChR currents. At 30 and 100 mM alcohol inhibited the currents only to 92 and 84% of the control, respectively (figure 2 of Aistrup et al. (40)). By contrast the α4β2 nAChR currents were much more sensitive to and potentiated by alcohol (Fig. 1). Alcohol at 10, 30, and 100 mM, the currents were augmented to 114, 127, and 155% of the control, respectively.

As is well known, alcohol exerts effects on most, if not all, neuroreceptors. In order to compare the effects on nAChRs with those on $GABA_A$Rs and NMDARs, the following experiments

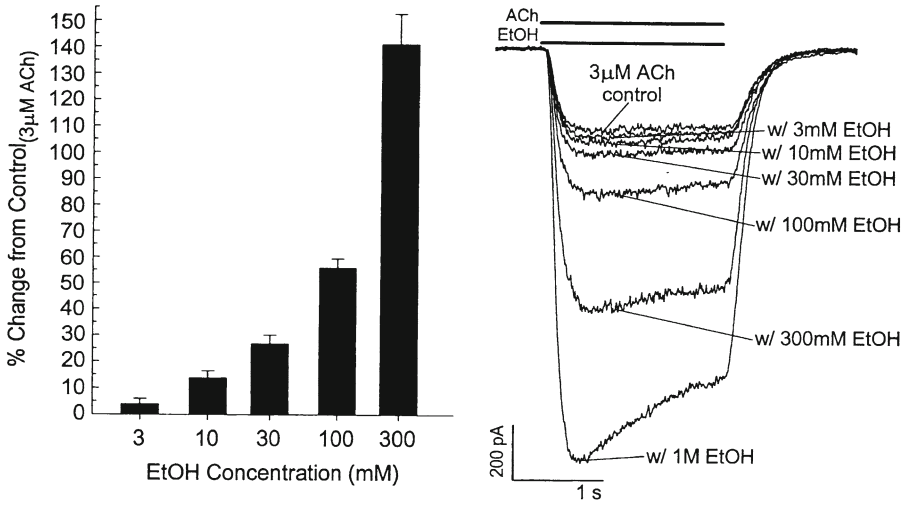

Fig. 1. Ethanol potentiation of ACh-induced currents in the rat cortical α4β2 nicotinic receptors in primary cultures. *Left*: Dose–response relationship for ethanol to increase the currents evoked by 3 μM ACh. *Right*: Sample current records induced by 3 μM ACh alone and those by ACh plus various concentrations of ethanol (Aistrup et al. (40) by permission).

were performed (40): Because the sensitivity of individual neurons varied, one and the same neuron was used to compare the alcohol sensitivity. GABA-induced currents were potentiated by 100 mM alcohol only 3 ± 3%, and modestly potentiated by 300 mM alcohol 18 ± 8%. In contrast, ACh-induced α4β2 currents were potentiated by 100 and 300 mM alcohol 61 ± 9% and 196 ± 63%, respectively. NMDA-induced currents were inhibited by 100 mM alcohol 35 ± 7%, an effect less efficacious than that on nAChRs (figure 5 of Aistrup et al. (40)). This experiment clearly illustrates that α4β2 nAChR currents are more sensitive to alcohol than GABA and NMDA currents.

3.2. Effects of Ethanol on Excitatory and Inhibitory Synaptic Transmission

Whereas there is no question that glutamate receptors are inhibited by alcohol (35, 40), alcohol modulation of $GABA_A$Rs has been a matter of controversies; potentiation, inhibition, and no effect by alcohol have been reported in the literature (41, 42). However, various behavior experiments clearly point out the importance of the GABAergic system as a target of alcohol. Since nAChRs have been highly sensitive to alcohol as described above, and also since nAChRs, when activated, facilitate the release of various transmitters (39), we proposed a hypothesis that alcohol stimulates the GABAergic system through potentiation of nAChRs.

In order to test the hypothesis, experiments with miniature excitatory postsynaptic currents (mEPSCs) and miniature inhibitory postsynaptic currents (mIPSCs) were performed using the patch clamp technique (43). Primary cultured rat cortical neurons were used. Synaptic networks were formed during cultures and spontaneous miniature currents could be recorded in the presence of 100 nM TTX to eliminate the activity of voltage-gated sodium channels and 20 nM atropine to block the muscarinic AChR currents. For recording of mEPSCs 20 μM bicuculline was added to eliminate mIPSCs, and for recording of mIPSCs 30 μM DL-2-amino-5-phosphonovaleric acid (APV) and 10 μM 6-cyano-7-nitroquinoxaline-2,3-dione (CNQX) were added to block mEPSCs. Two types of neurons were recognized in the cultures: one was bipolar neurons and the other multipolar neurons. Bipolar neurons possessed nAChRs, while multipolar neurons lacked nAChRs. As expected, the presence and absence of nAChRs are reflected in the action of alcohol.

Examples of mEPSCs and mIPSCs recorded from bipolar neurons in the presence and absence of ACh and/or ethanol are shown in Fig. 2. Analyses of these results in terms of the amplitude and frequency of mEPSCs and mIPSCs are illustrated in Fig. 3. ACh at 30 nM generated a steady current in bipolar neurons (Fig. 2), which was not produced in multipolar neurons (figure 8 of Moriguchi et al. (43)). This observation implies the presence and absence of nAChRs in bipolar and multipolar

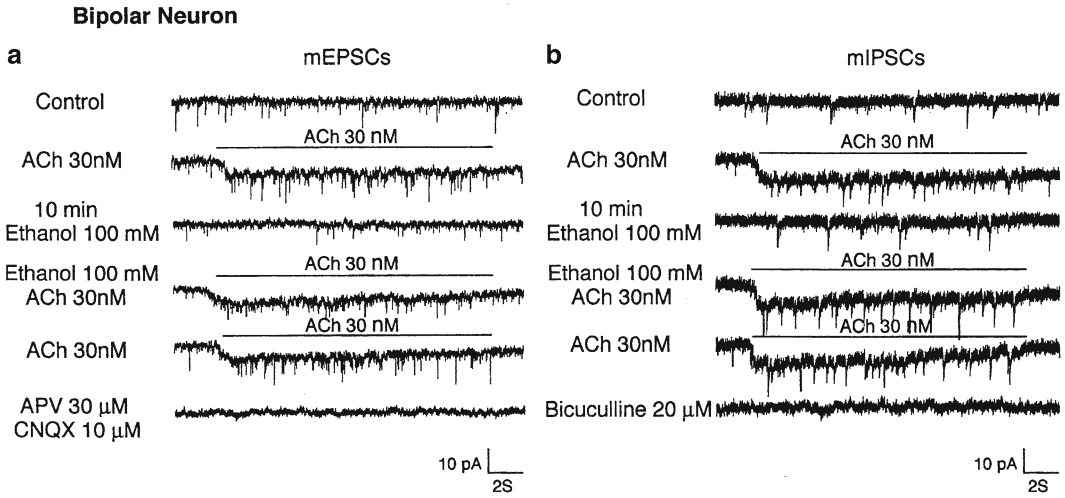

Fig. 2. Records of spontaneous miniature excitatory postsynaptic currents (mEPSCs) and miniature inhibitory postsynaptic currents (mIPSCs) in the primary cultured rat cortex bipolar neurons in the presence of 100 nM tetrodotoxin (TTX). ACh at 30 nM was applied via a U-tube system. (**a**) mEPSCs before (control), with 30 nM ACh, with 100 mM ethanol, with 100 mM ethanol plus 30 nM ACh, with 30 nM ACh, and with 30 μM DL-2-amino-5-phosphonovaleric acid (APV) plus 10 μM 6-cyano-7-nitroquinoxaline-2,3-dione (CNQX). (**b**) mIPSCs before (control), with 30 nM ACh, with 100 mM ethanol, with 100 mM ethanol plus 30 nM ACh, with 30 nM ACh, and with 20 μM bicuculine (Moriguchi et al. (43) by permission).

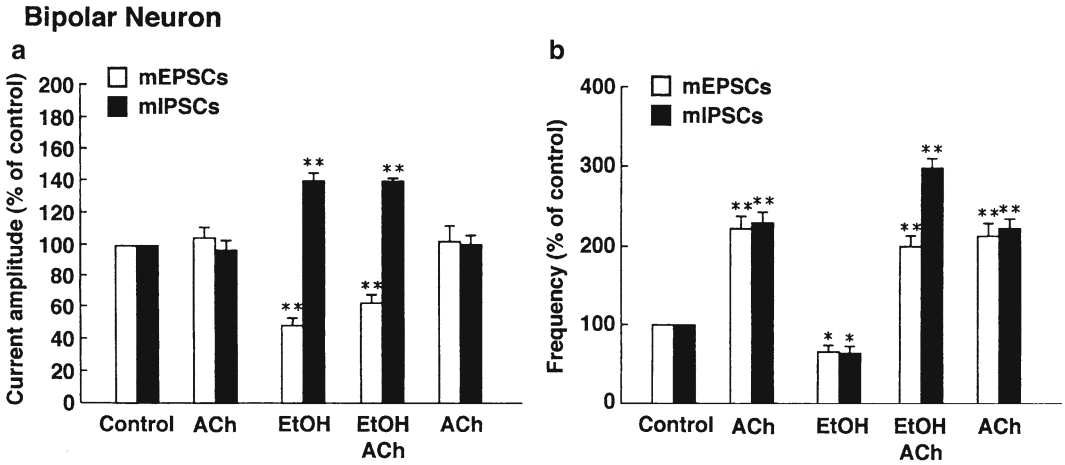

Fig. 3. Effects of ACh and ethanol on the amplitude and frequency of mEPSCs and mIPSCs in primary cultured rat cortical bipolar neurons. Data are normalized to the control values. (**a**) ACh 30 nM had no effect on the amplitude of mEPSCs and mIPSCs. Ethanol 100 mM or 100 mM ethanol plus 30 nM ACh decreased the amplitude of mEPSCs and increased the amplitude of mIPSCs. (**b**) ACh 30 nM increased the frequency of mEPSCs and mIPSCs. During 100 mM ethanol perfusion, 30 nM ACh increased the frequency of mEPSCs beyond the control level but to the same level as that achieved by ACh alone. However, the frequency of mIPSCs increased beyond the control and ACh level. $^{*}p < 0.05$, $^{**}p < 0.01$ (Moriguchi et al. (43) by permission).

neurons, respectively. Although ACh alone at 30 nM did not change the amplitude of either mEPSCs or mIPSCs in bipolar neurons, it greatly increased the frequency of both mEPSCs and mIPSCs reflecting the increase in the release of glutamate and GABA, respectively, as a result of stimulation of nAChRs (Fig. 3). These effects of ACh on the frequency were not seen in multipolar neurons due to the lack of nAChRs (figure 9 of Moriguchi et al. (43)).

Ethanol alone at 100 mM greatly increased the amplitude of mIPSCs in bipolar neurons and decreased the amplitude of mEPSCs reflecting the direct effects of ethanol on the GABA and glutamate receptors, respectively (Fig. 3). The frequency of both mEPSCs and mIPSCs was decreased by ethanol, probably due to a presynaptic effect (Fig. 3). Similar changes in both amplitude and frequency were produced by ethanol in multipolar neurons (figure 9 of Moriguchi et al. (43)). A combined application of 100 mM ethanol and 30 nM ACh also increased the amplitude of mIPSCs and decreased the amplitude of mEPSCs in bipolar neurons (Fig. 3), and similar changes were seen in multipolar neurons (figure 9 of Moriguchi et al. (43)). The effects of a combined application of 100 mM ethanol and 30 nM ACh on the frequency in bipolar neurons were complex somewhat (Fig. 3). The frequency of mIPSCs was increased more than the increase caused by ACh alone indicating ethanol potentiation of nAChRs. However, the increase in the frequency of mEPSCs was slightly less than that observed by ACh alone, probably due to a presynaptic effect of ethanol. It remains to be seen why mIPSCs and mEPSCs responded differently in bipolar neurons. In multipolar neurons, ethanol + ACh and ethanol alone caused similar changes in the frequency, slightly decreasing the frequency as compared with the control (figure 9 of Moriguchi et al. (43)).

The results of this study clearly show that ethanol modulates the release of glutamate and GABA through activation of nAChRs. Thus, regardless of the presence or absence of direct ethanol stimulation of GABARs, the GABAergic system is modulated by ethanol via stimulation of nAChRs.

3.3. Ethanol Modulation of Single nAChR Channels

Whereas a variety of neuroreceptor channels are modulated by ethanol, nAChRs of α4β2 type are particularly sensitive being augmented potently by ethanol (40). The maximum potentiation of the nAChRs by ACh is further increased by ethanol (40). However, the underlying mechanism remains to be seen. We propose that ethanol stabilizes the channel open state either by an increase in the channel open rate constant β and/or by a decrease in the closing rate constant α (44).

In order to test the hypothesis, single-channel patch clamp experiments were performed using the α4β2 nAChRs stably expressed in human embryonic kidney (HEK) cells (45). In an

attempt to decrease the occurrence of overlapping single-channel currents, we used a low concentration of ACh at 30 nM. Two conductance state currents, 1.5 and 2.6 pA, were frequently observed. The single-channel currents were blocked by 100 nM dihydro-β-erythroidine-HBr (DHβE), indicating that the currents are mediated by neuronal nAChRs. High and low conductances are calculated to be 40.5 and 21.9 pS, respectively.

Ethanol at 100 mM had no effect on the amplitude of either high- or low-conductance component of nAChR currents. The open time distributions were analyzed by the method of Sigworth and Sine (46). The number of events in each bin is plotted on a linear ordinate and the time axis is drawn on a logarithmic scale so that the effective bin width increases exponentially from left to right. This displays a multiexponential distribution as a series of skewed bell-shaped curves whose peaks overlie the time constants of several exponential components (see Fig. 4).

Details of single-channel analysis of nAChRs as affected by ethanol are described by Zuo et al. (45). It is of vital importance to relate single-channel data to whole-cell data. One of the unique aspects of ethanol-induced enhancement of whole-cell currents is that even the maximum current evoked by high concentrations of ACh is further increased by ethanol (40, 44). This could be either due to an increase in single-channel conductance or to more receptors staying open. The latter could arise from an increase in channel opening rate constant β and/or a decrease in the closing rate α (44). The experiments were designed to answer these questions.

Patch clamp experiments have revealed two conductance states in the ACh-induced opening of single channels. However, no change in single-channel conductance was discovered by application of 100 mM ethanol (figure 3 of Zuo et al. (45)). The probability of opening (P_{open}) was increased from 0.023 before to 0.029 after application of ethanol (figure 7 of Zuo et al. (45)). A question is how this increase in P_{open} occurs. The increase could be due to an increase in the mean open time and/or to a decrease in the mean closed time. The mean open time was found to increase in the high conductance channels, which amounted to 80–85% of the total population, from 9.0 to 15.5 ms, but no change occurred in the open time of low-conductance channels, which amounted to only 15–20% (figure 4 of Zuo et al. (45)). Furthermore, ethanol almost doubled the burst duration and the mean open time within bursts, and caused little or no change in the mean closed time within bursts (Fig. 4). Thus, it was concluded that ethanol stabilizes the open state of the receptors by decreasing the closing rate α.

3.4. Insecticide Modulation of Ion Channels

Pyrethroids are synthetic derivatives of pyrethrins which are toxic components contained in the flowers of some *Chrysanthemum* species and are used extensively as insecticides due to their potent

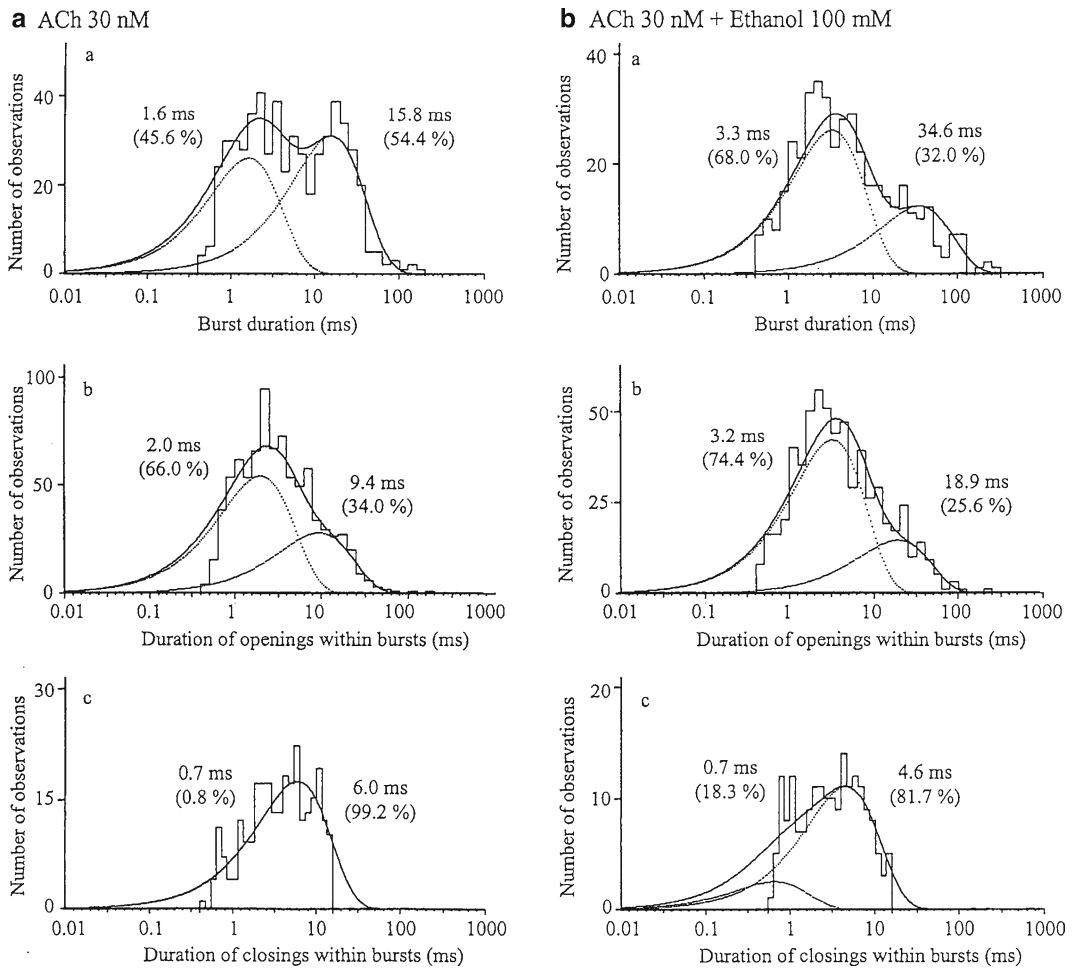

Fig. 4. Burst analysis in the absence and presence of ethanol. Outside-out patches were held at −70 mV. The distributions are displayed on a logarithmic time axis, and the best fits of exponential functions are shown. (**A**) Currents induced by 30 nM ACh. (**A**a) Burst duration. The time constants for distribution of burst durations are estimated to be 1.6 ms (45.6% of a total of 562 events, 5 separate patches combined) and 15.8 ms (54.4%). (**A**b) Open time within burst. The time constants for distribution of open time within bursts are estimated to be 2.0 ms (66.0% of a total of 838 events, 5 separate patches combined) and 9.4 ms (34.0%). (**A**c) Closed time within burst. The time constants for distribution of closed time within bursts are estimated to be 0.7 ms (0.8% of a total of 276 events, 5 separate patches combined) and 6.0 ms (99.2%). (**B**) Currents induced by co-application of 30 nM ACh and 100 mM ethanol. (**B**a) Burst duration. The time constants for distribution of burst durations are estimated to be 3.3 ms (68.0% of a total of 420 events, 5 separate patches combined) and 34.6 ms (32.0%). (**B**b) Open time within burst. The time constants for distribution of open time within bursts are estimated to be 3.2 ms (74.4% of a total of 618 events, 5 separate patches combined) and 18.9 ms (25.6%). (**B**c) Closed time within burst. The time constants for distribution of closed time within bursts are estimated to be 0.7 ms (18.3% of a total of 190 events, 5 separate patches combined) and 4.6 ms (81.7%) (Zuo et al. (45) by permission).

insect killing action, low mammalian toxicity, and biodegradability. Their toxic action is characterized by hyperexcitation followed by paralysis and death. Pyrethroids are primarily neurotoxicants and their mechanism of action has been studied by many investigators (see reviews (38, 47–56)). The primary target site of pyrethroids is

sodium channels which are kept open for an unusually long time leading to repetitive firing of the nerve. Only a few unique features of the mechanism of action of pyrethroids on sodium channels are described here.

The first demonstration that DDT, which was found to exhibit the very similar mechanism of action to that of pyrethroids (57), increased the depolarizing after-potential was made by Yamasaki and Ishii [Narahashi] (58) using the external recording technique as applied to cockroach nerve fibers (figure 1 of Narahashi (49)). This notion was later verified by intracellular microelectrode recording and voltage clamp and patch clamp experiments with pyrethroids have clearly shown that opening of single sodium channels is prolonged resulting in long-lasting whole-cell currents (19) and eventually causing hyperactivity of the nervous system (49).

One of the most intriguing aspects of pyrethroid modulation of sodium channels is that only a small population of sodium channels in the nerve membrane needs to be modified by pyrethroids to cause hyperexcitation. The method for counting pyrethroid-modified sodium channels in the membrane was developed by Tatebayashi and Narahashi (59).

Since the amplitude of peak sodium current is not changed by application of the pyrethroids tetramethrin, it is produced by unaltered normal sodium channels (Figs. 5 and 6a). Slowly rising and slowly decaying tail currents upon repolarization of the membrane are produced only in the presence of tetramethrin, so that they are due to the activity of pyrethroid-modified sodium channels

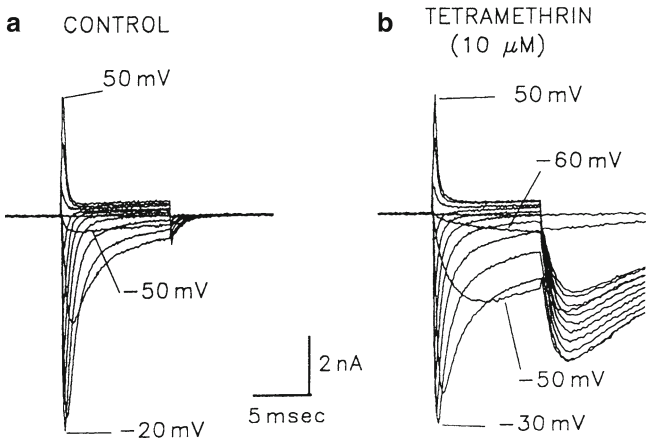

Fig. 5. Effects of 10 μM tetramethrin on the currents recorded from TTX-sensitive sodium channels in a primary cultured rat cerebellar Purkinje neuron. Currents were evoked by 10-ms depolarizations to test potentials ranging from −80 to +50 mV in 5 mV increments from a holding potential of −110 mV at a frequency of 0.1 Hz. (**a**) Currents under control condition. (**b**) After exposure to 10 μM tetramethrin (Song and Narahashi (19) by permission).

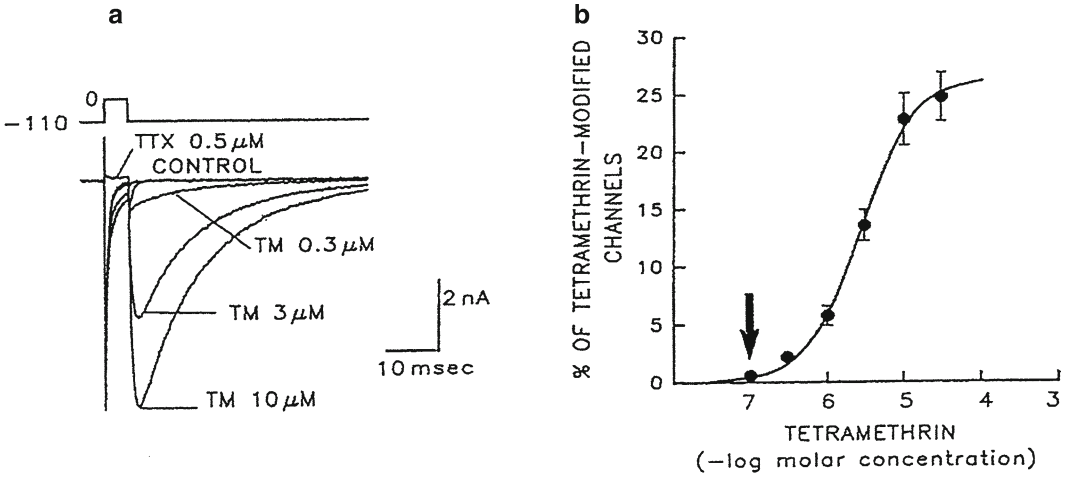

$$M = \{[I_{tail}/(E_h - E_{Na})]/[I_{Na}/(E_t - E_{Na})]\} \times 100$$

Fig. 6. Concentration-dependent effect of tetramethrin on TTX-sensitive sodium currents recorded from a primary cultured rat cerebellar Purkinje neuron. (**a**) Currents evoked by a 5-ms step depolarization to 0 mV from a holding potential of −110 mV under control condition and in the presence of tetramethrin at concentrations of 0.3, 3 and 10 μM. TTX at 0.5 μM completely blocked both the peak current and tetramethrin-induced tail current. (**b**) The concentration–response relationship for induction of tail current. Each point indicates the mean ± S.E.M (n=6). Data were fitted by the Hill equation. The percentage of channels modified by 100 nM tetramethrin is 0.62 ± 0.15% (*arrow*). The equation to calculate the percentage of the sodium channels modified by tetramethrin (M) (59) is as follows: $M = \{[I_{tail}/(E_h - E_{Na})]/[I_{Na}/(E_t - E_{Na})]\} \times 100$, where I_{tail} is the initial amplitude of the slowly decaying tail current that is extrapolated to the moment of repolarization, E_h is the potential to which the membrane is repolarized, E_{Na} is the equilibrium potential for sodium ions that is obtained as the reversal potential for sodium current, I_{Na} is the amplitude of the peak sodium current during depolarization, and E_t is the potential of step depolarization (Song and Narahashi (19) by permission).

(Figs. 5 and 6b). Thus, an equation was developed and the dose–response curve for pyrethroids modification of sodium channels was constructed (Fig. 6). Experiments to record action potentials showed that 100 nM tetramethrin, with which only 0.6% of sodium channels are modified, was the threshold concentration to initiate repetitive discharge. Thus, pyrethroids toxicity is greatly amplified through this mechanism from the sodium channel level to whole animal level.

Since the effects of deltamethrin in modifying sodium channels are irreversible, single-channel experiments were performed with primary cultured rat hippocampal neurons pretreated with deltamethrin (21). Examples of single sodium channel currents are shown in Fig. 7.

The experiments commenced 5–20 min after the treatment of inside-out membrane patches with 10 μM deltamethrin. Sometimes very brief openings were observed during a depolarization to −60 mV (second trace of Fig. 7a). However, often very

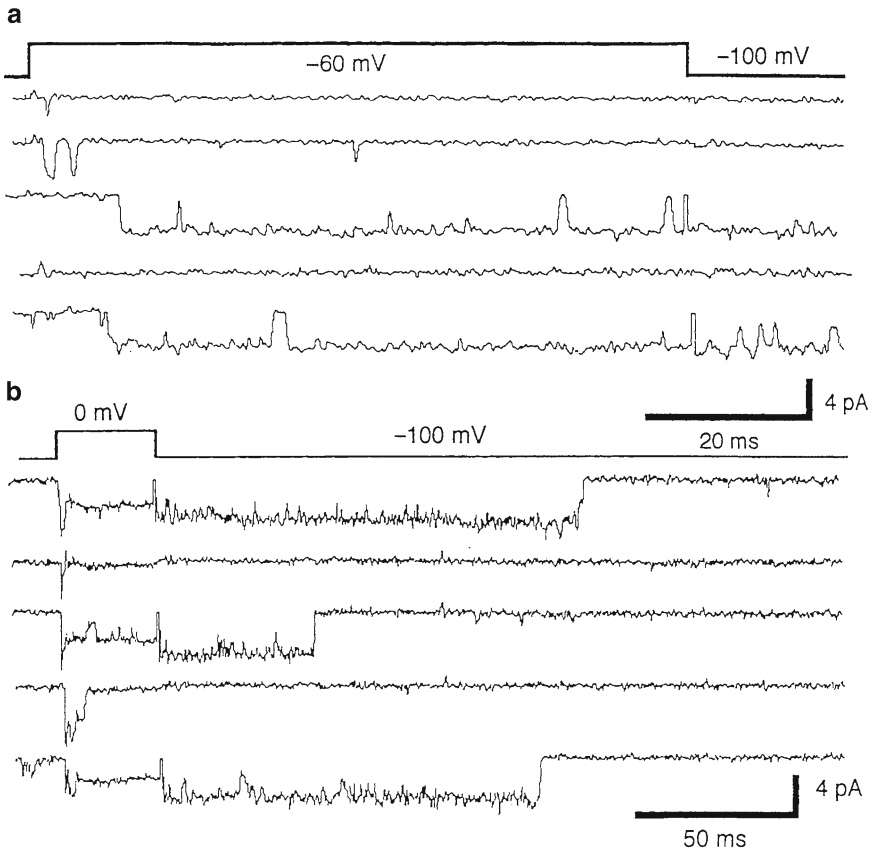

Fig. 7. Single sodium channel currents after treatment with 10 μM deltamethrin in primary cultured rat hippocampal neurons. (**a**) Inside-out membrane patch was depolarized to −60 mV for 80 ms and subsequently repolarized to −100 mV. Brief openings seen in the second record are from normal unmodified channels, and prolonged openings in the third and fifth records are from deltamethrin-modified sodium channels. (**b**) Inside-out membrane patch was depolarized to 0 mV for 30 ms and subsequently repolarized to 100 mV. Prolonged openings occurred during and after depolarization. The final cut-off frequencies of filtering were 1 and 2 kHz in (**a**) and (**b**), respectively (Motomura and Narahashi (21) by permission).

prolonged openings were observed. These occurred during the 80 ms depolarizing pulse and even continued after termination of the depolarization (third and fifth traces of Fig. 7a). Analyses of open time indicate that very brief openings are due to the activity of normal, unmodified sodium channels (figure 1 of Motomura and Narahashi (21)), whereas prolonged openings derive from deltamethrin-modified sodium channels. Very prolonged openings that continued after repolarization are even more clearly seen in Fig. 7b in which a 30 ms depolarizing pulse to 0 mV was followed by repolarization to −100 mV. Sodium channels were kept open for as long as 50 ms to more than 100 ms after repolarization. Continued opening after repolarization is reflected in the whole-cell tail current commonly observed in pyrethroid-treated cells (Figs. 5 and 6).

3.5. Differential Sensitivity of Ion Channels to Insecticides as the Basis for Selective Toxicity

Selective toxicity of insects over mammals is a very important characteristic of insecticide. It was previously thought that the ability of mammals to detoxify insecticides more effectively than insects was a major mechanism responsible for the selective toxicity between insects and mammals. Another serious problem for insecticides is that insects could gain resistance to insecticides. It has become increasingly clear that the differences in target site sensitivity play a major role in the selective toxicity of insects over mammals and the resistance of insects to insecticides.

Detoxication of insecticides was previously thought to be a major factor for insecticide resistance. We demonstrated for the first time that the nerve sensitivity was an important factor as the resistance mechanism. The nerve of the housefly strain normally sensitive to DDT, BHC (lindane), and dieldrin elicited repetitive discharges at lower concentrations of these insecticides than the nerve from the resistant strain of housefly (60). This discovery has eventually led to the concept of knockdown resistance *kdr* strain of insects. Various mutations of sodium channels have now been identified by many investigators (61).

Thus, for both the selective toxicity of insecticides in insects over mammals and for the decreased toxicity in insects resistant to insecticides, the nerve sensitivity to insecticides is an important factor. An example is shown here for a unique case of fipronil, a popular insecticide for which the GluCls are an important target site. GluCls are present only in invertebrate animals such as insects and *Caenorhabditis elegans* and absent in mammals, so that they are an ideal target site for insecticides.

Neurons in the thoracic ganglia of American cockroach *P. americana* were patch clamped to record ion channel currents (24–26, 62). At least two kinds of GluCls were recorded from cockroach neurons: one was a fast-desensitizing GluCl current and the other was a slow-desensitizing GluCl current. Very often a mixed type of current was recorded (Fig. 8). It is sometimes difficult to obtain one of the two types, and we have found the ways to inhibit one type so that only the other type of GluCl can be recorded (63). Application of trypsin at a concentration of 0.5 mg/mL for 10 min completely eliminated the slow-desensitizing GluCl component leaving the fast-desensitizing component intact. Whereas papain at a concentration of 0.5 mg/mL or bovine serum albumin at 0.5 mg/mL had no effect on either fast-desensitizing or slow-desensitizing GluCls, either 0.5 mg/mL soybean trypsin inhibitor or 5% polyvinylpyrrolidone selectively and reversibly blocked the fast-desensitizing component revealing the slow-desensitizing current.

Fipronil also blocked GABA-induced currents in rat DRG neurons with an IC_{50} of 1,600 nM (64) and cockroach neurons with an IC_{50} of 73 nM (62). It inhibited the fast-desensitizing GluCls with an IC_{50} of 800 nM and the slow-desensitizing GluCls

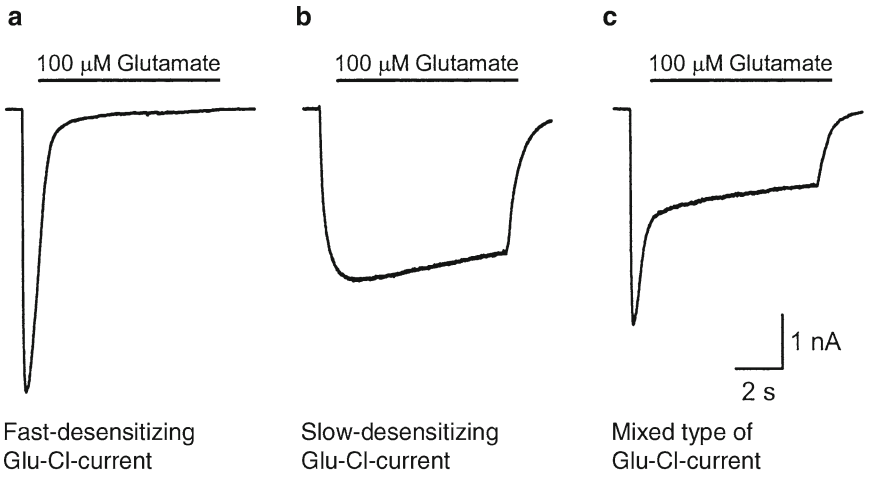

Fig. 8. Two components of glutamate-activated chloride currents (GluCls) recorded from primary cultured cockroach thoracic ganglion neurons. (**a**) Fast-desensitizing GluCl. (**b**) Slow-desensitizing GluCl. (**c**) Mixed type of GluCl.

with an IC_{50} of 10 nM (24). Thus, fipronil inhibition of both cockroach GABA currents and GluCls, especially those of the slow-desensitizing component, contributes significantly to the selective toxicity of fipronil to insects over mammals.

References

1. Shanes AM (1958) Electrochemical aspects of physiological and pharmacological actions in excitable cells. I. The resting cell and its alteration by extrinsic factors. Pharmacol Rev 10:59–164
2. Shanes AM (1958) Electrochemical aspects of physiological and pharmacological actions in excitable cells. II. The action potential and excitation. Pharmacol Rev 10:165–273
3. Cole KS (1949) Dynamic electrical characteristics of the squid axon membrane. Arch Sci Physiol 3:253–258
4. Hodgkin AL, Huxley AF (1952) Currents carried by sodium and potassium ions through the membrane of the giant axon of *Loligo*. J Physiol 116:449–472
5. Hodgkin AL, Huxley AF (1952) The components of membrane conductance in the giant axon of *Loligo*. J Physiol 116:473–496
6. Hodgkin AL, Huxley AF (1952) The dual effect of membrane potential on sodium conductance in the giant axon of *Loligo*. J Physiol 116:497–506
7. Hodgkin AL, Huxley AF (1952) A quantitative description of membrane current and its application to conduction and excitation in nerve. J Physiol 117:500–544
8. Hodgkin AL, Huxley AF, Katz B (1952) Measurement of current-voltage relations in the membrane of the giant axon of *Loligo*. J Physiol 116:424–448
9. Tasaki I, Hagiwara S (1957) Demonstration of two stable potential states in the squid giant axon under tetraethylammonium chloride. J Gen Physiol 40:859–885
10. Taylor RE (1959) Effect of procaine on electrical properties of squid axon membrane. Am J Physiol 196:1071–1078
11. Shanes AM, Freygang WH, Grundfest H, Amatniek E (1959) Anesthetic and calcium action in the voltage clamped squid giant axon. J Gen Physiol 42:793–802
12. Narahashi T, Deguchi T, Urakawa N, Ohkubo Y (1960) Stabilization and rectification of muscle fiber membrane by tetrodotoxin. Am J Physiol 198:934–938
13. Narahashi T, Moore JW, Scott WR (1964) Tetrodotoxin blockage of sodium conductance increase in lobster giant axons. J Gen Physiol 47:965–974

14. Neher E, Sakmann B (1976) Single-channel current recorded from membrane of denervated frog muscle fibres. Nature 260:779–802
15. Hamill OP, Marty A, Neher E, Sakmann B, Sigworth FJ (1981) Improved patch clamp techniques for high-resolution current recording from cells and cell-free membrane patches. Pflugers Arch 391:85–100
16. Roy M-L, Narahashi T (1992) Differential properties of tetrodotoxin-sensitive and tetrodotoxin-resistant sodium channels in rat dorsal root ganglion neurons. J Neurosci 12:2104–2111
17. Song J-H, Nagata K, Tatebayashi H, Narahashi T (1996) Interactions of tetramethrin, fenvalerate and DDT at the sodium channel site in rat dorsal root ganglion neurons. Brain Res 708:29–37
18. Kay AR, Wong RKS (1986) Isolation of neurons suitable for patch clamping from adult mammalian central nervous system. J Neurosci Methods 16:227–238
19. Song J-H, Narahashi T (1996) Modulation of sodium channels of rat cerebellar Purkinje neurons by the pyrethroid tetramethrin. J Pharmacol Exp Ther 277:445–453
20. Motomura H, Narahashi T (2000) Temperature dependence of pyrethroid modification of single sodium channels of rat hippocampal neurons. J Membr Biol 177:23–39
21. Motomura H, Narahashi T (2001) Interaction of tetramethrin and deltamethrin at the single sodium channel in rat hippocampal neurons. Neurotoxicology 22:329–339
22. Moriguchi S, Zhao X, Marszalec W, Yeh JZ, Narahashi T (2005) Modulation of *N*-methyl-D-aspartate receptors by donepezil in rat cortical neurons. J Pharmacol Exp Ther 315:125–135
23. Marszalec W, Narahashi T (1993) Use-dependent pentobarbital block of kainate and quisqualate currents. Brain Res 608:7–15
24. Zhao X, Yeh JZ, Salgado VL, Narahashi T (2004) Fipronil is a potent open channel blocker of glutamate-activated chloride channels in cockroach neurons. J Pharmacol Exp Ther 310:192–201
25. Zhao X, Salgado VL, Yeh JZ, Narahashi T (2004) Kinetic and pharmacological characterization of desensitizing and non-desensitizing glutamate-gated chloride channels in cockroach neurons. Neurotoxicology 25:967–980
26. Zhao X, Yeh JZ, Salgado VL, Narahashi T (2005) Sulfone metabolite of fipronil blocks γ-aminobutyric acid- and glutamate-activated chloride channels in mammalian and insect neurons. J Pharmacol Exp Ther 314:363–373
27. Quandt FN, Narahashi T (1982) Modification of single Na^+ channels by batrachotoxin. Proc Natl Acad Sci U S A 79:6732–6736
28. Tsunoo A, Yoshii M, Narahashi T (1986) Block of calcium channel by enkephalin and somatostatin in neuroblastoma-glioma hybrid NG108-15 cells. Proc Natl Acad Sci U S A 83:9832–9836
29. Twombly DA, Yoshii M, Narahashi T (1988) Mechanisms of calcium channel block by phenytoin. J Pharmacol Exp Ther 246:189–195
30. Chinn K, Narahashi T (1986) Stabilization of sodium channel states by deltamethrin in mouse neuroblastoma cells. J Physiol 380:191–207
31. Kimhi Y, Palfrey C, Spector I, Barak Y, Littauer UZ (1976) Maturation of neuroblastoma cells in the presence of dimethylsulfoxide. Proc Natl Acad Sci U S A 73:462–466
32. Meyer HH (1899) Zur Theorie der Alkoholnarkose. I. Mitt welche Eigenschaft der Aneasthetika bedingt ihre narkotische Wirkung? Arch Exp Pathol Pharmakol 42:109–118
33. Meyer HH (1901) Zur Theorie der Alkoholnarkose. III. Mitt der Einfluss wechselnder Temperatur auf Wirkungsstarke und Teilungskoefficient der Narkotika. Arch Exp Pathol Pharmakol 46:338–346
34. Overton E (1901) Studien uber die Narkose Zugleich ein Beitrag zur Allgemeinen Phamakologie. Fischer, Jena
35. Woodward JJ (1999) Ionotropic glutamate receptors as sites of action for ethanol in the brain. Neurochem Int 35:107–113
36. Mihic SJ (1999) Acute effects of ethanol on $GABA_A$ and glycine receptor function. Neurochem Int 35:115–123
37. Lovinger DM (1999) $5\text{-}HT_3$ receptors and the neural actions of alcohols: an increasingly exciting topic. Neurochem Int 35:125–130
38. Narahashi T, Aistrup GL, Marszalec W, Nagata K (1999) Neuronal nicotinic acetylcholine receptors: a new target site of ethanol. Neurochem Int 35:131–141
39. Wonnacott S (1997) Presynaptic nicotinic ACh receptors. Trends Neurosci 20:92–98
40. Aistrup GL, Marszalec W, Narahashi T (1999) Ethanol modulation of nicotinic acetylcholine receptor currents in cultured cortical neurons. Mol Pharmacol 55:39–49
41. Yamashita M, Marszalec W, Yeh JZ, Narahashi T (2006) Effects of ethanol on tonic GABA

currents in cerebellar granule cells and mammalian cells recombinantly expressing GABAa receptors. J Pharmacol Exp Ther 319: 431–438

42. Borghese CM, Harris RA (2007) Studies of ethanol actions on recombinant delta-containing gamma-aminobutyric acid type A receptors yield contradictory results. Alcohol 41:155–162
43. Moriguchi S, Zhao X, Marszalec W, Yeh JZ, Narahashi T (2007) Effects of ethanol on excitatory and inhibitory synaptic transmission in rat cortical neurons. Alcohol Clin Exp Res 31:89–99
44. Zuo Y, Aistrup GL, Marszalec W, Gillespie A, Chavez-Noriega LE, Yeh JZ, Narahashi T (2001) Dual action of n-alcohols on neuronal nicotinic acetylcholine receptors. Mol Pharmacol 60:700–711
45. Zuo Y, Nagata K, Yeh JZ, Narahashi T (2004) Single-channel analyses of ethanol modulation of neuronal nicotinic acetylcholine receptors. Alcohol Clin Exp Res 28:688–696
46. Sigworth FJ, Sine FM (1987) Data transformations for improved display and fitting of single-channel dwell time histograms. Biophys J 52:1047–1054
47. Narahashi T (1992) Nerve membrane Na^+ channels as targets of insecticides. Trends Pharmacol Sci 13:236–241
48. Narahashi T (1996) Neuronal ion channels as the target sites of insecticides. Pharmacol Toxicol 78:1–14
49. Narahashi T (2000) Neuroreceptors and ion channels as the basis for drug action: past, present, and future. The 2000 ASPET Otto Krayer Award Lecture. J Pharmacol Exp Ther 294:1–26
50. Narahashi T (2002) Nerve membrane ion channels as the target site of insecticides. Mini Rev Med Chem 2:419–432
51. Narahashi T, Ginsburg KS, Nagata K, Song J-H, Tatebayashi H (1998) Ion channels as targets for insecticides. Neurotoxicology 19:581–590
52. Ray DE, Fry JR (2006) A reassessment of the neurotoxicity of pyrethroids insecticides. Pharmacol Ther 111:174–193
53. Shafer TJ, Meyer DA, Crofton KM (2005) Developmental neurotoxicity of pyrethroids insecticides: critical review and future research needs. Environ Health Perspect 113: 123–136
54. Soderlund DM, Smith TJ, Lee SH (2000) Differential sensitivity of sodium channel isoforms and sequence variants to pyrethroid insecticides. Neurotoxicology 21:127–137
55. Vais H, Williamson MS, Devonshire AL, Usherwood PN (2001) The molecular interactions of pyrethroids insecticides with insect and mammalian sodium channels. Pest Manag Sci 57:877–888
56. Bradberry SM, Cage SA, Proudfoot AT, Vale JA (2005) Poisoning due to pyrethroids. Toxicol Rev 24:93–106
57. Lund AE, Narahashi T (1981) Interaction of DDT with sodium channels in squid giant axon membranes. Neuroscience 6:2253–2258
58. Yamasaki T, Ishii [Narahashi] T (1952) Studies on the mechanism of action of insecticides (V). The effects of DDT on the synaptic transmission in the cockroach. Oyo-Kontyu (J Nippon Soc Appl Entomol) 8:111–118
59. Tatebayashi H, Narahashi T (1994) Differential mechanism of action of the pyrethroid tetramethrin on tetrodotoxin-sensitive and tetrodotoxin-resistant sodium channels. J Pharmacol Exp Ther 270:595–603
60. Yamasaki T, Narahashi T (1958) Resistance of house flies to insecticides and the susceptibility of nerve to insecticides. Studies on the mechanism of action of insecticides (XVII). Botyu-Kagaku (Scientific Insect Control) 23:146–157
61. Soderlund DM (2008) Pyrethroids, knockdown resistance and sodium channels. Pest Manag Sci 64:610–616
62. Ikeda T, Zhao X, Kono Y, Yeh JZ, Narahashi T (2003) Fipronil modulation of glutamated-induced chloride currents in cockroach thoracic ganglion neurons. Neurotoxicology 24:807–815
63. Zhao X, Salgado VL, Yeh JZ, Narahashi T (2007) Mechanism of selective toxicity of alpha-endosulfan in insects and mammals. In: Proceedings of the 46th annual meeting of the society of toxicology, Charlotte, NC.
64. Ikeda T, Zhao X, Nagata K, Kono Y, Shono T, Yeh JZ, Narahashi T (2001) Fipronil modulation of the γ-aminobutyric $acid_A$ receptors in rat dorsal root ganglion neurons. J Pharmacol Exp Ther 296:914–921

Chapter 24

Neurotoxicity Assessment by Recording Electrical Activity from Neuronal Networks on Microelectrode Array Neurochips

Dieter G. Weiss

Abstract

Neuronal networks cultured on microelectrode array (MEA) neurochips provide a testing platform for neuroactive compounds such as neurotoxicants and neuropharmaceuticals. Electrical network activity is recorded, quantified, characterized and classified at the level of spike and burst patterns, yielding concentration–response curves of a multitude of activity-describing parameters for monitoring the effects on defined network activity states. The system allows highly complex studies of cellular behavior which can give new insight into the molecular mechanisms of drug or toxicant action. The MEA neurochip technology is suitable to study network electrical activity maturation (weeks 1–4), the long-term functioning of the active networks (many months), and give a precise characterization of toxicant or drug-induced effects on the electrical activity pattern.

Key words: Neurotoxicology, Safety pharmacology, Combination drugs, Phytopharmaceuticals, Electrophysiology endpoints, High content screening

1. Introduction

The function of the nervous system is special as it cannot be explained by studying individual neurons. Its function depends on the network and multicellular communication is the function. Testing for effects on single endpoints, i.e., a certain type of ion channel, would miss all other potentially also relevant functional components. Therefore, complex endpoints of multicellular ensembles are adequate for testing the effects of chemicals on the CNS.

Because nervous tissues express patterns of electrical activity as their normal function, any major interference with these

Michael Aschner et al. (eds.), *Cell Culture Techniques*, Neuromethods, vol. 56,
DOI 10.1007/978-1-61779-077-5_24, © Springer Science+Business Media, LLC 2011

patterns may generate behavioral and/or autonomic malfunctions in response to treatment with chemicals. The cessation of electrical activity (functional neurotoxicity), even if not associated with cell death (cytotoxicity), can lead to the death of the organism. Also, major changes in pattern generation can severely alter the performance of organisms without necessarily threatening survival. Whole network responses yield global information on a compound's interaction with all receptors present in the network and are, therefore, closer to the animal situation than data from single cell or single ion channel electrophysiology.

The technology was developed to its present form in 1977 by Guenter W. Gross when he devised a functional microelectrode array of 64 gold electrodes on glass slides/plates and recorded from a group of neurons in a snail ganglion placed on top (1). Later, he developed a system suitable for growing mammalian nerve cells on microelectrode arrays with transparent indium-tin oxide leads that allows to control the network's morphology by microscopy (2, 3).

Multicellular neuronal networks grown on substrate-embedded microelectrode arrays (MEA neurochips) provide a testing platform based on spontaneously active and self-organized complex networks with neuronal connectivity functional for many months (4–8). MEA neurochips allow the simultaneous and direct monitoring of action potentials of up to 100 or more individual neurons in acute or the long-term exposure studies over days and months. MEA neurochips are suitable to reveal the neuroactive potential of single or complex mixtures of compounds including those with unknown or multiple targets.

The system is used for analyzing the mechanisms of action of neuroactive chemicals and for drug screening. It yields in a global way in the native condition a very detailed description of the electrical communication in the network and then allows a distinction between cytotoxicity of neurons and glial cells (irreversible damage and cell loss) and functional neurotoxicity of compounds interacting temporarily and reversibly with receptors and ion channels. MEA neurochips are used for multiple single-cell electrophysiology of functional neuronal networks from dissociated embryonic mouse CNS areas, such as spinal cord or brain areas, cultured directly on glass/ITO 64 electrode arrays. The cell–electrode coupling remains stable for several months (2).

Neuronal networks retain tissue-specificity and respond to transmitter receptor blockers and other neurotoxic compounds in a substance-specific, dose-dependent manner and when analyzed by advanced multi-parametric data analysis and pattern analysis, they provide a powerful tool for functional neurotoxicity testing, pharmacology and safety pharmacology. Their sensitive and quantitative responses have made such platforms very

useful broadband biosensors for high content screening. The main fields of application are:

- Safety pharmacology (exclusion of adverse neuronal effects of non-nervous system-directed drugs)
- Drug profiling
- Toxicity testing of single and complex mixtures of chemicals
- Target identification and target validation in drug development
- Decision making between different lead compounds of similar quality, by comparison with related drugs

Given the complexity of the nervous system and the multitude of potentially toxic mechanisms, it is clear that a whole battery of tests is required for in vitro neurotoxicity testing. This also implies that it is not trivial to distinguish between pharmacological actions and toxicity responses, although this discrimination is required for risk management. For a comparison of different in vitro models for CNS toxicity testing see (9).

2. Materials

2.1. Chemicals

1. 5-Fluoro-2′-deoxyuridine + uridine (FDU): Sigma-Aldrich Chemical GmbH (Taufkirchen, Germany).
2. Poly-D-lysine MW 30–70 kDa: Sigma-Aldrich Chemical GmbH (Taufkirchen, Germany).
3. DNAse I (from bovine pancreas): Roche (Mannheim, Germany).
4. Accutase: PAA (Germany).
5. Laminin: Roche (Mannheim, Germany).
6. Fetal bovine serum: Pan Biotech GmbH (Aidenbach, Germany).
7. Horse serum: GIBCO BRL (Paisley, UK).
8. Minimum essential medium (MEM) and Dulbecco's modified essential medium (DMEM): GIBCO BRL (Paisley, UK).
9. Dissociation buffer: NaCl 135 mM, KCl 5 mM, Na_2HPO_4 0.3 mM, KH_2PO_4 0.2 mM, glucose 16.6 mM, saccharose 22 mM, HEPES 9.9 mM, DNase I (8,000 U/ml), accutase (10 U/ml), pH 7,3, sterile filtered.

2.2. Microelectrode Array Neurochips

The here used MEA neurochips and the chambers for culturing the networks were provided by the Center for Network Neuroscience (CNNS) at the University of North Texas (www.

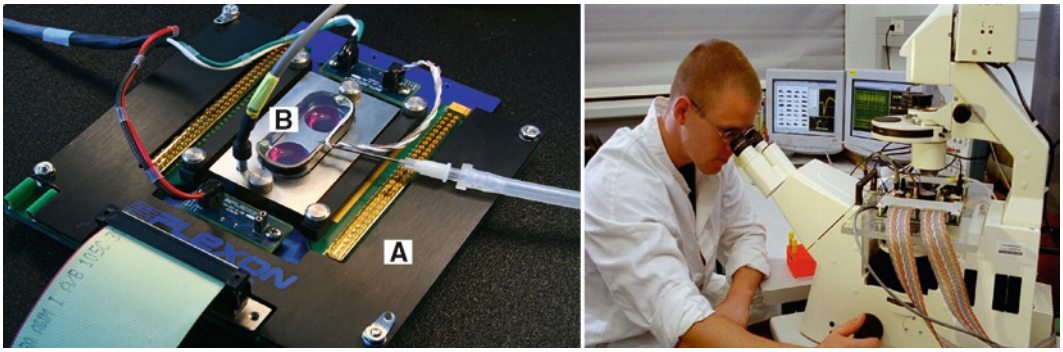

Fig. 1. (**a**) Preamplifier board of the Plexon Inc. MEA Workstation with 64-channel data cable and MEA neurochip in culture chamber. (**b**) Preamplifier board on a Zeiss Axiovert microscope for continuous optical control of the culture.

cnns.org) (Note 1). These 5 × 5 cm glass chips have a central recording matrix with 64 passive electrodes and indium-tin oxide conductors which are insulated by polysiloxane and end as gold-plated free electrodes. The electrode diameter is 20 µm, the electrode spacing ranges in different chip variants from 40 to 200 µm (www.cnns.org). The electrodes are typically arranged in a grid that covers about 2 mm^2. Each electrode extends to the periphery of the chip that makes contact with an external amplifier, which relays the spatiotemporal pattern of extracellular action potentials to a computer for data storage. If MEA neurochips are treated carefully and cleaned thoroughly, they may be re-used ten or more times. In order to increase throughput, several suppliers have introduced multiple recording matrices on one chip (Note 2).

2.3. Recording Equipment

MEA neurochips are housed in a recording chamber (both from CNNS) which is placed on a preamplifier board (Plexon, Inc., Dallas, TX, USA) containing temperature control devices and 64 preamplifiers (Fig. 1a). Recording and data analysis is performed with the multichannel acquisition processor system, a computer-controlled 64-channel amplifier system (Plexon, Inc.) providing programmable amplification, filtering, switching, and digital signal processing of MEA neurochip signals. When using glass/ITO MEA neurochips, it is possible and advisable to permanently control the network culture on an inverted microscope (Fig. 1b).

3. Methods

3.1. Preparation of MEA Neurochips

The hydrophobic insulation material surface is activated by brief (1 s) flaming with a hand-held butane burner through a stainless steel mask (5 mm diameter). This allows cell attachment on a confined hydrophilic region centered on the electrode array. The activated surface regions were coated with poly-D-lysine

(25 μg/ml; 30–70 kDa) and laminin (16 μg/ml) by applying one drop on the activated region overnight.

3.2. Preparation of Cells from Murine Frontal Cortex

Frontal cortex (FC) tissue is obtained from embryonic day 15–16 chr:NMRI mice (spinal cord SC at day 14). For other brain region tissues see Note 3. After ethyl ether anesthesia, mice were sacrificed by cervical dislocation according to National Animal Protection laws. The tissue is dissociated mechanically with two scalpels and transfer pipettes and subsequently enzymatically by incubation of the finely minced tissue for 15 min at 37° in dissociation buffer containing DNAse I (800 U/ml) and accutase (10U/ml). The cells are resuspended in DMEM10/10 (FC) or MEM10/10 (SC) (10% horse and 10% fetal calf serum) at a density of 1.0×10^6 cells/ml, and 300 μl were seeded onto MEA surfaces.

3.3. Neuronal Network Culture

Cultures were incubated at 37°C in a 10% CO_2 atmosphere until ready for use, which is 4 weeks after seeding (Fig. 2). Culture media were replenished three times a week with DMEM or MEM containing 10% horse serum. Like in the tissue of origin, networks develop from a mixture of different types of postmitotic neurons and glial cells. The glial cells have important auxiliary functions for the metabolism and for supplying the neurons with ions and nutrients. While neurons are postmitotic, glia cells are allowed to proliferate for 3–5 days up to a certain cell density, before overgrowing the monolayer. To stop further growth of glia cells, the developing co-cultures are then treated with 5-fluoro-2′-deoxyuridine (25 μM) and uridine (63 μM) for 48 h to prevent further proliferation.

The cells grow directly on the neurochips as self-organized neuronal networks. They are composed of a mixture of different neuronal cell types and glial cells comparable to the tissue of origin. The neurons couple electrically to the neurochip electrodes whereby the action potentials of the cells can be recorded (extracellular recording). At day 3–5, in vitro electrical activity starts spontaneously and develops into a pattern of partially oscillatory and partially synchronized fashion. After 4 weeks, the electrical activity in the network stabilizes. The activity patterns then remain stable for months during which period experiments can be performed. Characteristic changes occur then only when the networks are stimulated with neuroactive substances. Networks grow in a flat manner with glia cells forming a carpet. The number of glia cells exceeds that of neurons ten or more fold (Fig. 2).

3.4. Experiment Schedule

General cytotoxicity is to be covered by general “cytotox” tests. Functional neurotoxicity means that neurotoxicants cause changes that do not affect cell viability, “only” synaptic transmission or action potential propagation are impaired. Many different mechanisms are at work by which neurotoxicants exert their influence

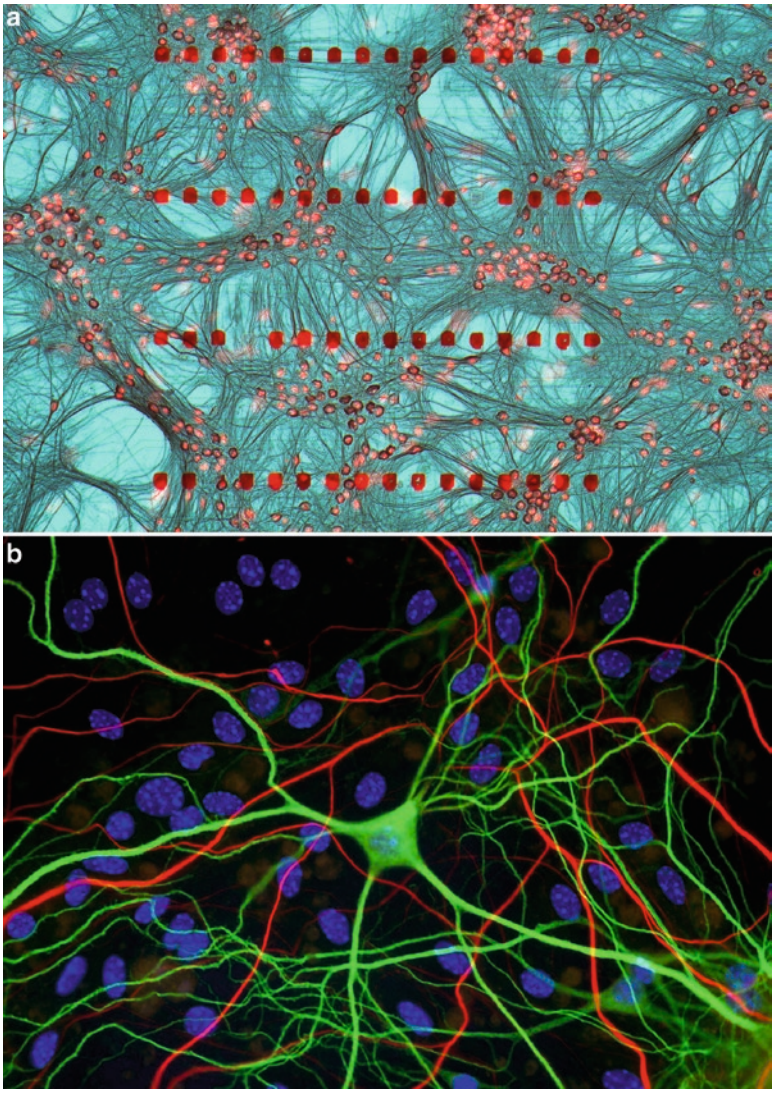

Fig. 2. (**a**) Frontal cortex network grown on a 64-electrode MEA neurochip 21 days in vitro. The culture was stained for neurons with DAB against neurofilament and MAP2. (**b**) Same at higher magnification to see the darker axonal (*red*) and the brighter dendritic (*green*) staining. Nuclei, mainly of glial cells, are *blue*. Micrographs by courtesy of Simone Stüwe, University of Rostock. Colors are seen in the online version.

on the nervous system. There are several conceivable endpoints which are useful to detect chemicals that impair the CNS functions:

1. Endpoint action potential propagation
2. Endpoint synaptic transmission, transmitter or peptide synthesis and release
3. Endpoint axonal transport

4. Endpoint glia function
5. Endpoint network development (developmental neurotoxicology)
6. Endpoint blood–brain barrier (BBB) integrity, i.e., all compounds need in parallel to be tested for BBB permeability for judging their toxic potential

Since impairments of mechanisms 1–5 will sooner or later also show up as changes of the network electrical patterns, this is the most direct and basic parameter and it can be studied relatively simply and at moderately high throughput using MEA neurochips. It is therefore that MEA neurochips are the testing platform with promise for future tests. Cultures can be acutely treated with test compounds or chronic pretreatment of the cultures is possible. In order to obtain concentration–response curves the neuronal networks are acutely treated, after recording the native activity pattern for 1 or 2 h as reference, with rising concentrations of the reference compounds for 30–60 min each. Reversibility tests are performed by washes with conditioned medium for 20–60 min (5, 6).

3.5. Data Recording

Recording is performed with the multichannel acquisition processor system, a computer-controlled 64-channel amplifier system (Plexon, Inc.) which delivers single neuron spike data and provides programmable amplification, filtering, switching, and digital signal processing of microelectrode signals. After setting the noise threshold, extracellular recordings of spike (action potential) and burst patterns are obtained simultaneously from each electrode. Furthermore, it is possible to discriminate signals from several neurons (units) which are picked up by the same electrode (Fig. 3). Spike identification and separation are accomplished by a template-matching algorithm in real time. This allows the simultaneous recording of up to 256 neurons (action potentials) from a 64-electrode MEA neurochip. The signals recorded are in the range of 15–1,800 μV. The total system amplification is 10 K and the sampling rate is 40 kHz. This high sampling rate provides in addition to the time mark for each action potential also the complete information about the wave form with its Na^+ and K^+ components typical for extracellular action potentials (Fig. 3 left) so that chemicals influencing the axonal Na^+ and K^+-channels can be discerned by causing changes of the waveform over time.

3.6. Data Analysis

The action potentials, or "spikes," are recorded as spike trains; they are clustered in groups, so-called bursts. Bursts are quantitatively described via spike train analysis using the program NeuroExplorer (Plexon Inc.). Bursts are defined by the beginning and end of a period characterized by short intervals between spike events. Maximum spike intervals defining the start of a burst

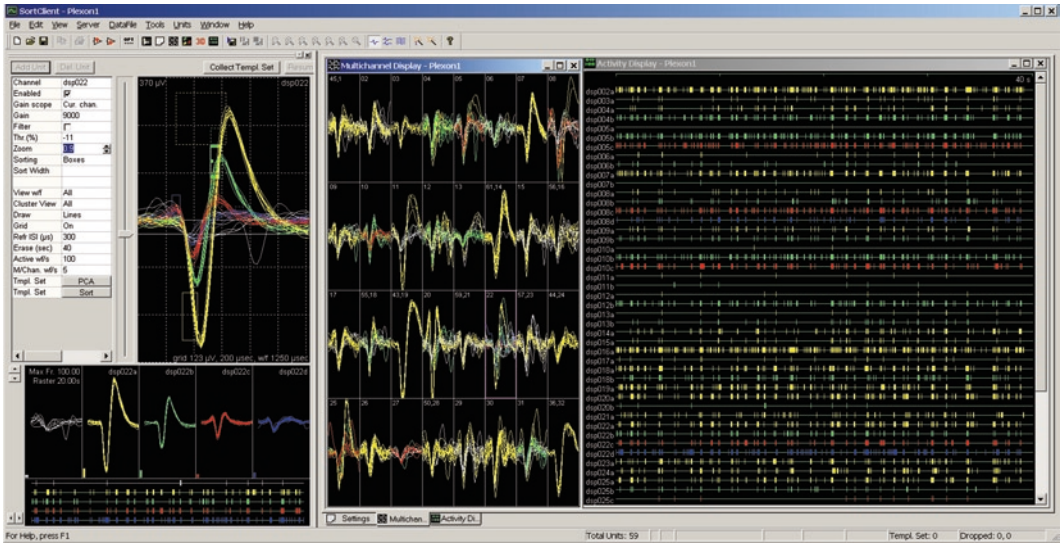

Fig. 3. Screenshot of the recording software SortClient (Plexon Inc.). *Left*: Waveforms of neurons recorded at one selected electrode at high temporal resolution. One electrode is able to record action potentials from several neurons (*top*) which are separated online on the basis of their amplitudes and waveforms and displayed in different colors by the software (*bottom left*). *Middle*: Overview of 32 of the recorded electrodes; some show multiple units (colors). *Right*: Activity pattern (40 s) of 43 recorded neurons after unit separation (*green*, *red* and *blue* indicate the second, third and fourth neuron detected on a given electrode). Forty seconds of spontaneous native electrical activity of a native frontal cortex culture. Each action potential is represented by a vertical tick. Colors are seen in the online version.

should be adjusted from 50 to 150 ms and maximum intervals that mark the end of a burst range from 100 to 300 ms depending on the type of tissue (spinal or cortical). Spike rate and burst rate values are derived from 60 s bin data and averaging over a period of at least 30 min of stable activity is recommended.

NeuroExplorer also allows one to perform high content analyses of the network activity patterns by providing a multi-parametric description, which quantitatively characterizes the whole action potential pattern of a given physiological state of the network as well as the changes exerted by the addition of neuroactive compounds. NeuroExplorer software provides 32 parameters which describe four categories of network activity features: overall activity, burst structure, synchronicity, and oscillatory behavior:

- The overall activity of an electrical pattern and its changes, i.e., upon addition of a neuroactive compound are described by parameters such as spike rate, burst rate, percent of spikes in burst, and total number of bursting neurons.
- A description of the structure of the bursts in an activity state is given by parameters such as mean spike frequency in bursts, peak spike frequency in bursts, interspike interval in bursts, burst period, number of spikes in bursts, burst duration, and

interburst interval. The also provided parameter "burst surprise" is a statistical measure of non-randomness of firing.

- Aspects of the oscillatory behavior that characterize the temporal dynamics of a network state are captured through the temporal coefficients of variation (CV_{TIME}) of the above burst rate, burst period, and spike rate parameters. These variation coefficients quantify the temporal behavior-reflecting temporal dynamics of the interactions within the network. The set of CV_{TIME} parameters characterizes the periodic behavior of single neuron activity patterns.
- The degree of coordination between different neurons in the network or degree of synchronicity in a given activity pattern is described by a set of spatial coefficients of variation ($CV_{NETWORK}$) calculated for the above mentioned basic parameters. They are a measure of firing synchronicity of a network.

These CVs, calculated in general by CV = SD/mean, describe the spatiotemporal behavior of the network activity. CV_{TIME} and $CV_{NETWORK}$ values are based on a parameter's values $p_{n,t}$, for each of the T bins in time and each of the N neurons in the network, calculated by:

$CV_{TIME} = (1/N)\sum_{n=1}^{N} \sigma_n / \mu_n$ with $\mu_n = (1/T)\sum_{t=1}^{T} p_{n,t}$ and σ_n, the associated standard deviation, and $CV_{NETWORK} = (i/T)\sum_{t=1}^{T} \sigma_t / \mu_t$ with $\mu_t = (1/N)\sum_{n=1}^{N} p_{n,t}$ and σ_t, the associated standard deviation.

Parameter values are typically derived from 60 s bin data over a period of at least 30 min of stable network activity. After adding or washing out test compounds it may take 5–15 min for a network to attain a stable firing pattern. For direct comparability, all parameters are normalized for each session and for each experimental treatment with regard to the corresponding values of the reference activity (native or after chronic pretreatment). The features' distributions were tested for normality. The level of significance after compound application is assessed using Student's paired *t*-test or ANOVA tests.

If the efficacy of a test compound is to be analyzed, a series of concentrations is applied to the networks and a concentration–response curve is obtained for each of the above parameters by fitting the data with the sigmoidal Hill equation. The changing parameter is fitted for each experiment as a function of the applied concentration to a single-sigmoidal or multiphasic-sigmoidal concentration–response curve given by the equation:

$$Y = y_{START} + (y_{END} - y_{START}) / (1 + 10^{[\log(EC_{50}) - \log(x)]*HC}).$$

From these concentration–response curves one can obtain the effective concentration causing 50% of the maximal response (EC_{50}) as well as the values for EC_{10}, EC_{20} or EC_{90} and the slope (Hill coefficient, nH). The data for concentration–response curves

are typically obtained by first performing a range finding experiment with cumulative addition of the test compound to one culture. In the concentration range found to influence the electrical activity 8–10 concentrations are further studied with 5–10 repeats. It is possible to use separate cultures for each concentration or apply the compound in rising concentrations to the same culture for each repeat experiment. In this case variation of the sequence, experiments of long-term stability of the culture over hours and reversibility should be performed to exclude non-additive behavior or adaptation effects of the network.

The set of concentration–response curves represents a detailed description of a compound's electrophysiological action profile indicating in the case of a potential drug candidate its efficacy, mode of action and a first hint on its therapeutic window. This information may be especially helpful in drug development studies when a group of compounds of similar action profiles is evaluated for selection of the most powerful lead compounds to be further developed. In neurotoxicity studies, a deviation in some parameters of more than 10 or 20% occurring in the low to intermediate concentration range indicates a potential neurotoxicant that deserves further attention and detailed study to decide on its exclusion, e.g., from drug development in safety pharmacology studies. Biological evaluation of a compound requires in all cases additional studies on permeability through or damaging effects on the blood–brain barrier.

Results are expressed as series means ± SEM. The absolute parameters' distributions are tested for normality. Using the SPSS v15 statistical software, significant changes induced by substance application are tested by analysis of variance (ANOVA) followed by Dunnett's multiple comparison post hoc test with the native activity as the common control. $P < 0.05$ is considered statistically significant. Variability of results between different MEA neurochips and different cultures are typically in the same range as in pharmacology and toxicology studies between individual test animals.

3.7. Database and Pattern Analysis

The sets of concentration–response curves obtained for a number of substances with known properties such as mode of action, established drugs or known toxicants can be combined into a substance database. The data represent compound-specific "fingerprints" which can be used to identify compounds by their activity patterns, or to find compounds of similar activity profiles. In this manner, additional evidence of substance or pattern features is assigned to the MEA neurochip data. These data sets are used to perform classification experiments by Pattern Analysis methods based on Bayesian classifiers, artificial neuronal networks, support vector machines (two classes, multiple classes, regression, using a selection of the best discriminating features and feature scores) (10). Result assessment is done by classifying a data set as if it were unknown. Such tests discriminate compounds

in the data set with an accuracy of 80% and more. Successful classification is the proof of reproducibility and a verification of the quality of the applied standard operating procedures. A large database with profiles of more than 100 neuroactive compounds is available at NeuroProof GmbH (Rostock, Germany, www.neuroproof.com) for custom screening.

Potentially neurotoxic effects may be exerted by compounds acting as ion channel blockers, axonal transport blockers, transmitter receptor blockers, opioids, narcotics, sedatives, anesthetics, and analgesics whose group pattern features can be determined. In a second step, the toxicity of new substances is classified for similarity to those characterized groups by their spike train responses in order to judge their toxic potential. The sensitivity and quantitative responses (7) make such platforms useful as broadband biosensors for in vitro CNS toxicity screening (11–17). The approach is a High Content Screening assay system also applicable for the late discovery and the early development phases in drug development, drug profiling, and safety pharmacology (18–21).

MEA neurochip technology is an alternative to animal experimentation (see Note 4). An overview of the properties of the technology is given in Note 5.

4. Notes

1. MEA neurochips can be made in house or purchased with different characteristics. Some alternative suppliers of MEA neurochip systems are Multichannel Systems GmbH, Reutlingen, Germany (www.multichannelsystems.com), Alpha MED Sciences Co. (www.med64.com) and Ayanda Biosystems SA, Lausanne Switzerland or Axion BioSystems (Atlanta, GA, USA). Some of these companies have focused on MEAs with a wider spacing for recording sum potentials from rat or murine brain slices. Several more systems are under development. For an overview see (22).
2. Increasing throughput. In 1998, the CNNS introduced a 2-network array where the normal 64 matrix was separated into two 32-electrode recording areas without changing the amplifier contacts, so that one can be used as a control. Tissue is seeded from the same dissociated cell pool onto both arrays, and a common medium bath is later separated by a two-compartment gasket. Alpha MED Sciences (Panasonic) has introduced a similar chip that contains two 32-electrode arrays separated by a chamber divider. Ayanda Biosystems (Lausanne, Switzerland) has introduced a four-well MEA chip compatible with the Multichannel Systems platform. Each recording area contains 15 microelectrodes and the four wells are spaced

approximately in conformity with a standard 96-well plate. Multichannel Systems has recently introduced a six-well chip wherein each well contains nine electrodes and a common ground.

3. In addition, tissue slices from Hippocampus, Cortex or other regions of interest can be placed onto MEA neurochips and analyzed; however, it cannot be expected that all brain regions will show self-igniting electrical activity (23–25). An extensive table of publications reporting on applications of MEA neurochip technology in neurotoxicity studies can be found in Appendix A of ref. (26).
4. Animal replacement and 3R's: The multielectrode neurochip technology offers a refinement by giving multi-parametric, fingerprint-like descriptions of the action of toxic compounds on nervous tissues. In addition, it reduces the number of animals required for neurotoxicity testing. From one parent mouse, neuronal tissue for 40–50 neurochips can be derived. Further, with each of these neurochips, dose–response series with 10–15 concentration steps, single dose repeats, or chronic experiments can be carried out. This will reduce the number of animal experiments needed for the study of toxic compounds by a factor of up to 500 and at the same time yield much more detailed information on the mode of action of the compounds. Additionally, cultures from knockout mice can replace in vivo animal disease models.
5. Overview over properties and applicability of MEA neurochip technology.
   - *Physiologically relevant information*: not single receptor information, but global information on effects on all cell types present with their synaptic and non-synaptic targets are obtained.
   - *Grown co-cultures*: self-organized networks including glia cells provide long-term stability through neuron–glia interactions, spontaneous activity, good intra-culture and inter-culture reproducibility.
   - *Tissue specificity*: various CNS regions can be studied which retain to a large extent their in vivo-like pharmacology and inventory of receptors.
   - *Long-term stability*: chronic experiments are possible due to non-invasive measurements and stable cell–electrode coupling.
   - *High data yield*: simultaneous recording of complex electrical network patterns from multiple electrodes.
   - *High-content screening*: quantitative multi-parametric analysis of spike trains, burst patterns, synchronicity and oscillations; in combination with high content imaging microscopy: Cytomics.

- *Global substance effects*: no prior knowledge of the mode of action or the target structures is needed and mixtures of compounds can be studied as well. The fact that neuroactive or neurotoxic substances often do not activate only a single receptor makes the "whole network" approach especially valuable for neurotoxicology studies.
- *Reference database*: classification according to known activity patterns and target receptors.

Acknowledgments

This research would not have been possible without the extensive discussions and continuous help and advice from Guenter W. Gross since he first introduced usable MEAs more than 30 years ago. The work was initially supported by the German Science Foundation DFG Innovationskolleg "Komplexe und Zelluläre Sensorsysteme" (INK 27), consecutively by the State Ministries of Education and of Economy of Mecklenburg-Vorpommern, and the European Community (ERDF) through the State Priority Research Program "Biosystems Technology." The author would like to thank the large number of collaborators and colleagues that have helped to establish and apply MEA neurochip technology in our laboratory, especially Alexandra Gramowski, Simone Stüwe, Konstantin Jügelt, Liane Mehnert and Willi Maile, as well as Kristine Gürtler and Bärbel Redlich for technical assistance. I am especially indebted to Olaf Schröder and his collaborators at Pattern Expert GmbH (Borsdorf, Germany) and NeuroProof GmbH (Rostock, Germany) for introducing us to machine-learning algorithms, Pattern Analysis and screenable database techniques, thus opening a new dimension of high-content screening to the field of MEA neurochip technology. The actual studies on special applications are supported by the European Union Grants NORMOLIFE and PREDICT i.v.

References

1. Gross GW, Rieske E, Kreutzberg GW, Meyer A (1977) A new fixed-array multi-microelectrode system designedfor long-term monitoring of extracellular single unit neuronal activity in vitro. Neurosci Lett 6:101–105
2. Gross GW, Wen W, Lin J (1985) Transparent indium-tin oxide patterns for extracellular, multisite recording in neuronal cultures. J Neurosci Meth 15:243–252
3. Gross GW, Rhoades BK, Azzazy HM, Wu MC (1995) The use of neuronal networks on multielectrode arrays asbiosensors. Biosens Bioelectron 10:553–567
4. Gross GW, Williams AN, Lucas JH (1982) Recording of spontaneous activity with photoetched microelectrode surfaces from mouse spinal neurons in culture. J Neurosci Methods 5:13–22
5. Gross GW, Harsch A, Rhoades BK, Göpel W (1997) Odor, drug and toxin analysis with neuronal networks in vitro: extracellular array recording of network responses. Biosens Bioelectron 12:373–393
6. Gross GW, Norton S, Gopal K, Schiffmann D, Gramowski A (1997) Nerve cell network in vitro: Applications to neurotoxicology,

drug development, and biosensors. Cell Eng 2:138–147

7. Gramowski A, Jügelt K, Weiss DG, Gross GW (2004) Substance identification by quantitative characterization of oscillatory activity in murine spinal cord networks on microelectrode arrays. Eur J Neurosci 19:2815–2825
8. Weiss DG, Gramowski A, Stüwe S, Jügelt K, Mehnert L, Schiffmann D, Schröder O (2006) Detecting neurotoxicity and neuropharmacological potential of compounds through electrical activity changes of neuronal networks on microelectrode arrays. In: Stett A (ed) Proceedings of Fifth International Meeting on Substrate-Integrated Microelectrodes, BIOPRO Stuttgart, 3-938345-02-0, 2006, pp 122–125
9. Bal-Price AK, Suñol C, Weiss DG, van Vliet E, Westerink RHS, Costa LG (2008) Application of in vitro neurotoxicity testing for regulatory purposes: symposium III summary and research needs. Neurotoxicology 29:520–531
10. Schroeder OH-U, Gramowski A, Jügelt K, Teichmann C, Weiss DG (2008) Spike train data analysis of substance-specific network activity: application to functional screening in preclinical drug development. In: Stett A (ed): Proceedings MEA Meeting 2008. BIOPRO edition vol. 5. Stuttgart: BIOPRO Baden-Württemberg GmbH, ISBN 3-938345-05-5, 113–116
11. Gramowski A, Schiffmann D, Gross GW (2000) Quantification of acute neurotoxic effects of trimethyltin using neuronal networks cultured on microelectrode arrays. Neurotoxicology 21:331–342
12. Gramowski A, Stüwe S, Jügelt K, Schiffmann D, Loock J, Schröder O, Gross GW, Weiss DG (2006) Detecting neurotoxicity through electrical activity changes of neuronal networks on multielectrode neurochips. In: Proceedings of the 5th World Congress on Alternatives and Animal Use in the Life Sciences, Berlin 2005. ALTEX, Spec. Issue 2006:414–419.
13. Keefer EW, Gramowski A, Stenger DA, Pancrazio JJ, Gross GW (2001) Characterization of acute neurotoxic effects of trimethylolpropane phosphate via neuronal network biosensors. Biosens Bioelectron 16:513–525
14. Parviz M, Gross GW (2007) Quantification of zinc toxicity using neuronal networks on microelectrode arrays. Neurotoxicology 28:520–531
15. Gopal KV, Miller BR, Gross GW (2007) Acute and sub-chronic functional neurotoxicity of methylphenidate on neuronal networks in vitro. J Neural Transm 114:1365–1375
16. Kulagina NV, O'Shaughnessy TJ, Ma W, Ramsdell JS, Pancrazio JJ (2004) Pharmacological effects of the marine toxins, brevitoxin and saxitoxin, on murine frontal cortex networks. Toxicon 44:669–679
17. Shafer TJ, Rijal SO, Gross GW (2008) Complete inhibition of spontaneous activity in neuronal networks by deltamethrin and permethrin. Neurotoxicology 2:203–212
18. Keefer EW, Gramowski A, Gross GW (2001) NMDA receptor-dependent periodic oscillations in cultured spinal cord networks. J Neurophysiol 86:3030–3042
19. Gramowski A, Jügelt K, Stüwe S, Schulze R, McGregor GP, Wartenberg-Demand A, Schröder O, Loock J, Weiss DG (2006) Functional screening of traditional antidepressants with primary cortical neuronal networks grown on multielectrode neurochips. Eur J Neurosci 24:455–465
20. Keefer EW, Norton SJ, Boyle NA, Talesa V, Gross GW (2001) Acute toxicity screening of novel AChE inhibitorsusing neuronal networks on microelectrode arrays. Neurotoxicology 22:3–12
21. Morefield SI, Keefer EW, Chapman KD, Gross GW (2000) Drug evaluations using neuronal networks cultured on microelectrode arrays. Biosens Bioelectron 15:383–396
22. Stett A (2008) Sixth International Meeting on Substrate-Integrated Microelectrodes, BIOPRO edition vol. 5. Stuttgart: BIOPRO Baden-Württemberg GmbH, 353 p. ISBN 3-938345-05-5
23. Xia Y, Gopal KV, Gross GW (2003) Differential acute effects of fluoxetine on frontal and auditory cortex networks in vitro. Brain Res 973:151–160
24. Gross GW, Gopal KV (2006) Emerging histiotypic properties of cultured neuronal networks. In: Taketani M, Baudry M (eds) Advances of network neurophysiology. pp 193–214
25. Ham MI, Bettencourt LM, McDaniel FD, Gross GW (2008) Spontaneous coordinated activity in cultured networks: analysis of multiple ignition sites, primary circuits, and burst phase delay distributions. J Comput Neurosci 24:346–357
26. Johnstone AFM, Gross GW, Weiss DG, Schroeder OH-U, Gramowski A, Shafer TJ (2010) Microelectrode arrays: A physiologically based neurotoxicity testing platform for the 21st Century, NeuroToxicology 31: 331–350

Chapter 25

$GABA_A$ Receptor Binding and Ion Channel Function in Primary Neuronal Cultures for Neuropharmacology/ Neurotoxicity Testing

Cristina Suñol and Daniel A. García

Abstract

$GABA_A$ receptor ($GABA_AR$) constitutes the main inhibitory receptor of the central nervous system. Due to the wide distribution and activity of its main neurotransmitter agonist, the γ-aminobutyric acid (GABA), its pharmacology has been thoroughly studied, given rise to the development of numerous drugs and of neuroactive compounds, some of the latest inducing neurotoxic effects.

In this chapter, we describe methods for studying the interaction of chemical agents with the $GABA_AR$ and the effects they produce on its function, by using mice cortical and cerebellar granule neurons that have been grown in vitro (cultured neurons). The methods described here include the evaluation of the binding of different agents such as GABA agonists, GABA antagonists or allosteric modulators of the receptor, and the assessment of the receptor functionality by analyzing the Cl^- flux induced by GABA.

Key words: Primary neuronal cultures, $GABA_A$ receptor, Muscimol binding, Flunitrazepam binding, TBPS binding, Chloride uptake, Allosteric modulation

1. Introduction

An excitatory neurotoxic effect, for example that induced by pesticides and marine toxins, is produced by different mechanisms: excessive activation of voltage-dependent Na^+ channels and of glutamate/acetylcholine receptor-operated channels or inactivation of Cl^- channels as those operated by the ionotropic $GABA_A$ receptor ($GABA_AR$) (1). The main chemical mediators in the central nervous system (CNS) are amino acids, like γ-aminobutyric acid (GABA), glycine and glutamate, which are in charge of inhibitory (GABA and glycine) and excitatory (glutamate) transmission signals between neurons. The gabaergic system mediates a series of physiological functions and neurological and psychiatric

Michael Aschner et al. (eds.), *Cell Culture Techniques*, Neuromethods, vol. 56,
DOI 10.1007/978-1-61779-077-5_25,

alterations. The neuronal gabaergic system is widely distributed in the CNS, where around 30–40% of the neurons release the neurotransmitter GABA. Due to the wide distribution and activity of GABA in the CNS, the pharmacology based on this neurotransmitter has been thoroughly studied, given rise to the development of numerous drugs and of neuroactive compounds, some of the latest inducing neurotoxic effects (for review of GABA neurotransmission see (2–7)). The development of selective pharmacological agents allowed to identify and to characterize two different types of GABA receptors, $GABA_A$ and $GABA_B$, which differ in their pharmacological, biochemical and electrophysiological properties. The $GABA_AR$ is a member of the superfamily of receptor ionic channels operated by ligand binding, whereas the $GABA_B$ receptor is a metabotropic receptor whose activation produces a cascade of second messengers. The $GABA_AR$ is an oligomeric protein, composed mainly of α, β, γ and δ subunits, that has separate but allosterically interacting binding sites for the endogenous neurotransmitter GABA, for benzodiazepines and for picrotoxinin-like convulsants among others. The activation of the $GABA_AR$ by GABA or their agonists leads to the opening of a channel permeable to Cl^- and generally induces a rapid inhibitory potential in the neuronal postsynaptic membrane. The Cl^- flux is increased by several types of depressing drugs, fundamentally benzodiazepines, barbiturates, steroids and anesthetics whereas it is reduced by convulsant agents like bicuculline and picrotoxinin. Other substances like alcohols, polychlorocycloalkane pesticides, convulsant β-carbolines, and metals (such as Zn^{2+}, mercury, lanthanum) interact with the $GABA_AR$. This wide spectrum of drugs, toxic agents, and metals modify the $GABA_AR$ function by directly interacting with the different binding sites or with other not yet well described sites present in the receptor complex. The binding sites for GABA and benzodiazepines at the $GABA_AR$ are located on the extracellular site of the receptor, at the interface of an α and a β subunit, and at the interface between an α and a γ2 subunit, respectively. The convulsants picrotoxinin and *t*-butyl bicyclophosphorothionate (TBPS), the barbiturates, the anesthetic propofol, and endogenous neuroesteroids bind to one or more sites located close to or within the chloride channel. All these binding sites are allosterically modulated. Allosteric ligands bind to the distinct sites of the $GABA_AR$ and modulate GABA-gated conductance changes. $GABA_AR$-positive allosteric modulators have anticonvulsants, anxiolytic, sedative, hypnotic and anesthetic activities, whereas those with negative allosteric actions have convulsant activities. Known allosteric binding modulations include the enhanced binding of benzodiazepine agonists by GABA, propofol, neurosteroids, thymol and barbiturates, the enhanced GABA-induced Cl^- flux by benzodiazepines, propofol, neurosteroids, thymol and barbiturates, and the different modifications of

[^{35}S]TBPS binding induced by GABA, benzodiazepines, and barbiturates.

$GABA_A$Rs are widely distributed in the brain and they have been reported to be expressed in primary neuronal cultures. In addition to their expression, their functionality, described as the ability to permeate Cl^-, has been well documented in mature primary cultured cells (8–12). In this chapter, we describe methods for studying the interaction of chemical agents with the different binding sites at the $GABA_A$R and the effects they produce on its function, by using mice cortical (CTX) and neuronal cerebellar granule cells (CGC) that have been grown in vitro (cultured neurons). Primary cultures of mice cortical neurons are constituted by around 40% of GABAergic neurons, which synthesize and release the neurotransmitter GABA. On the other hand, primary cultures of mice cerebellar granule cells (CGC) are mainly constituted by glutamatergic neurons and a minority of GABAergic neurons (6%) (13, 14). Both cultured cell types express α, β and γ $GABA_A$R subunits mimicking those found in vivo (15, 16). These primary neuronal cultures constitute in vitro models that are extensively used in neuropharmacological and neurotoxicological studies involving GABA and glutamate neurotransmission, neurodegeneration, and neuroprotection mechanisms.

2. Materials

2.1. Neuronal Cultures

Primary cultures of mice cortical neurons (CTX) are grown for 6–9 days in vitro and primary cultures of mice CGC are grown for 7–12 days in vitro. Cell suspension of CTX or CGC (around 1.6×10^6 cells/mL) are seeded in 24-multi-well plates. The preparation of the cultures is described in a different chapter of this book.

2.2. Radioligand Binding at the $GABA_A$ Receptor

This section lists the materials that are necessary to perform the radioligand binding assays at the GABA, benzodiazepine, and picrotoxinin recognition sites.

HEPES buffered saline solution (HBSS): 136 mM NaCl, 5.4 mM KCl, 1.2 mM $CaCl_2$, 1.4 mM $MgCl_2$, 1 mM NaH_2PO_4, 10 mM HEPES and 9 mM glucose, adjusted at pH 7.4. It can be kept at 4°C for short periods of time.

Tris–Citrate buffered saline solution (TCBSS): 50 mM Tris–Citrate and 200 mM NaCl, adjusted at pH 7.4. It can be kept at 4°C for short periods of time.

Radioligands: (^{3}H)muscimol (≈36.5 Ci/mmol) and [^{3}H] flunitrazepam (≈88 Ci/mmol) working solutions are prepared daily in HBSS at 200–250 nM and 10–20 nM, respectively. [^{35}S]-*t*-Butylbicyclophosphorothionate solution ([^{35}S]TBPS)

(≈90–180 Ci/mmol during the experimental period – note that the half life of ^{35}S is 89 days) is prepared in TCBSS buffer at 15–30 nM. These concentrations are 10× the final ones used in the assay. Take the solutions up and down with a pipette for a complete homogenization or use the vortex very gently (to avoid wetting the inner part of the cap tube) (see Note 1).

GABA: freshly stock solution prepared at 10 mM in HBSS. It is diluted at the necessary concentration in HBSS.

Diazepam: stock solution of 20 mM in dimethyl sulfoxide (DMSO). It can be kept at room temperature for several weeks. It is diluted 1/1,000 with HBSS just before the experiment.

Picrotoxinin: stock solution of 2 mM in HBSS or TCBSS (store in aliquots at −20°C). It is diluted 1/10 with HBSS or TCBSS just before the experiment.

Test Agent solutions. Test agents are diluted according to their solubility in HBSS or TCBSS (more hydrophilic compounds) or in DMSO (more hydrophobic). The solutions are freshly prepared at double concentration when dissolved in HBSS or TCBSS, or at 200× concentrated when dissolved in DMSO. The latest solutions are diluted 1/100 in HBSS or TCBSS immediately before the experiment. The maximum final percentage of vehicle in the incubation buffer must be ≤0.5% (this quantity of DMSO does not show difference with the controls in the three types of binding assays described).

2.3. $GABA_A$ Receptor Functionality

This section lists the materials that are necessary to perform the $^{36}Cl^-$ uptake assay.

Earle's balanced salt solution (EBSS): 116 mM NaCl, 1.8 mM $CaCl_2$, 0.8 mM $MgSO_4$, 1 mM NaH_2PO_4 and 15.2 mM $NaHCO_3$, adjusted at pH 7.4. It can be kept at 4°C for 1 week. The same day of the experiment add 5.5 mM glucose and control the pH.

Test agent solutions. Prepare as double concentrated in HBSS and in EBSS (if preincubation with the agent is included). DMSO must be ≤1%.

$^{36}Cl^-$ stock solution. Prepare a stock solution of $^{36}Cl^-$ by diluting ~1 μCi $^{36}Cl^-$ in 230 μL HBSS (per assay plate). Take the solution up and down with a pipette for a complete homogenization (see Notes 1 and 2).

$^{36}Cl^-$ working solution. In a 2 mL Eppendorf tube add 125 μL HBSS, 125 μL of test agent solutions double concentrated and 25 μL $^{36}Cl^-$ stock solution. Take the solution up and down with a pipette for a complete homogenization. This allows preparing eight conditions per assay plate that will be done in triplicate (see Note 2).

2.4. Radioactivity Measurement and Determination of $GABA_AR$ Parameters

- Liquid scintillation cocktail.
- Liquid scintillation counter.
- Scientific and statistical analysis software.

3. Methods

3.1. Neuronal Cultures

Primary cultures of cortical neurons or of CGC are cultured for 6–10 days in vitro. Assess cell viability and morphology by phase contrast optic microscopy before performing the assay. The assays are performed in attached cells, allowing the study of the interaction of agents with membrane receptors in a physiological milieu (physiological buffers and temperature).

3.2. Radioligand Binding at the $GABA_A$ Receptor

Binding assays are performed in living cells grown in 24-well plates. Seven concentrations of the test agent can be analyzed in triplicate, together with the nonspecific binding and a positive control (when necessary). Ligands of choice for the GABA, benzodiazepine, and the convulsant picrotoxinin binding sites are [^{3}H]muscimol, [^{3}H]flunitrazepam, and [^{35}S]TBPS, respectively (see Note 3). The protocol requires washing of the cells, incubation of the cells with the test agent and the radioligand, elimination of the unbound radioligand, disaggregation and collection of the cells, and determination of bound radioactivity by liquid scintillations counting.

3.2.1. Binding at the GABA Recognition Site

This binding is performed according to García et al. (11).

(a) Rinse the cultures with ≈0.5 mL pre-warmed (37°C) HBSS to eliminate traces of the culture medium (three times). Do not use vacuum in this step; simply remove the medium by careful inversion of the plate (i.e., "dump") over an appropriate receptacle.

(b) Completely remove HBSS from the cells by careful inversion of the plate. Gently blot the plate on a paper towel so that the monolayer is not disrupted. Make sure that the wells do not contain medium.

(c) Immediately add 0.125 mL of fresh pre-warmed HBSS buffer to all wells. Label the plate (bottom and lid).

(d) Add 0.125 mL of double concentrated test-agent solutions in HBSS to the corresponding wells. Control solutions must contain the same proportion of vehicle than test-agent solutions. Include one well for the nonspecific binding, containing 1 mM GABA, and two wells for the positive control (see Note 4).

(e) Preincubate the cells for 10 min at 25°C. This step is recommended when testing antagonists. Otherwise, it can be deleted.

(f) Add 25 μL of [^{3}H]muscimol 10× solution. Final concentration in the assay: 20–25 nM. Carefully shake the plate by drawing a simulated number 8.

(g) Incubate the cells for 20 min at 25°C.

(h) Remove the solution of the wells by vacuum aspiration. Quickly rinse three times with 1.5 mL cold HBSS solution.

(i) Observe the plate under optic microscope for changes in cell viability.

(j) Digest the cells in 0.2 mL 0.2 M NaOH overnight (or 4 h at room temperature with shaking).

(k) Take the whole content of each well into a 3 mL scintillation tube. Add 2 mL Optiphase 2 to each tube. Cap the tubes and vortex them.

(l) Count radioactivity in a liquid scintillation counter.

(m) Substract nonspecific binding from the counts of each well (it accounts for around 29% of the total binding). Determine binding with respect to the control condition, in the absence of the test agent.

3.2.2. Binding at the Benzodiazepine Recognition Site

This binding is performed according to Suñol et al. (10) and García et al. (11).

(a–c) Proceed like binding at the GABA site.

(d) Proceed like binding at the GABA site, but using 10 μM diazepam for the nonspecific binding instead of 1 mM GABA (see Note 4 for positive controls).

(e) Proceed like binding at the GABA site.

(f) Add 25 μL of [^{3}H]flunitrazepam 10× solution. Final concentration in the assay: 1–2 nM. Carefully shake the plate by drawing a simulated number 8.

(g) Incubate the cells for 30 min at 25°C.

(h–m) Proceed like binding at the GABA site.

(n) Substract nonspecific binding from the counts of each well (it accounts for around 10% of the total binding). Determine binding with respect to the control condition, in the absence of the test agent.

[^{3}H]Flunitrazepam binding parameters (K_d and B_{max}) in living cultured neurons are shown in Table 1 and Fig. 1. Determination of these parameters in neuronal cultures exposed to drug and chemicals can be used to evaluate changes of the $GABA_AR$ status. To determine K_d and B_{max}, the cells are incubated with different concentrations of (^{3}H]flunitrazepam (in the range 0.5–25 nM) in HBSS buffer (saturation binding experiment). Nonspecific binding in the presence of 10 μM diazepam is determined for a couple of [^{3}H]flunitrazepam concentrations, and that corresponding to the other concentrations is obtained by lineal interpolation. K_d and B_{max} values are obtained after fitting specific binding values to a hyperbolic equation by a nonlinear regression analysis.

Table 1
Parameters of [^{3}H]flunitrazepam binding in primary cultures of cortical neurons (CTX) and of cerebellar granule cells (CGC)

	CTX[a]	CGC[b]
K_d (nM)	7.4 ± 1.8	3.3 ± 0.2
B_{max} (fmol/mg protein)	731 ± 31	730 ± 60

[a,b] From (11, 19) respectively

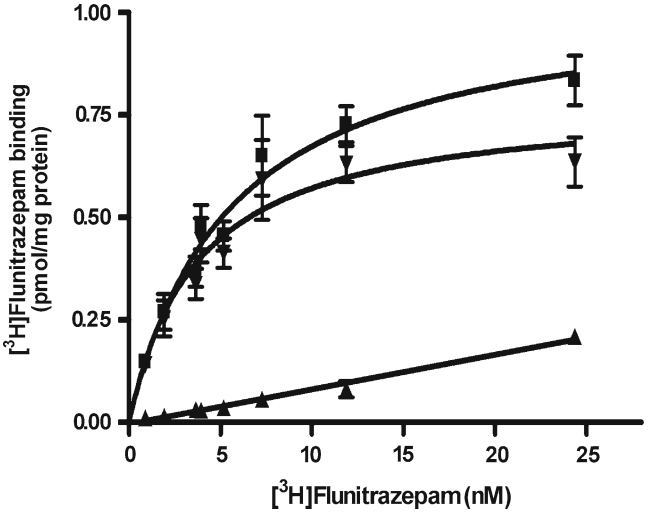

Fig. 1. [^{3}H]Flunitrazepam binding to the benzodiazepine site at the GABA$_A$ receptor (GABA$_A$R) using primary cultures of cortical neurons. *Filled square* total binding; *filled triangle* nonspecific binding; *filled inverted triangle* specific binding. Values are expressed as mean ± sem (reprinted from (11), with permission from Elsevier).

3.2.3. Binding at the Convulsant/Picrotoxinin Site

This binding is performed according to Pomés et al. (17) and García et al. (18).

(a) Rinse the cultures with ≈0.5 mL pre-warmed (37°C) HBSS to eliminate traces of the culture medium (three times). Do not use vacuum in this step; simply remove the medium by careful inversion of the plate (i.e., "dump") over an appropriate receptacle.

(b) Preincubate the cells for 10 min at 25°C with HBSS.

(c) Completely remove HBSS from the cells by careful inversion of the plate. Gently blot the plate on a paper towel so that the monolayer is not disrupted. Make sure that the wells do not contain medium.

(d) Immediately add 0.125 mL of fresh pre-warmed TCBSS buffer to all wells. Label the plate (bottom and lid).

(e) Add 0.125 mL of double concentrated test-agent solutions in TCBSS to the corresponding wells. Control solutions must contain the same proportion of vehicle than test-agent solutions. Include 3 wells for the nonspecific binding, containing 100 µM picrotoxinin.

(f) Add 25 µL of [^{35}S]TBPS 10× solution. Final concentration in the assay: 1.5–3 nM. Carefully shake the plate by drawing a simulated 8.

(g) Incubate the cells for 30 min at 25°C.

(h–m) Follow with steps (h–m) of the previous sections.

(n) Substract nonspecific binding from the counts of each well (it accounts for around 35% of the total binding). Determine binding with respect to the control condition, in the absence of the test agent.

3.2.4. Determining Direct and Allosteric Interactions at the GABA$_A$ Receptor

Compounds interacting with a binding site at the GABA$_A$R will produce an inhibition of the radioligand binding to this site. This is the case for GABA, GABA agonists and competitive GABA antagonists on [^{3}H]muscimol binding; for diazepam on [^{3}H]flunitrazepam binding; and for picrotoxinin or polychlorocycloalkane pesticides on [^{35}S]TBPS binding (Fig. 2).

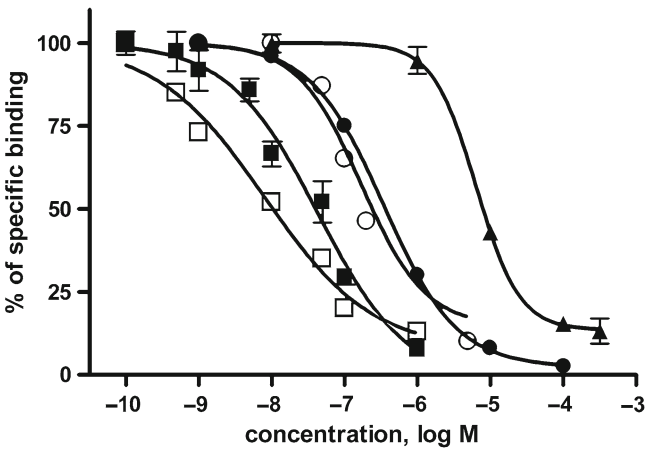

Fig. 2. Interaction of drugs and chemicals with binding sites at the GABA$_A$R. Inhibition of [^{3}H]muscimol binding by the endogenous neurotransmitter γ-aminobutyric acid (GABA) (*filled triangle*), of [^{3}H]flunitrazepam binding by the benzodiazepine diazepam (*filled square*), and of [^{35}S]TBPS binding by picrotoxinin (*filled circle*), and the chlorinated pesticides α-endosulfan (*open square*) and γ-hexachlorocyclohexane (lindane, *open circle*). Results are expressed as mean values. Error bars are not included for clarity (data extracted from (11, 17, 19)).

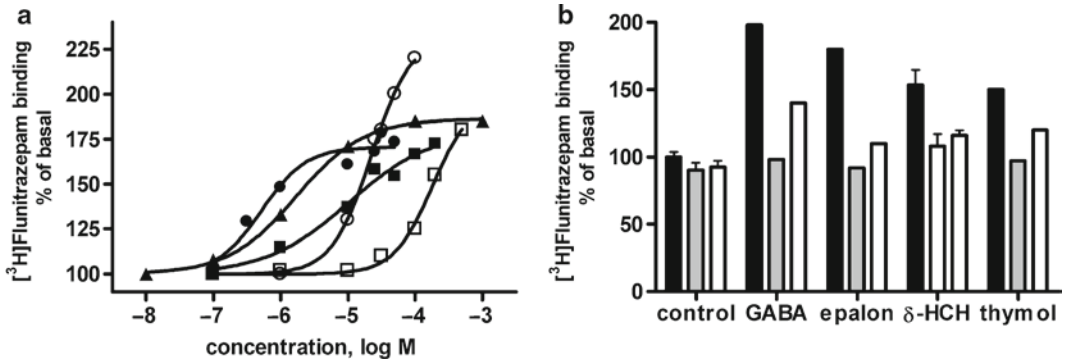

Fig. 3. Allosteric modulation at the GABA$_A$R. (**a**) (^{3}H)Flunitrazepam binding is increased by GABA (*filled triangle*) and positive allosteric modulators: the neurosteroid allopregnanolone (epalon, *filled circle*), the environmental contaminants δ-hexachlorocyclohexane (*filled square*) and methylmercury (*open circle*), and the plant extract thymol (*open square*). (**b**) The increase of [^{3}H]flunitrazepam binding by positive allosteric modulators (*black bars*) is reverted by the GABA$_A$R antagonists bicuculline (*gray bars*) and picrotoxinin (*white bars*) (data extracted from (10, 11, 19, 21)).

Furthermore, the binding sites at the GABA$_A$R are allosterically modulated, and the binding of an agent to its specific site will produce changes on the binding properties of the other sites at the receptor. Allosteric modulations include the enhanced binding of benzodiazepine agonists induced by GABA, propofol, neurosteroids, thymol, and barbiturates (Fig. 3a). The increase of [^{3}H] flunitrazepam induced by these agents is inhibited by competitive and noncompetitive GABA$_A$R antagonists (Fig. 3b). This reversion is indicative of an action of these compounds at one or several sites at the GABA$_A$R. [^{35}S]TBPS binding is allosterically modified by GABA, benzodiazepines, thymol, barbiturates, and other positive modulators of the GABA$_A$R. The binding of [^{35}S] TBPS is inhibited by these compounds when the incubation medium contains low micromolar concentrations of GABA, while it may be increased in the absence of GABA (18).

3.3. GABA$_A$ Receptor Functionality

The potentiation or inactivation of the GABA$_A$R can be determined by analyzing the Cl^- flux induced by GABA. In mature neurons, GABA and agonists induce a Cl^- influx that is increased by benzodiazepines, barbiturates, neurosteroids and ethanol, while it is reduced by competitive antagonists and by compounds that recognize the picrotoxinin site (1–6). This Cl^- flux can be evaluated by electrophysiology, $^{36}Cl^-$ uptake or fluorimetric determinations. Here we describe the $^{36}Cl^-$ uptake assay in living cells, according to previous publications (10–12).

(a) Replace culture medium with 0.5 mL pre-warmed EBSS solution (37°C) and incubate the cells inside the cell incubator for 30 min. Repeat this procedure and incubate the cells for 15 min twice.

(b) Completely remove EBSS by blotting the plate on a paper towel so that the monolayer is not disrupted. Add 250 μL EBSS to the whole plate. Label the plate (bottom and lid). Incubate the cells at room temperature and atmosphere for 10 min. Test agents dissolved in EBSS can be included in this step.

(c) Position the plate behind the methacrylate screen. Uptake of $^{36}Cl^-$ is performed well after well, in a sequential order. Remove medium from each well with vacuum aspiration and immediately add 0.240 mL of the corresponding working $^{36}Cl^-$ solution containing $^{36}Cl^-$, GABA (100 μM for $GABA_AR$ inhibition or 5 μM for $GABA_AR$ potentiation) and the test compound. The cells are incubated for 10 s. The incubation medium is removed with the pipette and returned to the eppendorf tube (the solution is reused for the replicates of the same concentration). The well is quickly rinsed four times with 1.5 mL cold HBSS solution. The rinsed solutions are removed by vacuum aspiration.

(d) Incubate the cells with 0.2 mL/well of distilled water during 1 h in agitation, in order to induce a hyposmotic shock and to release the $^{36}Cl^-$ molecules trapped in the cells.

(e) Collect the solution containing $^{36}Cl^-$ in a scintillation vial, add 4 mL of scintillation liquid and count radioactivity.

(f) GABA-induced $^{36}Cl^-$ uptake is determined by subtracting the basal Cl^- uptake in cells incubated in the absence of GABA or in the presence of 100 μM bicuculline ($GABA_AR$ antagonist).

$GABA_AR$ antagonists will inhibit GABA-induced Cl^- influx, whereas positive allosteric modulators will enhance it. Figure 4 shows the dose–response curve for GABA-inducing Cl^- influx and the inhibitory effects of several $GABA_AR$ antagonists.

3.4. Assessing Neuroactive Compounds Acting at the $GABA_A$ Receptor

Alcohols like isopropyl alcohol, depressant drugs like diazepam, phenobarbital, and chloral hydrate, the endogenous neurosteroid allopregnanolone, the plant extract thymol and the depressant environmental contaminant δ-HCH increase GABA-induced $^{36}Cl^-$ uptake in primary cultures of cortical neurons (9–11). Among these compounds, those not directly interacting with the benzodiazepine binding site also increase (^{3}H]flunitrazepam binding in primary cultured neurons, as it has been demonstrated for neurosteroids, thymol, barbiturates and δ-HCH (Fig. 3; (10–12, 19)). The effects of barbiturates, neurosteroids and δ-HCH on $GABA_AR$ function are in agreement with their depressant CNS activity in humans and experimental animals. Some other compounds like bicuculline, picrotoxinin and the pesticides lindane, dieldrin and α-endosulfan, inhibit the GABA-induced $^{36}Cl^-$ uptake in primary cultured neurons. They also inhibit the increase of

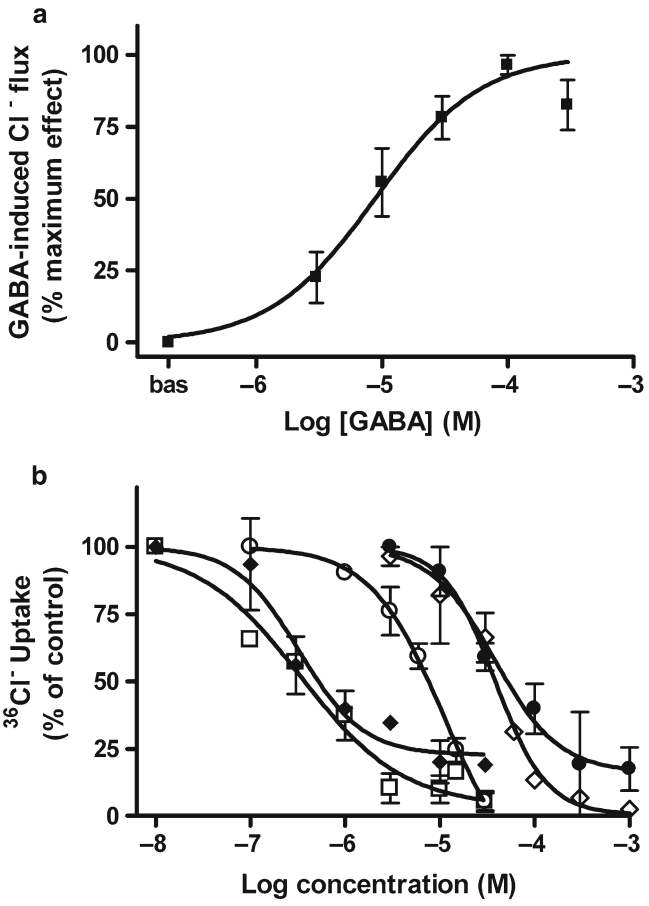

Fig. 4. Dose–response curve for GABA-inducing Cl^- influx and the inhibitory effects of GABA$_A$R antagonists. (**a**) GABA induces a Cl^- influx with an EC_{50} value of 8 μM (11) and a maximum effect attained at around 100 μM GABA (reprinted from (11), with permission from Elsevier). (**b**) 100 μM GABA-induced Cl^- influx is inhibited by competitive and noncompetitive GABA$_A$R antagonists. Bicuculline (*open diamond*), picrotoxinin (*filled circle*) and the chlorinated pesticides α-endosulfan (*open square*), γ-HCH (lindane, *open circle*) and dieldrin (*filled diamond*) (data extracted from (12, 20)).

[^{3}H]flunitrazepam induced by GABA (Fig. 3; (12, 19, 20)). The effects of these compounds on GABA$_A$R function are in agreement with their convulsant activity in humans and experimental animals. Both positive and negative modulators of the GABA$_A$R inhibit [^{35}S]TBPS binding in the presence of GABA. Therefore, both the direct assay of $^{36}Cl^-$ influx and the indirect assays based on the allosteric modifications of the bindings of [^{3}H]flunitrazepam and of [^{35}S]TBPS can be used as testing assays for compounds acting at the GABA$_A$R. Standardization of these methods and further validation could give rise to a high-throughput assay for the activity of chemicals on the GABA$_A$R.

3.5. Interpretation of Data

Subtract nonspecific binding and basal $^{36}Cl^-$ uptake to obtain specific binding and GABA-induced $^{36}Cl^-$ uptake. Refer these values to the control ones, obtained in the absence of the test agent. Fit the values to a sigmoid curve by using nonlinear regression and/or use the appropriate statistics.

4. Notes

1. Use protective personnel equipment (gloves, eyeglasses, and lab coat) when preparing and using radioactive solutions. Strictly follow the rules governing the amount of radioactivity that can be used in the lab bench and the waste policies for each radionuclide. The use of methacrylate screens is not necessary when working with ^{3}H or ^{35}S. It is strictly required when working with ^{36}Cl.
2. ^{36}Cl has a high energy (710 keV). Working with it requires the use of methacrylate screens and tube-holders to protect the analyst against the high β-radiation emitted by ^{36}Cl.
3. [^{3}H]muscimol is the preferred radioligand for the GABA site at the $GABA_AR$, since it is not taken by the GABA transport system. Instead, the use of [^{3}H]GABA in living cells would produce a radioactive measure related to neuronal GABA uptake more than to GABA receptor binding, according to the density of GABA transporters and receptors in the membrane.
4. As positive control, use a compound with known effect on the parameter to be studied. For the GABA recognition site, use an agonist or an antagonist that will reduce the binding of the radioligand. For the benzodiazepine recognition site, use a different benzodiazepine that will reduce the binding of [^{3}H]flunitrazepam binding, or a positive modulator like GABA or allopregnanolone that will increase [^{3}H]flunitrazepam binding. Results from a plate assay where the positive control does not act as expected will not be taken into consideration.

Acknowledgments

This work was supported by grants PI 06/1212, PI 10/0453 (Spanish Ministry of Health), LSHB-CT-2004-512051 from European Commission and SECyT-UNC, ANPCyT and CONICET (Argentina). DAG is a member of CONICET-Argentina.

References

1. Narahashi T (2000) Neuroreceptors and ion channels as the basis for drug action: past, present, and future. J Pharmacol Exp Ther 294:1–26
2. MacDonald RL, Olsen RW (1994) $GABA_A$ receptor channels. Annu Rev Neurosci 17:569–602
3. Dalby NO (2003) Inhibition of gamma-aminobutyric acid uptake: anatomy, physiology and effects against epileptic seizures. Eur J Pharmacol 479:127–137
4. Lambert JJ, Belelli D, Peden DR, Vardy AW, Peters JA (2003) Neurosteroid modulation of $GABA_A$ receptors. Prog Neurobiol 71:67–80
5. Whiting PJ (2003) $GABA_A$ receptor subtypes in the brain: a paradigm for CNS drug discovery? Drug Discov Today 8:445–450
6. Kalueff AV (2007) Mapping convulsants' binding to the $GABA_A$ receptor chloride ionophore: a proposed model for channel binding sites. Neurochem Int 50:61–68
7. Olsen RW, Sieghart W (2008) International Union of Pharmacology. LXX. Subtypes of γ-aminobutric $acid_A$ receptors: classification on the basis of subunit composition, pharmacology, and function. Update. Pharmacol Rev 60:243–260
8. Nagata K, Narahashi T (1994) Dual action of the cyclodiene insecticide dieldrin on the α-aminobutyric acid receptor-chloride channel complex of rat dorsal root ganglion neurons. J Pharmacol Exp Ther 269:164–171
9. Pomés A, Rodríguez-Farré E, Suñol C (1994) Disruption of GABA-dependent chloride flux by cyclodienes and hexachlorocyclohexanes in primary cultures of cortical neurons. J Pharmacol Exp Ther 271:1616–1623
10. Suñol C, García DA, Bujons J, Krištofíková Z, Matyas L, Babot Z, Kasal A (2006) Activity of B-nor analogues of neurosteroids on $GABA_A$ receptor in primary neuronal cultures. J Med Chem 49:3225–3234
11. García DA, Bujons J, Vale C, Suñol C (2006) Allosteric positive interaction of thymol with the $GABA_A$ receptor in primary cultures of mouse cortical neurons. Neuropharmacology 50:25–35
12. Galofré M, Babot Z, García DA, Iraola S, Rodríguez-Farré E, Forsby A, Suñol C (2010) $GABA_A$ receptor and cell membrane potential as functional endpoints in cultured neurons to evaluate chemicals for human acute toxicity. Neurotoxicol Teratol 32:52–61
13. Sonnewald U, Olstad E, Qu H, Babot Z, Cristòfol R, Suñol C, Schousboe A, Waagepetersen H (2004) First direct demonstration of extensive GABA synthesis in mouse cerebellar neuronal cultures. J Neurochem 91:796–803
14. Suñol C, Babot Z, Fonfría E, Galofré M, García D, Herrera N, Iraola S, Vendrell I (2008) Studies with neuronal cells: from basic studies of mechanisms of neurotoxicity to the prediction of chemical toxicity. Toxicol In Vitro 22(5):1350–1355
15. Poulter MO, Ohannesian L, Larmet Y, Feltz P (1997) Evidence that $GABA_A$ receptor subunit mRNA expression during development is regulated by $GABA_A$ receptor stimulation. J Neurochem 68:631–639
16. Hansen SL, Ebert B, Fjalland B, Kristiansen B (2001) Effects of $GABA_A$ receptor partial agonists in primary cultures of cerebellar granule neurons and cerebral cortical neurons reflect different receptor subunit compositions. Br J Pharmacol 133:539–549
17. Pomés A, Rodriguez-Farré E, Suñol C (1993) Inhibition of *t*-(^{35}S]butylbicyclophosphorothionate binding by convulsant agents in primary cultures of cerebellar neurons. Dev Brain Res 73:85–90
18. García DA, Vendrell I, Galofre M, Suñol C (2008) GABA released from cultured cortical neurons influences the modulation of *t*-[^{35}S] butylbicyclophosphorothionate binding at the $GABA_A$ receptor. Effects of thymol. Eur J Pharmacol 600:26–31
19. Vale C, Pomés A, Rodríguez-Farré E, Suñol C (1997) Allosteric interactions between γ-aminobutyric acid, benzodiazepine and picrotoxinin binding sites in primary cultures of cerebellar granule cells. Differential effects induced by γ- and δ-hexachlorocyclohexanes. Eur J Neurosci 319:343–353
20. Vale C, Fonfría E, Bujons J, Messeguer A, Rodríguez-Farré E, Suñol C (2003) The organochlorine pesticides gamma-hexachlorocyclohexane (lindane), alpha-endosulfan and dieldrin differentially interact with $GABA_A$ and glycine-gated chloride channels in primary cultures of cerebellar granule cells. Neuroscience 117:397–403
21. Fonfría E, Rodríguez-Farré E, Suñol C (2001) Mercury interaction with the $GABA_A$ receptor modulates the benzodiazepine binding site in primary cultures of cerebellar granule cells. Neuropharmacology 41:819–833

INDEX

Michael Aschner et al. (eds.), *Cell Culture Techniques*, Neuromethods, vol. 56,
DOI 10.1007/978-1-61779-077-5, © Springer Science+Business Media, LLC 2011

F

G

H

I

L

M

N

O

P

R

S

T

V

W